INFORMATION TO USERS

This manuscript has been reproduced from the microfilm master. UMI films the text directly from the original or copy submitted. Thus, some thesis and dissertation copies are in typewriter face, while others may be from any type of computer printer.

The quality of this reproduction is dependent upon the quality of the copy submitted. Broken or indistinct print, colored or poor quality illustrations and photographs, print bleedthrough, substandard margins, and improper alignment can adversely affect reproduction.

In the unlikely event that the author did not send UMI a complete manuscript and there are missing pages, these will be noted. Also, if unauthorized copyright material had to be removed, a note will indicate the deletion.

Oversize materials (e.g., maps, drawings, charts) are reproduced by sectioning the original, beginning at the upper left-hand corner and continuing from left to right in equal sections with small overlaps.

Photographs included in the original manuscript have been reproduced xerographically in this copy. Higher quality 6" x 9" black and white photographic prints are available for any photographs or illustrations appearing in this copy for an additional charge. Contact UMI directly to order.

ProQuest Information and Learning
300 North Zeeb Road, Ann Arbor, MI 48106-1346 USA
800-521-0600

DISSERTATION

MEMBRANE BEHAVIOR AND COUPLED SOLUTE TRANSPORT THROUGH A GEOSYNTHETIC CLAY LINER

Submitted by:

Michael Adam Malusis

Department of Civil Engineering

In partial fulfillment of the requirements

for the Degree of Doctor of Philosophy

Colorado State University

Fort Collins, CO

Summer 2001

UMI Number: 3032693

UMI Microform 3032693

ProQuest Information and Learning Company
300 North Zeeb Road
P.O. Box 1346
Ann Arbor, MI 48106-1346

COLORADO STATE UNIVERSITY

April 19, 2001

WE HEREBY RECOMMEND THAT THE DISSERTATION PREPARED UNDER OUR SUPERVISION BY MICHAEL A. MALUSIS ENTITLED "MEMBRANE BEHAVIOR AND COUPLED SOLUTE TRANSPORT THROUGH A GEOSYNTHETIC CLAY LINER" BE ACCEPTED AS FULFILLING, IN PART, THE REQUIREMENTS FOR THE DEGREE OF DOCTOR OF PHILOSOPHY.

COMMITTEE ON GRADUATE WORK

Advisor

Department Head

ABSTRACT OF DISSERTATION

MEMBRANE BEHAVIOR AND COUPLED SOLUTE TRANSPORT THROUGH A GEOSYNTHETIC CLAY LINER

The ability of a geosynthetic clay liner (GCL) to act as a semi-permeable membrane that restricts migration of solutes, and the influence of this membrane behavior on solute transport through a GCL, are evaluated in this research. A coupled solute transport model that accounts for membrane behavior (i.e., salt-sieving, chemico-osmotic counter flow) in clay soils is developed. In addition, laboratory chemico-osmotic/ diffusion and column tests are conducted on specimens of a GCL subjected to potassium chloride (KCl) solutions. Measured chemico-osmotic efficiency coefficients (ω) range from 0.14 to 0.63, and effective salt-diffusion coefficients (D_s^*) range from 2.38 x 10^{-10} m^2/s to 7.83 x 10^{-11} m^2/s for 10-mm-thick GCL specimens subjected to KCl source concentrations ranging from 0.0039 M to 0.047 M. The results indicate that two coupling effects limit KCl diffusion through the GCL: (1) an explicit coupling effect due to salt-sieving, as predicted by the coupled flux transport theory; and (2) implicit coupling characterized by a concentration-dependent decrease in D_s^* that ts related to the apparent tortuosity factor (τ_a). These effects are correlated with measured ω values for the GCL. Comparison of experimental results from column tests with model simulations based on independently measured values of ω and D_s^* (or τ_a) indicate that implicit coupling is more significant than explicit coupling for reducing solute flux through the GCL under diffusion-dominated conditions.

The results of theoretical simulations indicate that lower values of solute flux and longer solute transit times through a soil membrane are predicted by coupled solute transport theory relative to advective-dispersive theory that neglects chemico-osmotic efficiency. The coupled transport model also provides better agreement with measured data from the column tests than advective-dispersive theory. Use of advective-dispersive theory to simulate solute transport through GCLs appears reasonable under diffusion-dominated conditions, provided that implicit coupling is included by using an appropriate value of D_s^* (or τ_a) that corresponds to the solute concentration.

Michael A. Malusis
Civil Engineering Department
Colorado State University
Fort Collins, CO 80523
Summer 2001

ACKNOWLEDGMENTS

This research marks the completion of a long, humbling, sometimes depressing, but ultimately rewarding journey for me. I would not have reached the end of this journey without the caring guidance and support of two amazing people. The first is my wife, Lisa, who somehow managed to put up with me and always encouraged me, even during the dark hours (and there were many) when I was ready to give it all up. I love you, and owe you - big time. The second is my advisor, Dr. Charles D. Shackelford. Thanks for always being there for me, Chuck. I can never repay you in kind for the support you have given me. I value the friendship we have developed over the past eight years, and especially appreciate your devoted efforts on my behalf. I look forward to collaborating with you in the years to come.

I would like to thank Dr. Harold W. (Hal) Olsen, for providing a wealth of knowledge and assistance, and for assisting in publication of this research. It has been a privilege to work with you, Hal. Also, I would also like to thank my other committee members, Dr. John Nelson and Dr. Branka Ladanyi, for their willing involvement in this endeavor.

In addition, I need to thank many other people that have helped me tremendously along the way, including Laurie Howard, Joe Wilmetti, Tarek Salem, Rich and Melanie Davis, Howie and Diana Perko, Mitch Majeski, Dean Durkee, Dr. Paul Heyliger, Dr. Tom Siller, Dr. Ken Reardon, Dr. Steven Strauss, Matt Odom, Art Willden, and my parents, John and Leah Malusis.

Finally, the support of this work by the National Science Foundation (NSF) and Dr. Jim Self at the CSU Soil Testing Lab is gratefully acknowledged.

TABLE OF CONTENTS

		Page
Chapter 1	**Introduction**	
1.1	**Background**	**1.1**
1.2	**Objectives of Research**	**1.4**
1.3	**References**	**1.7**
Chapter 2	**A Laboratory Apparatus To Measure Chemico-Osmotic Efficiency Coefficients For Clay Soils**	
2.1	**Introduction**	**2.2**
2.2	**Background**	**2.4**
2.3	**New testing apparatus and procedures**	**2.7**
2.3.1	Testing cell	2.7
2.3.2	Flow-pump system	2.7
2.3.3	Flow-pump actuators	2.8
2.3.4	Measurement of chemico-osmotic efficiency	2.10
2.3.5	Measurement of solute transport parameters	2.11
2.4	**Example results**	**2.13**
2.4.1	Chemico-osmotic efficiency coefficient	2.14
2.4.2	Effective diffusion coefficient, D^*	2.17
2.4.3	Retardation factor, R_d	2.17
2.5	**Discussion**	**2.18**
2.5.1	Soil-solution interaction	2.18
2.5.2	Circulation rate	2.19
2.6	**Summary and conclusions**	**2.21**
2.7	**References**	**2.23**
Chapter 3	**Chemico-Osmotic Efficiency of a Geosynthetic Clay Liner**	
3.1	**Introduction**	**3.2**
3.2	**Materials and methods**	**3.4**
3.2.1	Geosynthetic clay liner	3.4
3.2.2	Liquids	3.4
3.2.3	Testing apparatus	3.5
3.2.4	Specimen assembly and disassembly	3.6
3.2.5	Measurement of ω	3.7
3.2.6	Correlation of solute concentrations with electrical conductance	3.10
3.2.7	Testing program	3.11
3.3	**Results**	**3.11**
3.3.1	Induced differential pressures	3.11
3.3.2	Determination of $\Delta\pi$	3.12
3.3.3	Chemico-osmotic efficiency coefficients	3.12

Chapter 3	(cont.)	Page
3.4	**Discussion**	**3.13**
3.4.1	Influence of porosity on chemico-osmotic efficiency	3.13
3.4.2	Influence of electrolyte concentration on chemico-osmotic efficiency	3.13
3.4.3	Practical significance	3.17
3.5	**Conclusions**	**3.19**
3.6	**References**	**3.20**

Chapter 4	Coupled Solute Diffusion for a Geosynthetic Clay Liner	
4.1	**Introduction**	**4.2**
4.2	**Theoretical background**	**4.5**
4.2.1	Diffusive solute flux	4.8
4.3	**Materials and experimental methods**	4.10
4.3.1	Geosynthetic clay liner	4.10
4.3.2	Liquids	4.11
4.3.3	Testing apparatus and procedure	4.11
4.3.4	Specimen preparation	4.13
4.3.5	Determination of chemico-osmotic efficiency	4.13
4.3.6	Determination of effective diffusion coefficients	4.14
4.3.7	Testing program	4.17
4.4	**Results**	**4.17**
4.4.1	Chemico-osmotic efficiency coefficients (ω)	4.17
4.4.2	Diffusion results	4.19
4.4.3	Effective diffusion coefficients (D^*)	4.19
4.5	**Discussion**	**4.20**
4.5.1	Relationship between D_s^* and ω	4.20
4.5.2	Restrictive tortuosity factor	4.22
4.5.3	Practical significance of results	4.25
4.6	**Conclusions**	**4.26**
4.7	**References**	**4.28**

Chapter 5	Coupled Solute Flux and Transport Through Clay Membrane Barriers	
5.1	**Introduction**	**5.2**
5.2	**Theoretical background**	**5.5**
5.2.1	Conceptual model	5.6
5.2.2	Dissipation of free energy	5.7
5.2.3	Coupled flux equations	5.8
5.2.4	Phenomenological coefficients, L_{ij}	5.10
5.3	**Theoretical development**	**5.12**
5.3.1	Coupled flux without applied current	5.13
5.3.2	Salt-diffusion coefficients	5.15
5.3.3	Total coupled solute flux	5.18
5.3.4	Coupled solute transport	5.19
5.3.5	Coupled solute transport with ion exchange	5.20
5.3.6	Coupled solute transport without membrane behavior	5.23
5.4	**Numerical modeling**	**5.26**
5.4.1	Initial and boundary conditions	5.26
5.4.2	Comparison of numerical and analytical solutions for $\omega = 0$	5.27
5.4.3	Theoretical analysis of coupled solute transport	5.29
5.4.3.1	Solute flux at $x = L$	5.33
5.4.3.2	Solute transit time	5.39

Chapter 5 (cont.) Page
5.5 Experimental assessment 5.40
5.5.1 Materials and methods 5.40
5.5.1.1 Bentomat® GCL 5.40
5.5.1.2 Liquids 5.40
5.5.1.3 Column testing apparatus 5.41
5.5.1.4 Specimen preparation 5.42
5.5.1.5 Testing conditions 5.42
5.5.2 Model simulations 5.43
5.5.3 Column test results and model comparisons 5.44
5.6 Conclusions 5.46
5.7 References 5.48

Chapter 6 Conclusions and Recommendations

6.1 Conclusions 6.1
6.2 Recommendations 6.4

Appendix A - Quantitative Assessment of the van't Hoff Expression for Evaluating Chemico-Osmotic Efficiency of Clay Soils

Appendix B - Development of Expression for Salt-Diffusion Coefficient of Ions in Mixed Electrolytes

Appendix C - Development of Finite Difference Model for Coupled Solute Transport through a Soil Membrane

Appendix D - Coupled Solute Transport Model Simulations

Appendix E - Chemico-Osmotic Test Data

Appendix F - Diffusion Test Data

Appendix G - Experimental Data and Coupled Solute Transport Model Simulations for Column Tests

LIST OF TABLES

Page

Chapter 2

2.1 Exchangeable cation concentrations for bentonite in Bentomat® GCL 2.27

Chapter 3

3.1 Measured properties of bentonite in Bentomat® GCL..... 3.24
3.2 Measured chemical properties of liquids used in study..... 3.25
3.3 Test results for GCL specimens..... 3.26

Chapter 4

4.1 Diffusion test results..... 4.33

Chapter 5

5.1 Self-diffusion and salt-diffusion coefficients for K^+, Na^+, and Cl^- system..... 5.54
5.2 Results of steady-state chemico-osmotic/diffusion tests for Bentomat® GCL..... 5.55
5.3 Input parameters for theoretical analysis..... 5.56
5.4 Input parameters for theoretical analysis (cont.)..... 5.57
5.5 Measured properties of bentonite in Bentomat® GCL..... 5.58
5.6 Column test conditions..... 5.59
5.7 Model simulations for comparison with column test data..... 5.60

LIST OF FIGURES

Page

Chapter 2

2.1 Measured head differences (ΔH) across a kaolinite specimen as a function of externally imposed flow rates (Q/t) and the ratio of NaCl concentrations at the specimen boundaries (C_B/C_T) (replotted after Olsen 1969) 2.28
2.2 Schematic of chemico-osmotic testing apparatus 2.29
2.3 Pictorial view of chemico-osmotic testing apparatus 2.30
2.4 Schematic of chemico-osmotic testing cell 2.31
2.5 Illustrations of flow-pump system: (a) pictorial view; (b) schematic cross-section 2.32
2.6 Schematics of flow-pump actuator: (a) top view; (b) cross-sectional view 2.33
2.7 Schematic of top and bottom actuators during constant-volume circulation of electrolyte solutions at soil specimen boundaries 2.34
2.8 Differential pressure measurement and data acquisition system: (a) schematic view; (b) pictorial view 2.35
2.9 Schematic illustration of steady-state diffusion test results 2.36
2.10 Pressure differences induced across 10-mm thick GCL specimens: (a) test 1; (b) test 2 ..... 2.37
2.11 Boundary concentrations of chloride (Cl^-) and potassium (K^+) over time for chemico-osmotic test 1 (C_{ot} = 0.0087 M KCl) 2.38
2.12 Boundary concentrations of chloride (Cl^-) and potassium (K^+) over time for chemico-osmotic test 2 (C_{ot} = 0.047 M KCl) 2.39
2.13 Measured electrical conductivity in circulation outflow from base pedestal versus time in chemico-osmotic tests 1 and 2 ..... 2.40
2.14 Results of steady-state method to evaluate the effective diffusion coefficient (D^*) and retardation factor (R_d) in chemico-osmotic test 1 for chloride and potassium (L = 0.010 m, C_{ot} = 0.0087 M, n = 0.79) 2.41
2.15 Hydraulic conductivity of GCL specimens before and after chemico-osmotic testing 2.42

Chapter 3

3.1 Schematic of Bentomat® GCL 3.27
3.2 Grain-size distributions for granular bentonite in Bentomat® GCL 3.28
3.3 Schematic of testing apparatus used in study 3.29
3.4 Correlation between KCl concentration and electrical conductance at 25 °C 3.30
3.5 Comparison of measured exit concentrations of K^+ and Cl^- from base pedestal (C_b) with estimated exit KCl concentrations based on electrical conductance (EC) measurements 3.31
3.6 Induced differential pressures measured across GCL specimens in single-stage chemico-osmotic tests (L = 1.0 cm) 3.32

Figures (cont.) Page

3.7 Induced differential pressures measured acrosss GCL specimens in multi-stage chemico-osmotic tests: (a) L = 0.8 cm; (b) L = 1.3 cm 3.33
3.8 Exit KCl concentrations (C_b and C_t) versus time for single-stage chemico-osmotic tests (L = 1.0 cm) 3.34
3.9 Exit KCl concentrations (C_b and C_t) versus time for multi-stage chemico-osmotic tests: (a) L = 0.8 cm; (b) L = 1.3 cm 3.35
3.10 Error in $\Delta\pi$ incurred by ignoring changes in boundary KCl concentrations due to diffusion 3.36
3.11 (a) Chemico-osmotic efficiency coefficients (ω_{ss}) versus porosity, n; (b) Initial hydraulic conductivity of GCL specimens permeated with processed tap water (PTW) 3.37
3.12 Chemico-osmotic efficiency of sodium bentonite as a function of salt concentration and porosity 3.38
3.13 Ratios of peak to steady-state differential pressures measured in chemico-osmotic tests 3.39
3.14 Effect of KCl concentration on hydraulic conductivity of GCL specimens tested in study 3.40
3.15 Simulated liquid flux through a 1.0-cm thick Bentomat GCL in the presence of KCl solutions 3.41

Chapter 4

4.1 Schematic of Bentomat® GCL 4.34
4.2 Schematic of testing apparatus used in study 4.35
4.3 Example illustration of steady-state diffusion test results 4.36
4.4 Induced differential pressures measured across GCL specimens 4.37
4.5 Measured chemico-osmotic efficiency coefficients of GCL specimens versus source KCl concentration (C_{ot}) 4.38
4.6 Measured exit concentrations of Cl^- and K^+ during diffusion tests 4.39
4.7 Steady-state diffusion results for Cl^-: (a) C_{ot} = 0.0039 M; (b) C_{ot} = 0.0087 M; (c) C_{ot} = 0.020 M; (d) C_{ot} = 0.047 M 4.40
4.8 Steady-state diffusion results for K^+: (a) C_{ot} = 0.0039 M; (b) C_{ot} = 0.0087 M; (c) C_{ot} = 0.020 M; (d) C_{ot} = 0.047 M 4.41
4.9 Comparison of D_s^* values based on K^+ versus Cl^- data 4.42
4.10 Comparison of D_ω^* versus D_s^* values obtained in study 4.43
4.11 Effective salt-diffusion coefficients versus (a) source KCl concentration; (b) chemico-osmotic efficiency coefficient 4.44
4.12 Tortuosity factors versus chemico-osmotic efficiency: (a) apparent tortuosity factor, τ_a; (b) restrictive tortuosity factor, τ_r 4.45
4.13 Measured D_ω^* values as a function of source concentration, C_o 4.46
4.14 Theoretical steady-state diffusive flux through Bentomat® GCL (L = 1.0 cm) 4.47

Chapter 5

5.1 Conceptual model of soil-water-electrolyte system (after Yeung 1990) 5.61
5.2 Natural containment versus engineered containment (after Shackelford 1996) 5.62

Figures (cont.) Page

5.3 Comparison of numerical and analytical solutions for exit flux of Cl^- (R_{da} = 1) and K^+ (R_{dc} = 5) through a non-membrane soil (ω = 0, L = 1 m, C_o = 0.1 M, τ_a = 0.1, k = 10^{-10} m/s, D_{oa} = 20.3 x 10^{-10} m^2/s) in which D_{ox} = D_{oc} = 19.6 x 10^{-10} m^2/s: (a) i_h = 0; (b) i_h = 10 ..... 5.63

5.4 Comparison of numerical and analytical solutions for exit flux of Cl^- (R_{da} = 1) and K^+ (R_{dc} = 5) through a non-membrane soil (ω = 0, L = 1 m, C_o = 0.1 M, τ_a = 0.1, k = 10^{-10} m/s, D_{oa} = 20.3 x 10^{-10} m^2/s) in which D_{oc} = 19.6 x 10^{-10} m^2/s and D_{ox} = 13.3 x 10^{-10} m^2/s: (a) i_h = 0; (b) i_h = 10 ..... 5.64

5.5 Schematic illustration of Bentomat® GCL 5.65

5.6 Relationship between chemico-osmotic efficiency (ω), source concentration (C_o), effective salt-diffusion coefficient (D_s^*), and apparent tortuosity factor (τ_a) for GCL specimens (L = 1.0 cm) subjected to KCl solutions: (a) ω versus Co; (b) D_s^* and τ_a versus ω 5.66

5.7 Theoretical KCl exit flux versus time (L = 1 m, C_o = 0.047 M, n = 0.78, k_h = 1.48 x 10^{-11} m/s) 5.67

5.8 Theoretical KCl exit flux versus time (L = 1 m, C_o = 0.020 M, n = 0.79, k_h = 2.06 x 10^{-11} m/s) 5.68

5.9 Theoretical KCl exit flux versus time (L = 1 m, C_o = 0.0087 M, n = 0.79, k_h = 1.33 x 10^{-11} m/s) 5.69

5.10 Theoretical KCl exit flux versus time (L = 1 m, C_o = 0.0039 M, n = 0.80, k_h = 1.65 x 10^{-11} m/s) 5.70

5.11 Peclet numbers as a function of hydraulic gradient 5.71

5.12 Theoretical steady-state concentration profiles inside soil barrier (L = 1 m, C_o = 0.047 M, n = 0.78, k_h = 1.48 x 10^{-11} m/s) 5.72

5.13 Theoretical steady-state concentration profiles inside soil barrier (L = 1 m, C_o = 0.020 M, n = 0.79, k_h = 2.06 x 10^{-11} m/s) 5.73

5.14 Theoretical steady-state concentration profiles inside soil barrier (L = 1 m, C_o = 0.0087 M, n = 0.79, k_h = 1.33 x 10^{-11} m/s) 5.74

5.15 Theoretical steady-state concentration profiles inside soil barrier (L = 1 m, C_o = 0.0039 M, n = 0.80, k_h = 1.65 x 10^{-11} m/s) 5.75

5.16 Normalized values of exit KCl flux at steady-state relative to the non-membrane (NM) condition 5.76

5.17 Normalized values of time to reach steady-state transport of KCl relative to the non-membrane (NM) condition 5.77

5.18 Schematic illustration of column testing apparatus 5.78

5.19 Comparison of measured exit K^+ and Cl^- fluxes from column tests on Bentomat GCL (L = 1.0 cm; C_o = 0.0087 M KCl) and predicted K^+ and Cl^- fluxes with either no coupling (NM) or both explicit and implicit coupling (EI) 5.79

5.20 Comparison of measured exit K^+ and Cl^- fluxes from column tests on Bentomat GCL (L = 1.0 cm, i_h = 703) and predicted K^+ and Cl^- fluxes with either no coupling (NM) or both explicit and implicit coupling (EI). 5.80

Figures (cont.) Page

5.21 Comparison of measured exit K^+ and Cl^- fluxes from column tests on Bentomat GCL (L = 1.0 cm, C_o = 0.0087 M KCl) and predicted K^+ and Cl^- fluxes with either implicit coupling only (I) or both explicit and implicit coupling (EI)..... 5.81

5.22 Comparison of measured and predicted steady-state exit solute fluxes for column tests on Bentomat GCL (L = 1.0 cm): (a) Column tests 1, 2, and 3 (C_o = 0.0087 M); and (b) Column tests 3 and 4 (i_h = 703)..... 5.82

LIST OF SYMBOLS

a = subscript denoting salt anion
A = cross-sectional area [L^2]
c = subscript denoting salt cation
C = molar solute concentration [$mol \cdot L^{-3}$]
C_o = source solute concentration [$mol \cdot L^{-3}$]
D^* = effective diffusion coefficient [L^2t^{-1}]
D_{sj} = salt-diffusion coefficient of solute j in free solution [L^2t^{-1}]
D^*_{sj} = effective salt-diffusion coefficient of solute j [L^2t^{-1}]
D^*_s = effective diffusion coefficient for salt [L^2t^{-1}]
D^*_ω = coupled effective salt-diffusion coefficient [L^2t^{-1}]
D_{so} = diffusion coefficient for salt in free solution [L^2t^{-1}]
D_{oj} = self-diffusion coefficient of solute j in free solution [L^2t^{-1}]
$\mathcal{F}$ = Faraday's constant [96,500 coulombs/equivalent]
h = hydraulic head [L]
i_h = hydraulic gradient [dimensionless]
i_π = chemico-osmotic gradient [dimensionless]
I = electrical current [$Coulomb \cdot L^{-2}t^{-1}$]
J = total solute flux [$mol \cdot L^{-2}t^{-1}$]
J_d = diffusive solute flux [$mol \cdot L^{-2}t^{-1}$]
J^a_j = advective flux of solute j [$mol \cdot L^{-2}t^{-1}$]
J^d_i = diffusive flux of solute i [$mol \cdot L^{-2}t^{-1}$]
k_e = electro-osmotic conductivity [$L^2t^{-1}Volt^{-1}$]
k_h = hydraulic conductivity [Lt^{-1}]
K_d = distribution coefficient [L^3M^{-1}]
L = soil barrier thickness [L]
L_{ij} = phenomenological coefficient
n = total soil porosity [dimensionless]
P = hydraulic (or liquid) pressure [$ML^{-1}t^{-2}$]
P_L = Peclet number [dimensionless]
q = total hydraulic liquid flux [Lt^{-1}]
q_h = hydraulic liquid flux [Lt^{-1}]
q_π = chemico-osmotic liquid flux [Lt^{-1}]
Q_j = total moles (aqueous and adsorbed phase) of solute j [$mol \cdot L^{-3}$]
Q_t = cumulative solute mass per unit cross-sectional area [ML^{-2}]
R = universal gas constant [8.314 J/mol·K]
R_d = retardation factor [dimensionless]
s = subscript denoting "salt"
ss = subscript denoting "steady state"

Symbols (cont.)

T = absolute temperature [T] or solute transit time [t]
T_L = time lag [t]
u = ionic mobility [$L^2t^{-1}Volt^{-1}$]
v_h = hydraulic seepage velocity [Lt^{-1}]
v_π = chemico-osmotic seepage velocity [Lt^{-1}]
V = volume [L^3]
w_A = atomic weight of solute [$M \cdot mol^{-1}$]
x = generic distance [L] or subscript denoting exchangeable cation
z = ion valence [dimensionless]

γ_w = unit weight of water [$Mt^{-2}L^{-2}$]
μ_i^c = chemical potential of solute i [$ML^2mol^{-1}t^{-2}$]
ν = number of ions per molecule of salt
π = chemico-osmotic pressure [$ML^{-2}t^{-2}$]
ρ_d = soil dry (bulk) density [ML^{-3}]
σ_e^* = effective electrical conductivity of the porous medium [$Coulomb \cdot t^{-1}L^{-1}Volt^{-1}$]
τ_a = apparent tortuosity factor [dimensionless]
τ_m = matrix tortuosity factor [dimensionless]
τ_r = restrictive tortuosity factor [dimensionless]
Ψ = electrical potential [Volt]
ω = chemico-osmotic efficiency coefficient [dimensionless]

CHAPTER 1

INTRODUCTION

1.1 BACKGROUND

The migration of solutes in fine-grained soils of low hydraulic conductivity has become an important consideration with respect to the design and performance of waste containment barriers that consist of these soils (e.g., liners, cutoff walls). Solute transport analyses for engineered barrier materials, such as compacted clay soils and geosynthetic clay liners (GCLs), typically are performed using solutions to the advective-dispersive equation (e.g., Shackelford 1988, Shackelford 1990). In these analyses, the advective term for solute flux in response to a hydraulic gradient is based on Darcy's law, and solute diffusion is described by Fick's first law for diffusive flux in response to a concentration gradient. Mechanical dispersion commonly is assumed to be negligible relative to diffusion for the low-flow conditions and the short distances of transport typically associated with waste containment barriers (Shackelford 1988, Mitchell 1993).

However, advective-dispersive transport theory represents a limiting case of the more general coupled flux transport theory that accounts for simultaneous fluxes of liquid, current, and ions through soil in response to hydraulic, electrical, and chemical gradients, respectively (e.g., Yeung 1990, Shackelford 1996). While the advective-dispersive approach is considered acceptable in the case of the relatively high flow rates commonly associated with contaminant transport through coarse-grained soils (e.g., aquifers), the use of advective-dispersive transport theory for clay barrier materials may not be appropriate.

In particular, the ability of fine-grained (i.e., clay) soils to act as semi-permeable membranes that inhibit the passage of solutes relative to liquid (i.e., water) is well documented (McKelvey and Milne 1962, Kemper and Rollins 1966, Olsen 1969, Marine and Fritz 1981, and Olsen et al. 1990). Restricted passage of charged solutes (ions) through the pores of a clay soil is attributed to electrostatic repulsion of the ions by electric fields associated with the diffuse double layers of adjacent clay particles (e.g., Marine and Fritz 1981, Fritz and Marine 1983, Fritz 1986, Keijzer et al. 1997). Non-electrolyte solutes (uncharged species), such as aqueous miscible organic compounds, also may be restricted from migrating through clay soils when the size of the molecule is greater than pore size of the clay soil (Grathwohl 1998).

Membrane behavior in clay soils results in chemico-osmosis, or the movement of liquid in response to a solute concentration gradient, as well as restricted diffusive flux of ions. Both of these processes are described by coupled flux theory (e.g., Katchalsky and Curran 1965, Greenberg et al. 1973, Yeung 1990, and Yeung and Mitchell 1993). Chemico-osmosis resulting from membrane behavior in clays has been shown to (1) influence volume change behavior (Mitchell et al. 1973, Barbour 1986, Barbour and Fredlund 1989), (2) cause apparent deviations from Darcy's law in laboratory hydraulic conductivity testing (Olsen 1985), (3) result in anomalous pore-fluid pressures in low-permeability geologic formations (Neuzil 2000), and (4) affect the rate of solute migration through aquitards (Greenberg et al. 1973).

The extent to which a clay soil acts as a membrane in the presence of a concentration gradient is termed chemico-osmotic efficiency and often is expressed quantitatively in terms of a chemico-osmotic efficiency coefficient, ω, or reflection coefficient, σ (e.g., Staverman 1952, Kemper and Rollins 1966, Olsen et al. 1990, Keijzer et al. 1997). The theoretical chemico-osmotic efficiency coefficient of an "ideal" membrane that completely restricts the movement of solutes is unity (i.e., $\omega = 1$), whereas $\omega = 0$ for a material that exhibits no solute restriction (e.g., Mitchell 1993). In most

cases, the pores in clay soils that exhibit membrane behavior vary over a range of sizes such that not all of the pores are restrictive. In such cases, ω typically falls within the range $0 < \omega < 1$. Thus, clay soils are referred to as "non-ideal" membranes (Kemper and Rollins 1966, Olsen 1969, Bresler 1973, Barbour 1986, Barbour and Fredlund 1989, Mitchell 1993, and Keijzer et al. 1997). The sizes of the pores in a clay soil and, therefore, the value of ω, are affected by several factors, including the state of stress on the soil, the types and amounts of clay minerals in the soil, and the types and concentrations of the solutes (Kemper and Rollins 1966, Bresler 1973, Olsen et al. 1990, Mitchell 1993).

The ability of sodium bentonite, in particular, to exhibit membrane behavior in the presence of common electrolytes (e.g., NaCl) has been illustrated extensively (e.g., Kemper and Rollins 1966, Kemper and Quirk 1972, Elrick et al. 1976, Fritz and Marine 1983, Keijzer et al. 1997). For example, Kemper and Rollins (1966) measured the chemico-osmotic membrane efficiency of compacted sodium bentonite pastes in the presence of NaCl and $CaCl_2$ solutions over a range of concentrations, and reported that the bentonite pastes exhibit membrane behavior that varies as a function of the soil porosity, electrolyte concentration, and ion valence.

Elrick et al. (1976) also studied membrane behavior in saturated bentonite pastes exposed to NaCl solutions and concluded that the rate of salt migration is reduced due to the permi-selective properties of the bentonite. More recently, Sawatsky et al. (1997) attributed a reduced diffusive solute flux of naphthalene, an aqueous miscible organic compound (non-electrolyte), through a montmorillonite-based shale to exclusion of the naphthalene from the pore space. Sawatsky et al. (1997) conclude that the observed membrane behavior will act to enhance the ability of the clay to limit contaminant flux. Similar solute exclusion effects for a variety of inorganic solutes have been reported in studies on compacted sodium bentonites (e.g., Murrinen 1990, Oscarson et al. 1992, Oscarson 1994, Oscarson and Hume 1994).

1.2 OBJECTIVES OF RESEARCH

Although the results of the aforementioned studies indicate that bentonite-rich soils may exhibit membrane behavior, and that this behavior can affect solute transport, no such correlation between membrane behavior and solute transport has been shown experimentally. In addition, since the application of advective-dispersive transport theory represents a limiting case in which the potential influence of membrane behavior is ignored, a direct comparison of solute transport based on advective-dispersive theory versus coupled solute transport theory that accounts for membrane behavior is needed. Such an evaluation may be important in waste containment applications, since bentonite-rich soils are desirable for use in engineered liners for landfills, surface impoundments, and waste piles (Oscarson et al. 1992, Gleason et al. 1997).

In particular, geosynthetic clay liners (GCLs) commonly are used either individually or as components of engineered waste containment liners and cover systems. Geosynthetic clay liners are factory-manufactured rolls consisting of thin layers (~ 5 to 10 mm) of bentonite clay (~ 5.0 kg/m^2) sandwiched between two geotextiles or bonded to a geomembrane. The preferential use of GCLs in containment applications relative to other alternatives, such as compacted clay liners, stems primarily from economic considerations and the extremely low hydraulic conductivities to water ($\leq 5 \times 10^{-11}$ m/s) typically measured for these materials (Daniel 1993, Koerner 1994). Except in the case of a GCL that contains a geomembrane, hydraulic and contaminant transport performance is governed by the bentonite component of a GCL. The relatively high bentonite content and low hydraulic conductivities typically associated with GCLs suggest that GCLs should exhibit membrane behavior. However, no such membrane behavior has been reported for GCLs. The existence of membrane behavior in GCLs may be important for evaluating the hydraulic and contaminant transport performance of GCLs used in waste containment applications.

Thus, the goal of this research is to evaluate the ability of a GCL to act as a semi-permeable membrane that restricts migration of solutes, and to evaluate the potential influence of this behavior on solute transport through the GCL. This goal will be accomplished by the following objectives: (1) to design and evaluate an experimental apparatus and testing procedure for measuring chemico-osmotic efficiency in clay soils; (2) to demonstrate experimentally the membrane properties of a GCL containing sodium bentonite; (3) to evaluate the influence of membrane behavior on solute diffusion through the GCL; (4) to develop a coupled solute transport model for transient solute migration through reactive (i.e., ion exchanging) clay membrane barriers; and (5) to demonstrate the validity of the coupled solute transport model versus traditional advective-dispersive transport theory for describing solute migration through a GCL.

The objectives listed above are accomplished by performing the following tasks:

(1) To develop a new laboratory apparatus and procedures for measuring the chemico-osmotic efficiency of clay soils in the presence of electrolyte solutions;

(2) To illustrate the performance of the testing apparatus for measuring simultaneously the chemico-osmotic efficiency coefficient (ω), the effective diffusion coefficient (D^*), and retardation factor (R_d) for a given soil and solute;

(3) To measure chemico-osmotic efficiency coefficients (ω) and solute transport parameters (D^* and R_d) for a GCL containing sodium bentonite subjected to potassium chloride (KCl) solutions;

(4) To evaluate the potential effects of porosity and solute concentration on the measured chemico-osmotic efficiency of the GCL;

(5) To discuss the potential significance of chemico-osmotic efficiency on liquid flow through the GCL;

(6) To evaluate the influence of membrane coupling (i.e., salt sieving) on the measured effective diffusion coefficients (D^*) for the GCL;

(7) To investigate the correlation between the measured D^* values for KCl at steady state and the measured chemico-osmotic efficiency coefficients (ω) for the GCL;

(8) To illustrate the potential significance of membrane behavior on solute diffusion through soil barriers in waste containment applications;

(9) To develop a coupled solute transport model that simulates transient, one-dimensional solute transport through reactive (i.e., ion exchanging) soil membranes;

(10) To perform a theoretical analysis using the coupled transport model and traditional advective-dispersive transport theory that illustrates the differences between the two theories and evaluates the factors affecting coupled solute transport in soil membranes; and

(11) To demonstrate the validity of the coupled transport theory versus advective-dispersive theory to model solute transport in soil membranes by comparing the two theories with experimental data obtained from column tests on the GCL.

1.3 REFERENCES

Barbour, S. L. (1986). "Osmotic flow and volume change in clay soils." *Ph.D. Dissertation*, University of Saskatchewan, Saskatoon, 255 p.

Barbour, S. L. and Fredlund, D. G. (1989). "Mechanisms of osmotic flow and volume change in clay soils." *Canadian Geotechnical Journal*, 26, 551-562.

Bresler, E. (1973). "Simultaneous transport of solutes and water under transient unsaturated flow conditions." *Water Resources Research*, 9(4), 975-986.

Daniel, D. E. (1993). "Clay liners." Chapter 7, *Geotechnical Practice for Waste Disposal*, D.E. Daniel, ed., Chapman and Hall, New York, 137-163.

Elrick, D. E., Smiles, D. E., Baumgartner, N., and Groenevelt, P. H. (1976). "Coupling phenomena in saturated homo-ionic montmorillonite: I. Experimental." *Soil Science Society of America Journal*, 40(4), 490-491.

Fritz, S. J. (1986). "Ideality of clay membranes in osmotic processes: A review." *Clays and Clay Minerals*, 34(2), 214-223.

Fritz, S. J., and Marine, I. W. (1983). "Experimental support for a predictive osmotic model of clay membranes." *Geochimica et Cosmochimica Acta*, 47, 1515-1522.

Gleason, M. H., Daniel, D. E., and Eykholt, G. R. (1997). "Calcium and sodium bentonite for hydraulic containment applications." *Journal of Geotechnical and Geoenvironmental Engineering*, ASCE, 123(5), 438-445.

Grathwohl, P. (1998). *Diffusion in Natural Porous Media, Contaminant Transport, Sortpion/Desorption and Dissolution Kinetics*. Kluwer Acadaemic Publ., Norwell, Massachusetts, 207 p.

Greenberg, J. A., Mitchell, J. K., and Witherspoon, P. A. (1973). "Coupled salt and water flows in a groundwater basin." *Journal of Geophysical Research*, 78(27), 6341-6353.

Katchalsky, A., and Curran, P. F. (1965). *Nonequilibrium Thermodynamics in Biophysics*. Harvard University Press, Cambridge, MA, 248 p.

Keijzer, Th. J. S., Kleingeld, P. J., and Loch, J. P .G. (1997). "Chemical osmosis in Compacted clayey material and the prediction of water transport." *Geoenvironmental Engineering, Contaminated Ground: Fate of Pollutants and Remediation*, R. N. Yong and H. R. Thomas, eds., Thomas Telford Publ., London, 199-204.

Kemper, W. D. and Quirk, J. P. (1972). "Ion mobilities and electric charge of external clay surfaces inferred from potential differences and osmotic flow." *Soil Science Society of America Proceedings*, 36, 426-433.

Kemper, W. D. and Rollins, J. B. (1966). "Osmotic efficiency coefficients across compacted clays." *Soil Science Society of America Proceedings*, 30, 529-534.

Koerner, R. M. (1994). *Designing with Geosynthetics*, 3rd Ed., Prentice-Hall, Englewood Cliffs, N. J., 783 p.

Marine, I. W., and Fritz, S. J. (1981). "Osmotic model to explain anomalous hydraulic heads." *Water Resources Research*, 17(1), 73-82.

McKelvey, J. G. and Milne, I. H. (1962). "The flow of salt solutions through compacted clay." *Clays and Clay Minerals*, 9. 248-259.

Mitchell, J. K. (1993). *Fundamentals of Soil Behavior*, 2nd Ed. John Wiley and Sons, New York, 437 p.

Mitchell, J. K., Greenberg, J. A., and Witherspoon, P. A. (1973). "Chemico-osmotic effects in fine-grained soils." *Journal of the Soil Mechanics and Foundations Division*, ASCE, 99(SM4), 307-322.

Muurinen, A. (1990). "Diffusion of uranium in compacted sodium bentonite." *Engineering Geology*, 28, 359-367.

Neuzil, C. E. (2000). "Osmotic generation of 'anomalous' fluid pressures in geological environments." *Nature*, 403(6766), 182-184.

Olsen, H. W. (1969). "Simultaneous fluxes of liquid and charge in saturated kaolinite." *Soil Science Society of America Proceedings*, 33, 338-344.

Olsen, H. W. (1985). "Osmosis: A cause of apparent deviations from Darcy's law." *Canadian Geotechnical Journal*, 22, 238-241

Olsen, H. W., Yearsley, E. N., and Nelson, K. R. (1990). "Chemico-osmosis versus diffusion-osmosis." *Transportation Research Record No. 1288*, Transportation Research Board, Washington D.C., 15-22.

Oscarson, D. W. (1994). Surface diffusion: is it an important transport mechanism in compacted clays?" *Clays and Clay Minerals*, 42, 534-543.

Oscarson, D. W. and Hume, H. B. (1994). "Diffusion of ^{14}C in dense saturated bentonite under steady-state conditions." *Transport in Porous Media*, 14, 73-84.

Oscarson, D. W., Hume, H. B., Sawatsky, N. G., and Cheung, S. C. H. (1992). "Diffusion of iodide in compacted bentonite." *Soil Science Society of America Journal*, Vol. 56(5), 1400-1406.

Sawatsky, N. Feng, Y., and Dudas, M. J. (1997). "Diffusion of 1-naphthol and naphthalene through clay materials: Measurement of apparent exclusion of solute from the pore space." *Journal of Contaminant Hydrology*, 27(1-2), 25-41.

Shackelford, C.D. (1988). "Diffusion as a transport process in fine-grained barrier materials." *Geotechnical News*, 6(2), 24-27.

Shackelford, C.D. (1990). "Transit time design of earthen barriers." *Engineering Geology*, 29, 79-94.

Staverman, A. J. (1952). "Non-equilibrium thermodynamics of membrane processes." Transactions of the Faraday Society, 48(2), 176-185.

Yeung, A. T. (1990). "Coupled flow equations for water, electricity and ionic contaminants through clayey soils under hydraulic, electrical, and chemical gradients." *Journal of Non-Equilibrium Thermodynamics*, 15, 247-267.

Yeung, A. T. and Mitchell, J. K. (1993). "Coupled fluid, electrical, and chemical flows in soil." *Geotechnique*, 43(1), 121-134.

CHAPTER 2

A LABORATORY APPARATUS TO MEASURE CHEMICO-OSMOTIC EFFICIENCY COEFFICIENTS FOR CLAY SOILS

ABSTRACT: A laboratory apparatus for measuring the chemico-osmotic efficiency coefficient, ω, for clay soils in the presence of electrolyte solutions is described. A chemico-osmotic experiment is conducted by establishing and maintaining a constant difference in electrolyte concentration across a soil specimen while preventing the flow of solution through the specimen. The chemico-osmotic efficiency coefficient is derived from a measured pressure difference induced across the specimen in response to the applied concentration difference. The effective diffusion coefficient (D^*) and retardation factor (R_d) of the electrolytes (solutes) also can be determined simultaneously by measuring the diffusive solute mass flux through the specimen until steady-state diffusion is achieved. Experimental results using specimens of a geosynthetic clay liner subjected to potassium chloride solutions indicate that the measurement of ω may be affected by soil-electrolyte interactions as well as by changes in the induced chemico-osmotic pressure difference due to solute diffusion. As a result, ω should be evaluated using the induced pressure difference at steady state. The time required to achieve a steady-state response in induced pressure difference is related to the time required to achieve steady net diffusion of total ions (i.e., anions plus cations) into the lower concentration boundary, and may be affected by the circulation rate at the specimen boundaries. The circulation rate should be sufficiently rapid to minimize changes in the boundary concentrations due to diffusion, but sufficiently slow to allow measurement of solute mass flux at the lower concentration boundary for evaluating D^* and R_d.

KEY WORDS: chemico-osmosis, chemico-osmotic pressure, chemico-osmotic efficiency coefficient, coupled phenomena, diffusion testing, effective diffusion coefficient, geosynthetic clay liners, reflection coefficient, retardation factor

2.1 INTRODUCTION

The ability of fine-grained (i.e., clay) soils to act as semi-permeable membranes that inhibit the passage of electrolytes, and thereby cause chemico-osmotic flow, has been recognized as a possible cause of anomalous *in situ* pore-pressure measurements and groundwater movement (Marine and Fritz 1981, Olsen et al. 1990). The degree to which a clay soil inhibits the entry of ions into the pore space is termed chemico-osmotic efficiency and often is expressed quantitatively in terms of a chemico-osmotic efficiency coefficient, ω, or reflection coefficient, σ (e.g., see Staverman 1951, Kemper and Rollins 1966, Olsen et al. 1990, Keijzer et al. 1999). The theoretical chemico-osmotic efficiency coefficient of an "ideal" membrane that completely restricts the movement of electrolytes is unity (i.e., $\omega = 1$), whereas $\omega = 0$ for a material that exhibits no electrolyte restriction (e.g., Mitchell 1993). Clay soils are considered "non-ideal" membranes, since ω typically falls within the range $0 < \omega < 1$ (Kemper and Rollins 1966, Olsen 1969, Fritz and Marine 1983). The value of ω for a given clay soil is influenced by several factors, including the types and amounts of clay minerals in the soil, the sizes of pores, and the types and concentrations of electrolytes (Kemper and Rollins 1966, Bresler 1973, Olsen et al. 1990, Mitchell 1993).

The influence of chemico-osmotic efficiency on liquid migration in porous media typically is described using general coupled flux theory based on principles of irreversible thermodynamics applied to charged membranes (e.g., Katchalsky and Curran 1965, Olsen 1972, Yeung 1990, Mitchell 1993). At steady state, the horizontal, one-dimensional flux of an electrolyte solution through a charged membrane under isothermal conditions with

no applied electrical current (i.e., I = 0) may be written as the sum of the Darcy flux, q_h, and a chemico-osmotic flux, q_π, as follows (Kemper and Rollins 1966, Barbour 1986):

$$q = q_h + q_\pi = -\frac{k_h}{\gamma_w}\frac{\Delta P}{\Delta x} + \omega\frac{k_h}{\gamma_w}\frac{\Delta \pi}{\Delta x} \tag{2.1}$$

where q is the total liquid flux, k_h is hydraulic conductivity, γ_w is the unit weight of water, P is liquid pressure, x is the direction of transport, and π is chemico-osmotic pressure. The chemico-osmotic pressure difference, $\Delta\pi$, represents the theoretical pressure difference across an "ideal" semi-permeable membrane (i.e., $\omega = 1$) that is required to prevent chemico-osmotic flux (e.g., see Olsen et al. 1990). Values of $\Delta\pi$ across a membrane separating ideal, dilute solutions containing N solutes of different concentration can be computed using the van't Hoff expression (Barbour and Fredlund 1989), or

$$\Delta\pi = RT\sum_{i=1}^{N}\Delta C_i \tag{2.2}$$

where R is the universal gas constant [8.314 $J \cdot mol^{-1}K^{-1}$], T is the absolute temperature [K], ΔC_i represents the concentration difference of solute i across the membrane [$mol \cdot L^{-3}$], and N is the total number of solute species. The van't Hoff expression is based on the limiting assumption that the electrolyte solutions are ideal and dilute and, therefore, provides only approximate values of the chemico-osmotic pressure difference. However, Fritz (1986) notes that the error associated with the van't Hoff expression does not exceed 5 percent for 1:1 electrolytes (e.g., NaCl, KCl) for concentrations ≤ 1.0 M.

An evaluation of the potential effect of chemico-osmotic flux, q_π, on liquid and solute migration through low-k_h clay soils with $\omega > 0$ based on Eq. 2.1 will require the measurement of the chemico-osmotic efficiency coefficient, ω. Such an evaluation may

be important, for example, with respect to the design and performance of low-k_h clay soils commonly used for waste containment. Thus, the purpose of this paper is to describe a new testing apparatus to measure chemico-osmotic efficiency of clay soils in the presence of electrolyte solutions.

2.2 BACKGROUND

Values of ω for clay soils have been measured in the laboratory using different methods. For example, Kemper and Rollins (1966) measured ω for sodium bentonite pastes with respect to different salts by conducting a two-staged test in which chemico-osmotic flux, q_π, and Darcy flux, q_h, were measured separately for a single test specimen. In the first stage, q_π was evaluated by placing a soil specimen into a testing cell located between two reservoirs containing solutions with different electrolyte concentrations (i.e., $\Delta\pi > 0$) under equal hydraulic pressure (i.e., $\Delta P = 0$). For these conditions, $q_h = 0$ such that, from Eq. 1,

$$q\big|_{\Delta P=0} = q_\pi = \omega \frac{k_h}{\gamma_w} \frac{\Delta\pi}{\Delta x} \tag{2.3}$$

The chemico-osmotic flux, q_π, was measured by monitoring the change in height of the solutions in standpipes connected to the reservoirs.

In the second stage, q_h was evaluated by permeating the same soil specimen with a solution containing equal parts of the solutions used in the chemico-osmotic stage (i.e., the average solution) under a controlled hydraulic pressure difference (i.e., $-\Delta P > 0$). Since $\Delta\pi = 0$ at steady state under these conditions, $q_\pi = 0$ such that, from Eq. 2.1,

$$q\big|_{\Delta\pi=0} = q_h = -\frac{k_h}{\gamma_w} \frac{\Delta P}{\Delta x} \tag{2.4}$$

The Darcy flux, q_h, was measured by monitoring liquid elevations in the standpipes. The expression used by Kemper and Rollins (1966) to calculate ω based on the results of the two testing stages is obtained by dividing Eq. 2.4 by Eq. 2.3, or

$$\omega = -\frac{q_\pi \Delta P}{q_h \Delta \pi} \tag{2.5}$$

The method proposed by Kemper and Rollins (1966) also was used by Letey et al. (1969) to measure ω of loams from natural deposits, and by Kemper and Quirk (1972) to measure ω of pure clays including illite, kaolinite, and sodium bentonite.

Although the test procedure proposed by Kemper and Rollins (1966) is simple to assemble and perform, two separate testing stages must be conducted to obtain measured values of ω. Also, variations in the applied chemico-osmotic pressure difference, $\Delta\pi$, will occur unless an attempt is made to maintain constant electrolyte concentrations at the specimen boundaries.

Olsen (1969) described a different approach for measuring ω. The apparatus used by Olsen (1969) to measure ω for saturated kaolinite specimens in the presence of NaCl solutions consisted of a confining cylinder with pistons to control the vertical stress on the specimen. The specimen was separated from the pistons with porous ceramic discs that transmit liquid between the clay and the piston channels (Olsen 1969). Solutions of different concentration of NaCl were introduced at the specimen boundaries through the piston channels, and flow through the specimen was superimposed using a syringe pump. Hydraulic head differences across the specimen were measured using a differential pressure transducer.

An example of the experimental results presented by Olsen (1969) is shown in Fig. 2.1 as a plot of head difference, ΔH, across the specimen versus the ratio of the solute concentrations at the bottom and top of the specimen, C_B/C_T. Separate curves are shown in Fig. 2.1 for each applied flow rate (designated as Q/t). The chemico-osmotic

efficiency coefficient, ω, is determined using the results in Fig. 2.1 in accordance with the following relationship (Olsen 1969):

$$\omega = \frac{\Delta H / \log(C_B / C_T)}{RTC_B / \gamma_w} \tag{2.6}$$

where the numerator in Eq. 2.6 represents the slope of the data shown in Fig. 2.1.

The method of Olsen (1969) represents a multi-stage approach to measure ω, since several different values of C_B/C_T must be applied to define the slopes shown in Fig. 2.1. Olsen (1969) indicated that the response time of the system was sufficiently rapid such that individual measurements were obtained within minutes after changing the boundary concentrations. As a result, measurement of ω using the approach of Olsen (1969) probably is more rapid than using the approach of Kemper and Rollins (1966). However, Olsen (1969) also notes that the system probably was not at a true steady state, since the measurement durations were much shorter than the time that would be required for sufficient diffusion of the electrolyte to establish a steady-state concentration distribution within the soil specimen.

The advantages of the testing apparatus and corresponding measurement approach described in this chapter relative to the existing systems include the ability to (1) measure chemico-osmotic efficiency based on the results of a one-stage test, (2) maintain constant boundary electrolyte concentrations and, thus, a constant chemico-osmotic pressure difference, $\Delta\pi$, throughout the testing duration, and (3) measure simultaneously both ω and the effective diffusion coefficient (D^*) and the retardation factor (R_d) of the solutes. The results of laboratory tests on a geosynthetic clay liner (GCL) using potassium chloride (KCl) solutions are presented to illustrate these measurements.

2.3 NEW TESTING APPARATUS AND PROCEDURES

The chemico-osmotic testing apparatus proposed in this study is illustrated schematically in Fig. 2.2 and pictorially in Fig. 2.3. The primary components of the apparatus include a testing cell, a flow-pump system with two stainless steel actuators, stainless steel tubing to control the circulation of electrolyte solutions at the boundaries of the soil specimen, a differential pressure transducer, and bladder accumulators to collect the circulated solutions and refill actuators. Additional details pertaining to these components follows.

2.3.1 Testing Cell

The chemico-osmotic testing cell consists of an acrylic cylinder (7.1-cm diameter), top piston, and base pedestal as shown in Fig. 2.4. The design is similar to that used by Olsen (1969). The top piston is used to control the vertical stress or void ratio of the soil specimen and can be locked in place to prevent soil expansion. The top piston and base pedestal are equipped with ports that enable circulation of separate electrolyte solutions through porous stones at the specimen boundaries to establish and maintain a constant concentration difference across the specimen. Additional ports are installed in the top piston and base pedestal to allow for measurement of differential pressure across the specimen.

2.3.2 Flow-Pump System

The electrolyte solutions are circulated through the porous stones at the ends of the specimen using a flow-pump system consisting of a dual-carriage syringe pump (Model 944, Harvard Apparatus, South Natick, MA) equipped with two custom actuators to provide circulation of separate solutions through the top piston and base pedestal. A schematic of the flow-pump system is shown in Fig. 2.5. The Model 944 syringe pump is the same as that described in Shackelford and Redmond (1994). The pump offers 12 gear

selections and an additional variable speed control to provide linear displacement rates ranging from approximately 2.1 x 10^{-8} to 1.1 x 10^{-3} m/s. The two individual plungers are connected to lead screws from a single pump motor that drives the plungers at the same rate through the actuators, displacing liquid at the selected rate. The plungers can be operated in the same direction (i.e., parallel motion) or in opposite directions (i.e., reciprocal motion).

2.3.3 Flow-Pump Actuators

The actuators (syringes) mounted on the syringe pump consist of an outer housing with an inner bore that contains the plunger, as shown in Fig. 2.5b. Electrolyte solution contained within the annular area around the plunger shaft is forced from the actuator by the plunger barrel, which contains a groove for an O-ring to create a seal between the barrel and the inner wall of the housing. Liquid is forced from the actuators through ports installed in the end-caps that are attached to the ends of the housing with screws as shown in Fig. 2.6a. All actuator parts were constructed with grade 316 stainless steel to minimize corrosion in the presence of strong electrolytes.

The dimensions and manufacturing tolerances of the actuator housing, plunger shaft, and plunger barrel are shown in Fig. 2.6b. The dimensions of the actuator parts were selected based on the size of the Model 944 pump carriage and the range of flow rates desired in this study and, therefore, may not be appropriate for other flow-pump systems or other applications in which a different range of flow rates is required. For example, the measured flow rates for the actuators used in this study ranged from 9.2 x 10^{-12} to 4.7 x 10^{-7} m^3/s. A lower desired range of flow rates requires a smaller bore size in the actuator housing or a larger plunger shaft. However, the manufacturing tolerances (Fig. 2.6b) associated with the diameter of the bore, plunger shaft, and plunger barrel are recommended for this actuator design, regardless of the dimensions, to ensure that a proper seal is maintained with the installed O-rings.

An advantage of this actuator design relative to other designs is the capability of infusing and withdrawing liquid at identical rates (see Olsen et al. 1991). For example, liquid can be expelled at one end of the housing and simultaneously collected at the same rate on the rear side of the plunger barrel through the port in the opposite end-cap. As a result of this capability, the two actuators are used in the chemico-osmotic test as individual circulation loops through the top piston and base pedestal to introduce fresh electrolyte solution continuously at the specimen boundaries, as shown in Fig. 2.7.

Once the plunger barrel reaches the end of the actuator housing, the actuator must be refilled with fresh electrolyte solution by reversing the pump direction and replenishing the actuator from an accumulator. The circulation outflow previously collected inside the actuator housing is purged simultaneously into a separate accumulator for subsequent chemical analysis (e.g., pH, electrical conductivity, and solute concentrations). All tubing used to circulate the solutions and refill the actuators is constructed with grade 316 stainless steel to minimize corrosion and to prevent volume change in the system.

Measured ion concentrations in the purged solutions are used to evaluate the solute flux entering the soil from the higher concentration boundary and exiting the soil into the lower concentration boundary due to diffusion. For example, if we assume in Fig. 2.7 that the solute concentration introduced into the top piston, C_{ot}, is greater than the solute concentration introduced into the base pedestal, C_{ob} (i.e., $C_{ot} > C_{ob}$), the difference in these concentrations represents a driving force for solute diffusion through the soil from the top piston to the base pedestal. As indicated in Fig. 2.7, the diffusive flux results in a lower concentration in circulation outflow from the top piston, C_t (i.e., $C_t < C_{ot}$), and a higher concentration in circulation outflow from the base pedestal, C_b (i.e., $C_b > C_{ob}$) as the solutions pass through the end-caps of the testing cell and back into the actuator housing. The measured concentrations, C_b and C_t, are used to compute the

chemico-osmotic pressure difference across the specimen, $\Delta\pi$, and to evaluate solute transport parameters (D^* and R_d).

2.3.4 Measurement of Chemico-Osmotic Efficiency

In order to measure the chemico-osmotic efficiency coefficient, the solutions are circulated through the specimen boundaries as shown in Fig. 2.7 to maintain a constant concentration difference across the specimen while maintaining a constant volume inside the testing cell (i.e., $\Delta V_{cell} = 0$). Since the volume of solution infused into either end of the testing cell is equal to the volume of solution withdrawn during circulation, no additional flux of solution can enter or exit the specimen boundaries. Therefore, solution flux through the soil cannot occur. This condition is represented mathematically by setting $q = 0$ in Eq. 2.1, or

$$-\frac{k_h}{\gamma_w}\frac{\Delta P}{\Delta x} + \frac{\omega k_h}{\gamma_w}\frac{\Delta \pi}{\Delta x} = 0 \qquad (2.7)$$

Rearrangement of Eq. 2.7 yields the following expression for the chemico-osmotic efficiency coefficient, ω (Katchalsky and Curran 1965, Groenevelt and Elrick 1976, and van Oort et al. 1996):

$$\omega = \left.\frac{\Delta P}{\Delta \pi}\right|_{q=0} \qquad (2.8)$$

The hydraulic pressure difference, ΔP, is induced across the specimen as a result of prohibiting the chemico-osmotic flux of solution that otherwise would occur in response to the applied concentration difference (e.g., see Keijzer et al. 1997). This induced pressure difference is measured with a differential pressure transducer (Model DP15, Validyne Engineering Sales Corp., Northridge, CA). The transducer is used in

conjunction with a demodulator (Model CD223, Validyne Engineering Sales Corp., Northridge, CA) for conversion of the transducer signal into units of pressure. An analog output channel on the demodulator was used to transmit the pressure data continuously to a personal computer equipped with an OMEGA Model 100A DAQ board (OMEGA Engineering Inc., Stamford, CT) and LabVIEW software (National Instruments Corp., Austin, TX, Version IV), as illustrated in Fig. 2.8.

The chemico-osmotic pressure difference, $\Delta\pi$, in Eq. 2.8 can be computed based on the solute concentrations in the opposite specimen boundaries in accordance with the van't Hoff expression (Eq. 2.2). Since $C_t < C_{ot}$ and $C_b > C_{ob}$ due to solute diffusion (see Fig. 2.7), we may define the average boundary concentrations of a solute species i, $\overline{C}_{t,i}$ and $\overline{C}_{b,i}$, as follows:

$$\overline{C}_{t,i} = \frac{C_{ot,i} + C_{t,i}}{2} \tag{9a}$$

$$\overline{C}_{b,i} = \frac{C_{ob,i} + C_{b,i}}{2} \tag{9b}$$

Based on these average concentrations, the average chemico-osmotic pressure difference, $\overline{\Delta\pi}$, can be written as follows in accordance with Eq. 2.2:

$$\overline{\Delta\pi} = RT\sum_{i=1}^{N}\left(\overline{C}_{b,i} - \overline{C}_{t,i}\right) \tag{2.10}$$

In accordance with Eq. 2.10, $\overline{\Delta\pi} < 0$ when $\overline{C}_{t,i} > \overline{C}_{b,i}$.

2.3.5 Measurement of Solute Transport Parameters

The effective diffusion coefficient, D^*, and retardation factor, R_d, for a solute species i is based on solute concentrations measured in the circulation outflow from the

lower concentration boundary (i.e., the base pedestal) during the test in a similar manner to that previously described by Jessberger and Onnich (1994). This approach to measuring D^* and R_d commonly is referred to as the steady state approach (Shackelford 1991).

In the steady-state approach, the measured concentrations for a given solute, C_b, typically are converted to cumulative mass per unit cross-sectional area, Q_t, or

$$Q_t = \frac{1}{A}\sum_{j=1}^{N_t}\Delta m_j = \frac{1}{A}\sum_{j=1}^{N_t}c_{b,j}\Delta V_j \qquad (2.11)$$

where Δm [M] is the incremental mass of the solute collected over a time increment (Δt), C_b [ML^{-3}] is the concentration of the solute in the incremental volume, ΔV [L^3], of circulation outflow from the base pedestal corresponding to the same Δt, and N_t is the number of incremental samples corresponding to the total elapsed time, t. The results are plotted in terms of Q_t versus t, as illustrated in Fig. 2.9. The curved portion of the example plot in Fig. 2.9 represents transient diffusion, while the linear portion of the data in Fig. 2.9 represents steady-state diffusion (Shackelford 1991). The analytical solution for Q_t at steady-state based on one-dimensional diffusion with a constant source concentration, C_{ot}, in the top piston and a perfectly flushing boundary condition in the base pedestal (i.e., $C_{ob} = 0$) is written as follows (Crank 1975, Shackelford 1991):

$$Q_t = \frac{nD^*c_{ot}}{L}t - \frac{nR_dLc_{ot}}{6} \qquad (2.12)$$

where n is the soil porosity [dimensionless], D^* is the effective diffusion coefficient [L^2t^{-1}], L is the specimen thickness [L], and R_d is the retardation factor [dimensionless]. By inspection, Eq. 2.12 represents a straight line through the steady-state data, as shown in Fig. 2.9. Typically, the slope, $\Delta Q_t/\Delta t$, in Fig. 2.9 is determined by best-fit linear

regression of the steady-state data and used to compute the effective diffusion coefficient, D^*, of the given solute species in accordance with Eq. 2.12, or

$$D^* = \left(\frac{\Delta Q_t}{\Delta t}\right)\left(\frac{L}{nc_{ot}}\right) \tag{2.13}$$

The retardation factor of the solute, R_d, is evaluated by determining the time tag, T_L, which represents the intercept of the regressed line through the steady-state data on the t-axis in Fig. 2.9. The intercept, T_L, is related to R_d by setting $Q_t = 0$ in Eq. 2.12 and re-arranging the resulting expression for R_d as follows (Shackelford 1991):

$$R_d = \frac{6D^*}{L^2}T_L \tag{2.14}$$

where D^* is determined previously from Eq. 2.13.

2.4 EXAMPLE RESULTS

Some example results illustrating the performance of the testing apparatus are presented herein based on two tests conducted on separate 0.010-m-thick geosynthetic clay liner (GCL) specimens. A GCL was chosen for testing due to the presence of sodium bentonite, which is expected to exhibit measurable chemico-osmotic efficiency based on previous studies (e.g., Kemper and Rollins 1966). In addition, GCLs commonly are used either individually or as components of waste containment liners and cover systems (Daniel 1993, Koerner 1994). The GCL used in this study is sold commercially under the trade name Bentomat® (Colloid Environmental Technologies Company (CETCO), Lovell, WY). The Bentomat® GCL consists of a layer of granular sodium bentonite between two non-woven polypropylene geotextiles held together by needle-punched fibers. Although the bentonite is regarded as a sodium bentonite, the results of

the exchangeable cation measurements presented in Table 2.1 indicate that an appreciable amount of calcium (Ca^{2+}) also is present on the exchange sites of the bentonite. The procedures associated with measurement of the exchangeable cations shown in Table 2.1 are described in detail by Shackelford and Redmond (1995).

Circular GCL specimens were cut from a larger GCL sheet, placed in the testing cell, and permeated under backpressure with a processed tap water (PTW) to saturate the specimen, remove excess soluble salts, and measure hydraulic conductivity. The PTW was processed by passing tap water through three Barnstead® ion exchange columns in series, resulting in no measurable potassium or chloride, a measured pH of 6.93, and a measured electrical conductivity (EC) of 0.32 mS/m at 25 °C. At the beginning of each test, PTW was circulated at both boundaries of the specimens (i.e., $C_{ot} = C_{ob} = 0$) at a flow rate of 4.2×10^{-10} m^3/s for approximately 4.5 days to establish a steady baseline pressure difference. The chemico-osmotic tests then were initiated by circulating 0.0087 M KCl ($= C_{ot}$) in the top piston in test 1 (L = 0.010 m, n = 0.79) and 0.047 M KCl ($= C_{ot}$) in test 2 (L = 0.010 m, n = 0.78), while maintaining $C_{ob} = 0$ in the base pedestal for both tests.

2.4.1 Chemico-Osmotic Efficiency Coefficient

Although the actual pressure differences, ΔP, induced across the GCL specimens are less than zero due to sign convention, the measured induced pressure differences are plotted as positive values (i.e., $-\Delta P > 0$) in Fig. 2.10. The baseline differential pressure, $-\Delta P_o$, during the first 4.5 days of PTW circulation at both specimen boundaries (i.e., $C_{ot} = C_{ob} = 0$) reached steady values of approximately 2.4 kPa and 4.0 kPa, respectively, in the two tests. Introduction of 0.0087 M KCl into the top piston in test 1 after 4.5 days resulted in an immediate and rapid increase in the pressure difference as shown in Fig. 2.10a, which reached a steady value, $-\Delta P_{ss}$, of 22.2 kPa. Introduction of 0.047 M KCl

into the top piston in test 2 after 4.5 days resulted in a steady value, $-\Delta P_{ss}$, of 32.0 kPa, as shown in Fig. 2.10b.

The non-zero baseline differential pressure measured while $C_{ot} = C_{ob} = 0$ in the two tests is similar to that observed by Olsen (1969) as indicated in Fig. 1 (i.e., $\Delta H > 0$ for $C_B/C_T = 1$ and $Q/t = 0$), and discussed by Olsen (1985) and Olsen et al. (1985). Possible reasons for this non-zero baseline pressure difference include the existence of very small flow rates through the specimen that constitute small deviations from the $q = 0$ condition assumed in the test (e.g., due to slight differences in the dimensions of the actuators), and/or differences in the hydraulic properties of the porous stones at the opposite ends of the specimen. In either case, this non-zero baseline pressure difference should not be included when evaluating chemico-osmotic efficiency. Therefore, evaluation of ω at steady state is based on a corrected $-\Delta P$ (i.e., $-(\Delta P_{ss} - \Delta P_o)$) of 19.7 kPa in test 1 and 28.0 kPa in test 2 (see Fig. 2.10).

The concentrations of K^+ and Cl^- in circulation outflow from the top piston and base pedestal in the two tests are shown in Figs. 2.11 and 2.12, respectively. The results for test 1 (i.e., $C_{ot} = 0.0087$ M KCl) in Fig. 2.11 show that the average concentrations in the top piston and base pedestal at steady state are $\overline{C}_t = 295$ mg/L and $\overline{C}_b = 10.5$ mg/L, respectively, for Cl^-, while $\overline{C}_t = 326$ mg/L and $\overline{C}_b = 11.0$ mg/L for K^+. The results of test 2 (i.e., $C_{ot} = 0.047$ M KCl) in Fig. 2.12 show that the average concentrations in the top piston and base pedestal at steady state are $\overline{C}_t = 1770$ mg/L and $\overline{C}_b = 118$ mg/L, respectively, for Cl^-, while $\overline{C}_t = 1950$ mg/L and $\overline{C}_b = 125$ mg/L for K^+. Based on these average concentrations, values of $\overline{\Delta\pi}$ across the specimens at steady state are 39.9 kPa in test 1 and 201 kPa in test 2 (see Eq. 2.10). The resulting values of ω at steady state are 0.49 (i.e., 19.7 kPa/39.9 kPa) in test 1 and 0.14 (i.e., 28.0 kPa/201 kPa) in test 2. These results are consistent with previous results for bentonite in that ω decreases with increasing average solute concentration across the soil (Kemper and Rollins 1966).

The time required to achieve a steady induced pressure difference response is approximately six days in test 1 (Fig. 2.10a) and 16 days in test 2 (Fig. 2.10b). This time also corresponds essentially to the time required to achieve steady electrical conductivity (EC) in the base pedestal in the two tests, as shown in Fig. 2.13. The steady EC indicates a steady concentration of total ions (i.e., anions plus cations) diffusing into the base pedestal. The correlation between steady differential pressure and steady EC is expected since the chemico-osmotic pressure difference, $\Delta\pi$, that controls the induced pressure difference for a given ω (i.e., $\Delta P = \omega\Delta\pi$) is a function of the difference in total ion concentration across the specimen in accordance with the van't Hoff expression (Eq. 2.2).

Diffusion of the non-reactive species (i.e., Cl^-) represents the contribution of anions to the measured EC values in the base pedestal shown in Fig. 2.13. However, diffusion of the reactive species (i.e., K^+) represents only a portion of the total cation contribution to the EC values in the base pedestal. For example, the results in Figs. 2.11 and 2.12 show that steady K^+ concentrations in the base pedestal are observed much later than steady Cl^- concentrations. Under the assumption that this delayed transport of K^+ is due to ion exchange, the adsorption of K^+ to the bentonite during this transient stage must be accompanied by desorption of the same number of equivalents of exchangeable cations in order to maintain electroneutrality in solution (e.g., see Shackelford et al. 1999). As previously noted in Table 2.1, the dominant exchangeable cations associated with the bentonite of the GCL used in this study are Na^+ and Ca^{2+}. Although K^+ is more likely to exchange with Na^+ relative to Ca^{2+} on the basis of valence (e.g., see Mitchell 1993), the desorption of either Na^+ or Ca^{2+} should result in a similar contribution to the overall EC in the base pedestal since the equivalent ionic conductances of Na^+ and Ca^{2+} are similar (Shackelford et al. 1999).

2.4.2 Effective Diffusion Coefficient, D*

The results of the steady-state method to determine the effective diffusion coefficient, D^*, and the retardation factor, R_d, for test 1 (i.e., C_{ot} = 0.0087 M KCl) are shown in Fig. 2.14. Steady-state diffusion into the base pedestal was observed after 144 hours (6 days) for Cl^- and after 912 hours (38 days) for K^+ based on the concentrations shown in Fig. 2.11. The slopes, $\Delta Q_t/\Delta t$, obtained based on linear regression of the steady-state data are 2.82 x 10^{-6} g/m^2/s for Cl^- and 2.43 x 10^{-6} g/m^2/s for K^+. The resulting D^* values for Cl^- and K^+ are 1.16 x 10^{-10} m^2/s and 0.907 x 10^{-10} m^2/s, respectively. The closeness in the D^* values for Cl^- and K^+ is consistent with the requirement that these D^* values must be the same at steady-state diffusion due to electroneutrality (Shackelford and Daniel 1991). In addition, these values are similar to the steady-state salt (KCl) D^* values reported by Jessberger and Onnich (1994) for sand/gravel/bentonite mixtures containing 14.4 percent sodium bentonite. For example, Jessberger and Onnich (1994) reported salt D^* values for 0.05 M KCl and 0.2 M KCl of 1.23 x 10^{-10} m^2/s and 1.34 x 10^{-10} m^2/s, respectively. However, the measured D^* values in this study do not account for coupling effects that result from the salt-sieving associated with clay membrane behavior (e.g., Groenevelt et al. 1980).

2.4.3 Retardation Factor, R_d

The T_L values for test 1 based on linear regression of the data for Cl^- and K^+ in Fig. 2.14 are 56.6 hr and 466 hr, respectively. Thus, from Eq. 2.12, the measured values of R_d are 1.4 for Cl^- and 9.1 for K^+. Values of R_d for non-reactive (i.e., non-adsorbing) solutes, typically for anions such as chloride (Cl^-) are expected to be unity (i.e., R_d = 1) (e.g., Shackelford 1993). Therefore, the measured value of R_d = 1.05 for Cl^- in Fig. 12a is close to that expected for Cl^-. Conversely, the measured value of R_d = 9.1 for K^+ in Fig. 2.12b is consistent with the behavior of a reactive (i.e., adsorbed) solute in which R_d

> 1. As noted earlier, the adsorption of K^+ transport in this test likely is due to ion exchange with Na^+ and/or Ca^{2+} at the clay particle surfaces.

2.5 DISCUSSION

2.5.1 Soil-Solution Interaction

Membrane behavior in a clay soil is characterized by the restriction of ions from the soil pores. This restriction is caused by electric fields associated with the adsorbed ion layers (i.e., diffuse double layers) surrounding adjacent clay particles that extend into the pore space (Marine and Fritz 1981). The degree of ion restriction and, thus, the chemico-osmotic efficiency of the soil is governed by the thicknesses of these adsorbed layers. For example, the degree of ion restriction is greatest (i.e., $\omega = 1$) when the adsorbed layers of adjacent particles overlap in the pore space, leaving no "free" space for solute transport.

The thickness of the adsorbed ion layer is influenced by pore fluid chemistry factors such as ion concentration, valence, dielectric constant, and temperature (Mitchell 1993). For example, an increase in ion concentration in the pore water causes a decrease in adsorbed layer thickness (Mitchell 1993). Therefore, an increase in solute concentration in the pore water of a soil during a chemico-osmotic test due to solute diffusion could result in a time-dependent decrease in chemico-osmotic efficiency.

In this study, the measured differential pressure, $-\Delta P$ (> 0), shown in Fig. 2.10b for chemico-osmotic test 2 (i.e., C_{ot} = 0.047 M KCl) increases to 40 kPa after approximately three days, but subsequently decreases before reaching a steady value of 32 kPa. The decrease in $-\Delta P$ in this test may be due a time-dependent decrease in chemico-osmotic efficiency of the specimen as the KCl diffuses from the top piston into the base pedestal. Conversely, a time-dependent decrease in ΔP was not observed in test 1 (see Fig. 2.10a), possibly because the solute concentration (i.e., 0.0087 M KCl) was not sufficiently large to cause a significant change in adsorbed layer thickness.

The potential for a time-dependent change in chemico-osmotic efficiency may be reflected indirectly through a change in hydraulic conductivity since an increase in electrolyte concentration also may result in an increase in hydraulic conductivity for relatively highly reactive clay soils, such as the sodium bentonites commonly used in GCLs (e.g., Shackelford et al. 2000). Therefore, the hydraulic conductivity of each GCL specimen was measured both before and after chemico-osmotic testing for comparison.

The results of these hydraulic conductivity measurements are shown in Fig. 2.15 for specimens subjected to C_{ot} = 0.0087 M KCl (test 1) and C_{ot} = 0.047 M KCl (test 2) during the chemico-osmotic tests. The results show that the hydraulic conductivity of the specimen subjected to 0.0087 M KCl during the chemico-osmotic test increased 36 percent from ~ 1.1 x 10^{-11} m/s before chemico-osmotic testing to ~ 1.5 x 10^{-11} m/s after chemico-osmotic testing. However, the hydraulic conductivity of the GCL specimen subjected to 0.047 M KCl during the chemico-osmotic test increased 61 percent from ~ 9.1 x 10^{-12} m/s before testing compared to ~ 1.5 x 10^{-11} m/s after testing. The slightly greater increase in k_h for the specimen subjected to the higher concentration of 0.047 M KCl is consistent with a greater decrease in adsorbed layer thickness during the chemico-osmotic test that also is likely responsible for the time-dependent decrease in -ΔP in Fig. 10b.

2.5.2 Circulation Rate

At t = 0 in a chemico-osmotic test, the initial difference in chemico-osmotic pressure, $\Delta\pi_o$, is computed in accordance with Eq. 2.2 based on the initial concentrations, C_{ot} and C_{ob}, of all solutes in the circulated solutions, or

$$\Delta\pi_o = RT\sum_{i=1}^{N}\left(C_{ob,i} - C_{ot,i}\right) \tag{2.15}$$

represents the maximum possible (absolute) value of $\Delta\pi$ that can be maintained across the specimen. At $t > 0$, the value of $\Delta\pi$ and, thus, the induced ΔP is related to the rate of diffusion relative to the circulation rate of the electrolyte solutions at the specimen boundaries. For example, "perfectly flushing" boundary conditions are applied by imposing a sufficiently rapid circulation rate such that the changes in solute mass at the specimen boundaries due to diffusion are negligible. In this case, $\overline{C}_t = C_{ot}$ and $\overline{C}_b = C_{ob}$, and $\overline{\Delta\pi} = \Delta\pi_o$ throughout the test. Conversely, if no attempt is made to maintain the boundary concentrations, diffusion will result in a decrease in solute mass in the top piston and an increase in solute mass in the base pedestal until $\overline{C}_t = \overline{C}_b$ and $\Delta\pi = 0$ at steady state. Likewise, any induced differential pressure, $-\Delta P$, that is generated during the transient stage of the test also will dissipate to zero at steady state (e.g., see Keijzer et al. 1997).

In this study, the circulation rate at the specimen boundaries was 4.2×10^{-10} m^3/s in both test 1 and test 2. This circulation rate is not sufficient to mimic "perfectly flushing" boundary conditions in either test, since $\overline{C}_t < C_{ot}$ and $\overline{C}_b > C_{ob}$ at steady state in both cases (see Figs. 2.11 and 2.12). However, the transient reduction in $\Delta\pi$ over time is greater in test 1 than in test 2. For example, values of $-\Delta\pi_o$ in test 1 (C_{ot} = 0.0087 M KCl and $C_{ob} = 0$) and test 2 (C_{ot} = 0.047 M KCl and $C_{ob} = 0$) are 43.0 kPa and 234 kPa, respectively. Therefore, at steady state, $-\overline{\Delta\pi}$ in test 1 (39.9 kPa) is 7.2 percent lower than $-\Delta\pi_o$, whereas $-\overline{\Delta\pi}$ (201 kPa) is 14 percent lower than $-\Delta\pi_o$ in test 2. The greater influence of diffusion on $-\overline{\Delta\pi}$ in test 2 is due to the higher concentration gradient and, thus, greater diffusive mass flux relative to test 1. The greater reduction in $\overline{\Delta\pi}$ in test 2 may be responsible, in part, for the increase and subsequent decrease in the transient differential pressure response (Fig. 10b), and the corresponding longer time required to achieve a steady ΔP (16 days) relative to test 1 (6 days).

Use of the initial chemico-osmotic pressure difference, $\Delta\pi_o$, rather than the average chemico-osmotic pressure difference, $\overline{\Delta\pi}$, to evaluate ω is more convenient,

since values of $\Delta\pi_o$ are computed easily based on the initial boundary solute concentrations (Eq. 2.15). Therefore, evaluation of ω based on $\Delta\pi_o$ eliminates the need to measure solute concentrations, C_b and C_t, in the circulation outflow from the base pedestal and top piston. For example, in this study, the values of ω based on $\Delta\pi_o$ rather than $\overline{\Delta\pi}$ are 0.46 (i.e., 19.7 kPa/43.0 kPa) in test 1 and 0.12 (i.e., 28.0 kPa/234 kPa) in test 2. These values of ω are slightly lower than the values of ω based on $\overline{\Delta\pi}$ (0.49 and 0.14, respectively). Nonetheless, the differences in these ω values represent the error associated with ignoring the influence of solute diffusion. This error can be reduced further by increasing the circulation rate to reduce changes in the boundary solute concentrations. A faster circulation rate also could reduce the time required to achieve steady-state conditions. However, a circulation rate that is too rapid will dilute the concentrations of solutes diffusing from the specimen such that the ability to measure solute mass flux into the base pedestal required for determination of D^* and R_d may be prohibited. Therefore, the optimal circulation rate should be sufficiently rapid to minimize changes in the boundary solute concentrations due to diffusion and to allow ω to be determined more conveniently based on $\Delta\pi_o$, but sufficiently slow to allow a measurable accumulation of solute mass into the base pedestal for determining D^* and R_d.

2.6 SUMMARY AND CONCLUSIONS

The design and performance of a testing apparatus to measure chemico-osmotic efficiency coefficients, ω, for clay soils in the presence of electrolytes is described. The testing cell that contains the soil specimen consists of a rigid cylinder, top piston, and base pedestal. The top piston and base pedestal are equipped with ports for measuring pressure differences and for continuous circulation of different electrolyte solutions at the specimen boundaries. Electrolyte circulation is provided under constant-volume conditions using a dual-carriage flow pump system with custom actuators (syringes) that

facilitate infusion and withdrawal of the solutions across opposite specimen boundaries at identical rates, while preventing flux of solution through the soil specimen. Thus, pressure differences are induced across the soil specimen due to the prevention of chemico-osmotic flux of solution through the soil that otherwise would occur as a result the controlled difference in electrolyte concentration. This concentration difference represents a difference in chemico-osmotic pressure across the specimen that can be estimated using the van't Hoff expression. The chemico-osmotic efficiency coefficient, ω, represents the ratio of the induced differential pressure, ΔP, versus the chemico-osmotic pressure difference, $\Delta\pi$.

The concentration difference applied by circulating the different electrolyte solutions at the specimen boundaries also represents a driving force for diffusion from the higher concentration boundary to the lower concentration boundary. Measured electrolyte concentrations in the circulation outflow from the lower concentration boundary can be used to determine the effective diffusion coefficient, D^*, and the retardation factor, R_d, for the solutes based on the steady-state approach.

The results of chemico-osmotic tests conducted on GCL specimens in the presence of KCl solutions indicate that the differential pressure response may be influenced by (1) time-dependent changes in chemico-osmotic efficiency due to changes in soil fabric, and (2) the circulation rate of the electrolyte solutions at the specimen boundaries relative to the rate of solute diffusion through the soil. The induced differential pressure is related directly to the difference in chemico-osmotic pressure, $\Delta\pi$, that is a function of the electrolyte concentrations circulated at the opposite specimen boundaries. Solute diffusion through the soil results in a decrease in electrolyte concentration at the higher concentration boundary and an increase in electrolyte concentration at the lower concentration boundary. The overall effect is a net decrease in $\Delta\pi$ that likely is responsible, in part, for the increase and subsequent decrease in the induced pressure difference across a GCL specimen subjected to 0.047 M KCl. A faster

circulation rate will reduce changes in $\Delta\pi$ due to diffusion, and may reduce the time required to achieve steady-state conditions. However, the circulation rate should be sufficiently slow to allow measurement of solute mass flux at the lower concentration boundary for evaluating the solute transport parameters (D^* and R_d).

2.7 REFERENCES

Barbour, S.L., 1986. Osmotic Flow and Volume Change in Clay Soils. *Ph.D. Dissertation*, University of Saskatchewan, Saskatoon, 255 p.

Barbour, S.L. and Fredlund, D.G., 1989. Mechanisms of Osmotic Flow and Volume Change in Clay Soils. *Canadian Geotechnical Journal*, Vol. 26, 551-562.

Bresler, E., 1973. Simultaneous Transport of Solutes and Water under Transient Unsaturated Flow Conditions. *Water Resources Research*, Vol. 9, No. 4, 975-986.

Crank, J., 1975. *The Mathematics of Diffusion.* 2nd Ed., Clarendon Press, Oxford, 414 p.

Daniel, D.E., 1993. Clay Liners. Chapter 7, *Geotechnical Practice for Waste Disposal*, D.E. Daniel, ed., Chapman and Hall, New York, 137-163.

Fritz, S.J., 1986. Ideality of Clay Membranes in Osmotic Processes: A Review. *Clays and Clay Minerals*, Vol. 34, No. 2, 214-223.

Fritz, S.J., and Marine, I.W., 1983. Experimental Support for a Predictive Osmotic Model of Clay Membranes. *Geochimica et Cosmochimica Acta*, Vol. 47, 1515-1522.

Groenevelt, P.H. and Elrick, D.E., 1976. Coupling Phenomena in Saturated Homo-ionic Montmorillonite: II. Theoretical. *Soil Science Society of America Journal*, Vol. 40, 820-823.

Groenevelt, P. H, Elrick, D. E., and Laryea, K. B., 1980. Coupling Phenomena in Saturated Homo-ionic Montmorillonite: IV. The Dispersion Coefficient. *Soil Science Society of America Journal*, Vol. 44, No. 6, 1168-1173.

Jessberger, H. L. and Onnich, K., 1994. Determination of Pollutant Transport Parameters by Laboratory Testing, *Proceedings, XIIIth ICSMFE*, New Delhi, India, 1547-1552.

Katchalsky, A., and Curran, P.F., 1965. *Nonequilibrium Thermodynamics in Biophysics.* Harvard University Press, Cambridge, MA, 248 p.

Keijzer, Th.J.S., Kleingeld, P.J., and Loch, J.P.G., 1997. Chemical Osmosis in Compacted Clayey Material and the Prediction of Water Transport. *Geoenvironmental Engineering, Contaminated Ground: Fate of Pollutants and Remediation*, R.N. Yong and H.R. Thomas, Eds., University of Wales, Cardiff, U.K., Sept. 6-12, Thomas Telford Publ., London, 199-204.

Kemper, W.D. and Quirk, J.P., 1972. Ion Mobilities and Electric Charge of External Clay Surfaces Inferred from Potential Differences and Osmotic Flow. *Soil Science Society of America Proceedings*, Vol. 36, 426-433.

Kemper, W.D. and Rollins, J.B., 1966. Osmotic Efficiency Coefficients Across Compacted Clays. *Soil Science Society of America Proceedings*, Vol. 30, 529-534.

Koerner, R.M., 1994. *Designing with Geosynthetics*, 3rd Ed., Prentice-Hall, Englewood Cliffs, NJ, 783 p.

Letey, J., Kemper, W.D., and Noonan, L., 1969. The Effect of Osmotic Pressure Gradients on Water Movement in Unsaturated Soil. *Soil Science Society of America Proceedings*, Vol. 33, 15-18.

Marine, I.W., and Fritz, S.J., 1981. Osmotic Model to Explain Anomalous Hydraulic Heads. *Water Resources Research*, Vol. 17, No. 1, 73-82.

Mitchell, J.K., 1993. *Fundamentals of Soil Behavior*, 2nd Ed., John Wiley and Sons, New York, 437 p.

Olsen, H.W., 1969. Simultaneous Fluxes of Liquid and Charge in Saturated Kaolinite. *Soil Science Society of America Proceedings*, Vol. 33, 338-344.

Olsen, H.W., 1972. Liquid Movement Through Kaolinite Under Hydraulic, Electric, and Osmotic Gradients. *American Association of Petroleum Geologists Bulletin*, Vol. 56, No. 10, 2022-2028.

Olsen, H.W., 1985. Osmosis: A Cause of Apparent Deviations from Darcy's Law. *Canadian Geotechnical Journal*, Vol. 22, 238-241.

Olsen, H.W., Nichols, R.W., and Rice, T.L., 1985. Low Gradient Permeability Measurements in a Triaxial System. *Geotechnique*, Vol. 35, No. 2, 145-157.

Olsen, H.W., Yearsley, E.N., and Nelson, K.R., 1990. Chemico-Osmosis Versus Diffusion-Osmosis. *Transportation Research Record No. 1288*, Transportation Research Board, Washington D.C., 15-22.

Olsen, H.W., Gill, J.D., Willden, A.T., and Nelson, K.R., 1991. Innovations in Hydraulic Conductivity Measurements. *Transportation Research Record No. 1309*, Transportation Research Board, Washington D.C., 9-17.

Redmond, P.L. and Shackelford, C.D., 1994. Design and Evaluation of a Flow Pump System for Column Testing. *ASTM Geotechnical Testing Journal*, Vol. 17, No. 3, 269-281.

Shackelford, C.D., 1991. Laboratory Diffusion Testing for Waste Disposal - A Review. *Journal of Contaminant Hydrology*, Vol. 7, No. 3, 177-217.

Shackelford, C. D. and Daniel, D. E., 1991. Diffusion in Saturated Soil: I. Background, *Journal of Geotechnical Engineering*, ASCE, Vol. 117, No. 3, 467-484.

Shackelford, C.D., 1993. Contaminant Transport. Chpater 3, *Geotechnical Practice for Waste Disposal*, D.E. Daniel, ed., Chapman and Hall, London, 33-65.

Shackelford, C.D. and Redmond, P.L., 1995. Solute Breakthrough Curves for Processed Kaolin at Low Flow Rates. *Journal of Geotechnical Engineering*, ASCE, Vol. 121, No. 1, 17-32.

Shackelford, C.D., Malusis, M.A., Majeski, M.J., and Stern, R.T., 1999. Electrical Conductivity Breakthrough Curves. *Journal of Geotechnical and Geoenvironmental Engineering*, ASCE, Vol. 125, No. 4, 260-270.

Shackelford, C.D., Benson, C.H., Katsumi, T., Edil, T.B., and Lin, L., 2000. Evaluating the Hydraulic Conductivity of GCLs Permeated with Non-Standard Liquids. *Geotextiles and Geomembranes*, Elsevier, Amsterdam, Vol. 18, Nos. 2/3, 133-161.

Staverman, A.J., 1951. Non-Equilibrium Thermodynamics of Membrane Processes. *Transactions of the Faraday Society*, Vol. 48, No. 2, 176-185.

Van Oort, E., Hale, A.H., Mody, F.K., and Roy, S., 1996. Transport in Shales and the Design of Improved Water-Based Shale Drilling Fluids. *SPE Drilling and Completion*, Society of Petroleum Engineers, Vol. 11, No. 3, 137-146.

Yeung, A.T., 1990. Coupled Flow Equations for Water, Electricity and Ionic Contaminants through Clayey Soils under Hydraulic, Electrical, and Chemical Gradients. *Journal of Non-Equilibrium Thermodynamics*, Vol. 15, 247-267.

Table 2.1 - Exchangeable cation concentrations for bentonite in Bentomat® GCL

Exchangeable Cation	Concentration (meq/100g dry soil)
K^+	0.8
Na^+	31.0
Ca^{2+}	20.8
Mg^{2+}	6.4

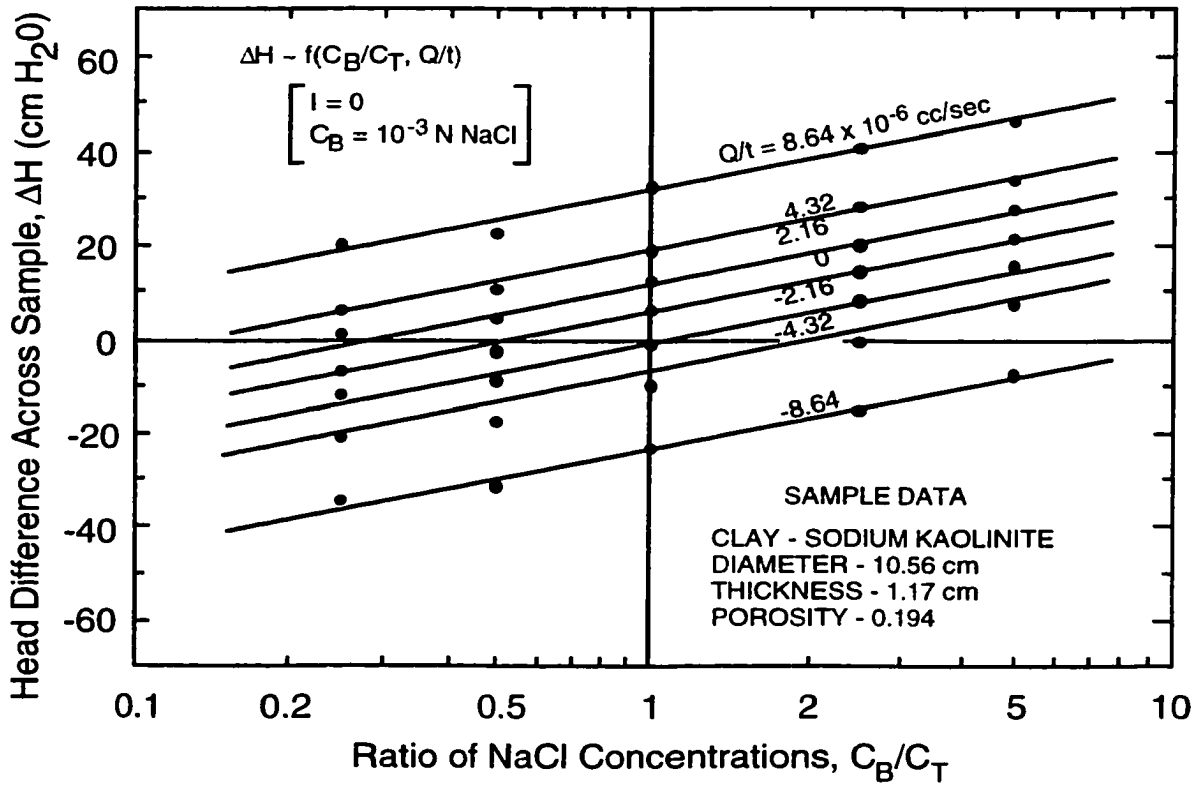

Fig. 2.1 - Measured head differences (ΔH) across a kaolinite specimen as a function of externally imposed flow rates (Q/t) and the ratio of NaCl concentrations at the specimen boundaries (C_B/C_T) (replotted after Olsen 1969).

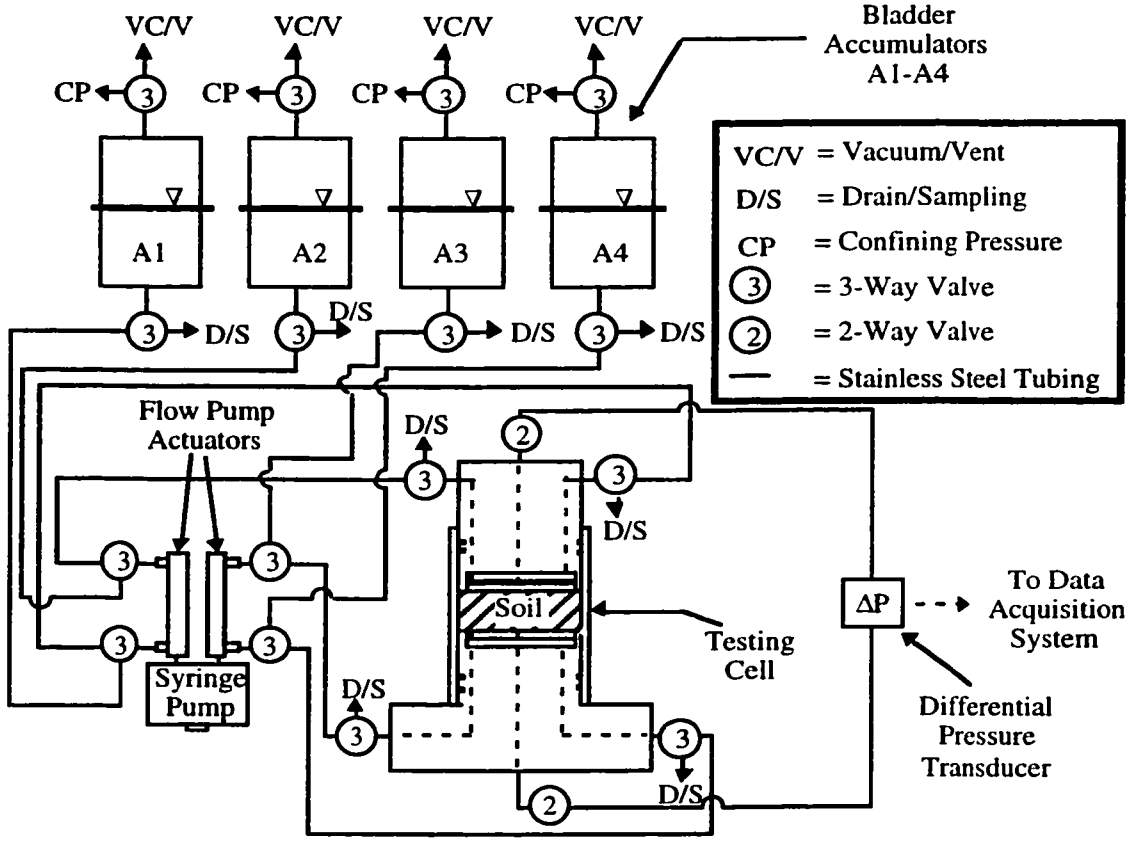

Fig. 2.2 - Schematic of chemico-osmotic testing apparatus.

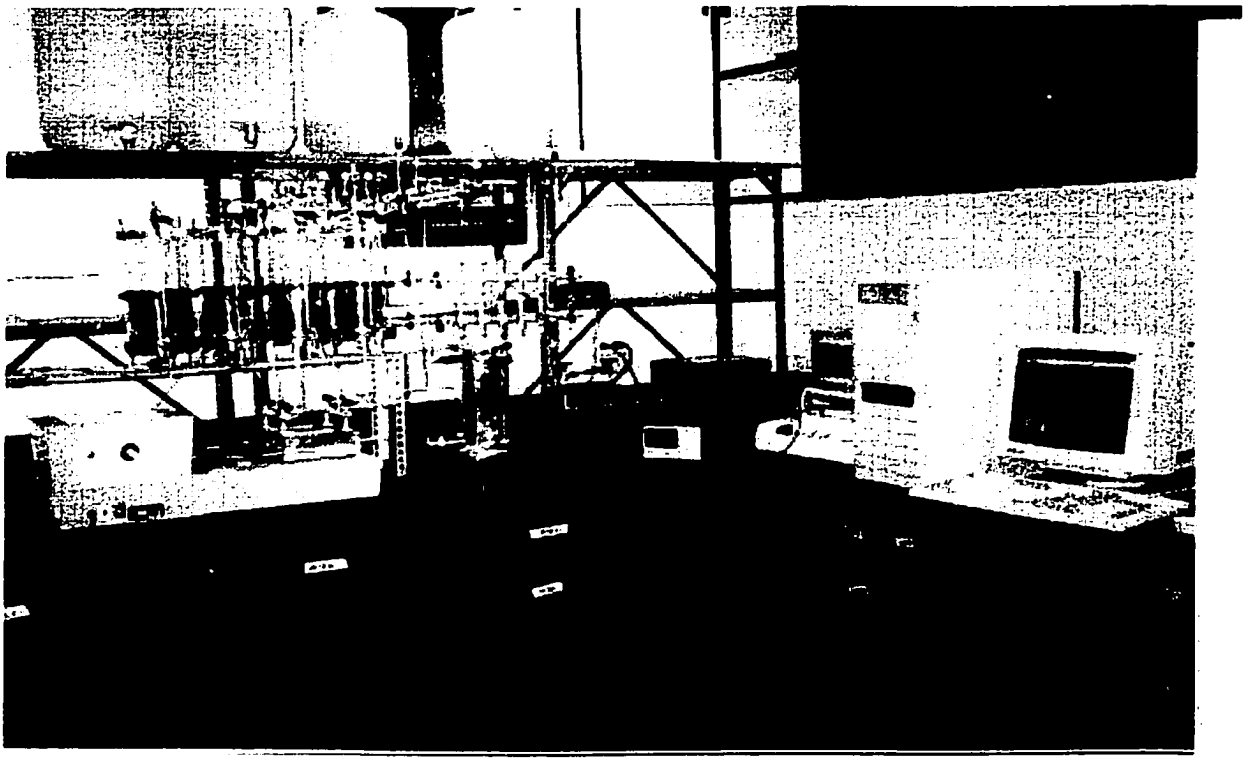

Fig. 2.3 – Pictorial view of chemico-osmotic testing apparatus.

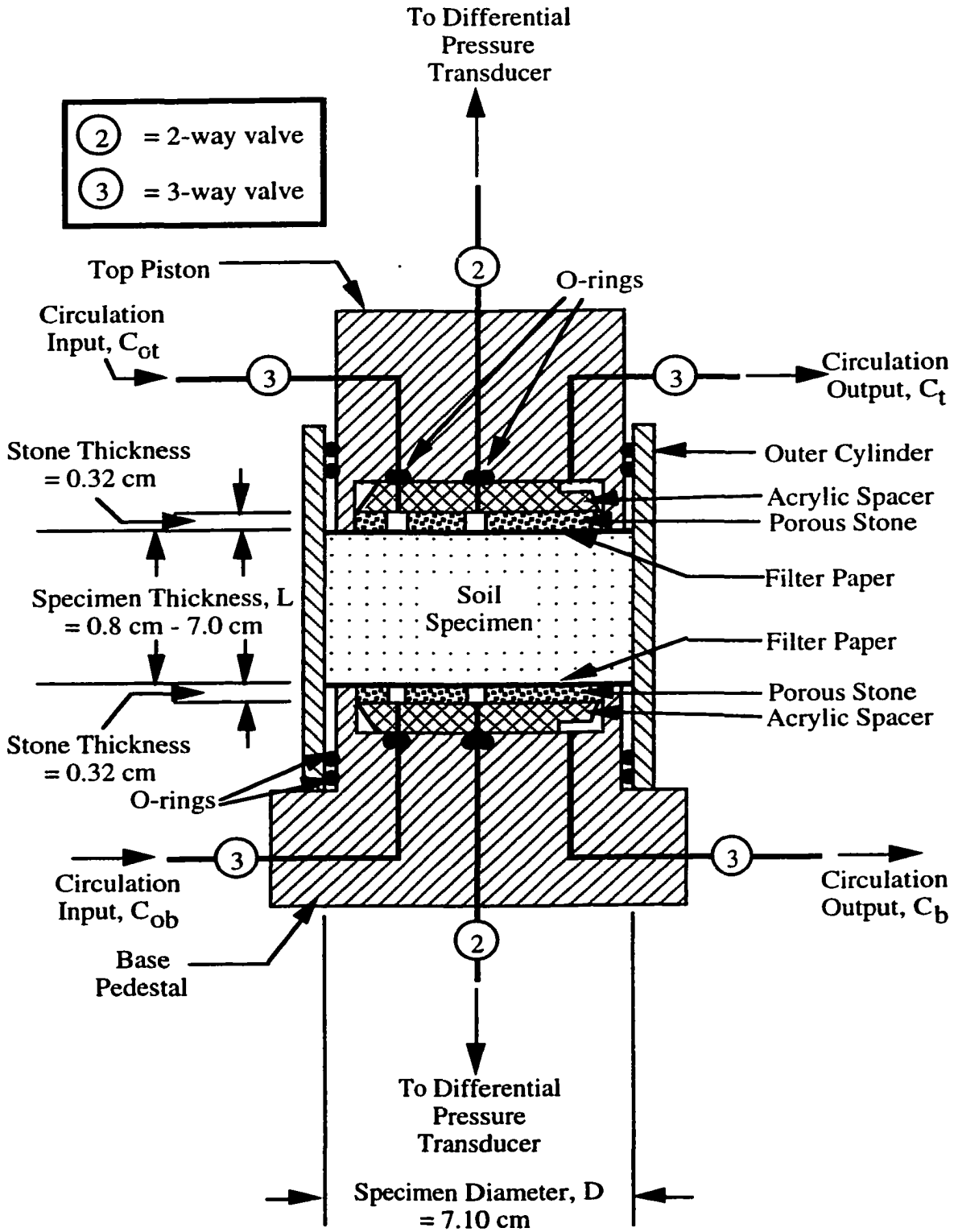

Fig. 2.4 - Schematic of chemico-osmotic testing cell.

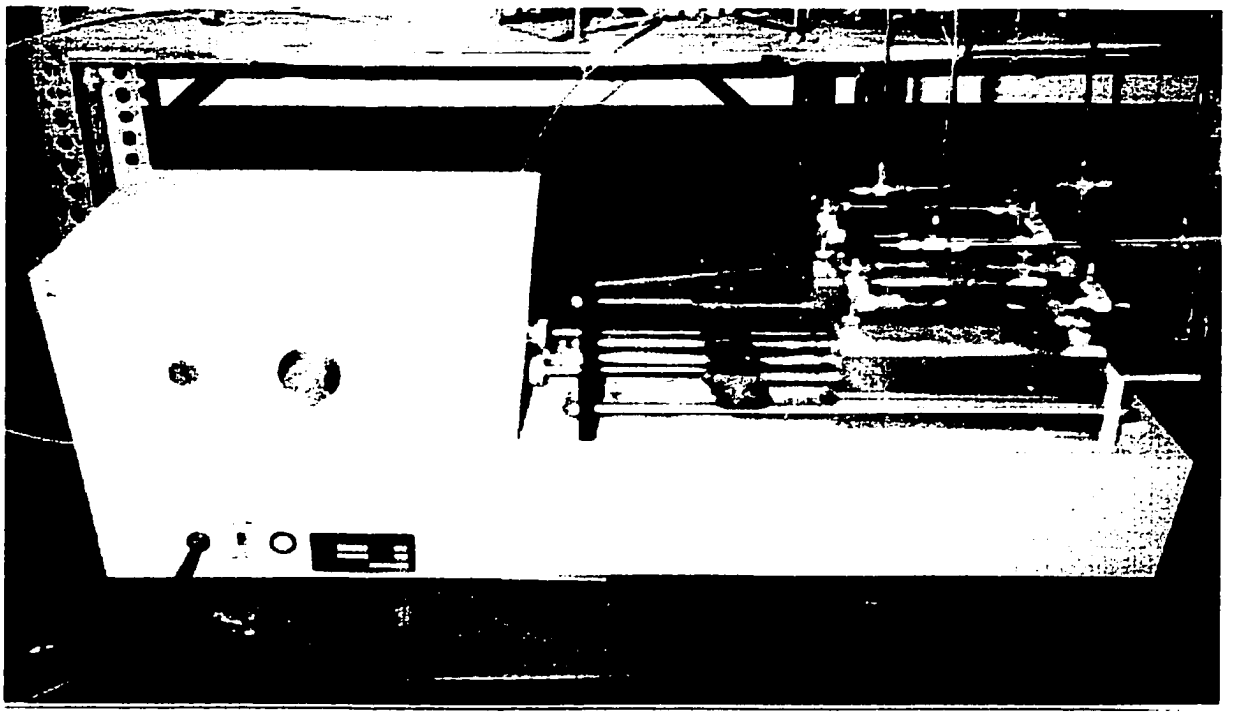

(a) Pictorial View

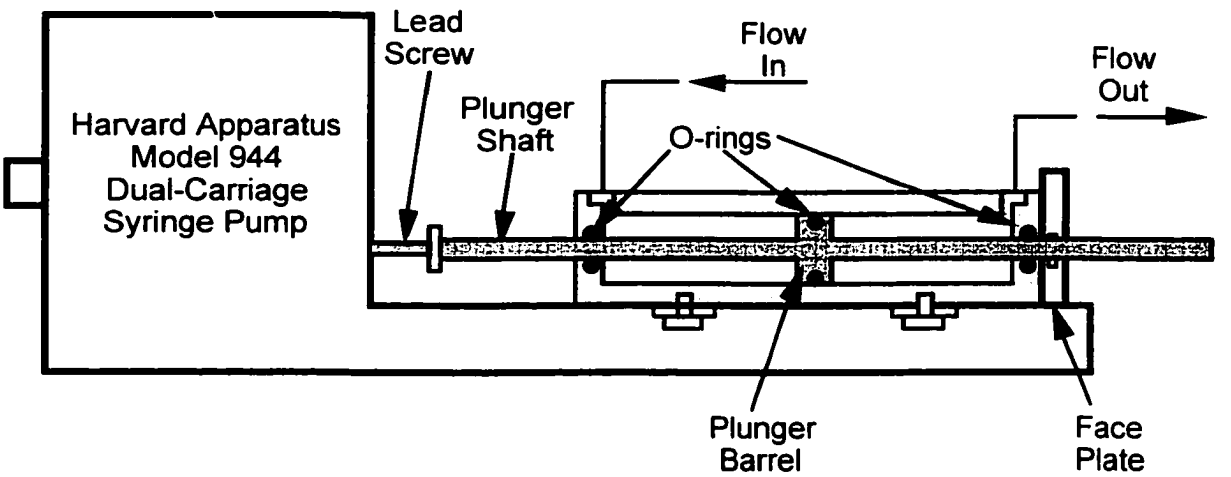

(b) Schematic Cross-Section

Fig. 2.5 - Illustrations of flow-pump system: (a) pictorial view; (b) schematic cross-section.

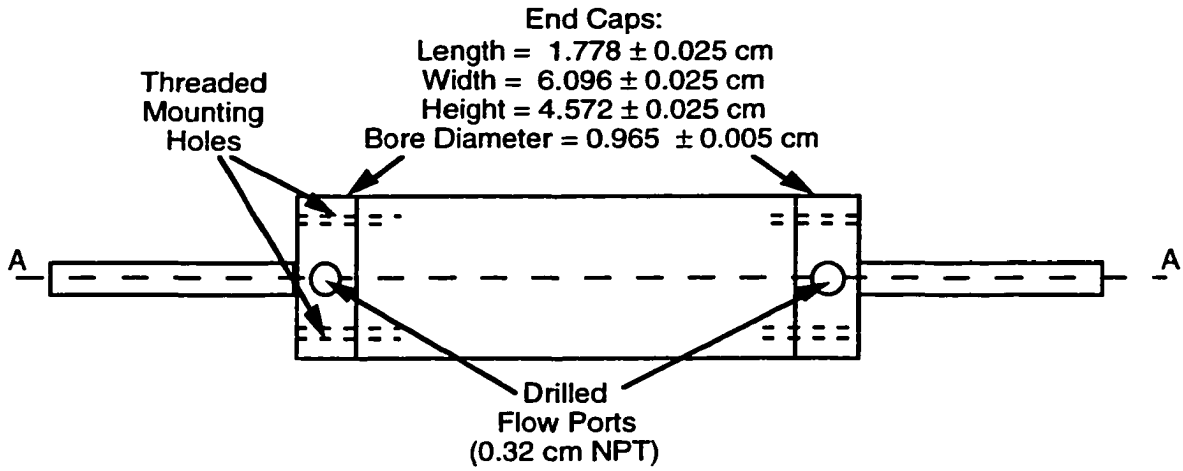

(a) Top View

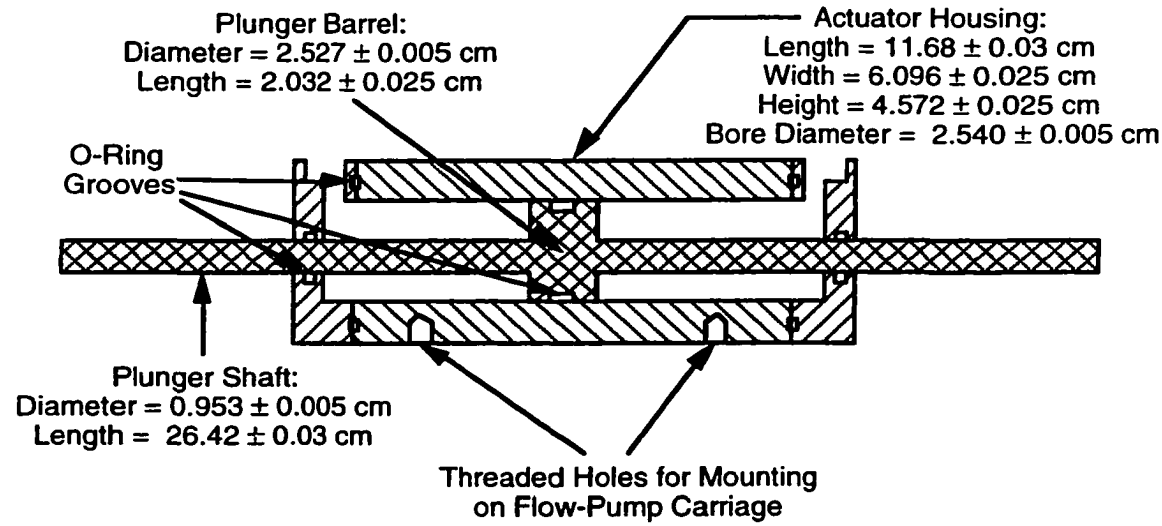

(b) Cross-sectional View (section A-A)

Fig. 2.6 - Schematics of flow-pump actuator: (a) top view; (b) cross-sectional view.

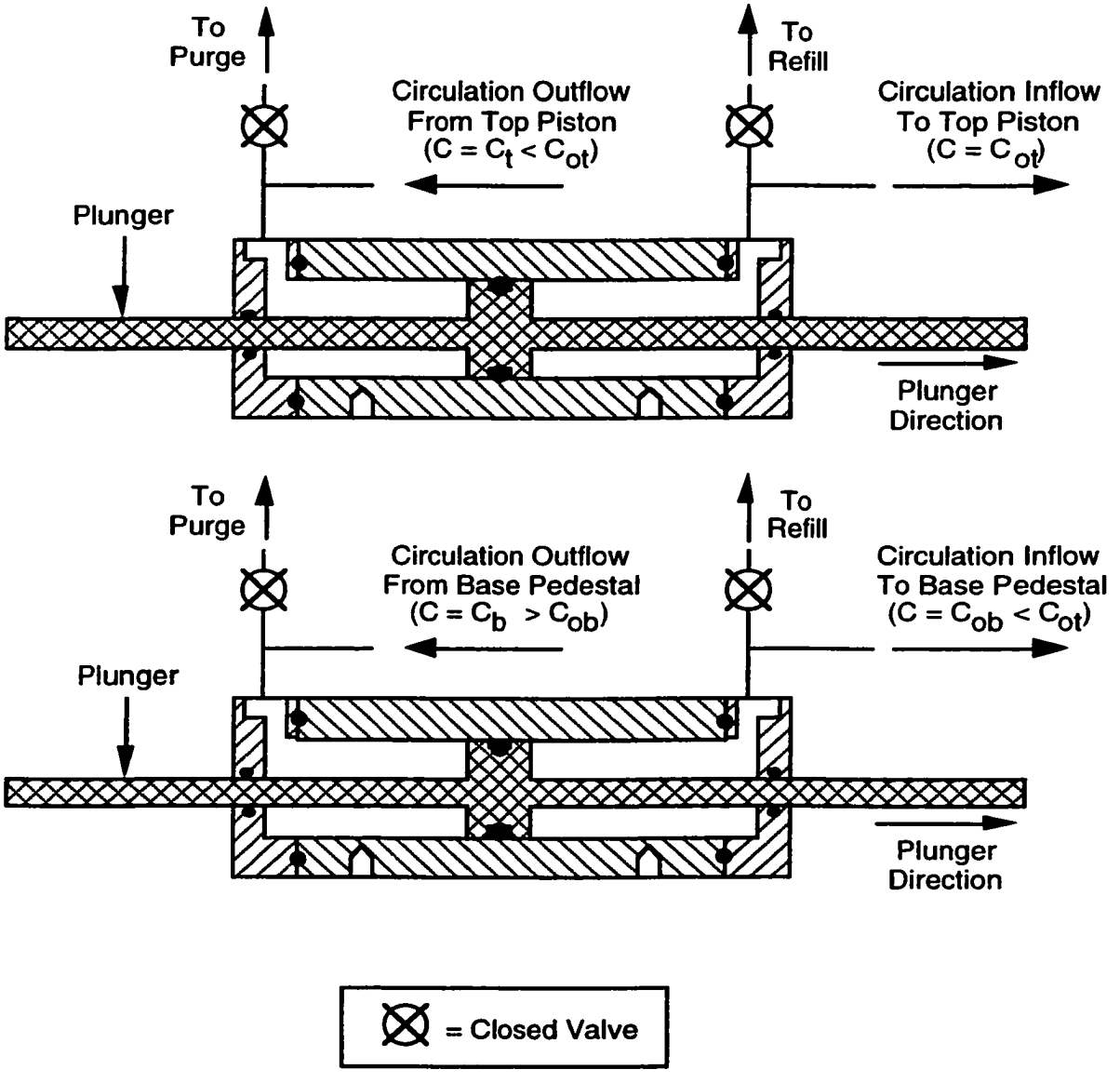

Fig. 2.7 - Schematic of top and bottom actuators during constant-volume circulation of electrolyte solutions at soil specimen boundaries.

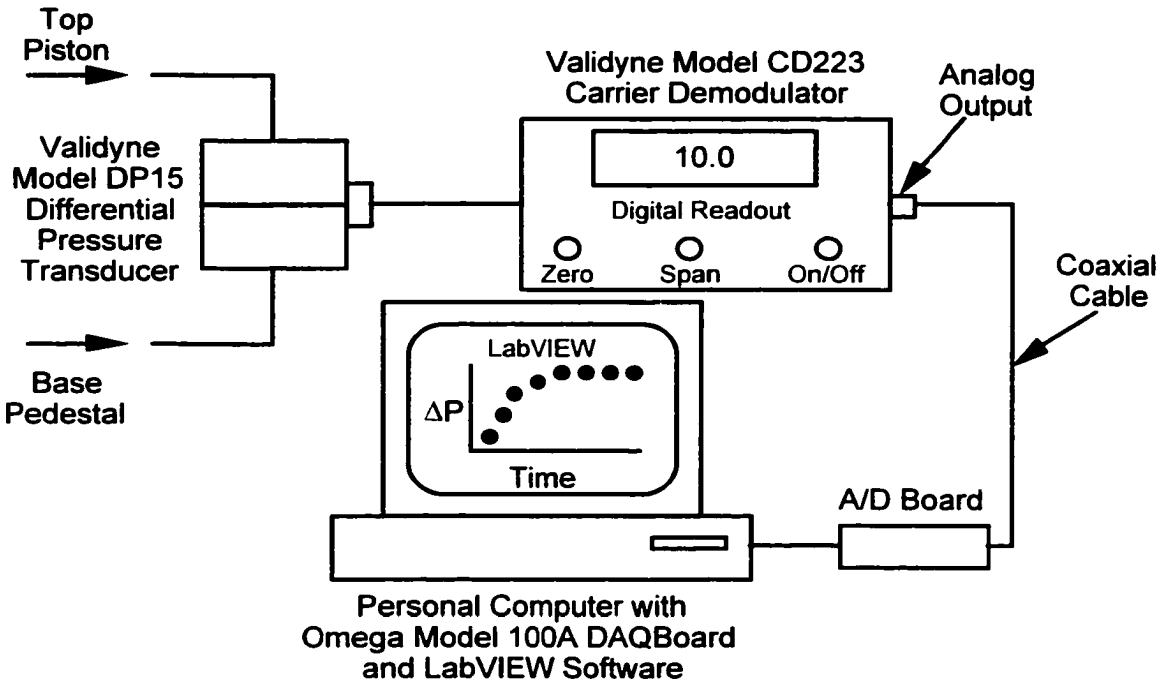

(a) Schematic View (not to scale)

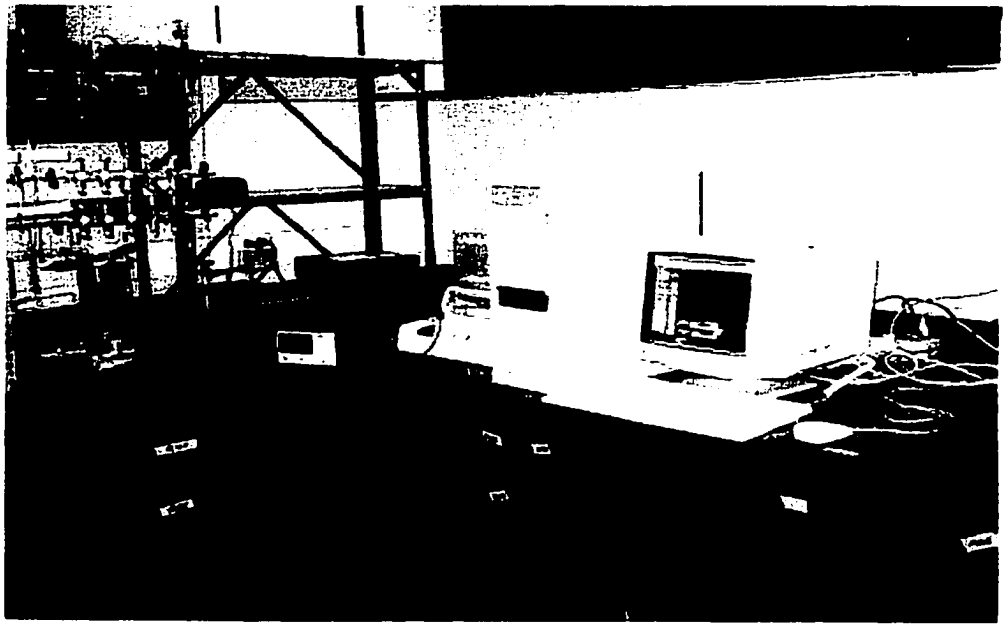

(a) Pictorial View

Fig. 2.8 - Differential pressure measurement and data acquisition system: (a) schematic view; (b) pictorial view.

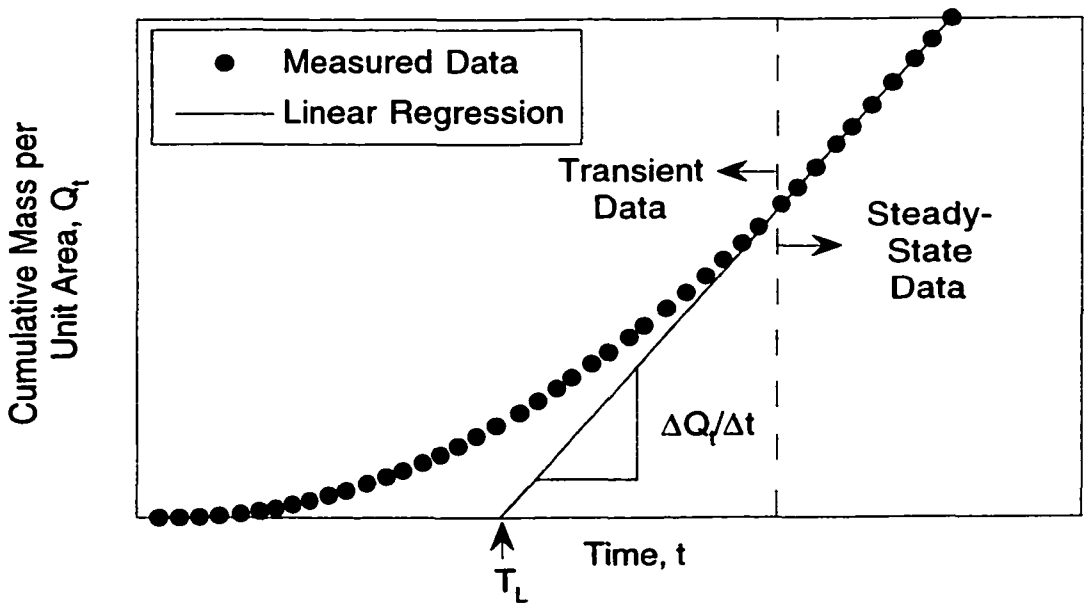

Fig. 2.9 - Schematic illustration of steady-state diffusion test results.

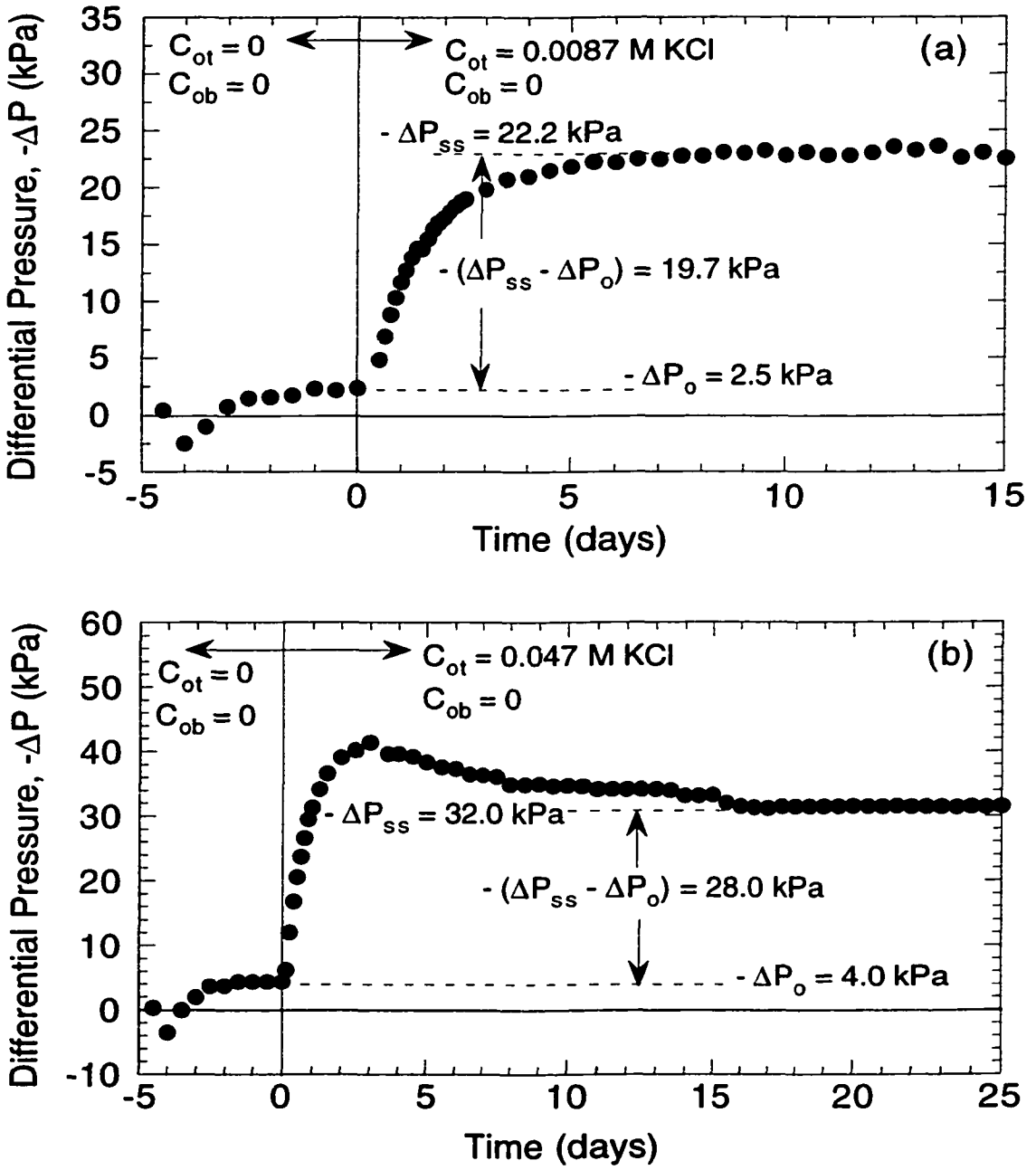

Fig. 2.10 - Pressure differences induced across 10-mm thick GCL specimens: (a) test 1; (b) test 2.

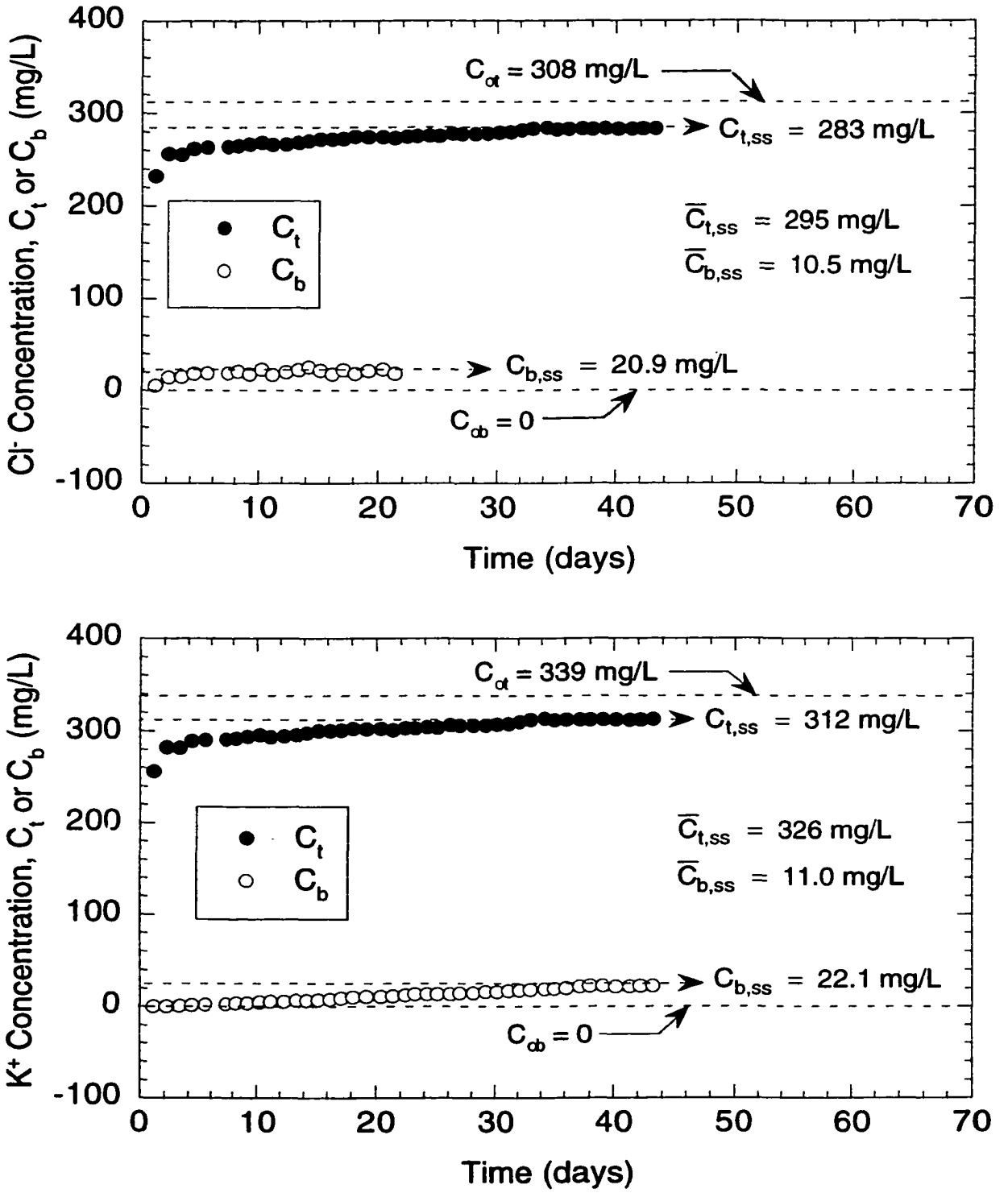

Fig. 2.11 - Boundary concentrations of chloride (Cl^-) and potassium (K^+) over time for chemico-osmotic test 1 (C_{ot} = 0.0087 M KCl).

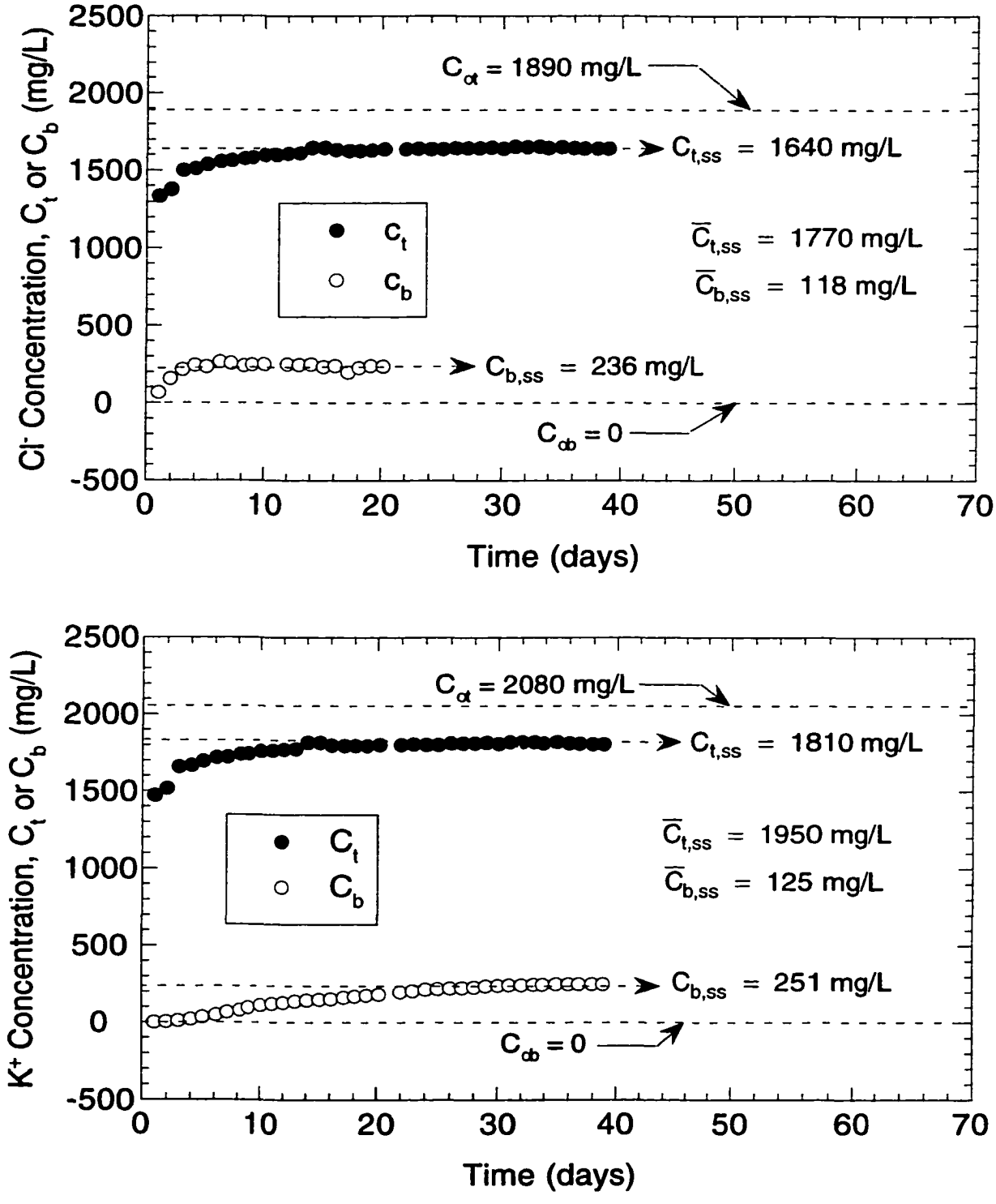

Fig. 2.12 - Boundary concentrations of chloride (Cl^-) and potassium (K^+) over time for chemico-osmotic test 2 (C_{ot} = 0.047 M KCl).

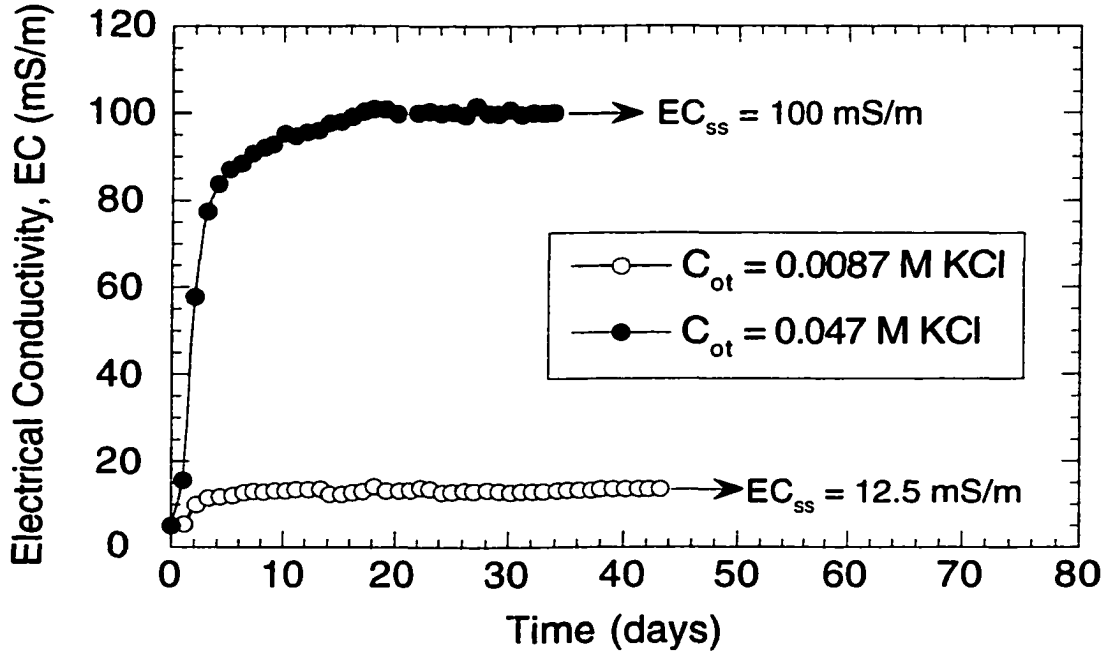

Fig. 2.13 - Measured electrical conductivity in circulation outflow from base pedestal versus time in chemico-osmotic tests 1 and 2.

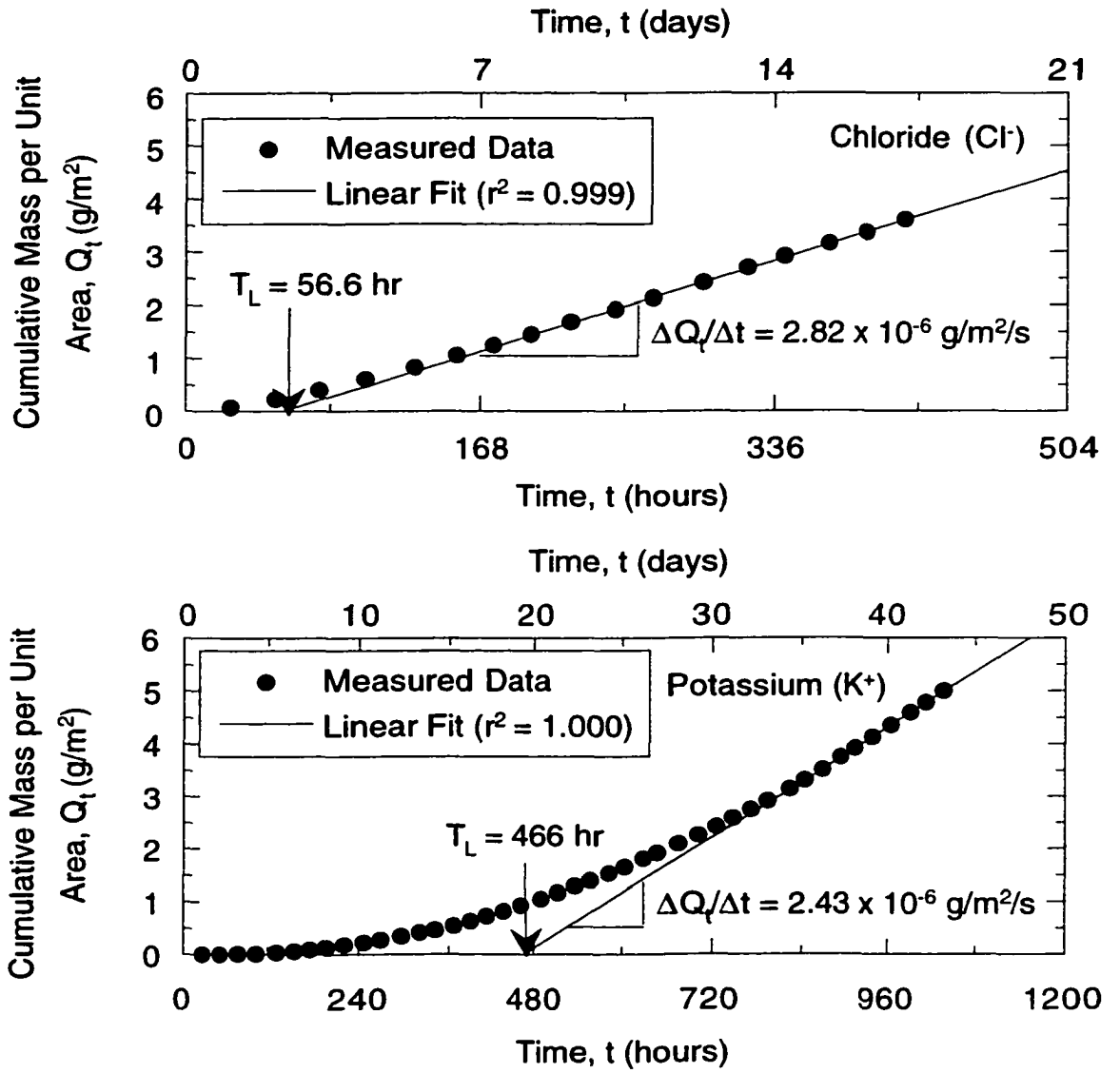

Fig. 2.14 - Results of steady-state method to evaluate the effective diffusion coefficient (D^*) and retardation factor (R_d) in chemico-osmotic test 1 for chloride and potassium (L = 0.010 m, C_{ot} = 0.0087 M, n = 0.79).

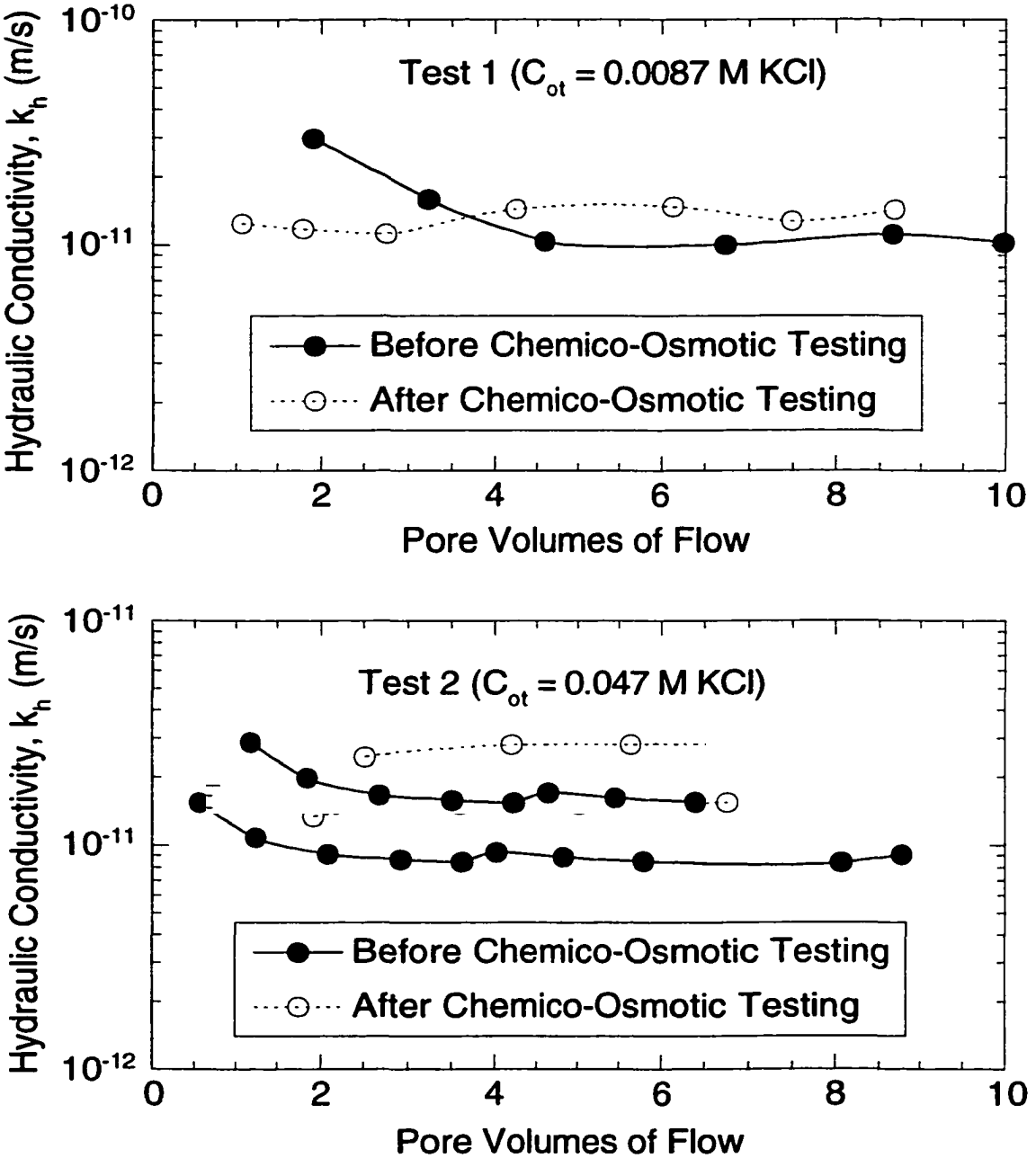

Fig. 2.15 - Hydraulic conductivity of GCL specimens before and after chemico-osmotic testing.

CHAPTER 3

CHEMICO-OSMOTIC EFFICIENCY OF A GEOSYNTHETIC CLAY LINER

ABSTRACT: Chemico-osmotic efficiency coefficients, ω, are determined from measured differential pressures induced across specimens of a geosynthetic clay liner (GCL) containing granular bentonite in response to applied differences in potassium chloride (KCl) concentrations under no-flow conditions. The results show that the GCL acts as a semi-permeable membrane with ω values at steady state, ω_{ss}, ranging from 0.08 to 0.69 for KCl concentration differences ranging from 0.0039 M to 0.047 M. The chemico-osmotic efficiency of the GCL decreases with increasing porosity and increasing KCl concentration. The decrease in ω_{ss} with increasing porosity is consistent with an increase in pore size reflected by an increase in measured hydraulic conductivity. The decrease in ω_{ss} with increasing KCl concentration is consistent with compression of the diffuse double layers surrounding the clay particles, and is reflected by a time-dependent decrease in the induced differential pressure as well as an increase in the hydraulic conductivity of the specimen. The practical implications of the study are illustrated through a simplified analysis of liquid flow through the GCL using the measured values of ω_{ss}.

KEY WORDS: bentonite, chemico-osmosis, coupled flow processes, geosynthetic clay liners, membranes, chemico-osmotic pressure, chemico-osmotic efficiency coefficient

3.1 INTRODUCTION

The ability of clay soils to act as membranes that restrict the passage of solutes is well documented (McKelvey and Milne 1962, Kemper and Rollins 1966, Olsen 1969, Marine and Fritz 1981, and Olsen et al. 1990). Restricted movement of charged solutes (ions) through the pores of a clay soil is attributed to electrostatic repulsion of the ions by electric fields associated with the diffuse double layers of adjacent clay particles (e.g., Hanshaw and Coplen 1973, Marine and Fritz 1981, Fritz and Marine 1983, Fritz 1986, Keijzer et al. 1997). This membrane behavior results in chemico-osmosis, or the movement of liquid in response to a solute concentration gradient, as well as restricted diffusive flux of ions as described by coupled flux theory (e.g., Katchalsky and Curran 1965, Greenberg et al. 1973, Yeung 1990, and Yeung and Mitchell 1993). Chemico-osmosis resulting from membrane behavior in clays has been shown to (1) influence volume change behavior (Mitchell et al. 1973, Barbour 1986, Barbour and Fredlund 1989), (2) cause apparent deviations from Darcy's law in laboratory hydraulic conductivity testing (Olsen 1985), (3) result in anomalous pore-fluid pressures in low-permeability geologic formations (Neuzil 2000), and (4) affect the rate of solute migration through aquitards (Greenberg et al. 1973).

The extent to which a clay soil acts as a membrane in the presence of a concentration gradient is termed chemico-osmotic efficiency and often is expressed quantitatively in terms of a chemico-osmotic efficiency coefficient, ω, or reflection coefficient, σ (e.g., Staverman 1952, Kemper and Rollins 1966, Olsen et al. 1990, Keijzer et al. 1997). The theoretical chemico-osmotic efficiency coefficient of an "ideal" membrane that completely restricts the movement of solutes is unity (i.e., $\omega = 1$), whereas $\omega = 0$ for a material that exhibits no solute restriction (e.g., Mitchell 1993). In most cases, the pores in clay soils that exhibit chemico-osmotic membrane behavior vary over a range of sizes such that not all of the pores are restrictive. In such cases, ω typically falls within the range $0 < \omega < 1$, and clay soils are referred to as "non-ideal" membranes

(Kemper and Rollins 1966, Olsen 1969, Bresler 1973, Barbour 1986, Barbour and Fredlund 1989, Mitchell 1993, and Keijzer et al. 1997). The sizes of the pores in a clay soil and, therefore, the value of ω, are affected by several factors, including the state of stress on the soil, the types and amounts of clay minerals in the soil, and the types and concentrations of the solutes (Kemper and Rollins 1966, Bresler 1973, Olsen et al. 1990, Mitchell 1993).

For example, Kemper and Rollins (1966) measured the chemico-osmotic efficiency of compacted sodium bentonite pastes in the presence of NaCl and $CaCl_2$ solutions over a range of concentrations, and reported that measured values of ω can vary over almost the entire range of $0 < \omega < 1$ depending on the soil porosity, solute concentration, and ion valence. Their results suggest that membrane behavior is significant in clay soils containing an appreciable amount of sodium bentonite.

Soils and soil mixtures containing sodium bentonite also are desirable for use in waste containment barriers (e.g. vertical cutoff walls, soil liner systems) due to the low hydraulic conductivity (e.g. $\leq 10^{-9}$ m/s) typically required in these applications. In particular, geosynthetic clay liners (GCLs) containing sodium bentonite commonly are used either individually or as components of waste containment liners and cover systems primarily due to the low hydraulic conductivities to water (e.g. $<\sim 10^{-11}$ m/s) typically measured for these materials (Daniel 1993, Koerner 1994).

Although the presence of sodium bentonite in GCLs and the low hydraulic conductivities typically associated with GCLs suggest that GCLs should exhibit membrane behavior, no such membrane behavior has been reported for GCLs. The existence of chemico-osmotic membrane behavior in GCLs may be important for evaluating the hydraulic and contaminant transport performance of GCLs used in waste containment applications. Thus, the overall objective of this study is to evaluate the potential for membrane behavior of a selected GCL by measuring the chemico-osmotic efficiency of the GCL in the presence of potassium chloride (KCl) solutions. The

potential effects of porosity and solute concentration on the chemico-osmotic efficiency of the GCL also are evaluated. Finally, the potential significance of the results is discussed within the context of a simplified analysis for liquid flow through the GCL.

3.2 MATERIALS AND METHODS

3.2.1 Geosynthetic Clay Liner

The geosynthetic clay liner (GCL) tested in this study is sold commercially under the trade name Bentomat® (Colloid Environmental Technologies Company (CETCO), Lovell, WY). A schematic cross-section of the Bentomat® GCL is shown in Fig. 3.1. Selected physical and chemical properties of the bentonite are given in Table 3.1.

The grain-size distributions of the GCL bentonite based both on a mechanical sieve analysis of the dry bentonite as well as the typical hydrometer (wet) analysis (ASTM D 422) are presented in Fig. 3.2. As shown in Fig. 3.2, the GCL bentonite is classified as a high-plasticity clay (CH) according to the Unified Soil Classification System (ASTM D 2487), or USCS, based on the results of the hydrometer analysis. However, the results from the mechanical sieve analysis indicate that the dry bentonite actually consists of assemblages or granules of individual clay particles and, therefore, is classified as poorly graded sand (SP). Shackelford et al. (2000) note that GCLs containing granular bentonite may have significantly different hydraulic conductivities relative to GCLs that contain powdered bentonite.

3.2.2 Liquids

The liquids used in this study consist of a processed tap water (PTW) and solutions of PTW and potassium chloride (KCl) (certified A.C.S., Fisher Scientific, Fair Lawn, NJ) dissolved in PTW at measured concentrations ranging from 0.0039 M to 0.047 M. The chloride (Cl^-) concentrations were measured using Ion Chromatography (IC), and the potassium (K^+) concentrations were measured using Inductively Coupled Plasma -

Optical Emissions Spectroscopy (ICP-OES). The PTW consists of tap water that is processed to remove ions by passage through three Barnstead® ion exchange columns. Measured values of pH and electrical conductance (EC) of the PTW and KCl solutions are given in Table 3.2.

3.2.3 Testing Apparatus

A schematic illustration of the testing apparatus is shown in Fig. 3.3. The testing cell consists of a rigid acrylic cylinder, top piston, and base pedestal. The top piston is locked in place to prevent soil expansion and to control the thickness and, therefore, the porosity of the soil specimen. The top piston and base pedestal are equipped with ports that enable circulation of separate electrolyte solutions through porous stones at the specimen boundaries to establish and maintain a constant concentration difference across the specimen. Additional ports are installed in the top piston and base pedestal to allow for measurement of differential pressure across the specimen. Further details regarding the testing apparatus are provided by Malusis et al. (2000).

The electrolyte solutions are circulated continuously through the porous stones at the ends of the specimen using a flow-pump system consisting of a dual-carriage syringe pump (Model 944, Harvard Apparatus, South Natick, MA) equipped with two customized actuators (i.e., syringes). In general, solutions containing initial concentrations of a given electrolyte, C_{ot} and C_{ob}, are expelled from each of the two actuators at the same, constant rate via the plunger that is attached to the flow-pump drive, and subsequently are infused through the porous stones across the top and bottom boundaries of the specimen. Circulation outflow from these boundaries is simultaneously collected at the same rate in order to maintain a constant volume inside the testing cell (i.e., $\Delta V_{cell} = 0$) and prevent liquid flux through the soil. All actuator parts, fittings, valves, and tubing are constructed with grade 316 stainless steel to minimize corrosion and volume change in the system.

The differences in solute (Cl^- and K^+) concentrations between the top and bottom boundaries of the specimen also result in solute diffusion from the higher concentration boundary (top) to the lower concentration boundary (bottom). This process of diffusion results in some solute mass flux into the specimen at the top boundary and the establishment of solute concentration profiles within the specimen. These concentration profiles eventually reach the bottom of the specimen such that some solute mass flux also exits the bottom of the specimen. If the replenishment rate of the source KCl solution through the top porous stone and PTW through the bottom porous stone is sufficiently greater than the diffusive rate through the specimen, then the upper and lower boundary conditions are maintained practically constant such that the outflow boundary concentrations are equal to the initial (source) concentrations (i.e., $C_t \approx C_{ot}$ and $C_b \approx C_{ob}$). However, if the replenishment rate is not sufficiently greater than the diffusive rate, then measurable differences in outflow concentrations will result (i.e., $C_t < C_{ot}$ and $C_b > C_{ob}$). As a result of this potential influence of diffusion on the test results, the circulation outflows also were collected and subsequently analyzed for concentrations (C_t and C_b) of the solutes, pH, and electrical conductance (EC).

3.2.4 Specimen Assembly and Disassembly

Circular specimens of the Bentomat® with nominal diameters of 71.1 mm were cut from a larger GCL sheet and placed on the base pedestal inside the testing cell. The cylinder then was filled with PTW to submerge the specimen, and the top piston was lowered into the cylinder to compress the GCL to the desired thickness. After completion of compression, the top piston was locked in place to prevent volume expansion of the specimen due to swelling of the bentonite.

Each specimen was permeated under backpressure with PTW before chemico-osmotic testing to saturate the specimen, remove the excess soluble salts, and measure the initial hydraulic conductivity. After permeation, PTW was circulated at the top and

bottom boundaries of the specimen at a flow rate of 4.2 x 10^{-10} m^3/s for approximately five days to establish a steady baseline differential pressure. The chemico-osmotic tests then were initiated by circulating KCl solution in the top piston (i.e., $C_{ot} > 0$) while continuing circulation of PTW in the base pedestal. Thus, in this study, the initial concentration of solute in the base pedestal was maintained at zero (i.e., $C_{ob} = 0$).

At the end of chemico-osmotic testing, the GCL specimen was permeated with the source solution until steady-state hydraulic conductivity was achieved. After permeation, the cell was disassembled, and the water content of the specimen was measured to determine the final degree of saturation of the specimen.

3.2.5 Measurement of ω

Since the thickness of the specimen is maintained constant during the chemico-osmotic test, the volume of the specimen inside the testing cell also is maintained constant (i.e., $\Delta V_{cell} = 0$). Also, as previously described, the volume of liquid infused into either end of the testing cell is equal to the volume of liquid withdrawn during circulation such that no flux of liquid can enter or exit the specimen boundaries during the test. As a result, the testing apparatus represents a closed system in that there is no volume change during the test and, therefore, no flow of liquid through the specimen. Also, electrical current is not applied across the specimen, and the non-conductive acrylic cell prevents short circuiting of the specimen. Under these conditions, the chemico-osmotic efficiency coefficient is defined as follows (Groenevelt and Elrick 1976, Malusis et al. 2000):

$$\omega = \left.\frac{\Delta P}{\Delta \pi}\right|_{q=0} \tag{3.1}$$

where ΔP is the measured differential pressure induced across the specimen as a result of prohibiting chemico-osmotic flux of solution, and $\Delta \pi$ is the theoretical chemico-osmotic

pressure difference across an "ideal" semi-permeable membrane (i.e., $\omega = 1$) subjected to an applied difference in solute (KCl) concentration (e.g., Olsen et al. 1990). In essence, ω as defined by Eq. 3.1 represents the ratio of the actual to maximum pressure difference that occurs across a membrane in a closed system in response to an applied concentration difference (i.e., as $\Delta P \rightarrow \Delta\pi$, $\omega \rightarrow 1$).

The induced differential pressure, ΔP, in Eq. 3.1 is measured using a differential pressure transducer (Model DP15, Validyne Engineering Sales Corp., Northridge, CA) that is located as shown in Fig. 3.3. The theoretical chemico-osmotic pressure difference, $\Delta\pi$, in Eq. 3.1 for a single-salt system can be calculated based on the salt concentrations at the specimen boundaries in accordance with the van't Hoff expression (Katchalsky and Curran 1965, Tinoco et al. 1995), or

$$\Delta\pi = \nu RT\Delta C = \nu RT(C_2 - C_1) \tag{3.2}$$

where ν is the number of ions per molecule of the salt, R is the universal gas constant [8.314 J mol $^{-1}$K^{-1}], T is the absolute temperature [K], C is the salt concentration (M), and subscripts 1 and 2 represent the individual compartments on either side of the soil specimen. For example, Eq. 2 for KCl solutions ($\nu = 2$) is written as follows:

$$\Delta\pi = 2RT(C_2 - C_1) \tag{3.3}$$

The van't Hoff expression is based on the limiting assumption that the electrolyte solutions are ideal and dilute and, therefore, provides only approximate values of the chemico-osmotic pressure difference. However, Fritz (1986) notes that the error associated with the van't Hoff expression is low (< 5 %) for 1:1 electrolytes (e.g., NaCl, KCl) and concentrations ≤ 1.0 M.

The initial difference in chemico-osmotic pressure, $\Delta\pi_o$, can be computed in accordance with Eq. 3.2 based on the initial KCl concentrations, C_{ot} and C_{ob}, or

$$\Delta\pi_o = 2RT(C_{ob} - C_{ot}) \tag{3.4}$$

Since $C_{ob} = 0$ in each test conducted in this study, Eq. 3.4 reduces to the following expression:

$$\Delta\pi_o = -2RTC_{ot} \tag{3.5}$$

The value $\Delta\pi_o$ based on Eq. 3.5 represents the maximum possible value of $\Delta\pi$ that can be maintained across the specimen during the test.

Calculation of chemico-osmotic efficiency based on $\Delta\pi_o$ is appropriate for "perfectly flushing" boundary conditions in which the circulation rate is sufficiently rapid relative to the diffusive rate such that changes in boundary KCl concentrations due to diffusion are negligible. However, when the circulation rate is not sufficiently rapid, changes in the boundary concentrations due to diffusion may result in a time-dependent reduction in $\Delta\pi$.

This potential effect of diffusion may be taken into account by basing the determination of ω on the average boundary KCl concentrations of a solute species, $\overline{C}_t$ and $\overline{C}_b$, defined as follows:

$$\overline{C}_t = \frac{C_{ot} + C_t}{2} \quad ; \quad \overline{C}_b = \frac{C_{ob} + C_b}{2} = \frac{C_b}{2} \tag{3.6}$$

Based on these average concentrations, an average chemico-osmotic pressure difference, $\Delta\overline{\pi}$, can be written for steady-state conditions as follows:

$$\Delta\bar{\pi}_{ss} = 2RT\left(\bar{C}_b - \bar{C}_t\right)_{ss} \quad (3.7)$$

where the subscript 'ss' refers to evaluation at steady state.

3.2.6 Correlation of Solute Concentrations with Electrical Conductance

Since the GCL specimens in this study were permeated with PTW before testing to remove the excess soluble salts, the electrical conductance (EC) of the electrolyte solutions in the circulation outflow from the specimen boundaries at steady state is assumed to be due solely to the contributions of Cl^- and K^+. Also, the relationship between EC and concentration of KCl solutions is linear over the range of concentrations used in this study, as shown in Fig. 3.4. As a result, KCl concentrations in the circulation outflow at steady state were determined based on EC measurements in accordance with the calibration shown in Fig. 3.4.

The validity of this assumption was verified in a test by measuring directly the concentrations of Cl^- and K^+ in the circulation outflow from the base pedestal and comparing these values to those calculated on the basis of EC using the calibration shown in Fig. 3.4. The results, shown in Fig. 3.5, indicate excellent agreement at steady state between the calculated KCl concentrations and the measured concentrations of Cl^- and K^+.

The results in Fig. 3.5 also indicate that the KCl values determined on the basis of EC tend to mimic closely the measured Cl^- concentrations. The closeness between the KCl concentrations based on EC and the measured Cl^- concentrations results from the requirement for electroneutrality in solution and the typical non-adsorbing behavior of Cl^- (Shackelford et al. 1999). As a result, the use of EC to estimate KCl concentration may reduce the testing duration since the steady-state KCl concentration is essentially the same as the steady-state Cl^- concentration that occurs much earlier than the steady-state concentration of K^+.

3.2.7 Testing Program

Both single-stage and multiple-stage chemico-osmotic tests were conducted in this study. In the single-stage tests, the differential pressure induced by introducing a single KCl solution into the top piston (i.e., C_{ot} = 0.0039 M, 0.0087 M, 0.020 M, or 0.047 M) was measured until steady-state conditions were reached (i.e., ΔP = constant). The multiple-stage tests consisted of five individual stages in which differential pressures corresponding to five different source KCl solutions (i.e. C_{ot} = 0.0039 M, 0.0060 M, 0.0087 M, 0.020 M, and 0.047 M) were measured across the same GCL specimen. Each stage was conducted until a steady differential pressure response across the specimen was observed. The thickness, L, of the GCL specimens was varied from 0.8 cm to 1.3 cm in the multiple-stage tests to evaluate the influence of porosity on chemico-osmotic efficiency.

3.3 RESULTS

3.3.1 Induced Differential Pressures

The measured differential pressures induced across the GCL specimens, $-\Delta P$ (> 0), in the single-stage tests are presented in Fig. 3.6. The baseline differential pressure, $-\Delta P_o$, during the first five days of DW circulation at both specimen boundaries (i.e., C_{ot} = C_{ob} = 0) ranged between 0.62 kPa and 4.0 kPa. This non-zero baseline differential pressure measured while $C_{ot} = C_{ob} = 0$ in the tests is attributed to slight differences in the hydraulic resistance of the porous stones at the opposite ends of the specimen and, therefore, is not included in the chemico-osmotic efficiency evaluation. Introduction of KCl into the top piston after the initial five days resulted in an immediate and rapid increase in the differential pressure in each test. Steady-state values of induced differential pressure, $-\Delta P_{ss}$, increased from 14.1 kPa to 32.0 kPa as the source KCl concentration, C_{ot}, increased from 0.0039 M to 0.047 M. Calculated values of ω at

steady-state, or ω_{ss}, are based on corrected, or effective, values of differential pressure, $-\Delta P_e$ ($= -\Delta P_{ss} - (-\Delta P_o)$) of 11.5 kPa, 19.7 kPa, 27.8 kPa, and 28.0 kPa, respectively, in the four tests.

The induced differential pressures measured in the multiple-stage tests are shown in Fig. 3.7. Values of $-\Delta P_e$ ranged from 13.1 kPa to 33.1 kPa in multiple-stage test 1 (L = 0.8 cm; Fig. 3.7a) and from 9.25 kPa to 21.1 kPa in multiple-stage test 2 (L = 1.3 cm; Fig. 3.7b). With the exception of the final stage of multiple-stage test 2 (Fig. 3.7b), the stepwise increase in the source KCl concentration, C_{ot}, results in a stepwise increase in $-\Delta P_e$.

3.3.2 Determination of $\Delta\pi$

The KCl concentrations in circulation outflows from the top and bottom specimen boundaries for the single-stage tests and the multiple-stage tests are shown in Figs. 3.8 and 3.9, respectively. These concentrations imply that the applied circulation rate used in this study of 4.2×10^{-10} m^3/s was not sufficient to mimic "perfectly flushing" boundary conditions. Based on these outflow concentrations, calculated values of $\Delta\pi_o$ (Eq. 3.5) in this study ranged from 1 to 20 percent greater than the calculated values of $\Delta\bar{\pi}$ (Eq. 3.7) for the range of KCl concentrations applied in the tests, as shown in Fig. 3.10. For a specimen with a given porosity (thickness), A greater difference between $\Delta\pi_o$ and $\Delta\bar{\pi}$ occurs for greater values of the source concentration, C_{ot}, and greater porosity, n.

3.3.3 Chemico-Osmotic Efficiency Coefficients

Measured osmotic efficiency coefficients at steady-state, ω_{ss}, based on the data in Figs. 3.6, 3.7, and 3.10 are shown in Table 3.3. Values of ω_{ss} based on $\Delta\pi_o$ are lower than values of ω_{ss} based on $\Delta\bar{\pi}_{ss}$ in all cases, since $\Delta\bar{\pi}_{ss} < \Delta\pi_o$ due to diffusion (see Fig. 3.10). However, the differences between ω_{ss} values based on $\Delta\bar{\pi}_{ss}$ versus $\Delta\pi_o$ are low in all cases (i.e., $\Delta\omega_{ss} \leq 0.04$), with lower differences typically occurring at higher

concentrations when ω_{ss} generally is low. Nonetheless, values of ω_{ss} based on $\Delta\overline{\pi}_{ss}$ are considered to be more accurate.

3.4 DISCUSSION

3.4.1 Influence of Porosity on Chemico-Osmotic Efficiency

Measured values of ω_{ss} from Table 3.3 based on $\Delta\overline{\pi}_{ss}$ are plotted versus the total porosity, n, of the GCL specimen as a function of the source KCl concentration (C_{ot}) and, therefore, the concentration difference (i.e., $\Delta C = C_{ot}$) in Fig. 3.11a. For comparison, the data from Olsen (1969) for tests performed using saturated kaolinite also are shown. The results indicate that values of ω_{ss} for the GCL specimens tend to decrease as the porosity increases for a given value of C_{ot}. The trend of decreasing ω_{ss} with increasing porosity in this study also is consistent with the trend in the measured, initial hydraulic conductivity of the GCL based on permeation with PTW shown in Fig. 3.11b insofar as an increase in hydraulic conductivity reflects an increase in pore size. Differences between the osmotic efficiencies of the GCL and saturated kaolinite shown in Fig. 3.11a can be attributed to differences in the stress conditions imposed on the test specimens as well as differences in the mineralogy of kaolinite versus the GCL bentonite.

3.4.2 Influence of Electrolyte Concentration on Osmotic Efficiency

Measured values of ω_{ss} from Table 3.3 based on $\Delta\overline{\pi}_{ss}$ are plotted versus the average salt concentration across the specimen in Fig. 3.12. For comparison, measured values of ω by Kemper and Rollins (1966) and Kemper and Quirk (1972) for < 2-μm sodium bentonite specimens subjected to NaCl and CsCl solutions also are shown in Fig. 3.12.

Although the differences in the chemico-osmotic efficiency coefficients reported in Fig. 3.12 probably can be attributed to several factors, at least three factors are readily apparent, viz. (1) differences in hydrated ionic radii of the solutes, (2) differences in

mineralogy of the bentonites, and (3) differences in the physical properties of the bentonites. In terms of hydrated ionic radii, the data in Fig. 3.12 indicate that, in general, the chemico-osmotic efficiency coefficient tends to decrease with the use of a different salt solution in the order NaCl > KCl > CsCl for bentonite specimens with the same average salt concentration and similar porosity. This trend is consistent with the expected effect of the hydrated ionic radius of the monovalent cation; i.e., ions with larger hydrated radii will be restricted from movement to a greater extent through pores of a given size (MacKay 1946). For example, the well-known lyotropic series indicates that the hydrated ionic radii of monovalent cations varies in the order $Na^+ > K^+ > Cs^+$ and, therefore, the chemico-osmotic efficiency coefficient should vary in the same order, i.e., all other factors being the same (MacKay 1946, Kharaka and Berry 1973). Thus, at least part of the differences in the data shown in Fig. 3.12 can be attributed to use of different salt solutions.

With respect to mineralogy, Kharka and Berry (1973) note that the chemico-osmotic efficiency increases with an increase in the exchange capacity of the material. The measured cation exchange capacity (CEC) for the GCL bentonite tested in this study is relatively low at 47.7 meq/100 g (Table 3.1). Thus, a higher montmorillonite content and/or better quality of montmorillonite in the bentonite used by Kemper and Rollins (1966) and Kemper and Quirk (1972) may have resulted in a higher CEC and, therefore, greater chemico-osmotic efficiency for their specimens. Although Kemper and Rollins (1966) did not report the mineralogy or the CEC of their bentonite, the sodium bentonite used by Kemper and Quirk (1972) had a reported CEC of 80 meq/100 g. Thus, some of the differences in the data reported in Fig. 3.12 may be attributed to differences in the mineralogy of the bentonites used in the different studies.

Finally, differences in the physical properties of the bentonite specimens may be contributing to differences in the data shown in Fig. 3.12. For example, Kemper and Rollins (1966) and Kemper and Quirk (1972) used a relatively tedious specimen

preparation process that involved sedimentation of the natural bentonite to remove the coarser fraction such that only the < 2 μm size particles remained. In contrast, no special bentonite processing was undertaken in this study such that GCL specimens were tested in their natural condition. As previously noted, the GCL bentonite in its natural state consists primarily of coarse-grained granules of clay particles (Fig. 3.2) that may have contributed to the existence of larger pores. This potential difference in pore size may be a factor contributing to the lower chemico-osmotic efficiencies reported for the GCL specimens in this study.

Although differences exist among the three sets of data reported in Fig. 3.12, the trends in all three sets of data are similar; i.e., the chemico-osmotic efficiency coefficient decreases with an increase in the average salt concentration across the specimen such that none of the specimens exhibit chemico-osmotic membrane behavior for average salt concentrations greater than approximately 0.2 M. The observed decrease in chemico-osmotic efficiency with increasing salt concentration shown in Fig. 3.12 is consistent with expected behavior based on diffuse double layer (Guoy-Chapman) theory (e.g., see Mitchell 1993). Based on this theory, the thickness of the double layers of adjacent clay particles and, thus, the extent of influence of the ion-restricting electric fields inside the soil pores decreases as the ion concentration in the pore water increases (e.g., Fritz 1986). In addition, the increase in solute concentration in the pore water due to solute diffusion during the osmotic tests likely is responsible for the time-dependent decrease in chemico-osmotic efficiency indicated by some of the differential pressure versus time data reported in Figs. 3.6 and 3.7.

For example, the measured differential pressure, $-\Delta P$, shown in Fig. 3.6 for C_{ot} = 0.047 M KCl increases to approximately 40 kPa after approximately three days, but subsequently decreases before reaching a steady value of 32 kPa. Similar trends are evident in the multiple-stage tests (Fig. 3.7), particularly for the higher KCl concentrations that would be expected to compress the double layers to a greater extent

relative to the lower KCl concentrations. Barbour (1986) noted similar pressure responses in his chemico-osmotic consolidation (open-system) tests resulting from expulsion of pore water due to diffusion of high concentration salts into the soil and 'collapse' of the double layers.

The greater tendency for time-dependent destruction of chemico-osmotic efficiency with increasing KCl concentration is illustrated by the ratio of peak differential pressure obtained during the chemico-osmotic tests, $-\Delta P_{peak}$, to the steady-state differential pressure, $-\Delta P_{ss}$ (i.e., $\Delta P_{peak}/\Delta P_{ss}$), as shown in Fig. 3.13. As indicated by the data in Fig. 3.13, this time-dependent effect is greatest for the GCL specimen at the highest porosity.

Compression of diffuse double layers during chemico-osmotic testing also may be reflected by a change in hydraulic conductivity, since an increase in salt concentration also may result in an increase in hydraulic conductivity, especially for relatively highly reactive clay soils such as the bentonites used in GCLs (Shackelford et al. 2000). For example, Whitworth and Fritz (1994) correlated reductions in membrane efficiency of compacted smectitic membranes in the presence of NaCl solutions with electrolyte-induced permeability effects. As a result, the ratios of the final hydraulic conductivity based on permeation with the source KCl solution after chemico-osmotic testing (k_{KCl}) to the initial hydraulic conductivity based on permeation with the processed tap water (k_{PTW}) for the six GCL specimens tested in this study are shown as a function of the KCL concentration in Fig. 3.14. The results indicate the expected trend (i.e., the higher the KCl concentration, the greater the increase in hydraulic conductivity) and, therefore, are consistent with the effects of KCl concentration on the chemico-osmotic efficiency of the GCL specimens observed in this study.

3.4.3 Practical Significance

The potential significance of chemico-osmotic efficiency on the movement of liquid through the GCL tested in this study is illustrated herein by considering the GCL as a liquid-containment barrier as shown in Fig. 3.15. The depth of ponded liquid above the GCL is assumed to be 30.5 cm (1.0 ft), in accordance with the maximum allowable leachate depth based on current U.S. regulatory standards. Also, the solute concentration in the leachate, C_o, is assumed to be greater than the solute concentration, C_e, at the exit boundary of the GCL (i.e., at x = L), and the GCL is assumed to be saturated by prehydration.

The total liquid flux through the GCL, q [Lt^{-1}], at steady state is represented by a hydraulic liquid flux, q_h [Lt^{-1}], in response to the difference in hydraulic head and a chemico-osmotic liquid flux, q_π [Lt^{-1}], in response to the difference in solute concentration, or (e.g., Katchalsky and Curran 1965, Kemper and Rollins 1966, Barbour 1986, Olsen et al. 1990, Whitworth and Fritz 1994)

$$q = q_h + q_\pi = -k\frac{\Delta h}{L} + \omega\frac{k}{\gamma_w}\frac{\Delta \pi}{L} \tag{3.8}$$

where Δh (< 0) represents the head loss across the GCL [L]. After substitution of Eq. 3.3, Eq. 3.8 becomes

$$q = -k\frac{\Delta h}{L} - \omega k\frac{2RT}{\gamma_w}\frac{(C_o - C_e)}{L} \tag{3.9}$$

The chemico-osmotic liquid flux through the GCL, q_π, occurs from lower solute concentration to higher solute concentration and, therefore, opposes the downward hydraulic liquid flux, q_h. Thus, if the effect of osmotic efficiency in the GCL is ignored

(i.e., $\omega = 0$) as usual, all liquid flow occurs as a downward hydraulic flux in accordance with Darcy's law.

The relative significance of chemico-osmosis on liquid flux through the GCL can be illustrated by considering the ratio, q/q_h, expressed as follows:

$$\frac{q}{q_h} = \frac{q}{q|_{\omega=0}} = 1 + \omega \frac{2RT}{\gamma_w \Delta h}(C_o - C_e) \tag{3.10}$$

As indicated by Eq. 3.10, $q/q_h = 1$ when either $C_o - C_e = 0$ or $\omega = 0$ since no chemico-osmosis occurs through the GCL. For $\omega > 0$ and $C_o - C_e > 0$, upward chemico-osmosis opposes the downward hydraulic liquid flux. Values of $q/q_h < 0$ indicate that the chemico-osmotic liquid flux is sufficiently high such that the net liquid flux is directed into the containment facility (i.e., upward), whereas values of $q/q_h > 0$ indicate that the net liquid flux is directed out of the containment facility (i.e., downward).

Values of q/q_h versus the difference in KCl concentration across the GCL (i.e., $C_o - C_e$) for ω_{ss} values measured in this study (Table 3) also are shown in Fig. 3.15. The results based on the measured data indicate that upward liquid flux is likely to occur through the GCL for the range of $C_o - C_e$ considered in this study. Values of $C_o - C_e$ greater than 0.05 M are expected to reduce the chemico-osmotic efficiency of the GCL such that the effect of chemico-osmosis eventually be destroyed and q/q_h would approach unity.

Net liquid flux into the containment facility results in negative advection (i.e., advection in the opposite direction of diffusion) and, thus, is potentially beneficial from the viewpoint of reducing the net rate of contaminant migration out of the containment facility. However, in addition to the limitations resulting from the simplifying assumptions previously noted, the results shown in Fig. 3.15 neglect the increase in solute concentration with depth due to diffusion and the potential for solute-clay interactions.

Both of these factors would tend to reduce and eventually eliminate this benefit as the concentration difference across the GCL is reduced due to diffusion and the chemico-osmotic efficiency decreases. In addition, upward chemico-osmotic liquid flux through the GCL in Fig. 3.15 could result in desiccation of the underlying foundation soil.

3.5 CONCLUSIONS

The results of an experimental investigation performed to determine the potential for chemico-osmotic membrane behavior of a geosynthetic lay liner (GCL) containing granular bentonite are reported. The results indicate that the GCL acts as a semi-permeable membrane in the presence of potassium chloride (KCl) solutions for KCl concentrations ranging from 0.0039 M to 0.047 M. Although this observed chemico-osmotic membrane behavior was expected on the basis of previous studies involving sodium bentonites, the existence of membrane behavior for GCLs heretofore has not been reported. The existence of such membrane behavior has important implications with respect to interpretation of test data involving GCLs and the use of GCLs in practical applications, such as liners in waste containment facilities.

Measured chemico-osmotic efficiency coefficients at steady state, ω_{ss}, for the GCL range from 0.08 to 0.69. These ω_{ss} values are based on the average difference in KCl concentration across the specimens that are corrected to account for changes in the boundary concentrations due to solute diffusion. Failure to account for solute diffusion resulted in slightly lower values of ω_{ss} (i.e., $\Delta\omega_{ss} \leq 0.04$).

The chemico-osmotic efficiency of the GCL decreases with increasing porosity and increasing KCl concentration. Both of these trends are consistent with the results of previous studies. The decrease in ω_{ss} with increasing porosity is consistent with an increase in pore size reflected by an increase in measured hydraulic conductivity. The decrease in ω_{ss} with increasing KCl concentration is consistent with compression of the diffuse double layers surrounding the clay particles, and is reflected by a time-dependent

decrease in the induced differential pressure as well as an increase in the hydraulic conductivity of the specimen.

The results of a simplified analysis of liquid flow through the GCL used as a liquid containment liner indicate that the observed chemico-osmotic membrane behavior of the GCL likely would result in a net liquid flux into the containment facility (i.e., upward) for the conditions assumed in the analyses. Since a net upward liquid flux would slow, or retard, the migration of contaminants out of the containment facility, the presence of such chemico-osmotic membrane behavior is potentially beneficial. However, this potential benefit is time dependent since the concentration difference across the GCL will decrease by solute diffusion resulting in an eventual destruction of the membrane behavior. This chemico-osmotic membrane behavior also could result in desiccation of the underlying foundation soil.

3.6 REFERENCES

Barbour, S. L. (1986). "Osmotic flow and volume change in clay soils." *Ph.D. Dissertation*, University of Saskatchewan, Saskatoon, 255 p.

Barbour, S. L. and Fredlund, D. G. (1989). "Mechanisms of osmotic flow and volume change in clay soils." *Canadian Geotechnical Journal*, 26, 551-562.

Bresler, E. (1973). "Simultaneous transport of solutes and water under transient unsaturated flow conditions." *Water Resources Research*, 9(4), 975-986.

Daniel, D. E. (1993). "Clay liners." Chapter 7, *Geotechnical Practice for Waste Disposal*, D.E. Daniel, ed., Chapman and Hall, New York, 137-163.

Fritz, S. J. (1986). "Ideality of clay membranes in osmotic processes: A review." *Clays and Clay Minerals*, 34(2), 214-223.

Fritz, S. J., and Marine, I. W. (1983). "Experimental support for a predictive osmotic model of clay membranes." *Geochimica et Cosmochimica Acta*, 47, 1515-1522.

Greenberg, J. A., Mitchell, J. K., and Witherspoon, P. A. (1973). "Coupled salt and water flows in a groundwater basin." *Journal of Geophysical Research*, 78(27), 6341-6353.

Groenevelt, P. H. and Elrick, D. E. (1976). "Coupling phenomena in saturated homo-ionic montmorillonite: II. Theoretical. " *Soil Science Society of America Journal*, 40, 820-823.

Hanshaw, B. B. and Coplen, T. B. (1973). Ultrafiltration by a compacted clay membrane – II. Sodium ion exclusion at various ionic strengths." *Geochimica et Cosmochimica Acta*, 37(10), 2311-2327.

Katchalsky, A., and Curran, P. F. (1965). *Nonequilibrium Thermodynamics in Biophysics*. Harvard University Press, Cambridge, MA, 248 p.

Keijzer, Th. J. S., Kleingeld, P. J., and Loch, J. P .G. (1997). "Chemical osmosis in Compacted clayey material and the prediction of water transport." *Geoenvironmental Engineering, Contaminated Ground: Fate of Pollutants and Remediation*, R. N. Yong and H. R. Thomas, eds., Thomas Telford Publ., London, 199-204.

Kemper, W. D. and Evans, N. A. (1963). "Movement of water as effected by free energy and pressure gradients III. Restriction of solutes by membranes." *Soil Science Society of America Proceedings*, 27(5), 426-433.

Kemper, W. D. and Quirk, J. P. (1972). "Ion mobilities and electric charge of external clay surfaces inferred from potential differences and osmotic flow." *Soil Science Society of America Proceedings*, 36, 426-433.

Kemper, W. D. and Rollins, J. B. (1966). "Osmotic efficiency coefficients across compacted clays." *Soil Science Society of America Proceedings*, 30, 529-534.

Kharaka, Y. K. and Berry, F. A. F. (1973). "Simultaneous flow of water and solutes through geological membranes – I. Experimental investigation." *Geochimica et Cosmochimica Acta*, 37(12), 2577-2603.

Koerner, R. M. (1994). *Designing with Geosynthetics*, 3rd Ed., Prentice-Hall, Englewood Cliffs, N. J., 783 p.

MacKay, R. A. (1946). "The control of impounding structures on ore deposition." *Economic Geology and the Bulletin of the Society of Economic Geologists*, The Economic Geology Publ. Co., New Haven, CT, 41, 13-46.

Malusis, M. A., Shackelford, C. D., and Olsen, H. W. (2000). "A laboratory apparatus to measure osmotic efficiency coefficients for clay soils." *Geotechnical Testing Journal*, ASTM, in press.

Marine, I. W., and Fritz, S. J. (1981). "Osmotic model to explain anomalous hydraulic heads." *Water Resources Research*, 17(1), 73-82.

McKelvey, J. G. and Milne, I. H. (1962). "The flow of salt solutions through compacted clay." *Clays and Clay Minerals*, 9. 248-259.

Mitchell, J. K. (1993). *Fundamentals of Soil Behavior*, 2nd Ed., John Wiley and Sons, New York, 437 p.

Mitchell, J. K., Greenberg, J. A., and Witherspoon, P. A. (1973). "Chemico-osmotic effects in fine-grained soils." *Journal of the Soil Mechanics and Foundations Division*, ASCE, 99(SM4), 307-322.

Neuzil, C. E. (2000). "Osmotic generation of 'anomalous' fluid pressures in geological environments." *Nature*, 403(6766), 182-184.

Olsen, H. W. (1969). "Simultaneous fluxes of liquid and charge in saturated kaolinite." *Soil Science Society of America Proceedings*, 33, 338-344.

Olsen, H. W. (1985). "Osmosis: A cause of apparent deviations from Darcy's law." *Canadian Geotechnical Journal*, 22, 238-241

Olsen, H. W., Yearsley, E. N., and Nelson, K. R. (1990). "Chemico-osmosis versus diffusion-osmosis." *Transportation Research Record No. 1288*, Transportation Research Board, Washington D.C., 15-22.

Shackelford, C. D. and Redmond, P. L. (1995). "Solute breakthrough curves for processed kaolin at low flow rates." *Journal of Geotechnical Engineering*, ASCE, 121(1), 17-32.

Shackelford, C. D., Malusis, M. A., Majeski, M. J., Stern, R. T. (1999). "Electrical conductivity breakthrough curves." *Journal of Geotechnical and Geoenvironmental Engineering*, ASCE, 125(4), 260-270.

Shackelford, C. D., Benson, C. H., Katsumi, T., Edil, T. B., and Lin, L. (2000). "Evaluating the hydraulic conductivity of GCLs permeated with non-standard liquids." *Geotextiles and Geomembranes*, 18(2/3), 133-161.

Staverman, A. J. (1952). "Non-equilibrium thermodynamics of membrane processes." Transactions of the Faraday Society, 48(2), 176-185.

Whitworth, T. M. and Fritz, S. J. (1994). "Electrolyte-induced solute permeability effects in compacted smectite membranes." *Applied Geochemistry*, 9(5), 533-546.

Yeung, A. T. (1990). "Coupled flow equations for water, electricity and ionic contaminants through clayey soils under hydraulic, electrical, and chemical gradients." *Journal of Non-Equilibrium Thermodynamics*, 15, 247-267.

Yeung, A. T. and Mitchell, J. K. (1993). "Coupled fluid, electrical, and chemical flows in soil." *Geotechnique*, 43(1), 121-134.

Table 3.1 – Measured properties of bentonite in Bentomat® GCL.

Property	Standard	Value
Liquid Limit, LL (%)	ASTM D 4318	478
Plasticity Index, PI (%)	ASTM D 4318	439
Specific Gravity, G_s	ASTM D 854	2.43
Principal Minerals (%):	a	
Montmorillonite		71
Mixed-Layer Illite/Smectite		7
Quartz		15
Other		7
Cation Exchange Capacity (meq/100 g)	b	47.7
Exchangeable Metals (meq/100 g):	b	
Ca		20.8
Mg		6.4
Na		31.0
K		0.8
Sum		59.0
Soluble Salts (mg/kg):	b, c	
Ca		443
Mg		407
Na		4636
K		263
Soil pH	b, d	9.2
Electrical Conductance (mS/m) @ 25°C	b, d	120

[a] Based on x-ray diffraction analyses performed by Mineralogy Inc., Tulsa, OK

[b] Procedures described in Shackelford and Redmond (1995).

[c] Measured from a 1 g:20 mL clay-water extract.

[d] Measured on a saturated soil paste.

Table 3.2 – Measured chemical properties of liquids used in study.

Liquid	KCl Concentration		pH	EC @ 25°C [a]
	(M)	(mg/L)		(mS/m)
Processed Tap Water (PTW)	0	0	6.93	0.32
KCl Solutions	0.0039	290	6.68	58.7
	0.0060	450	6.67	90.0
	0.0087	650	6.73	123
	0.020	1,500	6.87	276
	0.047	3,500	6.91	682

[a] EC = electrical conductance

Table 3.3 – Test results for GCL specimens.

Test No.	Test Conditions [a]				Chemico-Osmotic Test Results [b]					Hydraulic Conductivity Results [c]		
	Type	L (cm)	n	C_{ot} (M)	$-\Delta P_e$ (kPa)	$-\Delta\pi_o$ (kPa)	$-\Delta\overline{\pi}_{ss}$ (kPa)	$\omega_{ss} = \Delta P_e/\Delta\pi_o$	$\omega_{ss} = \Delta P_e/\Delta\overline{\pi}_{ss}$	Initial, k_{PTW} (m/s)	Final, k_{KCl} (m/s)	k_{KCl}/k_{PTW}
1	SS	1.0	0.80	0.0039	11.5	19.4	18.4	0.59	0.63	1.63×10^{-11}	1.65×10^{-11}	1.01
2	SS	1.0	0.79	0.0087	19.7	43.0	39.9	0.46	0.49	1.10×10^{-11}	1.33×10^{-11}	1.21
3	SS	1.0	0.79	0.020	27.8	99.1	86.4	0.28	0.32	1.52×10^{-11}	2.06×10^{-11}	1.36
4	SS	1.0	0.78	0.047	28.0	234	201	0.12	0.14	8.73×10^{-12}	1.48×10^{-11}	1.70
5	MS	0.8	0.74	0.0039	13.1	19.4	18.9	0.68	0.69	3.86×10^{-12}	6.24×10^{-12}	1.62
				0.0060	16.6	29.7	28.4	0.56	0.58			
				0.0087	21.8	43.0	41.1	0.51	0.53			
				0.020	29.6	99.1	91.2	0.30	0.32			
				0.047	33.1	234	211	0.14	0.16			
6	MS	1.3	0.86	0.0039	9.25	19.4	17.9	0.48	0.52	2.98×10^{-11}	4.74×10^{-11}	1.59
				0.0060	11.4	29.7	27.3	0.38	0.42			
				0.0087	16.4	43.0	38.8	0.38	0.42			
				0.020	21.1	99.1	81.8	0.21	0.26			
				0.047	15.9	234	189	0.07	0.08			

[a] SS = single-stage test, MS = multiple-stage test; L = specimen thickness; n = specimen porosity; C_{ot} = KCl source concentration

[b] $-\Delta P_e$ = Net differential pressure measured across specimen at steady state; $-\Delta\pi_o$ = theoretically maximum osmotic pressure difference based on difference in initial (source) concentrations; $-\Delta\overline{\pi}_{ss}$ = theoretically maximum chemico-osmotic pressure difference based on difference in boundary concentrations at steady state; ω_{ss} = chemico-osmotic efficiency coefficient at steady state.

[c] k_{PTW} based on permeation with processed tap water (PTW); k_{KCl} based on permeation with final source KCl solution at end of test.

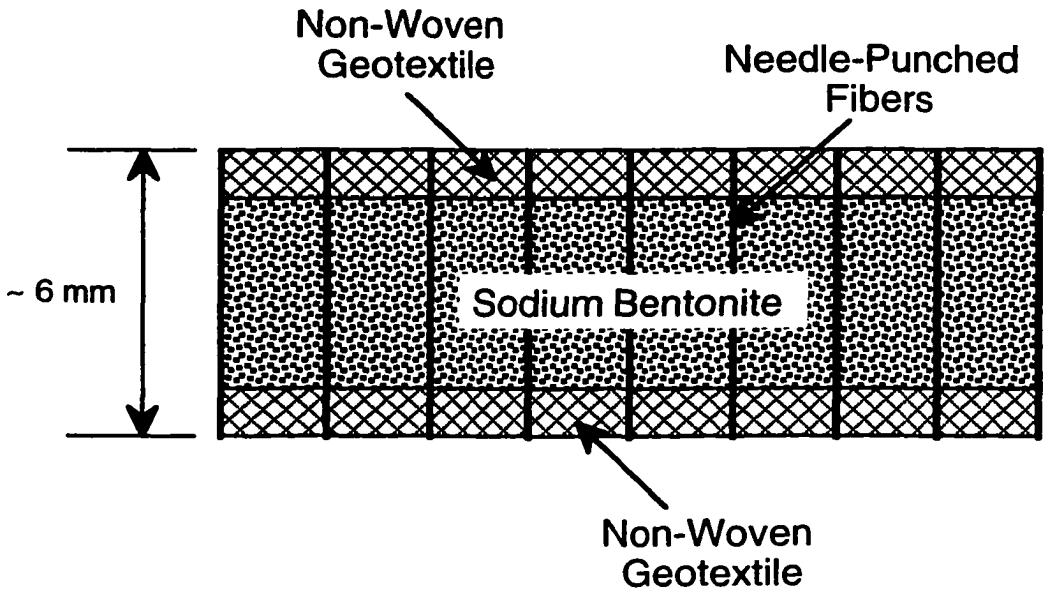

Fig. 3.1 - Schematic of Bentomat® GCL.

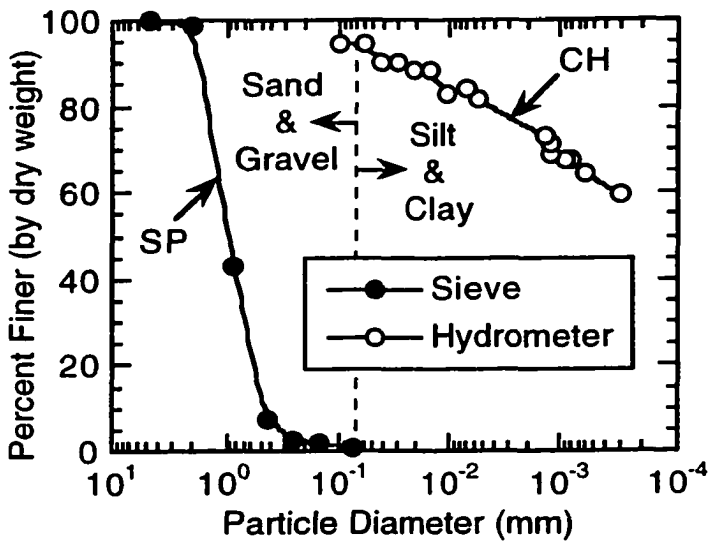

Fig. 3.2 - Grain-size distributions for granular bentonite in Bentomat® GCL.

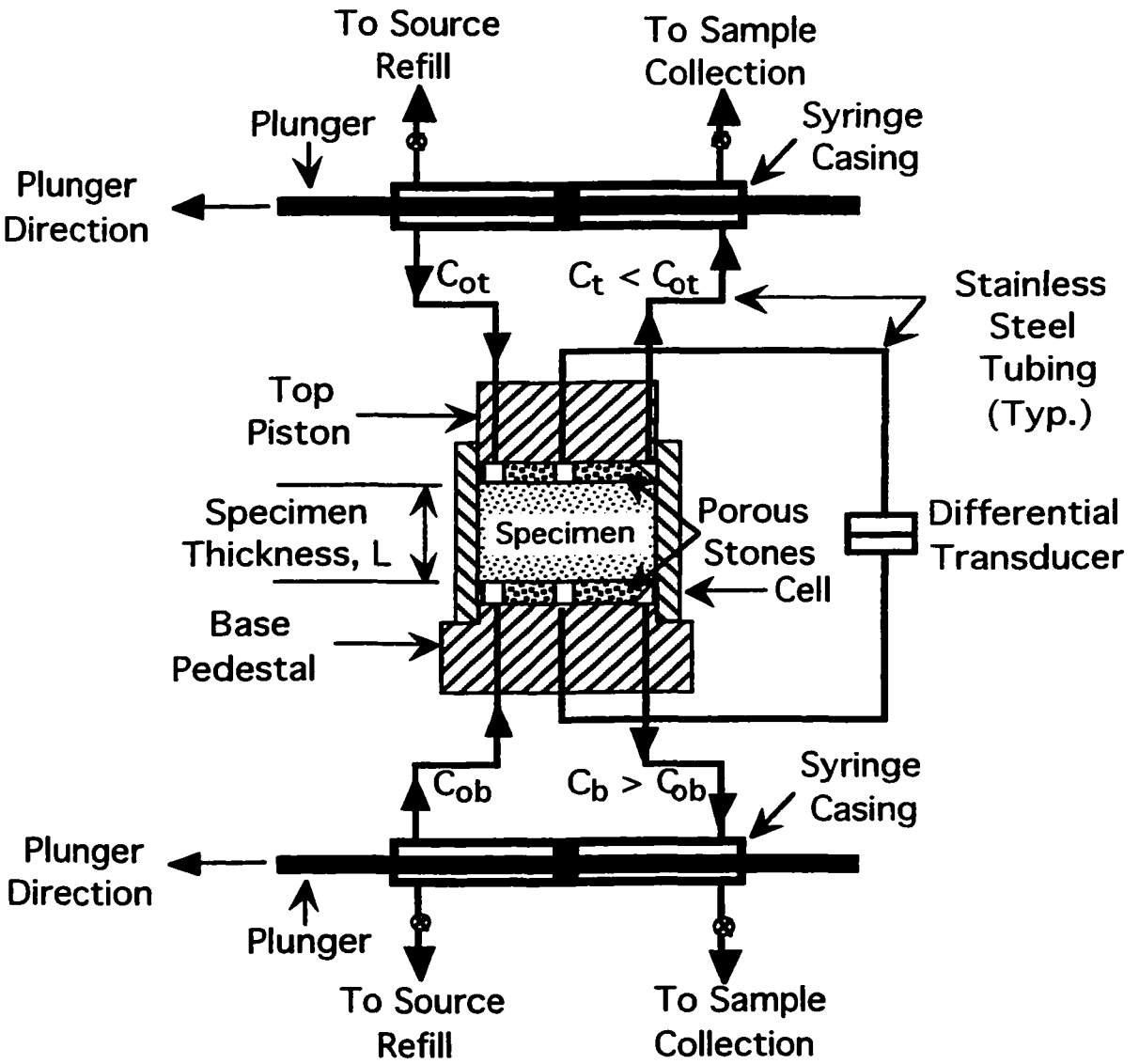

Fig. 3.3 - Schematic of testing apparatus used in study.

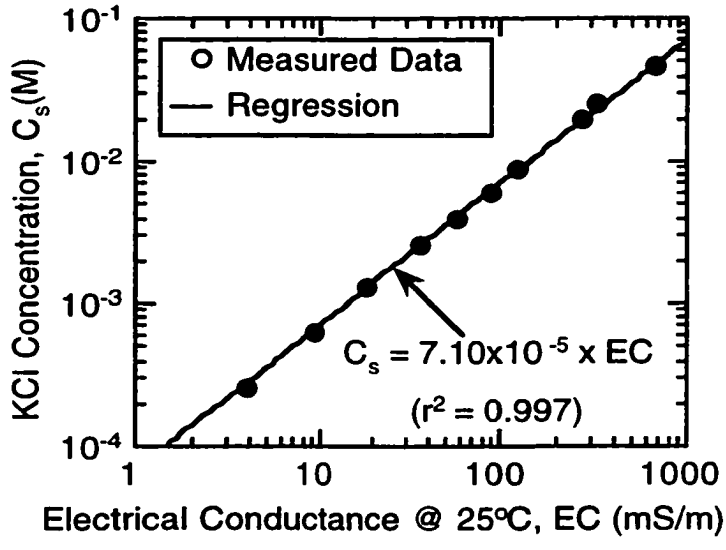

Fig. 3.4 - Correlation between KCl concentration and electrical conductance at 25 °C.

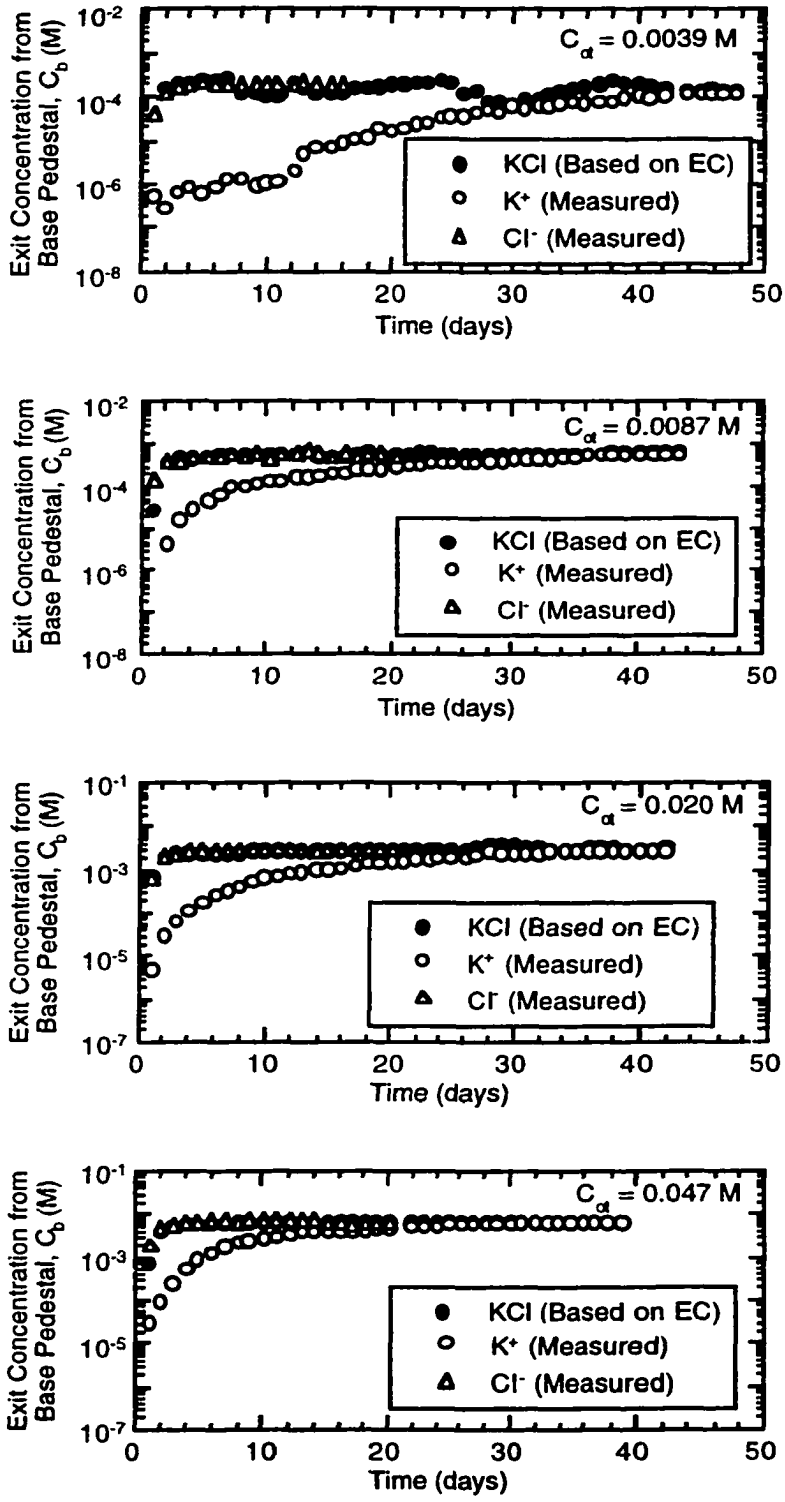

Fig. 3.5 - Comparison of measured exit concentrations of K^+ and Cl^- from base pedestal (C_b) with estimated exit KCl concentrations based on electrical conductance (EC) measurements.

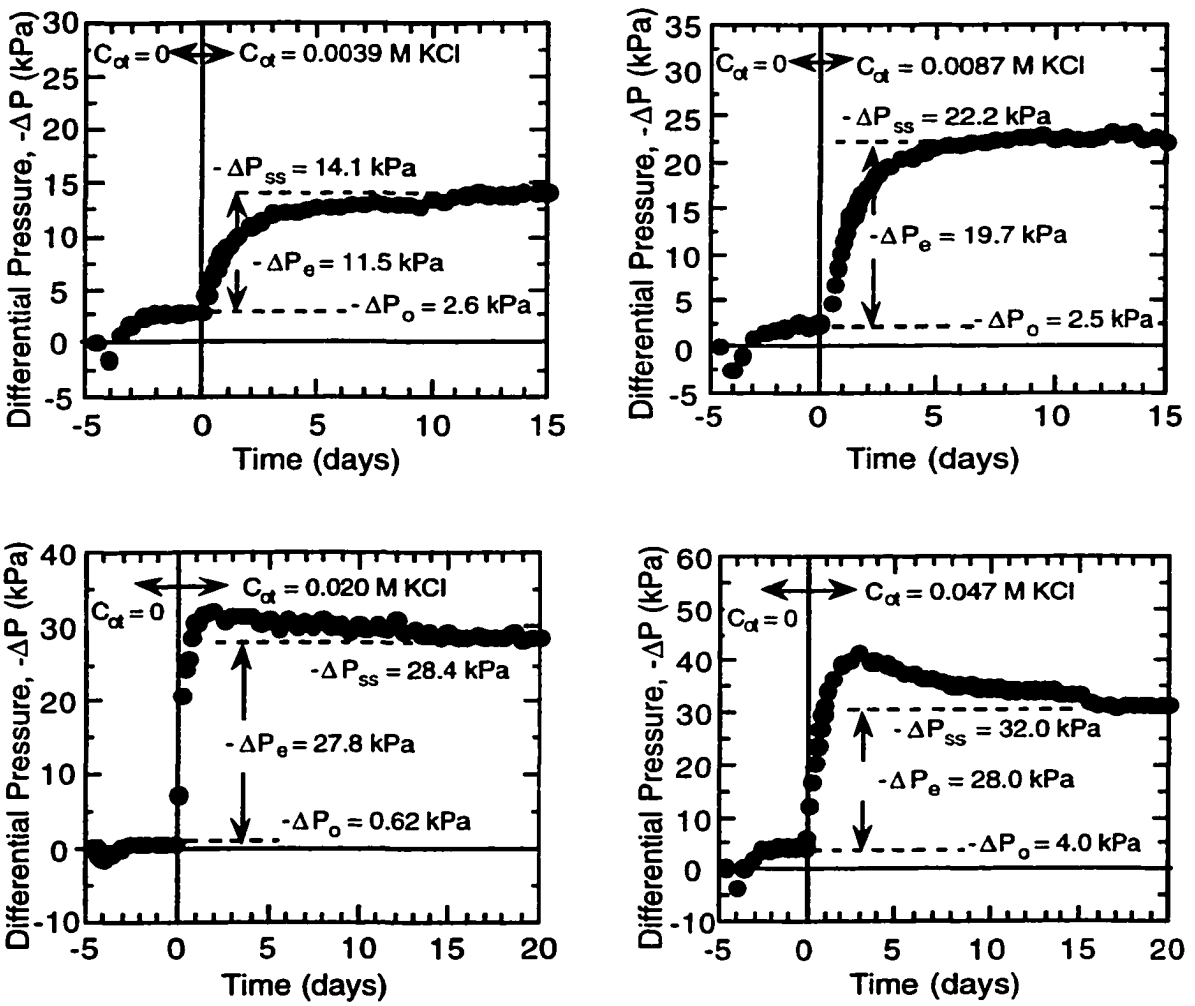

Fig. 3.6 - Induced differential pressures measured across GCL specimens in single-stage chemico-osmotic tests (L = 1.0 cm).

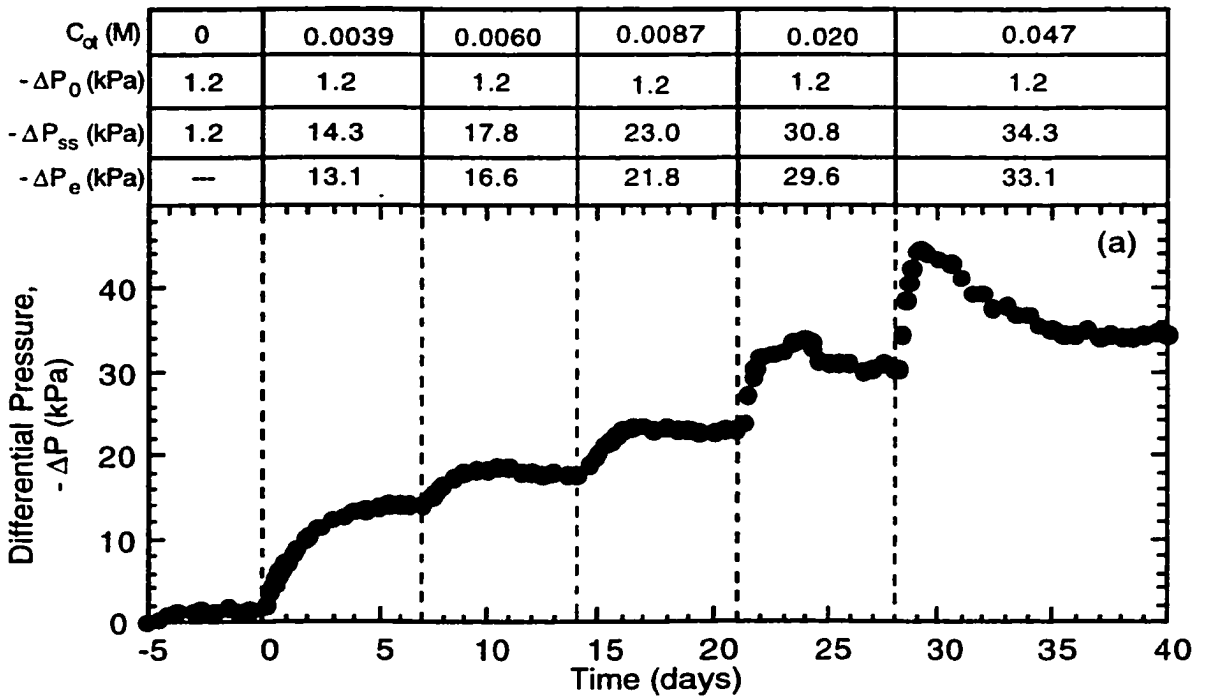

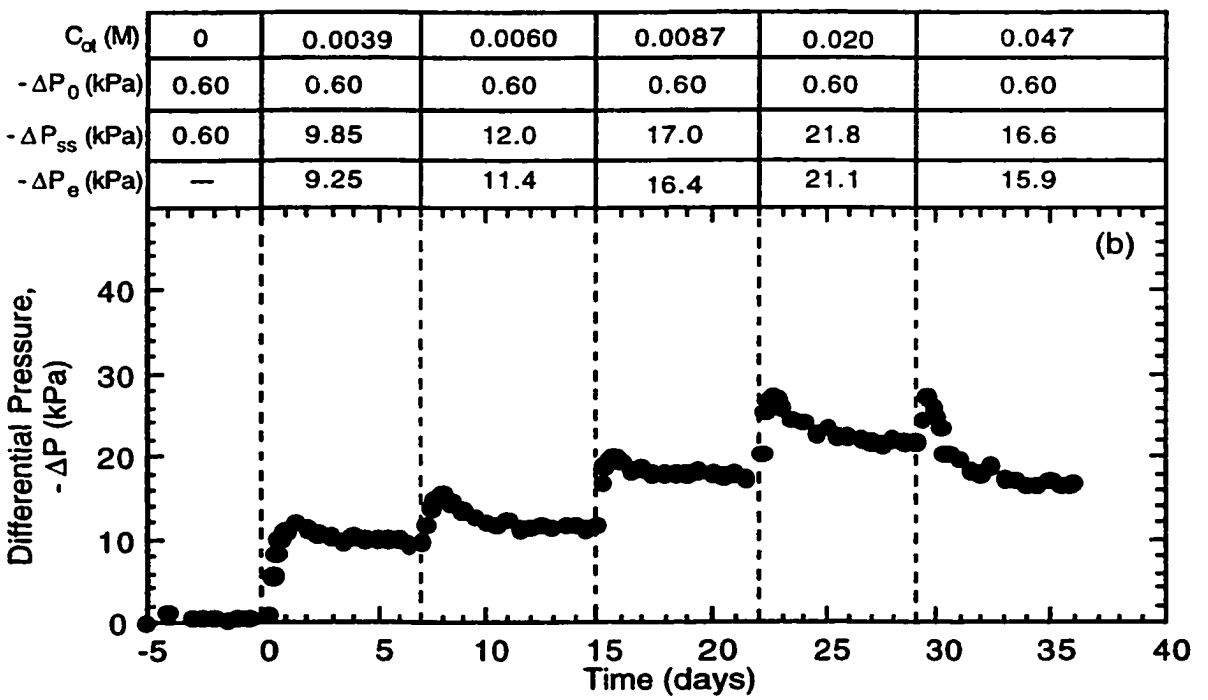

Fig. 3.7 - Induced differential pressures measured acrosss GCL specimens in multi-stage chemico-osmotic tests: (a) L = 0.8 cm; (b) L = 1.3 cm.

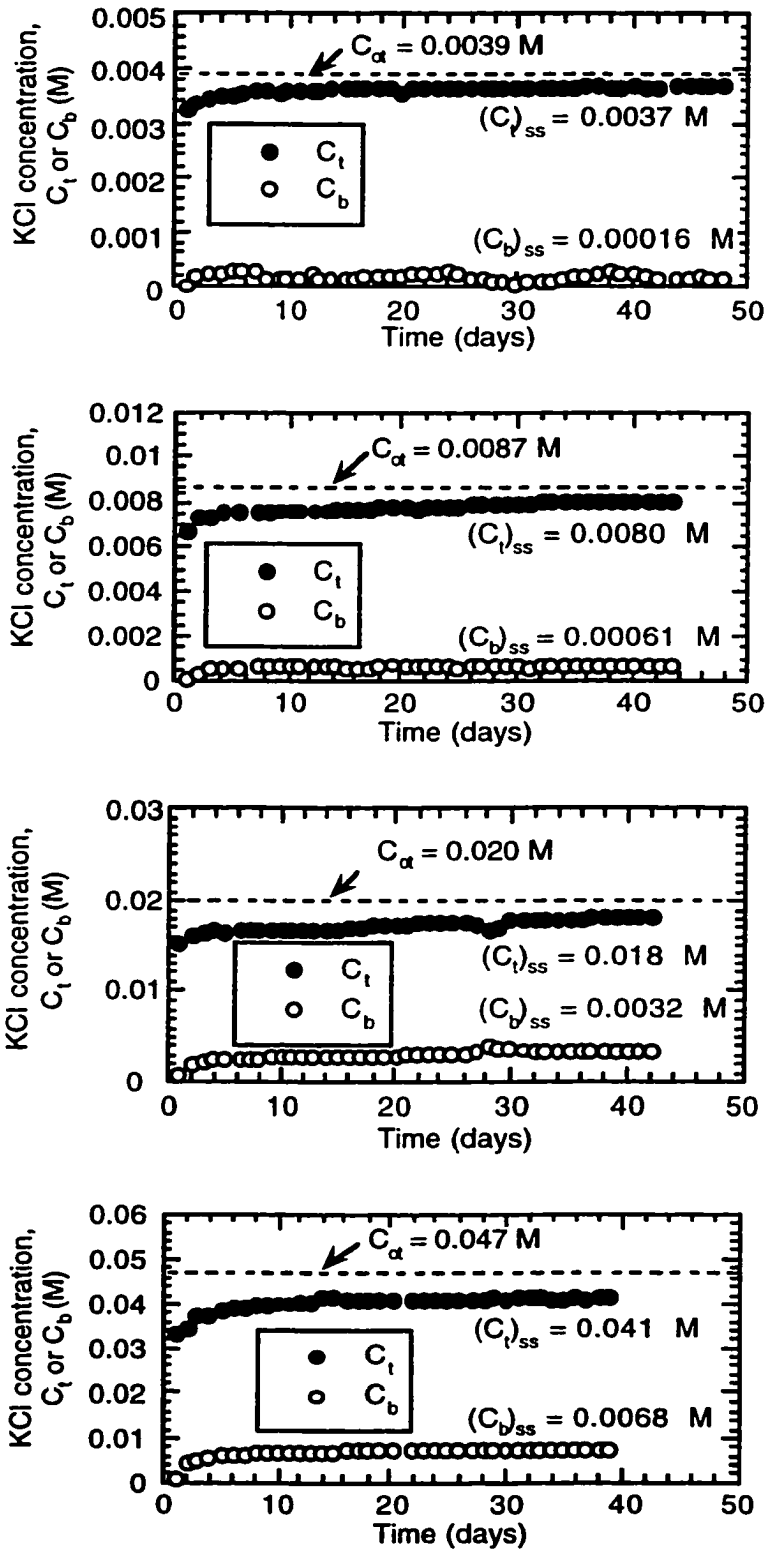

Fig. 3.8 - Exit KCl concentrations (C_b and C_t) versus time for single-stage chemico-osmotic tests (L = 1.0 cm).

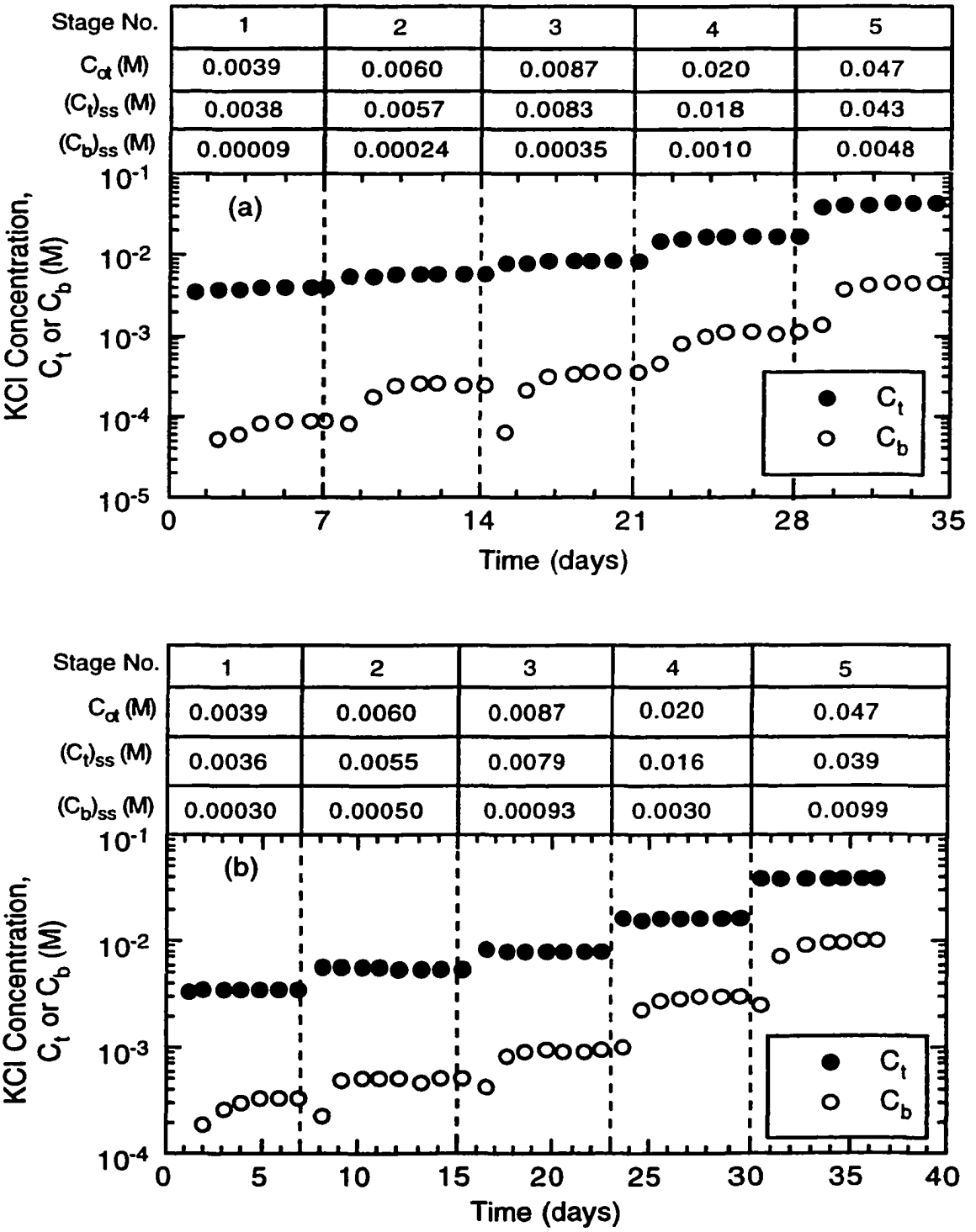

Fig. 3.9 - Exit KCl concentrations (C_b and C_t) versus time for multi-stage chemico-osmotic tests: (a) L = 0.8 cm; (b) L = 1.3 cm.

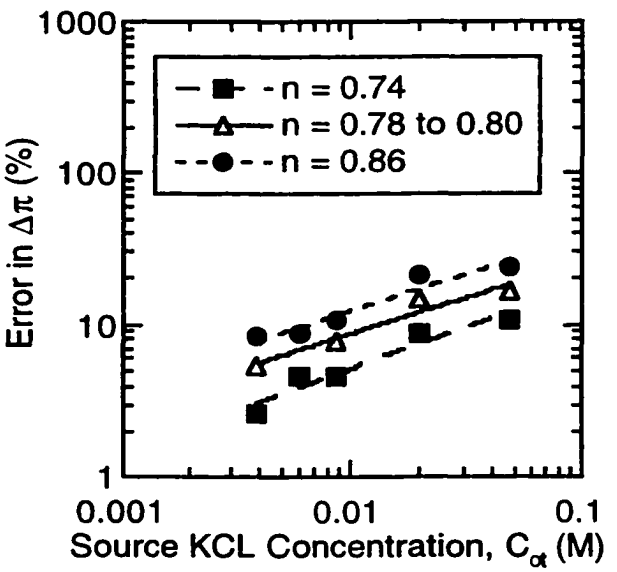

Fig. 3.10 - Error in $\Delta\pi$ incurred by ignoring changes in boundary KCl concentrations due to diffusion.

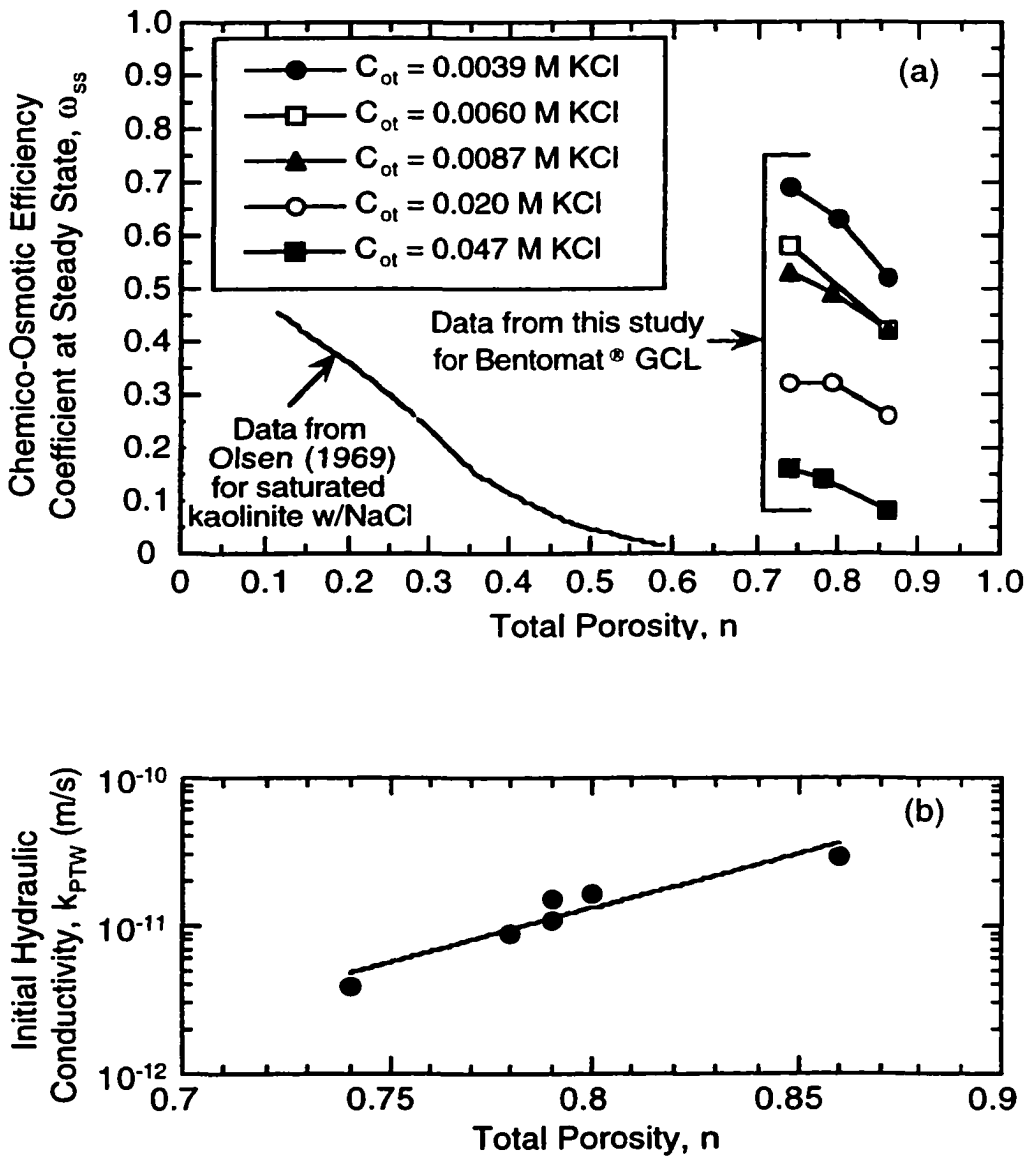

Fig. 3.11 - (a) Chemico-osmotic efficiency coefficients (ω_{ss}) versus porosity, n; (b) Initial hydraulic conductivity of GCL specimens permeated with processed tap water (PTW).

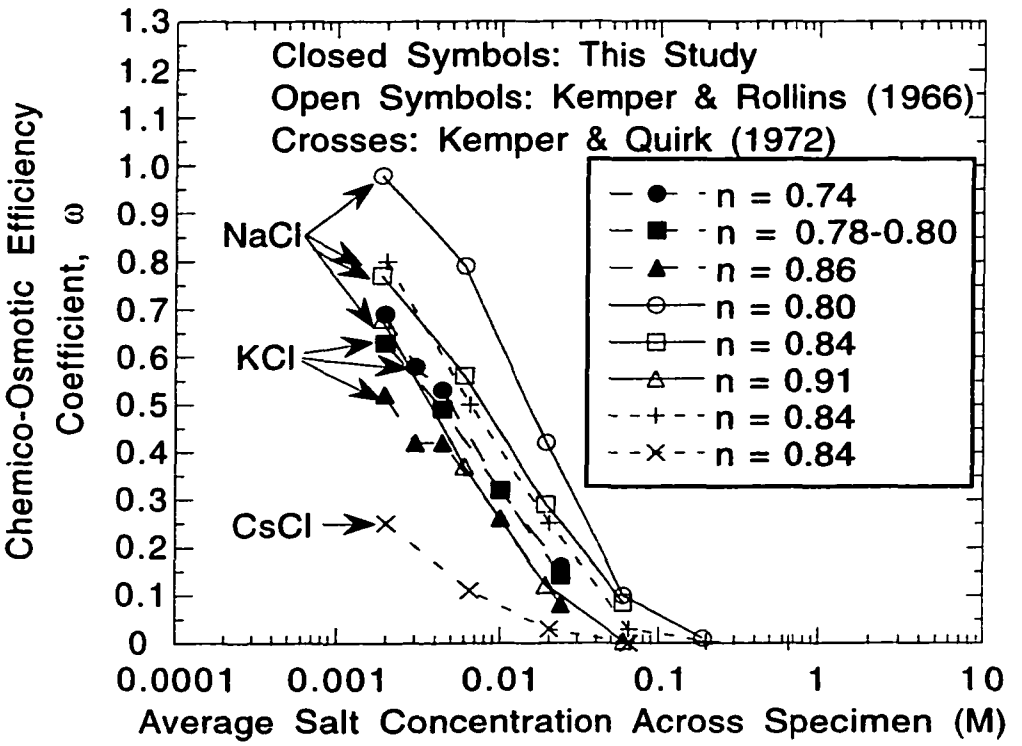

Fig. 3.12 - Chemico-osmotic efficiency of sodium bentonite as a function of salt concentration and porosity.

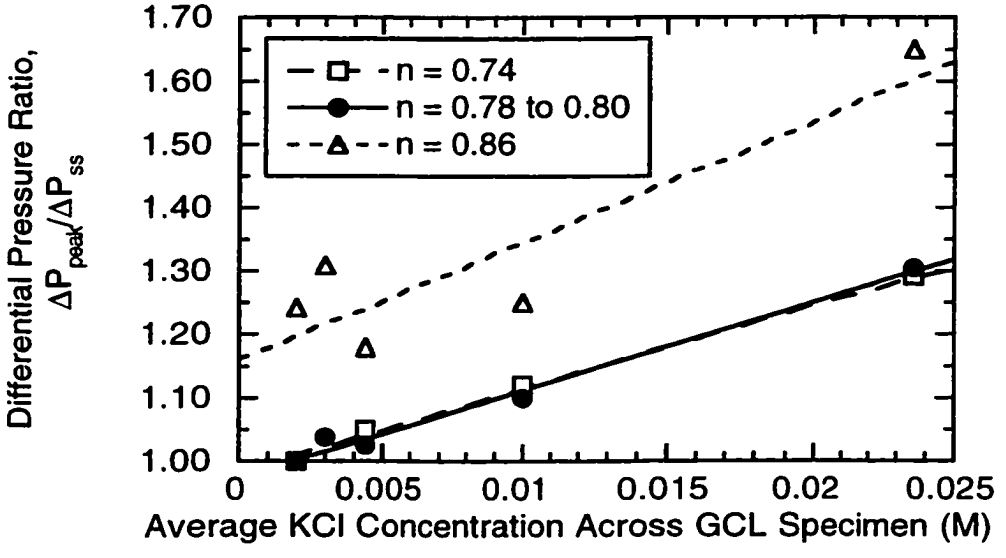

Fig. 3.13 - Ratios of peak to steady-state differential pressures measured in chemico-osmotic tests.

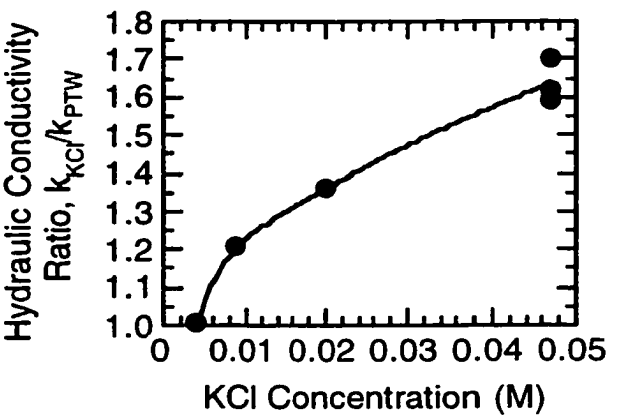

Fig. 3.14 - Effect of KCl concentration on hydraulic conductivity of GCL specimens tested in study.

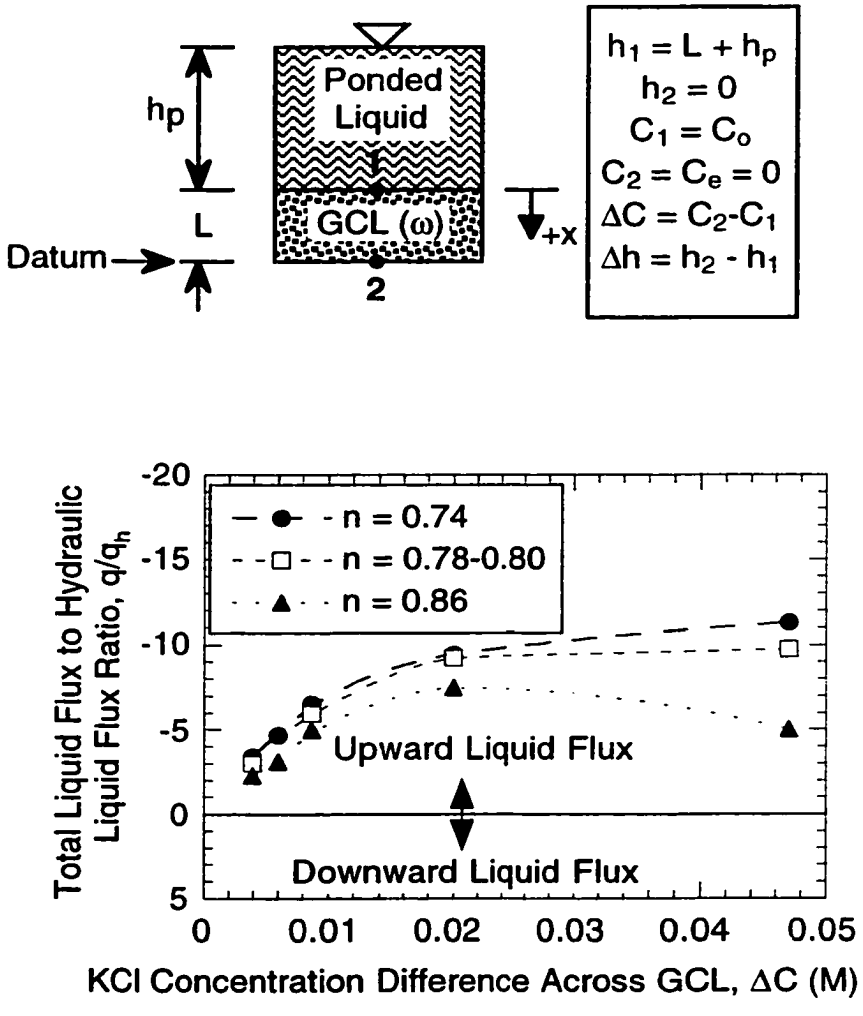

Fig. 3.15 - Simulated liquid flux through a 1.0-cm-thick Bentomat GCL in the presence of KCl solutions.

CHAPTER 4

COUPLED SOLUTE DIFFUSION FOR A GEOSYNTHETIC CLAY LINER

ABSTRACT: The influence of coupling effects associated with soil membrane behavior on the diffusion of potassium chloride (KCl) through a geosynthetic clay liner (GCL) containing sodium bentonite is investigated. These effects are evaluated on the basis of the results of steady-state diffusion tests under no-flow conditions in which measured effective salt-diffusion coefficients (D_s^*) are determined using coupled flux transport theory. The test results indicate that two separate coupling effects act to reduce KCl diffusion through the GCL: (1) a direct coupling effect due to salt-sieving, as predicted by the coupled flux transport theory; and (2) an empirical (indirect) coupling effect characterized by a concentration-dependent decrease in D_s^*. Both of these coupling effects are correlated with measured chemico-osmotic efficiency coefficients (ω) for the GCL. Examination of the coupled flux transport theory reveals that the salt-sieving effect can be expressed in terms of a coupled salt-diffusion coefficient, D_ω^*, that is less than D_s^* when $\omega > 0$. Differences between D_ω^* and D_s^* are less than 10 percent for all tests, indicating that the direct coupling is not significant in this study. The indirect coupling effect is marked by a ~300 percent decrease in D_s^* (i.e., 2.38×10^{-10} m^2/s to 7.83×10^{-11} m^2/s) corresponding to a decrease in source KCl concentration, C_o, from 0.047 M to 0.0039 M. Based on these results, a restrictive tortuosity factor, τ_r, is defined and correlated with chemico-osmotic efficiency to account for solute restriction effects. The implications of these results are discussed within the context of predicting solute flux through waste containment barriers.

KEY WORDS: bentonite, chemico-osmosis, chemico-osmotic efficiency, coupled processes, geosynthetic clay liners, diffusion, effective diffusion coefficient, membrane behavior, tortuosity

4.1 INTRODUCTION

Geosynthetic clay liners (GCLs) commonly are used as components in engineered liners for hydraulic containment applications, such as landfills, surface impoundments, and waste piles (Gleason et al. 1997). Geosynthetic clay liners are factory-manufactured rolls consisting of thin layers (~ 5 to 10 mm) of bentonite clay (~ 5.0 kg/m^2) sandwiched between two geotextiles or bonded to a geomembrane. The structural integrity of a GCL is maintained by stitching or needle-punching through the geotextiles and bentonite, and/or by adding an adhesive compound to the bentonite to bind the bentonite to the geotextile or geomembrane. The primary differences among the GCLs currently available pertain to the mineralogy (e.g., montmorillonite content), type (e.g., sodium versus calcium), and form (e.g., powder versus granular) of the bentonite used in the GCL, the type of geotextile (e.g., woven versus non-woven geotextiles), and the nature of the structural integrity. The preferential use of GCLs in containment applications relative to other alternatives, such as compacted clay liners, stems primarily from economic considerations and the extremely low hydraulic conductivities to water (i.e., $\leq 5 \times 10^{-11}$ m/s) typically measured for these materials (Daniel 1993, Koerner 1994). Except in the case of a GCL that contains a geomembrane, the low hydraulic conductivity of GCLs is attributed to the bentonite component of the GCL and, therefore, the hydraulic performance of GCLs without geomembranes is governed by the bentonite component of the GCL.

While the use of GCLs in containment applications has been based primarily on the favorable hydraulic performance and economic considerations, other factors may be important in terms of the overall performance of GCLs in containment applications. In

particular, Rowe et al. (1997a) report that breakthrough of contaminants through GCLs could occur in less than one day as a result of solute (liquid-phase) diffusion. Also, Petrov et al. (1997) conclude that the premature arrival of a salt (2.0 N NaCl) front through a needle-punched GCL during permeation at low flow rates likely was due to the dominance of diffusive transport. Finally, Rowe et al. (1997b) measured effective diffusion coefficients, D^*, for chloride diffusing through a needle-punched GCL as part of an evaluation of the equivalency of two composite liner systems, a geomembrane over a GCL and geomembrane over a compacted clay liner. On the basis of consideration of the relative leakage through holes in the geomembrane, the clay-leachate compatibility, and the diffusion of contaminants, Rowe et al. (1997b) conclude that the two composite liner systems were essentially equivalent for the conditions assumed in the comparison. Thus, diffusion apparently is an important, if not dominant, process in determining the rate of aqueous miscible contaminant migration through GCLs.

Membrane behavior, or the ability of clay soils to impede the passage of solutes, also could affect contaminant migration through GCLs. Restricted passage of charged solutes (ions) through the pores of a clay soil is attributed to electrostatic repulsion of the ions by electric fields associated with the diffuse double layers of adjacent clay particles (e.g., Marine and Fritz 1981, Fritz and Marine 1983, Fritz 1986, Keijzer et al. 1997). Non-electrolyte solutes (uncharged species), such as aqueous miscible organic compounds, also may be restricted from migrating through clay soils when the size of the molecule is greater than pore size of the clay soil (Grathwohl 1998). In addition to restricting the passage of solutes, membrane behavior also results in chemico-osmosis, or the movement of liquid in response to a solute concentration gradient (e.g., Mitchell 1993).

The ability of sodium bentonite, in particular, to exhibit membrane behavior in the presence of common electrolytes (e.g., NaCl) has been illustrated extensively (e.g., Kemper and Rollins 1966, Kemper and Quirk 1972, Elrick et al. 1976, Fritz and Marine

1983, Keijzer et al. 1997). For example, Kemper and Rollins (1966) measured the chemico-osmotic membrane efficiency of compacted sodium bentonite pastes in the presence of NaCl and $CaCl_2$ solutions over a range of concentrations, and reported that the bentonite pastes exhibit membrane behavior that varies as a function of the soil porosity, electrolyte concentration, and ion valence. Elrick et al. (1976) also studied membrane behavior in saturated bentonite pastes exposed to NaCl solutions and concluded that the rate of salt migration is reduced due to the permi-selective properties of the bentonite. More recently, Sawatsky et al. (1997) attributed a reduced diffusive solute flux of napthalene, an aqueous miscible organic compound (non-electrolyte), through a montmorillonite-based shale to exclusion of the napthalene from the pore space. Sawatsky et al. (1997) conclude that the observed membrane behavior will act to enhance the ability of the clay to limit contaminant flux. Similar solute exclusion effects for a variety of inorganic solutes have been reported for studies involving the use of compacted sodium bentonites being considered for use as containment barriers for nuclear waste repositories (e.g., Murrinen 1990, Oscarson et al. 1992, Oscarson 1994, Oscarson and Hume 1994). Although the results of all of these studies indicate that bentonite-rich soils may exhibit membrane behavior (i.e., solute exclusion), and that this behavior can affect solute diffusion, no such membrane behavior has been reported for bentonite-based GCLs, and no correlation between membrane behavior and solute diffusion has been shown experimentally.

Based on the aforementioned considerations, the objective of this chapter is to evaluate the potential influence of membrane behavior on the diffusion of potassium chloride (KCl) through a GCL. The diffusion of KCl through a GCL is evaluated on the basis of the results of steady-state diffusion tests and coupled flux transport theory that accounts for the effects of membrane behavior on solute diffusion. Also, the correlation between the measured effective diffusion coefficients (D^*) for KCl at steady state and the measured chemico-osmotic efficiency coefficients (ω) is investigated. Finally, the

potential significance of the results is evaluated within the context of diffusive solute transport through low-permeability soil barriers typically used in containment applications.

4.2 THEORETICAL BACKGROUND

Consider a system in which two aqueous solutions are separated by a charged membrane. Each compartment may contain a different pressure (P), electrical potential (Ψ), chemical potential (μ^c), and/or solution temperature (T) such that hydraulic, electrical, chemical, and/or thermal gradients are maintained across the membrane. For the special case pertaining to isothermal conditions in which the soil solution contains a single cation species and a single anion species resulting from complete dissociation of a binary electrolyte (e.g., NaCl), the equations for simultaneous flux of liquid, electrical current, and ions may be written in terms of flux per unit *total* cross-sectional area (i.e., solids plus voids) as follows (Yeung 1990, Mitchell 1993, and Yeung and Mitchell 1993):

$$q = -\left(\frac{k_h}{\gamma_w} + \frac{k_e^2}{n\sigma_e^*}\right)\frac{dP}{dx} - k_e\frac{d\Psi}{dx} + \left(\frac{\omega C_c k_h}{\gamma_w} - \frac{k_e C_c u_c^*}{\sigma_e^*}\right)\frac{d\mu_c^c}{dx} + \left(\frac{\omega C_a k_h}{\gamma_w} + \frac{k_e C_a u_a^*}{\sigma_e^*}\right)\frac{d\mu_a^c}{dx} \quad (4.1a)$$

$$I = -k_e\frac{dP}{dx} - n\sigma_e^*\frac{d\Psi}{dx} - nC_c u_c^*\frac{d\mu_c^c}{dx} + nC_a u_a^*\frac{d\mu_a^c}{dx} \quad (4.1b)$$

$$J_{dc} = \left(\frac{\omega C_c k_h}{\gamma_w} - \frac{k_e C_c u_c^*}{\sigma_e^*}\right)\frac{dP}{dx} - nC_c u_c^*\frac{d\Psi}{dx} - \frac{nD_c^* C_c}{RT}\frac{d\mu_c^c}{dx} \quad (4.1c)$$

$$J_{da} = \left(\frac{\omega C_a k_h}{\gamma_w} + \frac{k_e C_a u_a^*}{\sigma_e^*}\right)\frac{dP}{dx} + nC_a u_a^*\frac{d\Psi}{dx} - \frac{nD_a^* C_a}{RT}\frac{d\mu_a^c}{dx} \quad (4.1d)$$

where q is liquid flux [Lt^{-1}], k_h is hydraulic conductivity [Lt^{-1}], γ_w is the unit weight of water [$Mt^{-2}L^{-2}$], k_e is electro-osmotic conductivity [$L^2t^{-1}V^{-1}$], σ_e^* is the effective electrical conductivity of the porous medium [Coulomb·$t^{-1}L^{-1}V^{-1}$], ω is the chemico-osmotic efficiency coefficient [dimensionless], C is molar solute concentration [mol·L^{-3}], u^* is effective ionic mobility [$L^2t^{-1}V^{-1}$], I is electrical current [Coulomb·$L^{-2}t^{-1}$], J_d is diffusive flux [mol·$L^{-2}t^{-1}$], D^* is the effective self-diffusion coefficient [L^2t^{-1}], R is the universal gas constant [8.314 J/mol·K], T is the absolute temperature, and the subscripts a and c represent the anion and cation, respectively. The "effective" coefficients (i.e., u^*, D^*, σ_e^*) account for the tortuous nature of the pathways for solute migration in soil systems and are related to the same coefficients in free solution as follows (e.g., see Alshawabkeh and Acar 1996):

$$\sigma_e^* = \tau_a \sigma_{eo} \; ; \qquad u^* = \tau_a u_o \qquad ; \qquad D^* = \tau_a D_o \tag{4.2}$$

where τ_a is the dimensionless apparent tortuosity factor (< 1) as defined by Shackelford and Daniel (1991).

The influence of soil membrane behavior on solute diffusion can be illustrated by considering a system in which no electrical current is applied across the soil. In this case, I = 0, and Eq. 4.1b can be rearranged to yield the following expression for the electrical potential gradient, $d\Psi/dx$:

$$\frac{d\Psi}{dx} = -\frac{k_e}{n\sigma_e^*}\frac{dP}{dx} - \frac{C_c u_c^*}{\sigma_e^*}\frac{d\mu_c^c}{dx} + \frac{C_a u_a^*}{\sigma_e^*}\frac{d\mu_a^c}{dx} \tag{4.3}$$

In addition, for dilute solutions (Yeung 1990, Yeung and Mitchell 1993):

$$\frac{d\mu_i^c}{dx} = \frac{RT}{C_i}\frac{dC_i}{dx} \tag{4.4}$$

Substitution of Eqs. 4.3 and 4.4 into Eqs. 4.1a, 4.1c, and 4.1d yields the following set of coupled flux equations:

$$q = q_h + q_\pi = -\frac{k_h}{\gamma_w}\frac{dP}{dx} + \frac{\omega k_h}{\gamma_w}\frac{d\pi}{dx} \tag{4.5a}$$

$$J_{dc} = \frac{\omega C_c k_h}{\gamma_w}\frac{dP}{dx} - n\left(D_c^* - \frac{C_c u_c^{*2} RT}{\sigma_e^*}\right)\frac{dC_c}{dx} - n\left(\frac{C_c u_c^* u_a^* RT}{\sigma_e^*}\right)\frac{dC_a}{dx} \tag{4.5b}$$

$$J_{da} = \frac{\omega C_a k_h}{\gamma_w}\frac{dP}{dx} - n\left(\frac{C_a u_c^* u_a^* RT}{\sigma_e^*}\right)\frac{dC_c}{dx} - n\left(D_a^* - \frac{C_a u_a^{*2} RT}{\sigma_e^*}\right)\frac{dC_a}{dx} \tag{4.5c}$$

where q_h [Lt^{-1}] represents hydraulic liquid flux in accordance with Darcy's law, q_π [Lt^{-1}] is chemico-osmotic liquid flux, and $d\pi/dx$ represents the gradient in chemico-osmotic pressure [$ML^{-2}t^{-2}$] in accordance with the differential form of the van't Hoff expression for dilute solutions, or

$$\frac{d\pi}{dx} = RT\left(\frac{dC_c}{dx} + \frac{dC_a}{dx}\right) \tag{4.6}$$

The chemico-osmotic liquid flux, q_π, represents the flux of liquid across a soil membrane from a lower solute concentration to a higher solute concentration, i.e., opposite to the direction of solute diffusion.

4.2.1 Diffusive Solute Flux

The effective ionic mobility of an ionic species i, u_i^*, is related to the effective self-diffusion coefficient, D_i^*, by the Nernst-Einstein equation as follows (Alshawabkeh and Acar 1996):

$$D_i^* = \frac{RTu_i^*}{|z_i|F} \tag{4.7}$$

where z_i is the valence of species i and F is Faraday's constant (96,485 C/mol of e^-). Also, the effective electrical conductivity, σ_e^*, of a soil solution containing a binary electrolyte is related to effective ionic mobility of each species in solution as follows (Alshawabkeh and Acar 1996):

$$\sigma_e^* = F\sum_{i=1}^{N} C_i|z_i|u_i^* \tag{4.8}$$

where N is the number of ionic species. Finally, the preservation of electroneutrality in solution results in the following relationship between the molar concentrations of the cation and the anion at any location in the system:

$$|z_c|C_c = |z_a|C_a \tag{4.9}$$

or, in differential form,

$$|z_c|\frac{dC_c}{dx} = |z_a|\frac{dC_a}{dx} \tag{4.10}$$

Substitution of Eqs. 4.7 through 4.10 into Eqs. 4.5b and 4.5c yields the following expressions for coupled diffusive flux of the cation and anion (e.g., Groenevelt et al. 1980)

$$J_{dc} = \frac{\omega C_c k_h}{\gamma_w}\frac{dP}{dx} - nD_s^*\frac{dC_c}{dx} \; ; \; J_{da} = \frac{\omega C_a k_h}{\gamma_w}\frac{dP}{dx} - nD_s^*\frac{dC_a}{dx} \qquad (4.11)$$

where the effective salt-diffusion coefficient, D_s^*, is given by the Nernst-Einstein expression (e.g., Robinson and Stokes 1959) modified for the tortuosity effect as follows:

$$D_s^* = \tau_a D_s = \tau_a \left\{\frac{RT}{F}\left[\frac{u_a u_c (|z_a| + |z_c|)}{(u_a + u_c)|z_a||z_c|}\right]\right\} \qquad (4.12)$$

The aqueous salt-diffusion coefficient, D_s, given in Eq. 4.12 is the same for both species, which is consistent with the requirement that the rate of diffusion of the cation and anion in an aqueous single-salt system must be the same to satisfy electroneutrality (e.g., Robinson and Stokes 1959). The identical diffusion rates of the cation and anion during salt-diffusion result from an electrical potential gradient generated between the cation and anion in response to different ionic mobilities that slows down the faster-moving ion and speeds up the slower moving ion. Therefore, the value of D_s represents an intermediate value between the effective self-diffusion coefficients D_a and D_c for the cation and anion, respectively (e.g., Shackelford and Daniel 1991).

However, the effective salt diffusion coefficient, D_s^*, as formulated by Eq. 4.12 is based on the explicit assumption that only one cation and one anion species are co-diffusing through the porous medium. Therefore, the use of Eq. 4.12 is valid only when (a) the porous medium is inert (i.e., no interaction with either chemical species), (b) there is no net exchange of either diffusing species with the porous medium (e.g., the cation

exchange sites of a clay soil are completely filled with the co-diffusing cation, and the anion is not sorbed), or (c) steady-state diffusive flux conditions have been reached.

The first term in Eqs. 4.11 is a diffusive coupling term that arises due to the soil membrane behavior, while the second term represents traditional diffusion in accordance with Fick's first law. The diffusive coupling term has been called *streaming current* (Mitchell 1993), *hyperfiltration* (de Marsily 1986), or *salt sieving* (McKelvey and Milne 1962, Groenevelt et al. 1980). If the soil exhibits no membrane behavior, then $\omega = 0$ and Eqs. 4.11 reduce to the traditional form for Fick's first law for the aforementioned conditions under which D_s^* is applicable (Shackelford and Daniel 1991). Equations 4.11 form the theoretical basis for the evaluation of the coupling of solute diffusion and chemico-osmosis for the GCL used in this study.

4.3 MATERIALS AND EXPERIMENTAL METHODS

4.3.1 Geosynthetic Clay Liner

The geosynthetic clay liner (GCL) tested in this study is sold commercially under the trade name Bentomat® (Colloid Environmental Technologies Company (CETCO), Lovell, WY). The Bentomat® GCL consists of a layer of granular sodium bentonite sandwiched between two non-woven polypropylene geotextiles held together by needle-punched fibers, as shown in Fig. 4.1. Grain-size analyses (ASTM D421, D422) indicate that the GCL bentonite consists of approximately 75 percent clay-, 19 percent silt-, and 6 percent sand-sized particles. The bentonite has a liquid limit (LL) of 478 percent and a plasticity index (PI) of 439 percent (ASTM D4318), and results of an X-ray diffraction analysis of the bentonite indicate that the predominant clay minerals are montmorillonite (71 %) and mixed illite/smectite (7 %).

The results of soil chemical measurements performed on the GCL bentonite using the procedures described by Shackelford and Redmond (1995) indicate a cation exchange capacity (CEC) of 47.7 meq/100 g, with the exchange complex consisting of

approximately 52 percent sodium (Na^+), 35 percent calcium (Ca^{2+}), 11 percent magnesium (Mg^{2+}), and 1 percent potassium (K^+). The measured soluble metals contents of the GCL bentonite were 4636 mg/kg Na, 443 mg/kg Ca, 407 mg/kg Mg, and 263 mg/kg K. The saturated-paste pH and electrical conductance (EC) at 25°C were measured as 9.35 and 200 mS/m, respectively.

4.3.2 Liquids

The liquids used in this study consist of a processed tap water (PTW) and solutions of PTW and potassium chloride (KCl) (certified A.C.S., Fisher Scientific, Fair Lawn, NJ) dissolved in PTW at measured KCl concentrations ranging from 0.0039 M to 0.047 M (290 mg/L to 3500 mg/L). The processed tap water (pH = 6.93; electrical conductance, EC, at 25°C = 0.32 mS/m) consists of tap water that is processed to remove ions by passage through three Barnstead® ion exchange columns placed in series. The chloride (Cl^-) concentrations in the KCl solutions were measured using ion chromatography (IC), whereas the potassium (K^+) concentrations were measured using inductively coupled plasma - optical emissions spectroscopy (ICP-OES). The measured pH of the KCl solutions ranged from 6.68 to 6.91, and the measured EC at 25°C for the KCl solutions ranged from 58.7 to 682 mS/m.

4.3.3 Testing Apparatus and Procedure

The testing cell used in this study, illustrated schematically in Fig. 4.2, consists of a rigid acrylic cylinder, base pedestal, and top piston that is used to control the void ratio of the soil specimen. The top piston and base pedestal are equipped with ports that enable circulation of separate chemical solutions at the specimen boundaries to establish and maintain a constant concentration difference across the specimen. Additional ports are installed in the top piston and base pedestal to allow for measurement of differential pressure across the specimen.

Tests are conducted by continuously circulating chemical solutions through the porous stones at the ends of the specimen using a flow-pump system consisting of a dual-carriage syringe pump (Model 944, Harvard Apparatus, South Natick, MA) equipped with two customized actuators (i.e., syringes). In general, chemical solutions containing different concentrations of a given solute are expelled from each of the two actuators at the same, constant rate via the plunger that is attached to the flow-pump drive, and subsequently infuse through the porous stones across the top and bottom boundaries of the specimen. Circulation outflow from these boundaries is simultaneously collected through the opposite (back) end of the actuator at the same rate in order to maintain a constant volume inside the testing cell (i.e., $\Delta V_{cell} = 0$) and prevent liquid flux through the soil (q=0). Under these no-flow conditions, the chemico-osmotic liquid flux, q_π, that occurs in a soil membrane in response to the applied concentration difference is balanced by an equal hydraulic liquid flux, q_h, in the opposite direction, resulting in the development of an induced pressure gradient, dP/dx. The relationship between this induced pressure gradient and the chemico-osmotic efficiency of the soil is given by substituting q = 0 into Eq. 4.5a, or (Groenevelt et al. 1980, Malusis et al. 2000):

$$\left.\frac{dP}{dx}\right|_{q=0} = \omega \frac{d\pi}{dx} \tag{4.13}$$

The generation of an induced pressure gradient across fine-grained soil specimens under q = 0 conditions in a closed system previously has been shown experimentally (Olsen 1969, Keijzer et al. 1997, Malusis et al. 2000).

In the present case, a source KCl solution is circulated through the top piston such that $C_{ot} > 0$ while PTW is circulated through the base pedestal such that $C_{ob} = 0$. The resulting differences in solute (Cl^- and K^+) concentrations between the top and bottom boundaries of the specimen also result in solute diffusion from the higher concentration boundary (top) to the lower concentration boundary (bottom) such that there is a loss of

solute mass from the circulated source solution and a gain in solute mass in the circulated PTW. As a result, the solute concentration in the circulation outflow from the top piston, C_t, is lower than the solute concentration in the source solution (i.e., $C_t < C_{ot}$), while the solute concentration in the circulation outflow from the base pedestal, C_b, is greater than the solute concentration in the PTW, i.e., $C_b > C_{ob} = 0$ (see Fig. 4.2). The collected circulation outflow is stored for subsequent chemical analysis (e.g., pH, electrical conductance, solute concentrations). All actuator parts and tubing used to circulate the solutions were constructed with grade 316 stainless steel to minimize corrosion in the presence of strong electrolytes and to minimize volume change in the system. Additional details regarding the apparatus and components are provided by Malusis et al. (2000).

4.3.4 Specimen Preparation

Circular specimens of the Bentomat® GCL were cut from a larger GCL sheet, placed on base pedestal inside the testing cell, and submerged in PTW. The top piston was lowered to compress the GCL to the desired thickness, and locked in place to prevent volume expansion of the specimens due to swelling of the bentonite. Each specimen was permeated under backpressure with PTW to saturate the specimen, remove excess soluble salts, and measure initial hydraulic conductivity.

4.3.5 Determination of Chemico-Osmotic Efficiency

Based on the above described testing procedure, the chemico-osmotic efficiency coefficient, ω, is determined in accordance with Eq. 4.13, or (e.g., Malusis et al. 2000):

$$\omega = \left.\frac{\Delta P}{\Delta \pi}\right|_{q=0} \tag{4.14}$$

where ΔP is the measured differential pressure induced across the specimen as a result of prohibiting chemico-osmotic flux of solution, and $\Delta \pi$ is the theoretical chemico-osmotic

pressure difference across an "ideal" semi-permeable membrane (i.e., $\omega = 1$) subjected to an applied difference in solute (KCl) concentration (e.g., Olsen et al. 1990). The induced differential pressure, ΔP, in Eq. 4.14 is measured using a differential pressure transducer (Model DP15, Validyne Engineering Sales Corp., Northridge, CA) that is located as shown in Fig. 4.2.

The chemico-osmotic pressure difference, $\Delta\pi$, in Eq. 4.14 can be computed based on the solute concentrations in the opposite specimen boundaries in accordance with the van't Hoff expression (e.g., see Malusis et al. 2000). Since $C_t < C_{ot}$ and $C_b > C_{ob}$ due to solute diffusion, the average boundary concentrations of a solute species i, $\overline{C}_{t,i}$ and $\overline{C}_{b,i}$, may be defined as follows:

$$\overline{C}_{t,i} = \frac{C_{ot,i} + C_{t,i}}{2} \quad ; \quad \overline{C}_{b,i} = \frac{C_{ob,i} + C_{b,i}}{2} \tag{4.15}$$

Based on these average concentrations, the average chemico-osmotic pressure difference, $\overline{\Delta\pi}$, can be expresed as follows (Malusis et al. 2000):

$$\overline{\Delta\pi} = RT\sum_{i=1}^{N}\left(\overline{C}_{t,i} - \overline{C}_{b,i}\right) \tag{4.16}$$

4.3.6 Determination of Effective Diffusion Coefficients

The determination of the effective diffusion coefficient, D^*, is based on the solute concentrations measured in the circulation outflow from the lower concentration boundary (i.e., the base pedestal) during the test in a similar manner to that previously described by Jessberger and Onnich (1994). This approach to measuring D^* commonly is referred to as the steady-state approach (e.g., see Shackelford 1991).

In the steady-state approach, the measured concentrations of a given solute species in the collection (exit) reservoir, C_e, typically are converted to cumulative mass per unit cross-sectional area, Q_t [ML^{-2}], or

$$Q_t = \int_0^t w_A J_d dt = \frac{1}{A}\sum_{j=1}^{N_t} \Delta m_j = \frac{1}{A}\sum_{j=1}^{N_t} C_{ej} w_A \Delta V_j \qquad (4.17)$$

where w_A is the atomic weight of the solute [$M \cdot mol^{-1}$], Δm_j [M] is the incremental mass of the solute collected over time increment j, C_{ej} [$mol \cdot L^{-3}$] is the concentration of the solute in the incremental volume, ΔV_j [L^3], of collected solution, and N_t is the number of incremental samples corresponding to the total elapsed time, t. The results are plotted in terms of Q_t versus t, as illustrated in Fig. 4.3. The curved portion of the example plot in Fig. 4.3 represents transient diffusion, while the linear portion of the data represents steady-state diffusion (Shackelford 1991). The slope of the steady-state portion of the data in Fig. 4.3, $\Delta Q_t/\Delta t$, is related to the diffusive solute flux as follows based on Eq. 4.17:

$$\frac{\Delta Q_t}{\Delta t} = w_A J_d \qquad (4.18)$$

For the special condition of no net liquid flux imposed in this study, the general expressions for diffusive flux of the cation and anion given by Eqs. 4.11 may be modified by substitution of the expression for the induced pressure gradient given by Eq. 4.13 as follows:

$$J_{dc} = \frac{\omega^2 C_c k_h}{\gamma_w}\frac{d\pi}{dx} - nD_s^*\frac{dC_c}{dx} \; ; \; J_{da} = \frac{\omega^2 C_a k_h}{\gamma_w}\frac{d\pi}{dx} - nD_s^*\frac{dC_a}{dx} \qquad (4.19)$$

or, upon substitution of Eqs. 4.6 and 4.10 and rearrangement,

$$J_{dc} = -nD_{\omega}^{*}\frac{dC_c}{dx} \; ; \; J_{da} = -nD_{\omega}^{*}\frac{dC_a}{dx} \tag{4.20}$$

where D_{ω}^{*} represents a coupled effective diffusion coefficient given by

$$D_{\omega}^{*} = D_s^{*} - \frac{\omega^2(C_a + C_c)k_h RT}{n\gamma_w} \tag{4.21}$$

Based on Eq. 4.21, the coupled effective diffusion coefficient, D_{ω}^{*}, always is less than D_s^{*} when $\omega > 0$ due to the salt-sieving associated with the membrane behavior of the soil. Thus, when a clay soil exhibits membrane behavior, the diffusive fluxes given by Eqs. 4.18 will be less than the fluxes given by Fick's first law in which D_s^{*} is used rather than D_{ω}^{*}. However, $D_{\omega}^{*} = D_s^{*}$ based on Eq. 4.21 for a soil that exhibits no membrane behavior (i.e., $\omega = 0$).

In the case where the boundary concentrations are maintained essentially constant, Eqs. 4.18 may be written as follows for steady-state diffusion:

$$J_{dc} = -nD_{\omega}^{*}\frac{\Delta C_c}{\Delta x} \quad ; \quad J_{da} = -nD_{\omega}^{*}\frac{\Delta C_a}{\Delta x} \tag{4.22}$$

where the coupled effective diffusion coefficient is written as

$$D_{\omega}^{*} = D_s^{*} - \frac{\omega^2(\overline{C}_a + \overline{C}_c)k_h RT}{n\gamma_w} \tag{4.23}$$

and the concentrations $\overline{C}_c$ and $\overline{C}_a$ represent arithmetic mean concentrations across the membrane, i.e., $\overline{C} = (C_o + C_e)/2$ (Katchalsky and Curran 1965, Fritz 1986, Whitworth and Fritz 1994).

In terms of the steady-state approach, substitution of the general form of Eq. 4.22 into Eq. 4.18 and rearrangement yields the following expression for the coupled effective diffusion coefficient, D_ω^*, for the salt:

$$D_\omega^* = -\left(\frac{\Delta Q_t}{\Delta t}\right)\frac{L}{n w_A \Delta C} \tag{4.24}$$

The slope, $\Delta Q_t/\Delta t$, in Eq. 4.24 can be determined by best-fit linear regression of the steady-state data. The true effective diffusion coefficient, D_s^*, then is determined by substituting D_ω^* obtained from Eq. 4.24 into Eq. 4.23.

4.3.7 Testing Program

Four diffusion tests were conducted in this study. In each test, the thickness, L, of the GCL specimen was 1.0 cm. The porosity, n, of the specimens ranged between 0.78 and 0.80. A different source KCl concentration, C_{ot}, was used in each test (i.e., C_{ot} = 0.0039 M, 0.0087 M, 0.020 M, and 0.047 M) in order to evaluate the influence of solute concentration on measured values of D^*. Values of C_b were measured using inductively coupled plasma-optical emissions spectroscopy (ICP-OES) for K^+ and ion chromatography (IC) for Cl^-. In addition, electrical conductance (EC) and pH of the circulated solutions at both the top and bottom specimen boundaries were monitored.

4.4 RESULTS

4.4.1 Chemico-osmotic Efficiency Coefficients (ω)

The measured differential pressures induced across the GCL specimens, $-\Delta P$ (> 0), during the diffusion tests are shown in Fig. 4.4. Before introduction of the KCl, PTW was circulated at both specimen boundaries (i.e., $C_{ot} = C_{ob} = 0$) for five days to establish a baseline differential pressure, $-\Delta P_o$. Measured values of $-\Delta P_o$ ranged between 0.62 kPa and 4.0 kPa in the four tests. Introduction of KCl into the top piston after the initial five

days resulted in steady-state values of induced differential pressure, $-\Delta P_{ss}$, ranging from 14.1 kPa to 32.0 kPa. The difference between $-\Delta P_{ss}$ and $-\Delta P_o$ represents the "effective" induced differential pressure, $-\Delta P_e$ (i.e., $-\Delta P_e = -\Delta P_{ss} - (-\Delta P_o)$), that is due solely to the membrane behavior of the GCL (see Malusis et al. 2000). Values of $-\Delta P_e$ in the four tests were 11.5 kPa, 19.7 kPa, 27.8 kPa, and 28.0 kPa, respectively, as shown in Fig. 4.4. The effective induced differential pressure values were used in Eq. 4.14 to calculate ω (i.e., $\Delta P = \Delta P_e$).

The differences in chemico-osmotic pressure, $-\Delta\pi$, across the GCL specimens due to the applied concentration differences of 0.0039 M, 0.0087 M, 0.02 M, and 0.047 M were 18.4 kPa, 39.9 kPa, 86.4 kPa, and 201 kPa, respectively. These values of $-\Delta\pi$ have been corrected to account for slight changes in the boundary concentrations due to diffusion (e.g., see Malusis and Shackelford 2000).

Values of ω based on Eq. 4.14 corresponding to C_{ot} = 0.0039 M, 0.0087 M, 0.02 M, and 0.047 M are 0.63, 0.49, 0.32, and 0.14, respectively, as shown in Fig. 4.5. Based on these results, it is apparent that the GCL exhibited membrane behavior in the presence of the KCl solutions during the diffusion tests. The decrease in ω with increasing salt concentration is consistent with results of previous studies (Kemper and Rollins 1966, Olsen 1969, Kemper and Quirk 1972), and is attributed to collapse of the adsorbed layers (i.e., diffuse double layers) of water and ions surrounding the clay particles caused by the higher ion concentrations in the pore space (Fritz 1986). The trend of the data in Fig. 4.5, when extrapolated to concentrations beyond the highest source concentration used in this study (i.e., $C_{ot} > 0.047$ M), indicates that the GCL is expected to exhibit virtually no chemico-osmotic membrane efficiency at concentrations beyond approximately 0.08 M (i.e., $\omega \rightarrow 0$ as $C_{ot} \rightarrow 0.08$ M KCl).

4.4.2 Diffusion Results

Measured exit concentrations of Cl^- and K^+ from the base pedestal (i.e., C_b) are illustrated versus time in Fig. 4.6. Essentially constant values of C_b eventually are obtained in each test as steady-state diffusion is achieved. Greater values of C_b at steady state correspond to greater values of the source concentration, C_{ot}, since a greater C_{ot} results in a greater rate of diffusion through the soil. The results also indicate that steady-state diffusion is achieved more rapidly for Cl^- than for K^+ apparently due to cation exchange of the reactive K^+.

The resulting plots of Q_t versus time for Cl^- and K^+ based on the measured concentrations in Fig. 4.6 are illustrated in Figs. 4.7 and 4.8, respectively. The slopes of the steady-state portion of the data, $\Delta Q_t/\Delta t$, based on best-fit linear regression of the steady-state data range from 0.000784 to 0.0263 $mg/m^2/s$ for Cl^- and 0.000538 to 0.0275 $mg/m^2/s$ for K^+. The increase in $\Delta Q_t/\Delta t$ with increasing source concentration, C_{ot}, indicates an increase in solute flux through the soil based on Eq. 4.18. The x-intercept of the linear fit through the steady-state data represents the time lag, T_L, that provides a measure of the attenuation of the solute due to ion exchange during transport through the soil. Values of T_L for the reactive K^+ (321.8 hr to 737.6 hr) are considerably greater than values of T_L for the non-reactive Cl^- (24.8 hr to 51.3 hr) as expected on the basis of cation exchange.

4.4.3 Effective Diffusion Coefficients (D^*)

Values of the coupled salt-diffusion coefficient, D^*_ω, and the "true" salt-diffusion coefficient, D^*_s, based on the Cl^- and K^+ data in Figs. 4.7 and 4.8, respectively, are given in Table 4.1. As previously indicated, D^*_s should be the same for both K^+ and Cl^- at steady state, in accordance with the requirement for electroneutrality in solution. In this study, values of D^*_s based on the Cl^- data are essentially equivalent to D^*_s based on the K^+ data in three of the four tests, as shown in Fig. 4.9. In the test with the lowest source

concentration (C_{ot} = 0.0039 M), D_s^* based on the K^+ data (i.e., D_s^* = 5.17 x 10^{-11} m/s) is slightly lower than D_s^* based on the Cl^- data (i.e., D_s^* = 7.83 x 10^{-11} m/s). This particular test had the longest duration (48 days) and may not have quite reached steady-state conditions with respect to diffusion of the reactive K^+. However, steady-state transport of Cl^- was achieved in all four tests (see Fig. 4.6a). Therefore, values of D_s^* and D_ω^* based on the Cl^- data are considered for the remainder of this discussion.

As mentioned earlier, the coupled effective diffusion coefficient, D_ω^*, for a salt in a soil that exhibits no membrane behavior (i.e., $\omega = 0$) theoretically is equal to the true effective diffusion coefficient, D_s^*, for the salt based on Eq. 4.23. However, the results in Table 4.1 indicate that, as expected, $D_\omega^* < D_s^*$ for all tests in this study due to the salt-sieving associated with the membrane behavior of the GCL. This relationship between D_ω^* and D_s^* (based on the Cl^- data) is illustrated in Fig. 4.10a. Values of D_ω^*, in essence, represent the values that would be obtained by analyzing the test data using Fick's law that inherently assumes $\omega = 0$. Therefore, effective salt-diffusion coefficients previously reported for sodium bentonites and/or other clay soils that typically are evaluated from test data based on Fick's law represent coupled coefficients (i.e., D_ω^*) rather than true coefficients (i.e., D_s^*) unless the soil is shown to exhibit no chemico-osmotic efficiency (i.e., $\omega = 0$). The error associated with using Fick's law to evaluate the true coefficient D_s^* for the GCL tested in this study, illustrated in Fig. 4.10b, increases with increasing chemico-osmotic efficiency. However, for practical purposes, the error in all cases is relatively small (i.e., < 10%).

4.5 DISCUSSION

4.5.1 Relationship Between D_s^* and ω

The more significant aspect of the influence of membrane behavior on the diffusion results in Table 4.1 is the apparent dependence of D_s^* and D_ω^* on the source KCl concentration (C_{ot}) used in the tests. The measured values of D_s^*, plotted versus C_{ot}

in Fig. 4.11a, increase by approximately 300 percent (i.e., from 7.83 x 10^{-11} m/s to 2.38 x 10^{-10} m/s) as C_{ot} increases from 0.0039 M to 0.047 M. Similar results are shown for D_{ω}^{*}. This increase in D_s^{*} and D_{ω}^{*} with increasing source KCl concentration may be related to the observed decrease in chemico-osmotic efficiency of the GCL with increasing source KCL concentration (see Fig. 4.5). For example, the measured values of D_s^{*} and D_{ω}^{*} based on the four different source concentrations, C_{ot}, are plotted versus the corresponding measured values of ω in Fig. 4.11b. These results illustrate that D_s^{*} and D_{ω}^{*} increase as the chemico-osmotic efficiency of the GCL decreases.

While the apparent relationship between D_{ω}^{*} (or D_s^{*}) and ω in Fig. 4.11b has not been shown in previous experimental studies, these results reflect the expected behavior of clay membranes based on the current understanding of the mechanisms associated with ion restriction in soil systems. For example, the degree of ion restriction is greatest when the double layers of adjacent clay particles overlap in the pore space, leaving no "free" solution for solute transport (Marine and Fritz 1981). In this case, the membrane is considered an "ideal" membrane such that $\omega = 1$. Since no solute transport can occur through an "ideal" membrane, $J_d = 0$ and, thus, $D_{\omega}^{*} = 0$ based on Eq. 4.22. In reality, clay soils are "non-ideal" membranes, since ω typically falls within the range $0 < \omega < 1$. The double layers of a "non-ideal" membrane extend over only a portion of the pore space, and ions travel through the remaining "free" solution such that $D_{\omega}^{*} > 0$.

The higher ion concentrations in the pore space associated with an increase in the source concentration, C_{ot}, causes contraction of the diffuse double layers that results in a decrease in chemico-osmotic efficiency and a corresponding increase in D_{ω}^{*} as more "free" solution is available for solute transport. If the solute concentration is sufficiently high that the diffuse double layers are contracted to the extent that $\omega = 0$, then D_{ω}^{*} would equal D_s^{*} and also would approach a maximum value. The estimated maximum value of D_{ω}^{*} (= D_s^{*}) at $\omega = 0$ in this study is ~ 2.4 x 10^{-10} m^2/s based on extrapolation of the measured trends in Fig. 4.11b.

Higher values of D_ω^* represent a less tortuous pathway for solute migration. Therefore, an increase in D_ω^* represents an increase in the apparent tortuosity factor, τ_a, as shown in Fig. 4.12a. These values of τ_a were computed based on the values of D_ω^* and D_S^* using Eq. 4.2, assuming that the salt-diffusion coefficient for KCl in free solution, D_{so} = 19.93 x 10^{-10} m^2/s at 25 °C (e.g., see Robinson and Stokes 1959, Shackelford and Daniel 1991). Values of τ_a based on D_ω^* are similar to the values of τ_a based on D_S^* since there is little difference between D_ω^* and D_S^* in this study (see Fig. 4.11).

While the correlation between τ_a and ω based on the experimental results extends only within the range $0.14 < \omega < 0.69$, the expected trend for higher values of ω is shown in Fig. 4.12a based on extrapolation of the data, since by definition τ_a must approach zero as ω approaches unity (i.e., as $\omega \rightarrow 1$, $\tau_a \rightarrow 0$). Conversely, τ_a is expected to approach a maximum value when the chemico-osmotic efficiency is zero (i.e., $\omega = 0$). The estimated maximum value τ_a at $\omega = 0$ is ~0.12 based on extrapolation of the measured trends in Fig. 4.12a. The threshold source concentration corresponding to $\omega = 0$ is not known exactly, but appears to be at least 0.08 M based on extrapolation of the data in Fig. 4.5. However, the relationships between τ_a, ω, and C_{ot} given in Figs. 4.5 and 4.12 likely are unique for the GCL and testing conditions used in this study.

4.5.2 Restrictive Tortuosity Factor

Based on Shackelford and Daniel (1991), τ_a may be defined as the product of a matrix tortuosity factor, τ_m ($0 \leq \tau_m \leq 1$), representing the tortuous nature of the actual diffusive pathways through the porous medium due to the geometry of the interconnected pores, and a generalized restrictive tortuosity factor, τ_r ($0 \leq \tau_r \leq 1$), or

$$\tau_a = \tau_m \tau_r = \prod_{i=1}^{N} \tau_i = \tau_m (\tau_1 \cdot \tau_2 \cdots \tau_N) \tag{4.25}$$

where τ_r represents the product of N other factors (τ_i) that contribute to the apparent tortuosity by acting to reduce or restrict the diffusive mass flux of solutes through the porous medium. For example, Kemper et al. (1964) included a factor, α ($= \tau_r$), to account for the reduction in diffusive mass transport due to the increased viscosity of the water adjacent to the clay mineral surfaces (i.e., the adsorbed water) relative to that of the bulk water. Kemper and van Schaik (1966) included both α and γ (i.e., $\tau_r = \alpha\gamma$), where γ is a factor to account for anion exclusion resulting from the existence of membrane behavior for electrolytes. Porter et al. (1960) lumped these two effects into a single factor, also represented by γ, such that $\tau_r = \gamma$, presumably due to the difficulty associated with distinguishing between the effects of viscosity and anion exclusion. Finally, in the case of the exclusion of aqueous phase organic compounds (non-electrolytes) from soil pores, $\tau_r = \delta$, where δ is referred to as a 'constrictivity factor' (e.g., Grathwohl 1998).

At $\omega = 0$, the diffuse double layers surrounding the clay particles likely are sufficiently compressed that both ion exclusion and viscosity effects are negligible. Based on this assumption, the restrictive tortuosity factor, τ_r, is unity (i.e., $\tau_r = 1$), and the matrix tortuosity factor, τ_m, is represented by the maximum value of τ_a as given by Fig. 4.12a, or

$$\tau_m = \tau_{a,max} = \tau_a\Big|_{\omega=0} \tag{4.26}$$

The resulting expression for the restrictive tortuosity factor, τ_r, is obtained by substitution of Eq. 4.26 into Eq. 4.25 to yield

$$\tau_r = \frac{\tau_a}{\tau_m} = \frac{\tau_a}{\tau_{a,max}} \tag{4.27}$$

Since each GCL tested in this study had a similar porosity (i.e., $0.78 \leq n \leq 0.80$), $\tau_m \approx 0.12$ for all specimens.

Values of τ_r based on Eq. 4.27 and $\tau_m = 0.12$ are plotted versus the chemico-osmotic efficiency coefficient, ω, in Fig. 4.12b. The results indicate that τ_r decreases (i.e., the migration pathway is more tortuous) as ω increases. This decrease in τ_r likely is due to increased ion restriction and/or increased viscosity effects associated with greater thickness of diffuse double layers surrounding the clay particles, since no distinction can be made between these two individual effects.

The validity of the use of Eq. 4.27 or. more specifically, use of the relationship between τ_m and $\tau_{a,max}$ in Eq. 4.26 to evaluate τ_r in the manner described above warrants further investigation, since no other correlations between τ_a and ω have been evaluated in previous diffusion studies on GCLs, bentonites, or other clay soils. However, the potential influence of solute concentration on measured effective diffusion coefficients has been examined in previous experimental studies on bentonites and GCLs (e.g., Cho et al. 1993, Lake and Rowe 2000, Rowe et al. 2000). For example, Cho et al. (1993) measured D^* for cesium (Cs^+) in Avonlea bentonite (i.e., 80% sodium montmorillonite) subjected to source concentrations (C_o) of 3.8×10^{-8} M and 3.8×10^{-6} M and reported values of D^* ranging from 2.9×10^{-12} m^2/s to 3.2×10^{-11} m^2/s. Although the higher values of D^* in this range were obtained using the higher of the two C_o values, Cho et al. (1993) concluded that the effect of source concentration was insignificant based on a statistical analysis of the data.

Lake and Rowe (2000) also investigated the influence of source concentration on effective diffusion coefficients for NaCl under constant volume conditions in granular sodium bentonite extracted from a GCL (Bentofix® B4000) by conducting a four-stage diffusion test on a single specimen ($n = 0.71$). The source NaCl concentrations in the four stages were 0.08 M (4.6 g/L), 0.16 M (9.1 g/L), 0.60 M (35.1 g/L), and 2.0 M (114.3 g/L). The values of D^* obtained by Lake and Rowe (2000), based on the average of D^*

values reported individually for Na^+ and Cl^-, are plotted versus the source concentration, C_o, in Fig. 4.13. These values of D^* should be considered D^*_ω values, since Lake and Rowe (2000) did not account for membrane effects in the analysis. Therefore, the D^*_ω values obtained in this study are shown in Fig. 4.13 for comparison. The results in Fig. 4.13 indicate that a similar trend of increasing D^*_ω with increasing C_o was obtained by Lake and Rowe (2000) relative to the results obtained in this study. Although Lake and Rowe (2000) did not report chemico-osmotic efficiency coefficients, the results in Fig. 4.5 suggest that membrane behavior probably wasn't significant for the range of NaCl concentrations used in their study (i.e., $C_o \varepsilon 0.08$ M). However, the relationship between ω and C_o for the granular bentonite tested by Lake and Rowe (2000) may not be the same as the relationship in Fig. 4.5 due, in part, to the different porosity of the specimens (n = 0.78 to 0.80 versus n = 0.71), different salts used in the tests (KCl versus NaCl), and the potentially different properties of the granular bentonites in the two GCLs (Bentomat® versus Bentofix® B4000).

4.5.3 Practical Significance of Results

The influence of diffusion on the transport of miscible contaminants through clay barriers has received growing attention in recent years due to increasing evidence suggesting that diffusion can be an important, if not dominant, transport mechanism in waste containment applications (e.g., Shackelford 1988). In these applications, steady-state diffusive flux of a solute typically is assumed to occur in accordance with Fick's first law, and the effective diffusion coefficient, D^*, is assumed to be constant regardless of the solute concentration. However, the results of this study suggest that prediction of steady-state diffusive flux through a clay barrier material that exhibits membrane behavior may be accurate only when the analysis is based on the value of D^* corresponding to the concentration level of the contaminants.

For example, the theoretical steady-state diffusive KCl flux, J_d, through the GCL in this study based on Eq. 20 is shown in Fig. 4.14 versus the concentration difference across the GCL, ΔC, based on a constant D^*_ω ($= D^*_s$) = 2.4 x 10^{-10} m^2/s corresponding to $\omega = 0$ in Fig. 4.11b. This value theoretically would be the same for all ΔC in the absence of membrane behavior. Values of J_d obtained using Eq. 20 based on the actual, concentration-dependent values of D^*_ω from Table 2 also are shown in Fig. 4.14 for comparison. The results indicate that the use of D^*_ω = 2.4 x 10^{-10} m^2/s overestimates J_d except in the higher range of ΔC that corresponds to a lower chemico-osmotic efficiency.

The source concentration of contaminants contained by an actual soil barrier may not be known *a priori*. Also, performance of multiple diffusion tests for different values of C_o to obtain a trend of D^*_ω versus C_o such as that shown in Fig. 11a for an actual soil barrier typically is not practical from an economic standpoint. However, the results in Fig. 4.14 suggest that prediction of diffusive solute flux based on a single value of D^*_ω will yield conservative estimates as long as the D^*_ω value used in the analysis corresponds to a concentration level sufficiently high that membrane behavior is negligible.

4.6 CONCLUSIONS

The influence of membrane behavior on the diffusion of potassium chloride (KCl) through a geosynthetic clay liner (GCL) containing sodium bentonite is investigated. This behavior is evaluated on the basis of the results of steady-state diffusion tests under no-flow conditions in which measured effective salt-diffusion coefficients (D^*_s) are determined using coupled flux transport theory. The diffusion tests are conducted on 1.0-cm thick specimens with source KCl concentrations ranging from 0.0039 M to 0.047 M.

Comparison of the coupled flux transport theory with Fick's law indicates that the use of Fick's law to evaluate diffusion test data *in lieu* of the coupled flux theory results in the determination of a coupled effective salt-diffusion coefficient, D^*_ω, that is less than

the true coefficient, D_s^*, when the soil exhibits chemico-osmotic efficiency (i.e., $\omega > 0$). This difference is attributed to a coupling effect (i.e., salt-sieving) that is described by the coupled flux transport theory. In this study, the difference between measured values of D_ω^* and D_s^* for the GCL increases with increasing chemico-osmotic efficiency but does not exceed 10 percent for the range of source KCl concentrations tested. Therefore, the influence of salt-sieving is not significant in this study.

The test results also indicate that a second, implicit (or indirect) coupling effect occurs in the diffusion tests that is characterized by a concentration-dependent decrease in D_s^*. This indirect coupling causes a decrease in D_s^* from 2.38×10^{-10} m^2/s to 7.83×10^{-11} m^2/s as the source KCl concentration, C_o, decreases from 0.047 M to 0.0039 M, which correlates with an increase in the chemico-osmotic efficiency coefficient (ω) from 0.14 to 0.63. These results reflect the expected behavior of clay membranes based on the current understanding of the mechanisms associated with ion restriction in soil systems. The lower ion concentrations in the pore space associated with a decrease in the source KCl concentration causes expansion of the diffuse double layers that results in an increase in chemico-osmotic efficiency and a corresponding decrease in D_s^* since less of the pore space is available for solute transport.

Based on these results, a restrictive tortuosity factor, τ_r, is defined and correlated with the chemico-osmotic efficiency coefficient, ω, to account for solute restriction effects. Determination of τ_r is based on the premise that the tortuosity factor in the absence of membrane behavior (i.e., $\omega = 0$) is a maximum and can be represented as the matrix tortuosity factor, τ_m, that is due solely to the geometry of the interconnected pores.

The implications of the indirect coupling effect for predicting diffusive solute flux through a GCL in waste containment applications is considered based on a steady-state analysis using the D_ω^* values obtained in this study. The results of this analysis indicates that prediction of steady-state diffusive flux through a clay barrier material that exhibits membrane behavior may be accurate only when the analysis is based on the value of D_ω^*

corresponding to the concentration level of the contaminants being contained. If this concentration level is not known, prediction of diffusive solute flux based on a single value of D_ω^* will yield conservative estimates as long as the D_ω^* value used in the analysis corresponds to a sufficiently high concentration level that membrane behavior can be neglected.

4.7 REFERENCES

Alshawabkeh, A. N. and Acar, Y. B (1996). "Electrokinetics remediation. II: Theoretical model." *Journal of Geotechnical and Geoenvironmental Engineering*, ASCE, 122(3), 186-196.

Cho, W. J., Oscarson, D. W., Gray, M. N., and Cheung, S. C. H. (1993). "Influence of diffusant concentration on diffusion coefficients in clay." *Radiochimica Acta*, 60, 159-163.

Daniel, D. E. (1993). "Clay liners." Chapter 7, *Geotechnical Practice for Waste Disposal*, D.E. Daniel, ed., Chapman and Hall, New York, 137-163.

de Marsily, G. (1986). *Quantitative Hydrogeology*. Academic Press, Orlando, FL.

Elrick, D. E., Smiles, D. E., Baumgartner, N., and Groenevelt, P. H. (1976). "Coupling phenomena in saturated homo-ionic montmorillonite: I. Experimental." *Soil Science Society of America Journal*, 40(4), 490-491.

Fritz, S. J. (1986). "Ideality of clay membranes in osmotic processes: A review." *Clays and Clay Minerals*, 34(2), 214-223.

Fritz, S. J., and Marine, I. W. (1983). "Experimental support for a predictive osmotic model of clay membranes." *Geochimica et Cosmochimica Acta*, 47, 1515-1522.

Gleason, M. H., Daniel, D. E., and Eykholt, G. R. (1997). "Calcium and sodium bentonite for hydraulic containment applications." *Journal of Geotechnical and Geoenvironmental Engineering*, ASCE, 123(5), 438-445.

Grathwohl, P. (1998). *Diffusion in Natural Porous Media, Contaminant Transport, Sortpion/Desorption and Dissolution Kinetics*. Kluwer Acadaemic Publ., Norwell, Massachusetts, 207 p.

Groenevelt, P. H, Elrick, D. E., and Laryea, K. B. (1980). "Coupling phenomena in saturated homo-ionic montmorillonite: IV. The dispersion coefficient." *Soil Science Society of America Journal*, 44(6), 1168-1173.

Jessberger, H. L. and Onnich, K. (1994). "Determination of pollutant transport parameters by laboratory testing." *Proceedings, XIIIth ICSMFE*, New Delhi, India, 1547-1552.

Katchalsky, A., and Curran, P. F. (1965). *Nonequilibrium Thermodynamics in Biophysics*. Harvard University Press, Cambridge, MA, 248 p.

Keijzer, Th. J. S., Kleingeld, P. J., and Loch, J. P .G. (1997). "Chemical osmosis in compacted clayey material and the prediction of water transport." *Geoenvironmental Engineering, Contaminated Ground: Fate of Pollutants and Remediation*, R. N. Yong and H. R. Thomas, eds., Thomas Telford Publ., London, 199-204.

Kemper, W. D., Maasland, D. E. L., and Porter, L. K. (1964). "Mobility of water adjacent to mineral surfaces." *Soil Science Society of America Proceedings*, 28(2), 164-167.

Kemper, W. D. and Quirk, J. P. (1972). "Ion mobilities and electric charge of external clay surfaces inferred from potential differences and osmotic flow." *Soil Science Society of America Proceedings*, 36, 426-433.

Kemper, W. D. and Rollins, J. B. (1966). "Osmotic efficiency coefficients across compacted clays." *Soil Science Society of America Proceedings*, 30, 529-534.

Kemper, W. D. and van Schaik, J. C. (1966). "Diffusion of salts in clay-water systems." *Soil Science Society of America Proceedings*, 30, 534-540.

Koerner, R. M. (1994). *Designing with Geosynthetics*, 3rd Ed., Prentice-Hall, Englewood Cliffs, N. J., 783 p.

Lake, C. and Rowe, R.K. (2000). "Diffusion of sodium and chloride through geosynthetic clay liners." *Geotextiles and Geomembranes*, 18(2-4), 103-131.

Malusis, M. A. and Shackelford, C. D. (2000). "Chemico-osmotic efficiency of a geosynthetic clay liner." *Journal of Geotechnical and Geoenvironmental Engineering*, ASCE, in review.

Malusis, M. A., Shackelford, C. D., and Olsen, H. W. (2000). "A laboratory apparatus to measure osmotic efficiency coefficients for clay soils." *Geotechnical Testing Journal*, ASTM, in press.

Marine, I. W., and Fritz, S. J. (1981). "Osmotic model to explain anomalous hydraulic heads." *Water Resources Research*, 17(1), 73-82.

McKelvey, J. G. and Milne, I. H. (1962). "The flow of salt solutions through compacted clay." *Clays and Clay Minerals*, 9. 248-259.

Mitchell, J. K. (1993). *Fundamentals of Soil Behavior*, 2nd Ed. John Wiley and Sons, New York, 437 p.

Muurinen, A. (1990). "Diffusion of uranium in compacted sodium bentonite." *Engineering Geology*, 28, 359-367.

Olsen, H. W. (1969). "Simultaneous fluxes of liquid and charge in saturated kaolinite." *Soil Science Society of America Proceedings*, 33, 338-344.

Olsen, H. W., Yearsley, E. N., and Nelson, K. R. (1990). "Chemico-osmosis versus diffusion-osmosis." *Transportation Research Record No. 1288*, Transportation Research Board, Washington D.C., 15-22.

Oscarson, D. W. (1994). Surface diffusion: is it an important transport mechanism in compacted clays?" *Clays and Clay Minerals*, 42, 534-543.

Oscarson, D. W. and Hume, H. B. (1994). "Diffusion of ^{14}C in dense saturated bentonite under steady-state conditions." *Transport in Porous Media*, 14, 73-84.

Oscarson, D. W., Hume, H. B., Sawatsky, N. G., and Cheung, S. C. H. (1992). "Diffusion of iodide in compacted bentonite." *Soil Science Society of America Journal*, Vol. 56(5), 1400-1406.

Petrov, R. J., Rowe, R. K., and Quigley, R. M. (1997). "Comparison of laboratory-measured GCL hydraulic conductivity based on three permeameter types." *Geotechnical Testing Journal*, ASTM, 20(1), 49-62.

Porter, L. K., Kemper, W. D., Jackson, R. D., and Stewart, B. A. (1960). "Chloride diffusion in soils as influenced by moisture content." *Soil Science Society of America Proceedings*, 24(6), 460-463.

Robinson, R.A., and Stokes, R.H., 1959. *Electrolyte Solutions*, 2nd Ed., Butterworth Scientific Publications, London, England, 571 pp.

Rowe, R. K., Petrov, R. P., and Lake, C. (1997a). "Compatibility testing and diffusion through GCLs." *Proceedings, 6th International Landfill Symposium*, Sardinia '97, Cagliari, Italy, Vol. 3, 301-310.

Rowe, R. K., Lake, C., von Maubeuge, K., and Stewart, D. (1997b). "Implications of diffusion of chloride through geosynthetic clay liners." *Proceedings, GeoEnvironment '97*, Bouazza, Kodikara, and Parker, eds., Balkema, Rotterdam, The Netherlands, 295-300.

Rowe, R. K., Lake, C., and Petrov, R. P. (2000). "Apparatus and procedures for assessing inorganic diffusion coefficients for geosynthetic clay liners." *Geotechnical Testing Journal*, ASTM, 23(2), 206-214.

Sawatsky, N. Feng, Y., and Dudas, M. J. (1997). "Diffusion of 1-naphthol and naphthalene through clay materials: Measurement of apparent exclusion of solute from the pore space." *Journal of Contaminant Hydrology*, 27(1-2), 25-41.

Shackelford, C.D. (1988). "Diffusion as a transport process in fine-grained barrier materials." *Geotechnical News*, 6(2), 24-27.

Shackelford, C.D. (1991). "Laboratory diffusion testing for waste disposal - A Review. *Journal of Contaminant Hydrology*, 7(3), 177-217.

Shackelford, C. D. and Daniel, D. E. (1991). "Diffusion in saturated soil: I. Background." *Journal of Geotechnical Engineering*, ASCE, Vol. 117(3), 467-484.

Shackelford, C. D. and Redmond, P. L. (1995). "Solute breakthrough curves for processed kaolin at low flow rates." *Journal of Geotechnical Engineering*, ASCE, 121(1), 17-32.

Whitworth, T. M. and Fritz, S. J. (1994). "Electrolyte-induced solute permeability effects in compacted smectite membranes." *Applied Geochemistry*, 9(5), 533-546.

Yeung, A. T. (1990). "Coupled flow equations for water, electricity and ionic contaminants through clayey soils under hydraulic, electrical, and chemical gradients." *Journal of Non-Equilibrium Thermodynamics*, 15, 247-267.

Yeung, A. T. and Mitchell, J. K. (1993). "Coupled fluid, electrical, and chemical flows in soil." *Geotechnique*, 43(1), 121-134.

Table 4.1 - Diffusion test results.

Test No.	Test Conditions [a]			Specimen Properties [b]				Diffusion Results [c]			
	C_{ot} (M)	$\overline{C}_{K^+}$ (M)	$\overline{C}_{Cl^-}$ (M)	n	k_h (m/s)	S_f (%)	ω	Element	$\Delta Q_t/\Delta t$ (mg/m^2/s)	D^*_ω (m^2/s)	D^*_s (m^2/s)
1	0.0039	0.0019	0.0019	0.80	1.65×10^{-11}	97.0	0.63	K^+	0. 000538	4.39×10^{-11}	5.20×10^{-11}
								Cl^-	0. 000784	7.05×10^{-11}	7.86×10^{-11}
2	0.0087	0.0044	0.0044	0.79	1.33×10^{-11}	99.4	0.49	K^+	0.00243	9.07×10^{-11}	9.96×10^{-11}
								Cl^-	0.00282	1.16×10^{-10}	1.25×10^{-10}
3	0.020	0.010	0.010	0.79	1.52×10^{-11}	97.5	0.32	K^+	0.0118	1.91×10^{-10}	2.01×10^{-10}
								Cl^-	0.0120	2.14×10^{-10}	2.24×10^{-10}
4	0.047	0.024	0.024	0.78	1.48×10^{-11}	96.3	0.14	K^+	0.0287	1.99×10^{-10}	2.03×10^{-10}
								Cl^-	0.0306	2.34×10^{-10}	2.38×10^{-10}

[a] C_{ot} = source KCl concentration; $\overline{C}_{K^+}$, $\overline{C}_{Cl^-}$ = average concentrations of K^+ and Cl^- across specimen (= $C_{ot}/2$)

[b] n = specimen porosity; k_h = hydraulic conductivity based on permeation with source KCl solution; S_f = final degree of saturation; ω = chemico-osmotic efficiency coefficient at steady-state induced pressure

[c] $\Delta Q_t/\Delta t$ = slope of steady-state diffusion data (Figs. 7, 8); D^*_ω = coupled effective salt-diffusion coefficient; D^*_s = true effective salt-diffusion coefficient

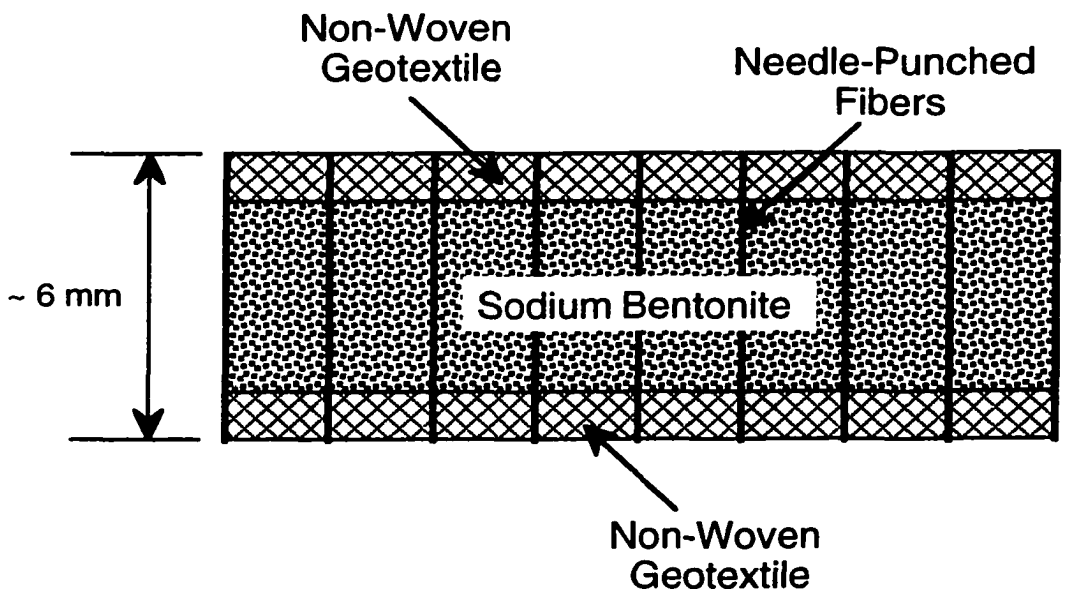

Fig. 4.1 - Schematic of Bentomat® GCL.

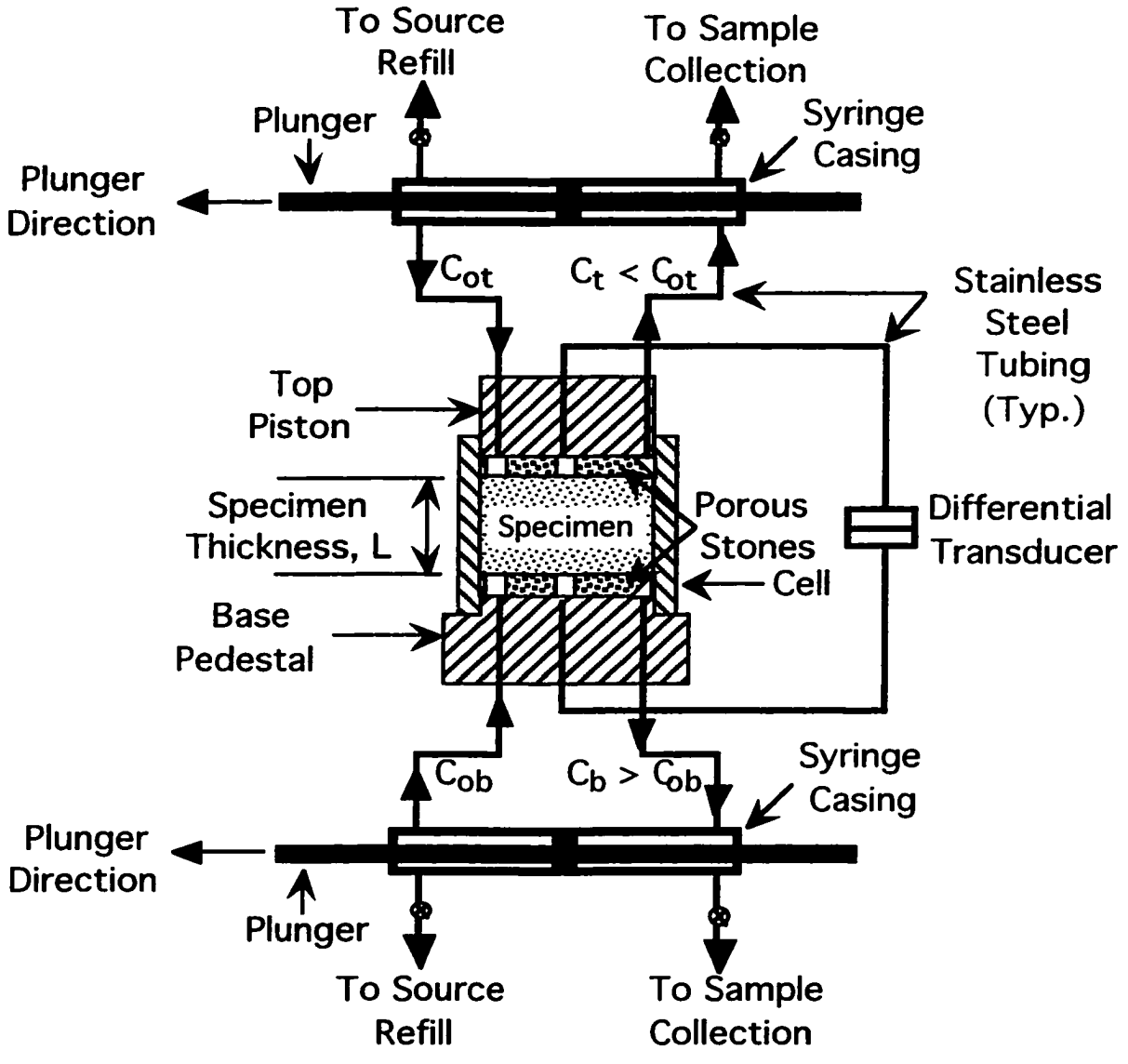

Fig. 4.2 - Schematic of testing apparatus used in study.

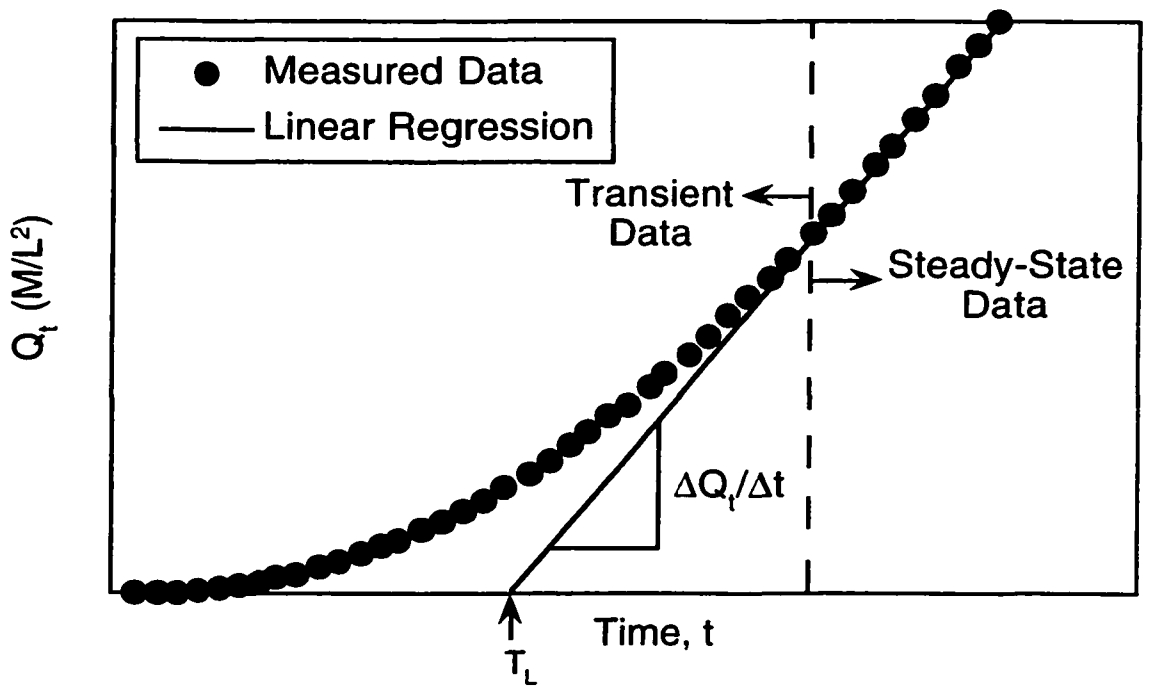

Fig. 4.3 - Example illustration of steady-state diffusion test results.

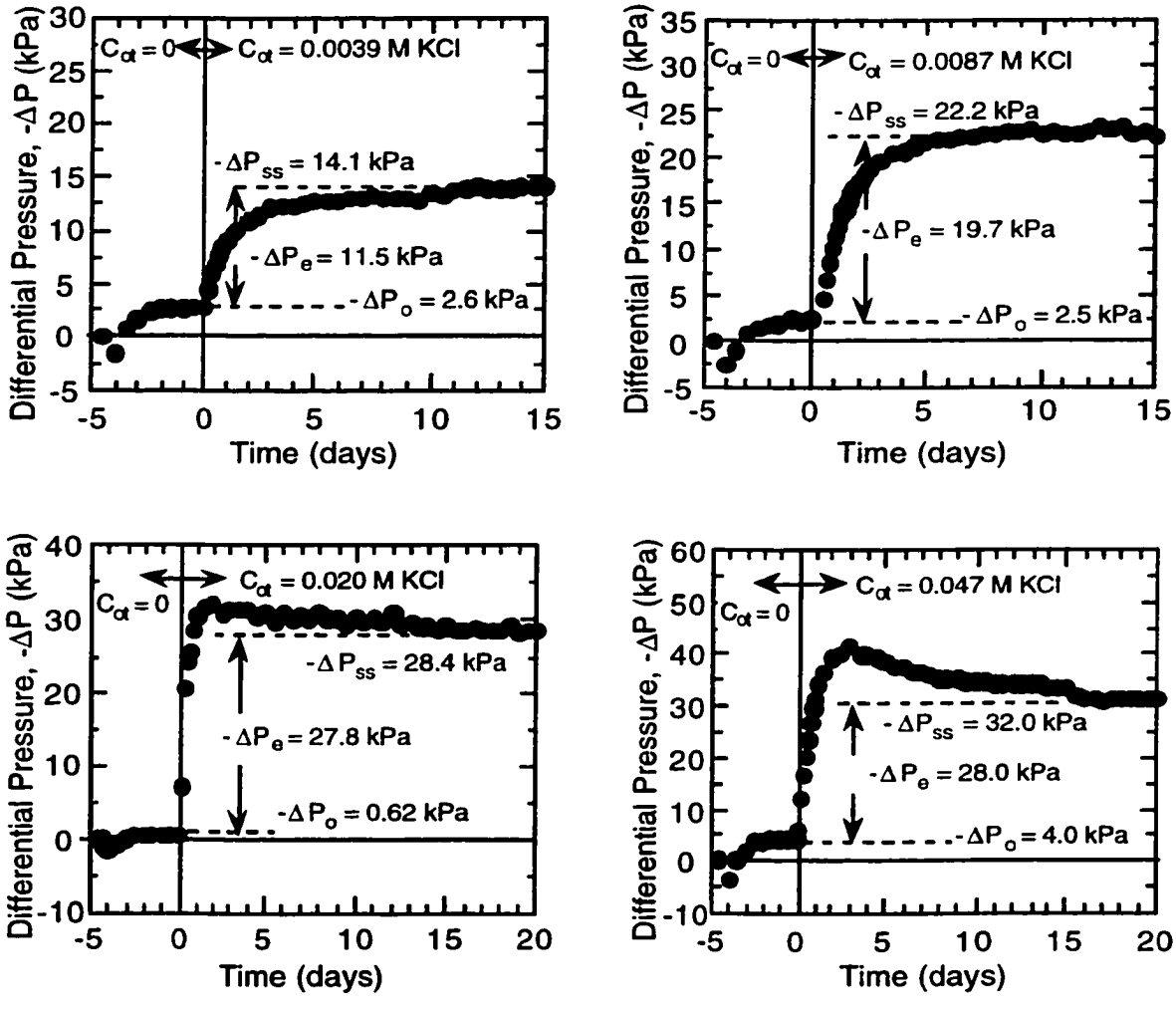

Fig. 4.4 - Induced differential pressures measured across GCL specimens.

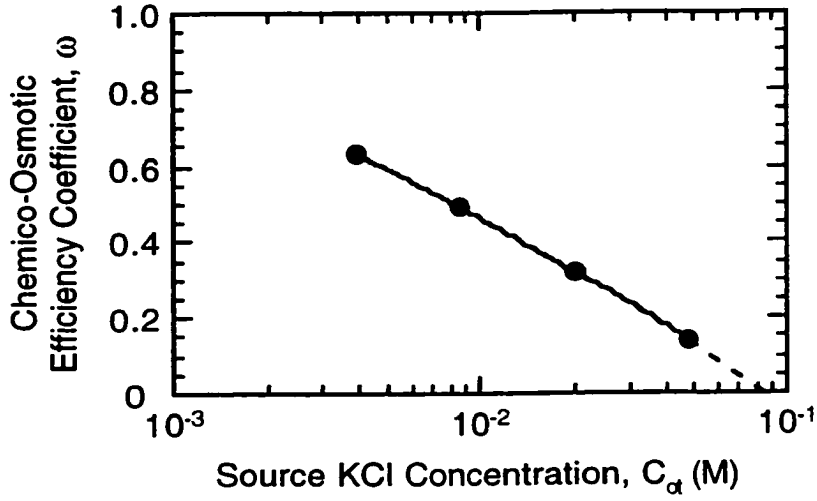

Fig. 4.5 - Measured chemico-osmotic efficiency coefficients of GCL specimens versus source KCl concentration (C_{ot}).

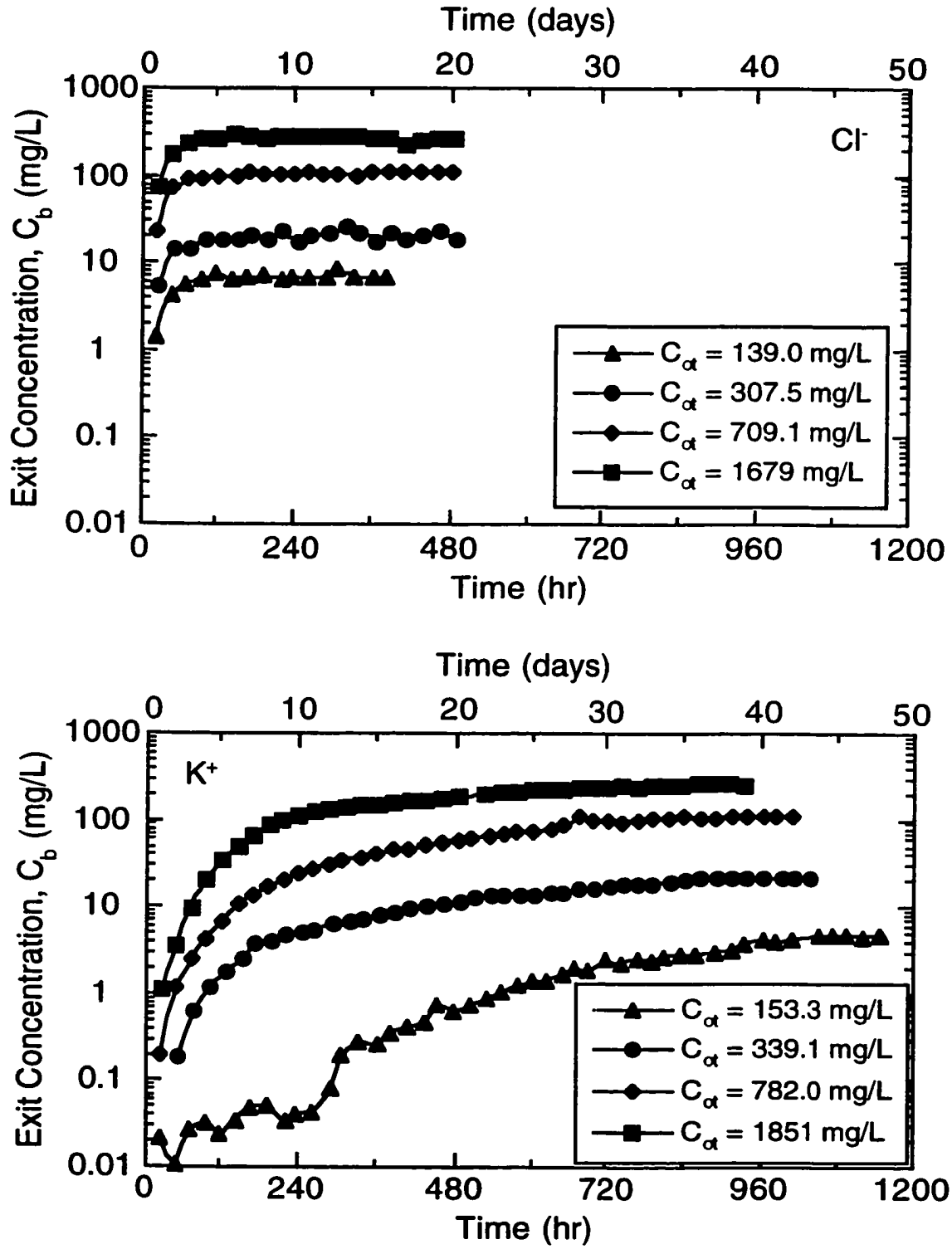

Fig. 4.6 - Measured exit concentrations of Cl^- and K^+ during diffusion tests.

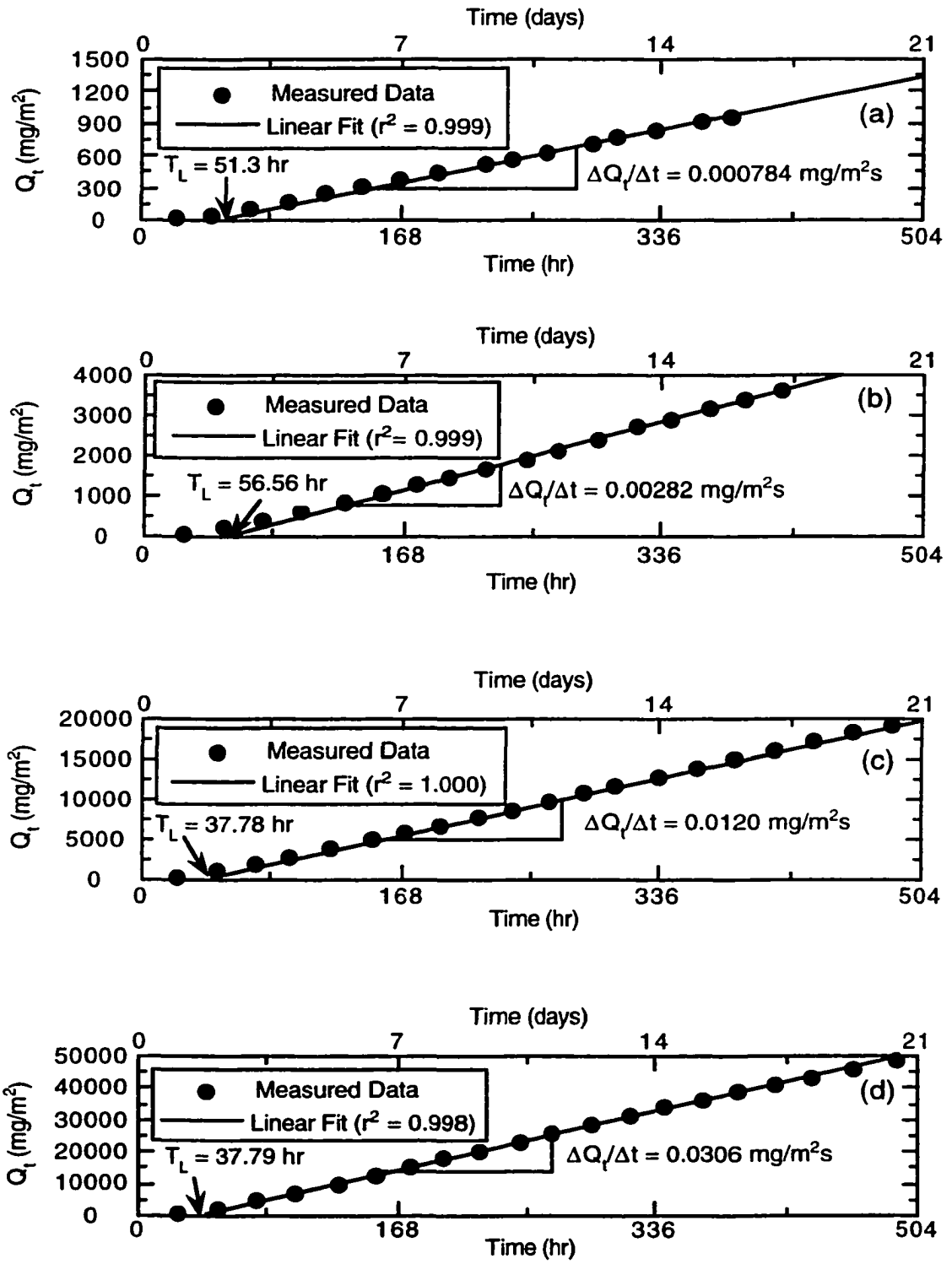

Fig. 4.7 - Steady-state diffusion results for Cl^-: (a) C_{ot} = 0.0039 M; (b) C_{ot} = 0.0087 M; (c) C_{ot} = 0.020 M; (d) C_{ot} = 0.047 M.

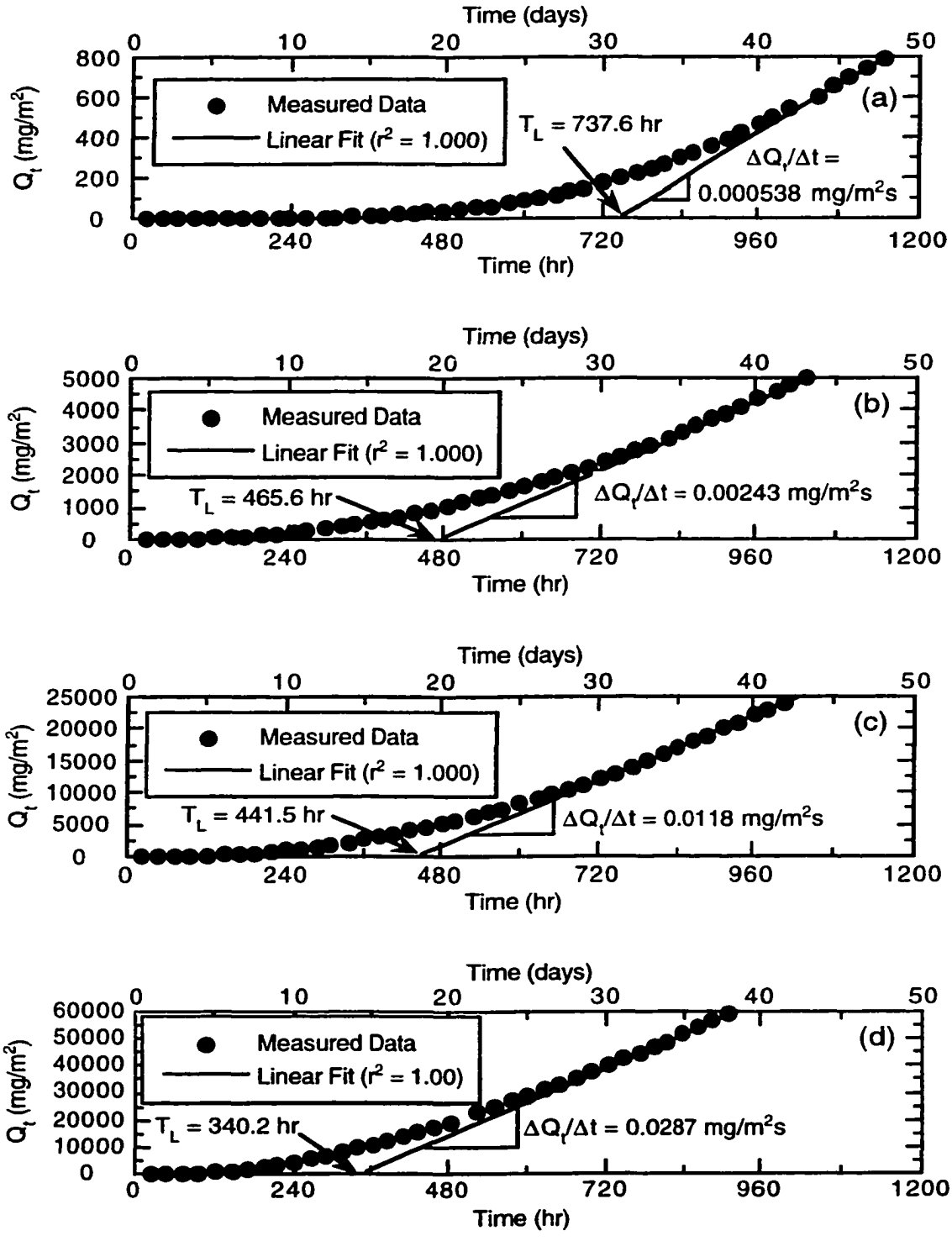

Fig. 4.8 - Steady-state diffusion results for K^+: (a) C_{ot} = 0.0039 M; (b) C_{ot} = 0.0087 M; (c) C_{ot} = 0.020 M; (d) C_{ot} = 0.047 M.

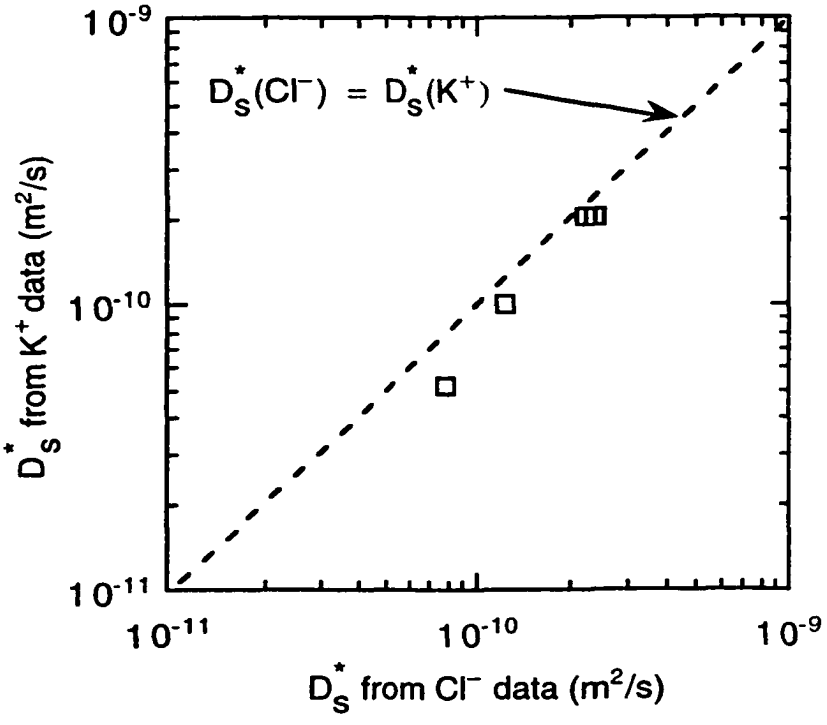

Fig. 4.9 - Comparison of D_s^* values based on K^+ versus Cl^- data.

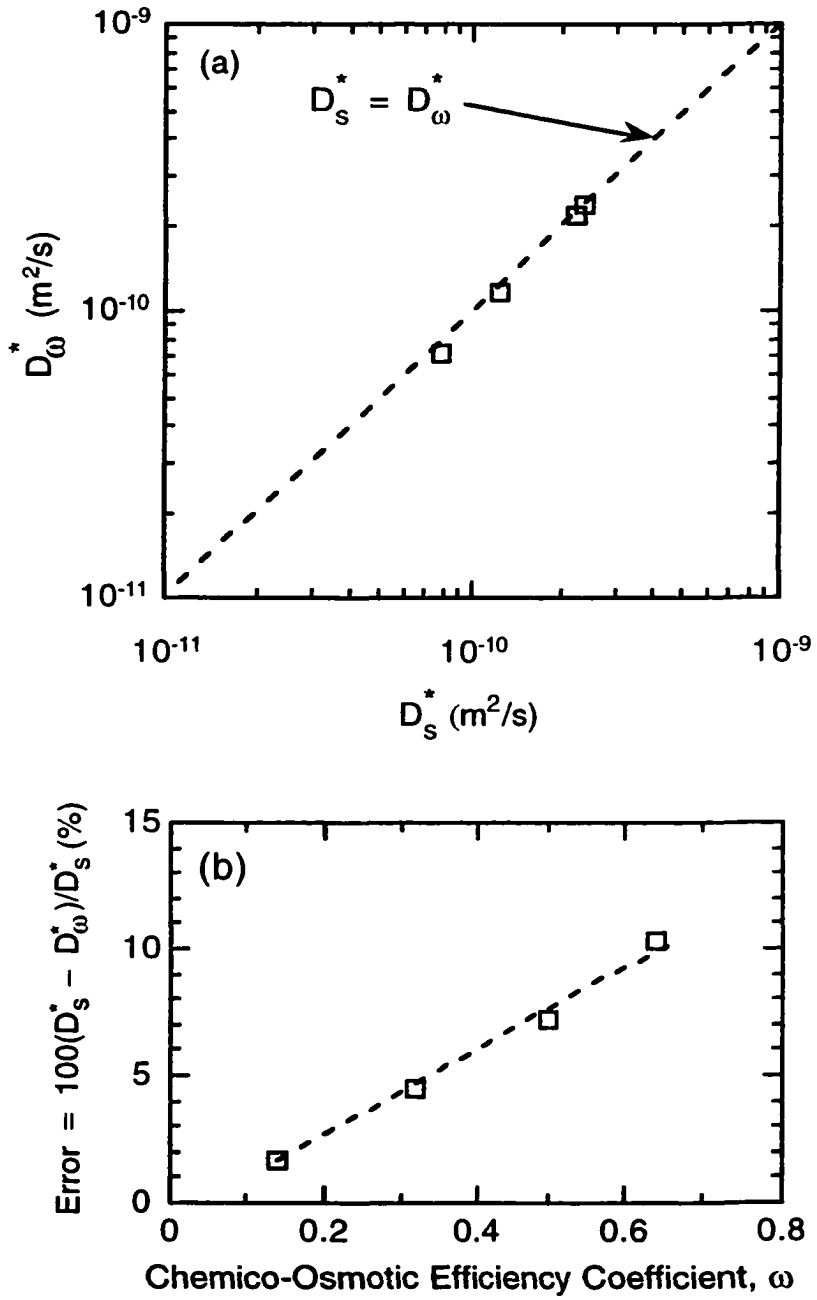

Fig. 4.10 - Comparison of D_ω^* versus D_s^* values obtained in study.

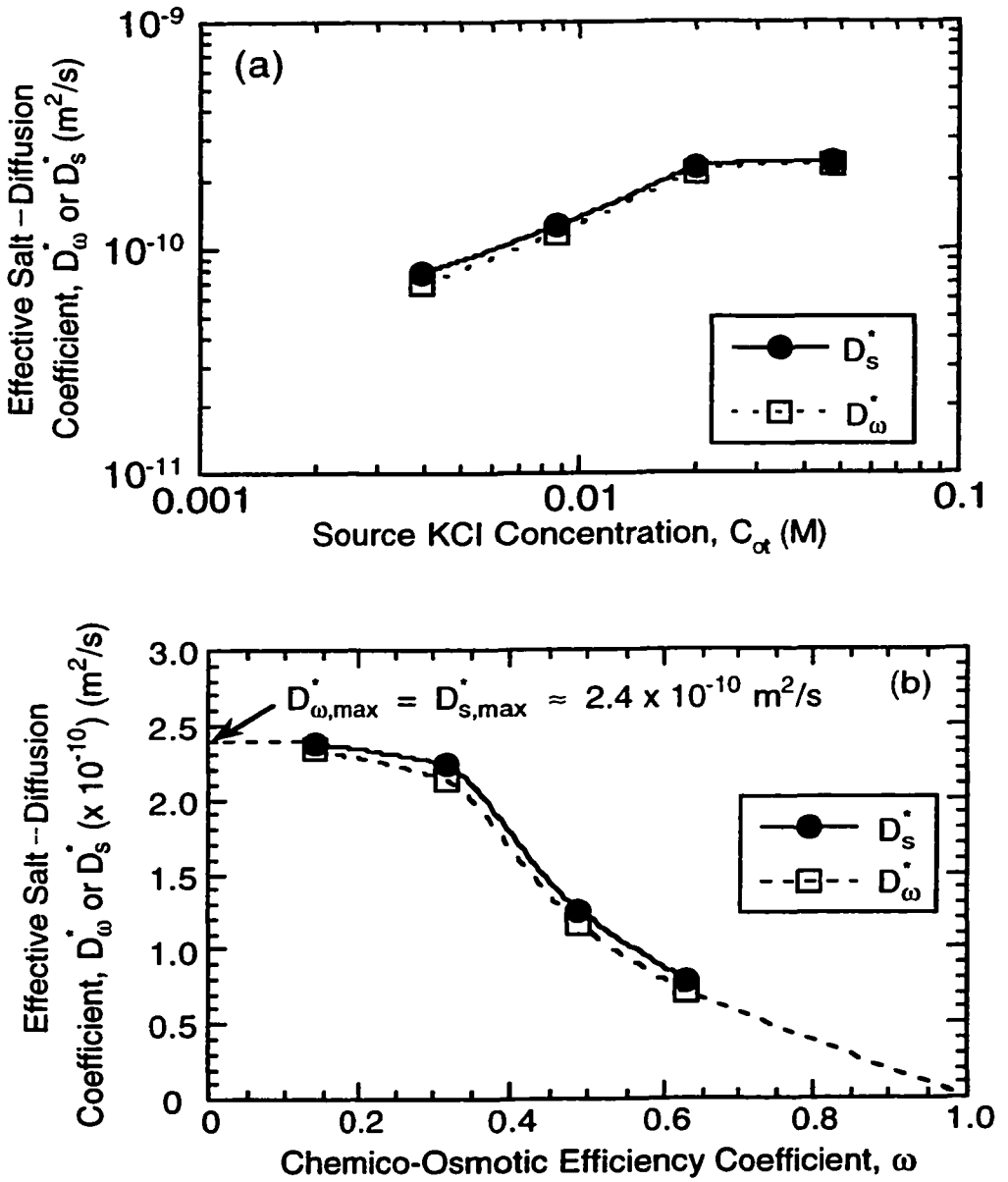

Fig. 4.11 - Effective salt-diffusion coefficients versus (a) source KCl concentration; (b) chemico-osmotic efficiency coefficient.

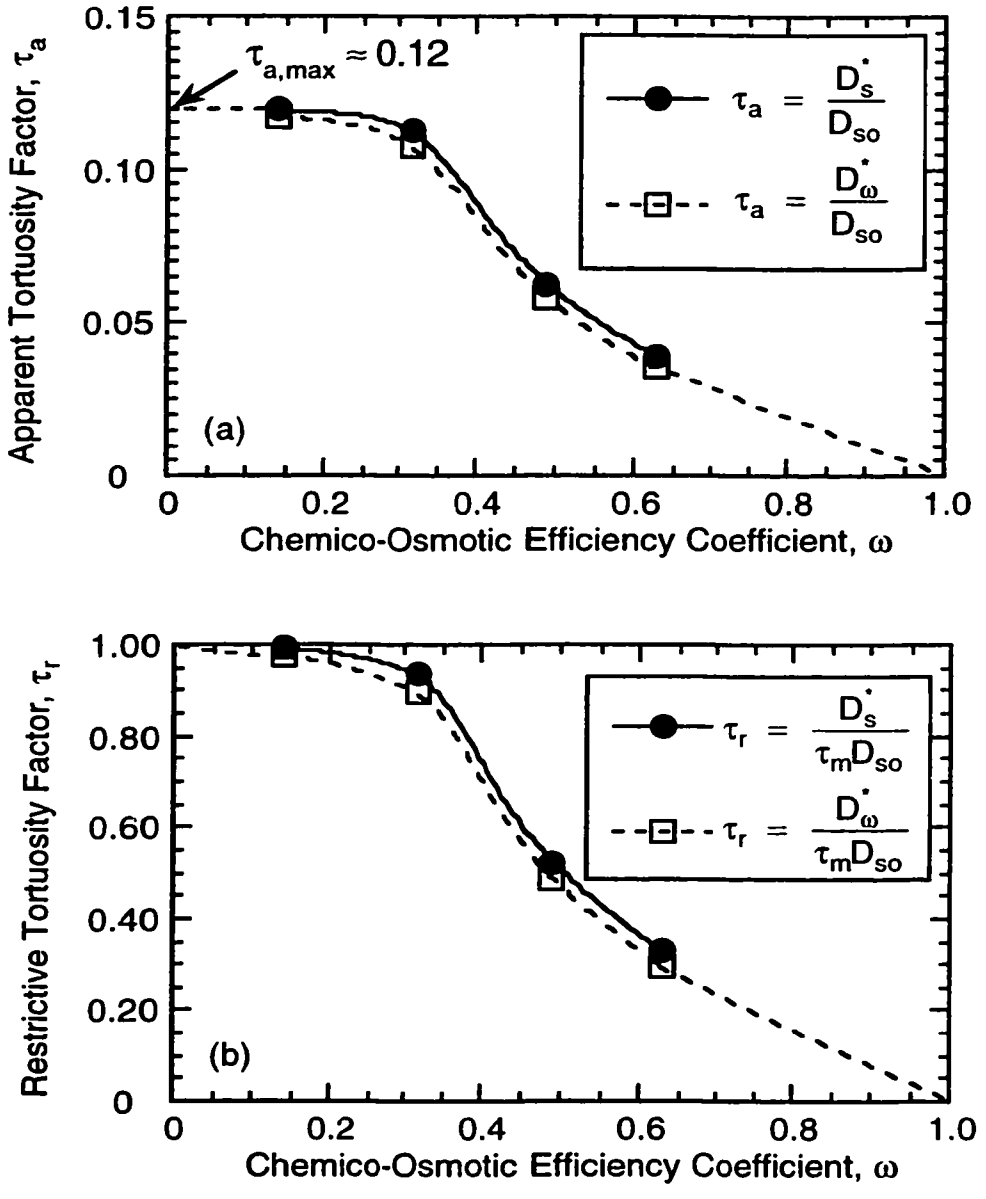

Fig. 4.12 - Tortuosity factors versus chemico-osmotic efficiency: (a) apparent tortuosity factor, τ_a; (b) restrictive tortuosity factor, τ_r.

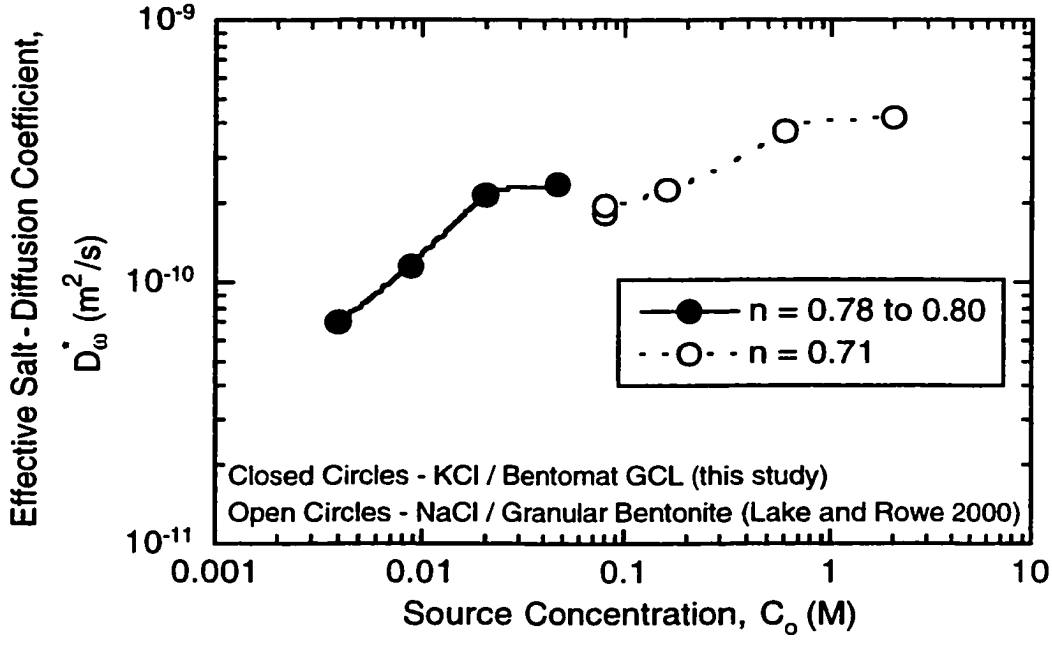

Fig. 4.13 - Measured D^*_ω values as a function of source concentration, C_o.

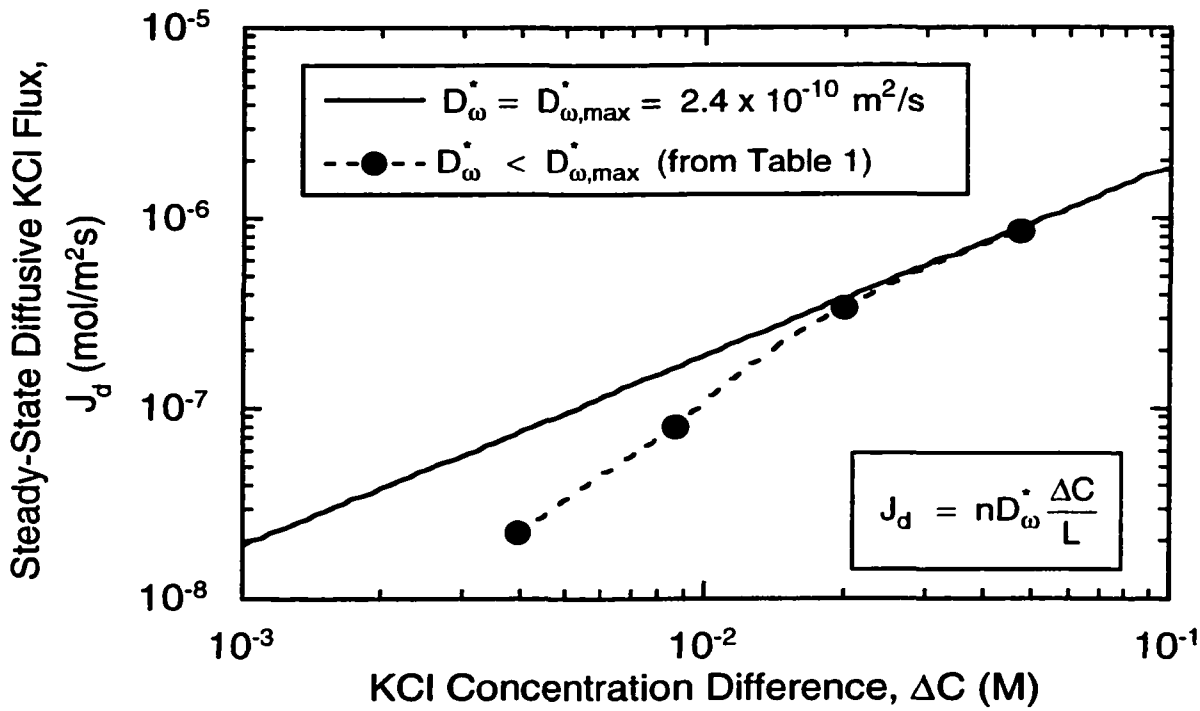

Fig. 4.14 - Theoretical steady-state diffusive flux through Bentomat® GCL (L = 1.0 cm).

CHAPTER 5

COUPLED SOLUTE FLUX AND TRANSPORT THROUGH CLAY MEMBRANE BARRIERS

ABSTRACT: A coupled solute transport model to simulate one-dimensional solute migration through reactive (i.e., ion exchanging) soil barriers is presented herein. The coupled model is based on principles of irreversible thermodynamics and accounts for explicit coupling effects (i.e., hyperfiltration and chemico-osmotic counter-advection) related to membrane behavior in the soil barrier. Theoretical simulations of coupled solute transport through a soil membrane are presented to illustrate the influence of these explicit coupling effects as well as an implicit (or empirical) coupling effect characterized by a decrease in apparent tortuosity factor, τ_a, with decreasing solute concentration and increasing chemico-osmotic efficiency of the soil. The results of the simulations are compared to the results of additional simulations based on advective-dispersive theory in which explicit coupling inherently is neglected. Solute fluxes predicted using both theories based on independently measured transport parameters are compared with measured solute fluxes from column tests on a geosynthetic clay liner (GCL) subjected to KCl solutions. The results of the theoretical analysis indicate that lower values of solute flux and longer solute transit times are predicted by coupled solute transport theory relative to advective-dispersive theory. The coupled transport model also provides better agreement with measured data from the column tests than advective-dispersive theory. However, use of advective-dispersive theory *in lieu* of the coupled theory to simulate solute transport through GCLs appears reasonable under diffusion-dominated conditions,

provided that implicit coupling is included by using a value of τ_a that corresponds to the source solute concentration.

KEY WORDS: bentonite, chemico-osmosis, chemico-osmotic efficiency, counter-advection, membrane behavior, diffusion, geosynthetic clay liner, hyperfiltration, membrane coupling effects

5.1 INTRODUCTION

The migration of solutes in fine-grained soils of low hydraulic conductivity has become an important consideration with respect to the design and performance of waste containment barriers that consist of these soils (e.g., liners, cutoff walls). For example, solute transport analyses for engineered barrier materials, such as compacted clay soils and geosynthetic clay liners (GCLs), typically are performed using solutions to the advective-dispersive equation (e.g., Shackelford 1988, Shackelford 1990). In these analyses, the advective term is based on Darcy's law for solution flux in response to a hydraulic gradient, and solute diffusion is described by Fick's first law for diffusive flux in response to a concentration gradient. Mechanical dispersion commonly is assumed to be negligible relative to diffusion for the low-flow conditions typically associated with these materials (Shackelford 1988, Mitchell 1993).

However, advective-dispersive transport theory represents a limiting case of the more general coupled flux transport theory in that coupling terms (e.g., chemico-osmosis) are assumed to be negligible (e.g., Yeung 1990, Shackelford 1996). While this approach is considered acceptable in the case of the relatively high flow rates commonly associated with coarse-grained soils (e.g., aquifers), the use of advective-dispersive theory for clay barrier materials may not be appropriate. For example, the results of several laboratory studies have shown that some clay soils have the ability to act as membranes that restrict

the passage of charged solutes (i.e., ions) (e.g., Kemper and Rollins 1966, Olsen 1969, Kemper and Quirk 1972, Fritz and Marine 1983). Such membrane behavior also results in chemico-osmosis, or the movement of liquid in response to a solute concentration gradient (Olsen 1969, Mitchell et al. 1973, Olsen 1985, Barbour 1986, Barbour and Fredlund 1989, Neuzil 2000).

Models that take into account restricted solute transport and/or chemico-osmotic flow resulting from the presence of soil membrane behavior have been developed (Bresler 1973, Greenberg et al. 1973, Barbour and Fredlund 1989, Yeung 1990, Yeung and Mitchell 1993). For example, Bresler (1973) developed a transport model accounting for chemico-osmosis during solute migration in unsaturated soils. Barbour and Fredlund (1989) used a similar approach as Bresler (1973) to characterize chemico-osmotic consolidation in clay soils. However, the diffusive solute flux in these models is governed solely by Fick's first law and does not include salt sieving effects associated with soil membranes.

Greenberg et al. (1973) presented a more rigorous transport model based on coupled flux theory to simulate the transient migration of water and salt (NaCl) in which both chemico-osmosis and restricted diffusion are included in the formulation. The model was used to simulate NaCl migration through a groundwater aquitard due to saltwater (seawater) intrusion. However, Greenberg et al. (1973) did not consider electrical coupling or the dissociation of the electrolyte into separate ionic species in the model formulation.

Yeung (1990) and Yeung and Mitchell (1993) improved on the model of Greenberg et al. (1973) by presenting a formal description of coupled flux equations for the simultaneous movement of liquid, electricity, and ions through soil membranes under isothermal conditions in which the phenomenological coefficients are expressed in terms of familiar and measurable hydraulic parameters (e.g., hydraulic conductivity). This model describes the simultaneous transport of a single cation and a single anion of a

strong (i.e., fully dissociating) electrolyte, and can be used to illustrate the effect of applied electrical current on solute transport that is relevant to applications such as electrokinetic remediation. However, the model is not valid for systems containing multiple cation or anion species, such as systems in which additional ionic species are introduced into the pore fluid due to ion exchange of reactive solutes during transient transport.

In all of these models, membrane behavior is represented by a chemico-osmotic efficiency coefficient, ω, or reflection coefficient, σ, that ranges from zero ($\omega = 0$) for non-membranes to unity ($\omega = 1$) for "ideal" membranes that completely restrict the passage of solutes (e.g., see Staverman 1952, Kemper and Rollins 1966, Olsen et al. 1990, Keijzer et al. 1997). Clay soils that exhibit membrane behavior typically only partially restrict the passage of solutes (i.e., $0 < \omega < 1$) and, therefore, are considered "non-ideal" membranes. The extent to which a clay soil behaves as a "non-ideal" membrane depends on the types and amounts of clay minerals in the soil, the sizes of pores, and the types and concentrations of solutes (Kemper and Rollins 1966, Olsen 1969, Bresler 1973, Fritz and Marine 1983, Olsen et al. 1990, Mitchell 1993).

Although the results of these theoretical studies indicate indirectly that membrane behavior may affect solute migration through engineered clay barrier materials in which $\omega > 0$, little experimental evidence of the potential effects of membrane behavior on solute transport currently is available. Since the application of the advective-dispersive equation for solute transport analysis represents a limiting case in which the potential influence of membrane coupling is ignored (i.e., $\omega = 0$), a direct comparison of solute transport based on advective-dispersive theory versus coupled solute transport theory that accounts for membrane behavior is needed.

The purpose of this chapter is to present the development of a coupled solute transport model extended from the work of Yeung (1990) and Yeung and Mitchell (1993) that can be used to simulate transient, one-dimensional solute transport through reactive

(i.e., ion exchanging) soil membranes. Theoretical analyses are presented to illustrate the factors affecting coupled solute transport. The results of these analyses also are compared to the results of analyses based on advective-dispersive theory to illustrate the differences between the two theories. Finally, the validity of the use of advective-dispersive theory to model solute transport in soil membranes *in lieu* of the coupled transport theory is examined by comparing the two theories with experimental data obtained from column tests on a geosynthetic clay liner (GCL) containing a sodium bentonite.

5.2 THEORETICAL BACKGROUND

The governing equations for coupled solute transport through a soil are derived from the simultaneous flux equations for water, current, ion, and heat migration across a charged membrane in response to hydraulic, electrical, chemical, and thermal gradients, respectively (e.g., see Katchalsky and Curran 1965). These flux equations are based on the second law of thermodynamics adapted for non-equilibrium systems in which irreversible processes occur. This approach is valid for irreversible processes provided that (1) local equilibrium is established such that any infinitesimal subsystem of the overall system is in equilibrium, (2) the fluxes are linearly related to the driving forces, and (3) Onsager's reciprocal law is valid for the system (Yeung and Mitchell 1993).

The linear relationship between fluxes J_i and driving forces X_i is expressed mathematically as follows:

$$\begin{aligned} J_1 &= L_{11}X_1 + L_{12}X_2 + \cdots + L_{1N}X_N \\ J_2 &= L_{21}X_1 + L_{22}X_2 + \cdots + L_{2N}X_N \\ &\vdots \qquad\qquad \vdots \\ J_N &= L_{N1}X_1 + L_{N2}X_2 + \cdots + L_{NN}X_N \end{aligned} \tag{5.1}$$

or

$$J_i = \sum_{j=1}^{N} L_{ij} X_j \tag{5.2}$$

where i = 1, 2, ... N and L_{ij} are phenomenological coefficients that relate the flux of type i to the gradient of type j. Evaluation of the phenomenological coefficients is necessary to provide a complete description of coupled flux processes, but becomes more difficult as the number of fluxes and driving forces increases. For example, a set of equations with three fluxes and driving forces contains nine coefficients, while a set of equations with four fluxes and driving forces contains 16 coefficients. In general, a system with N fluxes and driving forces contains N^2 phenomenological coefficients that must be evaluated. However, this matrix of coefficients can be considered symmetric in accordance with Onsager's reciprocal law, or

$$L_{ij} = L_{ji} \tag{5.3}$$

Therefore, the number of independent coefficients is reduced from N^2 to [(N+1)N]/2. The validity of Eq. 5.3 with respect to chemical coupling and electrical coupling in soil systems has been demonstrated experimentally in previous research by Abd-el-Aziz and Taylor (1965) and Olsen (1969), respectively.

5.2.1 Conceptual Model

The thermodynamics associated with the movement of water, current, ions, and heat in a soil system is considered based on a simple conceptual model that consists of two compartments separated by a homogeneous charged membrane of thickness L, as shown in Fig. 5.1. Each compartment may contain a different pressure (P), electrical

potential (Ψ), chemical potential (μ), and/or solution temperature (T) such that hydraulic, electrical, chemical, and thermal gradients, respectively, are maintained across the membrane. However, no gradients exist in either compartment (Katchalsky and Curran 1965, Yeung 1990).

The system in Fig. 5.1 can be considered as either a continuous or discontinuous system for the purpose of describing the dissipation of free energy due to irreversible processes. The state variables in a continuous system are functions of both time and space, and the driving forces at any point within a continuous system are represented by the gradients of the state variables at that location at a given time. Conversely, the state variables in a discontinuous system are only functions of space. In practical terms, the continuous approach represents the transient case, whereas the discontinuous approach represents the steady-state case (i.e., the gradient of each state variable is constant throughout the membrane). A continuous system is considered in this study in accordance with Yeung (1990).

5.2.2 Dissipation of Free Energy

The rate of dissipation of free energy by irreversible processes in a continuous, one-dimensional soil membrane is described by the dissipation function, Φ [$ML^{-1}t^{-3}$], that can be written for isothermal conditions as follows (Yeung 1990):

$$\Phi = -q\frac{\partial P}{\partial x} - I\frac{\partial \Psi}{\partial x} - \sum_{i=1}^{N} J_i^d \frac{\partial \mu_i^c}{\partial x} \tag{5.4}$$

where q is liquid flux [Lt^{-1}], P is the liquid pressure [$ML^{-1}t^{-2}$], I is electrical current [Coulomb$\cdot L^{-2}t^{-1}$], Ψ is electrical potential [Volt], J_i^d is the molar diffusive flux of solute i [mol $L^{-2}t^{-1}$], μ_i^c is the chemical potential of solute i [$ML^2mol^{-1}t^{-2}$], and the variable N in the summation represents the total number of ionic species in the system.

5.2.3 Coupled Flux Equations

The dissipation function in Eq. 5.4 assumes the following general form in terms of fluxes J_i and driving forces X_i:

$$\Phi = \sum_{i=1}^{N} J_i \cdot X_i \tag{5.5}$$

Therefore, we may write a set of N coupled flux equations for a system containing M (= N - 2) ionic species in accordance with the postulate of linear phenomenological equations (Eq. 5.2) as follows:

$$\begin{aligned}
q &= -L_{11}\frac{\partial P}{\partial x} - L_{12}\frac{\partial \Psi}{\partial x} - L_{13}\frac{\partial \mu_1^c}{\partial x} - L_{14}\frac{\partial \mu_2^c}{\partial x} - \ldots - L_{1N}\frac{\partial \mu_N^c}{\partial x} \\
I &= -L_{21}\frac{\partial P}{\partial x} - L_{22}\frac{\partial \Psi}{\partial x} - L_{23}\frac{\partial \mu_1^c}{\partial x} - L_{24}\frac{\partial \mu_2^c}{\partial x} - \ldots - L_{2N}\frac{\partial \mu_N^c}{\partial x} \\
J_1^d &= -L_{31}\frac{\partial P}{\partial x} - L_{32}\frac{\partial \Psi}{\partial x} - L_{33}\frac{\partial \mu_1^c}{\partial x} - L_{34}\frac{\partial \mu_2^c}{\partial x} - \ldots - L_{3N}\frac{\partial \mu_N^c}{\partial x} \\
J_2^d &= -L_{41}\frac{\partial P}{\partial x} - L_{42}\frac{\partial \Psi}{\partial x} - L_{43}\frac{\partial \mu_1^c}{\partial x} - L_{44}\frac{\partial \mu_2^c}{\partial x} - \ldots - L_{4N}\frac{\partial \mu_N^c}{\partial x} \\
&\vdots \qquad\qquad \vdots \\
J_M^d &= -L_{N1}\frac{\partial P}{\partial x} - L_{N2}\frac{\partial \Psi}{\partial x} - L_{N3}\frac{\partial \mu_1^c}{\partial x} - L_{N4}\frac{\partial \mu_2^c}{\partial x} - \ldots - L_{NN}\frac{\partial \mu_N^c}{\partial x}
\end{aligned} \tag{5.6}$$

or, in summation form,

$$q = -L_{11}\frac{\partial P}{\partial x} - L_{12}\frac{\partial \Psi}{\partial x} - \sum_{i=1}^{M} L_{1,i+2}\frac{\partial \mu_i^c}{\partial x} \tag{5.7a}$$

$$I = -L_{21}\frac{\partial P}{\partial x} - L_{22}\frac{\partial \Psi}{\partial x} - \sum_{i=1}^{M} L_{2,i+2}\frac{\partial \mu_i^c}{\partial x} \tag{5.7b}$$

$$J_j^d = -L_{j+2,1}\frac{\partial P}{\partial x} - L_{j+2,2}\frac{\partial \Psi}{\partial x} - \sum_{i=1}^{M} L_{j+2,i+2}\frac{nD_j^* c_j}{RT}\frac{\partial \mu_j^c}{\partial x} \; ; \; j = 1, 2, ..., M \tag{5.7c}$$

Equations 5.7a to 5.7c represent the most general case for coupled flux under isothermal conditions. The degree of complexity associated with the solution of these equations is related to the number of ionic species that are present in the system; i.e., an increase in the number of ionic species in a system increases the number of coefficients L_{ij} that must be evaluated as well as the number of equations necessary to define the system. As a result, previous theoretical development of coupled flux equations has been limited to migration of a single salt (Abd-el-Aziz and Taylor 1965, Groenevelt and Bolt 1969, Olsen 1969, Greenberg et al. 1973, Groenevelt and Elrick 1976, Yeung 1990, Yeung and Mitchell 1993).

For example, Yeung (1990) and Yeung and Mitchell (1993) present coupled flux equations for a soil system containing a single anion and a single cation of a strong (i.e., fully dissociating), binary electrolyte (e.g., NaCl). In this case, M = 2 and Eq. 5.6 reduces to

$$q = -L_{11}\frac{\partial P}{\partial x} - L_{12}\frac{\partial \Psi}{\partial x} - L_{13}\frac{\partial \mu_c^c}{\partial x} - L_{14}\frac{\partial \mu_a^c}{\partial x} \tag{5.8a}$$

$$I = -L_{21}\frac{\partial P}{\partial x} - L_{22}\frac{\partial \Psi}{\partial x} - L_{23}\frac{\partial \mu_c^c}{\partial x} - L_{24}\frac{\partial \mu_a^c}{\partial x} \tag{5.8b}$$

$$J_c^d = -L_{31}\frac{\partial P}{\partial x} - L_{32}\frac{\partial \Psi}{\partial x} - L_{33}\frac{\partial \mu_c^c}{\partial x} - L_{34}\frac{\partial \mu_a^c}{\partial x} \tag{5.8c}$$

$$J_a^d = -L_{41}\frac{\partial P}{\partial x} - L_{42}\frac{\partial \Psi}{\partial x} - L_{43}\frac{\partial \mu_c^c}{\partial x} - L_{44}\frac{\partial \mu_a^c}{\partial x} \tag{5.8d}$$

where subscripts c and a represent the cation (solute 1) and anion (solute 2), respectively.

5.2.4 Phenomenological Coefficients, L_{ij}

Yeung (1990) and Yeung and Mitchell (1993) also provide a detailed derivation of the relationships between the phenomenological coefficients L_{ij} and measurable soil parameters. These relationships, written herein with respect to the total cross-sectional area of the soil, are as follows (Yeung 1990):

$$L_{11} = \frac{k_h}{\gamma_w} + \frac{k_e^2}{\sigma_e^*} \tag{5.9}$$

$$L_{12} = L_{21} = k_e \tag{5.10}$$

$$L_{22} = n\sigma_e^* \tag{5.11}$$

$$L_{13} = L_{31} = -\frac{\omega C_c k_h}{\gamma_w} + \frac{k_e C_c u_c^*}{\sigma_e^*} \tag{5.12}$$

$$L_{23} = L_{32} = nC_c u_c^* \tag{5.13}$$

$$L_{14} = L_{41} = -\frac{\omega C_a k_h}{\gamma_w} - \frac{k_e C_a u_a^*}{\sigma_e^*} \tag{5.14}$$

$$L_{24} = L_{42} = -nC_a u_a^* \tag{5.15}$$

$$L_{34} = L_{43} = 0 \tag{5.16}$$

$$L_{33} = \frac{nD_c^* C_c}{RT} \tag{5.17}$$

$$L_{44} = \frac{nD_a^* C_a}{RT} \tag{5.18}$$

where k_h is hydraulic conductivity [Lt^{-1}], γ_w is the unit weight of water [$Mt^{-2}L^{-2}$], k_e is electro-osmotic conductivity [$L^2t^{-1}Volt^{-1}$], σ_e^* is the effective electrical conductivity of the porous medium [$Coulomb \cdot t^{-1}L^{-1}Volt^{-1}$], C is molar solute concentration [$mol \cdot L^{-3}$], u^* is effective ionic mobility [$L^2t^{-1}Volt^{-1}$], D^* is the effective self-diffusion coefficient [L^2t^{-1}], R is the universal gas constant [8.314 J/mol·K], T is the absolute temperature [T], n is the total soil porosity, and the subscripts a and c represent the anion and cation, respectively. The "effective" coefficients (i.e., u^*, D^*, σ_e^*) account for the tortuous nature of the pathways for solute migration in soil systems and are related to the coefficients in free solution as follows (e.g., see Alshawabkeh and Acar 1996):

$$\sigma_e^* = \tau_a \sigma_{eo} \; ; \qquad u^* = \tau_a u_o \qquad ; \qquad D^* = \tau_a D_o \tag{5.19}$$

where τ_a is the dimensionless apparent tortuosity factor (< 1) as defined by Shackelford and Daniel (1991).

As stated earlier, Eq. 5.8 is based on the explicit assumption that only one cation and one anion species are migrating through the porous medium. Therefore, the formulation of Yeung (1990) and Yeung and Mitchell (1993) is valid only when (a) no additional solutes are present in the porous medium or the external solutions, (b) the

porous medium is inert (i.e., no interaction with either chemical species), (c) there is no net exchange of either species with the porous medium (e.g., the cation exchange sites of a clay soil are completely filled with the transported cation, and the anion is not sorbed), or (d) steady-state transport has been reached (i.e., ion exchange processes are complete). These limitations can be significant with respect to engineered soil barriers used for waste containment, considering that leachates, mine wastes, and other contaminant sources often contain mixtures of chemical species, and ion exchange during transient transport through a clay barrier is a common and desirable process for retarding the movement of potentially harmful chemical species.

5.3 THEORETICAL DEVELOPMENT

The theory developed by Yeung (1990) and Yeung and Mitchell (1993) can be extended by accounting for additional ionic species in accordance with the general coupled flux equations (Eq. 5.7), and by defining the phenomenological coefficients to describe any solute species. For example, phenomenological coefficients $L_{j+2,1}$ and $L_{1,j+2}$ in Eqs. 5.7 can be defined for any solute j in accordance with Eqs. 5.12 and 5.14 as follows:

$$L_{j+2,1} = L_{1,j+2} = \frac{-\omega C_j k_h}{\gamma_w} \pm \frac{k_e C_j u_j^*}{\sigma_e^*} \tag{5.20}$$

Similarly, the coefficients $L_{j+2,2}$ and $L_{2,j+2}$ can be defined in accordance with Eqs. 5.13 and 5.15 as follows:

$$L_{j+2,2} = L_{2,j+2} = \pm n C_j u_j^* \tag{5.21}$$

where the "±" terms in Eqs. 5.20 and 5.21 are positive if species j is a cation and negative if species j is an anion. Finally, the coefficients $L_{j+2,i+2}$ can be defined in accordance with Eqs. 5.16 through 5.18 as follows:

$$L_{j+2,i+2} = \begin{cases} 0 & ; \; j \neq i \\ \dfrac{nD_j^* C_j}{RT} & ; \; j = i \end{cases} \tag{5.22}$$

Substitution of Eqs. 5.9 - 5.11 and Eqs. 5.20 - 5.22 into Eqs. 5.7 yields the following set of coupled flux equations for M solutes:

$$q = -\left(\frac{k_h}{\gamma_w} + \frac{k_e^2}{n\sigma_e^*}\right)\frac{\partial P}{\partial x} - k_e \frac{\partial \Psi}{\partial x} - \sum_{i=1}^{M}\left(-\frac{\omega C_i k_h}{\gamma_w} \pm \frac{k_e C_i u_i^*}{\sigma_e^*}\right)\frac{\partial \mu_i^c}{\partial x} \tag{5.23a}$$

$$I = -k_e \frac{\partial P}{\partial x} - n\sigma_e^* \frac{\partial \Psi}{\partial x} - \sum_{i=1}^{M}\left(\pm n C_i u_i^*\right)\frac{\partial \mu_i^c}{\partial x} \tag{5.23b}$$

$$J_j^d = -\left(-\frac{\omega C_j k_h}{\gamma_w} \pm \frac{k_e C_j u_j^*}{\sigma_e^*}\right)\frac{\partial P}{\partial x} - \left(\pm n C_j u_j^*\right)\frac{\partial \Psi}{\partial x} - \frac{nD_j^* C_j}{RT}\frac{\partial \mu_j^c}{\partial x}; \; j = 1,2,...,M \tag{5.23c}$$

5.3.1 Coupled Flux without Applied Current

The specific case involving the influence of soil membrane behavior on solute transport can be illustrated by considering a system in which no electrical current is applied across the soil. In this case, I = 0, and Eq. 5.23b can be rearranged to yield the following expression for the electrical potential gradient, $\partial\Psi/\partial x$:

$$\left.\frac{\partial \Psi}{\partial x}\right|_{I=0} = -\frac{k_e}{n\sigma_e^*}\frac{\partial P}{\partial x} - \sum_{i=1}^{M}\left(\pm\frac{C_i u_i^*}{\sigma_e^*}\right)\frac{\partial \mu_i^c}{\partial x} \tag{5.24}$$

In addition, for dilute solutions (Yeung 1990, Yeung and Mitchell 1993)

$$\frac{\partial \mu_i^c}{\partial x} = \frac{RT}{C_i}\frac{\partial C_i}{\partial x} \tag{5.25}$$

Substitution of Eqs. 5.24 and 5.25 into Eqs. 5.23a and 5.23c yields the following set of coupled flux equations for M solutes:

$$q = q_h + q_\pi = k_h i_h + k_\pi i_\pi = -\frac{k_h}{\gamma_w}\frac{\partial P}{\partial x} + \frac{\omega k_h}{\gamma_w}\frac{\partial \pi}{\partial x} \tag{5.26a}$$

$$J_j^d = \frac{\omega C_j k_h}{\gamma_w}\frac{\partial P}{\partial x} + n\left[-D_j^*\frac{\partial C_j}{\partial x} \pm \frac{C_j u_j^*}{\sigma_c^*} RT \sum_{i=1}^{m}\left(\pm u_i^*\right)\frac{\partial C_i}{\partial x}\right]; \; j = 1, 2, ..., M \tag{5.26b}$$

where q_h [Lt^{-1}] represents hydraulic liquid flux in accordance with Darcy's law, q_π [Lt^{-1}] is chemico-osmotic liquid flux, i_h is the hydraulic gradient, i_π is the chemico-osmotic gradient, and π represents chemico-osmotic pressure [$ML^{-2}t^{-2}$] in accordance with the van't Hoff expression for dilute solutions, or

$$\pi = RT\sum_{i=1}^{M} C_i \tag{5.27}$$

The chemico-osmotic liquid flux, q_π, represents the flux of liquid across a soil membrane from a lower solute concentration to a higher solute concentration, i.e., opposite to the direction of solute diffusion.

The summation term in Eq. 5.26b also can be separated into individual summation terms for the cation and anion species to yield

$$J_j^d = \frac{\omega C_j k_h}{\gamma_w}\frac{\partial P}{\partial x} - n\left[D_j^*\frac{\partial C_j}{\partial x} \pm \frac{C_j u_j^*}{\sigma_e^*}RT\left(\sum\left(u_-^*\right)\frac{\partial C_-}{\partial x} - \sum\left(u_+^*\right)\frac{\partial C_+}{\partial x}\right)\right] \quad (5.28)$$

where the subscripts "+" and "-" represent cations and anions, respectively. The effective electrical conductance, σ_e^*, also can be expressed in terms of the individual mobilities of the cations and anions as follows (Alshawabkeh and Acar 1996):

$$\sigma_e^* = F\left(\sum|z_-|u_-^*C_- + \sum|z_+|u_+^*C_+\right) \quad (5.29)$$

where $\mathcal{F}$ is Faraday's constant (= 96,500 coulombs/equivalent). Furthermore, the self-diffusion coefficient is related to the ionic mobility by the Nernst equation, that can be written in "effective" form for diffusion in soil (see Eq. 5.19) as follows (Alshawabkeh and Acar 1996):

$$D_j^* = \frac{u_j^* RT}{F|z_j|} \quad (5.30)$$

Substitution of Eqs. 5.29 and 5.30 into Eq. 5.28 yields the following diffusive flux expression:

$$J_j^d = \frac{\omega C_j k_h}{\gamma_w}\frac{\partial P}{\partial x} - n\left[D_j^*\frac{\partial C_j}{\partial x} \pm D_j^* C_j|z_j|\frac{\left(\sum D_-^*|z_-|\frac{\partial C_-}{\partial x} - \sum D_+^*|z_+|\frac{\partial C_+}{\partial x}\right)}{\left(\sum D_-^*|z_-|^2 C_- + \sum D_+^*|z_+|^2 C_+\right)}\right] \quad (5.31)$$

5.3.2 Salt-Diffusion Coefficients

The effective diffusion coefficients, D^*, in Eq. 5.31 are self-diffusion coefficients based on the individual mobility of each species without regard to the requirement for

electroneutrality in solution (e.g., see Yeung 1990). However, diffusive migration of ionic species in a typical waste containment scenario represents a salt-diffusion process whereby the ions travel together in the same direction through the soil (Shackelford and Daniel 1991). The "±" term in Eq. 5.31 represents the interaction among ionic species to maintain electroneutrality during salt diffusion. This interaction is characterized by electrical potential gradients generated between the cations and anions in response to different ionic mobility of each species, which slows down the faster-moving ions and speeds up the slower moving ions (Robinson and Stokes 1959).

Vinograd and McBain (1941) developed a general expression for the salt-diffusion coefficient of an ionic species, D_{sj}, in a free solution containing multiple solutes as a function of the self-diffusion coefficients of all species in the solution. This expression can be written for one-dimensional diffusion in aqueous solution as follows (see Appendix B):

$$D_{sj} = D_j \pm \frac{D_j C_j |z_j| \left(\sum D_- |z_-| \partial C_- - \sum D_+ |z_+| \partial C_+ \right)}{\partial C_j \left(\sum D_- |z_-|^2 C_- + \sum D_+ |z_+|^2 C_+ \right)} \tag{5.32a}$$

or, for solute diffusion in soil,

$$D^*_{sj} = \tau_a D_{sj} = \left[D^*_j \pm \frac{D^*_j C_j |z_j| \left(\sum D^*_- |z_-| \partial C_- - \sum D^*_+ |z_+| \partial C_+ \right)}{\partial C_j \left(\sum D^*_- |z_-|^2 C_- + \sum D^*_+ |z_+|^2 C_+ \right)} \right] \tag{5.32b}$$

Substitution of Eq. 5.32b into Eq. 5.31 yields the final expression for the diffusive solute flux of any solute species j in a soil system containing M solutes:

$$J^d_j = \frac{\omega C_j k_h}{\gamma_w} \frac{\partial P}{\partial x} - n D^*_{sj} \frac{\partial C_j}{\partial x} \tag{5.33}$$

The first term in Eq. 5.33 represents a diffusive coupling term that arises due to the soil membrane behavior, while the second term represents traditional diffusion in accordance with Fick's first law. The diffusive coupling term has been called *streaming current* (Mitchell 1993), *hyperfiltration* (de Marsily 1986), or *salt sieving* (McKelvey and Milne 1962, Groenevelt et al. 1980). The form of Eq. 5.33 is essentially the same as that previously reported by Groenevelt et al. (1980), although their approach in deriving Eq. 5.33 differed from the current approach. If the soil exhibits no membrane behavior, then $\omega = 0$ and Eq. 5.33 reduces to the traditional form for Fick's first law, or

$$J_j^d\Big|_{\omega=0} = -nD_{sj}^* \frac{\partial C_j}{\partial x} \tag{5.34}$$

The effective diffusion coefficient in Fick's first law typically is assumed to be constant for a given soil and solute, provided that the soil is homogeneous. However, Eq. 5.32 indicates that D_{sj} is a function of the absolute concentration and concentration gradient of each solute as well as the self-diffusion coefficient of each solute. Therefore, the value of D_{sj} is influenced by interactions among species j and all other ionic species in order to maintain electroneutrality in solution, and these interactions tend to be dominated by the species with greater concentration and/or concentration gradient. In practical terms, Eq. 5.32 suggests that D_{sj} and, therefore, D_{sj}^* may vary with both time and location within a homogeneous soil during transient transport. The significance of this effect will be discussed in greater detail later in this chapter.

5.3.3 Total Coupled Solute Flux

The total flux of a solute species j, or J_j [mol·L^{-2}t^{-1}], in a fine-grained soil (neglecting mechanical dispersion) is represented by the combined processes of advection and diffusion, or

$$J_j = J_j^a + J_j^d = qC_j + J_j^d \tag{5.35}$$

where J_j^a is the advective flux [mol·L^{-2}t^{-1}]. Therefore, the general expression for total coupled flux of a solute j is obtained by substituting Eqs. 5.26a and 5.33 into Eq. 5.35 to yield (e.g., see Mitchell 1993)

$$J_j = (1-\omega)q_h C_j + q_\pi C_j - nD_{sj}^* \frac{\partial C_j}{\partial x} \tag{5.36}$$

The first term in Eq. 5.36 represents the advective term that is reduced by a factor of 1-ω due to the membrane behavior of the soil. In physical terms, the factor 1-ω is considered to represent the process of hyperfiltration whereby solutes are filtered out of solution as the solution passes through the membrane under a hydraulic gradient (e.g., see Fritz and Marine 1983). The second term in Eq. 5.36 represents counter advection of solutes due to chemico-osmosis that typically occurs opposite to the direction of the hydraulic liquid flux. The remaining term in Eq. 5.36 represents solute diffusion in the form of Fick's first law. Under the condition that the soil does not exhibit membrane behavior (i.e., $\omega = 0$), $q_\pi = 0$ and Eq. 5.36 reduces to the traditional advective-diffusive solute flux, or

$$J_j\Big|_{\omega=0} = q_h C_j - nD_{sj}^* \frac{\partial C_j}{\partial x} \tag{5.37}$$

5.3.4 Coupled Solute Transport

The governing partial differential equations (PDE) for one-dimensional, coupled transport of an ionic species, j, under transient conditions is obtained by substituting Eq. 5.36 into the following mass balance expression:

$$\frac{\partial Q_j}{\partial t} = -\nabla \cdot J_j = -\frac{\partial}{\partial x}\left[(1-\omega)q_h C_j + q_\pi C_j - nD^*_{sj}\frac{\partial C_j}{\partial x}\right] \tag{5.38}$$

where Q_j [mol·L^{-3}] represents the total moles (aqueous and solid (adsorbed) phase) of species j per unit total volume of porous medium (i.e., solids and voids), that can be expressed as

$$Q_j = nC_j + \rho_d K_{dj} C_j \tag{5.39}$$

where ρ_d is the dry density of the soil [ML^{-3}] and K_{dj} is the distribution coefficient [L^{3}M^{-1}] that accounts for linear, reversible, and instantaneous partitioning of species j between the soil solids and the aqueous solution. Assuming steady hydraulic liquid flux (i.e., q_h = constant) through a homogeneous, incompressible soil (i.e., n = constant), Eq. 5.38 can be written as follows upon substitution on Eq. 5.39:

$$R_{dj}\frac{\partial C_j}{\partial t} = (\omega - 1)v_h\frac{\partial C_j}{\partial x} - v_\pi\frac{\partial C_j}{\partial x} - C_j\frac{\partial v_\pi}{\partial x} + D^*_{sj}\frac{\partial^2 C_j}{\partial x^2} + \frac{\partial D^*_{sj}}{\partial x}\frac{\partial C_j}{\partial x} \tag{5.40}$$

where v_h is the hydraulic seepage velocity (=q_h/n), v_π is the chemico-osmotic seepage velocity (=q_π/n), and R_{dj} represents the retardation factor of species j (Freeze and Cherry 1979), or

$$R_{dj} = 1 + \frac{\rho_d K_{dj}}{n} \tag{5.41}$$

The value of R_{dj} for nonreactive (non-adsorbing) solutes (e.g., Cl^-) is unity (i.e., $R_d = 1$), whereas R_d for reactive (adsorbing) solutes is greater than unity (i.e., $R_d > 1$).

5.3.5 Coupled Solute Transport with Ion Exchange

The primary advantage of the model presented herein relative to the model developed by Yeung (1990) and Yeung and Mitchell (1993) is the ability to simulate the more general and typically more appropriate case of salt migration through a clay barrier in which the cation species is reactive (i.e., $R_d > 1$) and, thus, undergoes ion exchange at the clay particle surfaces. For example, consider the coupled flux of the cation (c) and anion (a) of a strong (i.e., fully dissociating) salt through a clay-water system in which the exchange sites of the clay particles are filled with a single exchangeable cation species (x) that may enter the solution phase as a result of ion exchange with the salt cation. In this analysis, the salt anion is assumed to be non-reactive (i.e., $R_d = 1$). The resulting total flux equations for the individual cation and anion species, in accordance with Eq. 5.36, are as follows:

$$J_c = (1-\omega)q_h C_c - q_\pi C_c - nD^*_{sc}\frac{\partial C_c}{\partial x} \tag{5.42a}$$

$$J_a = (1-\omega)q_h C_a - q_\pi C_a - nD^*_{sa}\frac{\partial C_a}{\partial x} \tag{5.42b}$$

$$J_x = (1-\omega)q_h C_x - q_\pi C_x - nD^*_{sx}\frac{\partial C_x}{\partial x} \tag{5.42c}$$

where, in accordance with Eqs. 5.26a and 5.27,

$$q_\pi = \frac{\omega k_h}{\gamma_w} RT\left(\frac{\partial C_c}{\partial x} + \frac{\partial C_a}{\partial x} + \frac{\partial C_x}{\partial x}\right) \tag{5.43}$$

and the effective salt-diffusion coefficients are based on Eq. 5.32 as follows:

$$D^*_{sc} = \tau_a D_{sc} = \tau_a\left[D_c + \frac{D_c C_c |z_c|}{\partial C_c}\frac{\left(D_a|z_a|\partial C_a - D_c|z_c|\partial C_c - D_x|z_x|\partial C_x\right)}{\left(D_a|z_a|^2 C_a + D_c|z_c|^2 C_c + D_x|z_x|^2 C_x\right)}\right] \tag{5.44a}$$

$$D^*_{sa} = \tau_a D_{sa} = \tau_a\left[D_a - \frac{D_a C_a |z_a|}{\partial C_a}\frac{\left(D_a|z_a|\partial C_a - D_c|z_c|\partial C_c - D_x|z_x|\partial C_x\right)}{\left(D_a|z_a|^2 C_a + D_c|z_c|^2 C_c + D_x|z_x|^2 C_x\right)}\right] \tag{5.44b}$$

$$D^*_{sx} = \tau_a D_{sx} = \tau_a\left[D_x + \frac{D_x C_x |z_x|}{\partial C_x}\frac{\left(D_a|z_a|\partial C_a - D_c|z_c|\partial C_c - D_x|z_x|\partial C_x\right)}{\left(D_a|z_a|^2 C_a + D_c|z_c|^2 C_c + D_x|z_x|^2 C_x\right)}\right] \tag{5.44c}$$

The resulting equations for transient transport of the salt cation and salt anion, based on Eq. 5.40, are

$$R_{dc}\frac{\partial C_c}{\partial t} = (\omega - 1)v_h\frac{\partial C_c}{\partial x} - v_\pi\frac{\partial C_c}{\partial x} - C_c\frac{\partial v_\pi}{\partial x} + D^*_{sc}\frac{\partial^2 C_c}{\partial x^2} + \frac{\partial D^*_{sc}}{\partial x}\frac{\partial C_c}{\partial x} \tag{5.45a}$$

and

$$\frac{\partial C_a}{\partial t} = (\omega - 1)v_h\frac{\partial C_a}{\partial x} - v_\pi\frac{\partial C_a}{\partial x} - C_a\frac{\partial v_\pi}{\partial x} + D^*_{sa}\frac{\partial^2 C_a}{\partial x^2} + \frac{\partial D^*_{sa}}{\partial x}\frac{\partial C_a}{\partial x} \tag{5.45b}$$

where, in accordance with Eq. 5.43,

$$v_\pi = \frac{q_\pi}{n} = \frac{\omega k_h}{n\gamma_w} RT\left(\frac{\partial C_c}{\partial x} + \frac{\partial C_a}{\partial x} + \frac{\partial C_x}{\partial x}\right) \tag{5.46}$$

A similar expression can be written for the exchangeable cation but is not necessary in the simple case of a single exchangeable cation since the pore-fluid concentration of the exchangeable cation C_x at any location and time can be determined based on the solution of Eqs. 5.45a and 5.45b using the following requirement for electroneutrality in solution:

$$C_x = \frac{C_a|z_a| - C_c|z_c|}{|z_x|} \tag{5.47}$$

Concentration profiles for the three ionic species may be obtained by simultaneous solution of Eqs. 5.45a, 5.45b and 5.47 using a numerical method, and can be used in conjunction with Eq. 5.42a-c to evaluate the total flux of each species for a given time and location in the system.

The above model is valid provided that the exchange sites of the clay are filled with a single cation species. In reality, most clay soils contain multiple species of exchangeable cations. For example, while many processed, commercially-available bentonites are considered sodium (Na) bentonites, these soils typically contain an appreciable amount of other exchangeable cations such as Ca^{2+}, K^+, and Mg^{2+} (Stern and Shackelford 1998, Shackelford et al. 2000). However, Ca tends to be attracted more strongly to the soil surface than Na due to a higher valence and, as a result, typically is not as readily exchangeable as Na (Mitchell 1993). A more rigorous analysis that includes the potential contribution of multiple exchangeable cations could be performed by expanding definition of q_π (Eq. 5.43), expanding the electroneutrality constraint (Eq. 5.47), and incorporating an ion exchange model to account for competition among ions for the exchange sites based on an order of replaceability (e.g., Mitchell 1993). Such

rigor requires a more complex model with more input parameters that is less practical to use.

5.3.6 Solute Transport without Membrane Behavior

For non-membrane behavior, the chemico-osmotic efficiency coefficient is zero (i.e., $\omega = 0$), so chemico-osmotic liquid flux does not occur (i.e., $q_\pi = v_\pi = 0$) and, consequently, $\partial v_\pi / \partial x = 0$. In this case, the resulting expressions for total flux of the salt cation, salt anion, and exchangeable cation are given as follows based on Eq. 5.37:

$$J_c\big|_{\omega=0} = q_h C_c - nD^*_{sc}\frac{\partial C_c}{\partial x} \tag{5.48a}$$

$$J_a\big|_{\omega=0} = q_h C_a - nD^*_{sa}\frac{\partial C_a}{\partial x} \tag{5.48b}$$

$$J_x\big|_{\omega=0} = q_h C_x - nD^*_{sx}\frac{\partial C_x}{\partial x} \tag{5.48c}$$

Similarly, the transport equations for the salt cation and salt anion are given as follows based on Eqs. 5.45a-b:

$$R_{dc}\frac{\partial C_c}{\partial t}\bigg|_{\omega=0} = v_h\frac{\partial C_c}{\partial x} + D^*_{sc}\frac{\partial^2 C_c}{\partial x^2} + \frac{\partial D^*_{sc}}{\partial x}\frac{\partial C_c}{\partial x} \tag{5.49a}$$

$$\frac{\partial C_a}{\partial t}\bigg|_{\omega=0} = v_h\frac{\partial C_a}{\partial x} + D^*_{sa}\frac{\partial^2 C_a}{\partial x^2} + \frac{\partial D^*_{sa}}{\partial x}\frac{\partial C_a}{\partial x} \tag{5.49b}$$

Equations 5.49a and 5.49b represent advective-dispersive transport, but are non-linear equations that must be solved numerically due to the variable nature of the effective salt-diffusion coefficients, D^*_{sc} and D^*_{sa}, resulting from the presence of the desorbed

exchangeable cation species (see Eqs. 5.44a and 5.44b). As steady-state transport is approached, ion exchange becomes complete and the exchangeable cation species eventually disappears from the soil (i.e., as $t \rightarrow \infty$, $C_x \rightarrow 0$). As a result, the electroneutrality constraint (Eq. 5.47) at steady-state reduces to

$$\left(C_a|z_a|\right)_{ss} = \left(C_c|z_c|\right)_{ss} \tag{5.50}$$

or, in differential form,

$$\left(\partial C_a|z_a|\right)_{ss} = \left(\partial C_c|z_c|\right)_{ss} \tag{5.51}$$

where the subscript 'ss' represents steady state. Substitution of Eqs. 5.50 and 5.51 along with $C_x = \partial C_x = 0$ into Eqs. 5.44a and 5.44b reveals that

$$\left(D^*_{sc}\right)_{ss} = \left(D^*_{sa}\right)_{ss} = D^*_s \tag{5.52}$$

where D^*_s is given by the Nernst-Einstein equation (Shackelford 1989) as follows:

$$D^*_s = \tau_a D_s = \tau_a \left[\frac{D_c D_a \left(|z_a| + |z_c|\right)}{\left(D_a|z_a| + D_c|z_c|\right)}\right] \tag{5.53}$$

Inspection of Eqs. 5.52 and 5.53 reveals that D^*_s is the same for both the cation and anion and is a constant value, provided that the apparent tortuosity factor, τ_a, is constant for the porous medium.

In ion exchanging systems, Eq. 5.53 and, therefore, Eqs. 5.49a-b are valid only after ion exchange processes are complete (i.e., at steady state). However, a common assumption in traditional advective-dispersive solute transport analyses is that the values

of D_{sc}^* and D_{sa}^* in Eqs. 5.47a and 5.47b can be represented by D_s^* during transient transport. Since D_s^* is constant, $\partial D_s^*/\partial x = 0$ and Eqs. 5.49a and 5.49b reduce to the traditional one-dimensional, advective-diffusive solute transport equations, or

$$R_{dc}\frac{\partial C_c}{\partial t}\bigg|_{\omega=0} = v_h\frac{\partial C_c}{\partial x} + D_s^*\frac{\partial^2 C_c}{\partial x^2} \tag{5.54a}$$

$$\frac{\partial C_a}{\partial t}\bigg|_{\omega=0} = v_h\frac{\partial C_a}{\partial x} + D_s^*\frac{\partial^2 C_a}{\partial x^2} \tag{5.54b}$$

The primary advantage of Eqs. 5.54a-b relative to Eqs. 5.49a-b is that closed-form analytical solutions of Eq. 5.54a-b are available for a variety of initial and boundary conditions. For example, the analytical solution for time-dependent diffusive flux (i.e., $v_h = 0$) of solute j [$ML^{-2}t^{-1}$] at the exit boundary of a soil (i.e., at x = L) based on a constant source concentration [i.e., $C_j(x=0,t) = C_{oj}$], perfectly flushing conditions [i.e., $C_j(x=L,t) = 0$], and no solutes initially in the soil [i.e., $C_j(0<x\leq L,t=0) = 0$] is given by Crank (1960) as follows:

$$J_j^d(L,t)\Big|_{\omega=0} = \frac{nD_s^*C_{oj}}{L} + \frac{2nD_s^*C_{oj}}{L}\sum_{m=1}^{\infty}\cos(m\pi)\exp\left(-\frac{D_s^*m^2\pi^2t}{R_{dj}L^2}\right) \tag{5.55}$$

or for advective-diffusive transport (i.e., $v_h > 0$) based on Rabideau and Khandelwal (1999) as follows:

$$J_j(L,t)\Big|_{\omega=0} = C_{oj}\exp\left(\frac{v_h L}{2D_s^*}\right)\left\{\frac{nv_h}{2\sinh\left(\frac{v_h L}{2D_s^*}\right)} + nD_s^*\left(\frac{2\pi^2}{L^3}\right)\sum_{m=1}^{\infty}\frac{(-1)^2 m^2}{\frac{v_h^2}{4D_s^{*2}} + \frac{m^2\pi^2}{L^2}}\exp\left[\left(\frac{v_h^2}{4D_s^{*2}} + \frac{D_s^* m^2\pi^2}{L^2}\right)\frac{t}{R_{dj}}\right]\right\} \quad (5.56)$$

where π is the operational constant (= 3.14159...). Again, these analytical solutions do not account for electroneutrality during transient transport in ion-exchanging systems.

5.4 NUMERICAL MODELING

Time-dependent concentration profiles for the salt cation and salt anion are obtained in this study by solving Eqs. 5.45a, 5.45b, and 5.47 iteratively using an implicit-in-time, centered-in-space finite difference algorithm. The clay barrier of length L is divided into cells of thickness Δx, and the transit time is divided into discrete intervals of length Δt. Values of Δx and Δt were chosen in order to maintain compliance with stability requirements for the implicit-in-time, centered-in-space approach, and the algorithm was adjusted properly to account for numerical dispersion (Smith 1985). All details regarding the finite difference algorithm and the associated FORTRAN program are contained in Appendix C.

5.4.1 Initial and Boundary Conditions

The initial and boundary conditions considered in this study are the constant source, perfectly-flushing conditions described previously in conjunction with Eqs. 5.55 and 5.56. Similar initial and boundary conditions were employed by Greenberg et al. (1973) to describe the coupled transport of NaCl through a clay aquitard below a salt-

water aquifer. The problem geometry for this situation, shown in Fig. 5.2a, is analogous to the problem geometry associated with containment of miscible pollutants with engineered clay barrier materials shown in Fig. 5.2b (Shackelford 1996). In addition, the perfectly-flushing exit boundary condition is recommended as a conservative approach for design of vertical barriers such as cutoff walls (Rabideau and Khandelwal 1999).

5.4.2 Comparison of Analytical and Numerical Solutions for $\omega = 0$

The finite difference solution of Eqs. 5.45 - 5.47 is used to obtain concentration time-dependent concentration profiles that can be used to compute flux values for the salt anion and salt cation based on Eqs. 5.42-5.44. This solution should produce similar results as the analytical solutions of the advective-dispersive equation given by Eqs. 5.55 and 5.56 for the limiting case in which $\omega = 0$ provided that $R_d = 1$ for the solutes or, if $R_d > 1$ for the salt cation, the free-solution self-diffusion coefficient for the exchangeable cation, D_{ox}, is equivalent to the free-solution self-diffusion coefficient for the salt cation, D_{oc} (i.e., $D_{ox} = D_{oc}$).

For example, consider the transport of potassium chloride (KCl) through a soil barrier (L = 1 m) in which chloride (Cl^-) is a non-reactive solute with $R_d = 1$ and potassium (K^+) is a reactive solute with $R_d = 5$. The free-solution self-diffusion coefficients, D_o, for Cl^- and K^+ and the free-solution salt-diffusion coefficient, D_s, for KCl are given in Table 5.1 (see Shackelford and Daniel 1991) along with resulting values for D_o^* and D_s^* based on $\tau_a = 0.1$. Diffusion coefficient values for Na^+ and NaCl also are given in Table 5.1 for comparison. The D_s (or D_s^*) values in Table 5.1 essentially represent the mean of the D_o (or D_o^*) values for the individual ionic species.

In this example, the numerical model accounts for desorption of an exchangeable cation species x that replaces the reactive K^+ in solution to satisfy electroneutrality. Therefore, the numerical model requires a value of the free-solution self-diffusion coefficient, D_{ox}, for exchangeable species x. The analytical solutions to the advective-

dispersive equation (Eqs. 5.55 and 5.56) require only the D_s^* value for the salt (i.e., KCl) and do not account for desorption of an exchangeable cation species. Thus, traditional advective-dispersive theory inherently violates electroneutrality during transient transport in ion-exchanging systems, as noted earlier. This inherent limitation in the traditional theory is avoided if we assume that $D_{ox} = D_{oc}$ (= 19.6 x 10^{-10} m^2/s) as shown by the exit flux values (i.e., J(x=L)) for Cl^- and K^+ in Fig. 5.3. The results in Fig. 5.3 indicate excellent agreement between the numerical solution and the analytical solutions for pure diffusion (i = 0; Fig. 3a) and advection-dispersion (i = 10; Fig. 3b), since there is no difference between the ionic mobility of the salt cation (K^+) and exchangeable cation species.

In real systems, the mobility of the exchangeable cation is not likely to be equivalent to the mobility of the salt cation. For example, sodium (Na^+) typically is the predominant exchangeable cation in fine-grained soils containing bentonite. The free-solution self-diffusion coefficient for Na^+ (13.3 x 10^{-10} m^2/s in Table 5.1) is considerably smaller than that for K^+. The resulting flux values versus time for this condition are illustrated in Fig. 5.4a for i = 0 and in Fig. 5.4b for i = 10. The results indicate that transport of Cl^- based on the numerical solution appears to be retarded relative to the results from the analytical solutions. This apparent retardation effect is due to the fact that some of the Cl^- also migrates with the slower Na^+ rather than K^+ until ion exchange is complete. In addition, the Cl^- flux for i = 10 displays initial leveling at a value less than the steady-state flux. Similar behavior was reported by Shackelford et al. (1999) in a theoretical study of electrical conductivity breakthrough curves associated with transport of $CaCl_2$ through a sodium (Na) saturated soil in which the mobility of the exchangeable cation (Na^+) was less than the mobility of the salt cation (Ca^{2+}). The results in Fig. 5.4 also show that flux values given by the analytical solutions are equivalent to the flux values given by the numerical solution after ion exchange is complete and steady-state

conditions have been established. At steady state, Na^+ no longer is released into solution, and, therefore, Cl^-, migrates with K^+ in accordance with the combined mobility for the two species (i.e., $D_s^* = 1.993 \times 10^{-10}$ m^2/s).

5.4.3 Theoretical Analysis of Coupled Solute Transport

Examination of the equation for coupled solute flux given in Eq. 5.36 indicates that solute flux may be affected by membrane behavior due to (1) hyperfiltration, whereby ions are filtered out as the solution passes through the membrane under a hydraulic gradient (i.e., the advective flux is reduced by a factor of 1 - ω), and (2) counter-advection of solutes (i.e., $q_\pi c_j$) due to chemico-osmotic liquid flux (q_π) opposite to the direction of the hydraulic liquid flux (q_h). These coupling effects are termed *explicit* coupling effects for the remainder of this chapter. In addition, results of steady-state diffusion tests presented in Chapter 4 for potassium chloride (KCl) and a geosynthetic clay liner (GCL) containing sodium bentonite (Bentomat®; see Fig. 5.5) show that an *implicit* (or indirect) coupling effect also occurs in soil membranes such that the apparent tortuosity factor, τ_a, decreases with an increase in the chemico-osmotic efficiency coefficient, ω. The increase in ω also is correlated with a decrease in solute concentration, C. Based on the current understanding of ion restriction in soil membranes, lower solute concentrations in the pore space likely correspond to larger diffuse double layers surrounding the clay particles resulting in an increase in ω and a corresponding decrease in τ_a, since less of the pore space is available for solute transport (see Chapter 4).

The results of the steady-state diffusion tests on the Bentomat® GCL specimens with KCl solutions are summarized in Table 5.2. In addition, the relationship between the source KCl concentration (C_o) and the chemico-osmotic efficiency coefficient, ω, is illustrated in Fig. 5.6a, while the relationship between D_s^* (and τ_a) and ω is illustrated in

Fig. 5.6b. The decrease in ω with increasing salt concentration is consistent with results of previous studies (Kemper and Rollins 1966, Olsen 1969, Kemper and Quirk 1972), and is attributed to collapse of diffuse double layers surrounding the clay particles as described previously. When extrapolated to concentrations beyond the highest source concentration (i.e., $C_o > 0.047$ M), the trend in Fig. 5.6a indicates that the GCL is expected to exhibit virtually no chemico-osmotic membrane efficiency at concentrations beyond approximately 0.1 M (i.e., $\omega \rightarrow 0$ as $C_o \rightarrow 0.1$ M KCl). The implicit coupling effect in Fig. 5.6b also diminishes as C_o increases (and as ω decreases) such that the apparent tortuosity factor, τ_a, approaches a maximum value as ω approaches zero (i.e., $\tau_a \rightarrow \tau_{a,max}$ as $\omega \rightarrow 0$). Therefore, the maximum apparent tortuosity factor, $\tau_{a,max}$, represents the matrix tortuosity factor, τ_m, that accounts for the tortuous nature of the solute migration pathway through a porous medium due solely to the geometry of the interconnected pores (see Chapter 4). Based on the results in Fig. 5.6b, $\tau_m = \tau_{a,max} = 0.12$. The data trend in Fig. 5.6b further indicates that τ_a approaches zero as ω approaches unity (i.e., $\tau_a \rightarrow 0$ as $\omega \rightarrow 1$). This condition represents the expected behavior of an "ideal" membrane that, by definition, completely restricts the passage of solutes.

The results in Table 5.2 and Fig. 5.6 form the basis for a theoretical analysis of the influence of explicit and implicit coupling on solute (KCl) transport through soil membranes. The R_d values in Table 5.2 also were measured in the steady-state diffusion tests in accordance with the time-lag approach (see Chapter 2). However, the theoretical analysis presented herein is performed assuming $R_d = 1$ for both Cl^- and K^+ in order to evaluate only the influence of the membrane coupling effects, without additional effects that may result from the presence of an exchangeable cation species as described previously in Fig. 5.4. Under this condition, migration of Cl^- and K^+ must occur at the same rate in order to maintain electroneutrality in solution. Thus, the individual flux of either Cl^- or K^+ is representative of the flux of the salt as a whole (i.e., KCl flux), and

each solute migrates at the same rate in accordance with the effective salt-diffusion coefficient, D_s^* ($= \tau_a D_{so}$). This condition is representative of a soil that is initially saturated with K^+ whereby no cation exchange would occur. In this case, the coupled solute flux equation (Eq. 5.36) can be written as

$$J_s = (1-\omega)q_h C_s - q_\pi C_s - nD_s^* \frac{\partial C_s}{\partial x} \tag{5.57}$$

and the resulting solute transport equation is

$$\frac{\partial C_s}{\partial t} = (\omega - 1)v_h \frac{\partial C_s}{\partial x} - v_\pi \frac{\partial C_s}{\partial x} - C_s \frac{\partial v_\pi}{\partial x} + D_s^* \frac{\partial^2 C_s}{\partial x^2} \tag{5.58}$$

where the subscript "s" refers to the salt. In addition, the chemico-osmotic seepage velocity, v_π, can be written as

$$v_\pi = \frac{q_\pi}{n} = \frac{\omega k_h}{n\gamma_w} \nu RT \left(\frac{\partial C_s}{\partial x}\right) \tag{5.59}$$

where ν represents the number of ions per molecule of salt (e.g., $\nu = 2$ for KCl). Substitution of Eq. 5.59 into Eqs. 5.57 and 5.58 and rearrangement yields the following flux and transport equations:

$$J_s = (1-\omega)q_h C_s - \frac{\omega k_h}{\gamma_w} \nu RT \left(\frac{\partial C_s}{\partial x}\right) C_s - nD_s^* \frac{\partial C_s}{\partial x} \tag{5.60}$$

and

$$\frac{\partial C_s}{\partial t} = \left[(\omega - 1)v_h - \frac{\omega k_h}{n\gamma_w} \nu RT \left(\frac{\partial C_s}{\partial x}\right)\right] \frac{\partial C_s}{\partial x} + \left(D_s^* - C_s \frac{\omega k_h}{n\gamma_w} \nu RT\right) \frac{\partial^2 C_s}{\partial x^2} \tag{5.61}$$

The simulations using this theory are performed for a 1-m thick soil barrier (L = 1 m, n = 0.8) for the same source concentrations, C_o, used in the diffusion tests. The different simulation cases considered the analysis are listed in Tables 5.3 and 5.4. Input parameters for these cases have been established based on the measured results in Table 5.2 with the exception that $R_d = 1$ is assumed for both Cl^- and K^+. Cases with prefix "EI" represent cases based on Eqs. 5.60 and 5.61 in which both explicit and implicit coupling effects are included. The explicit coupling effects are included by using the appropriate value of ω (> 0) corresponding to the value of C_o. The implicit coupling effect is included by using the appropriate value of τ_a ($< \tau_m$) corresponding to the value of C_o. For example, in case EI3 (C_o = 0.0087 M), the appropriate values of ω and τ_a are 0.49 and 0.063, respectively, based on the results in Table 5.2. Cases with prefix "E" are cases based on Eqs. 5.60 and 5.61 in which explicit coupling is included (i.e., $\omega > 0$) but implicit coupling is ignored. Implicit coupling is ignored by assuming that membrane behavior does not affect the tortuosity of the soil barrier and, thus, τ_a is equal to the matrix tortuosity, τ_m, for all C_o. In case E3, for example, $\omega = 0.14$ but $\tau_a = \tau_m = 0.12$.

Cases with prefix "I" and "NM" both are cases in which the chemico-osmotic efficiency of the soil is ignored (i.e., $\omega = 0$). For these cases, Eqs. 5.60 and 5.61 reduce to the advective-dispersive equations (e.g., see Eqs. 5.48 and 5.54). The "I" cases represent advective-dispersive transport that includes implicit coupling ($\tau_a < \tau_m$), whereas the "NM" cases represent "non-membrane" cases in which the soil would exhibit no chemico-osmotic efficiency and the tortuosity of the solute migration pathway is solely a function of pore geometry. Thus, neither explicit nor implicit coupling effects occur in the "non-membrane" cases. For example, $\omega = 0$ and $t_a = 0.063$ in case I3, while w = 0 and $\tau_a = \tau_m = 0.12$ in case NM3.

The effect of hydraulic gradient, i_h, is examined by considering three different values in the simulations (i_h = 0, 10, 100). Values of the Peclet number, P_L, for each case are related to i_h and τ_a as follows:

$$P_L = \frac{v_h L}{D_s^*} = \frac{k_h i_h L}{n\tau_a D_{so}} \tag{5.62}$$

These values of P_L represent the relative significance of advection versus diffusion. For example, values of $P_L < 20$ are representative of a diffusion-dominated system, whereas advection tends to be more significant relative to diffusion at higher values of P_L (Shackelford 1995). Since implicit coupling is characterized by a reduction in τ_a, values of P_L for the cases in which implicit coupling is included in the analysis (i.e., the "I" and "EI" cases) are higher than P_L values for cases with the same hydraulic gradient in which implicit coupling is ignored (i.e., the "E" and "NM" cases). However, explicit coupling does not affect P_L, since Eq. 5.62 is independent of ω.

5.4.3.1 Solute Flux at x = L

The influence of membrane coupling effects are examined in this study based on the exit flux of salt from the soil, $J_s(x=L)$. Theoretical values of $J_s(x=L)$ for C_o = 0.047 M, 0.020 M, 0.0087 M, and 0.0039 M based on the cases given in Table 5.3 and 5.4 are illustrated versus time in Figs. 5.7, 5.8, 5.9, and 5.10, respectively. The theoretical condition corresponding to $J_s(x=L) = 0$ for an "ideal" membrane that completely restricts the passage of solutes also is shown for comparison. The results indicate that the highest values of exit flux for a given C_o and hydraulic gradient, i_h, typically occur for the non-membrane cases (i.e., $\omega = 0$, $\tau_a = 0.12$), whereas the lowest values of exit flux occur for cases in which both explicit and implicit membrane coupling are considered in the analysis. In addition, the reduction in exit flux due to combined explicit and implicit coupling relative to the non-membrane case is greater as C_o decreases, since ω increases and τ_a decreases with decreasing C_o. Thus, as C_o decreases, the values of exit flux

corresponding to the cases that include both explicit and implicit coupling effects approach more closely the "ideal" membrane condition in which $J_s(x=L) = 0$.

For the cases in which $C_o = 0.047$ M (Fig. 5.7) and $C_o = 0.02$ M (Fig. 5.8), the reduction in exit flux is primarily due to explicit coupling associated with $\omega = 0.14$ (for $C_o = 0.047$ M) and $\omega = 0.32$ (for $C_o = 0.02$ M). Implicit coupling has little or no effect on exit flux in Figs. 5.7 and 5.8, since the τ_a values corresponding to these source concentrations (0.119 and 0.112, respectively) are only slightly lower than the maximum tortuosity factor of 0.12 corresponding to $\omega = 0$.

For the lower source concentrations (i.e., $C_o = 0.0087$ M in Fig. 5.9 and $C_o = 0.0039$ M in Fig. 5.10), explicit and implicit coupling effects both contribute to the reduction in exit flux. The values of ω corresponding to $C_o = 0.0087$ M and $C_o = 0.0039$ M are 0.49 and 0.63, respectively, while the τ_a values are 0.063 and 0.039, respectively. However, the relative contribution of explicit and implicit coupling in these cases appears to be dependent upon the hydraulic gradient, i_h, and the Peclet number, P_L. For example, a majority of the reduction in exit flux in Figs. 5.9 and 5.10 appears to be due to implicit coupling when $i_h = 0$ (and thus, $P_L = 0$), whereas the significance of explicit coupling increases as i_h (and P_L) increases.

For $i_h = 100$, the exit flux values in Figs. 5.9 and 5.10 for the cases that include only implicit coupling (i.e., $\tau_a < \tau_m$ and $\omega = 0$) are as high or higher than the exit flux values for a non-membrane (i.e., $\tau_a = \tau_m$ and $\omega = 0$). If we consider that C_s approaches zero as x approaches L due to the perfectly-flushing condition established at the exit boundary of the soil barrier (i.e., $C_s \rightarrow 0$ as $x \rightarrow L$), the flux equation at $x = L$ can be approximated as follows based on Eq. 5.60:

$$J_s(x=L) \approx - nD_s^* \left.\frac{\partial C_s}{\partial x}\right|_{x=L} = -n\tau_a D_{so} \left.\frac{\partial C_s}{\partial x}\right|_{x=L} \qquad (5.63)$$

Equation 5.63 is not utilized in these simulations, but is presented to illustrate that the exit salt flux for a soil with a given porosity, n, and for a solute with a given free-solution salt diffusion coefficient, D_{so}, is governed by the apparent tortuosity factor, τ_a, and gradient in salt concentration, $\partial C_s/\partial x$, at the exit boundary. Therefore, the aforementioned results for $i_h = 100$ in Figs. 5.9 and 5.10 seem counterintuitive, since implicit coupling (i.e., a decrease in τ_a) is expected to result in a lower exit flux based on Eq. 5.63. However, the lower τ_a values associated with implicit coupling also results in an increase in the Peclet number, P_L, as shown in Fig. 5.11. The results in Fig. 5.11 also show that values of P_L also increase with increasing i_h as suggested by Eq. 5.62. Higher P_L values are representative of more advection-dominated solute transport, which results in a higher gradient in salt concentration at the exit boundary. Thus, the implicit effect is only significant for diffusion-dominated systems.

For example, salt concentration profiles inside the soil barrier at steady state (i.e., $t \rightarrow \infty$) are presented for each case in Figs. 5.12 ($C_o = 0.047$ M), 5.13 ($C_o = 0.02$ M), 5.14 ($C_o = 0.0087$ M), and 5.15 ($C_o = 0.0039$ M). The results illustrate that the greater significance of advection relative to diffusion, due to either an increase in i_h or a decrease in τ_a, results in a higher exit concentration gradient because the salt front extends further into the soil. The exit concentration gradients corresponding to $i_h = 100$ in Figs. 5.9 and 5.10 for the cases that include only implicit coupling (i.e., $\tau_a < \tau_m$ and $\omega = 0$) are higher than the exit concentration gradient for the a non-membrane case (i.e., $\tau_a = \tau_m$ and $\omega = 0$). Thus, the similar exit flux values at steady-state for these cases in Figs. 5.10 and 5.11 reflect the competing effects of a reduction in exit flux associated with a lower τ_a and an increase in exit flux due to a higher exit concentration gradient associated with a decrease in P_L.

The concentration profiles in Figs. 5.12 through 5.15 also indicate that the exit concentration gradient is lower for the cases that include explicit coupling (i.e., $\omega > 0$) relative to the cases in which explicit coupling is ignored (i.e., $\omega = 0$). As explained

earlier, explicit coupling terms are negligible in the salt flux equation at $x = L$ (Eq. 5.63) because $C_s = 0$ at $x = L$ in accordance with the perfectly-flushing exit boundary condition. However, the influence of explicit coupling becomes more significant at locations up-gradient of the exit boundary (i.e., at $x < L$) where $C_s > 0$. In particular, the greatest influence of explicit coupling effects on solute migration occurs at the entry boundary of the soil barrier ($x = 0$) where C_s is a maximum. Steady-state concentration profiles in Figs. 5.12 through 5.15 for all cases in which $\omega > 0$ are marked by a discontinuity in salt concentration at $x = 0$ such that C_s is less than the source concentration, C_o. Conversely, no discontinuity is observed at $x = 0$ for the cases in which explicit coupling is ignored (i.e., $\omega = 0$). In addition, salt-concentration profiles for $i_h = 0$ are linear for cases in which $\omega = 0$ but non-linear (i.e., concave) for cases in which $\omega > 0$. Thus, although explicit coupling effects appear to be negligible at $x = L$ based on Eq. 5.63, the influence of explicit coupling at $x < L$ ultimately causes a decrease in exit concentration gradient and a reduced exit flux.

The discontinuity in salt concentration at $x = 0$ for cases in which $\omega > 0$ in Figs. 5.12 through 5.15 is consistent with evidence from previous studies that clay membranes partially restrict entry of solutes into the pore space (e.g., Kemper and Maasland 1964, Kemper and van Schaik 1966, Kharaka and Berry 1973, Ishiguro et al. 1996, Sawatsky et al. 1997). For example, Kemper and van Schaik (1966) performed diffusion tests ($i_h = 0$) on bentonite pastes ($L = 2.0$ cm) with salt solutions (NaCl, $CaCl_2$). After steady-state diffusion of the salt was achieved, the specimens were cut into ~1-mm sections and pore fluid concentrations of salt were measured in each section. Kemper and van Schaik (1966) observed that the salt concentration immediately inside the specimens (i.e., $x = 0$ to 1 mm) was considerably lower than the source concentration, C_o, even in tests with C_o as high as 1.0 M NaCl. Non-linear steady-state concentration profiles also were observed in some of these tests. Kemper and van Schaik (1966) attributed this behavior to osmotic flow and partial exclusion of the salt from the clay but did not investigate the potential

relationship between this behavior and chemico-osmotic efficiency coefficients for the bentonite.

Typically, restriction of solutes at the entry interface of clay membranes is attributed to hyperfiltration under a hydraulic gradient, in accordance with the reduction factor $(1 - \omega)$ in Eq. 5.60 (e.g., see Fritz 1986, Kharaka and Smalley 1986). However, the results in Figs. 5.12 through 5.15 indicate that the discontinuity in salt concentration at the entry boundary also occurs for the cases in which $i = 0$ (and, thus, $(1 - \omega)q_h = 0$). In addition, discontinuities in salt concentration reported for bentonite pastes by Kemper and van Schaik (1966) were measured in diffusion tests in which $i_h = 0$. These results suggest that the apparent solute restriction may be related to the counter-advection term in Eq. 5.60. However, no definite conclusion can be made in this regard, so further investigation of the effects of explicit coupling on solute concentration profiles inside a soil membrane as a function of hydraulic gradient is warranted.

Reduction of salt flux due to membrane coupling effects also is illustrated in Fig. 5.16 based on the ratio of the steady-state exit flux with coupling included (explicit and/or implicit) to the steady-state exit flux for the non-membrane case (i.e., no coupling). With reference to Fig. 5.16, the steady-state exit fluxes with only explicit coupling, only implicit coupling, both explicit and implicit coupling, and no coupling (non-membrane) are denoted as J_E, J_I, J_{EI}, and J_{NM}, respectively.

The results in Fig. 5.16 indicate that the greatest reduction in steady-state exit flux occurs when both explicit and implicit coupling are included in the analysis. Extrapolation of the data trends given by J_{EI}/J_{NM} beyond $\omega = 0.63$ indicates that the salt flux approaches zero (i.e., $J_{EI}/J_{NM} \rightarrow 0$) as the chemico-osmotic efficiency coefficient approaches unity (i.e., as $\omega \rightarrow 1$). Thus, these simulations show that the expected behavior for an "ideal" membrane that completely restricts entry of solutes into the pore space is approached provided that both explicit and implicit coupling are included in the analysis.

When only explicit or only implicit coupling is included, the steady-state exit flux generally is reduced to a lesser degree. Moreover, some of the trends in the simulation results for J_E/J_{NM} and J_I/J_{NM} do not appear to approach zero as ω approaches unity, suggesting that salt can be transported through an "ideal" membrane. Since solute transport through an "ideal" membrane is not physically possible, the results in Fig. 5.16 illustrate the importance of considering both explicit and implicit coupling effects when modeling salt flux through soil barriers that exhibit membrane behavior.

The results in Fig. 5.16 also illustrate that, in the absence of a hydraulic gradient (i.e., $i_h = 0$), implicit coupling is more significant than explicit coupling with respect to reduction of salt flux for the higher values of ω (i.e., $\omega \geq 0.49$) in which τ_a is considerably lower than the matrix tortuosity factor, τ_m. The relative dominance of implicit coupling when $i_h = 0$ is responsible for the convergence of the data trends given by J_I/J_{NM} and J_{EI}/J_{NM} as ω increases beyond 0.49. However, for $\omega \leq 0.32$, implicit coupling is negligible and the trends given by J_I/J_{NM} and J_{EI}/J_{NM} diverge. As stated earlier, measured values of τ_a corresponding to $\omega \leq 0.32$ are only slightly lower than τ_m. Nonetheless, the results for $i_h = 0$ indicate that salt flux through soil membranes under diffusion-dominated conditions can be modeled conservatively over the range $0 < \omega < 1$ by considering only implicit coupling and neglecting explicit coupling.

The advantages of neglecting explicit coupling when evaluating solute transport through soil membranes are two-fold: (1) values of ω are assumed to be zero and, therefore, do not have to be measured; and (2) when $\omega = 0$, the coupled flux equations reduce to traditional advective-dispersive theory, for which numerous analytical solutions are available (e.g., see van Genuchten and Alves 1982). However, while use of advective-dispersive theory with implicit coupling seems reasonable for $i_h = 0$, the results in Fig. 5.16 also indicate that the influence of implicit coupling becomes less significant as i_h (and, thus, P_L) increases. At $i_h = 100$, implicit coupling is essentially negligible and explicit coupling is responsible for nearly all of the reduction in solute flux. As discussed

earlier, the reduction in exit flux due to a lower τ_a is negated by an increase in exit flux due to a higher exit concentration gradient associated with an increase in P_L as i_h increases and the system becomes more advection-dominated. Thus, use of advective-dispersive theory with implicit coupling does not appear to be sufficient for modeling advection-dominated solute transport through a soil membrane.

5.4.3.2 Solute Transit Time

Based on the time-dependent exit flux values in Figs. 5.7 through 5.10, membrane behavior also appears to result in a retardation effect such that a longer time is required to reach steady-state transport of KCl relative to the non-membrane case. Longer transit times are particularly evident in Fig. 5.10 for C_o = 0.0039 M, presumably due to the high ω (0.63) and low τ_a (0.039) for this case. To illustrate this effect, the time corresponding to steady-state transport of KCl was estimated for each case based on Figs. 5.7 through 5.10. These steady-state times, T, for solute transport with only explicit coupling, only implicit coupling, both explicit and implicit coupling, and no coupling (non-membrane) are denoted as T_E, T_I, T_{EI}, and T_{NM}, respectively.

Normalized values of steady-state time relative to the non-membrane case (i.e., T_E/T_{NM}, T_I/T_{NM}, T_{EI}/T_{NM}) are plotted as a function of chemico-osmotic efficiency in Fig. 5.17. The results show that the longer transit times for cases in which $i_h = 0$ or $i_h = 10$ are primarily due to implicit coupling, as indicated by the similar trends for T_I/T_{NM} and T_{EI}/T_{NM} as well as the fact that T_E/T_{NM} is only slightly greater than unity for the range of ω values considered in this study. Conversely, longer transit times for cases in which $i_h = 100$ are primarily due to explicit coupling since implicit coupling has little effect on transit time when solute transport is dominated by advection. These results are consistent with the exit flux results presented earlier, in that explicit coupling is dominant at high values of P_L and implicit coupling is dominant at low values of P_L.

5.5 EXPERIMENTAL ASSESSMENT

The validity of using the coupled solute transport model and advective-dispersive theory for predicting solute transport through a soil membrane is illustrated herein based on measured exit flux values of Cl^- and K^+ from four (4) column tests conducted on separate 10-mm-thick Bentomat® GCL specimens. These measured fluxes are compared with predicted Cl^- and K^+ exit fluxes given by either the coupled solute transport model or the advective-dispersive theory. Details regarding the column test specimens, KCl solutions, testing apparatus, and procedures are provided below.

5.5.1 Materials and Methods

5.5.1.1 Bentomat® GCL

The Bentomat® GCL consists of a layer of granular sodium bentonite between two non-woven polypropylene geotextiles held together by needle-punched fibers (see Fig. 5.5). Selected physical and chemical properties of the bentonite portion of the GCL are given in Table 5.5. The bentonite is regarded as a sodium bentonite due to the dominance of Na on the exchange sites, although the results of the exchangeable metal measurements presented in Table 5.5 indicate that an appreciable amount of exchangeable calcium (Ca) also is present.

5.5.1.2 Liquids

The liquids used in the column tests consist of a processed tap water (PTW) and solutions of PTW and potassium chloride (KCl) (certified A.C.S., Fisher Scientific, Fair Lawn, NJ) dissolved in PTW at measured concentrations of either 0.0087 M or 0.047 M. The PTW consists of tap water that is processed to remove ions by passage through three Barnstead® ion exchange columns. Measured values of pH and electrical conductance (EC) of the PTW and KCl solutions were reported previously in Table 3.2.

5.5.1.3 Column Testing Apparatus

A schematic illustration of the column testing apparatus is shown in Fig. 5.18. The testing cell consists of a rigid acrylic cylinder, top piston, and base pedestal. The top piston is locked in place to prevent soil expansion and to control the thickness and, therefore, the porosity of the soil specimen. The top piston and base pedestal are equipped with ports that enable circulation of separate electrolyte solutions through porous stones at the specimen boundaries to establish and maintain a constant concentration at each boundary. Further details regarding the testing cell are provided in Chapter 2.

The column testing apparatus is similar to the chemico-osmotic/diffusion test apparatus described in Chapter 2, except that electrolyte solutions are circulated at the ends of the specimen using variable-speed peristaltic pumps. The circulated solutions are collected in separate reservoirs for subsequent chemical analysis. A hydraulic gradient can be applied across the test specimen by pressurizing the sample collection reservoir at the source end of the specimen.

Experimental evaluation of exit flux of a solute j is predicated on the ability to measure the moles of solute exiting the specimen, ΔM_j, over a known time interval, Δt, in accordance with the following expression:

$$J_j(x = L) = \frac{\Delta M_j}{A\Delta t} = \frac{C_j \Delta V_s}{A\Delta t} \tag{5.64}$$

where C_j is the molar solute concentration and ΔV_s is the incremental sample volume of liquid collected over Δt. As a result, the circulation rate was selected carefully to simulate as closely as possible a "perfectly flushing" exit boundary condition without diluting the exit boundary to the extent that would prohibit measurement of C_j.

5.5.1.4 Specimen Preparation

Circular specimens of the Bentomat® with nominal diameters of 71.1 mm were placed on the base pedestal inside the testing cell. The cylinder then was filled with PTW to submerge the specimen, and the top piston was lowered into the cylinder to compress the specimen to the desired thickness. After completion of compression, the top piston was locked in place to prevent volume expansion of the specimen due to swelling of the bentonite.

Each specimen was permeated under backpressure with PTW before column testing to saturate the specimen, remove the excess soluble salts, and measure the initial hydraulic conductivity. After permeation, column tests were initiated by circulating the source KCl solution ($C_s = C_o$) at one end of the specimen, and circulating PTW ($C_s = 0$) at the other end of the specimen. Samples of circulated PTW collected over time increments, Δt, were analyzed for concentrations of Cl^- and K^+ in order to evaluate exit flux in accordance with Eq. 5.64. At the end of column testing, each specimen was permeated with the source KCl solution to evaluate the final hydraulic conductivity.

5.5.1.5 Testing Conditions

Testing conditions in the four column tests are given in Table 5.6. Three of the column tests were conducted with a source KCl concentration, C_o, of 0.0087 M, but with different applied hydraulic gradients (i_h = 0, 70.3, and 703). These values of i_h correspond to applied differences in hydraulic pressure across the specimens, ΔP, of 0, 10 psi, and 100 psi, respectively. The fourth column test was conducted with $i_h = 703$ (ΔP = 10 psi) and C_o = 0.047 M. Measured values of ω, τ_a, and R_d from the steady-state chemico-osmotic/diffusion tests corresponding to the same values of C_o also are given in Table 5.6. These values are assumed to be applicable for the column test specimens, given the similar thickness and porosity of the column test specimens relative to the

chemico-osmotic/diffusion test specimens and the similar C_o values used in the column tests. Values of n and k_h given in Table 5.6 are the actual measured values for the column test specimens. The k_h values are based on permeation of the column test specimens with the source KCl solution (i.e., 0.0087 M KCl or 0.047 M KCl) after completion of the column tests.

Values of R_d for K^+ given in Table 5.6 are much greater than unity. Therefore, K^+ is expected to be adsorbed during the column tests, resulting in desorption primarily of Na^+ or Ca^{2+} based on the exchangeable cation analysis presented in Table 5.5. Since the coupled solute transport model given by Eqs. 5.42 - 5.47 accounts for the desorption of only a single exchangeable cation species, and K^+ is more likely to displace Na^+ relative to Ca^{2+} on the basis of valence (e.g., Mitchell 1993), all desorbed cations are assumed to be Na^+ for the purpose of this analysis. Thus, the free-solution diffusion coefficients, D_o, for Cl^-, K^+, and Na^+ given in Table 5.1 are required as model inputs. No additional anions are assumed to enter the solution phase, although measured values of R_d for Cl^- are greater than unity (i.e., 1.53 for C_o = 0.0087 M KCl and 1.94 for C_o = 0.047 M KCl). The reason for measured values of $R_d > 1$ for Cl^- is likely due to the fact that the time-lag expression used to evaluate the R_d values (see Table 5.2) does not account for slower Cl^- migration during transient transport with Na^+ relative to steady-state transport with K^+, as shown theoretically in Fig. 5.4.

5.5.2 Model Simulations

The model simulations used for comparison of the column test data are given in Table 5.7. The model simulations include cases using the coupled solute transport theory with both explicit and implicit coupling ("EI"; $\omega > 0$ and $\tau_a < \tau_m$) and "non-membrane" cases using advective-dispersive theory ("NM"; $\omega = 0$ and $\tau_a = \tau_m$). The non-membrane cases represent fluxes predicted by advective-dispersive theory for a soil in which the

tortuosity is governed solely by pore geometry such that τ_a is equivalent to the matrix tortuosity factor, τ_m, of 0.12. Values of the Peclet number, P_L, shown for each of the "EI" and "NM" cases in Table 5.7 are relatively low ($P_L \leq 1.02$) even for the cases in which $i_h = 703$, primarily because the test specimens are extremely thin (i.e., L = 10 mm). The relatively low P_L values suggest that the column tests were conducted under diffusion-dominated conditions. To assess the effect of the implicit coupling indicated in Fig. 5.6, additional simulations were performed for the C_o = 0.0087 M tests using advective-dispersive theory in which only implicit coupling was considered ("I"; $\omega = 0$ and $\tau_a < \tau_m$). Performance of an "I" simulation for the C_o = 0.047 M test is not necessary, since there is essentially no difference between the "I" case ($\omega = 0$, $\tau_a = 0.119$) and the non-membrane ("NM") case ($\omega = 0$, $\tau_a = \tau_m = 0.12$) for $C_o = 0.047$ M.

5.5.3 Column Test Results and Model Comparisons

Measured values of exit flux for Cl^- and K^+ for column tests 1 through 3 (C_o = 0.0087 M) are shown in Fig. 5.19 along with simulated coupled ("EI") fluxes (i.e., ω = 0.49, $\tau_a = 0.063$) and the advective-dispersive ("NM") fluxes (i.e., $\omega = 0$, $\tau_a = \tau_m = 0.12$). The results indicate that the coupled transport model, in general, provides a better match to the experimental data for both Cl^- and K^+ than the advective-dispersive theory in each of the tests. The greater accuracy of the coupled model is based on better agreement with the steady-state exit flux and transit time. Use of advective-dispersive theory ($\omega = 0$) and the matrix tortuosity factor ($\tau_a = \tau_m = 0.12$) results in overestimation of the steady-state flux and underestimation of the transit time required to reach steady state conditions. Neither model is particularly effective at matching the measured transient K^+ flux values for column test 1 ($i_h = 0$). However, for the tests in which i_h = 70.3 and 703, the coupled model provides a reasonably good match to the measured K^+ flux values. These results

suggest that the R_d value for K^+ obtained from the chemico-osmotic/diffusion test (i.e., $R_d = 12.57$) is not accurate with respect to the results of the column test for $i_h = 0$.

The results of column test 4 ($C_o = 0.047$ M) are shown in Fig. 5.20 along with results of column test 3 ($C_o = 0.0087$ M), which was conducted at the same hydraulic gradient ($i_h = 703$). Less discrepancy is apparent between the theoretical fluxes given by the coupled transport model and advective-dispersive theory for $C_o = 0.047$ M relative to $C_o = 0.0087$ M. The similarity of the results from the two models for $C_o = 0.047$ M is attributed to the fact that the ω value for this case is only 0.14, and implicit coupling is not a factor in column test 4 because of the similarity between the apparent tortuosity factor, τ_a (0.119) and the matrix tortuosity factor, τ_m (0.12).

Measured values of exit flux for Cl^- and K^+ for column tests 1 through 3 ($C_o = 0.0087$ M) are shown again in Fig. 5.21 along with simulated coupled (EI) fluxes (i.e., $\omega = 0.49$, $\tau_a = 0.063$) advective-dispersive fluxes with implicit (I) coupling (i.e., $\omega = 0$, $\tau_a = 0.063$). The advective-dispersive model with implicit (I) coupling produces only slightly higher simulated values of solute flux at a given time than the coupled model that includes both explicit and implicit (EI) coupling. Overall, both models appear to provide reasonable matches to the experimental data.

Measured and predicted values of steady-state flux for the column tests based on the results in Figs. 5.19 through 5.21 are summarized in Fig. 5.22. For all tests, predicted steady-state fluxes based on the coupled solute transport theory (i.e., the EI cases) are closest to the measured steady-state fluxes. For column tests 1 through 3 in which $C_o = 0.0087$ M, advective-dispersive theory provides a relatively poor match to the measured steady-state fluxes when implicit coupling is neglected (i.e., the NM cases), but a reasonable match to the measured steady-state fluxes when implicit coupling is included (i.e., the I cases). For column test 4 in which $C_o = 0.047$ M, predicted steady-state fluxes based on advective-dispersive theory with implicit coupling (I) and without implicit

coupling (NM) are the same. As stated earlier, implicit coupling is not a factor in column test 4 because of the similarity between the apparent tortuosity factor, τ_a (0.119) and the matrix tortuosity factor, τ_m (0.12).

In general, the results in Fig. 5.22 suggest that use of advective-dispersive theory *in lieu* of the coupled solute transport theory is sufficient to model solute transport through the GCL specimens provided that implicit coupling is included in the analysis, even though ω is relatively high in these tests (i.e., $\omega = 0.49$). These results are attributed primarily to diffusion-dominated conditions in the column tests (based on the low P_L values shown in Table 5.7). Explicit coupling effects (i.e., hyperfiltration and chemico-osmotic counter-advection) associated with $\omega > 0$ may be more significant in advective-dominated systems, although it is not likely that advection would be very significant relative to diffusion in a GCL. For example, the minimum hydraulic head difference, Δh, across a GCL that would be required to achieve $P_L (= k_h \Delta h / n \tau_a D_{so}) > 20$ (assuming $\tau_a = 0.12$, $n = 0.8$, $k_h = 2 \times 10^{-11}$ m/s, $D_{so} = 10^{-9}$ m^2/s) is 96 m, which is not representative of conditions in field waste containment applications.

5.6 CONCLUSIONS

The development of a coupled solute transport model to describe one-dimensional solute migration through soil barriers exhibiting membrane behavior is described in this chapter. The model is based on principles of irreversible thermodynamics applied to charged membranes under isothermal conditions under the assumption that no electrical current is applied across the soil. The primary advantage of this model relative to other models developed previously is the ability to simulate the more general case of salt migration through a clay barrier in which the cation species is reactive (i.e., $R_d > 1$) and, thus, undergoes ion exchange at the clay particle surfaces and is replaced in solution by an exchangeable cation species. This case typically is more appropriate for describing solute transport in waste containment applications, considering that ion exchange during

transient transport through a clay barrier is a common and desirable process for retarding the movement of potentially harmful chemical species.

The results of a theoretical analysis indicate that exit solute flux, J(x=L), may be reduced and solute transit times through a soil may be increased as a result of membrane behavior due to both explicit and implicit (or empirical) coupling effects. Explicit coupling effects include hyperfiltration, whereby solutes are filtered out as the solution passes through the membrane under a hydraulic gradient, and counter-advection of solutes due to chemico-osmotic liquid flux opposite to the direction of the hydraulic liquid flux. Implicit coupling is characterized by a decrease in the apparent tortuosity factor, τ_a, with an increase in the chemico-osmotic efficiency coefficient, ω, such that τ_a is less than the matrix tortuosity factor for the soil, τ_m, that represents the tortuosity due solely to the geometry of the interconnected pores (i.e., $\tau_a < \tau_m$). The increase in ω also is correlated with a decrease in solute concentration, C, as shown based on results of steady-state chemico-osmotic/diffusion tests presented for potassium chloride (KCl) and a geosynthetic clay liner (GCL) containing sodium bentonite. Based on the current understanding of ion restriction in soil membranes, lower solute concentrations in the pore space likely correspond to larger diffuse double layers surrounding the clay particles resulting in an increase in ω and a corresponding decrease in τ_a, since less of the pore space is available for solute transport.

Traditional advective-dispersive solute transport theory is based on the limiting assumption that $\omega = 0$ and, thus, inherently neglects explicit coupling effects. Implicit coupling may be included when using advective-dispersive theory by using an appropriate value of τ_a ($< \tau_m$) that corresponds to the source concentration, C_o, or may be neglected by assuming that $\tau_a = \tau_m$ for all C_o. Comparison of theoretical exit solute fluxes obtained using the coupled solute transport theory with theoretical exit solute fluxes obtained using advective-dispersive theory indicates that implicit coupling is more significant than explicit coupling in reducing solute flux under diffusion-dominated

conditions. Under such conditions, use of advective-dispersive theory *in lieu* of coupled theory may be sufficient for modeling solute transport through soil membranes, provided that implicit coupling is included in the analysis.

Predicted values of exit solute flux obtained using both the coupled theory and advective-dispersive theory are compared with measured values of exit flux for Cl^- and K^+ from column tests on a GCL subjected to KCl solutions. The predicted fluxes are based on independently measured transport parameters from previous chemico-osmotic/diffusion tests conducted on specimens of the same GCL. The results indicate that the coupled solute transport model provides better agreement with the experimental data than advective-dispersive theory. Advective-dispersive theory overestimates solute flux and underestimates transit times relative to the measured data. However, advective-dispersive theory provides reasonably accurate fluxes relative to the measured data for the GCL when the appropriate value of τ_a ($< \tau_m$) is used to account for implicit coupling, primarily due to diffusion-dominated conditions in the column tests. Explicit coupling effects associated with $\omega > 0$ may be more significant in advective-dominated systems and, thus, use of coupled theory may be more appropriate to describe solute transport in such systems. However, advection is not likely to be dominant relative to diffusion in GCLs under typical field conditions in waste containment applications.

5.7 REFERENCES

Abd-El-Aziz, M.H. and Taylor, S.A. (1965). "Simultaneous flow of water and salt through unsaturated porous media." *Soil Science Society of America Proceedings*, 29, 141-143.

Alshawabkeh, A. N. and Acar, Y. B (1996). "Electrokinetics remediation. II: Theoretical model." *Journal of Geotechnical and Geoenvironmental Engineering*, ASCE, 122(3), 186-196.

Barbour, S.L. (1986). *Osmotic Flow and Volume Change in Clay Soils*. Ph.D. Dissertation, University of Saskatchewan, Saskatoon, 255 p.

Barbour, S.L. and Fredlund, D.G. (1989). "Mechanisms of osmotic flow and volume change in clay soils." *Canadian Geotechnical Journal*, 26, 551-562.

Bresler, E. (1973). "Simultaneous transport of solutes and water under transient unsaturated flow conditions." *Water Resources Research*, 9(4), 975-986.

Crank, J. (1975). *The Mathematics of Diffusion*. 2nd Ed., Clarendon Press, Oxford, 414 p.

de Marsily, G. (1986). *Quantitative Hydrogeology*. Academic Press, Orlando, FL.

Freeze, R.A., and Cherry, J.A. (1979). *Groundwater*. Prentice-Hall, Inc., Englewood Cliffs, NJ.

Fritz, S. J. (1986). "Ideality of clay membranes in osmotic processes: A review." *Clays and Clay Minerals*, 34(2), 214-223.

Fritz, S.J., and Marine, I.W. (1983). "Experimental support for a predictive osmotic model of clay membranes." *Geochimica et Cosmochimica Acta*, 47, 1515-1522.

Greenberg, J.A., Mitchell, J.K., and Witherspoon, P.A. (1973). "Coupled salt and water flows in a groundwater basin." *Journal of Geophysical Research*, 78(27), 6341-6353.

Groenevelt, P.H. and Bolt, G.H. (1969). "Non-equilibrium thermodynamics of the soil-water system: Review paper." *Journal of Hydrology*, 7, 358-388.

Groenevelt, P.H. and Elrick, D.E. (1976). "Coupling phenomena in saturated homo-ionic montmorillonite: II. theoretical." *Soil Science Society of America Journal*, 40, 820-823.

Groenevelt, P. H, Elrick, D. E., and Laryea, K. B. (1980). "Coupling phenomena in saturated homo-ionic montmorillonite: IV. The dispersion coefficient." *Soil Science Society of America Journal*, 44(6), 1168-1173.

Ishiguro, M., Matsuura, T., and Detellier, C. (1996). "A study on the solute separation and the pore size distribution of a montmorillonite membrane." *Separation Science and Technology*, 31(4), 545-556.

Katchalsky, A., and Curran, P.F. (1965). *Nonequilibrium Thermodynamics in Biophysics.* Harvard University Press, Cambridge, MA, 248 p.

Keijzer, Th. J. S., Kleingeld, P. J., and Loch, J. P .G. (1997). "Chemical osmosis in compacted clayey material and the prediction of water transport." *Geoenvironmental engineering, contaminated ground: Fate of pollutants and remediation*, R. N. Yong and H. R. Thomas, eds., Thomas Telford Publ., London, 199-204.

Kemper, W.D. and Maasland, D.E.L. (1964). "Reduction of salt content of solution on passing through thin films adjacent to charged surfaces." *Soil Science Society of America Proceedings*, 28, 318-323.

Kemper, W.D. and Quirk, J.P. (1972). "Ion mobilities and electric charge of external clay surfaces inferred from potential differences and osmotic flow." *Soil Science Society of America Proceedings*, 36, 426-433.

Kemper, W.D. and Rollins, J.B. (1966). "Osmotic efficiency coefficients across compacted clays." *Soil Science Society of America Proceedings*, 30, 529-534.

Kemper, W. D. and van Schaik, J. C. (1966). "Diffusion of salts in clay-water systems." *Soil Science Society of America Proceedings*, 30, 534-540.

Kharaka, Y.K. and Berry, F.A. (1973). "Simultaneous flow of water and solutes through geologic membranes, I. Experimental investigation." *Geochimica et Cosmochimica Acta*, 37, 2577-2603.

Kharaka, Y.K. and Smalley, W.C. (1976). "Flow of water and solutes through compacted clays." *The American Association of Petroleum Geologists Bulletin*, 60(6), 973-980.

McKelvey, J. G. and Milne, I. H. (1962). "The flow of salt solutions through compacted clay." *Clays and Clay Minerals*, 9, 248-259.

Mitchell, J.K. (1993). *Fundamentals of Soil Behavior*, 2nd Ed., John Wiley and Sons, New York, 437 p.

Mitchell, J.K., Greenberg, J.A., and Witherspoon, P.A. (1973). "Chemico-osmotic effects in fine-grained soils." *Journal of the Soil Mechanics and Foundations Division*, ASCE, 99(SM4), 307-322.

Neuzil, C.E. (2000). "Osmotic generation of 'anomalous' fluid pressures in geologic environments." *Nature*, 403(6766), 182-184.

Olsen, H.W. (1969). "Simultaneous fluxes of liquid and charge in saturated kaolinite." *Soil Science Society of America Proceedings*, 33, 338-344.

Olsen, H.W. (1985). "Osmosis: a cause of apparent deviations from Darcy's Law." *Canadian Geotechnical Journal*, 22, 238-241.

Olsen, H.W., Yearsley, E.N., and Nelson, K.R. (1990). "Chemico-osmosis versus diffusion-osmosis." *Transportation Research Record No. 1288*, Transportation Research Board, Washington D.C., 15-22.

Rabideau, A. and Khandelwal, A. (1998). "Boundary conditions for modeling transport in vertical barriers." *Journal of Environmental Engineering*, ASCE, 124(11), 1135-1139.

Robinson, R.A., and Stokes, R.H. (1959). *Electrolyte Solutions*, 2nd Ed., Butterworth Scientific Publications, London, England, 571 p.

Sawatsky, N., Feng, Y., and Dudas, M.J. (1997). "Diffusion of 1-naphthol and naphthalene through clay materials: Measurement of apparent exclusion of solute from the pore space." *Journal of Contaminant Hydrology*, 27(1), 25-41.

Shackelford, C.D. (1988). "Diffusion as a transport process in fine-grained barrier materials." *Geotechnical News*, 6(2), 24-27.

Shackelford, C.D. (1989). "Diffusion of contaminants through waste containment barriers." *Transportation Research Record No. 1219*, Transportation Research Board, National Research Council, Washington, DC, 169-182.

Shackelford, C.D. (1990). "Transit time design of earthen barriers." *Engineering Geology*, 29, 79-94.

Shackelford, C.D. (1995) "Critical concepts for column testing." *Journal of Geotechnical Engineering*, ASCE, 120(10), 1804-1828.

Shackelford, C.D. (1996). "Modeling in environmental geotechnics: applications and limitations." *Second International Congress on Environmental Geotechnics, IS-Osaka '96*, Osaka, Japan, Nov. 5-8.

Shackelford, C. D. and Daniel, D. E. (1991). "Diffusion in saturated soil: I. Background." *Journal of Geotechnical Engineering*, ASCE, 117(3), 467-484.

Shackelford, C. D.and Redmond, P.L. (1995). "Solute breakthrough curves for processed kaolin at low flow rates." *Journal of Geotechnical Engineering*, ASCE, 121(1), 17-32.

Shackelford, C. D., Malusis, M. A., Majeski, M. J., Stern, R. T. (1999). "Electrical conductivity breakthrough curves." *Journal of Geotechnical and Geoenvironmental Engineering*, ASCE, 125(4), 260-270.

Shackelford, C. D., Benson, C. H., Katsumi, T., Edil, T. B., and Lin, L. (2000). "Evaluating the hydraulic conductivity of GCLs permeated with non-standard liquids." *Geotextiles and Geomembranes*, 18(2/3), 133-161.

Smith, G.D. (1985). *Numerical Solutions of Partial Differential Equations: Finite Difference Methods*, 3rd Edition, Oxford University Press, 337 p.

Staverman, A. J. (1952). "Non-equilibrium thermodynamics of membrane processes." *Transactions of the Faraday Society*, 48(2), 176-185.

Stern, R.T. and Shackelford, C.D. (1998). "Permeation of sand-processed clay mixtures with calcium chloride solutions." *Journal of Geotechnical and Geoenvironmental Engineering*, ASCE, 124(3), 231-241.

van Genuchten, M.Th. and Alves, W.J. (1982). "Analytical solutions of the one-dimensional convective-dispersive solute transport equation." *Agrigultural Research Service Technical Bulletin No. 1661*, United States Department of Agriculture, 148 p.

Vinograd, J.R., and McBain, J.W. (1941). "Diffusion of electrolytes and of the ions in their mixtures." *Journal of the American Chemical Society*, 63, 2008-2015.

Yeung, A.T. (1990). "Coupled flow equations for water, electricity and ionic contaminants through clayey soils under hydraulic, electrical, and chemical gradients." *Journal of Non-Equilibrium Thermodynamics*, 15, 247-267.

Yeung, A.T. and Mitchell, J.K. (1993). "Coupled fluid, electrical, and chemical flows in soil." *Geotechnique*, 43(1), 121-134.

Table 5.1 - Self-diffusion and salt-diffusion coefficients for K^+, Na^+, and Cl^- system.

Chemical Species	Free-solution Self-Diffusion Coefficient[1], $D_o \times 10^{10}$ (m^2/s)	Free-solution Salt-Diffusion Coefficient[1], $D_{so} \times 10^{10}$ (m^2/s)	Effective Self-Diffusion Coefficient[2], $D_o^* \times 10^{10}$ (m^2/s)	Free-solution Salt-Diffusion Coefficient[2], $D_s^* \times 10^{10}$ (m^2/s)
K^+	19.6	---	1.96	---
Na^+	13.3	---	1.33	---
Cl^-	20.3	---	2.03	---
KCl	---	19.93	---	1.993
NaCl	---	16.10	---	1.610

[1] Limiting values at 25 °C (from Shackelford and Daniel 1991)
[2] $D_s^* = \tau_a D_{so}$ and $D_o^* = \tau_a D_o$ where $\tau_a = 0.1$

Table 5.2 - Results of steady-state chemico-osmotic/diffusion tests for Bentomat® GCL[1].

Test No.	n	C_o (M)	k_h[2] x 10^{11} (m/s)	ω	D_s^*[3] x 10^{10} (m^2/s)	τ_a[4]	Chloride (Cl^-)		Potassium (K^+)	
							T_L (hours)	R_d[5]	T_L (hours)	R_d[5]
1	0.80	0.0039	1.65	0.63	0.786	0.0394	51.30	0.87	737.6	12.52
2	0.79	0.0087	1.33	0.49	1.25	0.0627	56.56	1.53	465.6	12.57
3	0.79	0.020	2.06	0.32	2.24	0.1123	37.78	1.83	441.5	21.36
4	0.78	0.047	1.48	0.14	2.38	0.1194	37.79	1.94	340.2	17.49

(1) Values based on results of steady-state diffusion tests from Chapter 3: n = porosity; C_o = source KCl concentration; k_h = hydraulic conductivity; ω = chemico-osmotic efficiency coefficient; D_s^* = effective salt-diffusion coefficient; τ_a = apparent tortuosity factor; T_L = time lag; R_d = retardation factor.

(2) Values of k based on permeation with the source KCl solution.

(3) Values of D_s^* evaluated based on steady-state diffusion test data for Cl^- (see Chapter 3).

(4) $\tau_a = D_s^*/D_{so}$ where D_{so} = 19.93 x 10-10 m^2/s @ 25 °C (Robinson and Stokes 1959).

(5) Based on time-lag approach, $R_d = 6D_s^*T_L/L^2$ where L = 1.0 cm for all tests.

Table 5.3 - Input parameters for theoretical analysis[1].

Case[2]	C_o (M)	ω	τ_a	i_h	$k_h \times 10^{11}$ (m/s)	v_h[3] $\times 10^{11}$ (m/s)	P_L[4]
EI1	0.047	0.14	0.119	0	1.48	0	0
EI2	0.047	0.14	0.119	10	1.48	18.5	0.78
EI3	0.047	0.14	0.119	100	1.48	185	7.8
NM1	0.047	0	0.12	0	1.48	0	0
NM2	0.047	0	0.12	10	1.48	18.5	0.774
NM3	0.047	0	0.12	100	1.48	185	7.74
EI4	0.020	0.32	0.112	0	2.06	0	0
EI5	0.020	0.32	0.112	10	2.06	25.8	1.15
EI6	0.020	0.32	0.112	100	2.06	258	11.5
NM4	0.020	0	0.12	0	2.06	0	0
NM5	0.020	0	0.12	10	2.06	25.8	1.08
NM6	0.020	0	0.12	100	2.06	258	10.8
EI7	0.0087	0.49	0.063	0	1.33	0	0
EI8	0.0087	0.49	0.063	10	1.33	16.6	1.33
EI9	0.0087	0.49	0.063	100	1.33	166	13.3
NM7	0.0087	0	0.12	0	1.33	0	0
NM8	0.0087	0	0.12	10	1.33	16.6	0.695
NM9	0.0087	0	0.12	100	1.33	166	6.95
EI10	0.0039	0.63	0.039	0	1.65	0	0
EI11	0.0039	0.63	0.039	10	1.65	20.6	2.63
EI12	0.0039	0.63	0.039	100	1.65	206	26.3
NM10	0.0039	0	0.12	0	1.65	0	0
NM11	0.0039	0	0.12	10	1.65	20.6	0.862
NM12	0.0039	0	0.12	100	1.65	206	8.62

(1) C_o = source KCl concentration; ω = chemico-osmotic efficiency coefficient; τ_a = apparent tortuosity factor; i_h = hydraulic gradient; k_h = hydraulic conductivity; v_h = hydraulic seepage velocity; P_L = Peclet number

(2) Cases with prefix "EI" account for both explicit and implicit coupling ($\omega > 0$, $\tau_a < \tau_m$); cases with prefix "NM" account for no coupling ($\omega = 0$, $\tau_a = \tau_m$)

(3) $v_h = k_h i_h / n$ where $n = 0.8$ in all cases

(4) $P_L = v_h L / \tau_a D_{so}$ where $L = 1.0$ m and $D_{so} = 19.93 \times 10^{-10}$ m^2/s in all cases

Table 5.4 - Input parameters for theoretical analysis (cont.)[1].

Case[2]	C_o (M)	ω	τ_a	i_h	$k_h \times 10^{11}$ (m/s)	v_h[3] $\times 10^{11}$ (m/s)	P_L[4]
I1	0.047	0	0.119	0	1.48	0	0
I2	0.047	0	0.119	10	1.48	18.5	0.78
I3	0.047	0	0.119	100	1.48	185	7.8
E1	0.047	0.14	0.12	0	1.48	0	0
E2	0.047	0.14	0.12	10	1.48	18.5	0.774
E3	0.047	0.14	0.12	100	1.48	185	7.74
I4	0.020	0	0.112	0	2.06	0	0
I5	0.020	0	0.112	10	2.06	25.8	1.15
I6	0.020	0	0.112	100	2.06	258	11.5
E4	0.020	0.32	0.12	0	2.06	0	0
E5	0.020	0.32	0.12	10	2.06	25.8	1.08
E6	0.020	0.32	0.12	100	2.06	258	10.8
I7	0.0087	0	0.063	0	1.33	0	0
I8	0.0087	0	0.063	10	1.33	16.6	1.33
I9	0.0087	0	0.063	100	1.33	166	13.3
E7	0.0087	0.49	0.12	0	1.33	0	0
E8	0.0087	0.49	0.12	10	1.33	16.6	0.695
E9	0.0087	0.49	0.12	100	1.33	166	6.95
I10	0.0039	0	0.039	0	1.65	0	0
I11	0.0039	0	0.039	10	1.65	20.6	2.63
I12	0.0039	0	0.039	100	1.65	206	26.3
E10	0.0039	0.63	0.12	0	1.65	0	0
E11	0.0039	0.63	0.12	10	1.65	20.6	0.862
E12	0.0039	0.63	0.12	100	1.65	206	8.62

(1) C_o = source KCl concentration; ω = chemico-osmotic efficiency coefficient; τ_a = apparent tortuosity factor; i_h = hydraulic gradient; k_h = hydraulic conductivity; v_h = hydraulic seepage velocity; P_L = Peclet number

(2) Cases with prefix "I" account for implicit coupling only ($\omega = 0$, $\tau_a < \tau_m$); cases with prefix "E" account for explicit coupling only ($\omega > 0$, $\tau_a = \tau_m$)

(3) $v_h = k_h i_h / n$ where $n = 0.8$ in all cases

(4) $P_L = v_h L / \tau_a D_{so}$ where $L = 1.0$ m and $D_{so} = 19.93 \times 10^{-10}$ m^2/s in all cases

Table 5.5 – Measured properties of bentonite in Bentomat® GCL.

Property	Standard	Value
Liquid Limit, LL (%)	ASTM D 4318	478
Plasticity Index, PI (%)	ASTM D 4318	439
Specific Gravity, G_s	ASTM D 854	2.43
Principal Minerals (%):	a	
Montmorillonite		71
Mixed-Layer Illite/Smectite		7
Quartz		15
Other		7
Cation Exchange Capacity (meq/100 g)	b	47.7
Exchangeable Metals (meq/100 g):	b	
Ca		20.8
Mg		6.4
Na		31.0
K		0.8
Sum		59.0
Soluble Salts (mg/kg):	b, c	
Ca		443
Mg		407
Na		4636
K		263
Soil pH	b, d	9.2
Electrical Conductance (mS/m) @ 25°C	b, d	120

[a] Based on x-ray diffraction analyses performed by Mineralogy Inc., Tulsa, OK

[b] Procedures described in Shackelford and Redmond (1995).

[c] Measured from a 1 g:20 mL clay-water extract.

[d] Measured on a saturated soil paste.

Table 5.6 - Column test conditions[1].

Test No.	n	C_o (M)	k_h[2] x 10^{11} (m/s)	i_h	ω	τ_a	R_d	
							Cl-	K+
1	0.79	0.0087	1.50	0	0.49	0.0627	1.53	12.57
2	0.81	0.0087	2.01	70.3	0.49	0.0627	1.53	12.57
3	0.79	0.0087	1.43	703	0.49	0.0627	1.53	12.57
4	0.78	0.047	2.37	703	0.14	0.1194	1.94	17.49

(1) n = porosity; C_o = source KCl concentration; k_h = hydraulic conductivity; i_h = hydraulic gradient; ω = chemico-osmotic efficiency coefficient; τ_a = apparent tortuosity factor; R_d = retardation factor.

(2) Values of k_h based on permeation with the source KCl solution after column testing.

Table 5.7 - Model simulations for comparison with column test data[1,2].

Case No.	n	C_o (M)	k_h[3] x 10^{11} (m/s)	i_h	P_L[4]	ω	τ_a	R_d	
								Cl^-	K^+
EI1	0.79	0.0087	1.50	0	0	0.49	0.063	1.53	12.57
EI2	0.81	0.0087	2.01	70.3	0.107	0.49	0.063	1.53	12.57
EI3	0.79	0.0087	1.43	703	1.02	0.49	0.063	1.53	12.57
EI4	0.78	0.047	2.37	703	0.898	0.14	0.119	1.94	17.49
NM1	0.79	0.0087	1.50	0	0	0	0.12	1.53	12.57
NM2	0.81	0.0087	2.01	70.3	0.073	0	0.12	1.53	12.57
NM3	0.79	0.0087	1.43	703	0.532	0	0.12	1.53	12.57
NM4	0.78	0.047	2.37	703	0.893	0	0.12	1.94	17.49
I1	0.79	0.0087	1.50	0	0	0	0.063	1.53	12.57
I2	0.81	0.0087	2.01	70.3	0.107	0	0.063	1.53	12.57
I3	0.79	0.0087	1.43	703	1.02	0	0.063	1.53	12.57

(1) n = porosity; C_o = source KCl concentration; k_h = hydraulic conductivity; i_h = hydraulic gradient; P_L = Peclet number; ω = chemico-osmotic efficiency coefficient; τ_a = apparent tortuosity factor; R_d = retardation factor.

(2) Na^+ is exchangeable cation in all cases (D_{ox} = 13.3 x 10^{-10} m^2/s).

(3) Values of k_h based on permeation with the source KCl solution after column testing.

(4) $P_L = k_h i_h L/n\tau_a D_{so}$ where L = 1.0 cm and D_{so} = 19.93 x 10^{-10} m^2/s in all cases.

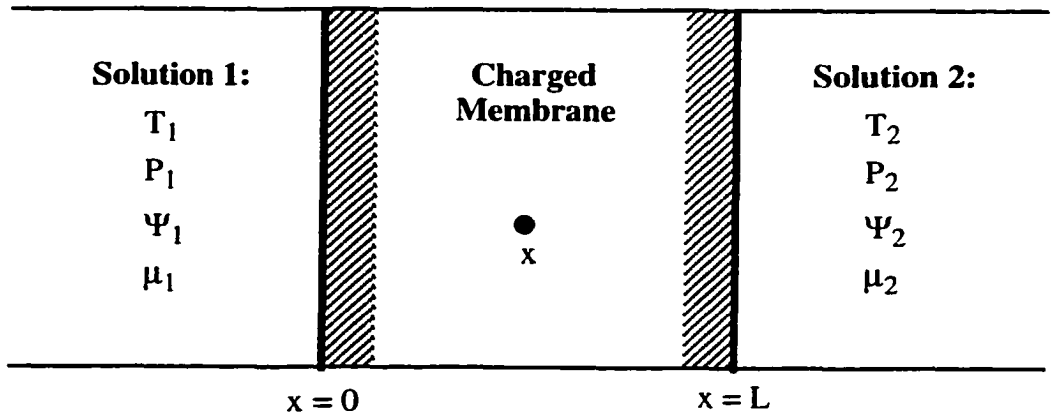

Fig. 5.1 - Conceptual model of soil-water-electrolyte system (after Yeung 1990).

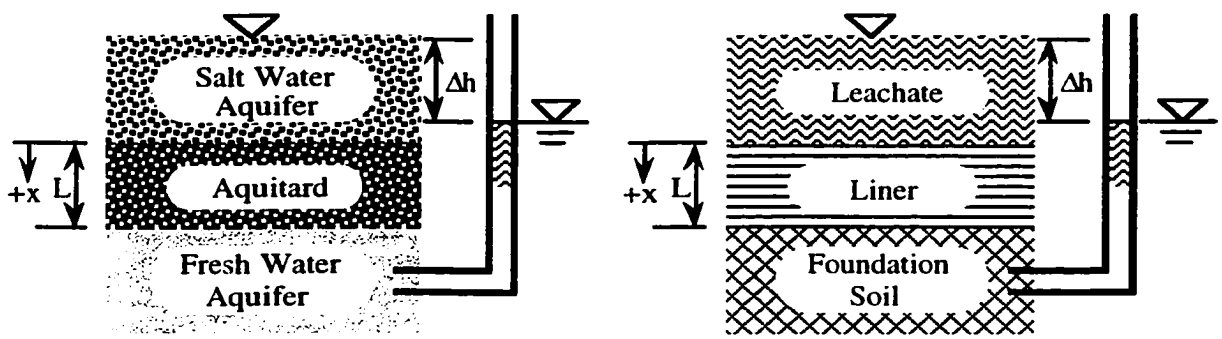

(a) Natural Containment

(b) Engineered Containment

Fig. 5.2 - Natural containment versus engineered containment (after Shackelford 1996).

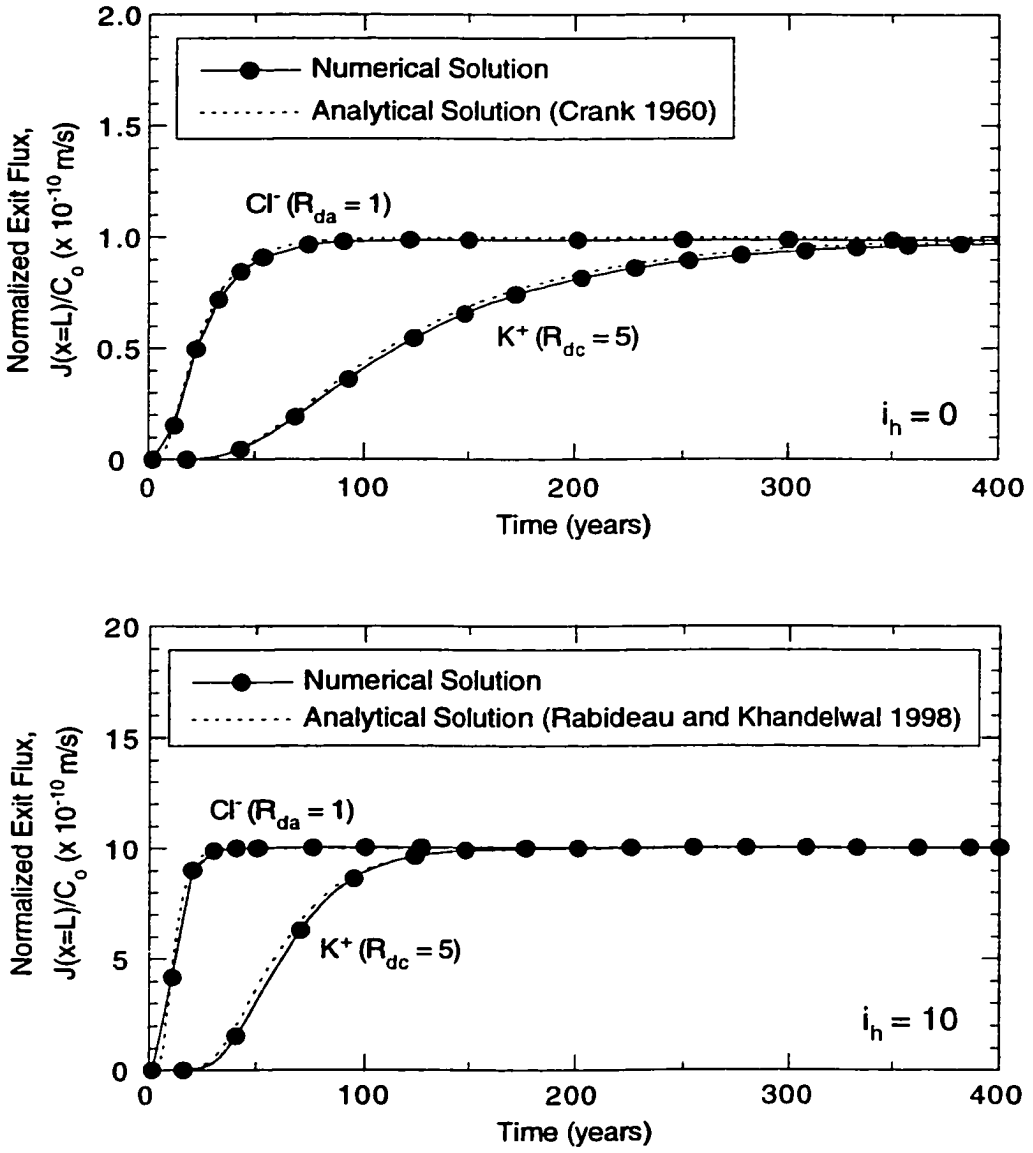

Fig. 5.3 - Comparison of numerical and analytical solutions for exit flux of Cl^- ($R_{da} = 1$) and K^+ ($R_{dc} = 5$) through a non-membrane soil ($\omega = 0$, L = 1 m, $C_o = 0.1$ M, $\tau_a = 0.1$, $k = 10^{-10}$ m/s, $D_{oa} = 20.3 \times 10^{-10}$ m^2/s) in which $D_{ox} = D_{oc} = 19.6 \times 10^{-10}$ m^2/s: (a) $i_h = 0$; (b) $i_h = 10$.

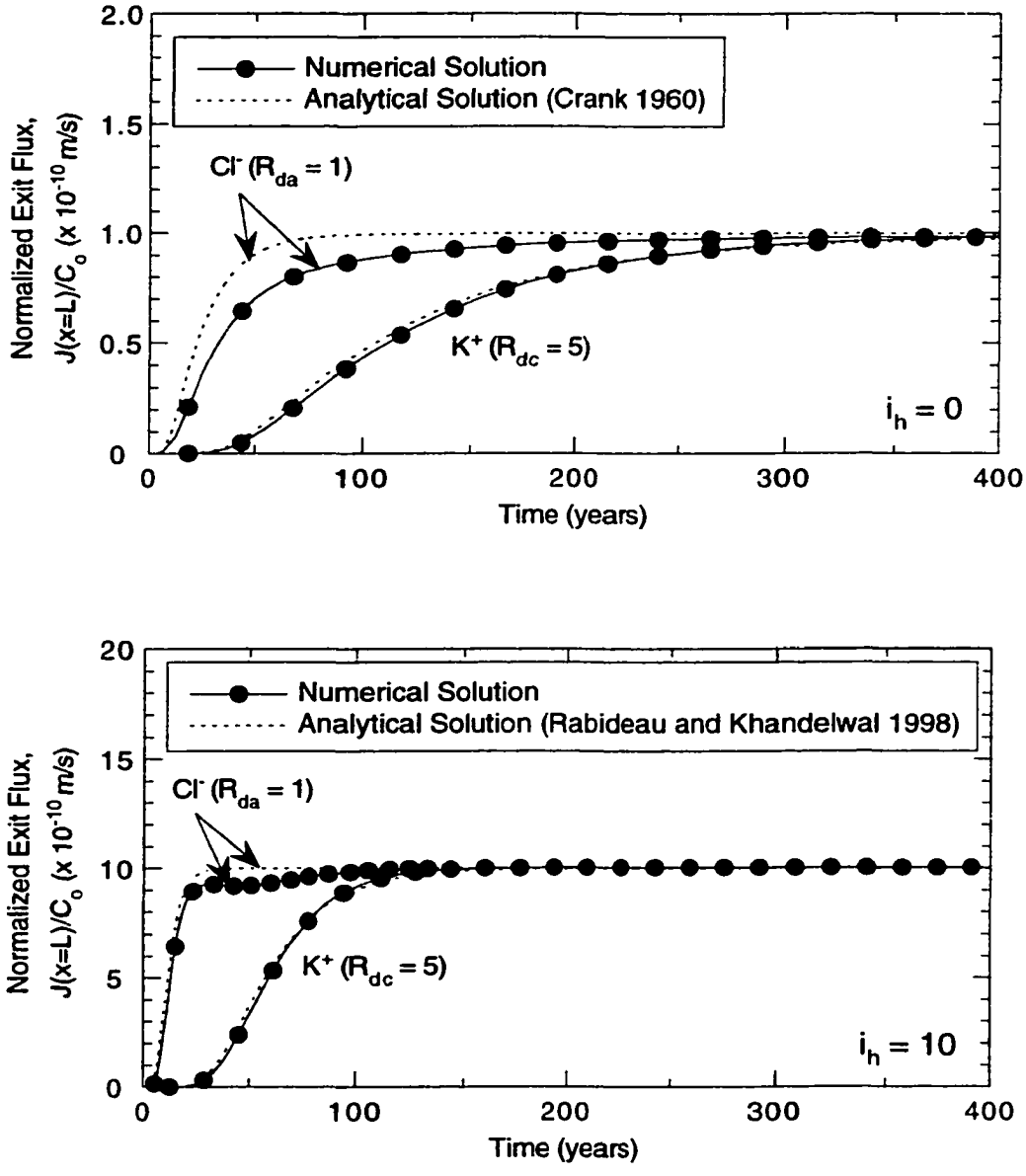

Fig. 5.4 - Comparison of numerical and analytical solutions for exit flux of Cl^- ($R_{da} = 1$) and K^+ ($R_{dc} = 5$) through a non-membrane soil ($\omega = 0$, L = 1 m, $C_o = 0.1$ M, $\tau_a = 0.1$, $k = 10^{-10}$ m/s, $D_{oa} = 20.3 \times 10^{-10}$ m^2/s) in which $D_{oc} = 19.6 \times 10^{-10}$ m^2/s and $D_{ox} = 13.3 \times 10^{-10}$ m^2/s: (a) $i_h = 0$; (b) $i_h = 10$.

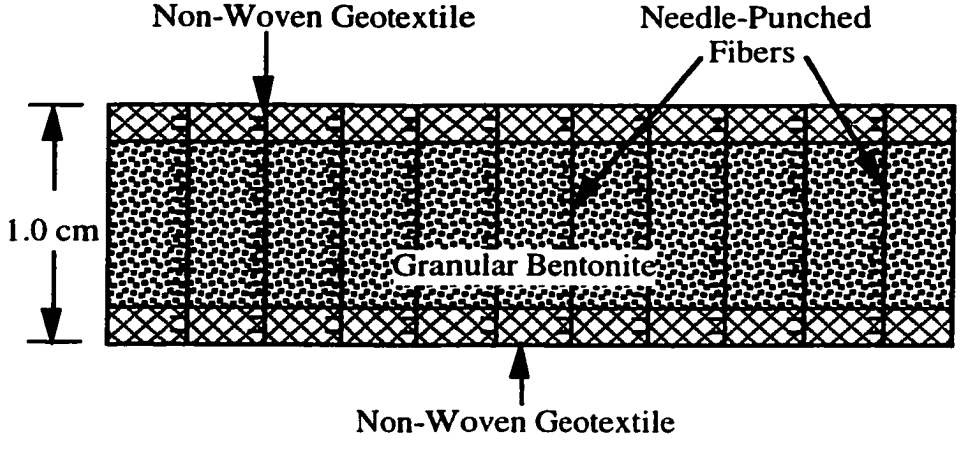

Fig. 5.5 - Schematic illustration of Bentomat® GCL.

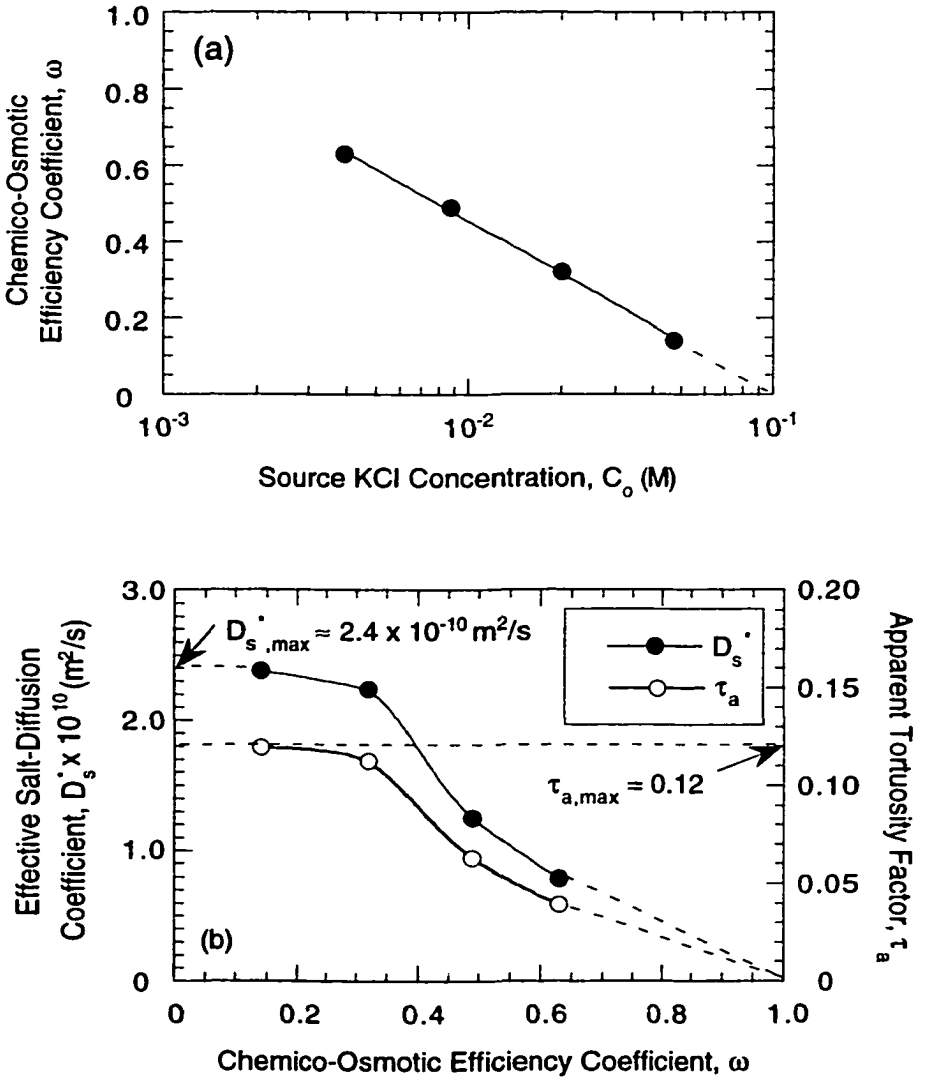

Fig. 5.6 - Relationship between chemico-osmotic efficiency (ω), source concentration (C_o), effective salt-diffusion coefficent (D_s^*), and apparent tortuosity factor (τ_a) for GCL specimens (L = 1.0 cm) subjected to KCl solutions: (a) ω versus C_o; (b) D_s^* and τ_a versus ω.

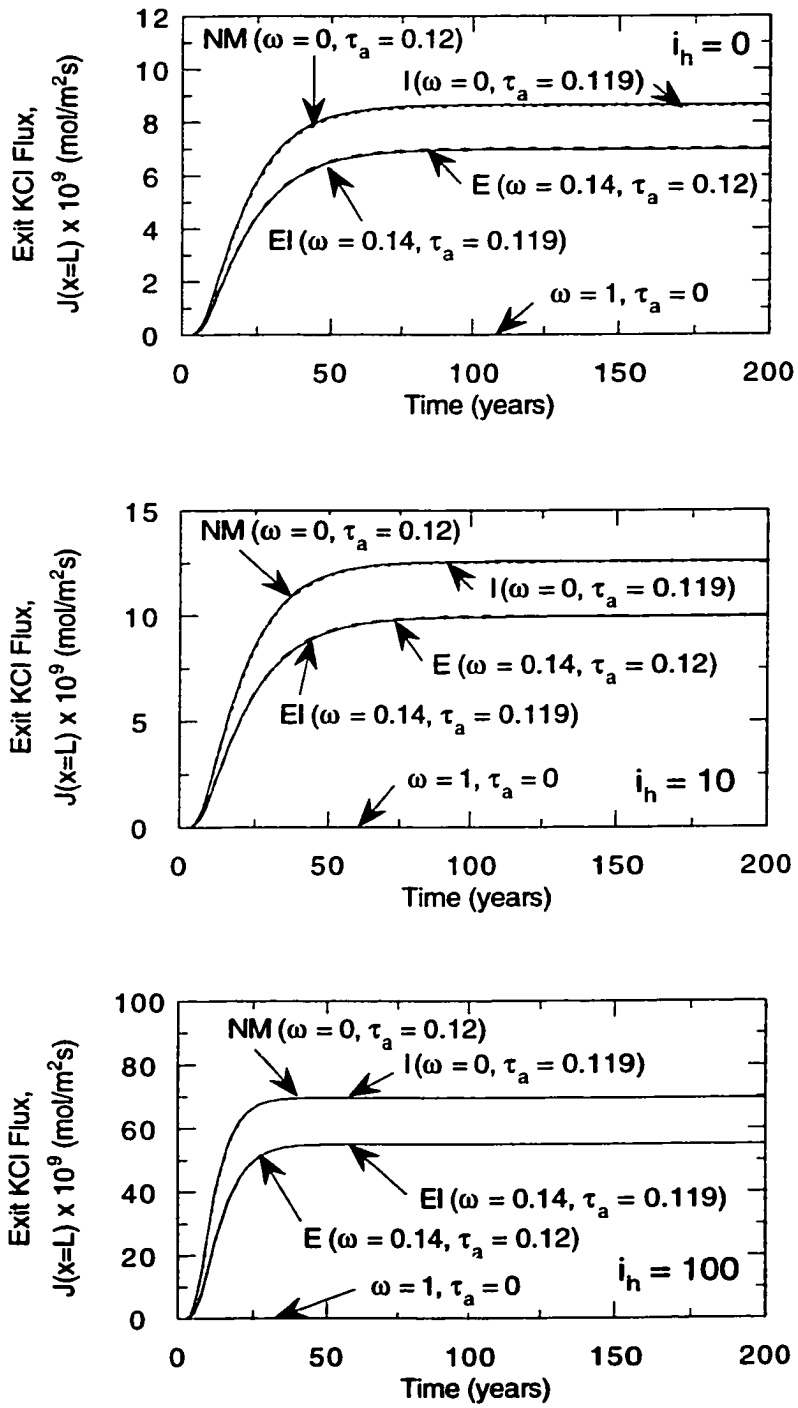

Fig. 5.7 - Theoretical KCl exit flux versus time (L = 1 m, C_o = 0.047 M, n = 0.78, k_h = 1.48 x 10^{-11} m/s).

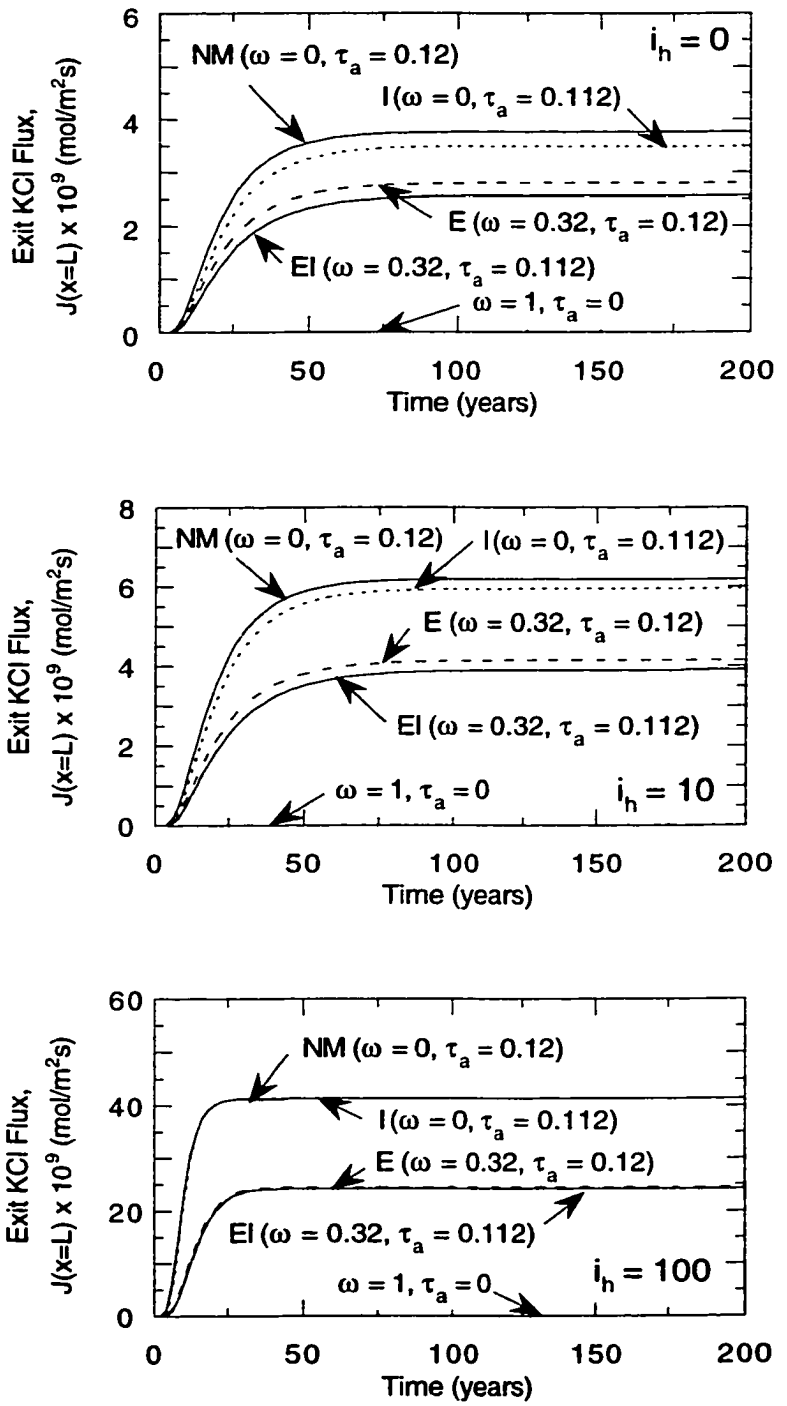

Fig. 5.8 - Theoretical KCl exit flux versus time (L = 1 m, C_o = 0.020 M, n = 0.79, k_h = 2.06 x 10^{-11} m/s).

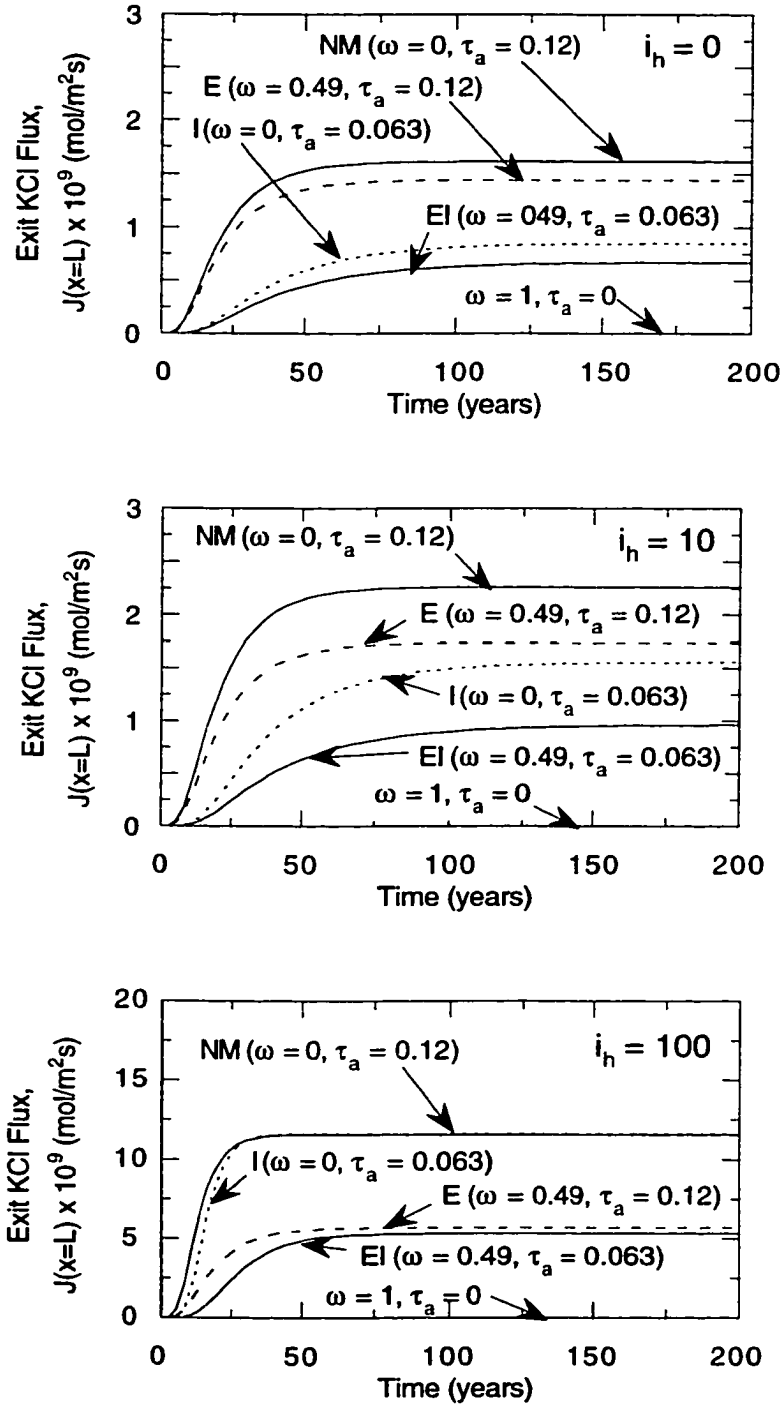

Fig. 5.9 - Theoretical KCl exit flux versus time (L = 1 m, C_o = 0.0087 M, n = 0.79, k_h = 1.33 x 10^{-11} m/s).

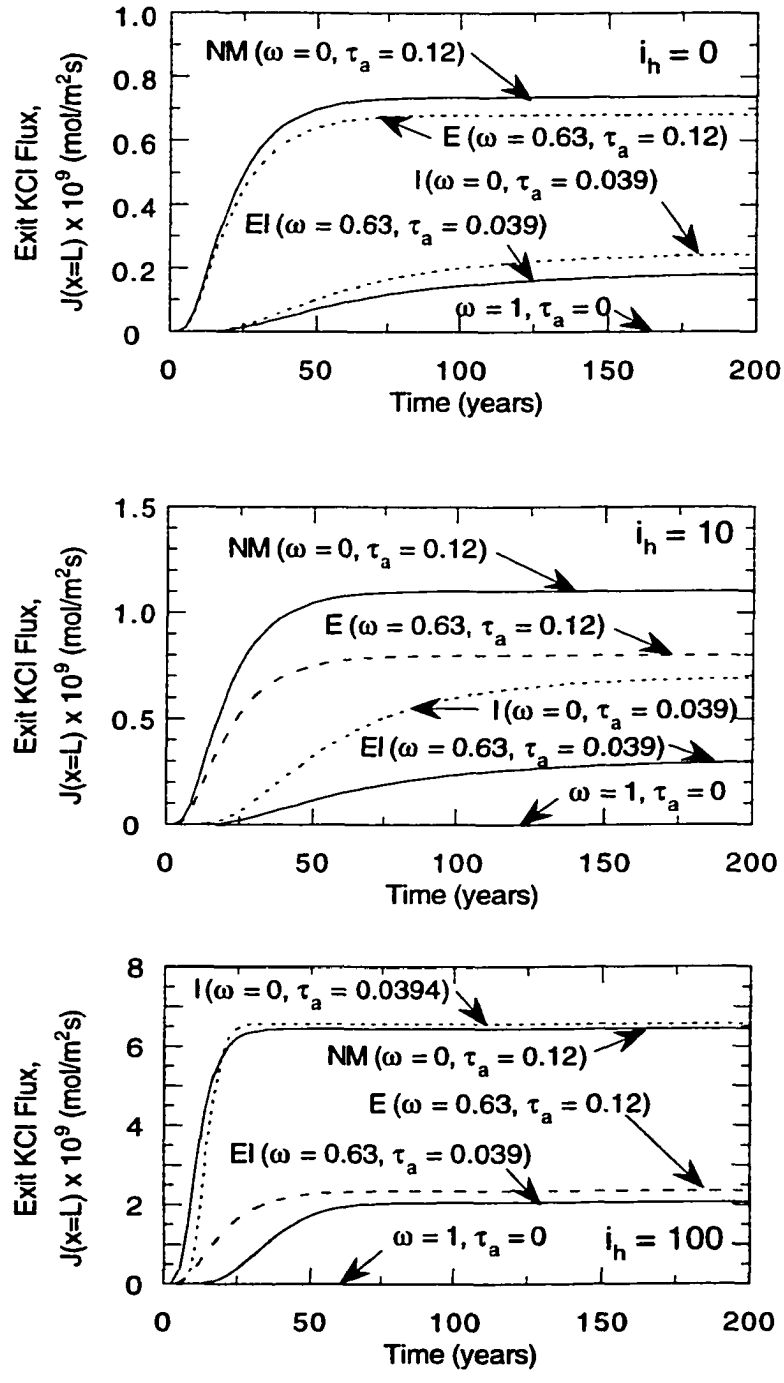

Fig. 5.10 - Theoretical KCl exit flux versus time (L = 1 m, C_o = 0.0039 M, n = 0.80, k_h = 1.65 x 10^{-11} m/s).

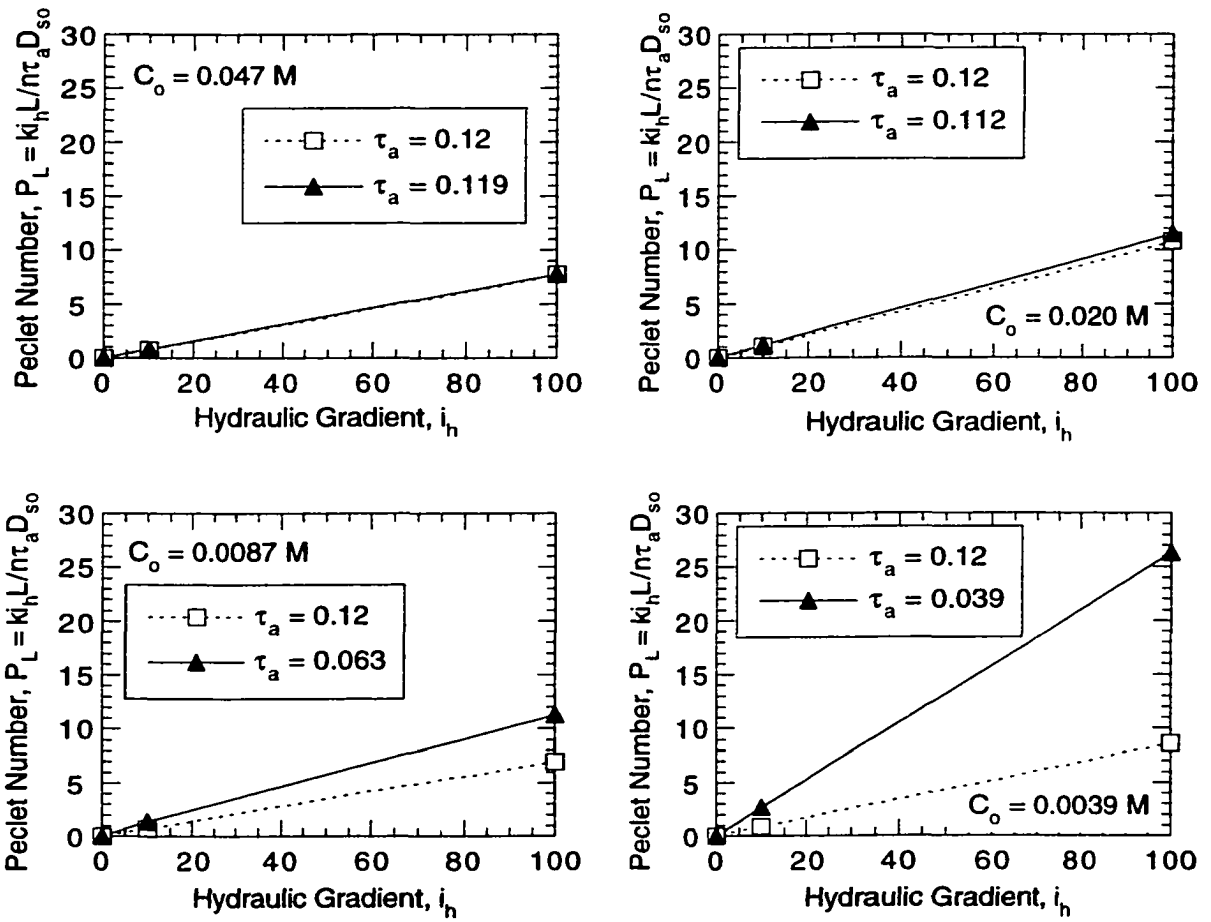

Fig. 5.11 - Peclet numbers as a function of hydraulic gradient.

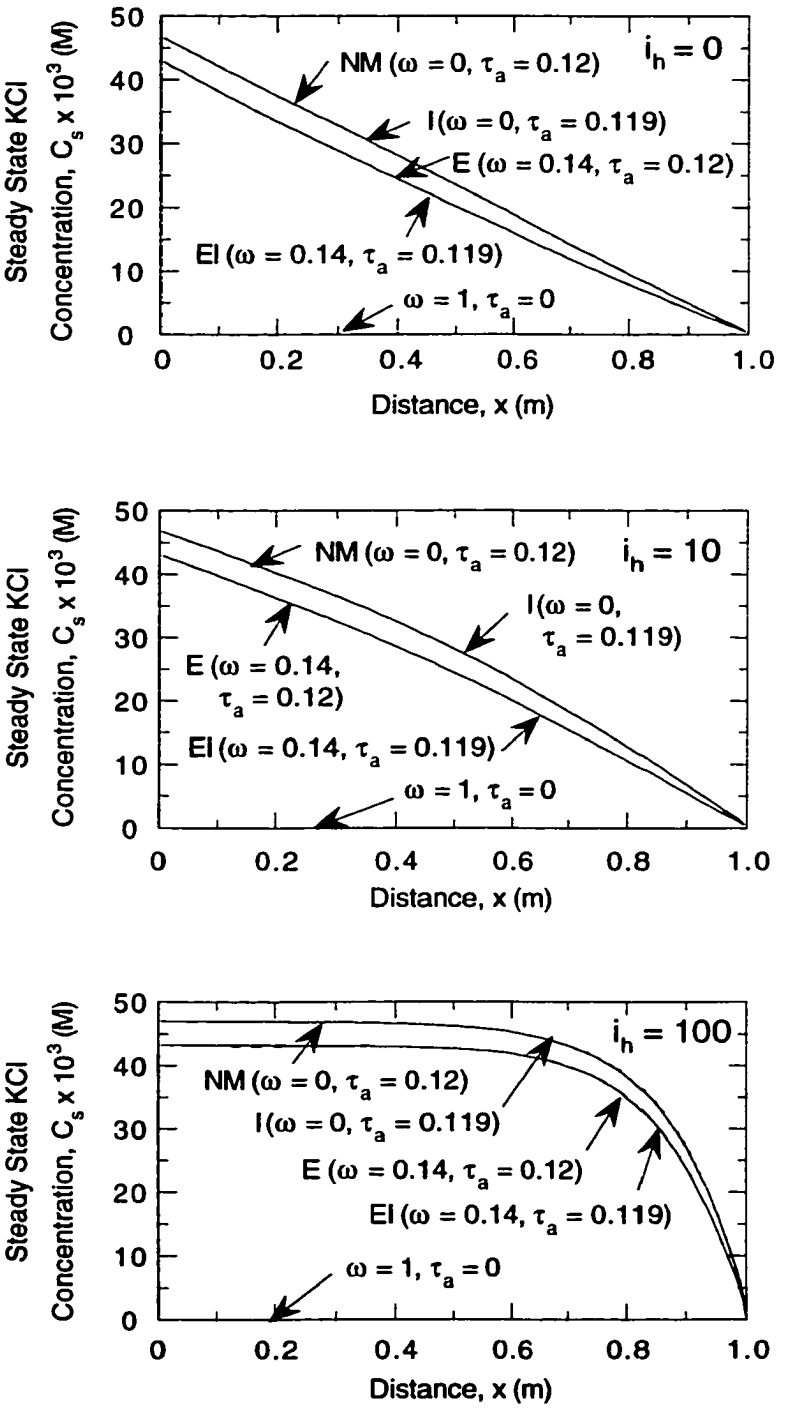

Fig. 5.12 - Theoretical steady-state concentration profiles inside soil barrier (L = 1 m, C_o = 0.047 M, n = 0.78, k_h = 1.48 x 10^{-11} m/s).

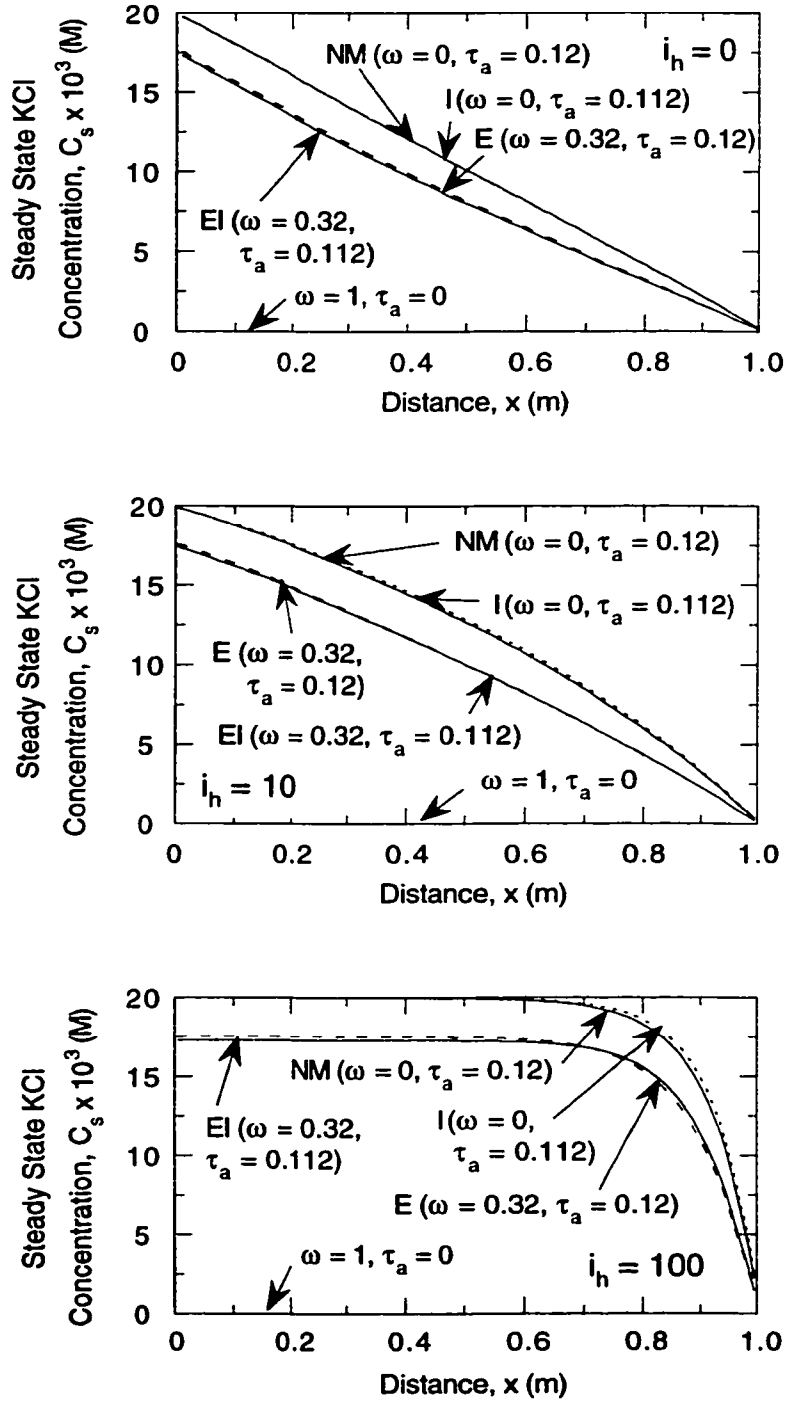

Fig. 5.13 - Theoretical steady-state concentration profiles inside soil barrier (L = 1 m, C_o = 0.020 M, n = 0.79, k_h = 2.06 x 10^{-11} m/s).

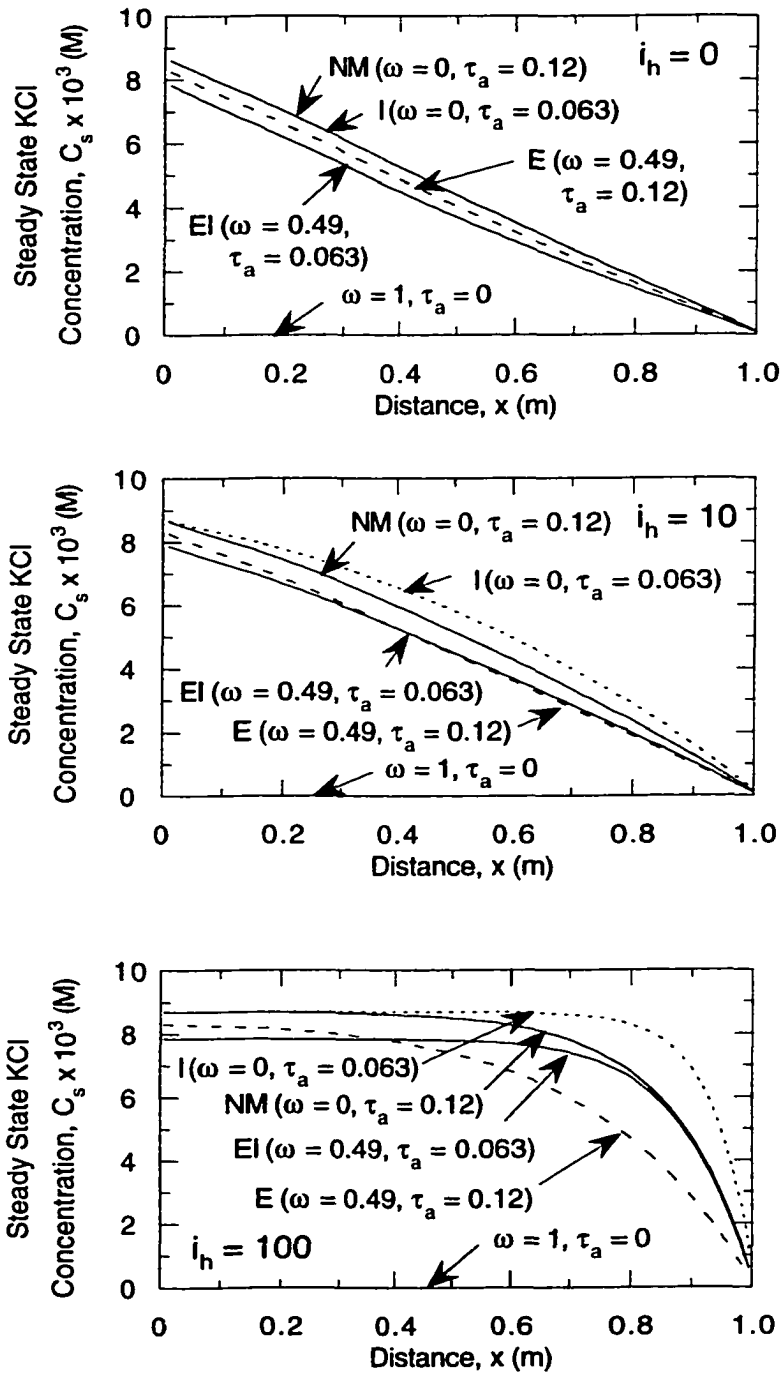

Fig. 5.14 - Theoretical steady-state concentration profiles inside soil barrier (L = 1 m, C_o = 0.0087 M, n = 0.79, k_h = 1.33 x 10^{-11} m/s).

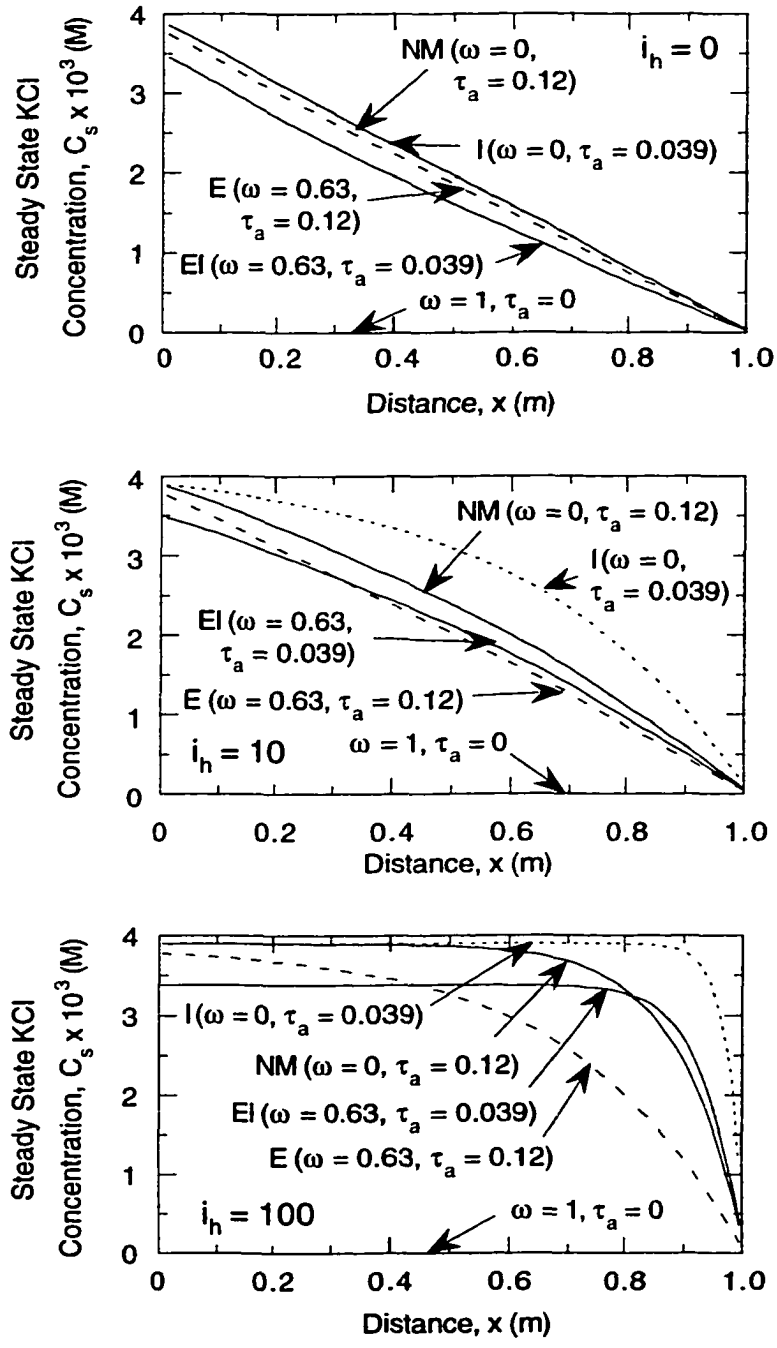

Fig. 5.15 - Theoretical steady-state concentration profiles inside soil barrier (L = 1 m, C_o = 0.0039 M, n = 0.80, k_h = 1.65 x 10^{-11} m/s).

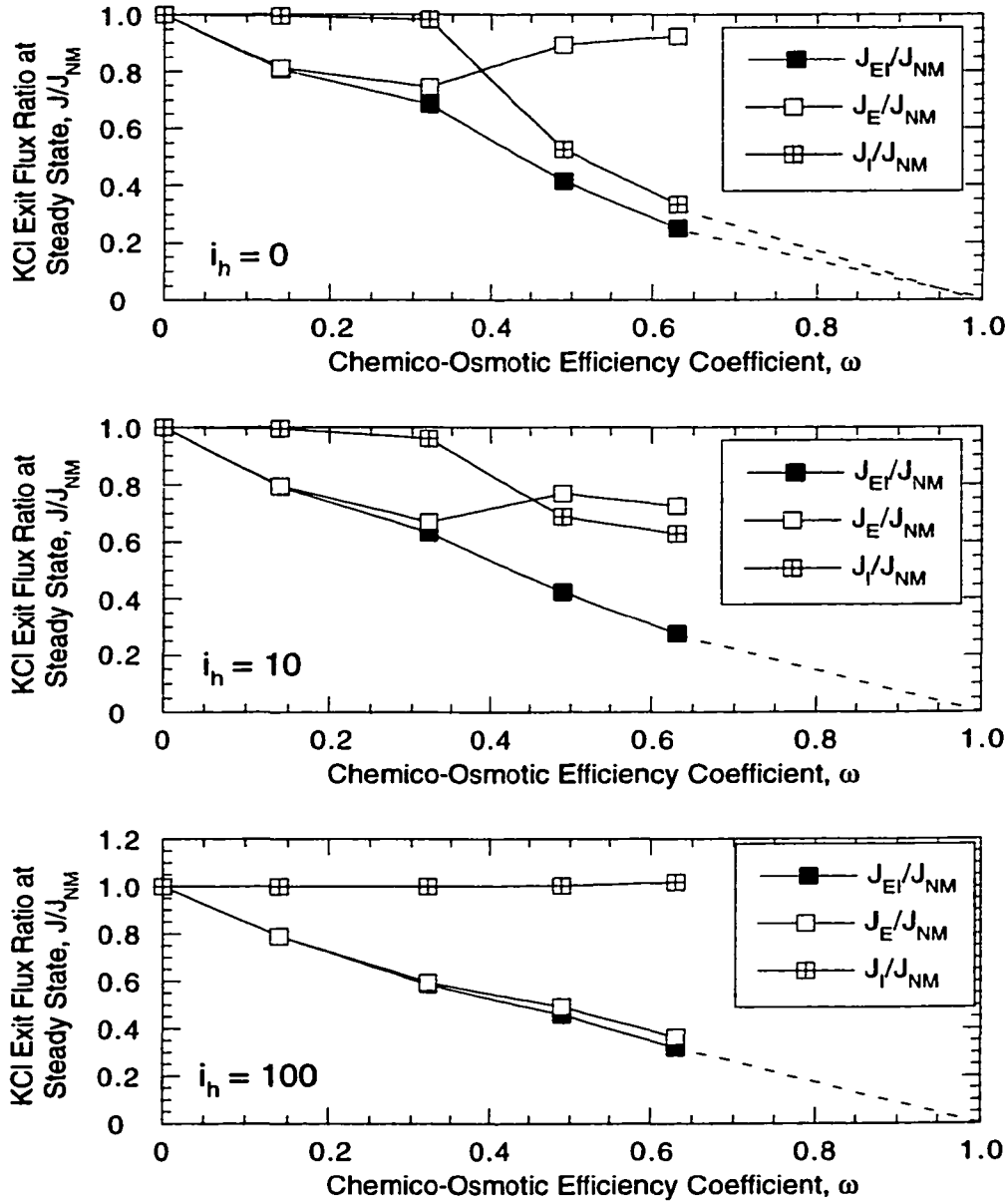

Fig. 5.16 - Normalized values of exit KCl flux at steady-state relative to the non-membrane (NM) condition.

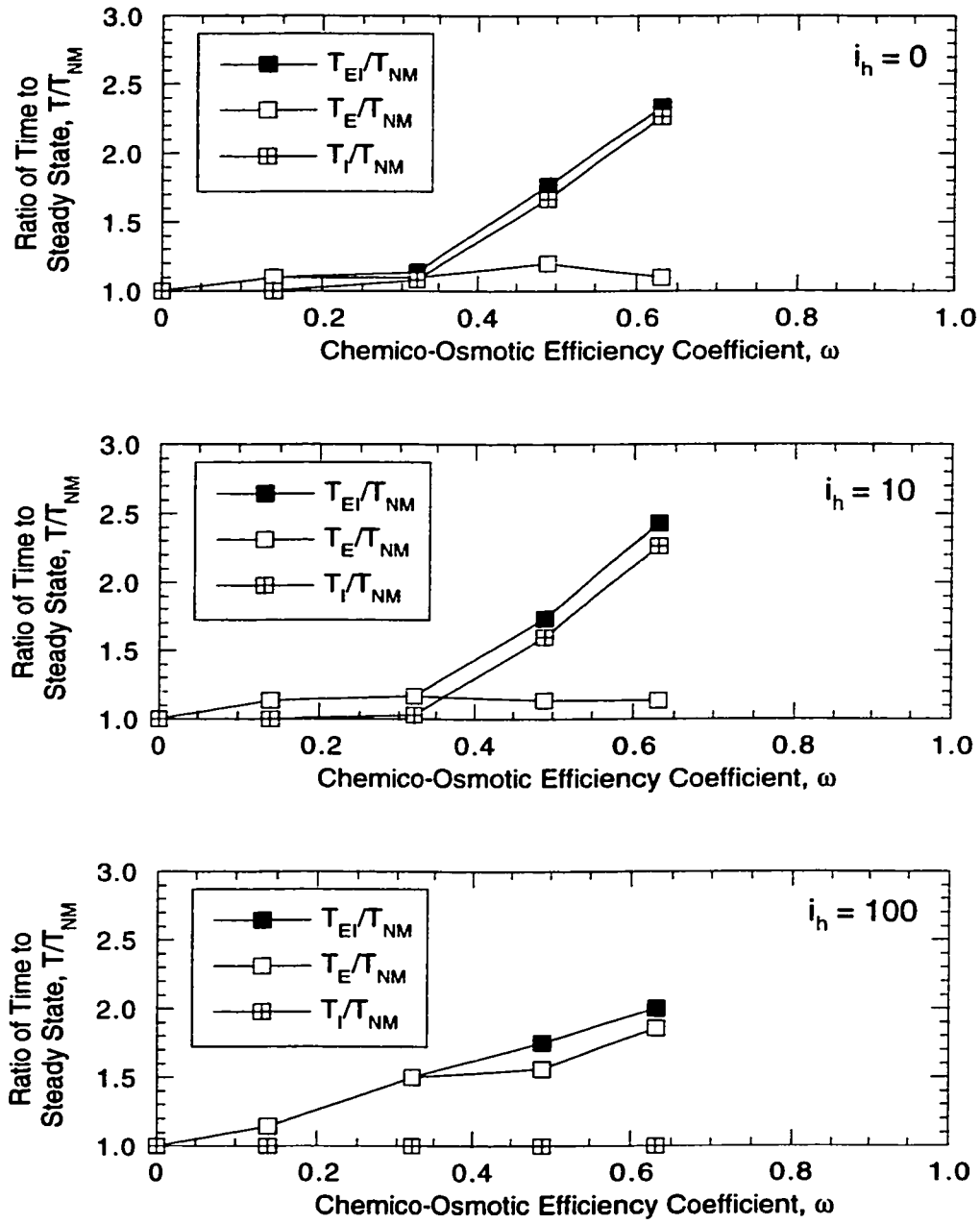

Fig. 5.17 - Normalized values of time to reach steady-state transport of KCl relative to the non-membrane (NM) condition.

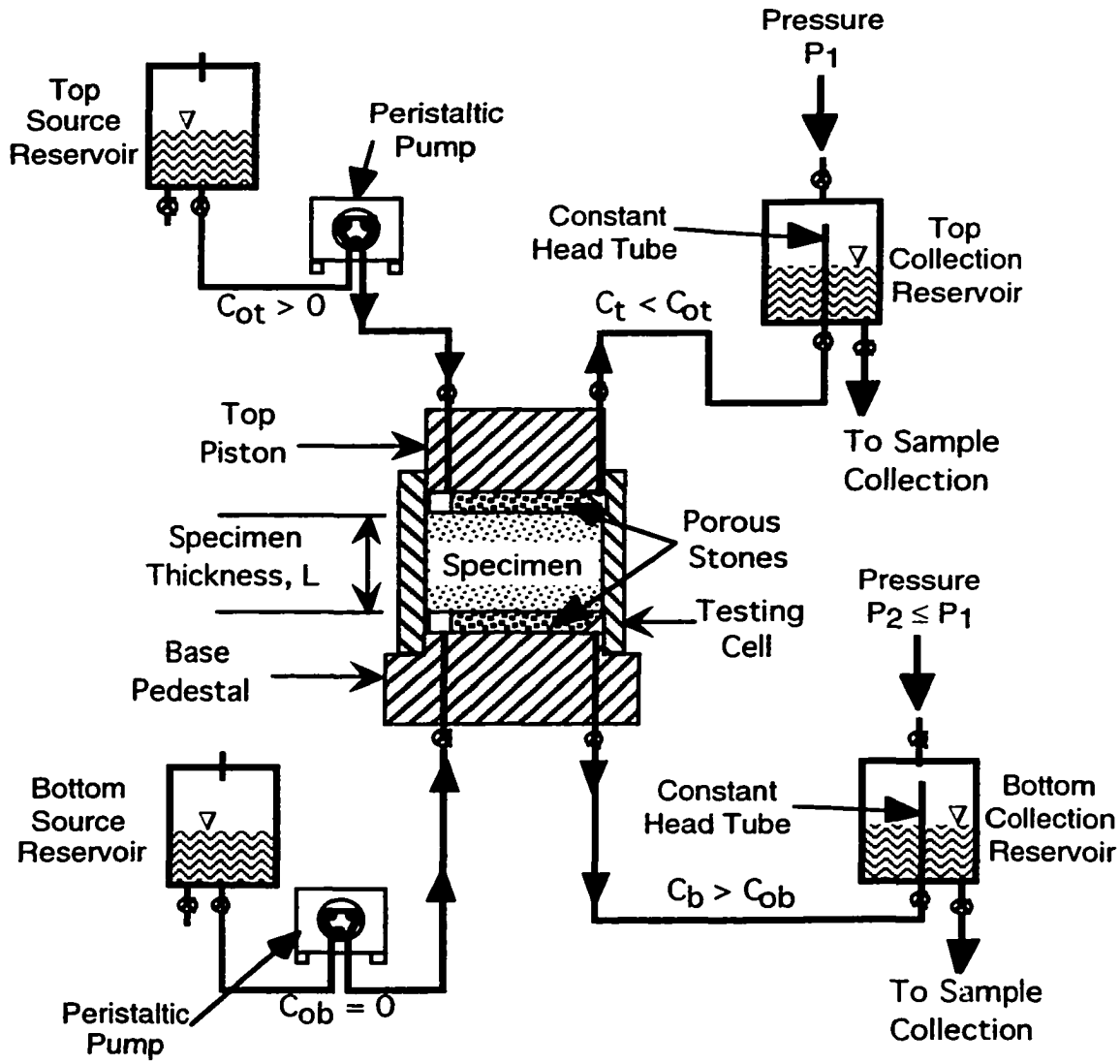

Fig. 5.18 - Schematic illustration of column testing apparatus.

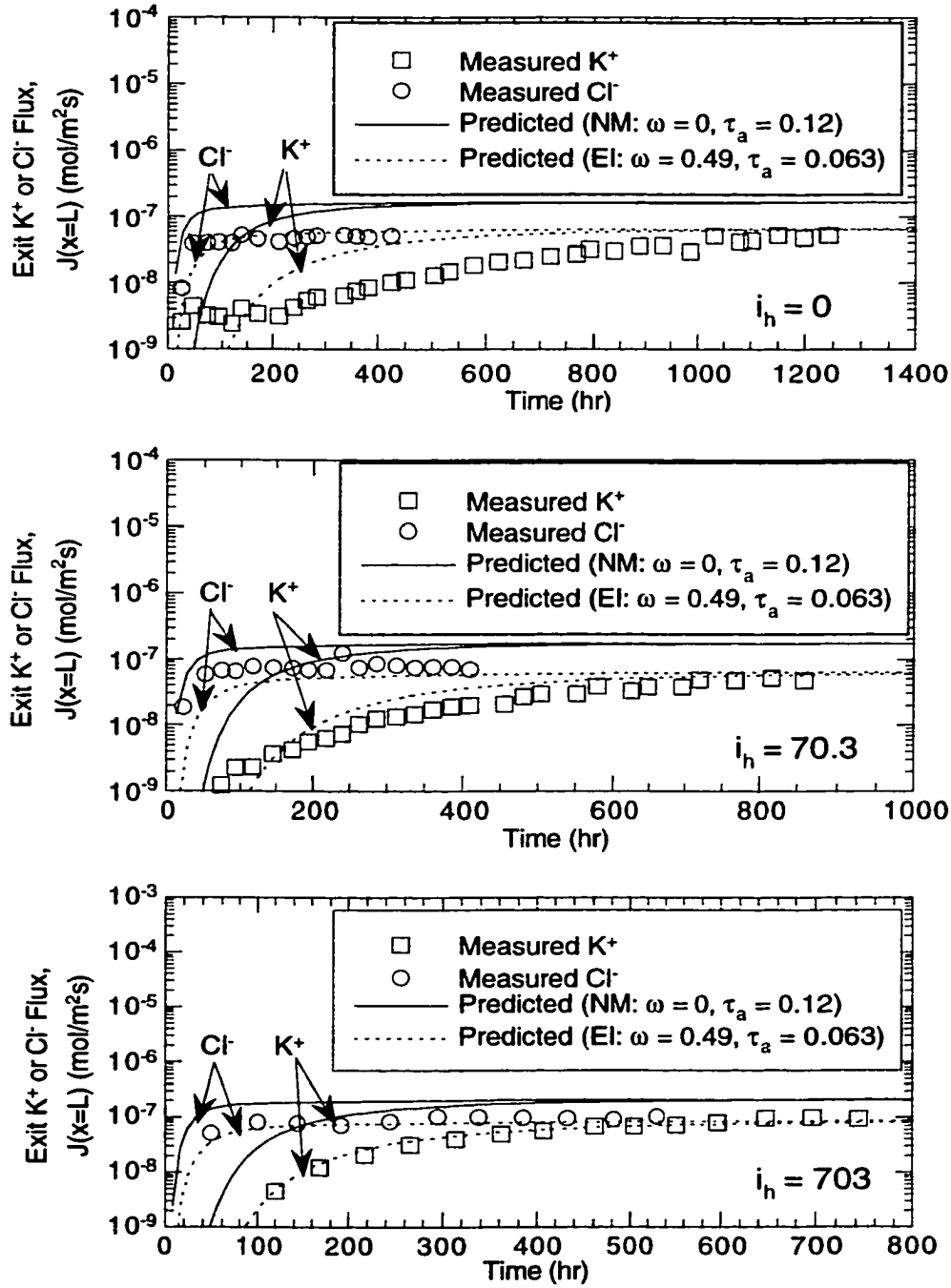

Fig. 5.19 - Comparison of measured exit K^+ and Cl^- fluxes from column tests on Bentomat GCL (L = 1.0 cm; C_o = 0.0087 M KCl) and predicted K^+ and Cl^- fluxes with either no coupling (NM) or both explicit and implicit coupling (EI).

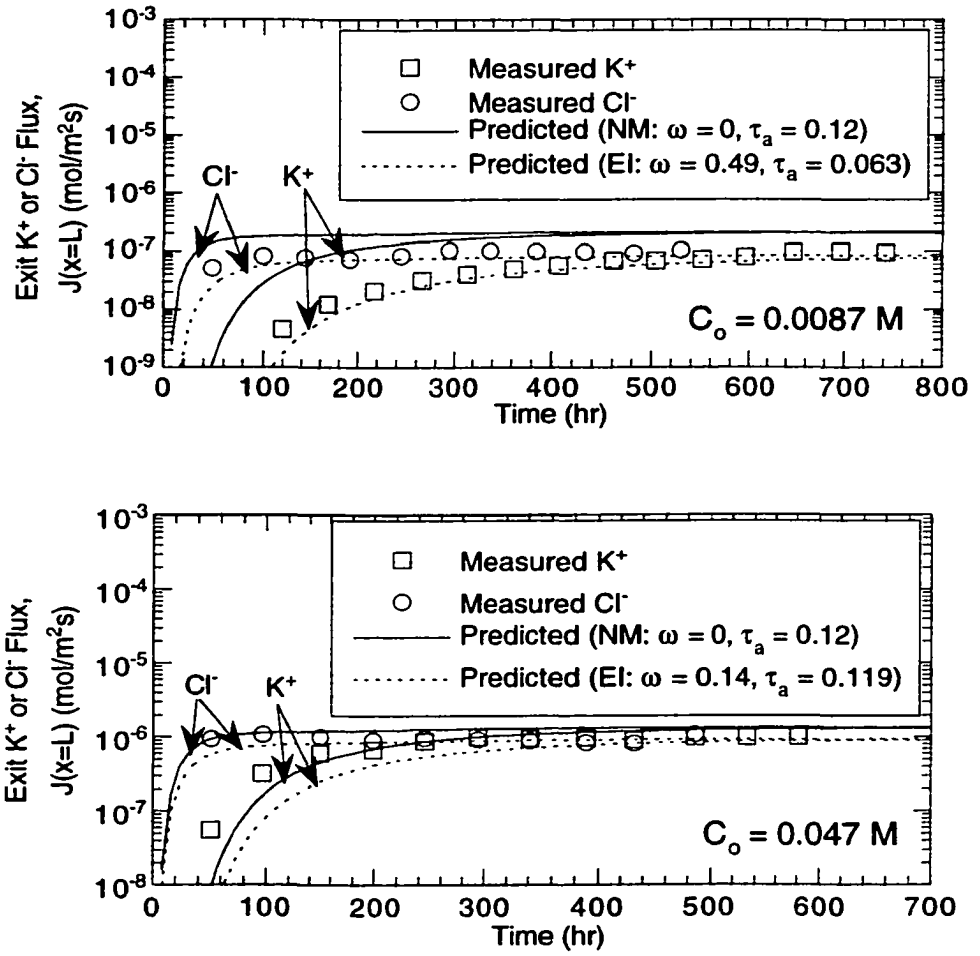

Fig. 5.20 - Comparison of measured exit K^+ and Cl^- fluxes from column tests on Bentomat GCL (L = 1.0 cm, i_h = 703) and predicted K^+ and Cl^- fluxes with either no coupling (NM) or both explicit and implicit coupling (EI).

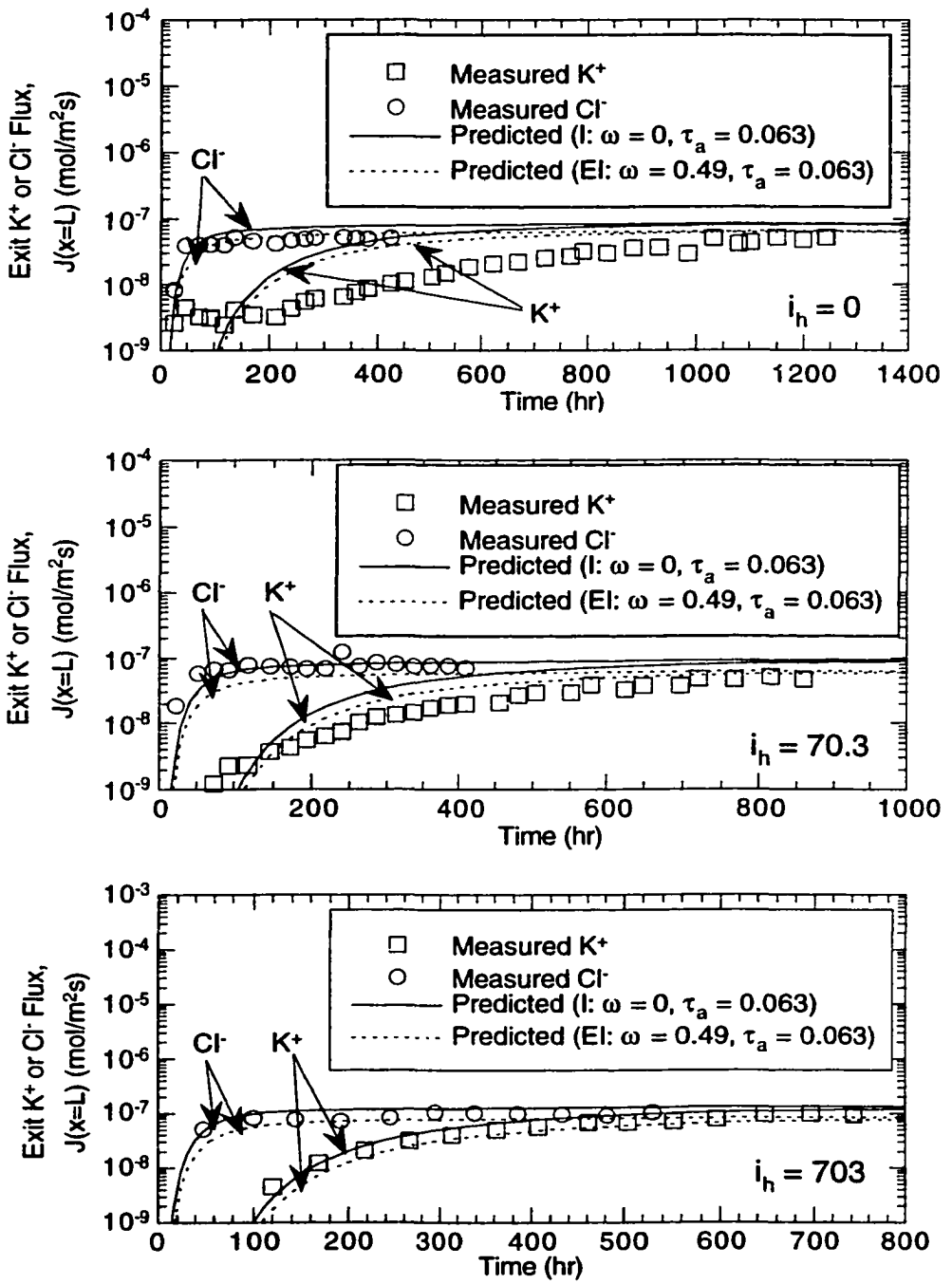

Fig. 5.21 - Comparison of measured exit K^+ and Cl^- fluxes from column tests on Bentomat GCL (L = 1.0 cm, C_o = 0.0087 M KCl) and predicted K^+ and Cl^- fluxes with either implicit coupling only (I) or both explicit and implicit coupling (EI).

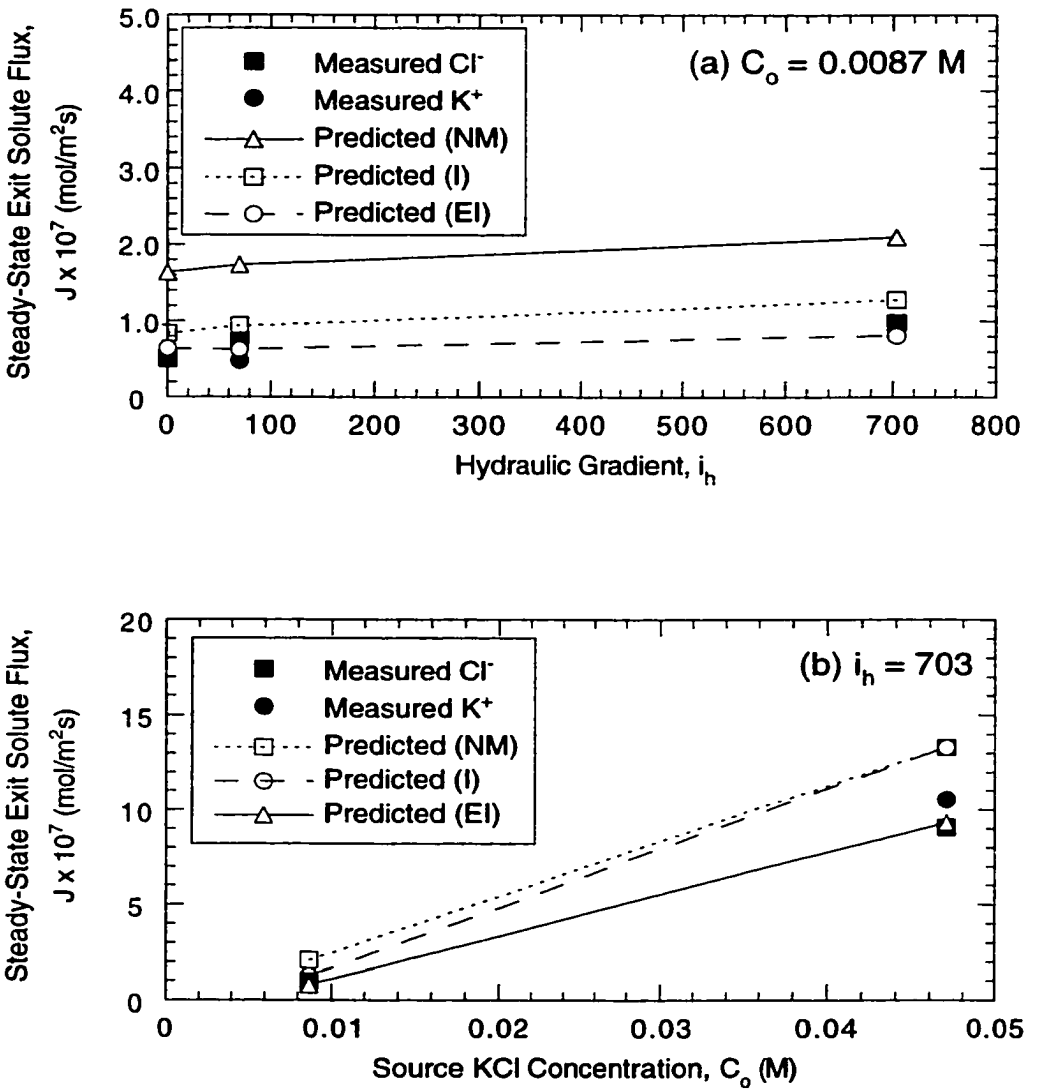

Fig. 5.22 - Comparison of measured and predicted steady-state exit solute fluxes for column tests on Bentomat GCL (L = 1.0 cm): (a) Column tests 1, 2, and 3 (C_o = 0.0087 M); and (b) Column tests 3 and 4 (i_h = 703).

APPENDIX A

QUANTITATIVE ASSESSMENT OF THE VAN'T HOFF EXPRESSION FOR EVALUATING CHEMICO-OSMOTIC EFFICIENCY OF CLAY SOILS

APPENDIX A

QUANTITATIVE ASSESSMENT OF THE VAN'T HOFF EXPRESSION FOR EVALUATING CHEMICO-OSMOTIC EFFICIENCY OF CLAY SOILS

ABSTRACT: The driving force for chemico-osmotic liquid flow in fine-grained soils (e.g., clays) often is described in terms chemico-osmotic pressure, π, that can be estimated using the van't Hoff expression. The van't Hoff expression relates π to molar salt concentration based on the limiting assumptions that the electrolyte solution is both *ideal* and *dilute*. The theoretical error in π resulting from use of the van't Hoff expression is a function of both electrolyte concentration and the type of electrolyte. For concentrations of 1:1 electrolytes NaCl and KCl ranging from 10^{-4} to 1.0 M, the van't Hoff expression overestimates π by as much as 8.5 percent and 11.2 percent, respectively, relative to the fundamental expression for real solutions. For concentrations of the 1:2 electrolyte $CaCl_2$ ranging from 10^{-4} to 1.0 M, the van't Hoff expression overestimates π by as much as 17 percent. The use of the van't Hoff expression results in greater than 5 percent overestimation in π for 1:1 electrolytes at concentrations greater than 0.05 M and for 1:2 electrolytes at concentrations greater than 10^{-3} M. The results of a six-stage osmotic test on a geosynthetic clay liner (GCL) subjected to potassium chloride (KCl) solutions indicates that the "true" osmotic efficiency coefficient is underestimated by as much as 5 percent for source KCl concentrations ranging from 0.0039 M to 0.047 M when the van't Hoff expression is used to compute the applied chemico-osmotic pressure difference across the GCL.

KEY WORDS: chemico-osmosis, chemico-osmotic pressure, electrolyte solution, osmotic coefficient, chemico-osmotic pressure, van't Hoff equation, water activity

A.1 INTRODUCTION

Chemico-osmosis, or the movement of solvent (e.g., water) from a solution of lower solute concentration to a solution of higher solute concentration, has been recognized as a possible source of anomalous pore-pressure measurements, water movement, and volume change in fine-grained soils (Marine and Fritz 1981, Barbour and Fredlund 1989, Olsen et al. 1990). Chemico-osmotic behavior is exhibited in a fine-grained soil-water-electrolyte system provided that the soil acts as a semi-permeable membrane, restricting the passage of electrolyte solutes through the soil pores (e.g., see Fritz 1986). Evaluation of this behavior typically is based on the concept of chemico-osmotic pressure.

For example, the driving force for chemico-osmotic liquid flux, q_π, in a soil-water-electrolyte system is the gradient in chemico-osmotic pressure, π, across the system (Kemper and Rollins 1966, Bresler 1973, Barbour and Fredlund 1989, Olsen et al. 1990, Basu and Sharma 1997), or

$$q_\pi = \omega \frac{k_h}{\rho_w g} \nabla \pi \qquad \text{(A.1)}$$

where q_π is the chemico-osmotic component of water flux, ω is the dimensionless osmotic efficiency coefficient ($0 \leq \omega \leq 1$), k_h is hydraulic conductivity [Lt^{-1}], g is the acceleration due to gravity [Lt^{-2}], and ρ_w is the density of water [ML^{-3}]. Typically, values of π are calculated using mathematical expressions derived from thermodynamics principles. The simplest of these expressions for π is the van't Hoff expression, which provides a linear relationship between chemico-osmotic pressure and molar solute concentration. The van't Hoff expression is presented in numerous chemistry and

engineering textbooks (e.g., Katchalsky and Curran 1965, Mitchell 1993, Tinoco et al. 1995), and has been used, for example, in theoretical and experimental studies on the effects of membrane behavior on water flow, solute migration, and volume change in fine-grained soil systems (Olsen 1969, Bresler 1973, Fritz and Marine 1983, Barbour and Fredlund 1989, Yeung 1990, Basu and Sharma 1997).

The van't Hoff expression is based on the limiting assumptions that the aqueous solution is both ideal and dilute. Electrolyte solutions generally are not ideal, but will approach ideal behavior as the solution becomes more dilute. Therefore, the van't Hoff equation represents an approximate solution for chemico-osmotic pressure of electrolyte solutions that is expected to become less accurate as electrolyte concentration increases. Although knowledge of this limitation in the van't Hoff expression is common, the error associated with application of the van't Hoff expression has not been quantified. Therefore, the purpose of this analysis is to quantify the error associated with the van't Hoff expression over a range of salt concentrations for some common electrolytes. Theoretical values of π obtained from the van't Hoff expression are compared against theoretical values obtained using the fundamental expression for π of real solutions. In addition, the implications of this error with regard to laboratory measurement of osmotic efficiency coefficients for a geosynthetic clay liner (GCL) is illustrated.

A.2 CHEMICO-OSMOTIC PRESSURE EXPRESSIONS

A.2.1 Real Electrolyte Solutions

The fundamental expression for π of real aqueous solutions is given by the following thermodynamic relation (Katchalsky and Curran 1965, Olsen et al. 1990, Tinoco et al. 1995):

$$\pi = -\frac{RT}{\overline{V}_w}\ln(a_w) \qquad (A.2)$$

where $\overline{V}_w$ is the partial molar volume of water [$L^3 mol^{-1}$], and a_w is the activity of water [mol L^{-3}]. Therefore, determination of π based on Eq. A.2 requires values of the activity of water in the solution. Water activity in a single-salt electrolyte solution can be expressed in terms of a dimensionless osmotic coefficient, ϕ, as follows (Rock 1983):

$$\ln(a_w) = -\phi \frac{X_s}{X_w} = -\phi M_w \nu m \tag{A.3}$$

where X_s is the mole fraction of the salt [dimensionless], X_w is the mole fraction of water [dimensionless], M_w is the molecular mass of water [$M \cdot mol^{-1}$], ν is the total number of ions per formula unit (e.g., $\nu = 2$ for KCl, $\nu = 3$ for $CaCl_2$), and m is the salt molality [$mol \cdot M^{-1}$]. Substitution of Eq. A.3 into Eq. A.2 yields the following relationship:

$$\pi = \phi \nu R T m \frac{M_w}{\overline{V}_w} \tag{A.4}$$

or, since $M_w / \overline{V}_w \approx 1$ for aqueous solutions at 25 C,

$$\pi \approx \phi \nu R T m \tag{A.5}$$

Equation A.5 indicates that π can be calculated for any salt solution provided that the osmotic coefficient, ϕ, corresponding to the particular salt concentration is known. Measured values of ϕ for different molalities of a limited number of electrolytes are tabulated in chemistry handbooks (e.g., Conway 1952, Robinson and Stokes 1959, Rock 1983). These published values of ϕ, if available, typically are limited to electrolyte concentrations greater than 0.1 m.

Kemper and Rollins (1966) indicate that ϕ may be calculated for a range of salt concentrations using the following differential equation relating ϕ with the mean activity coefficient of the electrolyte, γ_s (Rock 1983):

$$d\phi = d\ln\gamma_s + \frac{(1-\phi)}{m}dm \qquad (A.6)$$

Values of mean activity coefficient for NaCl, KCl, and $CaCl_2$ are shown for a range of concentrations in Fig. A.1. The data in Fig. A.1 indicate that solute activity tends to decrease as electrolyte concentration increases to approximately 0.5 m. In addition, the mean activity coefficient of the 1:2 electrolyte $CaCl_2$ is lower than that for the 1:1 electrolytes NaCl and KCl for a given molal concentration less than 1.0 m. The lower mean activity coefficient for $CaCl_2$ relative to NaCl and KCl results from a higher ionic strength, I, as predicted by the Debye-Huckel limiting law (e.g., see Rock 1983). The increase in mean activity coefficient at concentrations greater than 0.5 m shown in Fig. A.1 is attributed to electrical interactions as the ions become more crowded in solution. This concentration range extends beyond the range of acceptability of $I < 10^{-2.3}$ M for the Debye-Huckel limiting law (Stumm and Morgan 1996). Mean activity coefficients at these higher concentrations typically are unique for each electrolyte, due to the different sizes of the ions, as indicated by the different values of γ_s for the 1:1 electrolytes NaCl and KCl in Fig. A.1.

Values of the osmotic coefficient, ϕ, follow a similar trend to the mean activity coefficient due to the relationship between the two parameters as shown in Eq. A.6. For example, Kemper and Rollins (1966) used Eq. A.6 to compute osmotic coefficients for NaCl and $CaCl_2$ over a wide range of electrolyte concentrations based on mean activity coefficient data. These results are shown in Fig. A.2a along with published values of ϕ for NaCl, KCl, and $CaCl_2$ from Conway (1952) and Rock (1983). Values of ϕ at lower concentrations decrease as the salt concentration increases, but increase at concentrations

extending into the higher range. Values of ϕ for NaCl and $CaCl_2$ can exceed 1.0 at concentrations beyond 1.0 M, as shown in Fig. A.2a. The corresponding values of water activity, a_w, shown in Fig. A.2b, are computed using Eq. A.3 based on the osmotic coefficient data given in Fig A.2a.

A.2.2 Ideal Electrolyte Solutions

Solutions in which the interactive forces between all solution components (i.e., solute-solute, solute-solvent, solvent-solvent) are the same are termed *ideal* solutions. Electrolyte solutions generally are not ideal, but will approach ideal behavior as the solution becomes more dilute. In this case, the activity of water may be approximated in accordance with Raoult's law, or

$$\ln(a_w) \cong \ln(X_w) \cong -M_w \nu m \tag{A.7}$$

Substitution of Eqs. A.5 and A.7 into Eq. A.2 yields the following expression for π in ideal solutions:

$$\pi \text{ (ideal)} = \nu RTm \tag{A.8}$$

Comparison of Eq. A.8 with Eq. A.5 reveals that the assumption of ideality in solution results in $\phi = 1$ for all concentrations. Therefore, the potential error in π associated with this assumption is related to the degree of deviation of ϕ from unity for a given salt concentration (see Fig. A.2a).

A.2.3 Ideal, Dilute Electrolyte Solutions

The expression of chemico-osmotic pressure for an ideal solution in Eq. A.8 also can be simplified if the solution is assumed sufficiently dilute such that the volume of the

solute can be neglected. In this case, the molar salt concentration, C [mol·L^{-3}], and molal salt concentration, m, can be assumed equal (i.e., C = m), resulting in the following expression for the chemico-osmotic pressure of ideal, dilute solutions:

$$\pi \text{ (ideal,dilute)} = \nu RTC = RT\sum_{i=1}^{N} C_i \qquad \text{(A.9)}$$

where C_i is the molar concentration of solute species i [mol·L^{-3}] and N is the total number of different solute species in the solution. Equation A.9 is the well-known van't Hoff expression in which the osmotic pressure of ideal, dilute electrolyte solutions is expressed simply as a linear function of the sum of molar solute concentrations.

A.3 LIMITATIONS OF THE VAN'T HOFF EXPRESSION

The van't Hoff expression (Eq. A.9) is more convenient for evaluation of chemico-osmotic pressure, π, of an electrolyte solution than the expression for real solutions (Eq. A.5) that requires knowledge of osmotic coefficients. However, a quantitative assessment of the error associated with the van't Hoff expression due to the limiting assumptions that the solution is both ideal and dilute has not been performed. According to Fritz (1986), values of π calculated using Eq. A.9 are within five percent of values of π calculated using Eq. A.5 for solutions less than 1.0 M containing 1:1 electrolytes (e.g., NaCl, KCl). However, no quantitative analysis has been presented in the literature either to support this statement by Fritz (1986) or to assess the error in π for 1:2 electrolytes (e.g., $CaCl_2$).

Values of π for real electrolyte solutions containing NaCl, KCl, or $CaCl_2$ were calculated using Eq. A.5 based on the data in Fig. A.2a. These values of π are compared to values of π computed for ideal solutions (Eq. A.8) and ideal, dilute solutions (Eq. A.9) for salt concentrations ranging from 10^{-4} M to 1.0 M in Fig. A.3. When necessary, molal

salt concentrations were converted to molar salt concentrations based on published crystal densities of 2.170, 1.988, and 2.150 g/cm^3 for NaCl, KCl, and $CaCl_2$, respectively (CRC Press 1999).

The results in Figs. A.3a and A.3b indicate that the use of the expression for an ideal solution (Eq. A.8) or the van't Hoff equation (Eq. A.9) results in overestimation of π relative to the fundamental expression for real solutions for the 1:1 electrolytes NaCl and KCl at concentrations between 10^{-4} M and 1.0 M, since values of ϕ for NaCl and KCl are below 1.0 in this concentration range (see Fig. A.2a). The van't Hoff expression results in greater overestimation of π for NaCl and KCl than Eq. A.8, since the contribution of solute volume to the overall volume of the solution is neglected. Values of π for $CaCl_2$ shown in Fig. A.3c are overestimated at concentrations less than approximately 0.6 M, but are underestimated at concentrations greater than approximately 0.6 M. The underestimation of π in this higher concentration range is due to the increase in ϕ above 1.0 as shown in Fig. A.2a.

The theoretical error in π associated with use of the van't Hoff equation for NaCl, KCl, and $CaCl_2$ is quantified in Fig. A.4. A positive error in Fig. A.4 corresponds to overestimation of π, while a negative error corresponds to underestimation of π. The results indicate that the error in π (i.e., overestimation) for NaCl based on the van't Hoff expression increases from zero percent to approximately 8.5 percent as the salt concentration increases from 10^{-4} M to 0.4 M. However, the van't Hoff expression becomes more accurate beyond 0.4 M, due to an increase in ϕ (see Fig. A.2a). For example, the error in π for NaCl is approximately 6.0 percent at a concentration of 1.0 M. A similar trend is evident for KCl, although the error in π is greater for KCl than for NaCl due to the lower values of ϕ for KCl. The maximum error in π for KCl is approximately 11 percent at a concentration of 0.7 M.

The results in Fig. A.4 also indicate that the error in π is greater for $CaCl_2$ than for the 1:1 electrolytes (NaCl, KCl) for concentrations ranging from 10^{-4} M to 0.4 M. The

greater error associated with $CaCl_2$ in this concentration range is due to the lower values of ϕ for $CaCl_2$. The lower values of ϕ for $CaCl_2$ are due to a lower mean activity coefficient in accordance with the Debye-Huckel limiting law (see Fig. A.1). The maximum error in π (i.e., overestimation) for $CaCl_2$ based on the van't Hoff expression is approximately 17 percent at a concentration of 0.1 M. The error in π for $CaCl_2$ decreases from approximately 17 percent to zero percent as the concentration increases from 0.1 M to 0.8 M due to an increase in ϕ for $CaCl_2$. Beyond a concentration of 0.8 M, the van't Hoff expression significantly underestimates π for $CaCl_2$. For example, the error in π at a $CaCl_2$ concentration of 1.0 M is approximately -7.0 percent.

The error in π based on an ideal solution (Eq. A.8) also is shown in Fig. A.4 to illustrate that the majority of the error associated with the van't Hoff expression is a result of the assumption of ideality. For example, the difference between the error in π for ideal solutions computed with Eq. A.8 and values of π for ideal, dilute solutions computed with Eq. A.9 for salt concentrations below 0.1 M is small (<1%). Equation A.9 provides greater estimates of π than Eq. A.8 at higher salt concentrations, since the contribution of the salt volume to the overall volume of solution becomes more significant. Therefore, the error in π based on Eq. A.9 for NaCl and KCl concentrations above 0.1 M is greater than the error in π based on Eq. A.8. However, the van't Hoff expression results in slightly better estimates of π than Eq. A.8 for $CaCl_2$ in the region from 0.8 to 1.0 M where π is underestimated.

The results in Fig. A.4 can be used as a guide to establish the range of salt concentrations over which the van't Hoff expression is acceptable for estimating π. This acceptable concentration range depends on the level of accuracy required for the application of interest. For example, if the maximum acceptable error in π is ±5 percent, the maximum acceptable concentration at which the van't Hoff expression can be used to calculate π is 0.05 M for the 1:1 electrolytes NaCl and KCl. For the 1:2 electrolyte $CaCl_2$, the acceptable range appears to include concentrations up to 10^{-3} M as well as

concentrations between 0.6 and 0.9 M. However, the van't Hoff expression may not be appropriate for all 1:2 electrolytes in the region from 0.6 M to 0.9 M since osmotic coefficients in this range likely are unique for a particular electrolyte.

A.4 MEASUREMENT OF SOIL CHEMICO-OSMOTIC EFFICIENCY

The total liquid flux, q, through a soil membrane in response to both gradients in hydraulic pressure, P, and chemico-osmotic pressure, π, is the sum of the chemico-osmotic flux, q_π, given by Eq. A.1 and the hydraulic flux, q_h, given by Darcy's law, or (Barbour 1986)

$$q = q_h + q_\pi = -\frac{k_h}{\rho_w g}\nabla P + \omega\frac{k_h}{\rho_w g}\nabla\pi \qquad (A.10)$$

Equation A.10 has been used in experimental studies as the basis for evaluating osmotic efficiency coefficients, ω, for clay membranes in the presence of electrolyte solutions (Kemper and Rollins 1966, Kemper and Quirk 1972, Malusis et al. 2001). For example, Malusis et al. (2001) describe a laboratory apparatus and testing procedure to evaluate ω for a geosynthetic clay liner (GCL) containing sodium bentonite (i.e., Bentomat®). In these tests, the GCL specimen is placed in the rigid testing cell illustrated schematically in Fig. A.5. The top piston and base pedestal surrounding the specimen are equipped with ports that enable circulation of separate electrolyte solutions at the specimen boundaries to establish and maintain a constant difference in solute concentration across the specimen. The solutions were circulated continuously at the same rate using a flow-pump system consisting of a dual-carriage syringe pump (Model 944, Harvard Apparatus, South Natick, MA) equipped with two customized actuators (i.e., syringes). Additional ports are installed in the top piston and base pedestal to allow for measurement of differential pressure, ΔP, across the specimen.

As shown in Fig. A.5, solutions containing initial concentrations of a given electrolyte, C_{ot} and C_{ob}, are infused through the porous stones across the top and bottom boundaries of the specimen. Circulation outflow from these boundaries is simultaneously collected at the same rate in order to maintain a constant volume inside the testing cell (i.e., $\Delta V_{cell} = 0$) and prevent liquid flux through the soil (i.e., $q = 0$). The expression for ω under these conditions is obtained by substituting $q = 0$ into Eq. A.10 and rearranging to yield

$$\omega = \left.\frac{\nabla P}{\nabla \pi}\right|_{q=0} \tag{A.11}$$

or, at steady state,

$$\omega_{ss} = \left.\frac{\Delta P}{\Delta \pi}\right|_{q=0} \tag{A.12}$$

The differential pressure, ΔP, in Eq. A.12 is induced across a soil membrane due to prevention of chemico-osmosis and is measured using a differential pressure transducer (Malusis et al. 2001). The difference in chemico-osmotic pressure can be calculated using either the differential form of the expression for real solutions in Eq. A.5, i.e.,

$$\Delta \pi = \nu RT \Delta(\phi m) = \nu RT(\phi_2 m_2 - \phi_1 m_1) \tag{A.13}$$

or the following differential form of the van't Hoff expression based on Eq. A.9:

$$\Delta \pi \approx \nu RT \Delta C = \nu RT(C_2 - C_1) \tag{A.14}$$

The potential error associated with use of the van't Hoff expression (Eq. A.14) for evaluating osmotic efficiency coefficients in accordance with Eq. A.12 is illustrated herein based on a six-stage osmotic test conducted on a 0.008-m-thick Bentomat® GCL specimen in the presence of KCl solutions using the apparatus and procedures described by Malusis et al. (2001). The differential pressure induced in response to an applied difference in KCl concentration was measured in each stage. The bottom reservoir contained no KCl during the test (i.e., $C_{ob} = 0$), while the top reservoir contained $C_{ot} = 0$, 0.0039 M, 0.006 M, 0.0087 M, 0.02 M, and 0.047 M KCl, respectively, in each of the six stages. Each stage was conducted until a steady differential pressure response across the specimen was observed.

The induced differential pressures, $-\Delta P$ (> 0), measured in each testing stage are presented in Fig. A.6. The differential pressure $-\Delta P$ = 1.2 kPa measured during the first stage in which $C_{ot} = C_{ob} = 0$ represents a baseline differential pressure, $-\Delta P_o$, that is attributed to slight differences in the hydraulic resistance of the porous stones at the opposite ends of the specimen and, therefore, is not included in the chemico-osmotic efficiency evaluation (e.g., see Malusis et al. 2001). Steady-state values of induced differential pressure, $-\Delta P_{ss}$, increased from 14.3 kPa to 34.3 kPa as the source KCl concentration, C_{ot}, was increased from 0.0039 M to 0.047 M. Calculated values of ω at steady-state, or ω_{ss}, are based on corrected, or effective, values of differential pressure, $-\Delta P_e$ ($= -\Delta P_{ss} - (-\Delta P_o)$) of 13.1 kPa, 16.6 kPa, 21.8 kPa, 29.6 kPa, and 33.1 kPa in the five stages corresponding to C_{ot} = 0.0039 M, 0.0060 M, 0.0087 M, 0.020 M, and 0.047 M, respectively.

Values of ω for the GCL based on the data in Fig. A.6 are given in Table A.1. Values of $\Delta\pi$ used in the evaluation of the ω values in Table A.1 are based on the average boundary KCl concentrations, $\overline{C}_t$ and $\overline{C}_b$, or

$$\overline{C}_t = \frac{C_{ot} + C_t}{2} \quad ; \quad \overline{C}_b = \frac{C_{ob} + C_b}{2} = \frac{C_b}{2} \tag{A.15}$$

where C_t and C_b represent the KCl concentration in the circulation outflow from the top piston and base pedestal, respectively. Diffusion in response to the applied concentration difference results in a decrease in KCl concentration in the top piston (i.e., $C_t < C_{ot}$) and an increase in KCl concentration in the base pedestal (i.e., $C_b > C_{ob}$). Unless the circulation rate is sufficiently rapid relative to the diffusive rate that changes in the boundary concentrations due to diffusion are negligible, the average boundary concentrations are more appropriate for calculating $\Delta\pi$ than the initial concentrations, C_{ot} and C_{ob}.

The results in Table 1 indicate that the "true" osmotic efficiencies based on the chemico-osmotic pressure expression for real solutions (Eq. A.13), ω_R, are slightly higher than osmotic efficiencies based on the van't Hoff expression of chemico-osmotic pressure for ideal, dilute solutions, ω_V (Eq. A.14). Therefore, use of the van't Hoff expression represents a slightly conservative approach for estimating osmotic efficiency of clay soils. However, the results in Fig. A.7 illustrate the error in ω caused by application of Eq. A.14 is relatively small (i.e., < 5%) for the range of source KCl concentrations used in the osmotic test (i.e., $C_{ot} \leq 0.047$ M).

A.5 CONCLUSIONS

Values of chemico-osmotic pressure, π, typically are computed using mathematical expressions derived from thermodynamics principles. The van't Hoff expression is a common and convenient expression for π of electrolyte solutions that is derived under the limiting assumptions that the solution is both ideal and dilute. These assumptions result in error when estimating π for real electrolyte solutions. For example, the van't Hoff expression overestimates π for the 1:1 electrolytes NaCl and KCl. The error for NaCl and KCl approaches 5 percent at a concentration of approximately 0.05 M. The error in π for NaCl increases to a maximum of 8.5 percent at a concentration of 0.4

M, while the maximum error in π for KCl is 11.2 percent at a concentration of 0.7 M. The different degrees of error for NaCl and KCl at these higher concentrations is due to the different osmotic coefficients of the two salts.

For the 1:2 electrolyte $CaCl_2$, a theoretical overestimation of π by 5 percent corresponds to a concentration of only 10^{-3} M. The overestimation of π for $CaCl_2$ increases to 17 percent at a concentration of 0.1 M, indicating that the van't Hoff equation is applicable over a wider concentration range for 1:1 electrolytes. The van't Hoff expression results in less than 5 percent error for $CaCl_2$ concentrations between 0.6 M and 0.9 M. Values of π are underestimated by the van't Hoff expression for $CaCl_2$ concentrations greater than 0.8 M, since the osmotic coefficient of $CaCl_2$ exceeds 1.0 in this region. However, the van't Hoff expression may not be appropriate for all 1:2 electrolytes from 0.6 to 0.9 M, since osmotic coefficients in this range typically are unique for a particular electrolyte.

The potential error caused by application of the van't Hoff expression to evaluate osmotic efficiency coefficients, ω, is illustrated based on the results of a six-stage osmotic test on a geosynthetic clay liner (GCL) subjected to KCl solutions. The results of this test indicate that slightly conservative (i.e., underestimated) values of ω are obtained when the van't Hoff expression is used to compute the chemico-osmotic pressure difference, $\Delta\pi$, across the soil. The error in ω based on the test results is less than 5 percent for applied differences in KCl concentration less than 0.045 M.

A.6 REFERENCES

Barbour, S. L., 1986. Osmotic flow and volume change in clay soils. *Ph.D. Dissertation*, University of Saskatchewan, Saskatoon, 255 p.

Barbour, S.L. and Fredlund, D.G., 1989. Mechanisms of Osmotic Flow and Volume Change in Clay Soils. *Canadian Geotechnical Journal*, Vol. 26, pp. 551-562.

Basu, S., and Sharma, M.M., 1997. An Improved Space-Charge Model for Flow Through Charged Microporous Membranes. *Journal of Membrane Science*, Vol. 124, pp. 71-91.

Bresler, E., 1973. Simultaneous Transport of Solutes and Water under Transient Unsaturated Flow Conditions. *Water Resources Research*, Vol. 9, No. 4, pp. 975-986.

CRC Press, 1999. *CRC Handbook of Chemistry and Physics, 80th Edition.* Section 4: Properties of the Elements and Inorganic Compounds, David R. Lide, Ed., CRC Press, Boca Raton, FL, pp. 4.35 - 4.98.

Conway, B.E., 1952. *Electrochemical Data.* Elsevier Publishing Co., Amsterdam, 374 pp.

Fritz, S.J., 1986. Ideality of Clay Membranes in Osmotic Processes: A Review. *Clays and Clay Minerals*, Vol. 34, No. 2, pp. 214-223.

Fritz, S.J., and Marine, I.W., 1983. Experimental Support for a Predictive Osmotic Model of Clay Membranes. *Geochimica et Cosmochimica Acta*, Vol. 47, pp. 1515-1522.

Katchalsky, A., and Curran, P.F., 1965. *Nonequilibrium Thermodynamics in Biophysics.* Harvard University Press, Cambridge, MA, 248 pp.

Kemper, W. D. and Quirk, J. P., 1972. Ion mobilities and electric charge of external clay surfaces inferred from potential differences and osmotic flow. *Soil Science Society of America Proc.*, Vol. 36, pp. 426-433.

Kemper, W.D. and Rollins, J.B., 1966. Osmotic Efficiency Coefficients Across Compacted Clays. *Soil Science Society of America Proceedings*, Vol. 30, pp. 529-534.

Malusis, M. A., Shackelford, C. D., and Olsen, H. W. (2001). "A laboratory apparatus to measure osmotic efficiency coefficients for clay soils." *Geotechnical Testing Journal*, ASTM, in press.

Mitchell, J.K., 1993. *Fundamentals of Soil Behavior*, 2nd Ed., John Wiley and Sons, New York, 437 pp.

Olsen, H.W., 1969. Simultaneous Fluxes of Liquid and Charge in Saturated Kaolinite. *Soil Science Society of America Proceedings*, Vol. 33, pp. 338-344.

Olsen, H.W., Yearsley, E.N., and Nelson, K.R., 1990. Chemico-Osmosis Versus Diffusion-Osmosis. *Transportation Research Record No. 1288*, Transportation Research Board, Washington D.C., pp. 15-22.

Robinson, R.A., and Stokes, R.H., 1959. *Electrolyte Solutions*, 2nd Ed., Butterworth Scientific Publications, London, England, 571 pp.

Rock, P.A., 1983. *Chemical Thermodynamics*. University Science Books, Mill Valley, CA, 351 pp.

Stumm, W. and Morgan, J.J., 1996. *Aquatic Chemistry*. John Wiley and Sons, Inc., New York, 1022 pp.

Tinoco, Jr., I., Sauer, K., and Wang, J.C., 1995. *Physical Chemistry*. Prentice-Hall, Upper Saddle River, NJ, 761 pp.

Yeung, A.T., 1990. Coupled Flow Equations for Water, Electricity and Ionic Contaminants through Clayey Soils under Hydraulic, Electrical, and Chemical Gradients. *Journal of Non-Equilibrium Thermodynamics*, Vol. 15, pp. 247-267.

Table A.1 - Results of six-stage osmotic test.(1)

Stage No.	C_{ot} (M)	$\overline{C}_t$ (M)	$\overline{C}_b$ (M)	ϕ_t	ϕ_b	$-\Delta\pi_R = -\nu RT\Delta(\phi m)$ (kPa)(2)	$-\Delta\pi_V = -\nu RT\Delta C$ (kPa)	$-\Delta P_e$ (kPa)	$\omega_R = \Delta P_e/\Delta\pi_R$	$\omega_V = \Delta P_e/\Delta\pi_V$
1	0	---	---	---	---	---	---	---	---	---
2	0.0039	0.0039	4.5×10^{-5}	0.984	1.000	18.8	18.9	13.1	0.697	0.693
3	0.0060	0.0059	1.2×10^{-4}	0.980	1.000	28.1	28.4	16.6	0.592	0.584
4	0.0087	0.0085	1.8×10^{-4}	0.977	1.000	40.3	41.1	21.8	0.542	0.530
5	0.020	0.019	5.0×10^{-4}	0.966	0.999	88.5	91.2	29.6	0.335	0.325
6	0.047	0.045	0.0024	0.952	0.989	201	211	33.1	0.165	0.157

(1) C_{ot} = source KCl concentration; $\overline{C}_t$ and $\overline{C}_b$ = average boundary KCl concentrations; ϕ = osmotic coefficient; $-\Delta\pi$ = chemico-osmotic pressure difference; $-\Delta P_e$ = effective differential pressure; ω = osmotic efficiency coefficient.

(2) $m \approx C$ for $C \leq 0.045$ M.

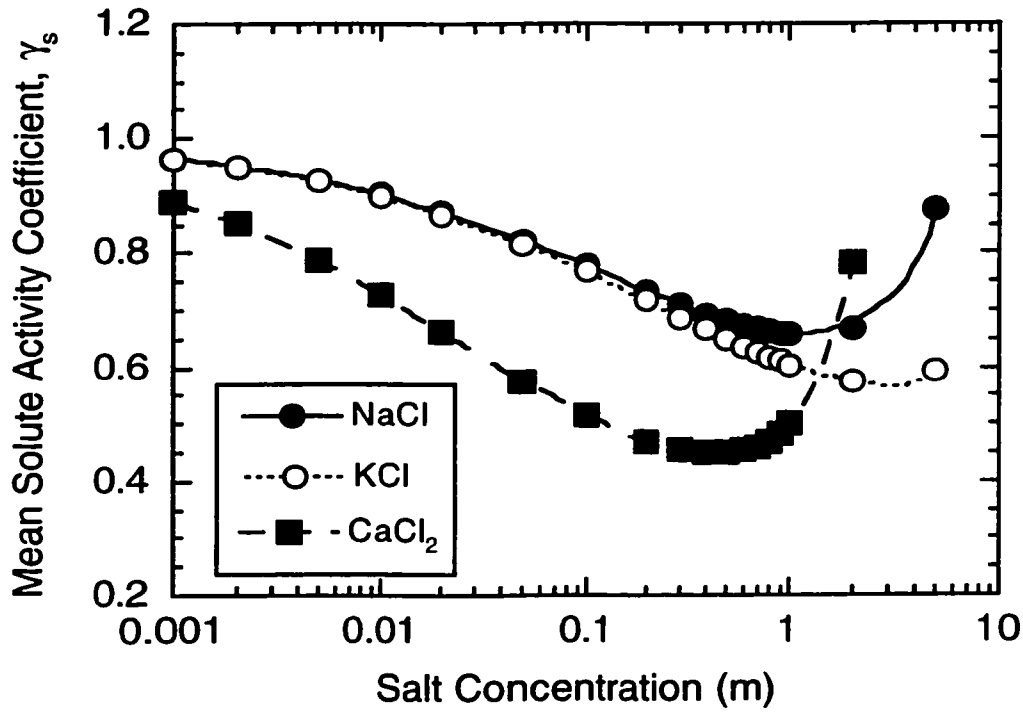

Fig. A.1 - Mean activity coefficients for NaCl, KCl, and $CaCl_2$ (data from CRC Press 1999).

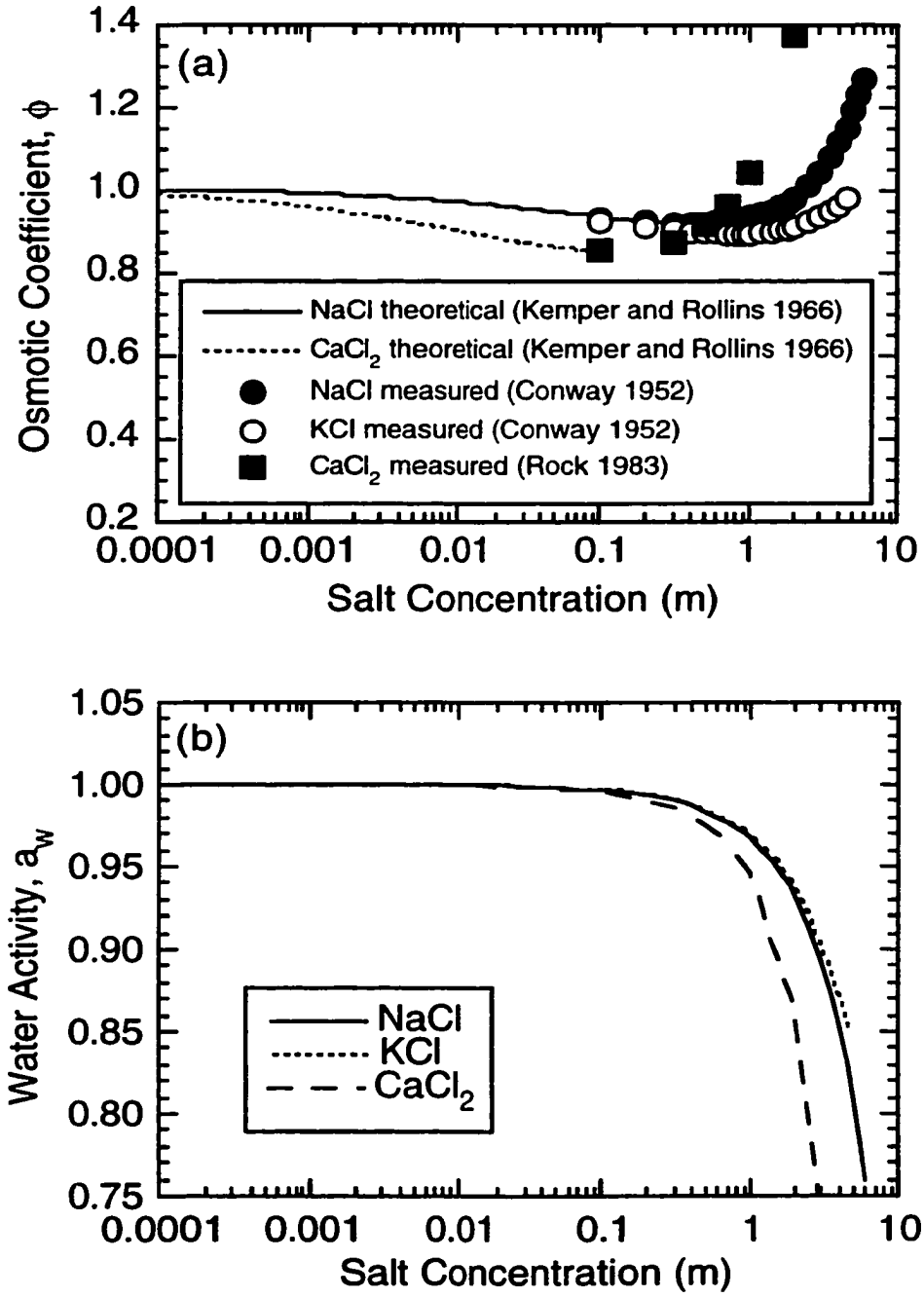

Fig. A.2 - (a) Osmotic coefficients and (b) water activities versus salt concentration for common electrolytes NaCl, KCl, and $CaCl_2$.

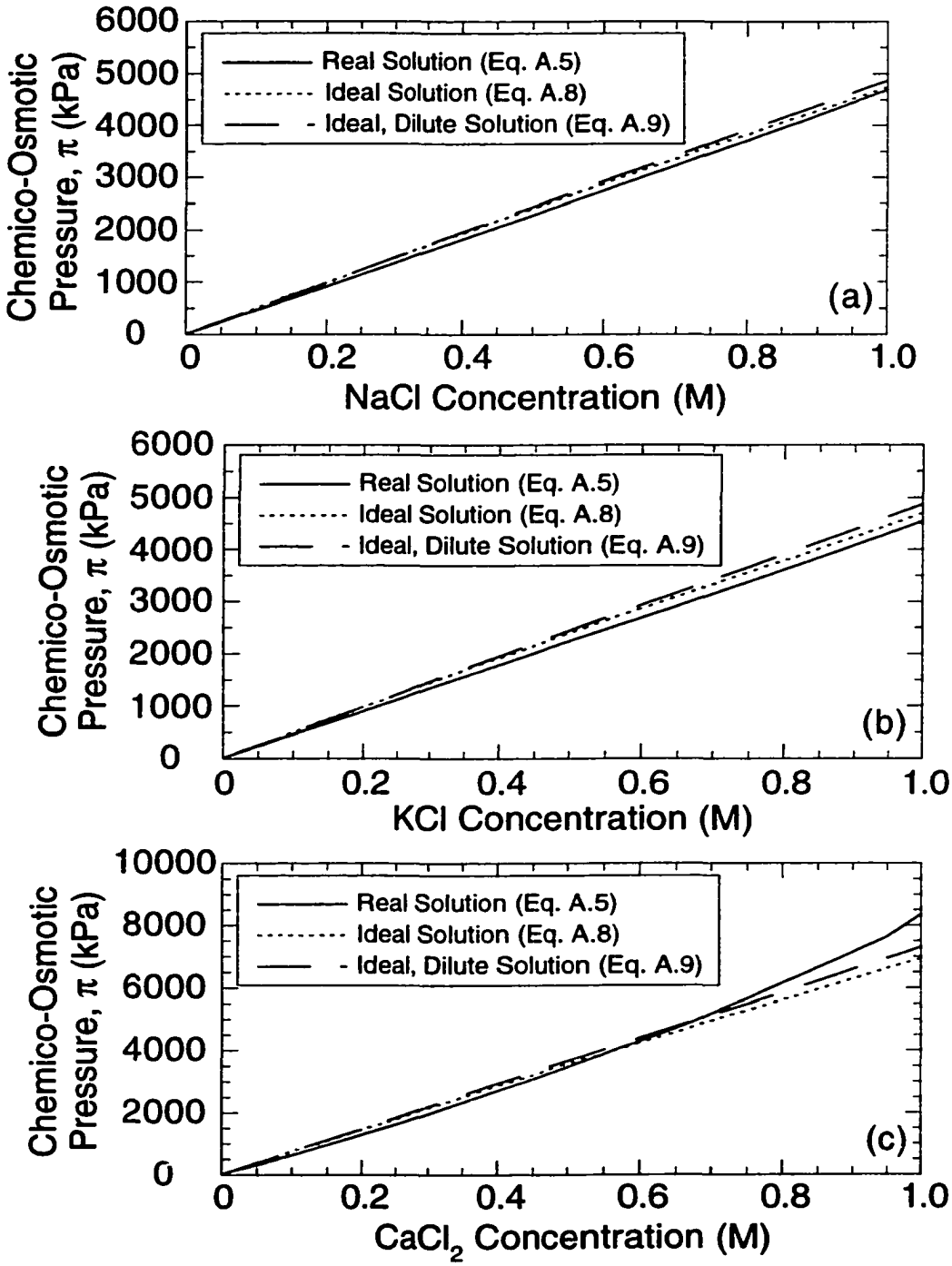

Fig. A.3 - Theoretical π values for real, ideal, and ideal, dilute solutions versus salt concentration: (a) NaCl; (b) KCl; (c) $CaCl_2$.

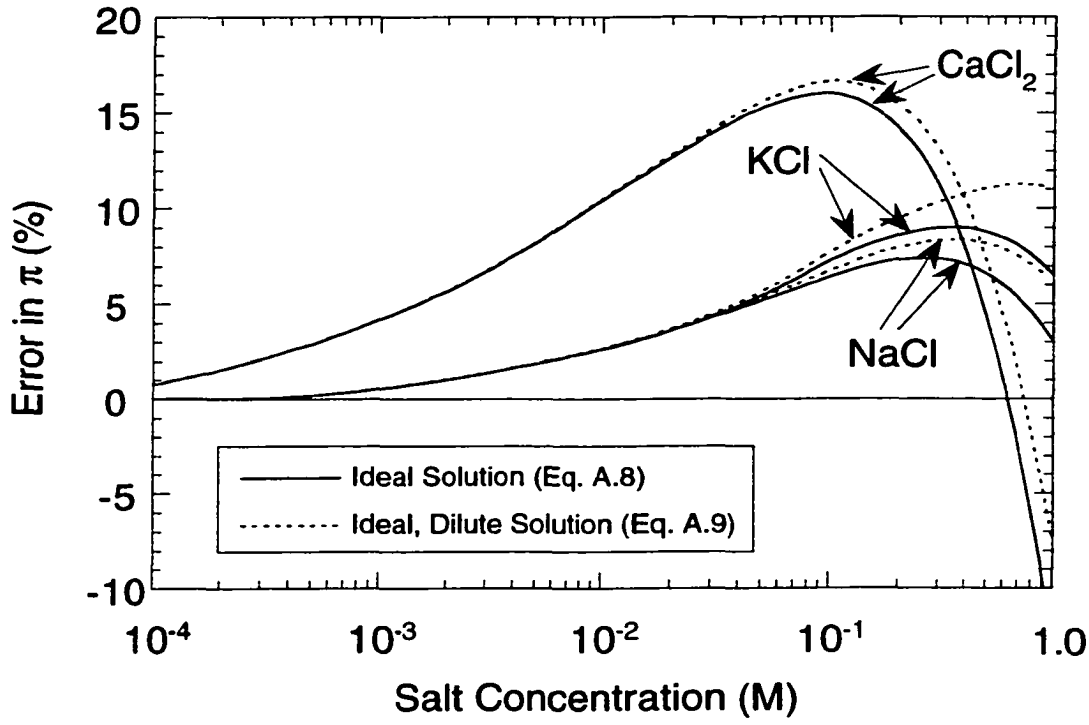

Fig. A.4 - Theoretical error in π for ideal solutions and ideal, dilute solutions of NaCl, KCl, and $CaCl_2$.

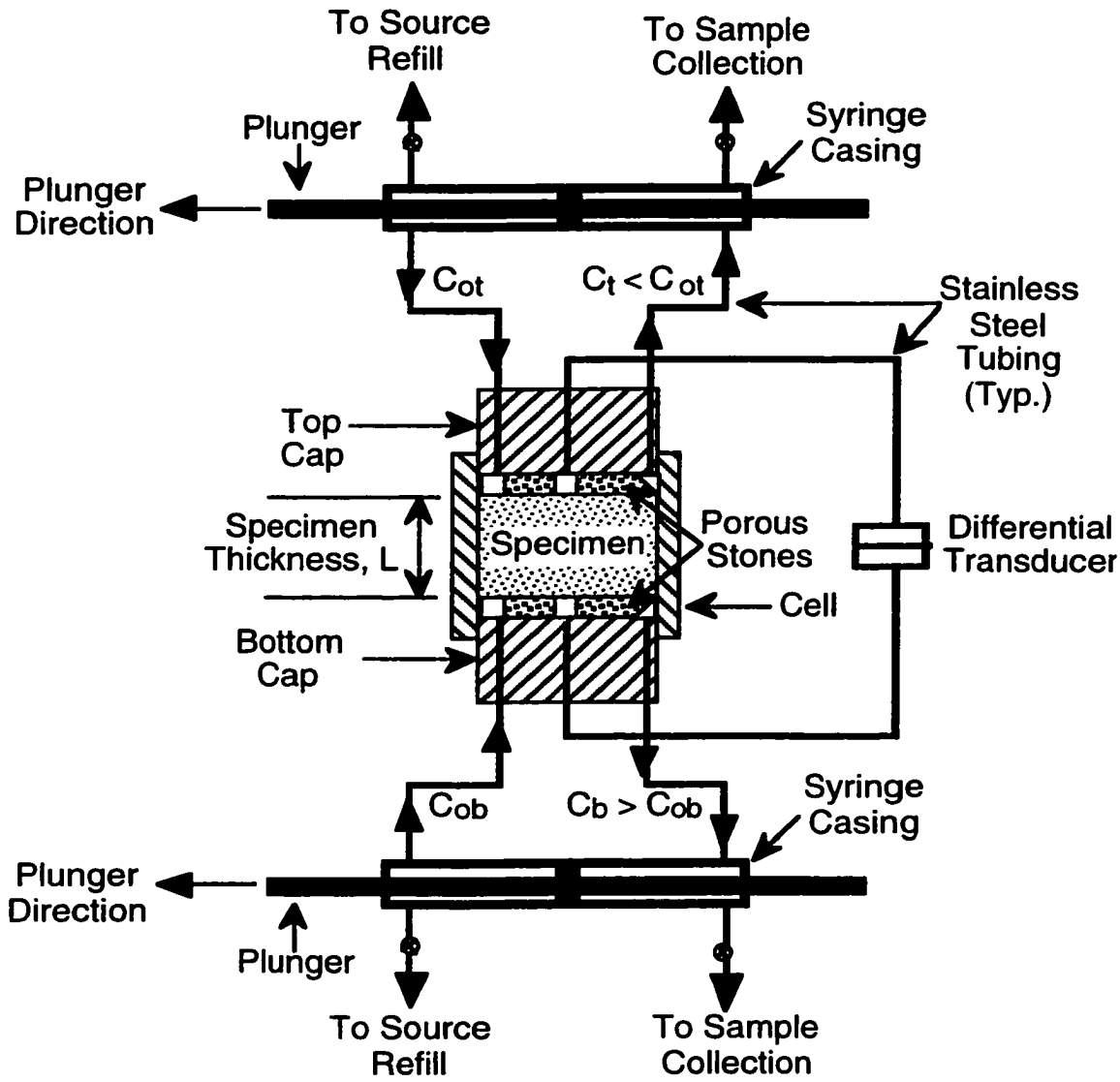

Fig. A.5 - Schematic of osmotic testing apparatus.

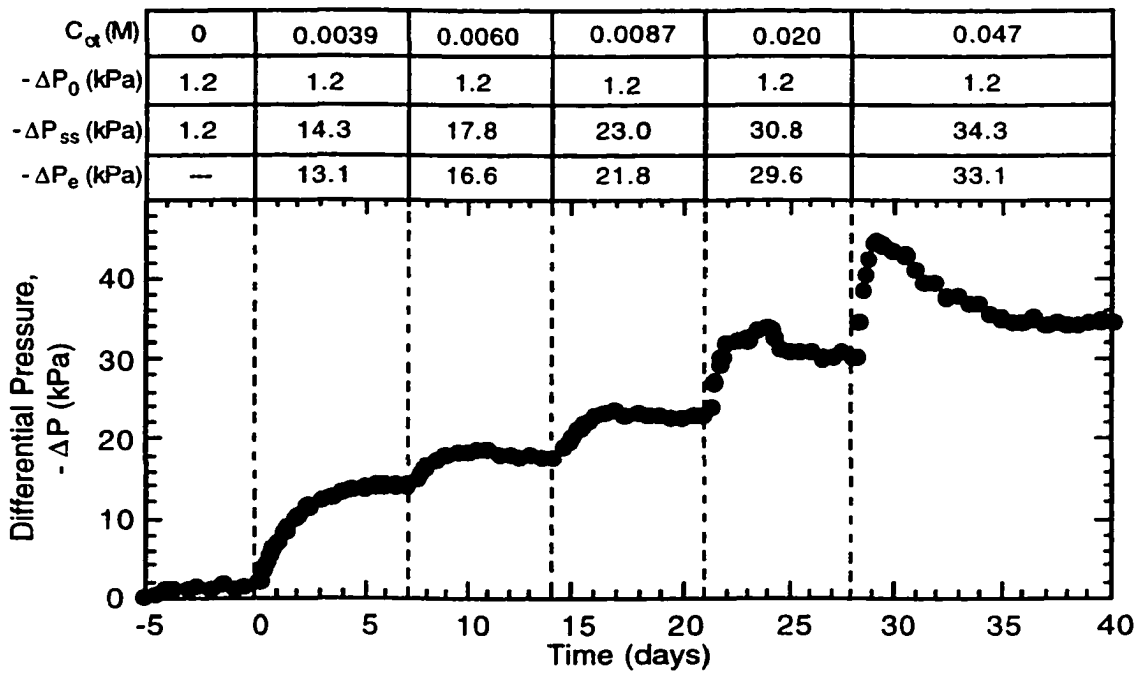

Fig. A.6 - Induced differential pressures measured across a 1.0-cm thick GCL subjected to KCl solutions.

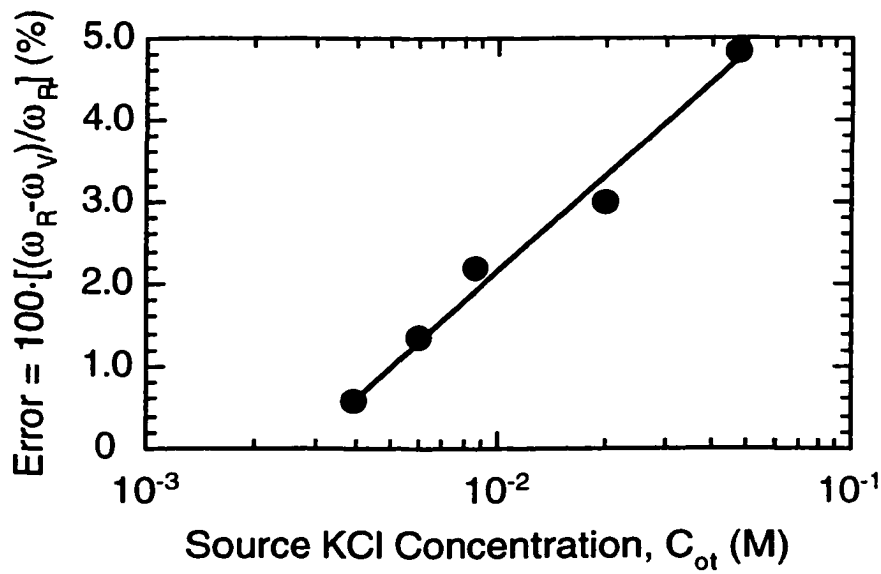

Fig. A.7 - Error in osmotic efficiency coefficients (ω) for 10-mm thick GCL.

APPENDIX B

DEVELOPMENT OF EXPRESSION FOR SALT-DIFFUSION COEFFICIENT OF IONS IN MIXED ELECTROLYTES

APPENDIX B

DEVELOPMENT OF EXPRESSION FOR SALT-DIFFUSION COEFFICIENT OF IONS IN MIXED ELECTROLYTES

6.1 Theoretical Development

Vinograd and McBain (1941) studied the diffusion of ions in free solutions containing mixed electrolytes. For the case in which the ions diffuse in the same direction (i.e., salt diffusion), Vinograd and McBain (1941) developed the following expression for the "practical" salt-diffusion coefficient of any cation in a mixture of ions:

$$D_{s+}\nabla N_+ = \frac{\lambda_+ \overline{R}T}{|z_+|}\left[\nabla N_+ + N_+|z_+|\left(\frac{\sum\lambda_-\frac{\nabla N_-}{|z_-|} - \sum\lambda_+\frac{\nabla N_+}{|z_+|}}{\sum\lambda_- N_- + \sum\lambda_+ N_+}\right)\right] \qquad \text{(B.1)}$$

where D_{s+} is the salt-diffusion coefficient of the cation of interest [L^2t^{-1}], N is solute concentration in normality, λ is equivalent conductance, $\overline{R}$ is a modified gas constant, T is absolute temperature, z is ion valence, and subscripts + and - represent cations and anions, respectively. The summation terms in Eq. B.1 account for all cationic and anionic species in the electrolyte mixture. Similarly, the salt-diffusion coefficient for an anion, D_{s-}, in a mixture of ions is as follows:

$$D_{s-}\nabla N_{-} = \frac{\lambda_{-}\overline{R}T}{|z_{-}|}\left[\nabla N_{-} - N_{-}|z_{-}|\left(\frac{\sum\lambda_{-}\frac{\nabla N_{-}}{|z_{-}|} - \sum\lambda_{+}\frac{\nabla N_{+}}{|z_{+}|}}{\sum\lambda_{-}N_{-} + \sum\lambda_{+}N_{+}}\right)\right] \qquad (B.2)$$

Based on Eqs. B.1 and B.2, we may write a general expression for the salt-diffusion coefficient of any ionic species j as follows:

$$D_{sj}\nabla N_{j} = \frac{\lambda_{j}\overline{R}T}{|z_{j}|}\left[\nabla N_{j} \pm N_{j}|z_{j}|\left(\frac{\sum\lambda_{-}\frac{\nabla N_{-}}{|z_{-}|} - \sum\lambda_{+}\frac{\nabla N_{+}}{|z_{+}|}}{\sum\lambda_{-}N_{-} + \sum\lambda_{+}N_{+}}\right)\right] \qquad (B.3)$$

where the "±" term is positive if species j is a cation and negative if species j is an anion.

The modified gas constant in Eq. B.3 is related to the universal gas constant, R, as follows:

$$\overline{R} = \frac{R}{\mathcal{F}^{2}} \qquad (B.4)$$

where $\mathcal{F}$ is Faraday's constant [96,500 coulombs]. Also, solute normality can be expressed in terms of molar concentration, C, based on the following expression:

$$N_{j} = |z_{j}|C_{j} \qquad (B.5)$$

Substitution of Eqs. B.4 and B.5 into Eq. B.3 yields

$$D_{sj}\nabla C_{j} = \frac{\lambda_{j}RT}{|z_{j}|\mathcal{F}^{2}}\left[\nabla C_{j} \pm C_{j}|z_{j}|\left(\frac{\sum\lambda_{-}\nabla C_{-} - \sum\lambda_{+}\nabla C_{+}}{\sum\lambda_{-}|z_{-}|C_{-} + \sum\lambda_{+}|z_{+}|C_{+}}\right)\right] \qquad (B.6)$$

Equivalent conductance, λ, is related to ionic mobility, u, as follows (Katchalsky and Curran 1965):

$$\lambda = Fu \tag{B.7}$$

Substitution of Eq. B.7 into Eq. B.6 and rearrangement yields

$$D_{sj}\nabla C_j = \frac{u_j RT}{|z_j|F}\nabla C_j \pm \frac{u_j RTC_j}{F}\left(\frac{\sum u_-\nabla C_- - \sum u_+\nabla C_+}{\sum u_+|z_+|C_+ + \sum u_-|z_-|C_-}\right) \tag{B.8}$$

Furthermore, the relationship between the self-diffusion coefficient for any species j, D_j, and its ionic mobility, u_j, is given by the Nernst equation (Shackelford and Daniel 1991), or

$$D_j = \frac{u_j RT}{F|z_j|} \tag{B.9}$$

Substitution of Eq. B.9 into Eq. B.8 yields the following expression for the "practical" salt-diffusion coefficient, D_{sj}:

$$D_{sj}\nabla C_j = D_j\nabla C_j \pm D_j|z_j|C_j\left(\frac{\sum D_-|z_-|\nabla C_- - \sum D_+|z_+|\nabla C_+}{\sum D_-|z_-|^2 C_- + \sum D_+|z_+|^2 C_+}\right) \tag{B.10}$$

or, for one-dimensional diffusion,

$$D_{sj}\frac{dC_j}{dx} = D_j\frac{dC_j}{dx} \pm D_j|z_j|C_j\left(\frac{\sum D_-|z_-|\frac{dC_-}{dx} - \sum D_+|z_+|\frac{dC_+}{dx}}{\sum D_-|z_-|^2 C_- + \sum D_+|z_+|^2 C_+}\right) \tag{B.11}$$

Consider the case of one-dimensional diffusion of the single cation and single anion of a strong (i.e., fully dissociating) binary electrolyte (e.g., NaCl, KCl). Based on Eq. B.11, we can write the following expressions for the cation (+) and the anion (-):

$$D_{s+}\frac{dC_+}{dx} = D_+\frac{dC_+}{dx} + D_+|z_+|C_+\left(\frac{D_-|z_-|\frac{dC_-}{dx} - D_+|z_+|\frac{dC_+}{dx}}{D_-|z_-|^2C_- + D_+|z_+|^2C_+}\right) \tag{B.12a}$$

$$D_{s-}\frac{dC_-}{dx} = D_-\frac{dC_-}{dx} - D_-|z_-|C_-\left(\frac{D_-|z_-|\frac{dC_-}{dx} - D_+|z_+|\frac{dC_+}{dx}}{D_-|z_-|^2C_- + D_+|z_+|^2C_+}\right) \tag{B.12b}$$

Based on the requirement for electroneutrality in solution, the molar concentration of the cation, C_+, is related to the molar concentration of the anion, C_-, at any given location as follows:

$$|z_+|C_+ = |z_-|C_- \tag{B.13}$$

or, in differential form,

$$|z_+|\frac{dC_+}{dx} = |z_-|\frac{dC_-}{dx} \tag{B.14}$$

Substitution of Eqs. B.13 and B.14 into Eqs. B.12a and B.12b yields the following expressions:

$$D_{s+} = D_+ + \frac{|z_+|D_+(D_- - D_+)}{D_-|z_-| + D_+|z_+|} \tag{B.15a}$$

$$D_{s-} = D_- - \frac{|z_-|D_-(D_- - D_+)}{D_-|z_-| + D_+|z_+|} \quad \text{(B.15b)}$$

or, upon rearrangement,

$$D_{s+} = \frac{D_+D_-(|z_-| + |z_+|)}{D_-|z_-| + D_+|z_+|} \quad \text{(B.16a)}$$

$$D_{s-} = \frac{D_+D_-(|z_-| + |z_+|)}{D_-|z_-| + D_+|z_+|} \quad \text{(B.16b)}$$

Inspection of Eqs. B.16a and B.16b reveals that $D_{s+} = D_{s-} = D_s$, which is consistent with the requirement that the rate of diffusion of the cation and anion in an aqueous single-salt system must be the same to satisfy electroneutrality (e.g., Robinson and Stokes 1959). Therefore, the value of D_s represents an intermediate value between the self-diffusion coefficients, D_- and D_+, for the anion and cation, respectively (e.g., Shackelford and Daniel 1991). Equations B.16a and B.16b are known traditionally as the Nernst-Einstein equation (Shackelford 1989).

B.2 REFERENCES

Katchalsky, A., and Curran, P.F., 1965. *Nonequilibrium Thermodynamics in Biophysics*. Harvard University Press, Cambridge, MA, 248 pp.

Robinson, R.A., and Stokes, R.H., 1959. *Electrolyte Solutions*, 2nd Ed., Butterworth Scientific Publications, London, England, 571 pp.

Shackelford, C.D., 1989. Diffusion of Contaminants Through Waste Containment Barriers. *Transportation Research Record No. 1219,* Transportation Research Board, National Research Council, Washington D.C., pp. 169-182.

Shackelford, C.D. and Daniel, D.E., 1991. Diffusion in Saturated Soil. I. Background. *Journal of Geotechnical Engineering*, ASCE, Vol. 117, No. 3, pp. 467-484.

Vinograd, J.R., and McBain, J.W., 1941. Diffusion of Electrolytes and of the Ions in Their Mixtures. *Journal of the American Chemical Society*, Vol. 63, pp. 2008-2015.

APPENDIX C

DEVELOPMENT OF FINITE DIFFERENCE MODEL FOR COUPLED SOLUTE TRANSPORT THROUGH A SOIL MEMBRANE

APPENDIX C

DEVELOPMENT OF FINITE DIFFERENCE MODEL FOR COUPLED SOLUTE TRANSPORT THROUGH A SOIL MEMBRANE

The equation for one-dimensional coupled transport of a solute, j, through a soil membrane in the absence of an electrical current and under isothermal conditions is given in Chapter 5 as follows:

$$R_{dj}\frac{\partial C_j}{\partial t} = (\omega - 1)v_h\frac{\partial C_j}{\partial x} - v_\pi\frac{\partial C_j}{\partial x} - C_j\frac{\partial v_\pi}{\partial x} + D^*_{sj}\frac{\partial^2 C_j}{\partial x^2} + \frac{\partial D^*_{sj}}{\partial x}\frac{\partial C_j}{\partial x} \qquad (C.1)$$

where R_d is the retardation factor, C is molar concentration, ω is the chemico-osmotic efficiency coefficient, v_h is the hydraulic seepage velocity, v_π is the chemico-osmotic seepage velocity, D^*_{sj} is the effective salt-diffusion coefficient, and x is the distance of transport. The chemico-osmotic seepage velocity, v_π, is given as follows:

$$v_\pi = \frac{\omega k_h}{n\gamma_w} RT \sum_{i=1}^{N} \frac{\partial C_i}{\partial x} \qquad (C.2)$$

where k_h is hydraulic conductivity, n is porosity, R is the universal gas constant (= 8.134 J/mol K), T is the absolute temperature, and N is the number of different solute species in the pore solution. Based on Eq. 5.32b, the effective salt-diffusion coefficient of species j is given as follows if j is a cation:

$$D_{sj}^{*} = \tau_a \left[D_j - \frac{D_j C_j |z_j|}{\partial C_j} \frac{\sum_{i=1}^{N} \left(\pm D_i |z_i| \partial C_i \right)}{\sum_{i=1}^{N} \left(D_i |z_i|^2 C_i \right)} \right] \tag{C.3}$$

or, if species j is an anion,

$$D_{sj}^{*} = \tau_a \left[D_j + \frac{D_j C_j |z_j|}{\partial C_j} \frac{\sum_{i=1}^{N} \left(\pm D_i |z_i| \partial C_i \right)}{\sum_{i=1}^{N} \left(D_i |z_i|^2 C_i \right)} \right] \tag{C.4}$$

where τ_a is the apparent tortuosity factor, D_j is the free-solution self-diffusion coefficient of species j, D_i is the free-solution self-diffusion coefficient of species i, z_j is the valence of species j, and j is a subset of i.

Consider the migration of a salt cation (c) and a salt anion (a) through a soil membrane. If we assume that the salt anion is conservative (i.e., $R_{da} = 1$) and the salt cation is reactive (i.e., $R_{dc} > 1$), then the salt cation may be replaced in solution by an exchangeable cation (x). Thus, N = 3 and we can write separate transport equations for the salt anion and salt cation as follows, in accordance with Eq. C.1:

$$\frac{\partial C_a}{\partial t} = (\omega - 1) v_h \frac{\partial C_a}{\partial x} - v_\pi \frac{\partial C_a}{\partial x} - C_a \frac{\partial v_\pi}{\partial x} + D_{sa}^{*} \frac{\partial^2 C_a}{\partial x^2} + \frac{\partial D_{sa}^{*}}{\partial x} \frac{\partial C_a}{\partial x} \tag{C.5a}$$

$$R_{dc} \frac{\partial C_c}{\partial t} = (\omega - 1) v_h \frac{\partial C_c}{\partial x} - v_\pi \frac{\partial C_c}{\partial x} - C_c \frac{\partial v_\pi}{\partial x} + D_{sc}^{*} \frac{\partial^2 C_c}{\partial x^2} + \frac{\partial D_{sc}^{*}}{\partial x} \frac{\partial C_c}{\partial x} \tag{C.5b}$$

where the subscripts c, a, and x represent the salt cation, salt anion, and exchangeable cation, respectively. The chemico-osmotic seepage velocity is written as follows based on Eq. C.2:

$$v_\pi = \frac{\omega k_h}{n\gamma_w} RT\left(\frac{\partial C_c}{\partial x} + \frac{\partial C_a}{\partial x} + \frac{\partial C_x}{\partial x}\right) \tag{C.6}$$

In addition, the effective salt-diffusion coefficient for the salt cation, D^*_{sc}, can be written as follows based on Eq. C.3:

$$D^*_{sc} = \tau_a\left[D_c + \frac{D_c C_c |z_c|}{\partial C_c}\left(\frac{D_a|z_a|\partial C_a - D_c|z_c|\partial C_c - D_x|z_x|\partial C_x}{D_a|z_a|^2 C_a + D_c|z_c|^2 C_c + D_x|z_x|^2 C_x}\right)\right] \tag{C.7}$$

and the effective salt-diffusion coefficient for the salt anion, D^*_{sa}, can be written as follows based on Eq. C.4:

$$D^*_{sa} = \tau_a\left[D_a - \frac{D_a C_a |z_a|}{\partial C_a}\left(\frac{D_a|z_a|\partial C_a - D_c|z_c|\partial C_c - D_x|z_x|\partial C_x}{D_a|z_a|^2 C_a + D_c|z_c|^2 C_c + D_x|z_x|^2 C_x}\right)\right] \tag{C.8}$$

Finally, the exchangeable cation concentration, C_x, is related to the concentrations of the salt cation (C_c) and salt anion (C_a) in accordance with the following requirement for electroneutrality in solution:

$$C_x = \frac{C_a|z_a| - C_c|z_c|}{|z_x|} \tag{C.9}$$

Equations C.5 through C.9 were solved numerically using an iterative implicit-in-time, centered-in-space finite difference algorithm. The soil membrane of thickness L was divided into N cells (i.e., k = 1...N) of thickness Δx, and the transport time was divided into NT time intervals (i.e., T = 1...NT) of duration Δt. The solute concentrations

(C_c, C_a, and C_x) were solved in each cell corresponding to an elapsed time, $t = T\Delta t$. The implicit-in-time approximation for the first derivative of variable X in cell k is given by

$$\frac{\partial X}{\partial t} \approx \frac{X_k^t - X_k^{t-\Delta t}}{\Delta t} \tag{C.10}$$

and the centered-in-space approximations for the first and second derivatives of X are given by

$$\frac{\partial X}{\partial x} \approx \frac{X_{k+1}^t - X_{k-1}^t}{2\Delta x} \quad ; \quad \frac{\partial^2 X}{\partial x^2} \approx \frac{X_{k+1}^t - 2X_k^t + X_{k-1}^t}{(\Delta x)^2} \tag{C.11}$$

Thus, Eqs. C.5a and C.5b can be written as follows:

$$\begin{aligned}\frac{C_{a,k}^t - C_{a,k}^{t-\Delta t}}{\Delta t} = {} & (\omega - 1)v_h \frac{C_{a,k+1}^t - C_{a,k-1}^t}{2\Delta x} - v_\pi \frac{C_{a,k+1}^t - C_{a,k-1}^t}{2\Delta x} \\ & - \alpha C_{a,k}^t + D_{sa}^* \frac{C_{a,k+1}^t - 2C_{a,k}^t + C_{a,k-1}^t}{(\Delta x)^2} + \beta_a \frac{C_{a,k+1}^t - C_{a,k-1}^t}{2\Delta x}\end{aligned} \tag{C.12a}$$

$$\begin{aligned}\frac{C_{c,k}^t - C_{c,k}^{t-\Delta t}}{\Delta t} = {} & (\omega - 1)v_h \frac{C_{c,k+1}^t - C_{c,k-1}^t}{2\Delta x} - v_\pi \frac{C_{c,k+1}^t - C_{c,k-1}^t}{2\Delta x} \\ & - \alpha C_{c,k}^t + D_{sc}^* \frac{C_{c,k+1}^t - 2C_{c,k}^t + C_{c,k-1}^t}{(\Delta x)^2} + \beta_c \frac{C_{c,k+1}^t - C_{c,k-1}^t}{2\Delta x}\end{aligned} \tag{C.12b}$$

and Eq. C.6 becomes

$$v_\pi = \frac{\omega k_h}{2n\gamma_w \Delta x} RT\left[(C_a + C_c + C_x)_{k+1}^t - (C_a + C_c + C_x)_{k-1}^t\right] \tag{C.13}$$

where

$$\alpha = \frac{\partial v_\pi}{\partial x} = \frac{\omega k_h}{n\gamma_w (\Delta x)^2} RT \left[\begin{array}{l} (C_a + C_c + C_x)^t_{k+1} \\ \quad - 2(C_a + C_c + C_x)^t_k + (C_a + C_c + C_x)^t_{k-1} \end{array} \right] \tag{C.14}$$

Also, coefficients β_a and β_b are

$$\beta_a = \frac{\partial D^*_{sa}}{\partial x} = \frac{D^{*t}_{sa,k+1} - D^{*t}_{sa,k-1}}{\Delta x} \; ; \; \beta_c = \frac{\partial D^*_{sc}}{\partial x} = \frac{D^{*t}_{sc,k+1} - D^{*t}_{sc,k-1}}{\Delta x} \tag{C.15}$$

where D^*_{sc} and D^*_{sa} are as follows based on Eqs. C.7 and C.8:

$$D^{*t}_{sc,k} = \tau_a D_c + \tau_a \frac{D_c C^t_{c,k} |z_c|}{C^t_{c,k+1} - C^t_{c,k-1}} \cdot \left[\frac{D_a |z_a| \left(C^t_{a,k+1} - C^t_{a,k-1}\right) - D_c |z_c| \left(C^t_{c,k+1} - C^t_{c,k-1}\right) - D_x |z_x| \left(C^t_{x,k+1} - C^t_{x,k-1}\right)}{D_a |z_a|^2 C^t_{a,k} + D_c |z_c|^2 C^t_{c,k} + D_x |z_x|^2 C^t_{x,k}} \right] \tag{C.16}$$

$$D^{*t}_{sa,k} = \tau_a D_a - \tau_a \frac{D_a C^t_{a,k} |z_a|}{C^t_{a,k+1} - C^t_{a,k-1}} \cdot \left[\frac{D_a |z_a| \left(C^t_{a,k+1} - C^t_{a,k-1}\right) - D_c |z_c| \left(C^t_{c,k+1} - C^t_{c,k-1}\right) - D_x |z_x| \left(C^t_{x,k+1} - C^t_{x,k-1}\right)}{D_a |z_a|^2 C^t_{a,k} + D_c |z_c|^2 C^t_{c,k} + D_x |z_x|^2 C^t_{x,k}} \right] \tag{C.17}$$

Rearrangement of Eqs. C.12a-b yields the following expressions:

$$C^{t-\Delta t}_{a,k} = [W_a] C^t_{a,k-1} + [X_a] C^t_{a,k} + [Y_a] C^t_{a,k+1} \tag{C.18a}$$

$$R_{dc} C^{t-\Delta t}_{c,k} = [W_c] C^t_{c,k-1} + [X_c] C^t_{c,k} + [Y_c] C^t_{c,k+1} \tag{C.18b}$$

where W, X, and Y are defined as follows:

$$[W_a] = \left[-\frac{(\omega-1)v_h\Delta t}{2\Delta x} + \frac{v_\pi \Delta t}{2\Delta x} + \frac{(D^*_{sa} - v_h^2\Delta t/2)\Delta t}{(\Delta x)^2} - \frac{\beta_a \Delta t}{2\Delta x} \right] \quad \text{(C.19a)}$$

$$[W_c] = \left[-\frac{(\omega-1)v_h\Delta t}{2\Delta x} + \frac{v_\pi \Delta t}{2\Delta x} + \frac{(D^*_{sc} - v_h^2\Delta t/2)\Delta t}{(\Delta x)^2} - \frac{\beta_c \Delta t}{2\Delta x} \right] \quad \text{(C.19b)}$$

$$[X_a] = \left[1 + \alpha\Delta t + \frac{2(D^*_{sa} - v_h^2\Delta t/2)\Delta t}{(\Delta x)^2} \right] \quad \text{(C.20a)}$$

$$[X_c] = \left[R_{dc} + \alpha\Delta t + \frac{2(D^*_{sc} - v_h^2\Delta t/2)\Delta t}{(\Delta x)^2} \right] \quad \text{(C.20b)}$$

$$[Y_a] = \left[\frac{(\omega-1)v_h\Delta t}{2\Delta x} - \frac{v_\pi \Delta t}{2\Delta x} + \frac{(D^*_{sa} - v_h^2\Delta t/2)\Delta t}{(\Delta x)^2} + \frac{\beta_a \Delta t}{2\Delta x} \right] \quad \text{(C.21a)}$$

$$[Y_c] = \left[\frac{(\omega-1)v_h\Delta t}{2\Delta x} - \frac{v_\pi \Delta t}{2\Delta x} + \frac{(D^*_{sc} - v_h^2\Delta t/2)\Delta t}{(\Delta x)^2} + \frac{\beta_c \Delta t}{2\Delta x} \right] \quad \text{(C.21b)}$$

The effective salt-diffusion coefficients in Eqs. C.19-21 are reduced by a factor ($-v_h\Delta t/2$) to account for numerical dispersion associated with the implicit-in-time approach.

Equations C.18a-b also can be written in expanded form as follows:

$$\begin{bmatrix} X_{a,1} & Y_{a,1} & 0 & 0 & 0 \\ W_{a,2} & X_{a,2} & Y_{a,2} & 0 & 0 \\ 0 & . & . & . & 0 \\ 0 & 0 & . & . & . \\ 0 & 0 & 0 & W_{a,N} & X_{a,N} \end{bmatrix} \begin{bmatrix} C^t_{a,1} \\ C^t_{a,2} \\ . \\ . \\ C^t_{a,N} \end{bmatrix} = \begin{bmatrix} C^{t-\Delta t}_{a,1} - W_{a,1}C_{ao} \\ C^{t-\Delta t}_{a,2} \\ . \\ . \\ C^{t-\Delta t}_{a,N} - Y_{a,N}C_{ae} \end{bmatrix} \quad \text{(C.22a)}$$

and

$$\begin{bmatrix} X_{c,1} & Y_{c,1} & 0 & 0 & 0 \\ W_{c,2} & X_{c,2} & Y_{c,2} & 0 & 0 \\ 0 & . & . & . & 0 \\ 0 & 0 & . & . & . \\ 0 & 0 & 0 & W_{c,N} & X_{c,N} \end{bmatrix} \begin{bmatrix} C'_{c,1} \\ C'_{c,2} \\ . \\ . \\ C'_{c,N} \end{bmatrix} = \begin{bmatrix} C_{c,1}^{t-\Delta t} - W_{c,1}C_{co} \\ C_{c,2}^{t-\Delta t} \\ . \\ . \\ C_{c,N}^{t-\Delta t} - Y_{c,N}C_{ce} \end{bmatrix} \qquad \text{(C.22b)}$$

The concentrations C_{ao} and C_{co} are the source concentrations (i.e., at x = 0) of the salt anion and salt cation, respectively, whereas C_{ae} and C_{ce} are the exit boundary concentrations (i.e., at x = L) of the salt cation and salt anion, respectively.

Solution of Eqs. C.22a and C.22b to obtain concentrations C_a and C_c in each cell is performed by inverting the tridiagonal matrices (see attached FORTRAN program). In the first iteration at each time step, Eqs. C.22a and C.22b are solved assuming that $C_x = v_\pi = \alpha = \beta_c = \beta_a = 0$ in all cells to obtain initial values of of C_a and C_c. The exchangeable cation concentrations, C_x, then are computed in accordance with the electroneutrality constraint given by Eq. C.9, or

$$C'_{x,k} = \frac{C'_{a,k}|z_a| - C'_{c,k}|z_c|}{|z_x|} \qquad \text{(C.23)}$$

Values of C_c, C_a, and C_x obtained in the initial iteration are used to compute new values of the tridiagonal matrix coefficients (i.e., the W, X, and Y values in Eqs. C.22a and C.22b) in accordance with Eqs. C.13 – C.17. Equations C.22a, C.22b, and C.23 then are re-solved based on the updated matrix coefficients to obtain new values of C_c, C_a, and C_x. The process is repeated until convergence is achieved such that the differences between the new values of C_c, C_a, and C_x and the C_c, C_a, and C_x values from the previous iteration are within a specified tolerance, TOL (typically, TOL = 0.001 in this study). Once convergence is achieved for salt anion and cation concentrations for successive time

intervals, values of coupled solute flux for the salt cation and salt anion in any cell, k, at time t can be computed in accordance with

$$J^t_{a,k} = n(1-\omega)v_h C^t_{a,k} - nv^t_{\pi,k} C^t_{a,k} - nD^{*t}_{sa,k}\left(\frac{C^t_{a,k+1} - C^t_{a,k+1}}{2\Delta x}\right) \qquad \text{(C.24)}$$

$$J^t_{c,k} = n(1-\omega)v_h C^t_{c,k} - nv^t_{\pi,k} C^t_{c,k} - nD^{*t}_{sc,k}\left(\frac{C^t_{c,k+1} - C^t_{c,k+1}}{2\Delta x}\right) \qquad \text{(C.25)}$$

All details regarding this algorithm are contained in the FORTRAN program and example input data file provided below. Output from model simulations is contained in Appendices D and G.

```
PROGRAM coupled
c*************************************************************************
c    This program solves coupled solute transport through a clay barrier
c    with perfectly flushing exit boundary condition.
c*************************************************************************
c         Variable definitions
c*************************************************************************
c         NC = Max allowable Number of cells
c         T = Max allowable Number of time steps
c         k,j,l,i,m = looping indices
c         nt = Number of time steps
c         n = Number of cells
c         W(i) = RHS of matrix
c         delx = cell size (m)
c         delt = Time step size (s)
c         dl = Free-solution salt-diffusion Coeff.(m^2/s)
c         da() = Anion diffusion coefficient minus numerical dispersion (m^2/s)
c         dc() = Cation diffusion coefficient minus numerical dispersion (m^2/s)
c         v = hydraulic seepage velocity (m/s)
c         Coa = Initial Anion Concentration (mol/m^3)
c         Coc = Initial Cation Concentration (mol/m^3)
c         tol = Tolerance for convergence
c         omega = osmotic efficiency coefficient (dimensionless)
c         kh = hydraulic conductivity (m/s)
c         temp = absolute temperature (Kelvin)
c         R = Universal gas const. 8.314 (J/mol-K)
c         Rda = Anion retardation factor (dimensionless)
c         Rdc = Cation retardation factor (dimensionless)
c         a(NC) = Anion concentration at time t (mol/m^3)
c         c(NC) = Cation concentration at time t (mol/m^3)
c         e(NC) = Exchangeable Cation concentration at time t (mol/m^3)
c         aa(NC,T) = Anion concentration at time t and cell i ((mol/m^3)
c         cc(NC,T) = Cation concentration at time t and cell i (mol/m^3)
c         ee(NC,T) = Exchangeable Cation concentration at time t and cell i (mol/m^3)
c         alpha(NC) = Osmotic term
c         Vpi = Osmotic seepage velocity
c         por  = porosity (dimensionless)
c         gw   = unit weight of water (N/M^3)
c         Za   = Anion Valence
c         Zc   = Cation Valence
c         Ze   = Exchangeable Cation Valence
c         UE(NC) = convergence vector
c         u(NC)  = dummy vector to store previous iteration
c         LB   = Barrier thickness (m)
c         qpi(NT) = chemico-osmotic water flux
c         Nout = The cell of output
c          Cbc  = Cation boundary concentration (mol/m^3)
c         Cba  = Anion boundary concentration (mol/m^3)
c         tau = apparent tortuosity factor (dimensionless)
c         dla = free-solution self-diffusion coeff. for anion (m^2/s)
c         dlc = free-solution self-diffusion coeff. for cation (m^2/s)
c         dle = free-solution self-diffusion coeff. for exchangeable cation (m^2/s)
```

```
c*************************************************************************
c       Variable declaration
c*************************************************************************
      INTEGER NC,T
      Real R,gw
      Parameter (NC=2100,T=6000)
      Parameter (R=8.314,gw=9806)
      INTEGER k,j,nt,ntt,n,l,i,m,f,Za,Zc,Ze,ii,Nout,TF
      REAL W(NC),Coa,Coc
      REAL d1,da(NC),dc(NC),Rda,Rdc,alpha(NC),Vpi(NC),por
      REAL delx,delt,v,dd,DIFF,tol,lb,d1a,d1c,d1e
      REAL omega,kh,temp, qpi(T), Cbc, Cba, tau
      REAL diag(NC),superd(NC),subd(NC),rhs(NC),a(NC),c(NC),e(NC)
      REAL UE(NC),TE(NC)
      REAL aa(NC,T),cc(NC,T),ee(NC,T),dda(NC,T),ddc(NC,T)
      REAL Ja(T), Jc(T)
      REAL Ja1(T), Ja2(T), Ja3(T)
      REAL Jc1(T), Jc2(T), Jc3(T)
c*************************************************************************
c       open files for input data, output data, and convergence data
c*************************************************************************
      open(7,file='input.dat',status='old')
      open(4,file='out2.dat',status='unknown')
      open(6,file='conv.dat',status='unknown')
c*************************************************************************
c       reading input data
c*************************************************************************
      read(7,*)
      read(7,*) nt
      read(7,*)
      read(7,*) n
      read(7,*)
      read(7,*) delx
      read(7,*)
      read(7,*) delt
      read(7,*)
      read(7,*) TF
      read(7,*)
      read(7,*) v
      read(7,*)
      read(7,*) Coa
      read(7,*)
      read(7,*) Coc
      read(7,*)
      read(7,*) tol
      read(7,*)
      read(7,*) omega
      read(7,*)
      read(7,*) kh
      read(7,*)
      read(7,*) temp
```

```
      read(7,*)
      read(7,*) Rda
      read(7,*)
      read(7,*) Rdc
      read(7,*)
      read(7,*) por
      read(7,*)
      read(7,*) Za
      read(7,*)
      read(7,*) Zc
      read(7,*)
      read(7,*) Ze
      read(7,*)
      read(7,*) LB
      read(7,*)
      read(7,*) Nout
      read(7,*)
      read(7,*) Cbc
      read(7,*)
      read(7,*) Cba
      read(7,*)
      read(7,*) tau
      read(7,*)
      read(7,*) d1a
      read(7,*)
      read(7,*) d1c
      read(7,*)
      read(7,*) d1e
c
c
C*************************************************************************
C    Parameter Initialization
C*************************************************************************
c
c

         f = 0
         do 1111 i=1,n
         a(i) = 0
         c(i) = 0
         e(i) = 0
         UE(i) = 0
         TE(i) = 0
         da(i) = tau*d1a - ((v*v*delt)/2)
         dc(i) = tau*d1c - ((v*v*delt)/2)
1111  continue
         do 1112 k=1,nt
         do 1112 i=1,n
         aa(i,k) = 0
         cc(i,k) = 0
         ee(i,k) = 0
1112  continue
c
c
```

```
c*************************************************************************
c  Start of Time loop
c*************************************************************************
c
c
      do 100 j=1,nt
          write(*,*) 'Time Step =', j
c
c
c*************************************************************************
c  Main iteration Start
c*************************************************************************
c
c
          Do 1000 ii=1,1000
c*************************************************************************
c  Start iterations to solve for anion concentrations
c*************************************************************************
c
C     Initialize arrays
c
      do 203 i=1,n
      UE(i) = 0
      alpha(i)= 0
          Vpi(i) = 0
203   continue
c
C         Matrix coefficient Calculations
c
      do 200 i=1,600
      do 201 l=1,5
      do 10 k=1,n
      alpha(k) = (omega * Kh * R * Temp * a(k))/(por*gw)
          Vpi(k) =  ((omega * Kh * R * Temp)/(por*gw*2*delx))*(a(k+1)
          * - a(k-1) + c(k+1) - c(k-1) + e(k+1) - e(k-1))
      w(k)=((alpha(k)*delt)/(delx**2))*(c(k+1) + c(k-1)+ e(k+1)
          * + e(k-1) - 2*c(k) - 2*e(k))
      diag(k) = ((2*da(k)*delt)/(delx**2)) - ((2*alpha(k)*delt)/(delx*
          **2)) + Rda
10    continue
      do 20 k=2,n
      subd(K) = -((Vpi(k)*delt)/(2*delx)) - ((da(k)*delt)/(delx**2))
     * - ((v*delt)/(2*delx)) + ((alpha(k)*delt/(delx**2))) + ((v * omega
     * * delt)/(2*delx)) + ((da(k)-da(k-1))/(2*delx**2))
20    continue
      do 30 k=1,n-1
        superd(K) = ((v*delt)/(2*delx)) + ((Vpi(k)*delt)/(2*delx))
     * - ((da(k)*delt)/(delx**2)) + (alpha(k)*delt/(delx**2)) - ((v *
     * omega * delt)/(2*delx)) - ((da(k+1)- da(k))/(2*delx**2))
30    continue
      do 40 k=2,n-1
      rhs(k)= (Rda * aa(k,j-1)*f) - w(k)
40    continue
```

```
      Vpi(1) = f*((omega * Kh * R * Temp)/(por*gw*2*delx))*(a(2) -
     * Coa + c(2) - Coc + e(2))
        rhs(1)= (Rda * aa(1,j-1)*f)
     * - ((alpha(1)*delt)/(delx**2))*(c(2)+Coc+e(2)-2*c(1)-2*e(1))
     * - Coa*(-((Vpi(1)*delt)/(2*delx)) - ((da(1)*delt)/(delx**2))
     * - ((v*delt)/(2*delx))  + ((alpha(1)*delt)/(delx**2))
     * + ((v * omega * delt)/(2*delx)) + ((da(2) - da(1))/(2*delx**2)))

      rhs(n)= (Rda * aa(n,j-1)*f) - ((alpha(n)*delt)/(delx**2))*
     * (cbc + c(n-1) + e(n-1) - 2*c(n) - 2*e(n)) - cba * (((v*delt)
     * /(2*delx)) + ((Vpi(n)*delt)/(2*delx)) - ((da(n)*delt)/(delx**2))
     * + (alpha(n)*delt/(delx**2)) - ((v * omega* delt)/(2*delx))
     * - (da(n)-da(n-1))/(2*delx**2))
c**************************************************************************
c       call tridiagonal solver to calculate anion concentrations
c**************************************************************************
        call tridag(subd,diag,superd,rhs,a,n)
201   continue
c
c     Convergence check for anion concentrations
c
      DIFF = 0.0
      DO 8 m = 1,n
      DD = ABS(a(m) - UE(m))
      DIFF = AMAX1(DIFF,DD)
      UE(m) = a(m)
 8    CONTINUE
c
c       if anions converge, start solving cation concentrations
c
     if (DIFF < tol)  goto 999
200   CONTINUE
c
c       non-convergence notification
c
      write(*,*) 'Anions: No Convergence ', 'Time Step =', j,'Res =',
          * DIFF
999   continue

c**************************************************************************
c  Start iterations to solve for cation concentrations
c**************************************************************************
c
C     Initialize arrays
c

      do 2030 i=1,n
          UE(i) = 0
          alpha(i) = 0
          Vpi(i) = 0
2030  continue
c
C       Matrix coefficient calculations
c
```

```
      do 2000 i=1,600
      do 2010 l=1,5
      do 110 k=1,n
      alpha(k) = (omega * Kh * R * Temp * c(k))/(por*gw)
      Vpi(k) =  ((omega * Kh * R * Temp)/(por*gw*2*delx))*(c(k+1) -
     * c(k-1) + a(k+1) - a(k-1) + e(k+1) - e(k-1))
      w(k)=((alpha(k)*delt)/(delx**2))*(a(k+1) + a(k-1) + e(k+1)
     * + e(k-1) - 2*a(k) - 2*e(k))
      diag(k) = ((2*dc(k)*delt)/(delx**2))-((2*alpha(k)*delt)/(delx**2))
          * + Rdc
110   continue
      do 220 k=2,n
      subd(K) = -((Vpi(k)*delt)/(2*delx)) - ((dc(k)*delt)/(delx**2))
     * - ((v*delt)/(2*delx)) + (alpha(k)*delt/(delx**2)) + ((v * omega
     * * delt)/(2*delx)) + ((dc(k)-dc(k-1))/(2*delx**2))
220   continue
      do 330 k=1,n-1
      superd(K) = ((v*delt)/(2*delx)) + ((Vpi(k)*delt)/(2*delx))
     * - ((dc(k)*delt)/(delx**2)) + (alpha(k)*delt/(delx**2)) - ((v *
     * omega * delt)/(2*delx)) - ((dc(k+1)-dc(k))/(2*delx**2))
330   continue
      do 440 k=2,n-1
      rhs(k)= (Rdc * cc(k,j-1)*f) - w(k)
440   continue
      Vpi(1) = f*((omega * Kh * R * Temp)/(por*gw*2*delx))*(a(2)-
     * Coa + c(2) - Coc + e(2))
c
       rhs(1)= (Rdc * cc(1,j-1)*f)
     * - ((alpha(1)*delt)/(delx**2))*(a(2)+Coa+e(2)-2*a(1)-2*e(1))
     * - Coc*(-((Vpi(1)*delt)/(2*delx)) - ((dc(1)*delt)/(delx**2))
     * - ((v*delt)/(2*delx))  + ((alpha(1)*delt)/(delx**2))
     * +((v * omega * delt)/(2*delx)) + ((dc(2) - dc(1))/(2*delx**2)))
c
       rhs(n)= (Rdc * cc(n,j-1)*f) - ((alpha(n)*delt)/(delx**2))*
     *(cba + a(n-1) + e(n-1) - 2*a(n) - 2*e(n)) - cbc * (((v*delt)
     * /(2*delx)) + ((Vpi(n)*delt)/(2*delx)) - ((dc(n)*delt)/(delx**2))
     * + (alpha(n)*delt/(delx**2)) - ((v * omega* delt)/(2*delx))
     * -(dc(n)-dc(n-1))/(2*delx**2))
c**************************************************************************
c        call tridiagonal solver to calculate cation concentrations
c**************************************************************************
      call tridag(subd,diag,superd,rhs,c,n)
2010  continue
c**************************************************************************
c     Convergence check for cation concentrations
c**************************************************************************

      DIFF = 0.0
      DO 80 m = 1,n
      DD = ABS(c(m) - UE(m))
      DIFF = AMAX1(DIFF,DD)
      UE(m) = c(m)
80    CONTINUE
c
```

```
c       if cations converge, solve exchangeable cation concentrations
c
    if (DIFF < tol)  goto 9990
2000  CONTINUE
c
c       non-convergence notification
c
    write(*,*) 'Cations: No Convergence ', 'Time Step =',j,',Res =',
        *DIFF
9990  continue


c**************************************************************************
c  Solving for Exchangeable Cation Concentrations
c**************************************************************************
c
c       electroneutrality constraint
c
    do 555 k=1,n
    e(k)= (Za*a(k) - Zc*c(k))/Ze
555   continue
c**************************************************************************
c    Check for convergence for exchangeable cation
c**************************************************************************
    DIFF = 0.0
    DO 81 m = 1,n
    DD = ABS(e(m) - TE(m))
    DIFF = AMAX1(DIFF,DD)
    TE(m) = e(m)
81    CONTINUE
        if (DIFF < tol)  goto 9991
c
c       updating matrix of diffusion coefficients
c
        do 82 m=2,n
        if (a(m)- a(m-1) .EQ. 0) goto 82
        if (a(m) .EQ. 0) goto 82
        da(m) = tau*(d1a + d1a*a(m)*Za*(d1c*Zc*((c(m)-c(m-1))/(delx))
   * + d1e*Ze*((e(m)-e(m-1))/(delx)) - d1a*Za*((a(m)-a(m-1))/
   * (delx)))/(((a(m)-a(m-1))/(delx))*(d1c*Zc**2*c(m) +
        * d1e*Ze**2*e(m) + d1a*Za**2*a(m)))) - ((v*v*delt)/2)
82      continue
        do 83 m = 2,n
        if (c(m)- c(m-1) .EQ. 0) goto 83
        if (c(m) .EQ. 0) goto 83
        dc(m) = tau*(d1c - d1c*c(m)*Zc*(d1c*Zc*((c(m)-c(m-1))/(delx))
   * + d1e*Ze*((e(m)-e(m-1))/(delx)) - d1a*Za*((a(m)-a(m-1))/
   * (delx)))/(((c(m)-c(m-1))/(delx))*(d1c*Zc**2*c(m) +
        * d1e*Ze**2*e(m) + d1a*Za**2*a(m)))) - ((v*v*delt)/2)
83      continue
        da(1) = tau*(d1a + d1a*a(1)*Za*(d1c*Zc*((c(1)- Coc)/(delx))
   * + d1e*Ze*((e(1)- 0)/(delx)) - d1a*Za*((a(1)- Coa)/
   * (delx)))/(((a(1)- Coa)/(delx))*(d1c*Zc**2*c(1) +
        * d1e*Ze**2*e(1) + d1a*Za**2*a(1)))) - ((v*v*delt)/2)
```

```
      dc(1) = tau*(d1c - d1c*c(1)*Zc*(d1c*Zc*((c(1)- Coc)/(delx))
     * + d1e*Ze*((e(1)- 0)/(delx)) - d1a*Za*((a(1)- Coa)/
     * (delx)))/(((c(1)- Coc)/(delx))*(d1c*Zc**2*c(1) +
      * d1e*Ze**2*e(1) + d1a*Za**2*a(1)))) - ((v*v*delt)/2)
1000  CONTINUE
     write(*,*) 'Over All: No Convergence ', 'Time Step =', j, 'Res = '
      *, DIFF
9991  continue
c
c     store converged concentrations and diffusion coeffs into 2-D array
c
     do 101 k=1,n
     aa(k,j)=a(k)
     cc(k,j)=c(k)
     ee(k,j)=e(k)
      dda(k,j) = da(k)
      ddc(k,j) = dc(k)
101   continue
     do 102 k=1,n
     TE(k) = 0
     f = 1
102   continue
100   continue
     do 491 k=1, nt
      cc(n+1,k) = cbc
      aa(n+1,k) = cba
      ee(n+1,k) = (Za*cba - Zc*cbc)/Ze
491   continue
     do 666 k = 1,nt
      qpi(k) =  ((omega * Kh * R * Temp)/(gw*2*delx))*(cc(Nout+1,k)
      * - cc(Nout-1,k) + aa(Nout+1,k) - aa(Nout-1,k) + ee(Nout+1,k)
    * - ee(nout-1,k))
     Jc1(k) = por * v * cc(Nout,k) - omega * por * v * cc(Nout,k)
      Jc2(k) = qpi(k)*cc(Nout,k)
      Jc3(k) = - por * (ddc(Nout,k)/(2*delx))*(cc(Nout+1,k)
      * - cc(Nout-1,k))
      Jc(k) = Jc1(k) + Jc2(k) + Jc3(k)
      Ja1(k) = por * v * aa(Nout,k) - omega * por * v * aa(Nout,k)
      Ja2(k) = qpi(k)*aa(Nout,k)
      Ja3(k) = - por * (dda(Nout,k)/(2*delx))*(aa(Nout+1,k)
      * - aa(Nout-1,k))
      Ja(k) = Ja1(k) + Ja2(k) + Ja3(k)
666   continue

      open(5,file='anions.dat',status='unknown')
      open(8,file='concx.dat',status='unknown')
      open(9,file='flux.dat',status='unknown')

      ntt = nt/10
      do 777 j = 1,ntt
     write(9,*) Ja(10*j)
777   continue
      do 7771 j = 1,ntt
     write(9,*) Jc(10*j)
```

```
7771  continue
        do 7772 k = 1,n
        write(8,*) cc(k,TF)
7772    continue
        do 7773 k = 1,n
c       Ja1(k) = por * v * aa(k,TF) - omega * por * v * aa(k,TF)
c       Ja2(k) = qpi(k)*aa(k,TF)
c       Ja3(k) = - por * (dda(k,TF)/(2*delx))*(aa(k+1,TF)
c       * - aa(k-1,TF))
c       Ja(k) = Ja1(k) + Ja2(k) + Ja3(k)
7773    continue
        do 7774 k = 1,n
c       write(8,*) Ja(k)
7774    continue
        do 7775 k = 1,n
c       write(5,*) Ja1(k)
7775    continue
        do 7776 k = 1,n
c       write(5,*) Ja2(k)
7776    continue
        do 7777 k = 1,n
c       write(5,*) Ja3(k)
7777    continue
        close(5)
        close(7)
    close(6)
    close(8)
    close(4)
        close(3)
    close(9)
        END
c*************************************************************
c    Tridiagonal Solver
c*************************************************************
    SUBROUTINE tridag(a,b,c,r,u,n)
    INTEGER n,NMAX
    REAL a(n),b(n),c(n),r(n),u(n)
    PARAMETER (NMAX=500)
    INTEGER j
    REAL bet,gam(NMAX)
    if(b(1).eq.0.)pause 'tridag: rewrite equations'
    bet=b(1)
    u(1)=r(1)/bet
    do 11 j=2,n
     gam(j)=c(j-1)/bet
     bet=b(j)-a(j)*gam(j)
     if(bet.eq.0.)pause 'tridag failed'
     u(j)=(r(j)-a(j)*u(j-1))/bet
11   continue
    do 12 j=n-1,1,-1
     u(j)=u(j)-gam(j+1)*u(j+1)
12   continue
    return
    END
```

EXAMPLE INPUT FILE

nt = Number of time steps
1000
n = Number of cells
100
delx = cell size (m)
0.0001
delt = Time step size (s)
2880
TF = Time step for examining J(x)
1000
v = seepage velocity (m/s)
1.2732e-8
Coa = Initial Anion Concentration (mol/m^3)
8.7
Coc = Initial Cation Concentration (mol/m^3)
8.7
tol = Tolerance for convergence
.001
omega = osmotic eff. coeff. (dimensionless)
0.49
kh = hydraulic conductivity (m/s)
1.43e-11
temp = absolute temperature (Kelvin)
298.15
Rda = Anion retardation factor (dimensionless)
1.53
Rdc = Cation retardation factor (dimensionless)
12.57
por = porosity (dimensionless)
0.79
Za = Anion Valence
1
Zc = Cation Valence
1
Ze = Exchangeable Cation Valence
1
LB = Barrier Thickness (meters)
0.01
Nout = The cell of output
100
Cbc = Cation boundary concentration (mol/m3)
0.0
Cba = Anion boundary concentration (mol/lm3)
0.0
tau = apparent tortuosity factor (dimensionless)
0.0627
dla = self-diffusion coefficient for anion (m2/s)
20.3e-10
dlc = self-diffusion coefficient for cation (m2/s)
19.6e-10
dle = self-diffusion coeff for exchangeable cation (m2/s)
13.3e-10

APPENDIX D

COUPLED SOLUTE TRANSPORT MODEL SIMULATIONS

C_o = 0.047 M	k_s = 0	L = 1.0 m	Δx = 0.01 m	n = 0.78
D_{oc} =19.6 x 10^{-10} m^2/s		D_{co} = 20.3e^{-10} m^2/s		$R_{dc} = R_{do}$ = 1
Case	NM	EI	E	I
ω	0.0	0.14	0.14	0.0
τ_o	0.120	0.119	0.120	0.119
Time (yr)	FLUX, J(x=L) mol/m^2s	FLUX, J(x=L) mol/m^2s	FLUX, J(x=L) mol/m^2s	FLUX, J(x=L) mol/m^2s
1 3699	9 937E-15	6 708E-15	7 140E-15	7 965E-15
2 7397	1 423E-12	1 398E-12	1 466E-12	1 717E-12
4 1096	2 838E-11	2 033E-11	2 112E-11	2 550E-11
5 4795	1 293E-10	9 621E-11	9 930E-11	1 223E 10
6 8493	3 461E-10	2 594E-10	2 665E 10	3 325E-10
8 2192	6 803E-10	5 103E-10	5 224E-10	6 576E-10
9 589	1 105E-09	8 293E 10	8 469E 10	1 073E-09
10 959	1 585E-09	1 191E-09	1 214E-09	1 544E-09
12 329	2 091E-09	1 575E-09	1 602E-09	2 043E 09
13 699	2 601E 09	1 961E 09	1 993E 09	2 546E 09
15 068	3 097E-09	2 341E-09	2 376E 09	3 038E 09
16 438	3 572E-09	2 705E-09	2 744E 09	3 508E 09
17 808	4 018E-09	3 049E-09	3 091E-09	3 951E 09
19 178	4 433E-09	3 372E-09	3 416E 09	4 365E-09
20 548	4 817E-09	3 672E-09	3 717E 09	4 747E 09
21 918	5 170E 09	3 950E-09	3 997E 09	5 099E-09
23 288	5 493E-09	4 206E 09	4 254E 09	5 422E 09
24 658	5 787E-09	4 442E-09	4 490E 09	5 717E-09
26 027	6 056E 09	4 658E-09	4 707E 09	5 985E-09
27 397	6 300E-09	4 856E-09	4 906E-09	6 230E 09
28 767	6 522E-09	5 037E-09	5 087E-09	6 452E-09
30 137	6 723E 09	5 203E-09	5 254E-09	6 654E-09
31 507	6 905E-09	5 355E-09	5 406E-09	6 838E-09
32 877	7 071E-09	5 494E-09	5 545E-09	7 004E-09
34 247	7 221E-09	5 621E-09	5 672E-09	7 155E 09
35 616	7 357E-09	5 737E-09	5 788E-09	7 292E 09
36 986	7 480E-09	5 843E-09	5 894E-09	7 416E-09
38 356	7 591E-09	5 940E 09	5 991E-09	7 529E 09
39 726	7 692E-09	6 029E-09	6 079E-09	7 630E-09
41 096	7 783E-09	6 110E-09	6 160E-09	7 723E-09
42 466	7 866E-09	6 185E-09	6 234E-09	7 807E 09
43 836	7 941E-09	6 253E-09	6 302E-09	7 882E-09
45 205	8 009E-09	6 315E-09	6 364E-09	7 951E-09
46 575	8 070E-09	6 371E 09	6 421E 09	8 013E 09
47 945	8 126E-09	6 423E-09	6 472E-09	8 070E 09
49 315	8 176E-09	6 471E-09	6 520E 09	8 121E 09
50 685	8 222E-09	6 514E-09	6 563E-09	8 167E-09
52 055	8 263E-09	6 554E-09	6 602E-09	8 209E-09
53 425	8 300E 09	6 591E-09	6 639E-09	8 247E 09
54 795	8 334E-09	6 624E 09	6 672E-09	8 282E 09
56 164	8 365E-09	6 655E-09	6 702E-09	8 313E-09
57 534	8 392E-09	6 683E-09	6 730E 09	8 341E 09
58 904	8 417E-09	6 708E-09	6 755E-09	8 367E 09
60 274	8 440E-09	6 732E-09	6 778E-09	8 390E 09
61 644	8 461E-09	6 753E-09	6 800E-09	8 411E 09
63 014	8 479E 09	6 773E 09	6 819E 09	8 430E-09
64 384	8 496E 09	6 791E-09	6 837E-09	8 447E-09
65 753	8 511E-09	6 807E-03	6 853E-09	8 463E 09
67 123	8 525E-09	6 822E-09	6 868E-09	8 477E-09
68 493	8 538E-09	6 836E-09	6 882E 09	8 490E 09
69 863	8 549E-09	6 849E-09	6 894E 09	8 502E 09
71 233	8 559E-09	6 860E 09	6 906E-09	8 512E 09
72 603	8 568E-09	6 871E 09	6 916E 09	8 522E-09
73 973	8 577E-09	6 881E-09	6 926E-09	8 530E 09
75 342	8 584E-09	6 889E-09	6 934E-09	8 538E 09
76 712	8 591E-09	6 898E-09	6 942E-09	8 545E 09
78 082	8 597E-09	6 905E-09	6 950E-09	8 552E-09
79 452	8 603E-09	6 912E-09	6 957E-09	8 558E-09
80 822	8 608E-09	6 918E-09	6 963E-09	8 563E 09
82 192	8 613E 09	6 924E-09	6 968E-09	8 568E-09
83 562	8 617E-09	6 929E-09	6 973E-09	8 572E-09
84 932	8 621E-09	6 934E-09	6 978E-09	8 576E 09
86 301	8 624E-09	6 938E-09	6 983E-09	8 579E 09
87 671	8 627E-09	6 942E-09	6 986E-09	8 583E 09
89 041	8 630E-09	6 946E-09	6 990E-09	8 586E-09
90 411	8 633E-09	6 949E-09	6 993E-09	8 588E-09
91 781	8 635E-09	6 953E-03	6 996E-09	8 591E-09
93 151	8 637E-09	6 955E-09	6 999E-09	8 593E-09
94 521	8 639E-09	6 958E-09	7 002E-09	8 595E 09
95 89	8 641E-09	6 960E-09	7 004E-09	8 597E-09
97 26	8 642E-09	6 963E-09	7 006E 09	8 598E 09
98 63	8 644E-09	6 965E-09	7 008E-09	8 600E-09
100	8 645E-09	6 966E-09	7 010E-09	8 601E-09
101 37	8 646E-09	6 968E-09	7 012E-09	8 602E 09
102 74	8 647E-09	6 970E-09	7 013E 09	8 603E-09
104 11	8 648E-09	6 971E-09	7 015E-09	8 604E-09
105 48	8 649E-09	6 972E-09	7 016E 09	8 605E 09
106 85	8 650E-09	6 973E-09	7 017E-09	8 606E-09
108 22	8 650E-09	6 975E-09	7 018E-09	8 607E-09
109 59	8 651E-09	6 976E-09	7 019E-09	8 607E-09
110 96	8 651E-09	6 976E-09	7 020E-09	8 608E-09
112 33	8 652E-09	6 977E-09	7 021E-09	8 609E-09
113 7	8 652E-09	6 978E-09	7 021E-09	8 609E-09
115 07	8 653E-09	6 979E-09	7 022E-09	8 609E-09
116 44	8 653E-09	6 979E-09	7 023E-09	8 610E-09
117 81	8 654E-09	6 980E-09	7 023E-09	8 610E 09
119 18	8 654E-09	6 980E-09	7 024E-09	8 611E-09
120 55	8 654E-09	6 981E-09	7 024E-09	8 611E-09
121 92	8 654E-09	6 981E-09	7 025E-09	8 611E-09
123 29	8 655E-09	6 982E-09	7 025E-09	8 611E-09
124 66	8 655E-09	6 982E-09	7 025E-09	8 612E-09
126 03	8 655E-09	6 983E-09	7 026E-09	8 612E-09
127 4	8 655E-09	6 983E-09	7 026E-09	8 612E-09
128 77	8 655E-09	6 983E-09	7 026E-09	8 612E-09
130 14	8 656E-09	6 983E-09	7 027E 09	8 612E-09
131 51	8 656E-09	6 984E-09	7 027E 05	8 612E-09
132 88	8 656E-09	6 984E-09	7 027E 09	8 613E-09
134 25	8 656E-09	6 984E-09	7 027E-09	8 613E-09
135 62	8 656E-09	6 984E-09	7 027E-09	8 613E-09
136 99	8 656E-09	6 984E-09	7 028E-09	8 613E-09
200	8 656E-09	6 984E-09	7 028E-09	8 613E-09

C_o = 0.047 M	k_s = 10	L = 1.0 m	Δx = 0.01 m	n = 0.78
D_{oc} =19.6 x 10^{-10} m^2/s		D_{co} = 20.3e^{-10} m^2/s		$R_{dc} = R_{do}$ = 1
Case	NM	EI	E	I
ω	0.0	0.14	0.14	0.0
τ_o	0.120	0.119	0.120	0.119
Time (yr)	FLUX, J(x=L) mol/m^2s	FLUX, J(x=L) mol/m^2s	FLUX, J(x=L) mol/m^2s	FLUX, J(x=L) mol/m^2s
1 3699	1 445E-14	9 429E-15	1 002E-14	1 184E-14
2 7397	2 193E-12	1 966E-12	2 059E-12	2 553E-12
4 1096	4 162E-11	2 860E-11	2 966E 11	3 790E-11
5 4795	1 911E-10	1 354E-10	1 395E-10	1 816E-10
6 8493	5 124E-10	3 648E 10	3 742E 10	4 934E-10
8 2192	1 007E-09	7 178E-10	7 337E 10	9 752E 10
9 589	1 633E-09	1 167E-09	1 189E-09	1 589E-09
10 959	2 342E-09	1 676E-09	1 706E-09	2 286E-09
12 329	3 087E-09	2 216E-09	2 251E-09	3 022E-09
13 699	3 836E-09	2 761E 09	2 802E-09	3 763E-09
15 068	4 566E 09	3 297E 09	3 341E 09	4 487E 09
16 438	5 261E 09	3 811E-09	3 859E-09	5 178E-09
17 808	5 914E-09	4 298E-09	4 349E-09	5 828E-09
19 178	6 521E-09	4 755E 09	4 809E-09	6 434E-09
20 548	7 081E 09	5 181E-09	5 236E 09	6 993E 09
21 918	7 595E 09	5 576E-09	5 632E-09	7 507E-09
23 288	8 065E-09	5 940E 09	5 997E 09	7 977E-09
24 658	8 493E-09	6 275E-09	6 333E-09	8 406E 09
26 027	8 883E-09	6 584E 09	6 642E-09	8 797E-09
27 397	9 236E-05	6 867E-09	6 925E-09	9 152E 09
28 767	9 557E-09	7 126E-09	7 185E-09	9 474E-09
30 137	9 847E-09	7 364E 09	7 423E-09	9 766E-09
31 507	1 011E-08	7 582E-09	7 641E-09	1 003E-08
32 877	1 035E 08	7 782E-09	7 841E-09	1 027E 08
34 247	1 056E-08	7 965E-09	8 023E-09	1 049E-08
35 616	1 076E 08	8 133E-09	8 191E-09	1 069E 08
36 986	1 094E-08	8 285E-09	8 344E-09	1 086E-08
38 356	1 109E-08	8 427E 09	8 484E 09	1 102E 08
39 726	1 124E-08	8 555E-09	8 612E-09	1 117E-08
41 096	1 137E-08	8 673E-09	8 729E-09	1 130E-08
42 466	1 149E-08	8 781E 09	8 837E-09	1 142E-08
43 836	1 159E-08	8 880E 09	8 935E 09	1 153E-08
45 205	1 169E-08	8 971E-09	9 025E 09	1 163E-08
46 575	1 178E-08	9 054E-09	9 108E-09	1 172E-08
47 945	1 185E-08	9 130E 09	9 183E-09	1 180E-08
49 315	1 193E-08	9 200E 09	9 253E-09	1 187E-08
50 685	1 199E-08	9 264E-09	9 316E-09	1 193E-08
52 055	1 205E 08	9 322E-09	9 374E 09	1 199E-08
53 425	1 210E-08	9 376E-09	9 428E-03	1 205E-08
54 795	1 215E-08	9 425E-09	9 476E-09	1 209E 08
56 164	1 219E-08	9 470E-09	9 521E-09	1 214E-08
57 534	1 223E-08	9 512E 09	9 562E 09	1 218E-08
58 904	1 226E 08	9 550E 09	9 600E-09	1 221E 08
60 274	1 230E-08	9 584E-09	9 634E-09	1 225E-08
61 644	1 232E-08	9 616E-09	9 666E-09	1 228E 08
63 014	1 235E 08	9 646E 09	9 694E-09	1 230E 08
64 384	1 237E 08	9 672E-09	9 721E-09	1 233E 08
65 753	1 240E-08	9 697E 09	9 745E-09	1 235E 08
67 123	1 241E 08	9 720E-09	9 768E-09	1 237E 08
68 493	1 243E 08	9 740E 09	9 788E 09	1 238E 08
69 863	1 245E-08	9 759E-09	9 807E-09	1 240E 08
71 233	1 246E-08	9 777E-09	9 824E-09	1 242E 08
72 603	1 247E-08	9 793E 09	9 840E-09	1 243E 08
73 973	1 249E-08	9 807E 09	9 854E-09	1 244E 08
75 342	1 250E-08	9 821E-09	9 867E-03	1 245E-08
76 712	1 251E 08	9 833E 09	9 880E-09	1 246E 08
78 082	1 251E-08	9 845E-09	9 891E 09	1 247E-08
79 452	1 252E-08	9 855E-09	9 901E-09	1 248E-08
80 822	1 253E-08	9 864E 09	9 910E-09	1 249E 08
82 192	1 253E-08	9 873E 09	9 919E-09	1 249E-08
83 562	1 254E-08	9 881E-09	9 927E-09	1 250E-08
84 932	1 255E-08	9 889E-09	9 934E-09	1 250E-08
86 301	1 255E-08	9 895E-09	9 941E-09	1 251E-08
87 671	1 255E-08	9 902E-09	9 947E 09	1 251E-08
89 041	1 256E-08	9 907E 09	9 952E-09	1 252E-08
90 411	1 256E-08	9 912E-09	9 957E-09	1 252E-08
91 781	1 256E-08	9 917E-09	9 962E-09	1 252E-08
93 151	1 257E-08	9 922E-09	9 966E-09	1 253E-08
94 521	1 257E-08	9 926E 09	9 970E-09	1 253E-08
95 89	1 257E-08	9 929E-09	9 974E-09	1 253E-08
97 26	1 257E-08	9 933E-09	9 977E-09	1 253E-08
98 63	1 258E-08	9 936E-09	9 980E-09	1 253E-08
100	1 258E-08	9 939E-09	9 983E-09	1 254E-08
101 37	1 258E-08	9 941E-09	9 985E-09	1 254E-08
102 74	1 258E-08	9 944E 09	9 988E-09	1 254E 08
104 11	1 258E-08	9 946E-09	9 990E-09	1 254E-08
105 48	1 258E-08	9 948E-09	9 992E-09	1 254E 08
106 85	1 258E-08	9 950E-09	9 994E-09	1 254E-08
108 22	1 259E-08	9 952E-09	9 995E-09	1 254E-08
109 59	1 259E-08	9 953E-09	9 997E-09	1 255E-08
110 96	1 259E-08	9 955E 09	9 998E-09	1 255E-08
112 33	1 259E-08	9 956E-09	1 000E-08	1 255E-08
113 7	1 259E-08	9 957E-09	1 000E-08	1 255E-08
115 07	1 259E-08	9 958E-09	1 000E-08	1 255E-08
116 44	1 259E-08	9 959E-09	1 000E-08	1 255E-08
117 81	1 259E-08	9 960E-09	1 000E-08	1 255E-08
119 18	1 259E-08	9 961E-09	1 001E-08	1 255E-08
120 55	1 259E-08	9 962E-09	1 001E-08	1 255E-08
121 92	1 259E-08	9 962E-09	1 001E-08	1 255E-08
123 29	1 259E 08	9 963E-09	1 001E-08	1 255E-08
124 66	1 259E-08	9 964E-09	1 001E-08	1 255E-08
126 03	1 259E-08	9 964E 09	1 001E-08	1 255E-08
127 4	1 259E-08	9 965E-09	1 001E-08	1 255E-08
128 77	1 259E-08	9 965E-09	1 001E-08	1 255E-08
130 14	1 259E-08	9 966E-09	1 001E-08	1 255E-08
131 51	1 259E-08	9 966E-09	1 001E-08	1 255E-08
132 88	1 259E-08	9 966E-09	1 001E-08	1 255E-08
134 25	1 259E-08	9 967E-09	1 001E-08	1 255E-08
135 62	1 259E-08	9 967E-09	1 001E-08	1 255E-08
136 99	1 259E-08	9 967E-09	1 001E-08	1 255E-08
200	1 259E-08	9 967E-09	1 001E-08	1 255E-08

C_o = 0.047 M	i_b = 100	L = 1.0 m	Δx = 0.01 m	n = 0.78
D_{ec} =19.6 x 10^{-10} m^2/s		D_{eo} = 20.3e^{-10} m^2/s		$R_{ec} = R_{eo} = 1$
Case	NM	EI	E	I
ω	0.0	0.14	0.14	0.0
τ_o	0.120	0.119	0.120	0.119
Time (yr)	FLUX, J(x=L) mol/m^2s	FLUX, J(x=L) mol/m^2s	FLUX, J(x=L) mol/m^2s	FLUX, J(x=L) mol/m^2s
1 3699	1 239E-13	2 708E-13	1 302E-13	2 424E-13
2 7397	2 658E-11	5 220E-11	2 751E-11	5 236E-11
4 1096	3 831E-10	7 783E-10	3 927E-10	7 483E-10
5 4795	1 760E-09	3 472E-09	1 792E-09	3 373E-09
6 8493	4 560E-09	8 670E-09	4 623E-09	8 517E-09
8 2192	8 597E-09	1 577E-08	8 684E-09	1 557E-08
9 589	1 339E-08	2 368E-08	1 350E-08	2 346E-08
10 959	1 845E-08	3 145E-08	1 858E-08	3 124E-08
12 329	2 344E-08	3 854E-08	2 356E-08	3 835E-08
13 699	2 810E-08	4 469E-08	2 822E-08	4 452E-08
15 068	3 233E-08	4 983E-08	3 244E-08	4 970E-08
16 438	3 607E-08	5 404E-08	3 617E-08	5 393E-08
17 808	3 932E-08	5 743E-08	3 941E-08	5 735E-08
19 178	4 209E-08	6 013E-08	4 217E-08	6 006E-08
20 548	4 443E-08	6 226E-08	4 450E-08	6 221E-08
21 918	4 639E-08	6 393E-08	4 645E-08	6 389E-08
23 288	4 802E-08	6 523E-08	4 807E-08	6 520E-08
24 658	4 935E-08	6 624E-08	4 940E-08	6 622E-08
26 027	5 045E-08	6 703E-08	5 049E-08	6 701E-08
27 397	5 134E-08	6 764E-08	5 138E-08	6 762E-08
28 767	5 207E-08	6 811E-08	5 211E-08	6 810E-08
30 137	5 266E-08	6 847E-08	5 269E-08	6 846E-08
31 507	5 313E-08	6 875E-08	5 316E-08	6 874E-08
32 877	5 351E-08	6 897E-08	5 354E-08	6 896E-08
34 247	5 381E-08	6 914E-08	5 384E-08	6 913E-08
35 616	5 406E-08	6 926E-08	5 409E-08	6 926E-08
36 986	5 425E-08	6 936E-08	5 428E-08	6 936E-08
38 356	5 441E-08	6 944E-08	5 444E-08	6 943E-08
39 726	5 453E-08	6 950E-08	5 456E-08	6 949E-08
41 096	5 463E-08	6 954E-08	5 466E-08	6 954E-08
42 466	5 471E-08	6 958E-08	5 474E-08	6 957E-08
43 836	5 478E-08	6 961E-08	5 480E-08	6 960E-08
45 205	5 483E-08	6 963E-08	5 485E-08	6 962E-08
46 575	5 487E-08	6 964E-08	5 489E-08	6 964E-08
47 945	5 490E-08	6 966E-08	5 493E-08	6 965E-08
49 315	5 492E-08	6 967E-08	5 495E-08	6 966E-08
50 685	5 494E-08	6 967E-08	5 497E-08	6 967E-08
52 055	5 496E-08	6 968E-08	5 499E-08	6 967E-08
53 425	5 497E-08	6 968E-08	5 500E-08	6 968E-08
54 795	5 498E-08	6 969E-08	5 501E-08	6 968E-08
56 164	5 499E-08	6 969E-08	5 502E-08	6 968E-08
57 534	5 500E-08	6 969E-08	5 502E-08	6 968E-08
58 904	5 500E-08	6 969E-08	5 503E-08	6 968E-08
60 274	5 500E-08	6 969E-08	5 503E-08	6 969E-08
61 644	5 501E-08	6 969E-08	5 504E-08	6 969E-08
63 014	5 501E-08	6 969E-08	5 504E-08	6 969E-08
64 384	5 501E-08	6 970E-08	5 504E-08	6 969E-08
65 753	5 501E-08	6 970E-08	5 504E-08	6 969E-08
67 123	5 502E-08	6 970E-08	5 504E-08	6 969E-08
68 493	5 502E-08	6 970E-08	5 504E-08	6 969E-08
69 863	5 502E-08	6 970E-08	5 505E-08	6 969E-08
71 233	5 502E-08	6 970E-08	5 505E-08	6 969E-08
72 603	5 502E-08	6 970E-08	5 505E-08	6 969E-08
73 973	5 502E-08	6 970E-08	5 505E-08	6 969E-08
75 342	5 502E-08	6 970E-08	5 505E-08	6 969E-08
76 712	5 502E-08	6 970E-08	5 505E-08	6 969E-08
78 082	5 502E-08	6 970E-08	5 505E-08	6 969E-08
79 452	5 502E-08	6 970E-08	5 505E-08	6 969E-08
80 822	5 502E-08	6 970E-08	5 505E-08	6 969E-08
82 192	5 502E-08	6 970E-08	5 505E-08	6 969E-08
83 562	5 502E-08	6 970E-08	5 505E-08	6 969E-08
84 932	5 502E-08	6 970E-08	5 505E-08	6 969E-08
86 301	5 502E-08	6 970E-08	5 505E-08	6 969E-08
87 671	5 502E-08	6 970E-08	5 505E-08	6 969E-08
89 041	5 502E-08	6 970E-08	5 505E-08	6 969E-08
90 411	5 502E-08	6 970E-08	5 505E-08	6 969E-08
91 781	5 502E-08	6 970E-08	5 505E-08	6 969E-08
93 151	5 502E-08	6 970E-08	5 505E-08	6 969E-08
94 521	5 502E-08	6 970E-08	5 505E-08	6 969E-08
95 89	5 502E-08	6 970E-08	5 505E-08	6 969E-08
97 26	5 502E-08	6 970E-08	5 505E-08	6 969E-08
98 63	5 502E-08	6 970E-08	5 505E-08	6 969E-08
100	5 502E-08	6 970E-08	5 505E-08	6 969E-08
101 37	5 502E-08	6 970E-08	5 505E-08	6 969E-08
102 74	5 502E-08	6 970E-08	5 505E-08	6 969E-08
104 11	5 502E-08	6 970E-08	5 505E-08	6 969E-08
105 48	5 502E-08	6 970E-08	5 505E-08	6 969E-08
106 85	5 502E-08	6 970E-08	5 505E-08	6 969E-08
108 22	5 502E-08	6 970E-08	5 505E-08	6 969E-08
109 59	5 502E-08	6 970E-08	5 505E-08	6 969E-08
110 96	5 502E-08	6 970E-08	5 505E-08	6 969E-08
112 33	5 502E-08	6 970E-08	5 505E-08	6 969E-08
1137	5 502E-08	6 970E-08	5 505E-08	6 969E-08
115 07	5 502E-08	6 970E-08	5 505E-08	6 969E-08
116 44	5 502E-08	6 970E-08	5 505E-08	6 969E-08
117 81	5 502E-08	6 970E-08	5 505E-08	6 969E-08
119 18	5 502E-08	6 970E-08	5 505E-08	6 969E-08
120 55	5 502E-08	6 970E-08	5 505E-08	6 969E-08
121 92	5 502E-08	6 970E-08	5 505E-08	6 969E-08
123 29	5 502E-08	6 970E-08	5 505E-08	6 969E-08
124 66	5 502E-08	6 970E-08	5 505E-08	6 969E-08
126 03	5 502E-08	6 970E-08	5 505E-08	6 969E-08
127 4	5 502E-08	6 970E-08	5 505E-08	6 969E-08
128 77	5 502E-08	6 970E-08	5 505E-08	6 969E-08
130 14	5 502E-08	6 970E-08	5 505E-08	6 969E-08
131 51	5 502E-08	6 970E-08	5 505E-08	6 969E-08
132 88	5 502E-08	6 970E-08	5 505E-08	6 969E-08
134 25	5 502E-08	6 970E-08	5 505E-08	6 969E-08
135 62	5 502E-08	6 970E-08	5 505E-08	6 969E-08
136 99	5 502E-08	6 970E-08	5 505E-08	6 969E-08
200	5 502E-08	6 970E-08	5 505E-08	6 969E-08

C_o = 0.020 M	i_b = 0	L = 1.0 m	Δx = 0.01 m	n = 0.79
D_{ec} =19.6 x 10^{-10} m^2/s		D_{eo} = 20.3e^{-10} m^2/s		$R_{ec} = R_{eo} = 1$
Case	NM	EI	E	I
ω	0.0	0.32	0.32	0.0
τ_o	0.120	0.112	0.120	0.112
Time (yr)	FLUX, J(x=L) mol/m^2s	FLUX, J(x=L) mol/m^2s	FLUX, J(x=L) mol/m^2s	FLUX, J(x=L) mol/m^2s
2 0548	2 709E-13	7 960E-14	1 534E-13	1 055E-13
4 1096	1 346E-11	6 305E-12	1 027E-11	8 728E-12
6 1644	1 018E-10	4 901E-11	7 189E-11	6 947E-11
8 2192	3 014E-10	1 532E-10	2 101E-10	2 201E-10
10 274	5 857E-10	3 102E-10	4 066E-10	4 489E-10
12 329	9 096E-10	4 970E-10	6 308E-10	7 218E-10
14 384	1 238E-09	6 931E-10	8 585E-10	1 008E-09
16 438	1 549E-09	8 851E-10	1 077E-09	1 287E-09
18 493	1 834E-09	1 066E-09	1 278E-09	1 548E-09
20 548	2 089E-09	1 232E-09	1 460E-09	1 786E-09
22 603	2 314E-09	1 382E-09	1 622E-09	1 999E-09
24 658	2 511E-09	1 516E-09	1 766E-09	2 188E-09
26 712	2 682E-09	1 636E-09	1 892E-09	2 355E-09
28 767	2 831E-09	1 743E-09	2 003E-09	2 501E-09
30 822	2 959E-09	1 837E-09	2 101E-09	2 629E-09
32 877	3 070E-09	1 921E-09	2 187E-09	2 741E-09
34 932	3 166E-09	1 995E-09	2 262E-09	2 838E-09
36 986	3 249E-09	2 061E-09	2 328E-09	2 923E-09
39 041	3 320E-09	2 118E-09	2 385E-09	2 997E-09
41 096	3 381E-09	2 170E-09	2 436E-09	3 061E-09
43 151	3 434E-09	2 215E-09	2 480E-09	3 118E-09
45 205	3 480E-09	2 255E-09	2 519E-09	3 166E-09
47 26	3 519E-09	2 291E-09	2 554E-09	3 209E-09
49 315	3 553E-09	2 322E-09	2 584E-09	3 246E-09
51 37	3 582E-09	2 350E-09	2 610E-09	3 278E-09
53 425	3 607E-09	2 375E-09	2 633E-09	3 306E-09
55 479	3 629E-09	2 397E-09	2 654E-09	3 331E-09
57 534	3 648E-09	2 416E-09	2 671E-09	3 352E-09
59 589	3 664E-09	2 433E-09	2 687E-09	3 370E-09
61 644	3 678E-09	2 449E-09	2 701E-09	3 386E-09
63 699	3 689E-09	2 462E-09	2 713E-09	3 400E-09
65 753	3 700E-09	2 474E-09	2 724E-09	3 412E-09
67 808	3 709E-09	2 485E-09	2 733E-09	3 423E-09
69 863	3 716E-09	2 494E-09	2 742E-09	3 432E-09
71 918	3 723E-09	2 503E-09	2 749E-09	3 440E-09
73 973	3 729E-09	2 510E-09	2 755E-09	3 447E-09
76 027	3 733E-09	2 517E-09	2 761E-09	3 453E-09
78 082	3 738E-09	2 523E-09	2 766E-09	3 459E-09
80 137	3 741E-09	2 528E-09	2 770E-09	3 463E-09
82 192	3 744E-09	2 533E-09	2 774E-09	3 467E-09
84 247	3 747E-09	2 537E-09	2 778E-09	3 471E-09
86 301	3 749E-09	2 540E-09	2 781E-09	3 474E-09
88 356	3 751E-09	2 544E-09	2 783E-09	3 476E-09
90 411	3 753E-09	2 546E-09	2 786E-09	3 479E-09
92 466	3 755E-09	2 549E-09	2 788E-09	3 481E-09
94 521	3 756E-09	2 551E-09	2 789E-09	3 482E-09
96 575	3 757E-09	2 553E-09	2 791E-09	3 484E-09
98 63	3 758E-09	2 555E-09	2 792E-09	3 485E-09
100 68	3 759E-09	2 557E-09	2 794E-09	3 486E-09
102 74	3 759E-09	2 558E-09	2 795E-09	3 487E-09
104 79	3 760E-09	2 559E-09	2 796E-09	3 488E-09
106 85	3 761E-09	2 561E-09	2 796E-09	3 489E-09
108 9	3 761E-09	2 561E-09	2 797E-09	3 490E-09
110 96	3 761E-09	2 562E-09	2 798E-09	3 490E-09
113 01	3 762E-09	2 563E-09	2 798E-09	3 491E-09
115 07	3 762E-09	2 564E-09	2 799E-09	3 491E-09
117 12	3 762E-09	2 564E-09	2 799E-09	3 491E-09
119 18	3 763E-09	2 565E-09	2 800E-09	3 492E-09
121 23	3 763E-09	2 566E-09	2 800E-09	3 492E-09
123 29	3 763E-09	2 566E-09	2 800E-09	3 492E-09
125 34	3 763E-09	2 566E-09	2 801E-09	3 493E-09
127 4	3 763E-09	2 567E-09	2 801E-09	3 493E-09
129 45	3 763E-09	2 567E-09	2 801E-09	3 493E-09
131 51	3 763E-09	2 567E-09	2 801E-09	3 493E-09
133 56	3 763E-09	2 567E-09	2 801E-09	3 493E-09
135 62	3 763E-09	2 568E-09	2 801E-09	3 493E-09
137 67	3 763E-09	2 568E-09	2 802E-09	3 493E-09
139 73	3 764E-09	2 568E-09	2 802E-09	3 493E-09
141 78	3 764E-09	2 568E-09	2 802E-09	3 493E-09
143 84	3 764E-09	2 568E-09	2 802E-09	3 494E-09
145 89	3 764E-09	2 568E-09	2 802E-09	3 494E-09
147 95	3 764E-09	2 569E-09	2 802E-09	3 494E-09
150	3 764E-09	2 569E-09	2 802E-09	3 494E-09
152 05	3 764E-09	2 569E-09	2 802E-09	3 494E-09
154 11	3 764E-09	2 569E-09	2 802E-09	3 494E-09
156 16	3 764E-09	2 569E-09	2 802E-09	3 494E-09
158 22	3 764E-09	2 569E-09	2 802E-09	3 494E-09
160 27	3 764E-09	2 569E-09	2 802E-09	3 494E-09
162 33	3 764E-09	2 569E-09	2 802E-09	3 494E-09
164 38	3 764E-09	2 569E-09	2 802E-09	3 494E-09
166 44	3 764E-09	2 569E-09	2 802E-09	3 494E-09
168 49	3 764E-09	2 569E-09	2 802E-09	3 494E-09
170 55	3 764E-09	2 569E-09	2 802E-09	3 494E-09
172 6	3 764E-09	2 569E-09	2 802E-09	3 494E-09
174 66	3 764E-09	2 569E-09	2 802E-09	3 494E-09
176 71	3 764E-09	2 569E-09	2 802E-09	3 494E-09
178 77	3 764E-09	2 569E-09	2 802E-09	3 494E-09
180 82	3 764E-09	2 569E-09	2 802E-09	3 494E-09
182 88	3 764E-09	2 569E-09	2 802E-09	3 494E-09
184 93	3 764E-09	2 569E-09	2 802E-09	3 494E-09
186 99	3 764E-09	2 569E-09	2 802E-09	3 494E-09
189 04	3 764E-09	2 569E-09	2 802E-09	3 494E-09
191 1	3 764E-09	2 569E-09	2 802E-09	3 494E-09
193 15	3 764E-09	2 569E-09	2 802E-09	3 494E-09
195 21	3 764E-09	2 569E-09	2 802E-09	3 494E-09
197 26	3 764E-09	2 569E-09	2 802E-09	3 494E-09
199 32	3 764E-09	2 569E-09	2 802E-09	3 494E-09
201 37	3 764E-09	2 569E-09	2 802E-09	3 494E-09
203 42	3 764E-09	2 569E-09	2 802E-09	3 494E-09
205 48	3 764E-09	2 569E-09	2 802E-09	3 494E-09

C_o = 0.020 M	i_b = 10	L = 1.0 m	Δx = 0.01 m	n = 0.79
D_{ec} =19.6 x 10^{-10} m^2/s		D_{ee} = 20.3e^{-10} m^2/s		$R_{ec} = R_{ee} = 1$
Case	NM	EI	E	I
ω	0.0	0.32	0.32	0.0
τ_p	0.120	0.112	0.120	0.112
Time (yr)	FLUX, J(x=L) mol/m^2s	FLUX, J(x=L) mol/m^2s	FLUX, J(x=L) mol/m^2s	FLUX, J(x=L) mol/m^2s
2 0548	4 374E-13	1 173E-13	2 207E-13	1 859E-13
4 1096	2 334E-11	9 308E-12	1 480E-11	1 545E 11
6 1644	1 733E-10	7 242E-11	1 037E-10	1 228E 10
8 2192	5 113E-10	2 255E-10	3 032E 10	3 883E 10
10 274	9 915E 10	4 550E-10	5 872E-10	7 905E-10
12 329	1 537E-09	7 360E-10	9 117E-10	1 268E 09
14 384	2 087E-09	1 027E-09	1 243E-09	1 767E 09
16 438	2 607E 09	1 313E-09	1 560E-09	2 252E 09
18 493	3 081E-09	1 583E-09	1 854E 09	2 702E 09
20 548	3 503E-09	1 832E-09	2 120E 09	3 111E 09
22 603	3 874E-09	2 058E-09	2 358E-09	3 476E 09
24 658	4 197E 09	2 261E-09	2 570E-09	3 799E 09
26 712	4 477E 09	2 443E-09	2 757E-09	4 081E 09
28 767	4 719E 09	2 605E-09	2 922E 09	4 328E 09
30 822	4 927E 09	2 750E-09	3 068E 09	4 543E 09
32 877	5 106E 09	2 878E 09	3 196E 09	4 730E 09
34 932	5 260E 09	2 992E 09	3 309E 09	4 892E 09
36 986	5 392E 09	3 093E 09	3 408E 09	5 033E 09
39 041	5 505E-09	3 183E-09	3 495E-09	5 155E 09
41 096	5 602E-09	3 263E 09	3 572E 09	5 261E 09
43 151	5 686E 09	3 334E-09	3 640E 09	5 353E 09
45 205	5 758E 09	3 397E-09	3 700E 09	5 432E 09
47 26	5 819E 09	3 453E-09	3 752E-09	5 501E-09
49 315	5 872E 09	3 503E-09	3 799E 09	5 561E 09
51 37	5 917E 09	3 547E-09	3 840E 09	5 612E 09
53 425	5 956E 09	3 587E 09	3 876E 09	5 657E 09
55 479	5 989E 09	3 622E-09	3 908E-09	5 696E 09
57 534	6 018E-09	3 653E 09	3 936E-09	5 729E-09
59 589	6 042E 09	3 681E 09	3 961E 09	5 758E 09
61 644	6 063E-09	3 706E-09	3 983E 09	5 783E 09
63 699	6 081E 09	3 728E-09	4 002E-09	5 805E-09
65 753	6 097E-09	3 748E-09	4 019E 09	5 824E 09
67 808	6 110E-09	3 765E 09	4 034E-09	5 840E 09
69 863	6 121E-09	3 781E 09	4 047E-09	5 855E-09
71 918	6 131E-09	3 795E-09	4 059E 09	5 867E 09
73 973	6 140E 09	3 807E-09	4 070E 09	5 877E 09
76 027	6 147E-09	3 819E-09	4 079E 09	5 887E 09
78 082	6 153E-09	3 828E-09	4 087E-09	5 895E 09
80 137	6 158E-09	3 837E 09	4 094E 09	5 901E 09
82 192	6 163E-09	3 845E-09	4 100E 09	5 907E 09
84 247	6 167E-09	3 852E-09	4 106E 09	5 913E 09
86 301	6 170E-09	3 858E-09	4 111E 09	5 917E 09
88 356	6 173E 09	3 864E-09	4 115E 09	5 921E-09
90 411	6 175E 09	3 869E 09	4 119E 09	5 924E 09
92 466	6 177E-09	3 874E-09	4 123E 09	5 927E-09
94 521	6 179E 09	3 877E-09	4 126E-09	5 930E 09
96 575	6 181E 09	3 881E-09	4 128E 09	5 932E 09
98 63	6 182E-09	3 884E-09	4 131E-09	5 934E-09
100 68	6 183E-09	3 887E-09	4 133E 09	5 935E 09
102 74	6 184E-09	3 890E-09	4 135E-09	5 937E 09
104 79	6 185E 09	3 892E-09	4 136E-09	5 938E 09
106 85	6 186E 09	3 894E-09	4 138E-09	5 939E 09
108 9	6 186E 09	3 896E 09	4 139E-09	5 940E 09
110 96	6 187E-09	3 897E-09	4 140E 09	5 941E-09
113 01	6 187E-09	3 899E 09	4 141E 09	5 942E-09
115 07	6 188E 09	3 900E-09	4 142E 09	5 942E-09
117 12	6 188E-09	3 901E 09	4 143E-09	5 943E 09
119 18	6 188E-09	3 902E-09	4 144E-09	5 943E-09
121 23	6 189E-09	3 903E-09	4 144E-09	5 944E 09
123 29	6 189E-09	3 904E-09	4 145E-09	5 944E 09
125 34	6 189E 09	3 904E 09	4 145E-09	5 944E-09
127 4	6 183E-09	3 905E-09	4 146E 09	5 944E 09
129 45	6 189E 09	3 906E-09	4 146E-09	5 945E-09
131 51	6 190E-09	3 906E-09	4 146E 09	5 945E-09
133 56	6 190E-09	3 907E-09	4 147E-09	5 945E-09
135 62	6 190E-09	3 907E 09	4 147E 09	5 945E 09
137 67	6 190E-09	3 907E-09	4 147E-09	5 945E 09
139 73	6 190E 09	3 908E-09	4 147E-09	5 945E-09
141 78	6 190E-09	3 908E-09	4 147E-09	5 945E-09
143 84	6 190E-09	3 908E-09	4 148E 09	5 946E 09
145 89	6 190E-09	3 908E-09	4 148E-09	5 946E-09
147 95	6 190E-09	3 909E-09	4 148E-09	5 946E 09
150	6 190E-09	3 909E-09	4 148E-09	5 946E 09
152 05	6 190E-09	3 909E-09	4 148E-09	5 946E-09
154 11	6 190E-09	3 909E-09	4 148E-09	5 946E-09
156 16	6 190E-09	3 909E-09	4 148E-09	5 946E-09
158 22	6 190E-09	3 909E-09	4 148E-09	5 946E-09
160 27	6 190E-09	3 910E-09	4 148E-09	5 946E-09
162 33	6 190E-09	3 910E-09	4 148E-09	5 946E-09
164 38	6 190E-09	3 910E-09	4 148E-09	5 946E-09
166 44	6 190E-09	3 910E-09	4 148E-09	5 946E-09
168 49	6 190E-09	3 910E-09	4 149E-09	5 946E-09
170 55	6 190E-09	3 910E-09	4 149E-09	5 946E-09
172 6	6 190E-09	3 910E-09	4 149E-09	5 946E-09
174 66	6 190E-09	3 910E-09	4 149E-09	5 946E-09
176 71	6 190E-09	3 910E-09	4 149E-09	5 946E-09
178 77	6 190E-09	3 910E-09	4 149E-09	5 946E-09
180 82	6 190E-09	3 910E-09	4 149E 09	5 946E-09
182 88	6 190E-09	3 910E-09	4 149E-09	5 946E-09
184 93	6 190E-09	3 910E-09	4 149E-09	5 946E-09
186 99	6 190E-09	3 910E-09	4 149E-09	5 946E-09
189 04	6 190E-09	3 910E-09	4 149E-09	5 946E-09
191 1	6 190E-09	3 910E-09	4 149E-09	5 946E-09
193 15	6 190E-09	3 910E-09	4 149E-09	5 946E-09
195 21	6 190E-09	3 910E-09	4 149E-09	5 946E-09
197 26	6 190E-09	3 910E-09	4 149E-09	5 946E-09
199 32	6 190E-09	3 910E-09	4 149E-09	5 946E-09
201 37	6 190E-09	3 910E-09	4 149E-09	5 946E-09
203 42	6 190E-09	3 910E 09	4 149E-09	5 946E-09
205 48	6 190E-09	3 910E-09	4 149E-09	5 946E-09

C_o = 0.020 M	i_b = 100	L = 1.0 m	Δx = 0.01 m	n = 0.79
D_{ec} =19.6 x 10^{-10} m^2/s		D_{ee} = 20.3e^{-10} m^2/s		$R_{ec} = R_{ee} = 1$
Case	NM	EI	E	I
ω	0.0	0.32	0.32	0.0
τ_p	0.120	0.112	0.120	0.112
Time (yr)	FLUX, J(x=L) mol/m^2s	FLUX, J(x=L) mol/m^2s	FLUX, J(x=L) mol/m^2s	FLUX, J(x=L) mol/m^2s
2 0548	1 448E-11	1 458E-12	2 415E-12	9 453E 12
4 1096	9 591E-10	1 328E 10	1 832E 10	7 642E-10
6 1644	5 958E-09	1 067E-09	1 319E 09	5 281E-09
8 2192	1 464E-08	3 280E 09	3 789E-09	1 376E-08
10 274	2 344E-08	6 397E-09	7 081E 09	2 275E 08
12 329	3 025E 08	9 792E-09	1 053E 08	2 986E 08
14 384	3 480E-08	1 301E 08	1 372E-08	3 464E-08
16 438	3 761E 08	1 580E-08	1 643E-08	3 758E-08
18 493	3 925E 08	1 808E-08	1 862E-08	3 928E 08
20 548	4 018E 08	1 986E 08	2 031E-08	4 024E 08
22 603	4 070E-08	2 115E-08	2 156E-08	4 076E 08
24 658	4 099E-08	2 216E-08	2 250E-08	4 104E 08
26 712	4 114E 08	2 284E 08	2 315E-08	4 119E-08
28 767	4 123E 08	2 331E 08	2 361E 08	4 127E 08
30 822	4 127E 08	2 363E-08	2 393E-08	4 131E 08
32 877	4 130E 08	2 385E 08	2 414E 08	4 133E 08
34 932	4 131E 08	2 399E 08	2 428E 08	4 134E 08
36 986	4 132E 08	2 408E-08	2 438E-08	4 135E 08
39 041	4 132E-08	2 414E-08	2 445E-08	4 135E 08
41 096	4 132E-08	2 418E-08	2 449E-08	4 135E-08
43 151	4 133E-08	2 421E-08	2 452E-08	4 135E 08
45 205	4 133E 08	2 422E-08	2 454E-08	4 135E 08
47 26	4 133E-08	2 423E-08	2 455E 08	4 135E 08
49 315	4 133E 08	2 424E-08	2 456E-08	4 135E-08
51 37	4 133E-08	2 424E 08	2 456E-08	4 135E 08
53 425	4 133E-08	2 425E-08	2 456E-08	4 135E 08
55 479	4 133E-08	2 425E-08	2 457E 08	4 135E-08
57 534	4 133E-08	2 425E-08	2 457E 08	4 135E 08
59 589	4 133E 08	2 425E 08	2 457E 08	4 135E 08
61 644	4 133E-08	2 425E 08	2 457E-08	4 135E 08
63 699	4 133E-08	2 425E 08	2 457E-08	4 135E 08
65 753	4 133E-08	2 425E 08	2 457E-08	4 135E 08
67 808	4 133E-08	2 425E 08	2 457E 08	4 135E 08
69 863	4 133E-08	2 425E-08	2 457E 08	4 135E-08
71 918	4 133E-08	2 425E-08	2 457E-08	4 135E 08
73 973	4 133E-08	2 425E-08	2 457E-08	4 135E-08
76 027	4 133E-08	2 425E 08	2 457E-08	4 135E-08
78 082	4 133E 08	2 425E-08	2 457E-08	4 135E-08
80 137	4 133E 08	2 425E-08	2 457E 08	4 135E-08
82 192	4 133E 08	2 425E 08	2 457E 08	4 135E 08
84 247	4 133E-08	2 425E-08	2 457E-08	4 135E-08
86 301	4 133E-08	2 425E-08	2 457E-08	4 135E 08
88 356	4 133E-08	2 425E-08	2 457E-08	4 135E-08
90 411	4 133E 08	2 425E-08	2 457E 08	4 135E-08
92 466	4 133E 08	2 425E 08	2 457E 08	4 135E 08
94 521	4 133E-08	2 425E-08	2 457E 08	4 135E-08
96 575	4 133E-08	2 425E-08	2 457E-08	4 135E-08
98 63	4 133E 08	2 425E 08	2 457E-08	4 135E 08
100 68	4 133E-08	2 425E-08	2 457E-08	4 135E 08
102 74	4 133E 08	2 425E-08	2 457E 08	4 135E-08
104 79	4 133E-08	2 425E-08	2 457E 08	4 135E-08
106 85	4 133E-08	2 425E 08	2 457E 08	4 135E-08
108 9	4 133E 08	2 425E 08	2 457E 08	4 135E 08
110 96	4 133E 08	2 425E-08	2 457E-08	4 135E 08
113 01	4 133E-08	2 425E-08	2 457E-08	4 135E 08
115 07	4 133E-08	2 425E 08	2 457E 08	4 135E-08
117 12	4 133E 08	2 425E-08	2 457E-08	4 135E 08
119 18	4 133E 08	2 425E-08	2 457E-08	4 135E 08
121 23	4 133E-08	2 425E-08	2 457E 08	4 135E-08
123 29	4 133E-08	2 425E-08	2 457E 08	4 135E-08
125 34	4 133E 08	2 425E-08	2 457E-08	4 135E 08
127 4	4 133E 08	2 425E 08	2 457E-08	4 135E 08
129 45	4 133E-08	2 425E-08	2 457E-08	4 135E 08
131 51	4 133E 08	2 425E-08	2 457E 08	4 135E-08
133 56	4 133E-08	2 425E 08	2 457E 08	4 135E 08
135 62	4 133E 08	2 425E-08	2 457E-08	4 135E 08
137 67	4 133E-08	2 425E 08	2 457E-08	4 135E 08
139 73	4 133E 08	2 425E-08	2 457E-08	4 135E 08
141 78	4 133E-08	2 425E-08	2 457E-08	4 135E 08
143 84	4 133E-08	2 425E-08	2 457E-08	4 135E-08
145 89	4 133E 08	2 425E-08	2 457E-08	4 135E 08
147 95	4 133E-08	2 425E-08	2 457E-08	4 135E-08
150	4 133E-08	2 425E-08	2 457E-08	4 135E 08
152 05	4 133E-08	2 425E-08	2 457E-08	4 135E-08
154 11	4 133E-08	2 425E-08	2 457E-08	4 135E 08
156 16	4 133E-08	2 425E-08	2 457E-08	4 135E 08
158 22	4 133E-08	2 425E-08	2 457E-08	4 135E-08
160 27	4 133E-08	2 425E-08	2 457E-08	4 135E-08
162 33	4 133E-08	2 425E-08	2 457E-08	4 135E-08
164 38	4 133E-08	2 425E-08	2 457E-08	4 135E-08
166 44	4 133E-08	2 425E-08	2 457E-08	4 135E-08
168 49	4 133E-08	2 425E-08	2 457E-08	4 135E-08
170 55	4 133E-08	2 425E-08	2 457E-08	4 135E-08
172 6	4 133E-08	2 425E-08	2 457E-08	4 135E-08
174 66	4 133E-08	2 425E-08	2 457E-08	4 135E-08
176 71	4 133E-08	2 425E-08	2 457E-08	4 135E-08
178 77	4 133E-08	2 425E-08	2 457E-08	4 135E-08
180 82	4 133E-08	2 425E-08	2 457E-08	4 135E-08
182 88	4 133E-08	2 425E 08	2 457E-08	4 135E-08
184 93	4 133E-08	2 425E-08	2 457E-08	4 135E-08
186 99	4 133E-08	2 425E-08	2 457E 08	4 135E-08
189 04	4 133E-08	2 425E-08	2 457E 08	4 135E-08
191 1	4 133E-08	2 425E-08	2 457E-08	4 135E-08
193 15	4 133E-08	2 425E-08	2 457E-08	4 135E-08
195 21	4 133E-08	2 425E-08	2 457E-08	4 135E-08
197 26	4 133E-08	2 425E-08	2 457E-08	4 135E-08
199 32	4 133E-08	2 425E-08	2 457E-08	4 135E-08
201 37	4 133E-08	2 425E-08	2 457E-08	4 135E-08
203 42	4 133E-08	2 425E-08	2 457E-08	4 135E-08
205 48	4 133E-08	2 425E-08	2 457E 08	4 135E-08

C_o = 0.0087 M	i_b = 0	L = 1.0 m	Δx = 0.01 m	n = 0.79
D_{oc} =19.6 x 10^{-10} m^2/s		D_{os} = 20.3e^{-10} m^2/s		$R_{dc} = R_{ds}$ = 1
Case	NM	EI	E	I
ω	0.0	0.49	0.49	0.0
τ_s	0.120	0.063	0.120	0.063
Time (yr)	FLUX, J(x=L) mol/m^2s	FLUX, J(x=L) mol/m^2s	FLUX, J(x=L) mol/m^2s	FLUX, J(x=L) mol/m^2s
2 7397	8 492E-13	1 114E-15	7 351E-13	1 408E-15
5 4795	3 035E-11	2 009E-13	2 466E-11	2 610E-13
8 2192	1 322E-10	2 655E-12	1 142E-10	3 502E-12
10 959	2 982E-10	1 177E-11	2 573E-10	1 567E-11
13 699	4 850E-10	3 033E-11	4 187E-10	4 059E-11
16 438	6 646E-10	5 772E-11	5 744E-10	7 751E-11
19 178	8 248E-10	9 151E-11	7 141E-10	1 231E-10
21 918	9 622E-10	1 290E-10	8 348E-10	1 736E-10
24 658	1 078E-09	1 679E-10	9 371E-10	2 259E-10
27 397	1 174E-09	2 066E-10	1 023E-09	2 778E-10
30 137	1 253E-09	2 440E-10	1 095E-09	3 278E-10
32 877	1 319E-09	2 796E-10	1 154E-09	3 750E-10
35 616	1 373E-09	3 129E-10	1 204E-09	4 191E-10
38 356	1 417E-09	3 439E-10	1 245E-09	4 598E-10
41 096	1 453E-09	3 726E-10	1 279E-09	4 971E-10
43 836	1 483E-09	3 989E-10	1 308E-09	5 312E-10
46 575	1 507E-09	4 230E-10	1 331E-09	5 622E-10
49 315	1 527E-09	4 451E-10	1 351E-09	5 903E-10
52 055	1 544E-09	4 652E-10	1 367E-09	6 158E-10
54 795	1 557E-09	4 836E-10	1 381E-09	6 389E-10
57 534	1 568E-09	5 004E-10	1 392E-09	6 597E-10
60 274	1 577E-09	5 157E-10	1 401E-09	6 785E-10
63 014	1 585E-09	5 296E-10	1 409E-09	6 955E-10
65 753	1 591E-09	5 423E-10	1 416E-09	7 108E-10
68 493	1 596E-09	5 538E-10	1 421E-09	7 246E-10
71 233	1 600E-09	5 644E-10	1 425E-09	7 371E-10
73 973	1 603E-09	5 739E-10	1 429E-09	7 483E-10
76 712	1 606E-09	5 827E-10	1 432E-09	7 584E-10
79 452	1 609E-09	5 906E-10	1 435E-09	7 676E-10
82 192	1 610E-09	5 979E-10	1 437E-09	7 758E-10
84 932	1 612E-09	6 045E-10	1 439E-09	7 832E-10
87 671	1 613E-09	6 105E-10	1 440E-09	7 899E-10
90 411	1 614E-09	6 160E-10	1 441E-09	7 959E-10
93 151	1 615E-09	6 210E-10	1 442E-09	8 013E-10
95 89	1 616E-09	6 256E-10	1 443E-09	8 062E-10
98 63	1 616E-09	6 257E-10	1 444E-09	8 106E-10
101 37	1 617E-09	6 335E-10	1 445E-09	8 146E-10
104 11	1 617E-09	6 370E-10	1 445E-09	8 182E-10
106 85	1 617E-09	6 401E-10	1 445E-09	8 214E-10
109 59	1 618E-09	6 430E-10	1 446E-09	8 243E-10
112 33	1 618E-09	6 456E-10	1 446E-09	8 270E-10
115 07	1 618E-09	6 480E-10	1 446E-09	8 293E-10
117 81	1 618E-09	6 502E-10	1 446E-09	8 315E-10
120 55	1 618E-09	6 522E-10	1 447E-09	8 334E-10
123 29	1 618E-09	6 540E-10	1 447E-09	8 351E-10
126 03	1 619E-09	6 557E-10	1 447E-09	8 367E-10
128 77	1 619E-09	6 572E-10	1 447E-09	8 381E-10
131 51	1 619E-09	6 586E-10	1 447E-09	8 393E-10
134 25	1 619E-09	6 598E-10	1 447E-09	8 405E-10
136 99	1 619E-09	6 610E-10	1 447E-09	8 415E-10
139 73	1 619E-09	6 620E-10	1 447E-09	8 424E-10
142 47	1 619E-09	6 630E-10	1 447E-09	8 433E-10
145 21	1 619E-09	6 639E-10	1 447E-09	8 440E-10
147 95	1 619E-09	6 647E-10	1 447E-09	8 447E-10
150 68	1 619E-09	6 654E-10	1 447E-09	8 453E-10
153 42	1 619E-09	6 661E-10	1 447E-09	8 459E-10
156 16	1 619E-09	6 667E-10	1 447E-09	8 464E-10
158 9	1 619E-09	6 672E-10	1 447E-09	8 468E-10
161 64	1 619E-09	6 677E-10	1 447E-09	8 472E-10
164 38	1 619E-09	6 682E-10	1 447E-09	8 476E-10
167 12	1 619E-09	6 685E-10	1 447E-09	8 479E-10
169 86	1 619E-09	6 690E-10	1 447E-09	8 482E-10
172 6	1 619E-09	6 693E-10	1 447E-09	8 485E-10
175 34	1 619E-09	6 697E-10	1 447E-09	8 487E-10
178 08	1 619E-09	6 700E-10	1 447E-09	8 489E-10
180 82	1 619E-09	6 702E-10	1 447E-09	8 491E-10
183 56	1 619E-09	6 705E-10	1 447E-09	8 493E-10
186 3	1 619E-09	6 707E-10	1 447E-09	8 495E-10
189 04	1 619E-09	6 709E-10	1 447E-09	8 496E-10
191 78	1 619E-09	6 711E-10	1 447E-09	8 497E-10
194 52	1 619E-09	6 712E-10	1 447E-09	8 498E-10
197 26	1 619E-09	6 714E-10	1 447E-09	8 500E-10
200	1 619E-09	6 715E-10	1 447E-09	8 500E-10
202 74	1 619E-09	6 717E-10	1 447E-09	8 501E-10
205 48	1 619E-09	6 718E-10	1 447E-09	8 502E-10
208 22	1 619E-09	6 719E-10	1 447E-09	8 503E-10
210 96	1 619E-09	6 720E-10	1 447E-09	8 503E-10
213 7	1 619E-09	6 721E-10	1 447E-09	8 504E-10
216 44	1 619E-09	6 722E-10	1 447E-09	8 504E-10
219 18	1 619E-09	6 722E-10	1 447E-09	8 505E-10
221 92	1 619E-09	6 723E-10	1 447E-09	8 505E-10
224 66	1 619E-09	6 724E-10	1 447E-09	8 506E-10
227 4	1 619E-09	6 724E-10	1 447E-09	8 506E-10
230 14	1 619E-09	6 725E-10	1 447E-09	8 506E-10
232 88	1 619E-09	6 725E-10	1 447E-09	8 507E-10
235 62	1 619E-09	6 726E-10	1 447E-09	8 507E-10
238 36	1 619E-09	6 726E-10	1 447E-09	8 507E-10
241 1	1 619E-09	6 726E-10	1 447E-09	8 507E-10
243 84	1 619E-09	6 727E-10	1 447E-09	8 507E-10
246 58	1 619E-09	6 727E-10	1 447E-09	8 508E-10
249 32	1 619E-09	6 727E-10	1 447E-09	8 508E-10
252 05	1 619E-09	6 728E-10	1 447E-09	8 508E-10
254 79	1 619E-09	6 728E-10	1 447E-09	8 508E-10
257 53	1 619E-09	6 728E-10	1 447E-09	8 508E-10
260 27	1 619E-09	6 728E-10	1 447E-09	8 508E-10
263 01	1 619E-09	6 728E-10	1 447E-09	8 509E-10
265 75	1 619E-09	6 729E-10	1 447E-09	8 508E-10
268 49	1 619E-09	6 729E-10	1 447E-09	8 508E-10
271 23	1 619E-09	6 729E-10	1 447E-09	8 508E-10
273 97	1 619E-09	6 729E-10	1 447E-09	8 509E-10

C_o = 0.0087 M	i_b = 10	L = 1.0 m	Δx = 0.01 m	n = 0.79
D_{oc} =19.6 x 10^{-10} m^2/s		D_{os} = 20.3e^{-10} m^2/s		$R_{dc} = R_{ds}$ = 1
Case	NM	EI	E	I
ω	0.0	0.49	0.49	0.0
τ_s	0.120	0.063	0.120	0.063
Time (yr)	FLUX, J(x=L) mol/m^2s	FLUX, J(x=L) mol/m^2s	FLUX, J(x=L) mol/m^2s	FLUX, J(x=L) mol/m^2s
2 7397	1 197E-12	1 555E-15	8 770E-13	2 722E-15
5 4795	4 245E-11	2 812E-13	2 945E-11	5 045E-13
8 2192	1 472E-10	3 720E-12	1 364E-10	6 761E-12
10 959	4 220E-10	1 651E-11	3 077E-10	3 020E-11
13 699	6 857E-10	4 256E-11	5 008E-10	7 805E-11
16 438	9 387E-10	8 104E-11	6 874E-10	1 487E-10
19 178	1 164E-09	1 286E-10	8 549E-10	2 366E-10
21 918	1 356E-09	1 813E-10	9 998E-10	3 314E-10
24 658	1 518E-09	2 361E-10	1 123E-09	4 303E-10
27 397	1 652E-09	2 907E-10	1 226E-09	5 279E-10
30 137	1 763E-09	3 436E-10	1 313E-09	6 216E-10
32 877	1 854E-09	3 939E-10	1 384E-09	7 097E-10
35 616	1 928E-09	4 412E-10	1 444E-09	7 915E-10
38 356	1 989E-09	4 852E-10	1 494E-09	8 667E-10
41 096	2 039E-09	5 259E-10	1 535E-09	9 353E-10
43 836	2 080E-09	5 634E-10	1 570E-09	9 977E-10
46 575	2 114E-09	5 979E-10	1 599E-09	1 054E-09
49 315	2 141E-09	6 295E-10	1 622E-09	1 105E-09
52 055	2 164E-09	6 584E-10	1 642E-09	1 151E-09
54 795	2 182E-09	6 848E-10	1 659E-09	1 193E-09
57 534	2 197E-09	7 089E-10	1 672E-09	1 230E-09
60 274	2 209E-09	7 309E-10	1 684E-09	1 263E-09
63 014	2 219E-09	7 510E-10	1 693E-09	1 293E-09
65 753	2 228E-09	7 694E-10	1 701E-09	1 320E-09
68 493	2 234E-09	7 861E-10	1 708E-09	1 345E-09
71 233	2 240E-09	8 014E-10	1 713E-09	1 366E-09
73 973	2 244E-09	8 154E-10	1 718E-09	1 386E-09
76 712	2 248E-09	8 281E-10	1 721E-09	1 403E-09
79 452	2 251E-09	8 398E-10	1 725E-09	1 419E-09
82 192	2 254E-09	8 504E-10	1 727E-09	1 433E-09
84 932	2 256E-09	8 601E-10	1 729E-09	1 446E-09
87 671	2 257E-09	8 690E-10	1 731E-09	1 457E-09
90 411	2 259E-09	8 770E-10	1 733E-09	1 467E-09
93 151	2 260E-09	8 844E-10	1 734E-09	1 477E-09
95 89	2 261E-09	8 912E-10	1 735E-09	1 485E-09
98 63	2 261E-09	8 974E-10	1 736E-09	1 492E-09
101 37	2 262E-09	9 030E-10	1 737E-09	1 499E-09
104 11	2 263E-09	9 082E-10	1 737E-09	1 505E-09
106 85	2 263E-09	9 129E-10	1 738E-09	1 510E-09
109 59	2 263E-09	9 172E-10	1 738E-09	1 515E-09
112 33	2 264E-09	9 211E-10	1 739E-09	1 519E-09
115 07	2 264E-09	9 247E-10	1 739E-09	1 523E-09
117 81	2 264E-09	9 280E-10	1 739E-09	1 525E-09
120 55	2 264E-09	9 310E-10	1 739E-09	1 529E-09
123 29	2 264E-09	9 337E-10	1 739E-09	1 532E-09
126 03	2 264E-09	9 363E-10	1 740E-09	1 534E-09
128 77	2 264E-09	9 386E-10	1 740E-09	1 537E-09
131 51	2 265E-09	9 407E-10	1 740E-09	1 539E-09
134 25	2 265E-09	9 426E-10	1 740E-09	1 540E-09
136 99	2 265E-09	9 443E-10	1 740E-09	1 542E-09
139 73	2 265E-09	9 459E-10	1 740E-09	1 544E-09
142 47	2 265E-09	9 474E-10	1 740E-09	1 545E-09
145 21	2 265E-09	9 488E-10	1 740E-09	1 546E-09
147 95	2 265E-09	9 500E-10	1 740E-09	1 547E-09
150 68	2 265E-09	9 511E-10	1 740E-09	1 548E-09
153 42	2 265E-09	9 521E-10	1 740E-09	1 549E-09
156 16	2 265E-09	9 531E-10	1 740E-09	1 550E-09
158 9	2 265E-09	9 539E-10	1 740E-09	1 550E-09
161 64	2 265E-09	9 547E-10	1 740E-09	1 551E-09
164 38	2 265E-09	9 555E-10	1 740E-09	1 551E-09
167 12	2 265E-09	9 561E-10	1 740E-09	1 552E-09
169 86	2 265E-09	9 567E-10	1 740E-09	1 552E-09
172 6	2 265E-09	9 573E-10	1 740E-09	1 553E-09
175 34	2 265E-09	9 578E-10	1 740E-09	1 553E-09
178 08	2 265E-09	9 582E-10	1 740E-09	1 553E-09
180 82	2 265E-09	9 587E-10	1 740E-09	1 554E-09
183 56	2 265E-09	9 590E-10	1 740E-09	1 554E-09
186 3	2 265E-09	9 594E-10	1 740E-09	1 554E-09
189 04	2 265E-09	9 597E-10	1 740E-09	1 554E-09
191 78	2 265E-09	9 600E-10	1 740E-09	1 554E-09
194 52	2 265E-09	9 603E-10	1 740E-09	1 555E-09
197 26	2 265E-09	9 605E-10	1 740E-09	1 555E-09
200	2 265E-09	9 608E-10	1 740E-09	1 555E-09
202 74	2 265E-09	9 610E-10	1 740E-09	1 555E-09
205 48	2 265E-09	9 612E-10	1 740E-09	1 555E-09
208 22	2 265E-09	9 613E-10	1 740E-09	1 555E-09
210 96	2 265E-09	9 615E-10	1 740E-09	1 555E-09
213 7	2 265E-09	9 616E-10	1 740E-09	1 555E-09
216 44	2 265E-09	9 618E-10	1 740E-09	1 555E-09
219 18	2 265E-09	9 619E-10	1 740E-09	1 556E-09
221 92	2 265E-09	9 620E-10	1 740E-09	1 556E-09
224 66	2 265E-09	9 621E-10	1 740E-09	1 556E-09
227 4	2 265E-09	9 622E-10	1 740E-09	1 556E-09
230 14	2 265E-09	9 623E-10	1 740E-09	1 556E-09
232 88	2 265E-09	9 624E-10	1 740E-09	1 556E-09
235 62	2 265E-09	9 624E-10	1 740E-09	1 556E-09
238 36	2 265E-09	9 625E-10	1 740E-09	1 556E-09
241 1	2 265E-09	9 626E-10	1 740E-09	1 556E-09
243 84	2 265E-09	9 626E-10	1 740E-09	1 556E-09
246 58	2 265E-09	9 627E-10	1 740E-09	1 556E-09
249 32	2 265E-09	9 627E-10	1 740E-09	1 556E-09
252 05	2 265E-09	9 627E-10	1 740E-09	1 556E-09
254 79	2 265E-09	9 628E-10	1 740E-09	1 556E-09
257 53	2 265E-09	9 628E-10	1 740E-09	1 556E-09
260 27	2 265E-09	9 628E-10	1 740E-09	1 556E-09
263 01	2 265E-09	9 629E-10	1 740E-09	1 556E-09
265 75	2 265E-09	9 629E-10	1 740E-09	1 556E-09
268 49	2 265E-09	9 629E-10	1 740E-09	1 556E-09
271 23	2 265E-09	9 630E-10	1 740E-09	1 556E-09
273 97	2 265E-09	9 630E-10	1 740E-09	1 556E-09

C_o = 0.0087 M	i_h = 100	L = 1.0 m	Δx = 0.01 m	n = 0.79
D_{oc} =19.6 x 10^{-10} m^2/s		D_{os} = 20.3e^{-10} m^2/s		$R_{dc} = R_{ds}$ = 1
Case	NM	EI	E	I
ω	0.0	0.49	0.49	0.0
τ_a	0.120	0.063	0.120	0.063
Time (yr)	FLUX, J(x=L) mol/m^2s	FLUX, J(x=L) mol/m^2s	FLUX, J(x=L) mol/m^2s	FLUX, J(x=L) mol/m^2s
2 7397	1 531E-11	1 048E-14	2 904E-12	2 493E-13
5 4795	5 136E-10	2 448E 12	1 062E-10	4 621E-11
8 2192	2 187E-09	3 534E-11	5 092E-10	5 489E-10
10 959	4 477E-09	1 699E 10	1 161E-09	2 033E-09
13 699	6 588E-09	4 448E-10	1 885E-09	4 232E-09
16 438	8 218E-09	8 437E-10	2 578E 09	6 458E-09
19 178	9 371E-09	1 319E-09	3 181E-09	8 268E-09
21 918	1 015E-08	1 823E-09	3 686E-09	9 554E-09
24 658	1 066E-08	2 318E-09	4 099E-09	1 039E 08
27 397	1 100E 08	2 782E 09	4 433E 09	1 091E 08
30 137	1 121E-08	3 201E-09	4 700E-09	1 122E-08
32 877	1 135E-08	3 570E-09	4 913E-09	1 140E-08
35 616	1 144E-08	3 885E-09	5 082E-09	1 150E-08
38 356	1 150E-08	4 159E 09	5 215E-09	1 156E-08
41 096	1 154E-08	4 385E-09	5 321E-09	1 159E-08
43 836	1 156E-08	4 572E-09	5 405E-09	1 161E-08
46 575	1 157E-08	4 725E-09	5 471E-09	1 162E-08
49 315	1 158E-08	4 849E-09	5 523E 09	1 162E 08
52 055	1 159E-08	4 949E 09	5 564E 09	1 162E 08
54 795	1 159E-08	5 029E 09	5 596E 09	1 163E 08
57 534	1 159E-08	5 093E 09	5 622E-09	1 163E-08
60 274	1 160E-08	5 143E-09	5 642E 09	1 163E-08
63 014	1 160E-08	5 183E-09	5 658E-09	1 163E-08
65 753	1 160E-08	5 215E 09	5 670E-09	1 163E-0A
68 493	1 160E-08	5 239E-09	5 680E-09	1 163E-08
71 233	1 160E-08	5 259E-09	5 688E 09	1 163E 08
73 973	1 160E-08	5 274E 09	5 694E-09	1 163E-08
76 712	1 160E-08	5 286E 09	5 699E-09	1 163E-0A
79 452	1 160E-08	5 295E-09	5 703E-09	1 163E-08
82 192	1 160E-08	5 302E 09	5 706E 09	1 163E 08
84 932	1 160E-08	5 307E-09	5 708E 09	1 163E-0A
87 671	1 160E-08	5 312E-09	5 710E-09	1 163E-08
90 411	1 160E-08	5 315E 09	5 711E-09	1 163E 08
93 151	1 160E 08	5 318E 09	5 712E-09	1 163E-08
95 89	1 160E-08	5 320E-09	5 713E 09	1 163E-08
98 63	1 160E-08	5 321E-09	5 714E 09	1 163E-08
101 37	1 160E-08	5 322E-09	5 715E-09	1 163E-08
104 11	1 160E-08	5 323E-09	5 715E-09	1 163E-08
106 85	1 160E-08	5 324E 09	5 715E 09	1 163E-08
109 59	1 160E-08	5 324E-09	5 716E-09	1 163E-08
112 33	1 160E-08	5 325E 09	5 716E 09	1 163E-08
115 07	1 160E-08	5 325E-09	5 716E-09	1 163E-08
117 81	1 160E-08	5 326E-09	5 716E 09	1 163E-08
120 55	1 160E-08	5 325E-09	5 716E-09	1 163E-08
123 29	1 160E-08	5 326E-09	5 716E-09	1 163E-08
126 03	1 160E-08	5 326E-09	5 717E-09	1 163E-08
128 77	1 160E-08	5 326E-09	5 717E-09	1 163E-08
131 51	1 160E-08	5 326E-09	5 717E-09	1 163E-08
134 25	1 160E-08	5 326E-09	5 717E-09	1 163E 08
136 99	1 160E-08	5 326E 09	5 717E 09	1 163E 08
139 73	1 160E-08	5 326E 09	5 717E 09	1 163E 08
142 47	1 160E 08	5 326E 09	5 717E 09	1 163E-0A
145 21	1 160E 08	5 326E 09	5 717E 09	1 163E-08
147 95	1 160E 08	5 326E 09	5 717E 09	1 163E 0A
150 68	1 160E-08	5 326E 09	5 717E-09	1 163E-08
153 42	1 160E 08	5 326E 09	5 717E-09	1 163E 08
156 16	1 160E 08	5 326E 09	5 717E-09	1 163E 08
158 9	1 160E-08	5 326E-09	5 717E-09	1 163E-08
161 64	1 160E-08	5 326E-09	5 717E-09	1 163E-08
164 38	1 160E-08	5 326E 09	5 717E-09	1 163E 0A
167 12	1 160E-08	5 326E 09	5 717E-09	1 163E 08
169 86	1 160E 08	5 326E 09	5 717E 09	1 163E-08
172 6	1 160E-08	5 326E-09	5 717E 09	1 163E 08
175 34	1 160E-08	5 326E-09	5 717E-09	1 163E-08
178 08	1 160E-08	5 326E 09	5 717E 09	1 163E-08
180 82	1 160E-08	5 326E 09	5 717E-09	1 163E-08
183 56	1 160E-08	5 326E-09	5 717E-09	1 163E-08
186 3	1 160E-08	5 326E-09	5 717E-09	1 163E-08
189 04	1 160E-08	5 326E-09	5 717E-09	1 163E-08
191 78	1 160E-08	5 326E-09	5 717E-09	1 163E-08
194 52	1 160E-08	5 326E-09	5 717E-09	1 163E-08
197 26	1 160E-08	5 326E-09	5 717E-09	1 163E-08
200	1 160E-08	5 326E-09	5 717E-09	1 163E-08
202 74	1 160E-08	5 326E-09	5 717E-09	1 163E-08
205 48	1 160E-08	5 326E-09	5 717E-09	1 163E-08
208 22	1 160E-08	5 326E-09	5 717E-09	1 163E-08
210 96	1 160E-08	5 326E-09	5 717E-09	1 163E-08
213 7	1 160E-08	5 326E-09	5 717E-09	1 163E-08
216 44	1 160E-08	5 326E-09	5 717E-09	1 163E-08
219 18	1 160E-08	5 326E-09	5 717E-09	1 163E-08
221 92	1 160E-08	5 326E-09	5 717E-09	1 163E-08
224 66	1 160E-08	5 326E-09	5 717E-09	1 163E-08
227 4	1 160E-08	5 326E-09	5 717E-09	1 163E-08
230 14	1 160E-08	5 326E 09	5 717E-09	1 163E-08
232 88	1 160E-08	5 326E-09	5 717E-09	1 163E-08
235 62	1 160E-08	5 326E-09	5 717E-09	1 163E-08
238 36	1 160E-08	5 326E-09	5 717E-09	1 163E-08
241 1	1 160E-08	5 326E-09	5 717E-09	1 163E-08
243 84	1 160E-08	5 326E-09	5 717E-09	1 163E-08
246 58	1 160E-08	5 326E-09	5 717E-09	1 163E-08
249 32	1 160E-08	5 326E-09	5 717E-09	1 163E-08
252 05	1 160E-08	5 326E-09	5 717E-09	1 163E-08
254 79	1 160E-08	5 326E-09	5 717E-09	1 163E-08
257 53	1 160E-08	5 326E-09	5 717E-09	1 163E-08
260 27	1 160E-08	5 326E-09	5 717E-09	1 163E-08
263 01	1 160E-08	5 326E-09	5 717E-09	1 163E-08
265 75	1 160E-08	5 326E-09	5 717E-09	1 163E-08
268 49	1 160E-08	5 326E-09	5 717E-09	1 163E-08
271 23	1 160E-08	5 326E-09	5 717E-09	1 163E-08
273 97	1 160E-08	5 326E-09	5 717E-09	1 163E-08
200	5 502E-08	6 970E-08	5 505E-08	6 969E-08

C_o = 0.0039 M	i_h = 0	L = 1.0 m	Δx = 0.01 m	n = 0.80
D_{oc} =19.6 x 10^{-10} m^2/s		D_{os} = 20.3e^{-10} m^2/s		$R_{dc} = R_{ds}$ = 1
Case	NM	EI	E	I
ω	0.0	0.63	0.63	0.0
τ_a	0.120	0.039	0.120	0.039
Time (yr)	FLUX, J(x=L) mol/m^2s	FLUX, J(x=L) mol/m^2s	FLUX, J(x=L) mol/m^2s	FLUX, J(x=L) mol/m^2s
2 7397	3 092E-13	8 539E-19	3 471E-13	2 701E-19
5 4795	1 355E 11	6 283E 16	1 169E 11	1 938E 15
8 2192	6 319E-11	2 209E-14	5 419E-11	7 063E-14
10 959	1 362E 10	1 947E-13	1 222E-10	2 383E-13
13 699	2 210E-10	8 215E-13	1 588E-10	9 201E-13
16 438	3 028E 10	2 253E-12	2 727E-10	2 507E-12
19 178	3 756E-10	4 719E-12	3 389E-10	6 334E 12
21 918	4 382E 10	8 267E-12	3 960E-10	1 153E-11
24 658	4 908E-10	1 280E-11	4 443E-10	1 806E-11
27 397	5 345E 10	1 816E-11	4 847E 10	2 574E-11
30 137	5 707E 10	2 413E 11	5 184E-10	3427E-11
32 877	6 005E-10	3 052E 11	5 463E-10	4 340E-11
35 616	6 250E 10	3 717E-11	5 695E-10	5 288E-11
38 356	6 451E 10	4 393E 11	5 886E 10	6 249E-11
41 096	6 616E-10	5 069E-11	6 045E 10	7 209E-11
43 836	6 752E 10	5 738E-11	6 175E 10	8 154E 11
46 575	6 863E-10	6 391E 11	6 285E-10	9 076E 11
49 315	6 954E-10	7 026E-11	6 375E-10	9 968E-11
52 055	7 029E-10	7 638E-11	6 450E 10	1 083E 10
54 795	7 091E-10	8 227E 11	6 512E-10	1 165E 10
57 534	7 141E 10	8 789E-11	6 563E 10	1 243E-10
60 274	7 182E-10	9 325E 11	6 605E-10	1 317E 10
63 014	7 216E 10	9 837E-11	6 640E-10	1 387E 10
65 753	7 244E-10	1 032E 10	6 669E 10	1 454E 10
68 493	7 267E 10	1 078E 10	6 693E 10	1 517E 10
71 233	7 285E 10	1 122E 10	6 713E-10	1 576E 10
73 973	7 301E 10	1 163E 10	6 730E 10	1 631E-10
76 712	7 313E 10	1 202E-10	6 743E 10	1 684E-10
79 452	7 324E 10	1 239E-10	6 755E 10	1 733E-10
82 192	7 332E 10	1 274E 10	6 764E-10	1 779E 10
84 932	7 339E 10	1 307E 10	6 772E 10	1 823E-10
87 671	7 345E 10	1 338E-10	6 778E 10	1 863E-10
90 411	7 349E-10	1 367E 10	6 783E 10	1 902E-10
93 151	7 353E-10	1 395E 10	6 788E-10	1 937E-10
95 89	7 356E 10	1 421E-10	6 792E-10	1 971E-10
98 63	7 359E 10	1 446E 10	6 795E-10	2 002E-10
101 37	7 361E-10	1 469E-10	6 797E-10	2 032E-10
104 11	7 363E-10	1 491E-10	6 799E-10	2 060E-10
106 85	7 364E-10	1 511E 10	6 801E-10	2 086E-10
109 59	7 365E-10	1 531E-10	6 802E-10	2 110E-10
112 33	7 366E 10	1 549E 10	6 803E-10	2 133E-10
115 07	7 367E-10	1 567E-10	6 804E 10	2 154E-10
117 81	7 368E-10	1 583E 10	6 805E-10	2 174E-10
120 55	7 368E 10	1 599E-10	6 806E-10	2 193E-10
123 29	7 369E 10	1 613E 10	6 807E 10	2 210E-10
126 03	7 369E 10	1 627E 10	6 807E 10	2 227E-10
128 77	7 369E-10	1 640E 10	6 807E 10	2 242E 10
131 51	7 370E 10	1 652E 10	6 808E 10	2 256E 10
134 25	7 370E-10	1 664E-10	6 808E 10	2 270E-10
136 99	7 370E 10	1 675E 10	6 808E 10	2 283E 10
139 73	7 370E 10	1 685E 10	6 808E-10	2 294E 10
142 47	7 370E-10	1 695E 10	6 808E 10	2 306E-10
145 21	7 370E-10	1 704E 10	6 809E 10	2 316E-10
147 95	7 370E 10	1 713E 10	6 809E 10	2 326E-10
150 68	7 371E-10	1 721E 10	6 809E-10	2 335E-10
153 42	7 371E 10	1 729E-10	6 809E 10	2 343E-10
156 16	7 371E 10	1 736E 10	6 809E 10	2 351E 10
158 9	7 371E 10	1 743E 10	6 809E-10	2 359E-10
161 64	7 371E 10	1 749E-10	6 809E 10	2 366E-10
164 38	7 371E-10	1 755E-10	6 809E-10	2 372E-10
167 12	7 371E 10	1 761E 10	6 809E 10	2 379E-10
169 86	7 371E-10	1 767E-10	6 809E 10	2 384E-10
172 6	7 371E-10	1 772E-10	6 809E-10	2 390E-10
175 34	7 371E-10	1 777E-10	6 809E-10	2 395E-10
178 08	7 371E 10	1 781E 10	6 809E 10	2 399E-10
180 82	7 371E-10	1 786E-10	6 809E-10	2 404E-10
183 56	7 371E 10	1 790E-10	6 809E-10	2 408E-10
186 3	7 371E 10	1 794E-10	6 809E-10	2 412E-10
189 04	7 371E-10	1 797E-10	6 809E-10	2 416E-10
191 78	7 371E 10	1 801E-10	6 809E-10	2 419E-10
194 52	7 371E 10	1 804E-10	6 809E-10	2 422E-10
197 26	7 371E 10	1 807E 10	6 809E 10	2 425E 10
200	7 371E-10	1 810E-10	6 809E 10	2 428E-10
202 74	7 371E-10	1 813E 10	6 809E-10	2 431E-10
205 48	7 371E-10	1 816E-10	6 809E-10	2 433E-10
208 22	7 371E-10	1 818E-10	6 809E-10	2 435E-10
210 96	7 371E-10	1 820E-10	6 809E-10	2 438E-10
213 7	7 371E 10	1 823E-10	6 809E-10	2 440E-10
216 44	7 371E-10	1 825E-10	6 809E-10	2 442E 10
219 18	7 371E-10	1 827E-10	6 809E 10	2 443E-10
221 92	7 371E-10	1 828E 10	6 809E-10	2 445E-10
224 66	7 371E-10	1 830E-10	6 809E-10	2 447E-10
227 4	7 371E-10	1 832E-10	6 809E-10	2 448E-10
230 14	7 371E-10	1 833E-10	6 809E-10	2 449E-10
232 88	7 371E-10	1 835E-10	6 809E-10	2 451E-10
235 62	7 371E-10	1 836E-10	6 809E-10	2 452E-10
238 36	7 371E-10	1 838E-10	6 809E-10	2 453E-10
241 1	7 371E-10	1 839E-10	6 809E-10	2 454E-10
243 84	7 371E-10	1 840E-10	6 809E-10	2 455E-10
246 58	7 371E-10	1 841E-10	6 809E-10	2 456E-10
249 32	7 371E-10	1 842E-10	6 809E-10	2 457E-10
252 05	7 371E-10	1 843E-10	6 809E-10	2 458E-10
254 79	7 371E-10	1 844E-10	6 809E-10	2 458E-10
257 53	7 371E-10	1 845E 10	6 809E-10	2 459E-10
260 27	7 371E-10	1 846E-10	6 809E-10	2 460E-10
263 01	7 371E-10	1 847E 10	6 809E-10	2 460E-10
265 75	7 371E 10	1 847E-10	6 809E-10	2 461E-10
268 49	7 371E 10	1 848E-10	6 809E-10	2 461E-10
271 23	7 371E-10	1 849E-10	6 809E-10	2 462E-10
273 97	7 371E-10	1 849E-10	6 809E-10	2 462E-10

C_o = 0.0039 M	k_h = 10	L = 1.0 m	Δx = 0.01 m	n = 0.80
D_{ac} =19.6 x 10^{-10} m^2/s	D_{as} = 20.3e^{-10} m^2/s			$R_{ac} = R_{as} = 1$

Case	NM	EI	E	I
ω	0.0	0.63	0.63	0.0
τ_n	0.120	0.039	0.120	0.039
Time (yr)	FLUX, J(x=L) mol/m^2s	FLUX, J(x=L) mol/m^2s	FLUX, J(x=L) mol/m^2s	FLUX, J(x=L) mol/m^2s
2.7397	4.875E-13	1.341E-18	4.051E-13	1.215E-18
5.4795	2.045E-11	9.936E-16	1.366E-11	5.370E-15
8.2192	9.530E-11	3.511E-14	6.341E-11	1.941E-13
10.959	2.077E-10	3.104E-13	1.431E-10	8.592E-13
13.699	3.366E-10	1.312E-12	2.325E-10	3.483E-12
16.438	4.603E-10	3.605E-12	3.196E-10	9.532E-12
19.178	5.703E-10	7.558E-12	3.972E-10	2.244E-11
21.918	6.644E-10	1.325E-11	4.643E-10	3.959E-11
24.658	7.432E-10	2.054E-11	5.211E-10	6.124E-11
27.397	8.085E-10	2.914E-11	5.686E-10	8.651E-11
30.137	8.623E-10	3.874E-11	6.083E-10	1.144E-10
32.877	9.065E-10	4.904E-11	6.412E-10	1.439E-10
35.616	9.427E-10	5.975E-11	6.685E-10	1.742E-10
38.356	9.723E-10	7.066E-11	6.911E-10	2.047E-10
41.096	9.966E-10	8.159E-11	7.098E-10	2.347E-10
43.836	1.016E-09	9.239E-11	7.254E-10	2.640E-10
46.575	1.033E-09	1.030E-10	7.382E-10	2.923E-10
49.315	1.046E-09	1.133E-10	7.489E-10	3.193E-10
52.055	1.057E-09	1.232E-10	7.577E-10	3.450E-10
54.795	1.066E-09	1.328E-10	7.650E-10	3.693E-10
57.534	1.073E-09	1.419E-10	7.711E-10	3.922E-10
60.274	1.079E-09	1.507E-10	7.761E-10	4.137E-10
63.014	1.083E-09	1.590E-10	7.802E-10	4.339E-10
65.753	1.087E-09	1.670E-10	7.837E-10	4.527E-10
68.493	1.091E-09	1.745E-10	7.866E-10	4.703E-10
71.233	1.093E-09	1.817E-10	7.889E-10	4.867E-10
73.973	1.095E-09	1.885E-10	7.909E-10	5.019E-10
76.712	1.097E-09	1.949E-10	7.925E-10	5.161E-10
79.452	1.099E-09	2.010E-10	7.939E-10	5.292E-10
82.192	1.100E-09	2.068E-10	7.950E-10	5.415E-10
84.932	1.101E-09	2.122E-10	7.959E-10	5.528E-10
87.671	1.102E-09	2.173E-10	7.967E-10	5.634E-10
90.411	1.102E-09	2.222E-10	7.973E-10	5.731E-10
93.151	1.103E-09	2.268E-10	7.979E-10	5.822E-10
95.89	1.103E-09	2.312E-10	7.983E-10	5.906E-10
98.63	1.104E-09	2.353E-10	7.987E-10	5.984E-10
101.37	1.104E-09	2.392E-10	7.990E-10	6.056E-10
104.11	1.104E-09	2.428E-10	7.992E-10	6.122E-10
106.85	1.104E-09	2.463E-10	7.994E-10	6.184E-10
109.59	1.104E-09	2.496E-10	7.996E-10	6.242E-10
112.33	1.105E-09	2.527E-10	7.997E-10	6.295E-10
115.07	1.105E-09	2.556E-10	7.998E-10	6.344E-10
117.81	1.105E-09	2.584E-10	7.999E-10	6.389E-10
120.55	1.105E-09	2.610E-10	8.000E-10	6.432E-10
123.29	1.105E-09	2.635E-10	8.001E-10	6.471E-10
126.03	1.105E-09	2.658E-10	8.002E-10	6.507E-10
128.77	1.105E-09	2.680E-10	8.002E-10	6.540E-10
131.51	1.105E-09	2.701E-10	8.002E-10	6.571E-10
134.25	1.105E-09	2.721E-10	8.003E-10	6.600E-10
136.99	1.105E-09	2.740E-10	8.003E-10	6.627E-10
139.73	1.105E-09	2.757E-10	8.003E-10	6.651E-10
142.47	1.105E-09	2.774E-10	8.003E-10	6.674E-10
145.21	1.105E-09	2.790E-10	8.003E-10	6.695E-10
147.95	1.105E-09	2.805E-10	8.004E-10	6.715E-10
150.68	1.105E-09	2.819E-10	8.004E-10	6.733E-10
153.42	1.105E-09	2.832E-10	8.004E-10	6.750E-10
156.16	1.105E-09	2.845E-10	8.004E-10	6.765E-10
158.9	1.105E-09	2.857E-10	8.004E-10	6.779E-10
161.64	1.105E-09	2.868E-10	8.004E-10	6.793E-10
164.38	1.105E-09	2.879E-10	8.004E-10	6.805E-10
167.12	1.105E-09	2.889E-10	8.004E-10	6.817E-10
169.86	1.105E-09	2.898E-10	8.004E-10	6.827E-10
172.6	1.105E-09	2.908E-10	8.004E-10	6.837E-10
175.34	1.105E-09	2.916E-10	8.004E-10	6.846E-10
178.08	1.105E-09	2.924E-10	8.004E-10	6.854E-10
180.82	1.105E-09	2.932E-10	8.004E-10	6.862E-10
183.56	1.105E-09	2.939E-10	8.004E-10	6.869E-10
186.3	1.105E-09	2.946E-10	8.004E-10	6.875E-10
189.04	1.105E-09	2.952E-10	8.004E-10	6.882E-10
191.78	1.105E-09	2.959E-10	8.004E-10	6.888E-10
194.52	1.105E-09	2.964E-10	8.004E-10	6.893E-10
197.26	1.105E-09	2.970E-10	8.004E-10	6.898E-10
200	1.105E-09	2.975E-10	8.004E-10	6.903E-10
202.74	1.105E-09	2.980E-10	8.004E-10	6.907E-10
205.48	1.105E-09	2.985E-10	8.004E-10	6.911E-10
208.22	1.105E-09	2.989E-10	8.004E-10	6.914E-10
210.96	1.105E-09	2.993E-10	8.004E-10	6.918E-10
213.7	1.105E-09	2.997E-10	8.004E-10	6.921E-10
216.44	1.105E-09	3.001E-10	8.004E-10	6.924E-10
219.18	1.105E-09	3.005E-10	8.004E-10	6.926E-10
221.92	1.105E-09	3.008E-10	8.004E-10	6.929E-10
224.66	1.105E-09	3.011E-10	8.004E-10	6.931E-10
227.4	1.105E-09	3.014E-10	8.004E-10	6.933E-10
230.14	1.105E-09	3.017E-10	8.004E-10	6.935E-10
232.88	1.105E-09	3.020E-10	8.004E-10	6.937E-10
235.62	1.105E-09	3.022E-10	8.004E-10	6.938E-10
238.36	1.105E-09	3.025E-10	8.004E-10	6.940E-10
241.1	1.105E-09	3.027E-10	8.004E-10	6.941E-10
243.84	1.105E-09	3.029E-10	8.004E-10	6.943E-10
246.58	1.105E-09	3.031E-10	8.004E-10	6.944E-10
249.32	1.105E-09	3.033E-10	8.004E-10	6.945E-10
252.05	1.105E-09	3.035E-10	8.004E-10	6.946E-10
254.79	1.105E-09	3.037E-10	8.004E-10	6.947E-10
257.53	1.105E-09	3.038E-10	8.004E-10	6.948E-10
260.27	1.105E-09	3.040E-10	8.004E-10	6.949E-10
263.01	1.105E-09	3.041E-10	8.004E-10	6.950E-10
265.75	1.105E-09	3.043E-10	8.004E-10	6.950E-10
268.49	1.105E-09	3.044E-10	8.004E-10	6.951E-10
271.23	1.105E-09	3.045E-10	8.004E-10	6.952E-10
273.97	1.105E-09	3.046E-10	8.004E-10	6.952E-10

C_o = 0.0039 M	k_h = 100	L = 1.0 m	Δx = 0.01 m	n = 0.80
D_{ac} =19.6 x 10^{-10} m^2/s	D_{as} = 20.3e^{-10} m^2/s			$R_{ac} = R_{as} = 1$

Case	NM	EI	E	I
ω	0.0	0.63	0.63	0.0
τ_n	0.120	0.039	0.120	0.039
Time (yr)	FLUX, J(x=L) mol/m^2s	FLUX, J(x=L) mol/m^2s	FLUX, J(x=L) mol/m^2s	FLUX, J(x=L) mol/m^2s
2.7397	1.108E-11	3.102E-18	9.410E-13	7.825E-15
5.4795	3.830E-10	4.834E-15	3.713E-11	6.486E-12
8.2192	1.576E-09	2.846E-13	1.864E-10	1.888E-10
10.959	3.073E-09	3.531E-12	4.373E-10	1.123E-09
13.699	4.317E-09	1.856E-11	7.255E-10	2.859E-09
16.438	5.172E-09	5.840E-11	1.004E-09	4.568E-09
19.178	5.707E-09	1.327E-10	1.252E-09	5.680E-09
21.918	6.026E-09	2.431E-10	1.462E-09	6.230E-09
24.658	6.211E-09	3.841E-10	1.636E-09	6.455E-09
27.397	6.316E-09	5.466E-10	1.778E-09	6.535E-09
30.137	6.376E-09	7.203E-10	1.893E-09	6.561E-09
32.877	6.409E-09	8.560E-10	1.986E-09	6.569E-09
35.616	6.428E-09	1.067E-09	2.061E-09	6.572E-09
38.356	6.439E-09	1.227E-09	2.121E-09	6.572E-09
41.096	6.445E-09	1.372E-09	2.169E-09	6.572E-09
43.836	6.448E-09	1.501E-09	2.207E-09	6.572E-09
46.575	6.450E-09	1.612E-09	2.238E-09	6.572E-09
49.315	6.451E-09	1.706E-09	2.262E-09	6.572E-09
52.055	6.451E-09	1.784E-09	2.282E-09	6.572E-09
54.795	6.452E-09	1.848E-09	2.297E-09	6.572E-09
57.534	6.452E-09	1.899E-09	2.310E-09	6.572E-09
60.274	6.452E-09	1.939E-09	2.320E-09	6.572E-09
63.014	6.452E-09	1.970E-09	2.328E-09	6.572E-09
65.753	6.452E-09	1.993E-09	2.334E-09	6.572E-09
68.493	6.452E-09	2.012E-09	2.339E-09	6.572E-09
71.233	6.452E-09	2.025E-09	2.344E-09	6.572E-09
73.973	6.452E-09	2.035E-09	2.347E-09	6.572E-09
76.712	6.452E-09	2.043E-09	2.349E-09	6.572E-09
79.452	6.452E-09	2.048E-09	2.351E-09	6.572E-09
82.192	6.452E-09	2.052E-09	2.353E-09	6.572E-09
84.932	6.452E-09	2.055E-09	2.354E-09	6.572E-09
87.671	6.452E-09	2.057E-09	2.355E-09	6.572E-09
90.411	6.452E-09	2.059E-09	2.356E-09	6.572E-09
93.151	6.452E-09	2.060E-09	2.357E-09	6.572E-09
95.89	6.452E-09	2.060E-09	2.358E-09	6.572E-09
98.63	6.452E-09	2.061E-09	2.358E-09	6.572E-09
101.37	6.452E-09	2.061E-09	2.358E-09	6.572E-09
104.11	6.452E-09	2.062E-09	2.359E-09	6.572E-09
106.85	6.452E-09	2.062E-09	2.359E-09	6.572E-09
109.59	6.452E-09	2.062E-09	2.359E-09	6.572E-09
112.33	6.452E-09	2.062E-09	2.359E-09	6.572E-09
115.07	6.452E-09	2.062E-09	2.359E-09	6.572E-09
117.81	6.452E-09	2.062E-09	2.359E-09	6.572E-09
120.55	6.452E-09	2.062E-09	2.359E-09	6.572E-09
123.29	6.452E-09	2.062E-09	2.359E-09	6.572E-09
126.03	6.452E-09	2.062E-09	2.359E-09	6.572E-09
128.77	6.452E-09	2.062E-09	2.360E-09	6.572E-09
131.51	6.452E-09	2.062E-09	2.360E-09	6.572E-09
134.25	6.452E-09	2.062E-09	2.360E-09	6.572E-09
136.99	6.452E-09	2.062E-09	2.360E-09	6.572E-09
139.73	6.452E-09	2.062E-09	2.360E-09	6.572E-09
142.47	6.452E-09	2.062E-09	2.360E-09	6.572E-09
145.21	6.452E-09	2.062E-09	2.360E-09	6.572E-09
147.95	6.452E-09	2.062E-09	2.360E-09	6.572E-09
150.68	6.452E-09	2.062E-09	2.360E-09	6.572E-09
153.42	6.452E-09	2.062E-09	2.360E-09	6.572E-09
156.16	6.452E-09	2.062E-09	2.360E-09	6.572E-09
158.9	6.452E-09	2.062E-09	2.360E-09	6.572E-09
161.64	6.452E-09	2.062E-09	2.360E-09	6.572E-09
164.38	6.452E-09	2.062E-09	2.360E-09	6.572E-09
167.12	6.452E-09	2.062E-09	2.360E-09	6.572E-09
169.86	6.452E-09	2.062E-09	2.360E-09	6.572E-09
172.6	6.452E-09	2.062E-09	2.360E-09	6.572E-09
175.34	6.452E-09	2.062E-09	2.360E-09	6.572E-09
178.08	6.452E-09	2.062E-09	2.360E-09	6.572E-09
180.82	6.452E-09	2.062E-09	2.360E-09	6.572E-09
183.56	6.452E-09	2.062E-09	2.360E-09	6.572E-09
186.3	6.452E-09	2.062E-09	2.360E-09	6.572E-09
189.04	6.452E-09	2.062E-09	2.360E-09	6.572E-09
191.78	6.452E-09	2.062E-09	2.360E-09	6.572E-09
194.52	6.452E-09	2.062E-09	2.360E-09	6.572E-09
197.26	6.452E-09	2.062E-09	2.360E-09	6.572E-09
200	6.452E-09	2.062E-09	2.360E-09	6.572E-09
202.74	6.452E-09	2.062E-09	2.360E-09	6.572E-09
205.48	6.452E-09	2.062E-09	2.360E-09	6.572E-09
208.22	6.452E-09	2.062E-09	2.360E-09	6.572E-09
210.96	6.452E-09	2.062E-09	2.360E-09	6.572E-09
213.7	6.452E-09	2.062E-09	2.360E-09	6.572E-09
216.44	6.452E-09	2.062E-09	2.360E-09	6.572E-09
219.18	6.452E-09	2.062E-09	2.360E-09	6.572E-09
221.92	6.452E-09	2.062E-09	2.360E-09	6.572E-09
224.66	6.452E-09	2.062E-09	2.360E-09	6.572E-09
227.4	6.452E-09	2.062E-09	2.360E-09	6.572E-09
230.14	6.452E-09	2.062E-09	2.360E-09	6.572E-09
232.88	6.452E-09	2.062E-09	2.360E-09	6.572E-09
235.62	6.452E-09	2.062E-09	2.360E-09	6.572E-09
238.36	6.452E-09	2.062E-09	2.360E-09	6.572E-09
241.1	6.452E-09	2.062E-09	2.360E-09	6.572E-09
243.84	6.452E-09	2.062E-09	2.360E-09	6.572E-09
246.58	6.452E-09	2.062E-09	2.360E-09	6.572E-09
249.32	6.452E-09	2.062E-09	2.360E-09	6.572E-09
252.05	6.452E-09	2.062E-09	2.360E-09	6.572E-09
254.79	6.452E-09	2.062E-09	2.360E-09	6.572E-09
257.53	6.452E-09	2.062E-09	2.360E-09	6.572E-09
260.27	6.452E-09	2.062E-09	2.360E-09	6.572E-09
263.01	6.452E-09	2.062E-09	2.360E-09	6.572E-09
265.75	6.452E-09	2.062E-09	2.360E-09	6.572E-09
268.49	6.452E-09	2.062E-09	2.360E-09	6.572E-09
271.23	6.452E-09	2.062E-09	2.360E-09	6.572E-09
273.97	6.452E-09	2.062E-09	2.360E-09	6.572E-09

C_o = 0.047 M	i_b = 0	L = 1.0 m	Δx = 0.01 m	n = 0.78
D_{ac} =19.6 x 10^{-10} m^2/s		D_{aa} = 20.3e^{-10} m^2/s		$R_{dc} = R_{da}$ = 1
Case	NM	EI	E	I
ω	0.0	0.14	0.14	0.0
τ_s	0.120	0.119	0.120	0.119
x (m)	Salt Conc Mol/m^3	Salt Conc Mol/m^3	Salt Conc Mol/m^3	Salt Conc Mol/m^3
0 005	46 535	42 771	42 794	46 535
0 015	46 069	42 276	42 299	46 069
0 025	45 604	41 783	41 806	45 604
0 035	45 138	41 292	41 315	45 138
0 045	44 673	40 802	40 825	44 673
0 055	44 208	40 315	40 338	44 207
0 065	43 742	39 829	39 852	43 742
0 075	43 277	39 344	39 367	43 277
0 085	42 811	38 861	38 885	42 811
0 095	42 346	38 380	38 404	42 346
0 105	41 881	37 901	37 925	41 880
0 115	41 415	37 423	37 447	41 415
0 125	40 950	36 947	36 971	40 949
0 135	40 485	36 473	36 496	40 484
0 145	40 019	36 000	36 023	40 019
0 155	39 554	35 529	35 552	39 553
0 165	39 088	35 059	35 082	39 088
0 175	38 623	34 591	34 614	38 622
0 185	38 158	34 124	34 148	38 157
0 195	37 692	33 659	33 682	37 691
0 205	37 227	33 195	33 219	37 226
0 215	36 761	32 733	32 757	36 761
0 225	36 296	32 273	32 296	36 295
0 235	35 831	31 814	31 837	35 830
0 245	35 365	31 356	31 379	35 364
0 255	34 900	30 899	30 922	34 899
0 265	34 435	30 445	30 467	34 433
0 275	33 969	29 991	30 014	33 968
0 285	33 504	29 539	29 561	33 503
0 295	33 038	29 088	29 111	33 037
0 305	32 573	28 639	28 661	32 572
0 315	32 108	28 191	28 213	32 106
0 325	31 642	27 744	27 766	31 641
0 335	31 177	27 299	27 321	31 176
0 345	30 712	26 855	26 877	30 710
0 355	30 246	26 412	26 434	30 245
0 365	29 781	25 971	25 992	29 779
0 375	29 315	25 531	25 552	29 314
0 385	28 850	25 092	25 113	28 849
0 395	28 385	24 655	24 675	28 383
0 405	27 919	24 218	24 239	27 918
0 415	27 454	23 783	23 804	27 453
0 425	26 989	23 350	23 370	26 987
0 435	26 523	22 917	22 937	26 522
0 445	26 058	22 486	22 505	26 056
0 455	25 593	22 055	22 075	25 591
0 465	25 127	21 626	21 645	25 126
0 475	24 662	21 199	21 217	24 660
0 485	24 197	20 772	20 791	24 195
0 495	23 731	20 347	20 365	23 730
0 505	23 266	19 922	19 940	23 264
0 515	22 801	19 499	19 517	22 799
0 525	22 335	19 077	19 095	22 334
0 535	21 870	18 656	18 673	21 868
0 545	21 405	18 236	18 253	21 403
0 555	20 939	17 818	17 834	20 938
0 565	20 474	17 400	17 416	20 472
0 575	20 009	16 984	17 000	20 007
0 585	19 543	16 568	16 584	19 542
0 595	19 078	16 154	16 169	19 076
0 605	18 613	15 741	15 756	18 611
0 515	18 147	15 328	15 343	18 146
0 625	17 682	14 917	14 932	17 681
0 635	17 217	14 507	14 521	17 215
0 645	16 751	14 098	14 112	16 750
0 655	16 286	13 690	13 704	16 285
0 665	15 821	13 283	13 296	15 819
0 675	15 355	12 877	12 890	15 354
0 685	14 890	12 472	12 485	14 889
0 695	14 425	12 068	12 080	14 423
0 705	13 959	11 665	11 677	13 958
0 715	13 494	11 263	11 274	13 493
0 725	13 029	10 862	10 873	13 028
0 735	12 563	10 462	10 472	12 562
0 745	12 098	10 062	10 073	12 097
0 755	11 633	9 664	9 674	11 632
0 765	11 167	9 267	9 277	11 166
0 775	10 702	8 871	8 880	10 701
0 785	10 237	8 475	8 484	10 236
0 795	9 771	8 081	8 089	9 771
0 805	9 306	7 687	7 696	9 305
0 815	8 841	7 295	7 303	8 840
0 825	8 376	6 903	6 910	8 375
0 835	7 910	6 512	6 519	7 910
0 845	7 445	6 122	6 129	7 444
0 855	6 980	5 733	5 739	6 979
0 865	6 514	5 345	5 351	6 514
0 875	6 049	4 958	4 963	6 048
0 885	5 584	4 571	4 576	5 583
0 895	5 118	4 186	4 190	5 118
0 905	4 653	3 801	3 805	4 653
0 915	4 188	3 417	3 421	4 187
0 925	3 722	3 034	3 038	3 722
0 935	3 257	2 652	2 655	3 257
0 945	2 792	2 271	2 273	2 792
0 955	2 327	1 890	1 892	2 326
0 965	1 861	1 511	1 512	1 861
0 975	1 396	1 132	1 133	1 396
0 985	0 931	0 754	0 755	0 931
0 995	0 465	0 376	0 377	0 465

C_o = 0.047 M	i_b = 10	L = 1.0 m	Δx = 0.01 m	n = 0.78
D_{ac} =19.6 x 10^{-10} m^2/s		D_{aa} = 20.3e^{-10} m^2/s		$R_{dc} = R_{da}$ = 1
Case	NM	EI	E	I
ω	0.0	0.14	0.14	0.0
τ_s	0.120	0.119	0.120	0.119
x (m)	Salt Conc Mol/m^3	Salt Conc Mol/m^3	Salt Conc Mol/m^3	Salt Conc Mol/m^3
0 005	46 695	42 935	42 957	46 696
0 015	46 388	42 513	42 634	46 390
0 025	46 078	42 290	42 310	46 082
0 035	45 766	41 964	41 983	45 771
0 045	45 451	41 636	41 655	45 457
0 055	45 134	41 306	41 324	45 141
0 065	44 815	40 974	40 991	44 822
0 075	44 492	40 640	40 656	44 501
0 085	44 167	40 303	40 319	44 177
0 095	43 840	39 964	39 979	43 851
0 105	43 510	39 624	39 638	43 522
0 115	43 177	39 281	39 294	43 190
0 125	42 842	38 935	38 948	42 856
0 135	42 504	38 588	38 600	42 519
0 145	42 164	38 239	38 250	42 180
0 155	41 820	37 887	37 898	41 837
0 165	41 474	37 533	37 543	41 492
0 175	41 125	37 177	37 187	41 144
0 185	40 774	36 819	36 828	40 793
0 195	40 420	36 458	36 467	40 440
0 205	40 062	36 096	36 104	40 084
0 215	39 702	35 731	35 738	39 724
0 225	39 339	35 364	35 371	39 362
0 235	38 973	34 995	35 001	38 997
0 245	38 605	34 623	34 629	38 629
0 255	38 233	34 250	34 255	38 258
0 265	37 858	33 874	33 879	37 884
0 275	37 481	33 496	33 500	37 508
0 285	37 100	33 116	33 120	37 128
0 295	36 717	32 734	32 737	36 745
0 305	36 330	32 349	32 352	36 359
0 315	35 940	31 962	31 965	35 970
0 325	35 547	31 573	31 575	35 577
0 335	35 151	31 182	31 184	35 182
0 345	34 752	30 789	30 790	34 783
0 355	34 350	30 393	30 394	34 382
0 365	33 944	29 995	29 996	33 977
0 375	33 535	29 595	29 595	33 568
0 385	33 123	29 193	29 193	33 157
0 395	32 708	28 789	28 788	32 742
0 405	32 289	28 382	28 381	32 324
0 415	31 867	27 973	27 972	31 902
0 425	31 442	27 562	27 560	31 478
0 435	31 013	27 149	27 147	31 049
0 445	30 581	26 734	26 731	30 618
0 455	30 146	26 316	26 313	30 182
0 465	29 707	25 896	25 893	29 744
0 475	29 264	25 474	25 471	29 301
0 485	28 818	25 050	25 046	28 856
0 495	28 369	24 623	24 620	28 406
0 505	27 916	24 195	24 191	27 953
0 515	27 459	23 764	23 760	27 497
0 525	26 999	23 331	23 326	27 037
0 535	26 534	22 896	22 891	26 573
0 545	26 067	22 458	22 453	26 105
0 555	25 595	22 018	22 014	25 634
0 565	25 120	21 577	21 572	25 158
0 575	24 641	21 133	21 127	24 679
0 585	24 158	20 686	20 681	24 197
0 595	23 672	20 238	20 233	23 710
0 605	23 181	19 787	19 782	23 219
0 615	22 687	19 335	19 329	22 725
0 625	22 188	18 880	18 874	22 226
0 635	21 686	18 422	18 417	21 724
0 645	21 180	17 963	17 957	21 217
0 655	20 669	17 502	17 496	20 706
0 665	20 155	17 038	17 032	20 192
0 675	19 636	16 572	16 566	19 673
0 685	19 114	16 104	16 098	19 150
0 695	18 587	15 634	15 628	18 622
0 705	18 056	15 162	15 156	18 091
0 715	17 521	14 687	14 681	17 555
0 725	16 981	14 210	14 205	17 015
0 735	16 437	13 732	13 726	16 471
0 745	15 889	13 251	13 245	15 922
0 755	15 337	12 767	12 762	15 369
0 765	14 780	12 282	12 277	14 811
0 775	14 219	11 795	11 789	14 249
0 785	13 653	11 305	11 300	13 683
0 795	13 083	10 813	10 808	13 112
0 805	12 508	10 320	10 315	12 536
0 815	11 928	9 824	9 819	11 956
0 825	11 344	9 326	9 321	11 371
0 835	10 756	8 825	8 821	10 781
0 845	10 162	8 323	8 319	10 186
0 855	9 564	7 819	7 814	9 587
0 865	8 961	7 312	7 308	8 983
0 875	8 354	6 803	6 800	8 374
0 885	7 741	6 293	6 289	7 761
0 895	7 124	5 780	5 776	7 142
0 905	6 502	5 265	5 262	6 518
0 915	5 874	4 748	4 745	5 890
0 925	5 242	4 228	4 226	5 256
0 935	4 605	3 707	3 705	4 617
0 945	3 963	3 184	3 182	3 973
0 955	3 315	2 658	2 657	3 324
0 965	2 663	2 131	2 129	2 670
0 975	2 005	1 601	1 600	2 011
0 985	1 342	1 070	1 069	1 346
0 995	0 674	0 536	0 535	0 676

C_o = 0.047 M	i_b = 100	L = 1.0 m	Δx = 0.01 m	n = 0.78
D_{ac} =19.6 x 10^{-10} m^2/s		D_{as} = 20.3e^{-10} m^2/s		$R_{ac} = R_{as} = 1$
Case	NM	EI	E	I
ω	0.0	0.14	0.14	0.0
τ_a	0.120	0.119	0.120	0.119
x (m)	Salt Conc Mol/m^3	Salt Conc Mol/m^3	Salt Conc Mol/m^3	Salt Conc Mol/m^3
0 005	46 999	43 196	43 219	46 999
0 015	46 998	43 196	43 218	46 998
0 025	46 997	43 195	43 218	46 997
0 035	46 995	43 195	43 217	46 996
0 045	46 994	43 194	43 217	46 995
0 055	46 992	43 193	43 216	46 993
0 065	46 991	43 193	43 215	46 992
0 075	46 989	43 192	43 214	46 990
0 085	46 987	43 191	43 213	46 988
0 095	46 985	43 190	43 212	46 986
0 105	46 982	43 189	43 211	46 984
0 115	46 980	43 188	43 210	46 982
0 125	46 977	43 186	43 209	46 979
0 135	46 974	43 185	43 207	46 976
0 145	46 971	43 183	43 205	46 973
0 155	46 967	43 182	43 204	46 970
0 165	46 964	43 180	43 202	46 967
0 175	46 960	43 178	43 199	46 963
0 185	46 955	43 175	43 197	46 959
0 195	46 950	43 173	43 194	46 954
0 205	46 945	43 170	43 191	46 949
0 215	46 939	43 167	43 188	46 944
0 225	46 933	43 164	43 185	46 938
0 235	46 926	43 160	43 181	46 932
0 245	46 919	43 156	43 177	46 925
0 255	46 911	43 151	43 172	46 917
0 265	46 903	43 146	43 167	46 909
0 275	46 893	43 141	43 161	46 900
0 285	46 883	43 135	43 155	46 890
0 295	46 872	43 128	43 148	46 880
0 305	46 860	43 121	43 141	46 869
0 315	46 848	43 113	43 133	46 856
0 325	46 834	43 105	43 124	46 843
0 335	46 818	43 095	43 114	46 828
0 345	46 802	43 085	43 103	46 812
0 355	46 784	43 073	43 091	46 795
0 365	46 764	43 060	43 078	46 776
0 375	46 743	43 046	43 063	46 756
0 385	46 720	43 031	43 048	46 734
0 395	46 695	43 014	43 030	46 710
0 405	46 668	42 996	43 011	46 684
0 415	46 639	42 975	42 990	46 655
0 425	46 607	42 953	42 967	46 625
0 435	46 573	42 928	42 942	46 591
0 445	46 535	42 901	42 914	46 555
0 455	46 494	42 872	42 884	46 515
0 465	46 450	42 839	42 850	46 473
0 475	46 402	42 803	42 813	46 426
0 485	46 350	42 764	42 773	46 375
0 495	46 294	42 720	42 729	46 320
0 505	46 232	42 673	42 680	46 261
0 515	46 166	42 621	42 627	46 196
0 525	46 093	42 563	42 568	46 126
0 535	46 015	42 500	42 503	46 049
0 545	45 930	42 431	42 433	45 966
0 555	45 837	42 355	42 355	45 876
0 565	45 737	42 272	42 270	45 778
0 575	45 628	42 180	42 177	45 671
0 585	45 510	42 079	42 074	45 555
0 595	45 381	41 969	41 962	45 430
0 605	45 242	41 848	41 839	45 293
0 615	45 091	41 715	41 704	45 145
0 625	44 927	41 569	41 555	44 984
0 635	44 749	41 409	41 393	44 809
0 645	44 555	41 234	41 215	44 619
0 655	44 345	41 042	41 020	44 413
0 665	44 118	40 831	40 807	44 188
0 675	43 870	40 600	40 573	43 945
0 685	43 602	40 347	40 317	43 680
0 695	43 310	40 071	40 037	43 393
0 705	42 994	39 768	39 731	43 081
0 715	42 651	39 436	39 396	42 742
0 725	42 278	39 074	39 030	42 373
0 735	41 874	38 678	38 631	41 973
0 745	41 435	38 245	38 195	41 539
0 755	40 958	37 772	37 719	41 067
0 765	40 441	37 257	37 200	40 554
0 775	39 879	36 694	36 634	39 997
0 785	39 270	36 082	36 018	39 392
0 795	38 608	35 415	35 348	38 735
0 805	37 890	34 690	34 619	38 021
0 815	37 111	33 901	33 828	37 246
0 825	36 265	33 045	32 969	36 404
0 835	35 347	32 116	32 038	35 489
0 845	34 350	31 110	31 030	34 495
0 855	33 268	30 020	29 939	33 416
0 865	32 094	28 843	28 761	32 244
0 875	30 819	27 572	27 489	30 970
0 885	29 436	26 201	26 119	29 587
0 896	27 934	24 725	24 644	28 084
0 905	26 304	23 139	23 060	26 452
0 915	24 534	21 436	21 360	24 680
0 925	22 614	19 611	19 539	22 754
0 935	20 529	17 658	17 591	20 662
0 945	18 266	15 573	15 511	18 390
0 955	15 810	13 349	13 295	15 922
0 965	13 145	10 983	10 937	13 242
0 975	10 251	8 469	8 432	10 330
0 985	7 110	5 803	5 777	7 167
0 996	3 701	2 981	2 967	3 732
	0 000	0 000	0 000	0 000

C_o = 0.020 M	i_b = 0	L = 1.0 m	Δx = 0.01 m	n = 0.79
D_{ac} =19.6 x 10^{-10} m^2/s		D_{as} = 20.3e^{-10} m^2/s		$R_{ac} = R_{as} = 1$
Case	NM	EI	E	I
ω	0.0	0.32	0.32	0.0
τ_a	0.120	0.112	0.120	0.112
x (m)	Salt Conc Mol/m^3	Salt Conc Mol/m^3	Salt Conc Mol/m^3	Salt Conc Mol/m^3
0 005	19 802	17 336	17 531	19 802
0 015	19 604	17 122	17 317	19 604
0 025	19 406	16 908	17 105	19 406
0 035	19 208	16 696	16 893	19 208
0 045	19 010	16 485	16 682	19 010
0 055	18 812	16 275	16 473	18 812
0 065	18 614	16 067	16 265	18 614
0 075	18 416	15 859	16 057	18 416
0 085	18 218	15 653	15 851	18 218
0 095	18 020	15 448	15 646	18 020
0 105	17 822	15 244	15 442	17 822
0 115	17 624	15 041	15 239	17 624
0 125	17 426	14 839	15 036	17 425
0 135	17 228	14 638	14 835	17 227
0 145	17 030	14 439	14 635	17 029
0 155	16 832	14 240	14 436	16 831
0 165	16 634	14 042	14 237	16 633
0 175	16 436	13 846	14 040	16 435
0 185	16 238	13 650	13 843	16 237
0 195	16 040	13 455	13 648	16 039
0 205	15 842	13 261	13 453	15 841
0 215	15 644	13 068	13 259	15 643
0 225	15 446	12 877	13 066	15 445
0 235	15 248	12 686	12 874	15 247
0 245	15 049	12 495	12 683	15 049
0 255	14 851	12 306	12 492	14 851
0 265	14 653	12 118	12 303	14 653
0 275	14 455	11 930	12 114	14 455
0 285	14 257	11 744	11 926	14 257
0 295	14 059	11 558	11 738	14 059
0 305	13 861	11 373	11 552	13 861
0 315	13 663	11 189	11 366	13 663
0 325	13 465	11 005	11 181	13 465
0 335	13 267	10 823	10 997	13 267
0 345	13 069	10 641	10 813	13 069
0 355	12 871	10 460	10 631	12 871
0 365	12 673	10 280	10 449	12 673
0 375	12 475	10 100	10 267	12 474
0 385	12 277	9 921	10 087	12 276
0 395	12 079	9 743	9 907	12 078
0 405	11 881	9 566	9 727	11 880
0 415	11 683	9 389	9 549	11 682
0 425	11 485	9 214	9 371	11 484
0 435	11 287	9 038	9 194	11 286
0 445	11 089	8 864	9 017	11 088
0 455	10 891	8 690	8 841	10 890
0 465	10 693	8 517	8 666	10 692
0 475	10 495	8 345	8 491	10 494
0 485	10 297	8 173	8 317	10 296
0 495	10 099	8 002	8 144	10 098
0 505	9 901	7 831	7 971	9 900
0 515	9 703	7 661	7 799	9 702
0 525	9 505	7 492	7 628	9 504
0 535	9 307	7 323	7 457	9 306
0 545	9 109	7 156	7 286	9 108
0 555	8 911	6 988	7 116	8 910
0 565	8 713	6 821	6 947	8 712
0 575	8 515	6 655	6 779	8 514
0 585	8 317	6 490	6 611	8 316
0 595	8 119	6 325	6 443	8 118
0 605	7 921	6 160	6 276	7 920
0 615	7 723	5 997	6 110	7 722
0 625	7 525	5 833	5 944	7 524
0 635	7 327	5 671	5 779	7 326
0 645	7 129	5 508	5 614	7 128
0 655	6 931	5 347	5 450	6 930
0 665	6 733	5 186	5 286	6 732
0 675	6 535	5 025	5 123	6 534
0 685	6 337	4 865	4 960	6 336
0 695	6 139	4 706	4 798	6 138
0 705	5 941	4 547	4 636	5 940
0 715	5 743	4 389	4 475	5 742
0 725	5 545	4 231	4 314	5 544
0 735	5 347	4 073	4 154	5 346
0 745	5 149	3 916	3 994	5 148
0 755	4 951	3 760	3 835	4 950
0 765	4 752	3 604	3 677	4 752
0 775	4 554	3 449	3 518	4 554
0 785	4 356	3 294	3 360	4 356
0 795	4 158	3 139	3 203	4 158
0 805	3 960	2 986	3 046	3 960
0 815	3 762	2 832	2 890	3 762
0 825	3 564	2 679	2 734	3 564
0 835	3 366	2 526	2 578	3 366
0 845	3 168	2 374	2 423	3 168
0 855	2 970	2 223	2 269	2 970
0 865	2 772	2 072	2 115	2 772
0 875	2 574	1 921	1 961	2 574
0 885	2 376	1 770	1 808	2 376
0 895	2 178	1 621	1 655	2 178
0 905	1 980	1 471	1 502	1 980
0 915	1 782	1 322	1 350	1 782
0 925	1 584	1 174	1 198	1 584
0 935	1 386	1 025	1 047	1 386
0 945	1 188	0 878	0 896	1 188
0 955	0 990	0 730	0 746	0 990
0 965	0 792	0 584	0 596	0 792
0 975	0 594	0 437	0 446	0 594
0 985	0 396	0 291	0 297	0 396
0 995	0 198	0 145	0 148	0 198

C_o = 0.020 M	i_h = 10	L = 1.0 m	Δx = 0.01 m	n = 0.79
D_{ac} =19.6 x 10^{-10} m^2/s		D_{ca} = 20.3e^{-10} m^2/s		$R_{ac} = R_{ca} = 1$
Case	NM	EI	E	I
ω	0.0	0.32	0.32	0.0
τ_2	0.120	0.112	0.120	0.112
x (m)	Salt Conc Mol/m^3	Salt Conc Mol/m^3	Salt Conc Mol/m^3	Salt Conc Mol/m^3
0.005	19.891	17.416	17.607	19.896
0.015	19.780	17.292	17.477	19.790
0.025	19.663	17.167	17.346	19.683
0.035	19.556	17.041	17.215	19.575
0.045	19.442	16.913	17.082	19.466
0.055	19.327	16.785	16.949	19.356
0.065	19.210	16.656	16.814	19.244
0.075	19.092	16.525	16.679	19.131
0.085	18.973	16.394	16.542	19.016
0.095	18.853	16.261	16.405	18.900
0.105	18.731	16.128	16.266	18.783
0.115	18.608	15.993	16.127	18.664
0.125	18.483	15.857	15.987	18.544
0.135	18.357	15.721	15.845	18.423
0.145	18.230	15.583	15.703	18.300
0.155	18.102	15.444	15.560	18.176
0.165	17.972	15.305	15.416	18.050
0.175	17.840	15.164	15.271	17.923
0.185	17.707	15.022	15.125	17.794
0.195	17.573	14.879	14.977	17.664
0.205	17.437	14.735	14.829	17.532
0.215	17.300	14.590	14.680	17.399
0.225	17.161	14.444	14.530	17.264
0.235	17.021	14.297	14.380	17.128
0.245	16.879	14.149	14.228	16.990
0.255	16.736	14.000	14.075	16.850
0.265	16.591	13.850	13.921	16.709
0.275	16.444	13.698	13.766	16.566
0.285	16.296	13.546	13.610	16.421
0.295	16.146	13.393	13.454	16.275
0.305	15.995	13.239	13.296	16.127
0.315	15.841	13.083	13.137	15.977
0.325	15.687	12.927	12.978	15.826
0.335	15.530	12.770	12.817	15.672
0.345	15.372	12.611	12.656	15.517
0.355	15.212	12.452	12.494	15.360
0.365	15.050	12.291	12.330	15.201
0.375	14.887	12.130	12.166	15.041
0.385	14.722	11.967	12.001	14.878
0.395	14.555	11.804	11.834	14.714
0.405	14.386	11.639	11.667	14.547
0.415	14.215	11.474	11.499	14.379
0.425	14.042	11.307	11.330	14.209
0.435	13.868	11.140	11.160	14.037
0.445	13.691	10.971	10.989	13.862
0.455	13.513	10.801	10.817	13.686
0.465	13.333	10.631	10.645	13.507
0.475	13.150	10.459	10.471	13.327
0.485	12.966	10.286	10.296	13.144
0.495	12.780	10.113	10.121	12.959
0.505	12.592	9.938	9.944	12.772
0.515	12.401	9.763	9.767	12.583
0.525	12.209	9.586	9.589	12.392
0.535	12.014	9.408	9.409	12.198
0.545	11.817	9.230	9.229	12.002
0.555	11.618	9.050	9.048	11.804
0.565	11.417	8.870	8.856	11.603
0.575	11.214	8.688	8.683	11.401
0.585	11.008	8.506	8.500	11.195
0.595	10.801	8.322	8.315	10.988
0.605	10.591	8.138	8.129	10.777
0.615	10.378	7.952	7.943	10.565
0.625	10.164	7.766	7.756	10.350
0.635	9.947	7.579	7.567	10.132
0.645	9.727	7.390	7.378	9.912
0.655	9.505	7.201	7.188	9.689
0.665	9.281	7.011	6.997	9.464
0.675	9.054	6.820	6.805	9.236
0.685	8.825	6.628	6.613	9.005
0.695	8.593	6.434	6.419	8.772
0.705	8.359	6.240	6.225	8.535
0.715	8.122	6.046	6.029	8.296
0.725	7.883	5.850	5.833	8.055
0.735	7.641	5.653	5.636	7.810
0.745	7.396	5.455	5.438	7.563
0.755	7.149	5.256	5.239	7.312
0.765	6.899	5.057	5.040	7.059
0.775	6.646	4.856	4.839	6.803
0.785	6.390	4.655	4.638	6.543
0.795	6.132	4.453	4.436	6.281
0.805	5.871	4.249	4.233	6.015
0.815	5.607	4.045	4.029	5.747
0.825	5.340	3.840	3.824	5.475
0.835	5.070	3.634	3.619	5.200
0.845	4.797	3.428	3.412	4.922
0.855	4.521	3.220	3.205	4.641
0.865	4.242	3.011	2.997	4.356
0.875	3.960	2.802	2.788	4.068
0.885	3.675	2.591	2.579	3.776
0.895	3.387	2.380	2.368	3.482
0.905	3.096	2.168	2.157	3.183
0.915	2.801	1.955	1.945	2.881
0.925	2.503	1.741	1.732	2.576
0.935	2.202	1.527	1.518	2.267
0.945	1.898	1.311	1.304	1.954
0.955	1.590	1.095	1.088	1.638
0.965	1.279	0.877	0.872	1.318
0.975	0.964	0.659	0.655	0.994
0.985	0.646	0.440	0.438	0.667
0.995	0.325	0.221	0.219	0.335

C_o = 0.020 M	i_h = 100	L = 1.0 m	Δx = 0.01 m	n = 0.79
D_{ac} =19.6 x 10^{-10} m^2/s		D_{ca} = 20.3e^{-10} m^2/s		$R_{ac} = R_{ca} = 1$
Case	NM	EI	E	I
ω	0.0	0.32	0.32	0.0
τ_2	0.120	0.112	0.120	0.112
x (m)	Salt Conc Mol/m^3	Salt Conc Mol/m^3	Salt Conc Mol/m^3	Salt Conc Mol/m^3
0.005	20.000	17.300	17.529	20.000
0.015	20.000	17.300	17.529	20.000
0.025	20.000	17.300	17.529	20.000
0.035	20.000	17.300	17.529	20.000
0.045	20.000	17.300	17.529	20.000
0.055	20.000	17.300	17.529	20.000
0.065	20.000	17.300	17.528	20.000
0.075	20.000	17.300	17.528	20.000
0.085	20.000	17.300	17.528	20.000
0.095	20.000	17.300	17.528	20.000
0.105	20.000	17.300	17.528	20.000
0.115	20.000	17.300	17.528	20.000
0.125	20.000	17.300	17.528	20.000
0.135	19.999	17.300	17.528	20.000
0.145	19.999	17.300	17.528	20.000
0.155	19.999	17.300	17.528	20.000
0.165	19.999	17.300	17.528	20.000
0.175	19.999	17.300	17.528	20.000
0.185	19.999	17.300	17.528	20.000
0.195	19.999	17.300	17.527	20.000
0.205	19.999	17.300	17.527	20.000
0.215	19.999	17.300	17.527	20.000
0.225	19.998	17.300	17.527	19.999
0.235	19.998	17.300	17.527	19.999
0.245	19.998	17.299	17.526	19.999
0.255	19.998	17.299	17.526	19.999
0.265	19.997	17.299	17.526	19.999
0.275	19.997	17.299	17.525	19.999
0.285	19.997	17.299	17.525	19.999
0.295	19.996	17.299	17.524	19.998
0.305	19.996	17.298	17.524	19.998
0.315	19.995	17.298	17.523	19.998
0.325	19.994	17.298	17.522	19.997
0.335	19.994	17.297	17.521	19.997
0.345	19.993	17.297	17.520	19.996
0.355	19.992	17.296	17.519	19.996
0.365	19.991	17.296	17.518	19.995
0.375	19.990	17.295	17.517	19.995
0.385	19.988	17.294	17.515	19.994
0.395	19.987	17.293	17.513	19.993
0.405	19.985	17.292	17.511	19.992
0.415	19.983	17.291	17.509	19.991
0.425	19.981	17.290	17.506	19.990
0.435	19.979	17.288	17.504	19.988
0.445	19.976	17.287	17.500	19.986
0.455	19.973	17.285	17.496	19.984
0.465	19.970	17.282	17.492	19.982
0.475	19.966	17.280	17.487	19.980
0.485	19.961	17.276	17.482	19.977
0.495	19.956	17.273	17.476	19.974
0.505	19.951	17.269	17.469	19.970
0.515	19.945	17.264	17.461	19.966
0.525	19.938	17.259	17.452	19.961
0.535	19.930	17.253	17.442	19.955
0.545	19.921	17.246	17.430	19.949
0.555	19.910	17.238	17.418	19.942
0.565	19.899	17.229	17.403	19.934
0.575	19.886	17.218	17.386	19.925
0.585	19.871	17.206	17.368	19.914
0.595	19.855	17.192	17.347	19.902
0.605	19.837	17.176	17.323	19.889
0.615	19.816	17.158	17.296	19.873
0.625	19.792	17.137	17.265	19.856
0.635	19.766	17.113	17.231	19.836
0.645	19.736	17.086	17.192	19.813
0.655	19.702	17.054	17.148	19.787
0.665	19.664	17.019	17.098	19.757
0.675	19.621	16.977	17.042	19.724
0.685	19.572	16.930	16.979	19.685
0.695	19.518	16.877	16.908	19.642
0.705	19.456	16.815	16.828	19.592
0.715	19.387	16.745	16.738	19.535
0.725	19.308	16.665	16.636	19.471
0.735	19.220	16.573	16.522	19.398
0.745	19.120	16.469	16.393	19.314
0.755	19.008	16.350	16.249	19.219
0.765	18.881	16.215	16.087	19.111
0.775	18.739	16.061	15.906	18.988
0.785	18.578	15.887	15.703	18.847
0.795	18.396	15.689	15.476	18.688
0.805	18.191	15.465	15.222	18.506
0.815	17.960	15.212	14.940	18.299
0.825	17.700	14.927	14.626	18.063
0.835	17.406	14.605	14.277	17.795
0.845	17.075	14.244	13.890	17.490
0.855	16.702	13.840	13.462	17.142
0.865	16.281	13.388	12.989	16.746
0.875	15.806	12.885	12.469	16.295
0.885	15.270	12.326	11.897	15.782
0.895	14.666	11.707	11.271	15.198
0.905	13.985	11.025	10.587	14.533
0.915	13.217	10.274	9.843	13.776
0.925	12.352	9.453	9.034	12.914
0.935	11.375	8.557	8.159	11.933
0.945	10.274	7.583	7.215	10.815
0.955	9.032	6.528	6.200	9.543
0.965	7.632	5.392	5.111	8.095
0.975	6.053	4.172	3.948	6.447
0.985	4.272	2.867	2.709	4.570
0.995	2.264	1.476	1.393	2.433
	0.000	0.000		

C_o = 0.0087 M	i_b = 0	L = 1.0 m	Δx = 0.01 m	n = 0.79
D_{ac} =19.6 x 10^{-10} m^2/s		D_{aa} = 20.3e^{-10} m^2/s		$R_{dc} = R_{da}$ = 1
Case	NM	EI	E	I
ω	0.0	0.49	0.49	0.0
τ_p	0.120	0.063	0.120	0.063
x (m)	Salt Conc Mol/m^3	Salt Conc Mol/m^3	Salt Conc Mol/m^3	Salt Conc Mol/m^3
0.005	8.614	7.837	8.248	8.614
0.015	8.528	7.745	8.159	8.528
0.025	8.442	7.653	8.070	8.442
0.035	8.355	7.562	7.981	8.355
0.045	8.269	7.471	7.892	8.269
0.055	8.183	7.380	7.803	8.183
0.065	8.097	7.290	7.715	8.097
0.075	8.011	7.200	7.626	8.011
0.085	7.925	7.111	7.538	7.925
0.095	7.839	7.022	7.450	7.839
0.105	7.753	6.933	7.362	7.752
0.115	7.666	6.844	7.274	7.666
0.125	7.580	6.756	7.187	7.580
0.135	7.494	6.669	7.099	7.494
0.145	7.408	6.581	7.012	7.408
0.155	7.322	6.494	6.925	7.322
0.165	7.236	6.407	6.838	7.236
0.175	7.150	6.321	6.751	7.149
0.185	7.063	6.234	6.664	7.063
0.195	6.977	6.149	6.578	6.977
0.205	6.891	6.063	6.491	6.891
0.215	6.805	5.978	6.405	6.805
0.225	6.719	5.893	6.319	6.719
0.235	6.633	5.808	6.233	6.633
0.245	6.547	5.724	6.147	6.546
0.255	6.460	5.640	6.062	6.460
0.265	6.374	5.556	5.976	6.374
0.275	6.288	5.472	5.891	6.288
0.285	6.202	5.389	5.806	6.202
0.295	6.116	5.306	5.720	6.116
0.305	6.030	5.224	5.635	6.030
0.315	5.944	5.141	5.551	5.943
0.325	5.857	5.059	5.466	5.857
0.335	5.771	4.977	5.381	5.771
0.345	5.685	4.896	5.297	5.685
0.355	5.599	4.814	5.213	5.599
0.365	5.513	4.733	5.129	5.513
0.375	5.427	4.653	5.045	5.427
0.385	5.341	4.572	4.961	5.340
0.395	5.254	4.492	4.877	5.254
0.405	5.168	4.412	4.793	5.168
0.415	5.082	4.332	4.710	5.082
0.425	4.996	4.253	4.627	4.996
0.435	4.910	4.173	4.543	4.910
0.445	4.824	4.094	4.460	4.824
0.455	4.738	4.016	4.377	4.737
0.465	4.651	3.937	4.295	4.651
0.475	4.565	3.859	4.212	4.565
0.485	4.479	3.781	4.129	4.479
0.495	4.393	3.703	4.047	4.393
0.505	4.307	3.625	3.965	4.307
0.515	4.221	3.548	3.882	4.221
0.525	4.135	3.471	3.800	4.134
0.535	4.049	3.394	3.718	4.048
0.545	3.962	3.317	3.637	3.962
0.555	3.876	3.240	3.555	3.875
0.565	3.790	3.164	3.473	3.790
0.575	3.704	3.088	3.392	3.704
0.585	3.618	3.012	3.311	3.618
0.595	3.532	2.937	3.230	3.531
0.605	3.446	2.861	3.149	3.445
0.615	3.359	2.786	3.068	3.359
0.625	3.273	2.711	2.987	3.273
0.635	3.187	2.636	2.906	3.187
0.645	3.101	2.562	2.825	3.101
0.655	3.015	2.487	2.745	3.015
0.665	2.929	2.413	2.665	2.929
0.675	2.843	2.339	2.584	2.842
0.685	2.756	2.265	2.504	2.756
0.695	2.670	2.192	2.424	2.670
0.705	2.584	2.118	2.345	2.584
0.715	2.498	2.045	2.265	2.498
0.725	2.412	1.972	2.185	2.412
0.735	2.326	1.899	2.106	2.326
0.745	2.240	1.827	2.026	2.239
0.755	2.153	1.754	1.947	2.153
0.765	2.067	1.682	1.868	2.067
0.775	1.981	1.610	1.789	1.981
0.785	1.895	1.538	1.710	1.895
0.795	1.809	1.466	1.631	1.809
0.805	1.723	1.395	1.552	1.723
0.815	1.637	1.323	1.473	1.637
0.825	1.551	1.252	1.395	1.550
0.835	1.464	1.181	1.317	1.464
0.845	1.378	1.110	1.238	1.378
0.855	1.292	1.040	1.160	1.292
0.865	1.206	0.969	1.082	1.206
0.875	1.120	0.899	1.004	1.120
0.885	1.034	0.829	0.926	1.034
0.895	0.948	0.759	0.848	0.947
0.905	0.861	0.689	0.771	0.861
0.915	0.775	0.619	0.693	0.775
0.925	0.689	0.550	0.616	0.689
0.935	0.603	0.481	0.538	0.603
0.945	0.517	0.412	0.461	0.517
0.955	0.431	0.343	0.384	0.431
0.965	0.345	0.274	0.307	0.345
0.975	0.258	0.205	0.230	0.258
0.985	0.172	0.137	0.153	0.172
0.995	0.086	0.068	0.077	0.086

C_o = 0.0087 M	i_b = 10	L = 1.0 m	Δx = 0.01 m	n = 0.79
D_{ac} =19.6 x 10^{-10} m^2/s		D_{aa} = 20.3e^{-10} m^2/s		$R_{dc} = R_{da}$ = 1
Case	NM	EI	E	I
ω	0.0	0.49	0.49	0.0
τ_p	0.120	0.063	0.120	0.063
x (m)	Salt Conc Mol/m^3	Salt Conc Mol/m^3	Salt Conc Mol/m^3	Salt Conc Mol/m^3
0.005	8.641	7.867	8.264	8.659
0.015	8.581	7.808	8.191	8.618
0.025	8.521	7.748	8.118	8.576
0.035	8.460	7.688	8.044	8.534
0.045	8.399	7.628	7.971	8.491
0.055	8.338	7.567	7.897	8.447
0.065	8.276	7.506	7.823	8.403
0.075	8.214	7.444	7.748	8.359
0.085	8.151	7.382	7.674	8.313
0.095	8.088	7.320	7.599	8.267
0.105	8.024	7.257	7.525	8.221
0.115	7.960	7.194	7.450	8.174
0.125	7.895	7.130	7.374	8.126
0.135	7.830	7.066	7.299	8.077
0.145	7.765	7.002	7.223	8.028
0.155	7.699	6.937	7.148	7.978
0.165	7.632	6.872	7.072	7.928
0.175	7.566	6.806	6.995	7.877
0.185	7.498	6.740	6.919	7.825
0.195	7.430	6.674	6.842	7.772
0.205	7.362	6.607	6.766	7.719
0.215	7.293	6.540	6.689	7.665
0.225	7.224	6.472	6.612	7.610
0.235	7.154	6.404	6.534	7.555
0.245	7.084	6.336	6.457	7.498
0.255	7.013	6.267	6.379	7.441
0.265	6.942	6.198	6.301	7.384
0.275	6.870	6.128	6.223	7.325
0.285	6.798	6.058	6.144	7.266
0.295	6.725	5.988	6.066	7.205
0.305	6.652	5.917	5.987	7.144
0.315	6.578	5.846	5.908	7.083
0.325	6.504	5.775	5.829	7.020
0.335	6.429	5.703	5.750	6.957
0.345	6.354	5.630	5.670	6.892
0.355	6.278	5.558	5.591	6.827
0.365	6.201	5.484	5.511	6.761
0.375	6.124	5.411	5.431	6.694
0.385	6.047	5.337	5.350	6.626
0.395	5.969	5.263	5.270	6.557
0.405	5.890	5.188	5.189	6.487
0.415	5.811	5.113	5.108	6.417
0.425	5.731	5.037	5.027	6.345
0.435	5.651	4.961	4.946	6.272
0.445	5.570	4.885	4.865	6.199
0.455	5.489	4.808	4.783	6.124
0.465	5.407	4.731	4.701	6.048
0.475	5.324	4.654	4.619	5.972
0.485	5.241	4.576	4.537	5.894
0.495	5.157	4.498	4.454	5.815
0.505	5.073	4.419	4.372	5.735
0.515	4.988	4.340	4.289	5.654
0.525	4.902	4.261	4.206	5.572
0.535	4.816	4.181	4.123	5.489
0.545	4.729	4.100	4.039	5.405
0.555	4.642	4.020	3.956	5.320
0.565	4.554	3.939	3.872	5.233
0.575	4.465	3.857	3.788	5.145
0.585	4.376	3.776	3.704	5.056
0.595	4.286	3.694	3.620	4.966
0.605	4.196	3.611	3.535	4.875
0.615	4.105	3.528	3.450	4.782
0.625	4.013	3.445	3.366	4.689
0.635	3.920	3.361	3.280	4.593
0.645	3.827	3.277	3.195	4.497
0.655	3.734	3.192	3.110	4.399
0.665	3.639	3.108	3.024	4.300
0.675	3.544	3.022	2.938	4.200
0.685	3.448	2.937	2.852	4.098
0.695	3.352	2.851	2.766	3.995
0.705	3.255	2.764	2.680	3.890
0.715	3.157	2.678	2.593	3.785
0.725	3.059	2.590	2.506	3.677
0.735	2.959	2.503	2.419	3.568
0.745	2.860	2.415	2.332	3.458
0.755	2.759	2.327	2.245	3.346
0.765	2.658	2.238	2.157	3.233
0.775	2.556	2.149	2.069	3.118
0.785	2.453	2.060	1.981	3.002
0.795	2.349	1.970	1.893	2.884
0.805	2.245	1.880	1.805	2.764
0.815	2.140	1.789	1.717	2.643
0.825	2.035	1.698	1.628	2.520
0.835	1.928	1.607	1.539	2.395
0.845	1.821	1.515	1.450	2.269
0.855	1.713	1.423	1.361	2.141
0.865	1.605	1.331	1.271	2.012
0.875	1.495	1.238	1.182	1.880
0.885	1.385	1.145	1.092	1.747
0.895	1.274	1.052	1.002	1.612
0.905	1.162	0.958	0.912	1.475
0.915	1.050	0.864	0.821	1.336
0.925	0.936	0.769	0.731	1.196
0.935	0.822	0.674	0.640	1.053
0.945	0.707	0.579	0.549	0.909
0.955	0.591	0.483	0.458	0.762
0.965	0.475	0.387	0.367	0.614
0.975	0.357	0.291	0.275	0.464
0.985	0.239	0.194	0.184	0.311
0.995	0.120	0.097	0.092	0.157

C_o = 0.0087 M	k_h = 100	L = 1.0 m	Δx = 0.01 m	n = 0.79
D_{oc} =19.6 x 10^{-10} m^2/s		D_{os} = 20.3e^{-10} m^2/s		$R_{dc} = R_{ds}$ = 1
Case	NM	EI	E	I
ω	0.0	0.49	0.49	0.0
τ_s	0.120	0.063	0.120	0.063
x (m)	Salt Conc Mol/m^3	Salt Conc Mol/m^3	Salt Conc Mol/m^3	Salt Conc Mol/m^3
0.005	8.700	7.847	8.311	8.700
0.015	8.699	7.847	8.306	8.700
0.025	8.699	7.847	8.300	8.700
0.035	8.698	7.847	8.295	8.700
0.045	8.698	7.847	8.289	8.700
0.055	8.697	7.847	8.282	8.700
0.065	8.697	7.847	8.276	8.700
0.075	8.696	7.847	8.269	8.700
0.085	8.695	7.847	8.262	8.700
0.095	8.695	7.847	8.254	8.700
0.105	8.694	7.847	8.246	8.700
0.115	8.693	7.847	8.238	8.700
0.125	8.692	7.847	8.230	8.700
0.135	8.691	7.847	8.221	8.700
0.145	8.690	7.846	8.211	8.700
0.155	8.689	7.846	8.202	8.700
0.165	8.688	7.846	8.191	8.700
0.175	8.686	7.846	8.181	8.700
0.185	8.685	7.846	8.170	8.700
0.195	8.684	7.846	8.158	8.700
0.205	8.682	7.845	8.146	8.700
0.215	8.680	7.845	8.133	8.700
0.225	8.678	7.845	8.120	8.700
0.235	8.676	7.845	8.106	8.700
0.245	8.674	7.844	8.091	8.700
0.255	8.671	7.844	8.076	8.700
0.265	8.669	7.843	8.060	8.700
0.275	8.666	7.843	8.043	8.700
0.285	8.663	7.842	8.026	8.700
0.295	8.660	7.842	8.008	8.700
0.305	8.656	7.841	7.989	8.700
0.315	8.653	7.840	7.969	8.700
0.325	8.649	7.840	7.948	8.700
0.335	8.644	7.839	7.927	8.700
0.345	8.640	7.838	7.904	8.700
0.355	8.635	7.837	7.880	8.699
0.365	8.629	7.835	7.856	8.699
0.375	8.624	7.834	7.830	8.699
0.385	8.617	7.832	7.803	8.699
0.395	8.611	7.831	7.775	8.699
0.405	8.603	7.829	7.746	8.699
0.415	8.595	7.827	7.715	8.699
0.425	8.587	7.824	7.683	8.698
0.435	8.578	7.822	7.649	8.698
0.445	8.568	7.819	7.615	8.698
0.455	8.558	7.815	7.578	8.698
0.465	8.546	7.812	7.540	8.697
0.475	8.534	7.808	7.500	8.697
0.485	8.521	7.803	7.459	8.696
0.495	8.507	7.798	7.415	8.696
0.505	8.491	7.792	7.370	8.695
0.515	8.475	7.786	7.323	8.694
0.525	8.457	7.779	7.274	8.693
0.535	8.438	7.772	7.222	8.692
0.545	8.418	7.763	7.169	8.691
0.555	8.396	7.754	7.113	8.690
0.565	8.372	7.743	7.054	8.688
0.575	8.346	7.731	6.994	8.686
0.585	8.319	7.718	6.930	8.684
0.595	8.289	7.704	6.864	8.681
0.605	8.257	7.687	6.795	8.678
0.615	8.222	7.669	6.723	8.674
0.625	8.185	7.649	6.648	8.670
0.635	8.145	7.627	6.570	8.665
0.645	8.102	7.603	6.488	8.660
0.655	8.056	7.575	6.403	8.653
0.665	8.006	7.545	6.315	8.646
0.675	7.952	7.511	6.222	8.637
0.685	7.894	7.474	6.126	8.627
0.695	7.831	7.432	6.026	8.615
0.705	7.764	7.386	5.922	8.602
0.715	7.692	7.336	5.814	8.586
0.725	7.614	7.279	5.701	8.568
0.735	7.530	7.217	5.584	8.546
0.745	7.439	7.148	5.461	8.522
0.755	7.342	7.072	5.334	8.493
0.765	7.237	6.988	5.202	8.459
0.775	7.124	6.895	5.065	8.421
0.785	7.002	6.793	4.922	8.376
0.795	6.871	6.680	4.773	8.323
0.805	6.730	6.556	4.619	8.263
0.815	6.578	6.420	4.459	8.192
0.825	6.414	6.271	4.292	8.110
0.835	6.238	6.107	4.119	8.015
0.845	6.048	5.928	3.939	7.905
0.855	5.843	5.732	3.753	7.776
0.865	5.623	5.518	3.560	7.627
0.875	5.385	5.286	3.359	7.454
0.885	5.130	5.033	3.151	7.253
0.895	4.855	4.759	2.936	7.020
0.905	4.558	4.462	2.712	6.749
0.915	4.239	4.140	2.481	6.435
0.925	3.895	3.794	2.241	6.069
0.935	3.525	3.422	1.993	5.645
0.945	3.126	3.022	1.736	5.153
0.955	2.697	2.594	1.470	4.580
0.965	2.235	2.137	1.195	3.916
0.975	1.736	1.649	0.911	3.145
0.985	1.200	1.131	0.617	2.249
0.995	0.622	0.582	0.314	1.208
200	5.502E-08	6.970E-08	5.505E-08	6.969E-08

C_o = 0.0039 M	k_h = 0	L = 1.0 m	Δx = 0.01 m	n = 0.80
D_{oc} =19.6 x 10^{-10} m^2/s		D_{os} = 20.3e^{-10} m^2/s		$R_{dc} = R_{ds}$ = 1
Case	NM	EI	E	I
ω	0.0	0.63	0.63	0.0
τ_s	0.120	0.039	0.120	0.039
x (m)	Salt Conc Mol/m^3	Salt Conc Mol/m^3	Salt Conc Mol/m^3	Salt Conc Mol/m^3
0.005	3.861	3.460	3.749	3.861
0.015	3.823	3.418	3.710	3.823
0.025	3.784	3.376	3.670	3.784
0.035	3.746	3.335	3.631	3.745
0.045	3.707	3.294	3.591	3.706
0.055	3.668	3.253	3.552	3.668
0.065	3.630	3.212	3.512	3.629
0.075	3.591	3.171	3.473	3.590
0.085	3.553	3.131	3.434	3.552
0.095	3.514	3.090	3.395	3.513
0.105	3.475	3.050	3.355	3.474
0.115	3.437	3.011	3.316	3.435
0.125	3.398	2.971	3.277	3.397
0.135	3.359	2.931	3.238	3.358
0.145	3.321	2.892	3.199	3.319
0.155	3.282	2.853	3.160	3.281
0.165	3.244	2.814	3.121	3.242
0.175	3.205	2.775	3.082	3.203
0.185	3.166	2.736	3.043	3.164
0.195	3.128	2.698	3.005	3.126
0.205	3.089	2.660	2.966	3.087
0.215	3.051	2.621	2.927	3.048
0.225	3.012	2.583	2.889	3.010
0.235	2.973	2.546	2.850	2.971
0.245	2.935	2.508	2.811	2.932
0.255	2.896	2.470	2.773	2.894
0.265	2.857	2.433	2.734	2.855
0.275	2.819	2.396	2.696	2.816
0.285	2.780	2.359	2.658	2.777
0.295	2.742	2.322	2.619	2.739
0.305	2.703	2.285	2.581	2.700
0.315	2.664	2.248	2.543	2.661
0.325	2.626	2.212	2.505	2.623
0.335	2.587	2.176	2.466	2.584
0.345	2.549	2.139	2.428	2.545
0.355	2.510	2.103	2.390	2.507
0.365	2.471	2.067	2.352	2.468
0.375	2.433	2.032	2.314	2.429
0.385	2.394	1.996	2.276	2.391
0.395	2.355	1.960	2.238	2.352
0.405	2.317	1.925	2.200	2.313
0.415	2.278	1.890	2.163	2.275
0.425	2.240	1.855	2.125	2.236
0.435	2.201	1.820	2.087	2.198
0.445	2.162	1.785	2.049	2.159
0.455	2.124	1.750	2.012	2.120
0.465	2.085	1.715	1.974	2.082
0.475	2.047	1.681	1.936	2.043
0.485	2.008	1.646	1.899	2.004
0.495	1.969	1.612	1.861	1.966
0.505	1.931	1.578	1.824	1.927
0.515	1.892	1.544	1.787	1.889
0.525	1.854	1.510	1.749	1.850
0.535	1.815	1.476	1.712	1.811
0.545	1.776	1.443	1.674	1.773
0.555	1.738	1.409	1.637	1.734
0.565	1.699	1.376	1.600	1.696
0.575	1.660	1.342	1.563	1.657
0.585	1.622	1.309	1.525	1.618
0.595	1.583	1.276	1.489	1.580
0.605	1.545	1.243	1.452	1.541
0.615	1.506	1.210	1.415	1.503
0.625	1.467	1.177	1.378	1.464
0.635	1.429	1.145	1.341	1.426
0.645	1.390	1.112	1.304	1.387
0.655	1.352	1.080	1.267	1.348
0.665	1.313	1.047	1.230	1.310
0.675	1.274	1.015	1.193	1.271
0.685	1.236	0.983	1.156	1.233
0.695	1.197	0.951	1.120	1.194
0.705	1.158	0.919	1.083	1.156
0.715	1.120	0.887	1.046	1.117
0.725	1.081	0.855	1.010	1.079
0.735	1.043	0.823	0.973	1.040
0.745	1.004	0.792	0.937	1.001
0.755	0.965	0.760	0.900	0.963
0.765	0.927	0.729	0.864	0.924
0.775	0.888	0.697	0.827	0.886
0.785	0.850	0.666	0.791	0.847
0.795	0.811	0.635	0.755	0.809
0.805	0.772	0.604	0.718	0.770
0.815	0.734	0.573	0.682	0.732
0.825	0.695	0.542	0.646	0.693
0.835	0.656	0.511	0.610	0.655
0.845	0.618	0.480	0.574	0.616
0.855	0.579	0.450	0.537	0.578
0.865	0.541	0.419	0.501	0.539
0.875	0.502	0.389	0.465	0.501
0.885	0.463	0.358	0.429	0.462
0.895	0.425	0.328	0.393	0.424
0.905	0.386	0.298	0.357	0.385
0.915	0.348	0.268	0.322	0.347
0.925	0.309	0.238	0.286	0.308
0.935	0.270	0.208	0.250	0.270
0.945	0.232	0.178	0.214	0.231
0.955	0.193	0.148	0.178	0.193
0.965	0.154	0.118	0.143	0.154
0.975	0.116	0.089	0.107	0.116
0.985	0.077	0.059	0.071	0.077
0.995	0.039	0.029	0.036	0.039

C_o = 0.0039 M	i_b = 10	L = 1.0 m	Δx = 0.01 m	n = 0.80
D_{ac} =19.6 x 10^{-10} m^2/s		D_{aa} = 20.3e^{-10} m^2/s		$R_{ac} = R_{aa} = 1$
Case	NM	EI	E	I
ω	0.0	0.63	0.63	0.0
τ_a	0.120	0.039	0.120	0.039
x (m)	Salt Conc Mol/m^3	Salt Conc Mol/m^3	Salt Conc Mol/m^3	Salt Conc Mol/m^3
0.005	3.876	3.477	3.756	3.892
0.015	3.851	3.456	3.722	3.884
0.025	3.826	3.434	3.689	3.876
0.035	3.802	3.412	3.655	3.867
0.045	3.776	3.389	3.622	3.859
0.055	3.751	3.367	3.588	3.850
0.065	3.725	3.344	3.554	3.840
0.075	3.700	3.321	3.521	3.831
0.085	3.674	3.297	3.487	3.821
0.095	3.647	3.274	3.453	3.811
0.105	3.621	3.250	3.419	3.801
0.115	3.594	3.226	3.384	3.790
0.125	3.567	3.201	3.350	3.780
0.135	3.540	3.177	3.316	3.769
0.145	3.512	3.152	3.281	3.757
0.155	3.485	3.127	3.247	3.746
0.165	3.457	3.101	3.212	3.734
0.175	3.429	3.075	3.177	3.721
0.185	3.400	3.050	3.143	3.709
0.195	3.372	3.023	3.108	3.696
0.205	3.343	2.997	3.073	3.682
0.215	3.314	2.970	3.038	3.669
0.225	3.284	2.943	3.003	3.655
0.235	3.255	2.916	2.968	3.640
0.245	3.225	2.889	2.932	3.625
0.255	3.195	2.861	2.897	3.610
0.265	3.164	2.833	2.861	3.595
0.275	3.133	2.805	2.826	3.579
0.285	3.102	2.776	2.790	3.562
0.295	3.071	2.747	2.755	3.545
0.305	3.040	2.718	2.719	3.528
0.315	3.008	2.689	2.683	3.510
0.325	2.976	2.659	2.647	3.492
0.335	2.944	2.630	2.611	3.473
0.345	2.911	2.599	2.575	3.454
0.355	2.878	2.569	2.539	3.434
0.365	2.845	2.538	2.502	3.414
0.375	2.812	2.507	2.466	3.393
0.385	2.778	2.476	2.429	3.372
0.395	2.744	2.445	2.393	3.350
0.405	2.709	2.413	2.356	3.327
0.415	2.675	2.381	2.319	3.304
0.425	2.640	2.349	2.283	3.281
0.435	2.605	2.316	2.246	3.256
0.445	2.569	2.283	2.209	3.231
0.455	2.533	2.250	2.172	3.206
0.465	2.497	2.217	2.134	3.179
0.475	2.461	2.183	2.097	3.152
0.485	2.424	2.149	2.060	3.125
0.495	2.387	2.115	2.022	3.096
0.505	2.349	2.080	1.985	3.067
0.515	2.312	2.046	1.947	3.037
0.525	2.274	2.011	1.910	3.006
0.535	2.235	1.975	1.872	2.974
0.545	2.196	1.940	1.834	2.942
0.555	2.157	1.904	1.796	2.908
0.565	2.118	1.868	1.758	2.874
0.575	2.078	1.831	1.720	2.839
0.585	2.038	1.795	1.682	2.803
0.595	1.998	1.758	1.643	2.766
0.605	1.957	1.720	1.605	2.728
0.615	1.916	1.683	1.567	2.689
0.625	1.874	1.645	1.528	2.649
0.635	1.832	1.607	1.489	2.608
0.645	1.790	1.568	1.451	2.565
0.655	1.748	1.530	1.412	2.522
0.665	1.705	1.491	1.373	2.477
0.675	1.661	1.452	1.334	2.432
0.685	1.618	1.412	1.295	2.385
0.695	1.573	1.372	1.256	2.337
0.705	1.529	1.332	1.217	2.287
0.715	1.484	1.292	1.177	2.236
0.725	1.439	1.251	1.138	2.184
0.735	1.393	1.210	1.098	2.131
0.745	1.347	1.169	1.059	2.076
0.755	1.301	1.128	1.019	2.020
0.765	1.254	1.086	0.979	1.962
0.775	1.207	1.044	0.940	1.902
0.785	1.159	1.002	0.900	1.841
0.795	1.111	0.959	0.860	1.779
0.805	1.063	0.916	0.820	1.714
0.815	1.014	0.873	0.779	1.648
0.825	0.964	0.829	0.739	1.581
0.835	0.915	0.786	0.699	1.511
0.845	0.864	0.742	0.658	1.440
0.855	0.814	0.697	0.618	1.366
0.865	0.763	0.653	0.577	1.291
0.875	0.711	0.608	0.537	1.214
0.885	0.659	0.563	0.496	1.135
0.895	0.607	0.518	0.455	1.053
0.905	0.554	0.472	0.414	0.969
0.915	0.501	0.426	0.373	0.884
0.925	0.447	0.380	0.332	0.795
0.935	0.393	0.333	0.291	0.705
0.945	0.338	0.286	0.249	0.612
0.955	0.283	0.239	0.208	0.517
0.965	0.227	0.192	0.167	0.419
0.975	0.171	0.144	0.125	0.318
0.985	0.115	0.097	0.084	0.215
0.995	0.058	0.048	0.042	0.109

C_o = 0.0039 M	i_b = 100	L = 1.0 m	Δx = 0.01 m	n = 0.80
D_{ac} =19.6 x 10^{-10} m^2/s		D_{aa} = 20.3e^{-10} m^2/s		$R_{ac} = R_{aa} = 1$
Case	NM	EI	E	I
ω	0.0	0.63	0.63	0.0
τ_a	0.120	0.039	0.120	0.039
x (m)	Salt Conc Mol/m^3	Salt Conc Mol/m^3	Salt Conc Mol/m^3	Salt Conc Mol/m^3
0.005	3.900	3.373	3.776	3.900
0.015	3.900	3.373	3.772	3.900
0.025	3.900	3.373	3.769	3.900
0.035	3.900	3.373	3.765	3.900
0.045	3.900	3.373	3.761	3.900
0.055	3.900	3.373	3.757	3.900
0.065	3.900	3.373	3.752	3.900
0.075	3.900	3.373	3.748	3.900
0.085	3.900	3.373	3.743	3.900
0.095	3.900	3.373	3.739	3.900
0.105	3.899	3.373	3.734	3.900
0.115	3.899	3.373	3.728	3.900
0.125	3.899	3.373	3.723	3.900
0.135	3.899	3.373	3.717	3.900
0.145	3.899	3.373	3.712	3.900
0.155	3.899	3.373	3.706	3.900
0.165	3.899	3.373	3.699	3.900
0.175	3.899	3.373	3.693	3.900
0.185	3.899	3.373	3.686	3.900
0.195	3.898	3.373	3.679	3.900
0.205	3.898	3.373	3.672	3.900
0.215	3.898	3.373	3.664	3.900
0.225	3.898	3.373	3.656	3.900
0.235	3.897	3.373	3.648	3.900
0.245	3.897	3.373	3.639	3.900
0.255	3.897	3.373	3.630	3.900
0.265	3.896	3.373	3.621	3.900
0.275	3.896	3.373	3.612	3.900
0.285	3.896	3.373	3.602	3.900
0.295	3.895	3.373	3.591	3.900
0.305	3.895	3.373	3.581	3.900
0.315	3.894	3.373	3.569	3.900
0.325	3.894	3.373	3.558	3.900
0.335	3.893	3.373	3.546	3.900
0.345	3.892	3.373	3.533	3.900
0.355	3.891	3.373	3.520	3.900
0.365	3.890	3.373	3.507	3.900
0.375	3.890	3.373	3.493	3.900
0.385	3.888	3.373	3.478	3.900
0.395	3.887	3.373	3.463	3.900
0.405	3.886	3.373	3.447	3.900
0.415	3.885	3.373	3.431	3.900
0.425	3.883	3.373	3.414	3.900
0.435	3.881	3.373	3.396	3.900
0.445	3.880	3.373	3.378	3.900
0.455	3.877	3.373	3.359	3.900
0.465	3.875	3.373	3.339	3.900
0.475	3.873	3.373	3.318	3.900
0.485	3.870	3.373	3.297	3.900
0.495	3.867	3.373	3.275	3.900
0.505	3.864	3.373	3.252	3.900
0.515	3.860	3.373	3.228	3.900
0.525	3.856	3.373	3.203	3.900
0.535	3.852	3.373	3.178	3.900
0.545	3.847	3.372	3.151	3.900
0.555	3.842	3.372	3.123	3.900
0.565	3.836	3.372	3.094	3.900
0.575	3.830	3.372	3.065	3.900
0.585	3.823	3.372	3.034	3.900
0.595	3.816	3.371	3.001	3.900
0.605	3.807	3.371	2.968	3.900
0.615	3.798	3.371	2.934	3.900
0.625	3.788	3.370	2.898	3.900
0.635	3.777	3.369	2.860	3.900
0.645	3.765	3.369	2.822	3.900
0.655	3.752	3.368	2.782	3.900
0.665	3.737	3.367	2.740	3.900
0.675	3.722	3.365	2.697	3.900
0.685	3.704	3.363	2.653	3.900
0.695	3.685	3.361	2.606	3.900
0.705	3.664	3.359	2.558	3.900
0.715	3.641	3.355	2.509	3.900
0.725	3.615	3.351	2.457	3.900
0.735	3.587	3.347	2.404	3.900
0.745	3.557	3.341	2.348	3.900
0.755	3.523	3.334	2.291	3.899
0.765	3.486	3.325	2.232	3.899
0.775	3.445	3.314	2.170	3.899
0.785	3.401	3.302	2.107	3.898
0.795	3.352	3.286	2.041	3.897
0.805	3.298	3.267	1.973	3.896
0.815	3.239	3.244	1.902	3.895
0.825	3.174	3.216	1.829	3.892
0.835	3.103	3.182	1.753	3.889
0.845	3.025	3.141	1.675	3.885
0.855	2.940	3.091	1.594	3.878
0.865	2.846	3.032	1.510	3.869
0.875	2.742	2.961	1.424	3.857
0.885	2.629	2.877	1.334	3.839
0.895	2.504	2.776	1.242	3.813
0.905	2.368	2.658	1.146	3.777
0.915	2.218	2.519	1.047	3.727
0.925	2.053	2.358	0.945	3.655
0.935	1.872	2.171	0.840	3.554
0.945	1.673	1.957	0.731	3.411
0.955	1.455	1.713	0.618	3.209
0.965	1.216	1.438	0.502	2.923
0.975	0.953	1.130	0.382	2.519
0.985	0.665	0.788	0.259	1.948
0.995	0.348	0.411	0.131	1.141

APPENDIX E

CHEMICO-OSMOTIC TEST DATA

DIFFERENTIAL PRESSURES FOR SINGLE-STAGE OSMOTIC TESTS (L = 1.0 cm)							
n = 0.80 Co = 0.0039 M KCl wf = 163.38% Swf = 97.03%		n = 0.79 Co = 0.0087 M KCl wf = 151.44% Swf = 99.36%		n = 0.79 Co = 0.020 M KCl wf = 151.29% Swf = 97.53%		n = 0.78 Co = 0.047 M KCl wf = 140.42% Swf = 96.3%	
Time (days)	P1-P2 (kPa)	Time (days)	P1-P2 (kPa)	Time (days)	P1-P2 (kPa)	Time (days)	P1-P2 (kPa)
-4.50	0	-4.50	0	-4.50	0	-4.50	0.304
-4.00	-1.4283	-4.00	-2.525	-4.00	-1.766	-4.00	-3.450
-3.50	0.6693	-3.50	-1.007	-3.50	-0.628	-3.50	-0.035
-3.00	1.7181	-3.00	0.731	-3.00	0.000	-3.00	1.973
-2.50	2.3253	-2.50	1.435	-2.50	0.386	-2.50	3.616
-2.00	2.6772	-2.00	1.566	-2.00	0.531	-2.00	3.740
-1.50	2.6289	-1.50	1.718	-1.50	0.642	-1.50	4.388
-1.00	2.6634	-1.00	2.318	-1.00	0.538	-1.00	4.388
-0.50	2.8842	-0.50	2.139	-0.50	0.635	-0.50	4.409
0.00	2.7807	0.00	2.381	0.00	0.628	0.00	4.382
0.17	4.3953	0.50	4.457	0.17	7.266	0.13	6.231
0.33	5.7132	0.63	6.548	0.33	20.452	0.25	12.068
0.50	6.8517	0.75	8.432	0.50	24.184	0.38	16.788
0.67	7.7211	0.88	9.929	0.67	25.530	0.50	20.597
0.83	8.3559	1.00	11.288	0.83	28.393	0.63	23.750
1.00	8.9286	1.13	12.372	1.00	30.532	0.75	26.627
1.17	9.1494	1.25	13.441	1.50	31.823	0.88	29.553
1.33	9.6324	1.38	14.269	2.00	32.251	1.00	31.312
1.50	9.9912	1.50	14.186	2.50	30.905	1.25	34.189
2.00	10.861	1.63	15.118	3.00	31.499	1.50	36.577
2.50	11.413	1.75	15.967	3.50	31.374	2.00	39.082
3.00	11.985	1.88	16.505	4.00	31.367	2.50	40.179
3.50	12.275	2.00	16.981	4.50	30.532	3.00	41.393
4.00	12.337	2.13	17.464	5.00	30.795	3.50	38.902
4.50	12.558	2.25	17.954	5.50	29.843	4.00	39.661
5.00	12.655	2.38	18.340	6.00	30.912	4.50	39.192
5.50	12.71	2.50	18.609	6.50	30.022	5.00	38.357
6.00	12.779	3.00	19.444	7.00	30.526	5.50	37.598
6.50	12.889	3.50	20.327	7.50	30.001	6.00	37.301
7.00	13.069	4.00	20.617	8.00	30.843	6.50	36.542
7.50	13.172	4.50	21.149	8.50	30.201	7.00	36.377
8.00	12.91	5.00	21.480	9.00	30.084	7.50	36.073
8.50	12.903	5.50	21.901	9.50	29.242	8.00	34.955
9.00	12.875	6.00	21.797	10.00	30.146	8.50	34.955
9.50	12.841	6.50	22.128	10.50	29.422	9.00	35.052
10.00	13.469	7.00	22.087	11.00	30.001	9.50	34.617
10.50	13.269	7.50	22.404	11.50	29.353	10.00	34.735
11.00	13.71	8.00	22.411	12.00	30.795	10.50	34.652
11.50	13.952	8.50	22.722	12.50	29.035	11.00	34.169

DIFFERENTIAL PRESSURES FOR SINGLE-STAGE OSMOTIC TESTS (Cont.)							
n = 0.80 Co = 0.0039 M KCl wf = 163.38% Swf = 97.03%		n = 0.79 Co = 0.0087 M KCl wf = 151.44% Swf = 99.36%		n = 0.79 Co = 0.020 M KCl wf = 151.29% Swf = 97.53%		n = 0.78 Co = 0.047 M KCl wf = 140.42% Swf = 96.3%	
Time (days)	P1-P2 (kPa)	Time (days)	P1-P2 (kPa)	Time (days)	P1-P2 (kPa)	Time (days)	P1-P2 (kPa)
12.00	14.159	9.00	22.604	13.00	29.566	11.50	34.189
12.50	13.814	9.50	22.853	13.50	28.739	12.00	34.141
13.00	13.903	10.00	22.439	14.00	29.042	12.50	34.162
13.50	13.931	10.50	22.708	14.50	28.525	13.00	34.203
14.00	14.062	11.00	22.473	15.00	29.035	13.50	33.996
14.50	14.045	11.50	22.439	15.50	28.552	14.00	33.175
15.00	14.014	12.00	22.660	16.00	28.607	14.50	33.217
		12.50	23.177	16.50	28.835	15.00	33.292
		13.00	22.894	17.00	28.366	15.50	32.000
		13.50	23.232	17.50	28.587	16.00	31.500
		14.00	22.266	18.00	28.525	16.50	31.300
		14.50	22.694	18.50	29.008	17.00	31.195
		15.00	22.156	19.00	28.290	17.50	31.519
				19.50	28.456	18.00	31.457
				20.00	28.504	18.50	31.505
						19.00	31.485
						19.50	31.499
						20.00	31.547

DIFFERENTIAL PRESSURES FOR MULTI-STAGE TEST 1 (L = 0.8 cm)							
n = 0.74		wf = 163.38%				Swf = 97.03%	
Time (days)	P1-P2 (kPa)	Time (days)	P1-P2 (kPa)	Time (days)	P1-P2 (kPa)	Time (days)	P1-P2 (kPa)
Co = 0		5.50	14.145	17.50	23.094	28.50	38.486
-5.00	0.145	6.00	14.235	18.00	23.370	28.67	40.486
-4.50	0.186	6.50	14.197	18.50	22.922	28.83	42.486
-4.00	0.842	7.00	14.254	19.00	22.880	29.00	44.367
-3.50	0.338	Co = 0.0060 M		19.50	22.539	29.17	44.788
-3.00	1.083	7.50	15.104	20.00	22.783	29.33	44.408
-2.50	0.324	7.67	15.656	20.50	22.973	29.50	44.160
-2.00	1.263	7.83	16.111	21.00	23.053	30.00	43.608
-1.50	1.746	8.00	16.505	Co = 0.020 M		30.50	43.028
-1.00	1.145	8.50	17.229	21.33	23.874	31.00	41.269
-0.50	1.542	9.00	17.919	21.50	26.972	31.50	39.296
0.00	0.524	9.50	18.209	21.67	29.014	32.00	39.323
Co = 0.0039 M		10.00	18.319	21.83	30.415	32.50	37.771
0.17	2.201	10.50	18.409	22.00	31.768	33.00	37.985
0.33	3.485	11.00	18.451	22.50	32.133	33.50	36.674
0.50	4.540	11.50	17.954	23.00	32.492	34.00	36.729
0.67	5.437	12.00	18.085	23.50	33.520	34.50	35.528
0.83	6.286	12.50	17.629	24.00	33.886	35.00	34.873
1.00	6.990	13.00	17.809	24.50	31.257	35.50	34.500
1.33	8.239	13.50	17.619	25.00	31.022	36.00	34.562
1.50	8.873	14.00	17.802	25.50	30.767	36.50	34.903
1.83	10.005	Co = 0.0087 M		26.00	30.848	37.00	34.258
2.00	10.426	14.50	18.023	26.50	30.152	37.50	34.458
2.50	11.482	14.83	19.817	27.00	30.380	38.00	34.265
3.00	12.261	15.00	20.348	27.50	30.772	38.50	34.114
3.50	12.710	15.50	21.673	28.00	30.319	39.00	34.376
4.00	13.179	16.00	22.825	Co = 0.047 M		39.50	34.724
4.50	13.531	16.50	23.336	28.17	30.374	40.00	34.486
5.00	13.952	17.00	23.591	28.33	34.486		

DIFFERENTIAL PRESSURES FOR MULTI-STAGE TEST 2 (L = 1.3 cm)							
n = 0.86		wf = 163.38%				Swf = 97.03%	
Time (days)	P1-P2 (kPa)	Time (days)	P1-P2 (kPa)	Time (days)	P1-P2 (kPa)	Time (days)	P1-P2 (kPa)
Co = 0		6.50	9.563	15.50	19.831	27.00	21.804
-5.00	0.000	7.00	9.833	15.67	20.058	27.50	21.521
-4.50	-1.394	Co = 0.0060 M		15.83	19.920	28.00	21.983
-4.00	1.111	6.50	14.197	16.00	19.568	28.50	21.866
-3.50	-0.269	7.00	14.254	16.50	18.175	29.00	21.818
-3.00	0.514	7.33	11.696	17.00	18.499	Co = 0.047 M	
-2.50	0.593	7.50	13.779	17.50	18.050	29.33	24.419
-2.00	0.635	7.67	14.780	18.00	17.892	29.50	27.365
-1.50	0.316	7.83	15.159	18.50	17.899	29.67	27.138
-1.00	0.628	8.00	15.456	19.00	17.912	29.83	25.979
-0.50	0.647	8.17	15.704	19.50	18.299	30.00	24.585
0.00	-0.269	8.33	14.435	20.00	17.933	30.17	23.412
Co = 0.0039 M		8.50	14.428	20.50	17.616	30.33	20.314
0.17	-0.421	9.00	13.552	21.00	17.912	30.50	20.300
0.33	0.890	9.50	12.696	21.50	17.485	31.00	19.755
0.50	5.610	10.00	12.061	Co = 0.020 M		31.50	18.326
0.67	8.301	10.50	11.889	22.17	20.452	32.00	18.016
0.83	9.971	11.00	12.227	22.33	25.261	32.50	18.947
1.00	10.930	11.50	11.302	22.50	26.869	33.00	17.222
1.50	12.206	12.00	11.509	22.67	27.117	33.50	17.174
2.00	11.095	12.50	11.840	22.83	26.882	34.00	16.608
2.50	10.743	13.00	11.627	23.00	25.765	34.50	16.408
3.00	10.247	13.50	11.861	23.50	24.329	35.00	16.933
3.50	9.688	14.00	11.813	24.00	24.150	35.50	16.401
4.00	10.302	14.50	11.295	24.50	22.742	35.83	16.608
4.50	10.012	15.00	11.682	25.00	23.446	36.00	16.643
5.00	9.922	Co = 0.0087 M		25.50	22.508		
5.50	9.867	15.17	16.719	26.00	22.239		
6.00	9.902	15.33	18.954	26.50	21.970		

APPENDIX F

DIFFUSION TEST DATA

DIFFUSION TEST 1
C_o = 0.0039 M KCl

Hydraulic conductivity before testing = 1.63 x 10^{-11} m/s
Hydraulic conductivity after testing = 1.65 x 10^{-11} m/s
Porosity = 0.80 Thickness = 1.0 cm Area, A = 39.726 cm^2

$$Q_{tj} = \frac{1}{A}\sum_{i=1}^{N} C_{j,i} V_i$$

Time (hr)	Cl^- Conc., C_e (mg/L)	K^+ Conc., C_c (mg/L)	Sample Volume, V (mL)	Cum. Mass/Unit Area, Q_t Cl^- (mg/m2)	K^+ (mg/m2)	Elec. Conductivity, EC top (mS/m)	bottom (mS/m)	pH top	bottom
23.77	1.40	0.022	38.335	13.51	0.212	49.20	0.00	6.79	7.05
46.43	4.30	0.011	36.902	53.45	0.314	50.90	2.09	6.92	7.24
71.85	5.70	0.027	40.887	112.10	0.589	52.00	2.64	6.90	7.31
95.77	6.50	0.032	38.706	175.40	0.898	52.30	2.94	6.98	7.36
119.68	7.50	0.024	38.692	248.50	1.132	52.80	3.30	6.99	7.37
143.13	6.40	0.035	37.748	309.30	1.460	52.90	3.33	7.05	7.31
166.17	6.90	0.049	37.435	374.30	1.922	53.70	3.83	7.01	7.24
191.18	7.00	0.051	40.217	445.20	2.438	53.80	1.69	7.00	7.24
221.12	6.50	0.035	47.369	522.70	2.855	53.30	1.66	7.10	7.29
238.70	6.60	0.040	29.675	572.00	3.154	53.50	1.58	7.11	7.24
262.17	6.70	0.044	38.023	636.10	3.575	53.80	1.51	7.06	7.16
292.42	6.70	0.082	47.122	715.60	4.548	53.70	3.01	7.07	7.28
308.75	8.70	0.193	25.891	772.30	5.806	53.70	2.01	7.04	7.34
333.73	6.70	0.272	40.046	839.80	8.548	54.00	1.63	6.97	7.24
363.32	6.70	0.256	46.894	918.90	11.569	54.20	1.63	6.96	7.23
382.23	6.70	0.350	29.429	968.60	14.162	54.20	1.69	7.01	7.19
405.77		0.415	36.991		18.027	54.30	2.11	7.01	7.17
431.93		0.468	42.145		22.992	54.40	2.23	7.03	7.16
453.37		0.733	31.808		28.861	54.30	2.27	7.07	7.25
477.12		0.640	37.567		34.913	53.40	2.58	7.08	7.26
504.00		0.729	40.923		42.422	54.00	2.63	7.11	7.25
528.83		0.898	38.903		51.216	54.10	2.82	7.12	7.25
552.97		1.044	38.291		61.279	54.40	3.12	7.03	7.24
577.38		1.229	39.044		73.358	54.50	3.27	7.07	7.21
599.90		1.398	36.212		86.102	54.60	2.88	7.06	7.23
622.92		1.448	36.913		99.556	54.80	1.64	7.05	7.15
648.28		1.716	41.408		117.443	54.50	1.85		
668.42		1.958	32.173		133.300	54.70	1.11	7.16	7.18
690.08		1.839	34.201		149.133	54.70	1.11	7.11	7.20
717.05		2.448	43.129		175.710	55.10	0.84	7.09	7.29
742.87		2.296	40.966		199.386	55.00	1.16	7.10	7.22
769.63		2.544	42.872		226.841	54.90	1.26	7.05	7.22
791.57		2.412	34.614		247.857	54.80	1.47	7.05	7.24
810.52		2.720	30.038		268.424	55.00	1.83	7.04	7.20
838.28		2.908	44.435		300.951	55.00	2.18	7.09	7.20
860.23		2.839	34.761		325.793	55.60	2.28	7.10	7.18
887.55		3.067	43.935		359.712	55.60	2.68	7.07	7.19
913.40		3.193	41.733		393.255	55.20	3.36	7.05	7.27
934.87		3.842	34.158		426.290	55.10	2.97	7.04	7.17
961.87		4.174	43.204		471.685	55.40	2.67	7.02	7.20
983.22		3.988	34.277		506.095	55.10	2.45		
1008.10		4.318	40.07		549.648	55.20	2.03	6.97	7.14
1050.20		4.707	46.775		605.071	55.40	1.85	7.10	7.11
1075.40		4.819	40.565		654.278	55.40	1.94	7.07	7.19
1098.10		4.889	36.419		699.098	55.30	2.11	7.02	7.26
1120.70		4.611	36.575		741.551	55.40	1.97	7.02	7.20
1146.50		4.845	41.269		791.883	55.40	1.87	7.14	7.24

DIFFUSION TEST 2
C_o = 0.0087 M KCl

Hydraulic conductivity before testing = 1.10×10^{-11} m/s
Hydraulic conductivity after testing = 1.33×10^{-11} m/s
Porosity = 0.79 Thickness = 1.0 cm Area = 39.726 cm^2

$$Q_{tj} = \frac{1}{A}\sum_{i=1}^{N} C_{j,i} V_i$$

Time (hr)	Cl^- Conc. C_a (mg/L)	K^+ Conc, C_c (mg/L)	Sample Volume, V (mL)	Cum. Mass/Unit Area, Q_t Cl^- (mg/m2)	K^+ (mg/m2)	Elec. Conductivity, EC top (mS/m)	bottom (mS/m)	pH top	bottom
27.20	6.40	0.000	43.51	70.10	0.000	94.60	0.36	6.99	7.29
52.85	15.10	0.181	41.815	229.04	1.905	103.20	4.89	7.08	7.34
77.97	17.60	0.612	39.623	404.58	8.009	102.90	6.53	7.12	7.50
103.20	19.50	1.166	40.647	604.10	19.940	105.30	6.78	7.15	7.42
130.57	20.90	1.822	43.671	833.86	39.969	105.80	7.11		
154.57	24.10	2.502	37.856	1063.51	63.811	105.90	7.70	7.15	7.48
175.90	22.95	3.862	33.643	1257.87	96.518	106.30	8.02	7.17	7.46
198.27	22.35	3.921	35.413	1457.10	131.471	106.90	7.78	7.12	7.44
221.47	25.55	4.688	36.776	1693.63	174.869	107.50	8.09	7.13	7.45
246.57	22.35	5.175	39.619	1916.53	226.480	106.70	8.13	7.11	7.44
268.40	24.65	5.294	34.65	2131.53	272.656	107.00	8.43	7.16	7.39
296.08	25.80	6.485	44.043	2417.57	344.553	107.50	8.42	7.24	7.35
321.10	28.35	6.846	39.687	2700.79	412.946	108.30	8.51	7.11	7.37
341.52	26.55	7.228	32.18	2915.86	471.496	108.90	7.31	7.22	7.31
367.10	24.05	7.994	40.539	3161.28	553.072	108.90	7.37	7.19	7.32
389.57	24.10	8.690	35.498	3376.63	630.723	109.10	7.58	7.28	7.35
412.37	24.35	9.791	36.916	3602.91	721.708	109.80	8.04	7.24	7.34
435.90		10.343	37.279		818.767	109.60	9.27	7.17	7.30
461.48		10.757	40.53		928.514	109.70	8.16	7.18	7.38
489.58		11.154	44.631		1053.826	109.20	8.16	7.20	7.31
512.78		12.622	36.694		1170.412	109.90	8.35	7.10	7.35
536.35		13.466	37.281		1296.784	110.00	8.92	7.18	7.34
556.25		13.521	31.381		1403.592	110.30	8.65	7.13	7.30
581.35		13.779	39.748		1541.458	110.10	7.64		
602.43		13.747	33.251		1656.521	111.00	7.82	7.24	7.32
628.40		14.762	40.939		1808.649	110.80	8.09	7.10	7.29
647.27		14.772	29.873		1919.731	110.80	8.05	7.21	7.30
675.27		15.732	43.867		2093.450	110.90	8.30	7.25	7.33
700.83		16.112	40.699		2258.516	111.30	8.02	7.22	7.33
724.82		16.996	38.069		2421.387	111.50	7.64	7.14	7.34
747.85		17.832	36.388		2584.723	112.30	7.94	7.11	7.29
771.70		18.160	37.519		2756.234	113.00	7.99	7.16	7.27
793.77		18.555	34.615		2917.912	113.30	7.91	7.15	7.27
823.05		19.271	46.53		3143.628	112.70	8.18		7.30
843.65		20.009	32.961		3309.645	112.90	8.20	7.13	7.31
867.35		21.380	37.832		3513.251	113.00	8.30	7.14	7.30
893.80		22.105	42.02		3747.066	112.90	8.34	7.14	7.26
913.50		22.139	30.723		3918.283	113.00	8.60	7.16	7.27
938.82		21.664	39.808		4135.370	112.90	8.58		7.29
964.75		21.879	40.9		4360.626	112.80	8.59	7.15	7.31
991.32		22.222	42.323		4597.373	113.00	8.60	7.12	7.30
1012.90		22.154	34.034		4787.171	113.10	8.55	7.05	7.32
1037.10		22.213	37.967		4999.465	113.00	8.57		

DIFFUSION TEST 3
C_o = 0.020 M KCl

Hydraulic conductivity before testing = 1.12×10^{-11} m/s
Hydraulic conductivity after testing = 1.52×10^{-11} m/s
Porosity = 0.79 Thickness = 1.0 cm Area = 39.726 cm^2

$$Q_{tj} = \frac{1}{A}\sum_{i=1}^{N} C_{j,i} V_i$$

Time (hr)	Cl^- Conc, C_a (mg/L)	K^+ Conc, C_c (mg/L)	Sample Volume, V (mL)	Cum. Mass/Unit Area, Q_t Cl^- (mg/m2)	K^+ (mg/m2)	Elec. Conductivity, EC top (mS/m)	bottom (mS/m)	pH top	bottom
23.52	22.90	0.191	39.757	229.18	1.911	208.00	9.08	6.92	7.11
49.90	73.90	1.167	43.988	1047.46	14.834	221.00	28.20	6.95	7.30
73.90	90.10	2.445	40.28	1961.03	39.624	222.00	32.40	6.97	7.36
96.42	95.10	4.366	37.436	2857.21	80.768	225.00	33.40	6.99	7.32
122.52	97.10	6.824	39.947	3833.61	149.387	224.00	34.30	6.98	7.33
149.97	100.00	10.933	43.829	4936.89	270.009	225.00	35.80	7.03	7.31
169.19	111.10	13.600	30.685	5795.05	375.058	227.00	35.80	7.02	7.24
192.89	104.20	16.966	37.592	6781.07	535.604	227.00	35.70	6.98	7.27
217.10	105.60	20.726	38.558	7806.02	736.770	227.00	37.30	7.00	7.27
240.00	103.20	24.838	35.933	8739.49	961.435	227.00	37.80	6.92	7.29
264.62	108.00	27.865	38.871	9796.24	1234.088	228.00	38.00	6.94	7.27
287.04	107.00	31.115	35.503	10752.50	-1512.162	230.00	38.40	6.93	7.29
308.64	104.80	35.029	34.769	11669.73	1818.743	231.00	38.80	6.96	7.20
336.00	100.20	37.509	44.765	12798.83	2241.410	231.00	37.90	6.96	7.24
360.72	112.70	41.574	39.338	13914.82	2653.090	231.00	38.40	6.97	7.30
384.31	108.40	44.991	37.735	14944.49	3080.451	232.00	38.30	6.99	7.28
409.08	112.70	46.963	39.206	16056.74	3543.934	232.00	37.80	7.01	7.29
434.59	109.50	51.845	41.255	17193.89	4082.338	236.00	39.00	7.01	7.29
458.26	111.00	54.994	37.137	18231.55	4596.438	236.00	39.10	7.02	7.27
483.34	108.10	58.354	39.554	19307.87	5177.452	238.00	39.90	7.03	7.24
505.34		61.967	34.72		5719.035	238.00	40.70	7.02	7.23
531.67		64.968	38.83		6354.062	239.00	40.80	7.04	7.24
555.91		68.746	38.363		7017.935	240.00	41.10	7.00	7.21
572.33		74.700	24.86		7485.398	239.00	40.10	7.01	7.19
599.33		74.213	42.242		8274.530	239.00	41.30	7.01	7.16
628.82		79.073	46.732		9204.711	241.00	41.70	7.05	7.80
649.49		85.793	19.983		9636.268	236.00	45.80	7.04	7.23
673.92		108.440	23.875		10287.983	230.00	55.10	7.06	7.22
696.94		99.849	34.483		11154.693	234.00	51.70	7.05	7.20
721.06		95.558	38.652		12084.439	243.00	51.90	7.05	7.24
745.06		94.994	38.2		12997.889	244.00	48.00	7.03	7.25
769.18		99.739	38.249		13958.196	244.00	46.00		
791.90		101.200	35.845		14871.330	244.00	44.40		
818.21		102.150	41.695		15943.460	244.00	43.80		
841.82		103.450	37.15		16957.636	245.00	44.20	7.03	7.20
866.02		104.170	38.236		17960.265	244.00	45.10	7.04	7.17
887.38		107.000	33.903		18873.426	246.00	44.90	7.04	7.16
914.38		108.090	42.834		20038.891	247.00	45.00	7.06	7.19
936.67		110.210	35.427		21021.726	246.00	44.80	7.07	7.19
961.22		109.910	38.672		22091.665	246.00	44.80	7.05	7.20
981.31		110.100	31.539		22965.763	246.00	44.80	7.02	7.16
1007.80		111.450	41.765		24137.467	248.00	44.90	7.05	7.16

DIFFUSION TEST 4
C_o = 0.047 M KCl

Hydraulic conductivity before testing = 8.73×10^{-12} m/s
Hydraulic conductivity after testing = 1.48×10^{-11} m/s
Porosity = 0.78 Thickness = 1.0 cm Area = 39.726 cm^2

$$Q_{tj} = \frac{1}{A}\sum_{i=1}^{N} C_{j,i} V_i$$

Time (hr)	Cl^- Conc, C_a (mg/L)	K^+ Conc, C_c (mg/L)	Sample Volume, V (mL)	Cum. Mass/Unit Area, Q_t Cl^- (mg/m2)	K^+ (mg/m2)	Elec. Conductivity, EC top (mS/m)	bottom (mS/m)	pH top	bottom
24.23	74.00	1.130	38.185	711.29	10.862	483.00	10.59	6.64	7.09
48.05	175.00	3.623	37.474	2362.09	45.038	498.00	52.70	6.67	7.15
72.35	238.00	9.749	38.158	4648.15	138.680	543.00	72.40	6.71	7.17
96.60	269.00	20.481	38.075	7226.36	334.978	546.00	78.80	6.67	7.20
120.60	259.00	33.617	37.758	9688.05	654.494	556.00	82.10	6.67	7.15
147.23	292.00	48.207	42.062	12779.75	1164.911	563.00	83.50	6.71	7.14
171.03	286.00	65.134	37.155	15454.66	1774.098	565.00	85.80	6.74	7.13
197.73	266.00	81.834	42.62	18308.44	2690.289	570.00	87.10	6.75	7.11
215.28	273.00	97.560	27.292	20183.96	3360.532	572.00	87.90	6.79	7.10
241.92	279.00	111.170	42.089	23139.92	4538.359	577.00	90.30	6.78	7.10
266.33	278.00	121.580	38.738	25850.78	5723.961	578.00	89.80	6.82	7.07
290.05	277.00	128.370	37.309	28452.25	6929.511	581.00	90.60	6.83	7.08
314.58	275.00	139.690	38.51	31118.07	8283.653	582.00	91.20	6.84	7.11
338.57	278.00	145.160	37.44	33738.10	9651.721	595.00	92.80	6.87	7.07
362.55	260.00	149.110	38.32	36246.08	11090.028	595.00	93.10	6.83	7.09
386.77	266.00	154.340	38.041	38793.25	12567.945	590.00	94.20	6.85	7.06
411.45	222.00	165.010	38.486	40943.96	14166.500	588.00	95.30	6 74	7.05
434.28	250.00	170.160	36.026	43211.11	15709.653	588.00	95.90	6.80	7.07
458.15	266.00	177.760	37.563	45726.28	17390.438	589.00	95.80	6.81	7.08
483.85	263.00	185.670	41.031	48442.68	19308.131	591.00	94.70	6.82	7.10
527.10		197.240	68.577		22712.951	591.00	95.10	6.81	7.09
551.85		205.330	38.85		24720.993	592.00	95.40	6.85	7.13
577.22		214.210	39.838		26869.183	591.00	94.90	6.80	7.07
600.92		219.720	37.349		28934.904	591.00	95.20	6.87	7.06
625.93		222.450	40.045		31177.277	594.00	94.50	6.86	7.05
649.30		225.850	36.446		33249.284	594.00	96.60	6.84	7.08
673.33		231.000	38.698		35493.624	594.00	94.90	6.83	7.09
696.15		235.010	36.595		37658.520	595.00	94.80	6.85	7 12
720.98		238.990	40.065		40068.774	593.00	95.60	6.79	7.13
744.73		243.340	38.584		42432.260	597.00	94.60	6.81	7.16
769.50		244.000	39.912		44783.236	596.00	95.10	6.82	7.14
793.40		245.760	37.998		47133.897	597.00	94.90	6.84	7.15
812.05		247.260	29.54		48942.763	594.00	95.10	6.84	7.17
838.57		249.970	42.754		51579.227	594.00	95.00	6.80	7.15
863.67		250.960	40.152		54176.372	595.00	95.50	6.78	7.15
885.05		252.040	34.17		56385.655	594.00	95.40	6.82	7.14
911.72		251.480	43.228		59260.177	595.00	95.50	6.77	7.13
933.97		249.310	35.871		61511.365	595.00	95.50	6.81	7.14

APPENDIX G

EXPERIMENTAL DATA AND COUPLED SOLUTE TRANSPORT MODEL SIMULATIONS FOR COLUMN TESTS

COLUMN TEST 1
C_o = 0.0087 M KCl
i_h = 0

$k_h = 1.50 \times 10^{-11}$ m/s
n = 0.79
L = 1.0 cm
A = 39.726 cm^2
W_A = 39.098 g/mol (K^+)
W_A = 35.453 g/mol (Cl^-)

$$J_{j,i} = \frac{C_{j,i} V_i W_{Ai}}{t_i - t_{i-1}}$$

Time, t (hr)	Cl^- Conc, C_a (mg/L)	K^+ Conc, C_c (mg/L)	Sample Volume, V (mL)	Exit solute Flux, J(x=L)	
				Cl^- (mol/m^2s)	K^+ (mol/m^2s)
24.97	3.10	1.062	33.629	8.235E-09	2.558E-09
46.70	12.10	1.493	36.238	3.979E-08	4.452E-09
72.53	9.70	0.849	54.433	4.031E-08	3.199E-09
94.18	12.70	1.049	35.861	4.149E-08	3.108E-09
120.25	13.20	0.865	40.717	4.067E-08	2.416E-09
139.27	9.50	0.830	53.033	5.225E-08	4.140E-09
171.05	8.10	0.677	90.985	4.573E-08	3.466E-09
211.30	9.90	0.827	86.085	4.176E-08	3.163E-09
239.57	11.60	1.170	58.121	4.704E-08	4.302E-09
265.03	11.40	1.411	55.155	4.870E-08	5.465E-09
283.87	12.70	1.656	38.356	5.101E-08	6.032E-09
335.48	14.00	1.925	97.075	5.193E-08	6.475E-09
359.10	13.70	2.299	43.700	5.000E-08	7.608E-09
381.98	14.30	2.773	39.693	4.892E-08	8.602E-09
424.73	14.40	3.196	77.215	5.130E-08	1.032E-08
452.30		3.618	47.714		1.120E-08
504.80		4.365	88.305		1.313E-08
532.42		5.215	44.059		1.488E-08
576.60		6.014	76.525		1.863E-08
621.83		6.989	74.925		2.070E-08
670.05		7.930	76.065		2.237E-08
719.95		9.503	74.975		2.554E-08
768.48		10.748	68.985		2.732E-08
792.45		11.765	37.002		3.248E-08
839.35		12.128	65.005		3.006E-08
887.78		13.682	71.955		3.635E-08
934.75		14.565	66.585		3.693E-08
985.77		15.105	56.345		2.984E-08
1031.60		16.332	79.805		5.089E-08
1079.30		17.653	64.135		4.239E-08
1102.70		18.762	30.411		4.361E-08
1150.10		18.453	74.565		5.191E-08
1198.60		19.664	66.755		4.845E-08
1241.60		21.297	58.805		5.203E-08

COLUMN TEST 2
C_o = 0.0087 M KCl
i_h = 70.34

$k_h = 2.01 \times 10^{-11}$ m/s
n = 0.81
L = 1.0 cm
A = 39.726 cm^2
W_A = 39.098 g/mol (K^+)
W_A = 35.453 g/mol (Cl^-)

$$J_{j,i} = \frac{C_{j,i} V_i W_{Ai}}{t_i - t_{i-1}}$$

Time, t (hr)	Cl^- Conc, C_a (mg/L)	K^+ Conc, C_c (mg/L)	Sample Volume, V (mL)	Exit solute Flux, J(x=L)	
				Cl^- (mol/m^2s)	K^+ (mol/m^2s)
22.83	7.20	0.246	30.373	1.889E-08	5.852E-10
52.05	23.30	0.204	37.244	5.858E-08	4.651E-10
74.05	25.60	0.525	28.898	6.632E-08	1.233E-09
92.82	28.10	1.085	22.055	6.513E-08	2.280E-09
117.70	32.00	1.039	30.954	7.851E-08	2.312E-09
145.62	28.90	1.555	36.905	7.535E-08	3.676E-09
171.97	28.20	1.844	34.223	7.224E-08	4.283E-09
193.62	27.80	2.489	26.857	6.802E-08	5.522E-09
217.93	28.20	2.885	29.755	6.806E-08	6.313E-09
240.22	49.60	3.289	28.332	1.244E-07	7.479E-09
262.42	28.30	4.380	29.407	7.394E-08	1.038E-08
286.22	29.20	4.762	35.114	8.497E-08	1.257E-08
312.88	30.40	5.644	35.163	7.906E-08	1.331E-08
337.12	28.80	6.261	31.663	7.422E-08	1.463E-08
360.90	29.90	7.391	30.564	7.579E-08	1.699E-08
385.72	29.30	8.052	32.617	7.595E-08	1.893E-08
409.43	27.50	8.776	30.473	6.969E-08	2.017E-08
455.80		10.224	53.430		2.107E-08
480.85		11.534	32.986		2.716E-08
504.80		12.726	31.136		2.959E-08
551.93		14.294	55.020		2.984E-08
579.30		16.074	36.598		3.844E-08
625.27		16.255	52.765		3.337E-08
648.75		16.549	29.962		3.776E-08
696.33		17.850	55.765		3.741E-08
719.70		20.556	30.305		4.768E-08
767.32		22.758	55.380		4.734E-08
815.55		24.003	57.460		5.114E-08
858.77		23.206	48.540		4.661E-08

COLUMN TEST 3
C_o = 0.0087 M KCl
i_h = 703.4

$k_h = 1.43 \times 10^{-11}$ m/s
n = 0.79
L = 1.0 cm
A = 39.726 cm^2
W_A = 39.098 g/mol (K^+)
W_A = 35.453 g/mol (Cl^-)

$$J_{j,i} = \frac{C_{j,i} V_i W_{Ai}}{t_i - t_{i-1}}$$

Time, t (hr)	Cl^- Conc, C_a (mg/L)	K^+ Conc, C_c (mg/L)	Sample Volume, V (mL)	Exit solute Flux, J(x=L)	
				Cl^- (mol/m^2s)	K^+ (mol/m^2s)
24.17	1.38	0.000	129.25	1.456E-08	---
49.07	4.95	0.000	131.75	5.166E-08	---
73.70	7.29	0.000	127.32	7.432E-08	---
100.35	8.09	0.188	136.88	8.195E-08	1.727E-09
119.77	8.30	0.547	88.77	7.484E-08	4.472E-09
143.75	8.15	0.870	115.93	7.770E-08	7.521E-09
168.47	8.44	1.477	116.68	7.858E-08	1.247E-08
192.03	8.31	1.944	102.70	7.142E-08	1.515E-08
217.42	8.64	2.449	120.26	8.074E-08	2.075E-08
245.17	8.75	2.825	134.02	8.335E-08	2.440E-08
265.83	9.33	4.025	90.57	8.064E-08	3.155E-08
295.58	10.50	4.516	148.16	1.031E-07	4.022E-08
313.97	10.80	5.212	80.44	9.321E-08	4.079E-08
338.53	10.70	5.678	118.06	1.014E-07	4.880E-08
362.53	11.40	6.026	110.02	1.031E-07	4.940E-08
385.37	11.10	6.792	101.88	9.768E-08	5.420E-08
407.58	10.90	7.121	100.40	9.715E-08	5.755E-08
432.90	11.20	7.802	109.21	9.529E-08	6.019E-08
462.17	11.50	8.468	132.98	1.031E-07	6.881E-08
482.33	12.10	9.147	77.91	9.220E-08	6.320E-08
504.98	11.10	9.175	94.42	9.126E-08	6.840E-08
530.07	12.40	9.798	107.20	1.045E-07	7.489E-08
551.92		9.918	89.43		7.260E-08
575.53		10.504	99.57		7.920E-08
596.22		10.982	84.01		7.977E-08
622.47		11.444	118.83		9.265E-08
647.77		11.995	113.19		9.597E-08
671.27		12.164	102.89		9.525E-08
696.83		12.286	114.93		9.877E-08
719.95		12.293	101.62		9.664E-08
743.42		12.285	100.87		9.444E-08

COLUMN TEST 4
C_o = 0.047 M KCl
i_h = 703.4

$k_h = 2.37 \times 10^{-11}$ m/s
n = 0.81
L = 1.0 cm
A = 39.726 cm^2
W_A = 39.098 g/mol (K^+)
W_A = 35.453 g/mol (Cl^-)

$$J_{j,i} = \frac{C_{j,i} V_i W_{Ai}}{t_i - t_{i-1}}$$

Time, t (hr)	Cl^- Conc, C_a (mg/L)	K^+ Conc, C_c (mg/L)	Sample Volume, V (mL)	Exit solute Flux, J(x=L)	
				Cl^- (mol/m^2s)	K^+ (mol/m^2s)
25.42	40.00	1.050	210.53	6.535E-07	1.555E-08
51.22	75.00	4.803	165.48	9.488E-07	5.509E-08
75.18	83.00	14.403	144.60	9.877E-07	1.554E-07
96.77	55.00	18.017	211.65	1.064E-06	3.160E-07
123.77	81.00	45.442	173.78	1.028E-06	5.231E-07
149.65	82.00	54.887	157.50	9.841E-07	5.973E-07
176.32	79.00	54.374	165.23	9.654E-07	6.025E-07
198.23	80.00	63.905	126.97	9.141E-07	6.621E-07
216.75	79.00	71.648	101.00	8.499E-07	6.989E-07
244.87	77.00	76.811	176.78	9.549E-07	8.637E-07
266.78	86.00	82.828	124.11	9.605E-07	8.388E-07
294.18	69.00	80.854	186.56	9.266E-07	9.845E-07
319.77	71.00	83.000	168.65	9.231E-07	9.785E-07
341.25	72.00	84.832	134.02	8.859E-07	9.464E-07
368.12	72.00	88.839	178.91	9.456E-07	1.058E-06
389.57	68.00	85.729	134.59	8.415E-07	9.620E-07
414.48	68.00	86.322	162.22	8.732E-07	1.005E-06
431.32	71.00	86.971	98.40	8.186E-07	9.092E-07
459.73	67.00	96.690	187.46	8.717E-07	1.141E-06
486.13	87.00	88.455	163.74	1.064E-06	9.812E-07
510.43		92.313	149.40		1.015E-06
532.82		89.306	136.73		9.756E-07
555.52		91.230	137.40		9.876E-07
581.28		87.948	165.61		1.011E-06
608.63		85.983	220.92		1.242E-06

COLUMN TEST 1

C_o = 0.0087 M KCl	i_b = 0	L = 1.0 cm	Δx = 0.01 cm	n = 0.79	R_{d+} =12.57	R_{d-} = 1.53
D_{m+} =19.6 x 10^{-10} m^2/s	D_{m-} = 20.3 x 10^{-10} m^2/s		D_m =13.3 x 10^{-10} m^2/s		k_s = 1.50 x 10^{-11} m/s	

Potassium (K^+)				Chloride (Cl^-)			
Case	NM	EI	I	Case	NM	EI	I
ω	0.0	0.49	0.0	ω	0.0	0.49	0.00
τ_o	0.120	0.063	0.063	τ_o	0.120	0.063	0.063
Time (hr)	Exit Flux mol/m^2s	Exit Flux mol/m^2s	Exit Flux mol/m^2s	Time (hr)	Exit Flux mol/m^2s	Exit Flux mol/m^2s	Exit Flux mol/m^2s
14	1.284E-13	5.307E-18	6.888E-18	14	1.378E-08	4.488E-10	6.203E-10
28	2.879E-11	8.471E-15	1.101E-14	28	5.758E-08	5.319E-09	7.537E-09
42	4.504E-10	5.588E-13	7.381E-13	42	9.143E-08	1.403E-08	1.988E-08
56	2.250E-09	8.010E-12	1.088E-11	56	1.111E-07	2.274E-08	3.231E-08
70	6.281E-09	4.908E-11	6.588E-11	70	1.221E-07	2.988E-08	4.234E-08
84	1.262E-08	1.785E-10	2.405E-10	84	1.288E-07	3.585E-08	4.984E-08
98	2.075E-08	4.708E-10	6.307E-10	98	1.328E-07	3.988E-08	5.554E-08
112	2.997E-08	9.888E-10	1.320E-09	112	1.358E-07	4.328E-08	5.984E-08
126	3.985E-08	1.785E-09	2.357E-09	126	1.384E-07	4.578E-08	6.285E-08
140	4.933E-08	2.815E-09	3.751E-09	140	1.405E-07	4.773E-08	6.488E-08
154	5.870E-08	4.121E-09	5.481E-09	154	1.425E-07	4.927E-08	6.680E-08
168	6.758E-08	5.651E-09	7.500E-09	168	1.443E-07	5.051E-08	6.795E-08
182	7.588E-08	7.388E-09	9.756E-09	182	1.460E-07	5.155E-08	6.904E-08
196	8.358E-08	9.223E-09	1.218E-08	196	1.475E-07	5.242E-08	6.997E-08
210	9.068E-08	1.118E-08	1.475E-08	210	1.488E-07	5.318E-08	7.078E-08
224	9.714E-08	1.320E-08	1.739E-08	224	1.501E-07	5.388E-08	7.150E-08
238	1.031E-07	1.528E-08	2.007E-08	238	1.513E-07	5.446E-08	7.217E-08
252	1.085E-07	1.732E-08	2.274E-08	252	1.523E-07	5.504E-08	7.278E-08
266	1.134E-07	1.938E-08	2.540E-08	266	1.533E-07	5.556E-08	7.337E-08
280	1.178E-07	2.137E-08	2.801E-08	280	1.541E-07	5.605E-08	7.392E-08
294	1.218E-07	2.334E-08	3.058E-08	294	1.548E-07	5.650E-08	7.445E-08
308	1.256E-07	2.525E-08	3.304E-08	308	1.556E-07	5.694E-08	7.495E-08
322	1.288E-07	2.711E-08	3.544E-08	322	1.563E-07	5.734E-08	7.543E-08
336	1.320E-07	2.888E-08	3.775E-08	336	1.569E-07	5.773E-08	7.589E-08
350	1.347E-07	3.061E-08	3.988E-08	350	1.574E-07	5.810E-08	7.633E-08
364	1.373E-07	3.226E-08	4.211E-08	364	1.579E-07	5.845E-08	7.674E-08
378	1.395E-07	3.385E-08	4.418E-08	378	1.583E-07	5.878E-08	7.714E-08
392	1.416E-07	3.538E-08	4.612E-08	392	1.587E-07	5.910E-08	7.753E-08
406	1.435E-07	3.686E-08	4.798E-08	406	1.591E-07	5.938E-08	7.788E-08
420	1.452E-07	3.818E-08	4.977E-08	420	1.594E-07	5.968E-08	7.824E-08
434	1.468E-07	3.948E-08	5.147E-08	434	1.598E-07	5.995E-08	7.857E-08
448	1.482E-07	4.074E-08	5.310E-08	448	1.600E-07	6.021E-08	7.888E-08
462	1.495E-07	4.193E-08	5.464E-08	462	1.603E-07	6.045E-08	7.918E-08
476	1.507E-07	4.307E-08	5.611E-08	476	1.605E-07	6.068E-08	7.947E-08
490	1.518E-07	4.414E-08	5.751E-08	490	1.607E-07	6.090E-08	7.974E-08
504	1.528E-07	4.517E-08	5.885E-08	504	1.608E-07	6.111E-08	8.000E-08
518	1.537E-07	4.615E-08	6.011E-08	518	1.611E-07	6.131E-08	8.025E-08
532	1.545E-07	4.707E-08	6.132E-08	532	1.612E-07	6.150E-08	8.048E-08
546	1.552E-07	4.795E-08	6.247E-08	546	1.614E-07	6.168E-08	8.070E-08
560	1.558E-07	4.878E-08	6.356E-08	560	1.615E-07	6.185E-08	8.092E-08
574	1.565E-07	4.958E-08	6.460E-08	574	1.616E-07	6.201E-08	8.112E-08
588	1.571E-07	5.035E-08	6.558E-08	588	1.617E-07	6.216E-08	8.131E-08
602	1.576E-07	5.107E-08	6.653E-08	602	1.618E-07	6.231E-08	8.149E-08
616	1.581E-07	5.175E-08	6.742E-08	616	1.619E-07	6.245E-08	8.167E-08
630	1.585E-07	5.240E-08	6.827E-08	630	1.620E-07	6.258E-08	8.183E-08
644	1.589E-07	5.302E-08	6.908E-08	644	1.621E-07	6.270E-08	8.198E-08
658	1.592E-07	5.361E-08	6.985E-08	658	1.622E-07	6.282E-08	8.214E-08
672	1.595E-07	5.417E-08	7.058E-08	672	1.622E-07	6.294E-08	8.228E-08
686	1.598E-07	5.470E-08	7.127E-08	686	1.623E-07	6.304E-08	8.241E-08
700	1.601E-07	5.520E-08	7.194E-08	700	1.623E-07	6.315E-08	8.254E-08
714	1.604E-07	5.568E-08	7.257E-08	714	1.624E-07	6.324E-08	8.266E-08
728	1.606E-07	5.614E-08	7.317E-08	728	1.624E-07	6.333E-08	8.278E-08
742	1.608E-07	5.657E-08	7.374E-08	742	1.625E-07	6.342E-08	8.289E-08
756	1.610E-07	5.698E-08	7.428E-08	756	1.625E-07	6.351E-08	8.300E-08
770	1.611E-07	5.738E-08	7.480E-08	770	1.625E-07	6.358E-08	8.310E-08
784	1.613E-07	5.775E-08	7.529E-08	784	1.626E-07	6.366E-08	8.319E-08
798	1.614E-07	5.811E-08	7.575E-08	798	1.626E-07	6.373E-08	8.328E-08
812	1.616E-07	5.845E-08	7.620E-08	812	1.626E-07	6.380E-08	8.337E-08
826	1.617E-07	5.877E-08	7.662E-08	826	1.626E-07	6.387E-08	8.345E-08
840	1.618E-07	5.908E-08	7.703E-08	840	1.627E-07	6.393E-08	8.353E-08
854	1.619E-07	5.937E-08	7.741E-08	854	1.627E-07	6.399E-08	8.360E-08
868	1.620E-07	5.965E-08	7.778E-08	868	1.627E-07	6.404E-08	8.368E-08
882	1.620E-07	5.991E-08	7.813E-08	882	1.627E-07	6.409E-08	8.374E-08
896	1.621E-07	6.016E-08	7.846E-08	896	1.627E-07	6.414E-08	8.381E-08
910	1.622E-07	6.040E-08	7.877E-08	910	1.627E-07	6.419E-08	8.387E-08
924	1.622E-07	6.063E-08	7.907E-08	924	1.627E-07	6.424E-08	8.393E-08
938	1.623E-07	6.084E-08	7.936E-08	938	1.628E-07	6.428E-08	8.398E-08
952	1.623E-07	6.105E-08	7.963E-08	952	1.628E-07	6.432E-08	8.403E-08
966	1.624E-07	6.125E-08	7.989E-08	966	1.628E-07	6.436E-08	8.408E-08
980	1.624E-07	6.143E-08	8.014E-08	980	1.628E-07	6.440E-08	8.413E-08
994	1.625E-07	6.161E-08	8.037E-08	994	1.628E-07	6.444E-08	8.418E-08
1008	1.625E-07	6.178E-08	8.060E-08	1008	1.628E-07	6.447E-08	8.422E-08
1022	1.625E-07	6.194E-08	8.081E-08	1022	1.628E-07	6.450E-08	8.426E-08
1036	1.626E-07	6.208E-08	8.101E-08	1036	1.628E-07	6.453E-08	8.430E-08
1050	1.626E-07	6.224E-08	8.121E-08	1050	1.628E-07	6.456E-08	8.434E-08
1064	1.626E-07	6.238E-08	8.139E-08	1064	1.628E-07	6.459E-08	8.438E-08
1078	1.626E-07	6.251E-08	8.157E-08	1078	1.628E-07	6.462E-08	8.441E-08
1092	1.627E-07	6.264E-08	8.173E-08	1092	1.628E-07	6.464E-08	8.444E-08
1106	1.627E-07	6.276E-08	8.189E-08	1106	1.628E-07	6.467E-08	8.447E-08
1120	1.627E-07	6.287E-08	8.205E-08	1120	1.628E-07	6.469E-08	8.450E-08
1134	1.627E-07	6.298E-08	8.219E-08	1134	1.628E-07	6.471E-08	8.453E-08
1148	1.627E-07	6.308E-08	8.233E-08	1148	1.628E-07	6.473E-08	8.456E-08
1162	1.627E-07	6.318E-08	8.246E-08	1162	1.628E-07	6.475E-08	8.458E-08
1176	1.627E-07	6.327E-08	8.258E-08	1176	1.628E-07	6.477E-08	8.461E-08
1190	1.628E-07	6.336E-08	8.270E-08	1190	1.628E-07	6.478E-08	8.463E-08
1204	1.628E-07	6.345E-08	8.282E-08	1204	1.628E-07	6.481E-08	8.466E-08
1218	1.628E-07	6.353E-08	8.293E-08	1218	1.628E-07	6.482E-08	8.467E-08
1232	1.628E-07	6.361E-08	8.303E-08	1232	1.628E-07	6.484E-08	8.469E-08
1246	1.628E-07	6.368E-08	8.313E-08	1246	1.628E-07	6.485E-08	8.471E-08
1260	1.628E-07	6.375E-08	8.322E-08	1260	1.628E-07	6.487E-08	8.473E-08
1274	1.628E-07	6.382E-08	8.331E-08	1274	1.628E-07	6.488E-08	8.475E-08
1288	1.628E-07	6.388E-08	8.339E-08	1288	1.628E-07	6.488E-08	8.476E-08
1302	1.628E-07	6.394E-08	8.347E-08	1302	1.628E-07	6.490E-08	8.476E-08
1316	1.628E-07	6.400E-08	8.355E-08	1316	1.628E-07	6.492E-08	8.478E-08
1330	1.628E-07	6.405E-08	8.362E-08	1330	1.628E-07	6.493E-08	8.481E-08
1344	1.628E-07	6.410E-08	8.369E-08	1344	1.628E-07	6.494E-08	8.482E-08
1358	1.628E-07	6.415E-08	8.376E-08	1358	1.628E-07	6.495E-08	8.484E-08
1372	1.628E-07	6.420E-08	8.382E-08	1372	1.628E-07	6.496E-08	8.485E-08
1386	1.628E-07	6.425E-08	8.388E-08	1386	1.628E-07	6.497E-08	8.486E-08
1400	1.628E-07	6.429E-08	8.394E-08	1400	1.628E-07	6.497E-08	8.487E-08

COLUMN TEST 2

C_o = 0.0087 M KCl	i_k = 70.34	L = 1.0 cm	Δx = 0.01 cm	n = 0.81	R_{ds} =12.57	R_{ds} = 1.53
D_{ss} =19.6 x 10^{-10} m^2/s	D_{ss} = 20.3 x 10^{-10} m^2/s		D_{ss} =13.3 x 10^{-10} m^2/s		k_h = 2.01 x 10^{-11} m/s	

Potassium (K^+)				Chloride (Cl^-)			
Case	NM	EI	I	Case	NM	EI	I
ω	0.0	0.49	0.0	ω	0.0	0.49	0.00
τ_o	0.120	0.063	0.063	τ_o	0.120	0.063	0.063
Time (hr)	Exit Flux mol/m^2s	Exit Flux mol/m^2s	Exit Flux mol/m^2s	Time (hr)	Exit Flux mol/m^2s	Exit Flux mol/m^2s	Exit Flux mol/m^2s
14	1.370E-13	5.231E-18	7.288E-18	14	1.475E-08	4.357E-10	6.928E-10
28	3.049E-11	8.275E-15	1.200E-14	28	6.186E-08	5.128E-09	8.413E-09
42	4.771E-10	5.429E-13	8.050E-13	42	9.788E-08	1.349E-08	2.230E-08
56	2.384E-09	7.758E-12	1.185E-11	56	1.189E-07	2.187E-08	3.602E-08
70	6.657E-09	4.748E-11	7.188E-11	70	1.308E-07	2.887E-08	4.717E-08
84	1.338E-08	1.735E-10	2.625E-10	84	1.374E-07	3.437E-08	5.580E-08
98	2.201E-08	4.549E-10	6.886E-10	98	1.418E-07	3.858E-08	6.179E-08
112	3.178E-08	9.530E-10	1.441E-09	112	1.450E-07	4.183E-08	6.630E-08
126	4.207E-08	1.705E-09	2.575E-09	126	1.476E-07	4.433E-08	6.980E-08
140	5.235E-08	2.721E-09	4.088E-09	140	1.498E-07	4.628E-08	7.204E-08
154	6.231E-08	3.985E-09	5.980E-09	154	1.518E-07	4.783E-08	7.388E-08
168	7.175E-08	5.488E-09	8.200E-09	168	1.536E-07	4.908E-08	7.533E-08
182	8.068E-08	7.132E-09	1.067E-08	182	1.555E-07	5.013E-08	7.649E-08
196	8.877E-08	8.934E-09	1.334E-08	196	1.571E-07	5.101E-08	7.747E-08
210	9.629E-08	1.084E-08	1.614E-08	210	1.585E-07	5.178E-08	7.832E-08
224	1.032E-07	1.280E-08	1.903E-08	224	1.598E-07	5.247E-08	7.908E-08
238	1.095E-07	1.480E-08	2.198E-08	238	1.610E-07	5.308E-08	7.976E-08
252	1.152E-07	1.681E-08	2.498E-08	252	1.621E-07	5.365E-08	8.043E-08
266	1.205E-07	1.882E-08	2.781E-08	266	1.631E-07	5.417E-08	8.104E-08
280	1.252E-07	2.077E-08	3.088E-08	280	1.640E-07	5.465E-08	8.162E-08
294	1.295E-07	2.288E-08	3.348E-08	294	1.648E-07	5.510E-08	8.217E-08
308	1.336E-07	2.456E-08	3.620E-08	308	1.656E-07	5.553E-08	8.270E-08
322	1.370E-07	2.637E-08	3.884E-08	322	1.663E-07	5.593E-08	8.321E-08
336	1.403E-07	2.812E-08	4.139E-08	336	1.668E-07	5.632E-08	8.369E-08
350	1.432E-07	2.980E-08	4.382E-08	350	1.675E-07	5.669E-08	8.416E-08
364	1.458E-07	3.141E-08	4.617E-08	364	1.680E-07	5.702E-08	8.460E-08
378	1.483E-07	3.288E-08	4.842E-08	378	1.684E-07	5.734E-08	8.502E-08
392	1.508E-07	3.444E-08	5.058E-08	392	1.688E-07	5.765E-08	8.543E-08
406	1.528E-07	3.585E-08	5.263E-08	406	1.693E-07	5.795E-08	8.582E-08
420	1.544E-07	3.720E-08	5.460E-08	420	1.698E-07	5.823E-08	8.619E-08
434	1.561E-07	3.849E-08	5.647E-08	434	1.698E-07	5.849E-08	8.654E-08
448	1.576E-07	3.971E-08	5.826E-08	448	1.702E-07	5.874E-08	8.687E-08
462	1.590E-07	4.088E-08	5.998E-08	462	1.705E-07	5.898E-08	8.719E-08
476	1.603E-07	4.198E-08	6.158E-08	476	1.707E-07	5.921E-08	8.750E-08
490	1.614E-07	4.304E-08	6.312E-08	490	1.709E-07	5.942E-08	8.779E-08
504	1.625E-07	4.404E-08	6.459E-08	504	1.711E-07	5.963E-08	8.807E-08
518	1.634E-07	4.500E-08	6.598E-08	518	1.713E-07	5.982E-08	8.833E-08
532	1.643E-07	4.591E-08	6.731E-08	532	1.715E-07	6.000E-08	8.858E-08
546	1.651E-07	4.677E-08	6.858E-08	546	1.716E-07	6.018E-08	8.882E-08
560	1.658E-07	4.759E-08	6.978E-08	560	1.718E-07	6.034E-08	8.905E-08
574	1.665E-07	4.837E-08	7.093E-08	574	1.719E-07	6.050E-08	8.926E-08
588	1.671E-07	4.911E-08	7.202E-08	588	1.720E-07	6.065E-08	8.947E-08
602	1.676E-07	4.981E-08	7.305E-08	602	1.721E-07	6.079E-08	8.966E-08
616	1.681E-07	5.048E-08	7.404E-08	616	1.722E-07	6.093E-08	8.985E-08
630	1.685E-07	5.112E-08	7.497E-08	630	1.723E-07	6.106E-08	9.003E-08
644	1.689E-07	5.172E-08	7.586E-08	644	1.724E-07	6.118E-08	9.019E-08
658	1.693E-07	5.230E-08	7.671E-08	658	1.725E-07	6.129E-08	9.035E-08
672	1.697E-07	5.284E-08	7.752E-08	672	1.725E-07	6.140E-08	9.051E-08
686	1.700E-07	5.336E-08	7.828E-08	686	1.726E-07	6.151E-08	9.065E-08
700	1.703E-07	5.386E-08	7.902E-08	700	1.726E-07	6.161E-08	9.079E-08
714	1.706E-07	5.433E-08	7.971E-08	714	1.727E-07	6.170E-08	9.092E-08
728	1.708E-07	5.477E-08	8.037E-08	728	1.727E-07	6.179E-08	9.105E-08
742	1.710E-07	5.520E-08	8.100E-08	742	1.728E-07	6.188E-08	9.117E-08
756	1.712E-07	5.560E-08	8.160E-08	756	1.728E-07	6.196E-08	9.128E-08
770	1.714E-07	5.598E-08	8.217E-08	770	1.729E-07	6.204E-08	9.139E-08
784	1.715E-07	5.635E-08	8.272E-08	784	1.728E-07	6.211E-08	9.149E-08
798	1.717E-07	5.670E-08	8.325E-08	798	1.729E-07	6.218E-08	9.159E-08
812	1.718E-07	5.703E-08	8.372E-08	812	1.728E-07	6.225E-08	9.168E-08
826	1.719E-07	5.734E-08	8.419E-08	826	1.730E-07	6.231E-08	9.177E-08
840	1.720E-07	5.764E-08	8.464E-08	840	1.730E-07	6.237E-08	9.185E-08
854	1.721E-07	5.793E-08	8.508E-08	854	1.730E-07	6.243E-08	9.193E-08
868	1.722E-07	5.820E-08	8.548E-08	868	1.730E-07	6.248E-08	9.201E-08
882	1.723E-07	5.845E-08	8.585E-08	882	1.730E-07	6.253E-08	9.208E-08
896	1.724E-07	5.870E-08	8.621E-08	896	1.731E-07	6.258E-08	9.215E-08
910	1.725E-07	5.893E-08	8.656E-08	910	1.731E-07	6.263E-08	9.222E-08
924	1.725E-07	5.915E-08	8.689E-08	924	1.731E-07	6.267E-08	9.228E-08
938	1.726E-07	5.937E-08	8.721E-08	938	1.731E-07	6.272E-08	9.234E-08
952	1.727E-07	5.957E-08	8.751E-08	952	1.731E-07	6.276E-08	9.240E-08
966	1.727E-07	5.976E-08	8.780E-08	966	1.731E-07	6.279E-08	9.245E-08
980	1.727E-07	5.994E-08	8.807E-08	980	1.731E-07	6.283E-08	9.250E-08
994	1.728E-07	6.011E-08	8.833E-08	994	1.731E-07	6.287E-08	9.255E-08
1008	1.728E-07	6.028E-08	8.858E-08	1008	1.731E-07	6.290E-08	9.260E-08
1022	1.728E-07	6.044E-08	8.881E-08	1022	1.731E-07	6.293E-08	9.264E-08
1036	1.728E-07	6.059E-08	8.904E-08	1036	1.731E-07	6.298E-08	9.269E-08
1050	1.728E-07	6.073E-08	8.925E-08	1050	1.732E-07	6.299E-08	9.273E-08
1064	1.728E-07	6.088E-08	8.945E-08	1064	1.732E-07	6.302E-08	9.278E-08
1078	1.730E-07	6.098E-08	8.965E-08	1078	1.732E-07	6.304E-08	9.280E-08
1092	1.730E-07	6.111E-08	8.983E-08	1092	1.732E-07	6.307E-08	9.284E-08
1106	1.730E-07	6.123E-08	9.001E-08	1106	1.732E-07	6.309E-08	9.287E-08
1120	1.730E-07	6.134E-08	9.018E-08	1120	1.732E-07	6.311E-08	9.290E-08
1134	1.730E-07	6.145E-08	9.034E-08	1134	1.732E-07	6.313E-08	9.293E-08
1148	1.731E-07	6.155E-08	9.049E-08	1148	1.732E-07	6.315E-08	9.296E-08
1162	1.731E-07	6.164E-08	9.063E-08	1162	1.732E-07	6.317E-08	9.299E-08
1176	1.731E-07	6.174E-08	9.077E-08	1176	1.732E-07	6.319E-08	9.301E-08
1190	1.731E-07	6.182E-08	9.090E-08	1190	1.732E-07	6.321E-08	9.304E-08
1204	1.731E-07	6.190E-08	9.103E-08	1204	1.732E-07	6.322E-08	9.306E-08
1218	1.731E-07	6.198E-08	9.114E-08	1218	1.732E-07	6.324E-08	9.308E-08
1232	1.731E-07	6.206E-08	9.126E-08	1232	1.732E-07	6.325E-08	9.311E-08
1246	1.731E-07	6.213E-08	9.137E-08	1246	1.732E-07	6.327E-08	9.313E-08
1260	1.731E-07	6.220E-08	9.147E-08	1260	1.732E-07	6.328E-08	9.315E-08
1274	1.731E-07	6.226E-08	9.157E-08	1274	1.732E-07	6.330E-08	9.317E-08
1288	1.731E-07	6.232E-08	9.166E-08	1288	1.732E-07	6.331E-08	9.318E-08
1302	1.732E-07	6.238E-08	9.175E-08	1302	1.732E-07	6.332E-08	9.320E-08
1316	1.732E-07	6.244E-08	9.183E-08	1316	1.732E-07	6.333E-08	9.322E-08
1330	1.732E-07	6.249E-08	9.191E-08	1330	1.732E-07	6.334E-08	9.323E-08
1344	1.732E-07	6.254E-08	9.198E-08	1344	1.732E-07	6.335E-08	9.325E-08
1358	1.732E-07	6.259E-08	9.207E-08	1358	1.732E-07	6.336E-08	9.326E-08
1372	1.732E-07	6.264E-08	9.213E-08	1372	1.732E-07	6.337E-08	9.327E-08
1386	1.732E-07	6.268E-08	9.220E-08	1386	1.732E-07	6.338E-08	9.328E-08
1400	1.732E-07	6.272E-08	9.226E-08	1400	1.732E-07	6.338E-08	9.330E-08

COLUMN TEST 3

C_o = 0.0087 M KCl	i_b = 703.4	L = 1.0 cm	Δx = 0.01 cm	n = 0.79	R_{dK} =12.57	R_{dCl} = 1.53
D_{eK} =19.6 x 10^{-10} m^2/s	D_{eK} = 20.3 x 10^{-10} m^2/s		D_{eCl} =13.3 x 10^{-10} m^2/s		k_b = 1.43 x 10^{-11} m/s	

Potassium (K^+)				Chloride (Cl^-)			
Case	NM	EI	I	Case	NM	EI	I
ε	0.0	0.49	0.0	ε	0.0	0.49	0.00
τ_o	0.120	0.063	0.063	τ_o	0.120	0.063	0.063
Time (hr)	Exit Flux mol/m^2s	Exit Flux mol/m^2s	Exit Flux mol/m^2s	Time (hr)	Exit Flux mol/m^2s	Exit Flux mol/m^2s	Exit Flux mol/m^2s
8	7.148E-17	1.087E-20	1.163E-22	8	2.488E-08	9.515E-11	3.782E-11
16	8.832E-14	5.378E-17	1.277E-18	16	2.548E-08	2.271E-09	1.541E-09
24	4.767E-12	6.588E-15	3.855E-16	24	6.175E-08	8.883E-09	7.975E-09
32	5.848E-11	2.441E-13	1.834E-14	32	9.470E-08	1.748E-08	1.919E-08
40	3.172E-10	2.580E-12	2.000E-13	40	1.198E-07	2.648E-08	3.250E-08
48	1.054E-09	1.432E-11	2.280E-12	48	1.379E-07	3.458E-08	4.575E-08
56	2.580E-09	5.281E-11	1.082E-11	56	1.505E-07	4.155E-08	5.783E-08
64	5.038E-09	1.480E-10	3.788E-11	64	1.593E-07	4.738E-08	6.835E-08
72	8.567E-09	3.284E-10	1.018E-10	72	1.655E-07	5.214E-08	7.727E-08
80	1.307E-08	6.344E-10	2.287E-10	80	1.698E-07	5.605E-08	8.471E-08
88	1.844E-08	1.083E-09	4.512E-10	88	1.732E-07	5.925E-08	9.085E-08
96	2.460E-08	1.723E-09	7.983E-10	96	1.758E-07	6.188E-08	9.589E-08
104	3.107E-08	2.535E-09	1.291E-09	104	1.778E-07	6.400E-08	1.000E-07
112	3.798E-08	3.527E-09	1.956E-09	112	1.798E-07	6.578E-08	1.034E-07
120	4.511E-08	4.692E-09	2.805E-09	120	1.812E-07	6.723E-08	1.061E-07
128	5.230E-08	6.017E-09	3.842E-09	128	1.826E-07	6.847E-08	1.083E-07
136	5.948E-08	7.482E-09	5.068E-09	136	1.840E-07	6.952E-08	1.101E-07
144	6.655E-08	9.070E-09	6.478E-09	144	1.852E-07	7.042E-08	1.116E-07
152	7.347E-08	1.076E-08	8.058E-09	152	1.865E-07	7.121E-08	1.129E-07
160	8.020E-08	1.253E-08	9.798E-09	160	1.876E-07	7.191E-08	1.139E-07
168	8.669E-08	1.437E-08	1.168E-08	168	1.887E-07	7.254E-08	1.148E-07
176	9.285E-08	1.625E-08	1.368E-08	176	1.898E-07	7.311E-08	1.155E-07
184	9.865E-08	1.816E-08	1.581E-08	184	1.908E-07	7.364E-08	1.162E-07
192	1.047E-07	2.008E-08	1.802E-08	192	1.918E-07	7.413E-08	1.168E-07
200	1.102E-07	2.202E-08	2.030E-08	200	1.928E-07	7.458E-08	1.173E-07
208	1.154E-07	2.395E-08	2.265E-08	208	1.937E-07	7.502E-08	1.178E-07
216	1.204E-07	2.588E-08	2.504E-08	216	1.945E-07	7.543E-08	1.183E-07
224	1.251E-07	2.775E-08	2.746E-08	224	1.953E-07	7.582E-08	1.187E-07
232	1.298E-07	2.961E-08	2.991E-08	232	1.961E-07	7.620E-08	1.192E-07
240	1.338E-07	3.144E-08	3.238E-08	240	1.968E-07	7.656E-08	1.196E-07
248	1.378E-07	3.324E-08	3.482E-08	248	1.975E-07	7.691E-08	1.200E-07
256	1.417E-07	3.498E-08	3.727E-08	256	1.982E-07	7.724E-08	1.203E-07
264	1.453E-07	3.670E-08	3.970E-08	264	1.988E-07	7.757E-08	1.207E-07
272	1.487E-07	3.837E-08	4.212E-08	272	1.994E-07	7.788E-08	1.211E-07
280	1.520E-07	4.000E-08	4.451E-08	280	2.000E-07	7.819E-08	1.214E-07
288	1.551E-07	4.157E-08	4.687E-08	288	2.005E-07	7.848E-08	1.218E-07
296	1.580E-07	4.311E-08	4.918E-08	296	2.011E-07	7.876E-08	1.221E-07
304	1.607E-07	4.458E-08	5.146E-08	304	2.015E-07	7.904E-08	1.225E-07
312	1.633E-07	4.603E-08	5.373E-08	312	2.020E-07	7.931E-08	1.228E-07
320	1.658E-07	4.743E-08	5.593E-08	320	2.024E-07	7.958E-08	1.231E-07
328	1.682E-07	4.878E-08	5.808E-08	328	2.029E-07	7.981E-08	1.235E-07
336	1.704E-07	5.008E-08	6.021E-08	336	2.032E-07	8.005E-08	1.238E-07
344	1.725E-07	5.136E-08	6.228E-08	344	2.036E-07	8.028E-08	1.241E-07
352	1.745E-07	5.258E-08	6.431E-08	352	2.040E-07	8.051E-08	1.244E-07
360	1.764E-07	5.376E-08	6.628E-08	360	2.043E-07	8.073E-08	1.247E-07
368	1.781E-07	5.490E-08	6.821E-08	368	2.048E-07	8.094E-08	1.250E-07
376	1.798E-07	5.601E-08	7.010E-08	376	2.049E-07	8.114E-08	1.253E-07
384	1.814E-07	5.707E-08	7.194E-08	384	2.052E-07	8.134E-08	1.256E-07
392	1.830E-07	5.810E-08	7.373E-08	392	2.056E-07	8.153E-08	1.259E-07
400	1.844E-07	5.910E-08	7.547E-08	400	2.057E-07	8.171E-08	1.261E-07
408	1.858E-07	6.006E-08	7.717E-08	408	2.060E-07	8.188E-08	1.264E-07
416	1.870E-07	6.098E-08	7.883E-08	416	2.062E-07	8.206E-08	1.267E-07
424	1.883E-07	6.188E-08	8.044E-08	424	2.064E-07	8.222E-08	1.269E-07
432	1.894E-07	6.274E-08	8.201E-08	432	2.066E-07	8.238E-08	1.272E-07
440	1.905E-07	6.358E-08	8.354E-08	440	2.068E-07	8.254E-08	1.274E-07
448	1.916E-07	6.438E-08	8.502E-08	448	2.070E-07	8.268E-08	1.276E-07
456	1.925E-07	6.516E-08	8.647E-08	456	2.072E-07	8.283E-08	1.278E-07
464	1.935E-07	6.591E-08	8.787E-08	464	2.073E-07	8.297E-08	1.281E-07
472	1.944E-07	6.663E-08	8.924E-08	472	2.075E-07	8.310E-08	1.283E-07
480	1.952E-07	6.733E-08	9.057E-08	480	2.076E-07	8.323E-08	1.285E-07
488	1.960E-07	6.800E-08	9.186E-08	488	2.078E-07	8.335E-08	1.287E-07
496	1.967E-07	6.865E-08	9.311E-08	496	2.079E-07	8.347E-08	1.289E-07
504	1.974E-07	6.928E-08	9.433E-08	504	2.080E-07	8.359E-08	1.291E-07
512	1.981E-07	6.988E-08	9.552E-08	512	2.082E-07	8.370E-08	1.293E-07
520	1.988E-07	7.047E-08	9.667E-08	520	2.083E-07	8.381E-08	1.295E-07
528	1.994E-07	7.103E-08	9.779E-08	528	2.084E-07	8.392E-08	1.297E-07
536	1.999E-07	7.158E-08	9.888E-08	536	2.085E-07	8.402E-08	1.298E-07
544	2.005E-07	7.210E-08	9.993E-08	544	2.086E-07	8.411E-08	1.300E-07
552	2.010E-07	7.261E-08	1.010E-07	552	2.087E-07	8.421E-08	1.302E-07
560	2.015E-07	7.310E-08	1.020E-07	560	2.088E-07	8.430E-08	1.304E-07
568	2.019E-07	7.357E-08	1.029E-07	568	2.088E-07	8.438E-08	1.305E-07
576	2.024E-07	7.403E-08	1.038E-07	576	2.088E-07	8.447E-08	1.307E-07
584	2.028E-07	7.447E-08	1.046E-07	584	2.090E-07	8.455E-08	1.308E-07
592	2.032E-07	7.489E-08	1.057E-07	592	2.091E-07	8.463E-08	1.310E-07
600	2.036E-07	7.530E-08	1.065E-07	600	2.091E-07	8.471E-08	1.311E-07
608	2.039E-07	7.570E-08	1.074E-07	608	2.092E-07	8.478E-08	1.313E-07
616	2.043E-07	7.608E-08	1.082E-07	616	2.093E-07	8.485E-08	1.314E-07
624	2.046E-07	7.645E-08	1.090E-07	624	2.093E-07	8.492E-08	1.315E-07
632	2.049E-07	7.681E-08	1.098E-07	632	2.094E-07	8.498E-08	1.317E-07
640	2.052E-07	7.715E-08	1.105E-07	640	2.094E-07	8.505E-08	1.318E-07
648	2.054E-07	7.748E-08	1.112E-07	648	2.095E-07	8.511E-08	1.319E-07
656	2.057E-07	7.780E-08	1.119E-07	656	2.095E-07	8.517E-08	1.320E-07
664	2.059E-07	7.811E-08	1.126E-07	664	2.096E-07	8.523E-08	1.321E-07
672	2.062E-07	7.841E-08	1.133E-07	672	2.096E-07	8.529E-08	1.322E-07
680	2.064E-07	7.870E-08	1.139E-07	680	2.096E-07	8.534E-08	1.323E-07
688	2.066E-07	7.898E-08	1.146E-07	688	2.097E-07	8.539E-08	1.325E-07
696	2.068E-07	7.925E-08	1.152E-07	696	2.097E-07	8.544E-08	1.326E-07
704	2.070E-07	7.951E-08	1.158E-07	704	2.098E-07	8.549E-08	1.327E-07
712	2.071E-07	7.976E-08	1.163E-07	712	2.098E-07	8.554E-08	1.327E-07
720	2.073E-07	8.000E-08	1.169E-07	720	2.098E-07	8.558E-08	1.328E-07
728	2.075E-07	8.024E-08	1.175E-07	728	2.098E-07	8.563E-08	1.329E-07
736	2.076E-07	8.046E-08	1.180E-07	736	2.098E-07	8.567E-08	1.330E-07
744	2.078E-07	8.068E-08	1.185E-07	744	2.098E-07	8.571E-08	1.331E-07
752	2.079E-07	8.089E-08	1.190E-07	752	2.098E-07	8.575E-08	1.332E-07
760	2.080E-07	8.109E-08	1.195E-07	760	2.098E-07	8.578E-08	1.333E-07
768	2.082E-07	8.128E-08	1.199E-07	768	2.100E-07	8.582E-08	1.334E-07
776	2.083E-07	8.146E-08	1.204E-07	776	2.100E-07	8.586E-08	1.334E-07
784	2.084E-07	8.166E-08	1.208E-07	784	2.100E-07	8.589E-08	1.335E-07
792	2.085E-07	8.184E-08	1.213E-07	792	2.100E-07	8.593E-08	1.336E-07
800	2.086E-07	8.201E-08	1.217E-07	800	2.100E-07	8.596E-08	1.336E-07

COLUMN TEST 4

C_o = 0.047 M KCl		t_b = 703.4	L = 1.0 cm	Δx = 0.01 cm	n = 0.78	R_{dK} =17.49	R_{dCl} = 1.94
D_{oK} =19.6 x 10^{-10} m^2/s		D_{oCl} = 20.3 x 10^{-10} m^2/s		D_{oCl} =13.3 x 10^{-10} m^2/s		k_o = 2.37 x 10^{-11} m/s	
Potassium (K^+)				Chloride (Cl^-)			
Case	NM	EI	I	Case	NM	EI	I
ω	0.0	0.14	0.00	ω	0.0	0.14	0.00
τ_o	0.120	0.119	0.119	τ_o	0.120	0.119	0.119
Time (hr)	Exit Flux mol/m^2s	Exit Flux mol/m^2s	Exit Flux mol/m^2s	Time (hr)	Exit Flux mol/m^2s	Exit Flux mol/m^2s	Exit Flux mol/m^2s
8	4.423E-16	4.408E-17	4.423E-16	8	1.647E-08	9.229E-09	1.647E-08
16	5.468E-13	7.888E-14	5.468E-13	16	1.685E-07	9.556E-08	1.685E-07
24	2.978E-11	5.447E-12	2.978E-11	24	4.075E-07	2.358E-07	4.075E-07
32	3.665E-10	8.251E-11	3.665E-10	32	6.230E-07	3.690E-07	6.230E-07
40	1.983E-09	5.278E-10	1.983E-09	40	7.881E-07	4.764E-07	7.881E-07
48	6.635E-09	1.888E-09	6.635E-09	48	9.019E-07	5.585E-07	9.019E-07
56	1.614E-08	5.384E-09	1.614E-08	56	9.818E-07	6.199E-07	9.818E-07
64	3.180E-08	1.157E-08	3.180E-08	64	1.037E-06	6.658E-07	1.037E-06
72	5.408E-08	2.111E-08	5.408E-08	72	1.074E-06	6.988E-07	1.074E-06
80	8.263E-08	3.425E-08	8.263E-08	80	1.101E-06	7.251E-07	1.101E-06
88	1.167E-07	5.088E-08	1.167E-07	88	1.120E-06	7.448E-07	1.120E-06
96	1.552E-07	7.088E-08	1.552E-07	96	1.134E-06	7.598E-07	1.134E-06
104	1.988E-07	9.320E-08	1.988E-07	104	1.146E-06	7.720E-07	1.146E-06
112	2.408E-07	1.178E-07	2.408E-07	112	1.156E-06	7.820E-07	1.156E-06
120	2.862E-07	1.442E-07	2.862E-07	120	1.164E-06	7.908E-07	1.164E-06
128	3.320E-07	1.716E-07	3.320E-07	128	1.173E-06	7.981E-07	1.173E-06
136	3.777E-07	1.987E-07	3.777E-07	136	1.180E-06	8.049E-07	1.180E-06
144	4.228E-07	2.282E-07	4.228E-07	144	1.187E-06	8.112E-07	1.187E-06
152	4.668E-07	2.568E-07	4.668E-07	152	1.194E-06	8.170E-07	1.194E-06
160	5.098E-07	2.848E-07	5.098E-07	160	1.201E-06	8.225E-07	1.201E-06
168	5.512E-07	3.128E-07	5.512E-07	168	1.208E-06	8.278E-07	1.208E-06
176	5.911E-07	3.387E-07	5.911E-07	176	1.214E-06	8.328E-07	1.214E-06
184	6.294E-07	3.661E-07	6.294E-07	184	1.220E-06	8.378E-07	1.220E-06
192	6.661E-07	3.917E-07	6.661E-07	192	1.226E-06	8.422E-07	1.226E-06
200	7.010E-07	4.164E-07	7.010E-07	200	1.231E-06	8.467E-07	1.231E-06
208	7.344E-07	4.403E-07	7.344E-07	208	1.237E-06	8.508E-07	1.237E-06
216	7.661E-07	4.632E-07	7.661E-07	216	1.242E-06	8.550E-07	1.242E-06
224	7.962E-07	4.852E-07	7.962E-07	224	1.246E-06	8.590E-07	1.246E-06
232	8.246E-07	5.063E-07	8.246E-07	232	1.251E-06	8.627E-07	1.251E-06
240	8.520E-07	5.265E-07	8.520E-07	240	1.256E-06	8.663E-07	1.256E-06
248	8.778E-07	5.458E-07	8.778E-07	248	1.260E-06	8.698E-07	1.260E-06
256	9.022E-07	5.643E-07	9.022E-07	256	1.264E-06	8.731E-07	1.264E-06
264	9.253E-07	5.820E-07	9.253E-07	264	1.268E-06	8.763E-07	1.268E-06
272	9.472E-07	5.988E-07	9.472E-07	272	1.271E-06	8.793E-07	1.271E-06
280	9.680E-07	6.148E-07	9.680E-07	280	1.275E-06	8.822E-07	1.275E-06
288	9.876E-07	6.302E-07	9.876E-07	288	1.278E-06	8.850E-07	1.278E-06
296	1.006E-06	6.448E-07	1.006E-06	296	1.281E-06	8.876E-07	1.281E-06
304	1.024E-06	6.587E-07	1.024E-06	304	1.284E-06	8.901E-07	1.284E-06
312	1.041E-06	6.720E-07	1.041E-06	312	1.287E-06	8.925E-07	1.287E-06
320	1.058E-06	6.846E-07	1.058E-06	320	1.289E-06	8.948E-07	1.289E-06
328	1.071E-06	6.967E-07	1.071E-06	328	1.292E-06	8.970E-07	1.292E-06
336	1.085E-06	7.082E-07	1.085E-06	336	1.294E-06	8.991E-07	1.294E-06
344	1.098E-06	7.191E-07	1.098E-06	344	1.297E-06	9.011E-07	1.297E-06
352	1.112E-06	7.295E-07	1.112E-06	352	1.299E-06	9.030E-07	1.299E-06
360	1.124E-06	7.395E-07	1.124E-06	360	1.301E-06	9.048E-07	1.301E-06
368	1.135E-06	7.490E-07	1.135E-06	368	1.303E-06	9.066E-07	1.303E-06
376	1.146E-06	7.580E-07	1.146E-06	376	1.304E-06	9.082E-07	1.304E-06
384	1.156E-06	7.666E-07	1.156E-06	384	1.306E-06	9.098E-07	1.306E-06
392	1.165E-06	7.748E-07	1.165E-06	392	1.308E-06	9.113E-07	1.308E-06
400	1.175E-06	7.826E-07	1.175E-06	400	1.309E-06	9.127E-07	1.309E-06
408	1.183E-06	7.900E-07	1.183E-06	408	1.311E-06	9.141E-07	1.311E-06
416	1.191E-06	7.971E-07	1.191E-06	416	1.312E-06	9.154E-07	1.312E-06
424	1.199E-06	8.038E-07	1.199E-06	424	1.314E-06	9.166E-07	1.314E-06
432	1.208E-06	8.103E-07	1.208E-06	432	1.315E-06	9.178E-07	1.315E-06
440	1.213E-06	8.164E-07	1.213E-06	440	1.316E-06	9.189E-07	1.316E-06
448	1.220E-06	8.223E-07	1.220E-06	448	1.317E-06	9.200E-07	1.317E-06
456	1.226E-06	8.278E-07	1.226E-06	456	1.318E-06	9.210E-07	1.318E-06
464	1.232E-06	8.331E-07	1.232E-06	464	1.319E-06	9.220E-07	1.319E-06
472	1.238E-06	8.382E-07	1.238E-06	472	1.320E-06	9.229E-07	1.320E-06
480	1.243E-06	8.430E-07	1.243E-06	480	1.321E-06	9.238E-07	1.321E-06
488	1.248E-06	8.476E-07	1.248E-06	488	1.322E-06	9.247E-07	1.322E-06
496	1.253E-06	8.520E-07	1.253E-06	496	1.323E-06	9.255E-07	1.323E-06
504	1.257E-06	8.562E-07	1.257E-06	504	1.323E-06	9.263E-07	1.323E-06
512	1.261E-06	8.602E-07	1.261E-06	512	1.324E-06	9.270E-07	1.324E-06
520	1.265E-06	8.640E-07	1.265E-06	520	1.325E-06	9.277E-07	1.325E-06
528	1.269E-06	8.676E-07	1.269E-06	528	1.326E-06	9.284E-07	1.326E-06
536	1.273E-06	8.711E-07	1.273E-06	536	1.326E-06	9.290E-07	1.326E-06
544	1.276E-06	8.744E-07	1.276E-06	544	1.327E-06	9.296E-07	1.327E-06
552	1.279E-06	8.775E-07	1.279E-06	552	1.327E-06	9.302E-07	1.327E-06
560	1.283E-06	8.805E-07	1.283E-06	560	1.328E-06	9.308E-07	1.328E-06
568	1.285E-06	8.834E-07	1.285E-06	568	1.328E-06	9.313E-07	1.328E-06
576	1.288E-06	8.861E-07	1.288E-06	576	1.328E-06	9.318E-07	1.328E-06
584	1.291E-06	8.887E-07	1.291E-06	584	1.329E-06	9.323E-07	1.329E-06
592	1.293E-06	8.911E-07	1.293E-06	592	1.330E-06	9.327E-07	1.330E-06
600	1.296E-06	8.935E-07	1.296E-06	600	1.330E-06	9.332E-07	1.330E-06
608	1.298E-06	8.958E-07	1.298E-06	608	1.330E-06	9.336E-07	1.330E-06
616	1.300E-06	8.979E-07	1.300E-06	616	1.331E-06	9.340E-07	1.331E-06
624	1.302E-06	9.000E-07	1.302E-06	624	1.331E-06	9.344E-07	1.331E-06
632	1.304E-06	9.019E-07	1.304E-06	632	1.332E-06	9.347E-07	1.332E-06
640	1.306E-06	9.038E-07	1.306E-06	640	1.332E-06	9.351E-07	1.332E-06
648	1.307E-06	9.056E-07	1.307E-06	648	1.332E-06	9.354E-07	1.332E-06
656	1.308E-06	9.072E-07	1.308E-06	656	1.332E-06	9.357E-07	1.332E-06
664	1.310E-06	9.088E-07	1.310E-06	664	1.333E-06	9.360E-07	1.333E-06
672	1.312E-06	9.104E-07	1.312E-06	672	1.333E-06	9.363E-07	1.333E-06
680	1.313E-06	9.118E-07	1.313E-06	680	1.333E-06	9.366E-07	1.333E-06
688	1.314E-06	9.133E-07	1.314E-06	688	1.333E-06	9.368E-07	1.333E-06
696	1.316E-06	9.146E-07	1.316E-06	696	1.334E-06	9.371E-07	1.334E-06
704	1.317E-06	9.159E-07	1.317E-06	704	1.334E-06	9.373E-07	1.334E-06
712	1.318E-06	9.171E-07	1.318E-06	712	1.334E-06	9.376E-07	1.334E-06
720	1.319E-06	9.183E-07	1.319E-06	720	1.334E-06	9.378E-07	1.334E-06
728	1.320E-06	9.194E-07	1.320E-06	728	1.334E-06	9.380E-07	1.334E-06
736	1.321E-06	9.204E-07	1.321E-06	736	1.334E-06	9.382E-07	1.334E-06
744	1.322E-06	9.214E-07	1.322E-06	744	1.335E-06	9.384E-07	1.335E-06
752	1.322E-06	9.224E-07	1.322E-06	752	1.335E-06	9.385E-07	1.335E-06
760	1.323E-06	9.233E-07	1.323E-06	760	1.335E-06	9.387E-07	1.335E-06
768	1.324E-06	9.242E-07	1.324E-06	768	1.335E-06	9.389E-07	1.335E-06
776	1.325E-06	9.250E-07	1.325E-06	776	1.335E-06	9.390E-07	1.335E-06
784	1.325E-06	9.258E-07	1.325E-06	784	1.335E-06	9.392E-07	1.335E-06
792	1.326E-06	9.266E-07	1.326E-06	792	1.335E-06	9.393E-07	1.335E-06
800	1.327E-06	9.273E-07	1.327E-06	800	1.335E-06	9.394E-07	1.335E-06